Electromagnetic separators

Ulli Köster

Institut Laue Langevin
Grenoble, France

Institut Laue Langevin

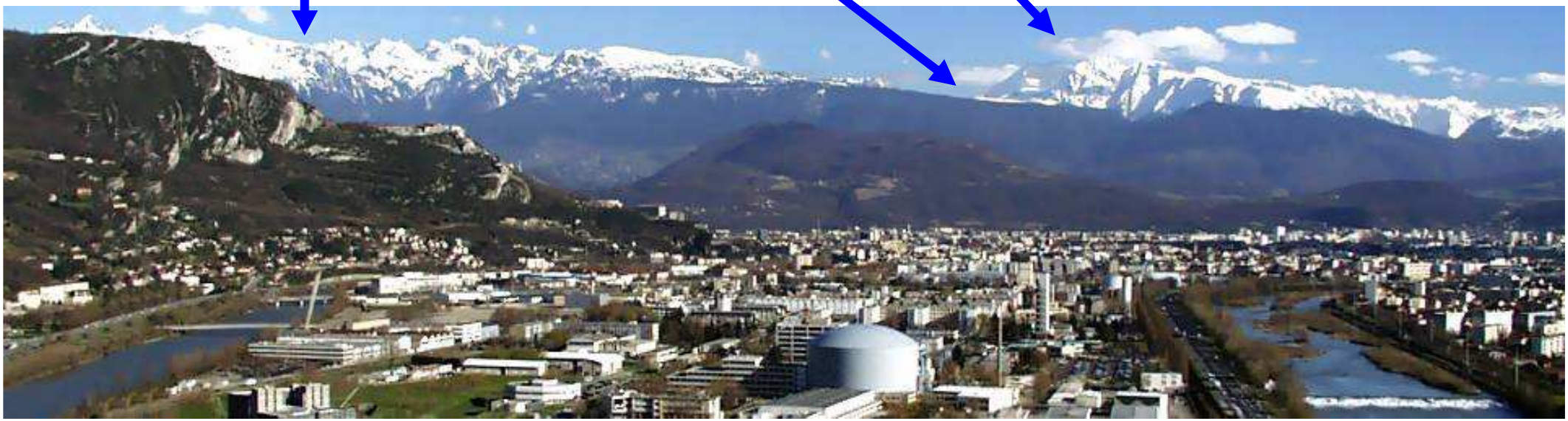

- **founded 1967**
- **today 13 member states**
- **operates most powerful neutron source of the world:**
  58 MW high flux reactor, $1.5 \cdot 10^{15}$ n./cm^2/s maximum neutron flux
- **over 40 instruments, mainly for neutron scattering**
- **user facility: 2000 scientific visitors from 45 countries per year**
- **Director General: Richard Wagner**
- **Nuclear physics instruments: LOHENGRIN, GAMS**

LOHENGRIN Setup

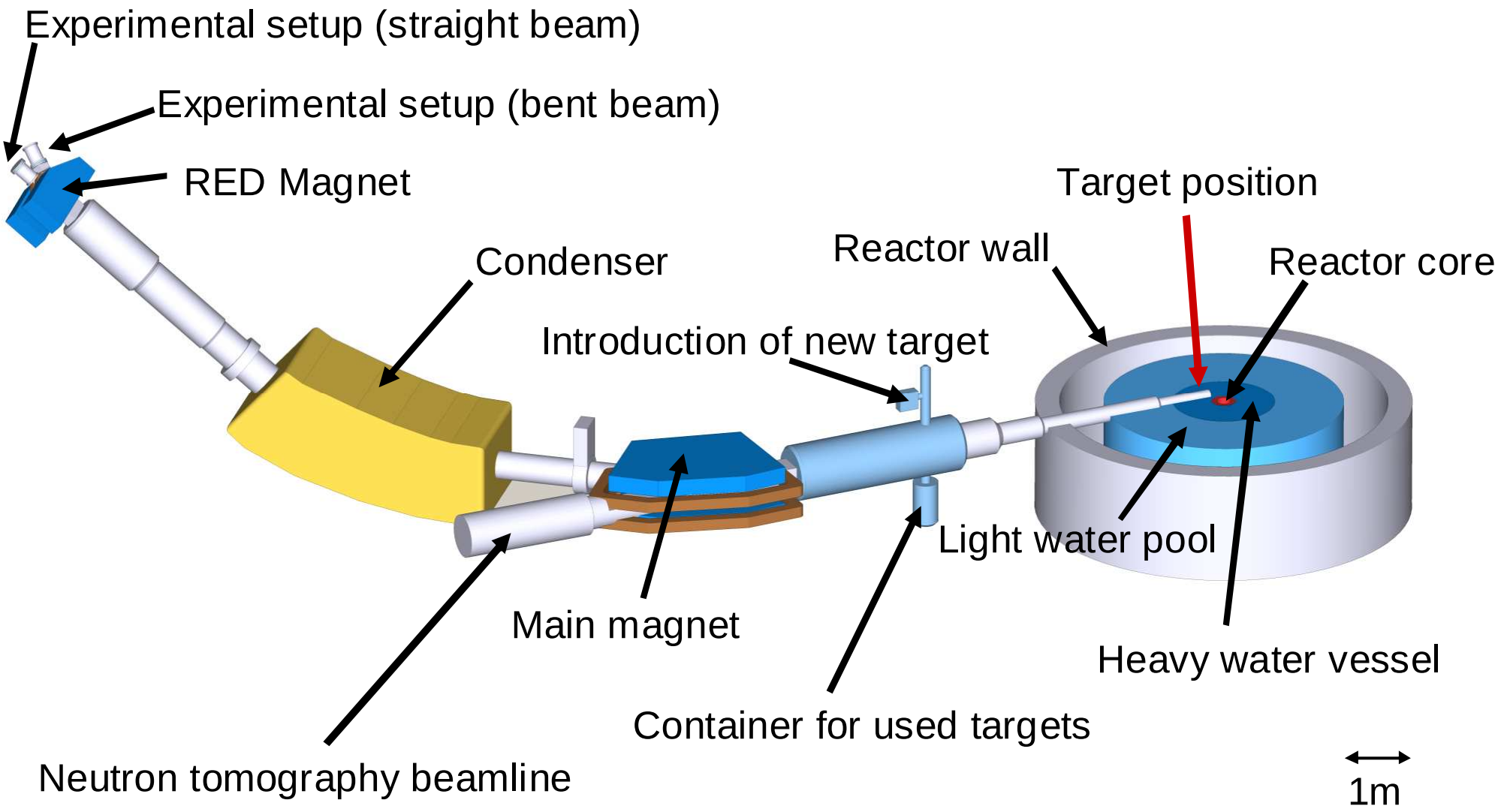

Outline

1. **Definitions and history**
2. **Basics of ion optics and dispersive elements**
3. **Static fields**
   a) deflection spectrometer
   b) retardation spectrometer
4. **Dynamic fields/separation**
   a) Time-of-Flight spectrometer
   b) Radiofrequency spectrometer
   c) Traps
5. **Technical realization (ion sources, etc.)**
6. **“Real examples” for nuclear physics applications**
   a) ISOL
   b) Recoil separators
   c) Fragment separators
   d) Spectrometer

Definitions

- **spectrometer: electrical detection**
- **spectrograph: photographic or other non-electrical detection**
- **also used: spectroscope**

- **mass / energy / isotope separator: assures a physical separation of different masses / energies / isotopes**

BigRIPS at RIBF Facility, RIKEN, Japan

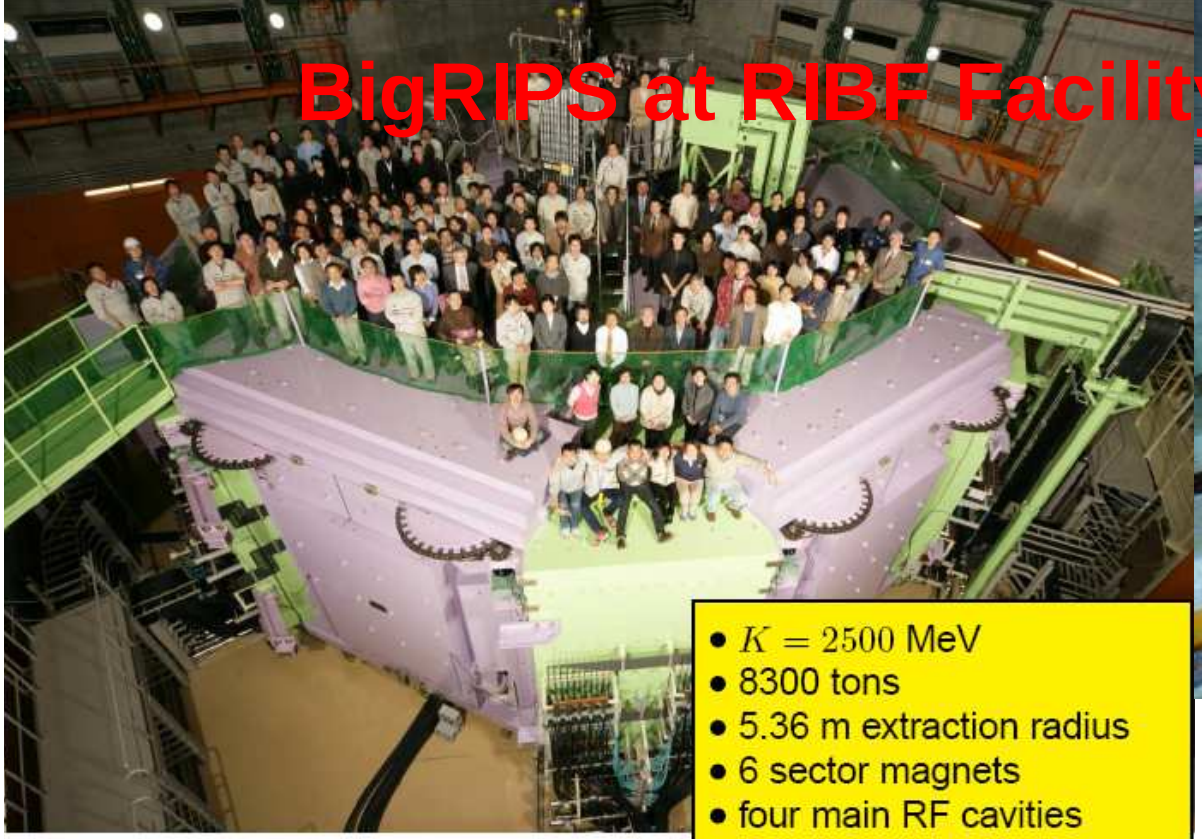

- $K = 2500$ MeV
- 8300 tons
- 5.36 m extraction radius
- 6 sector magnets
- four main RF cavities

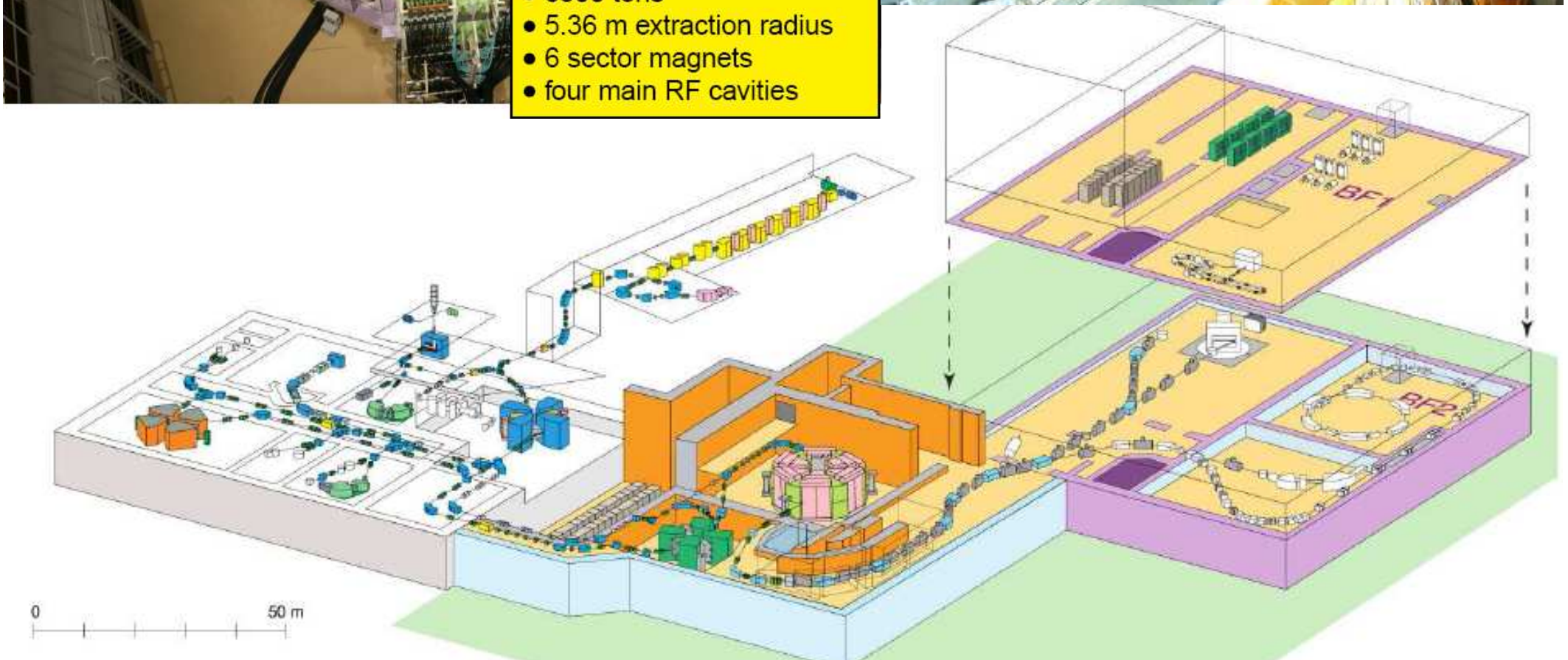

Super-FRS at FAIR, Germany

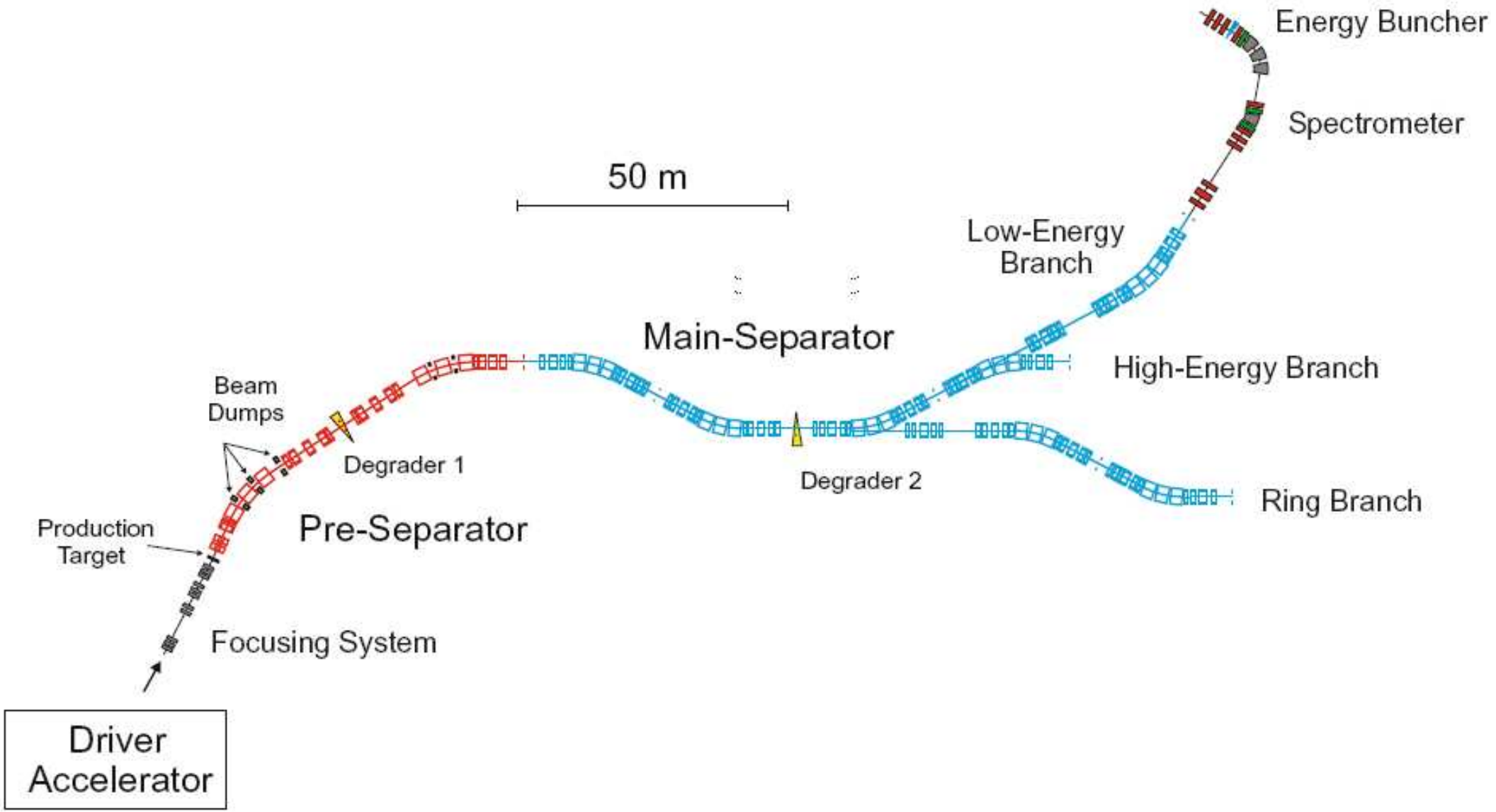

Importance of electromagnetic spectrometers

Thomson 1897: cathode rays

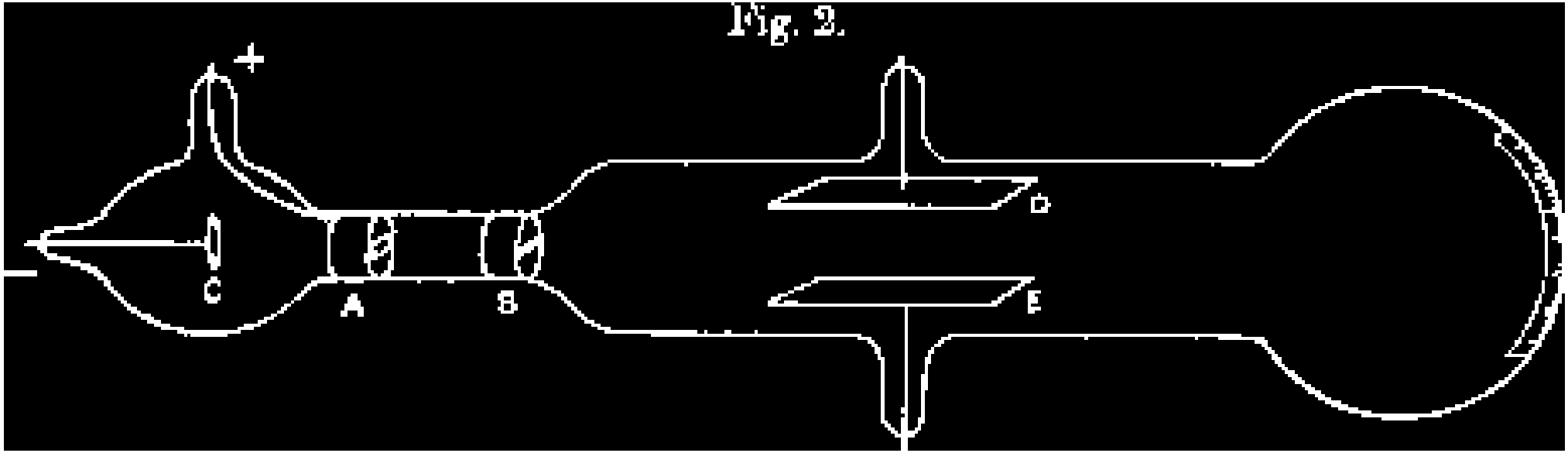

"Cathode rays", J.J. Thompson, Phil. Mag. 44 (1897) 293.

Noble prize in physics 1906 for discovery of the electron and the determination of its m/q ratio.

Goldstein 1886: *Kanalstrahlen*

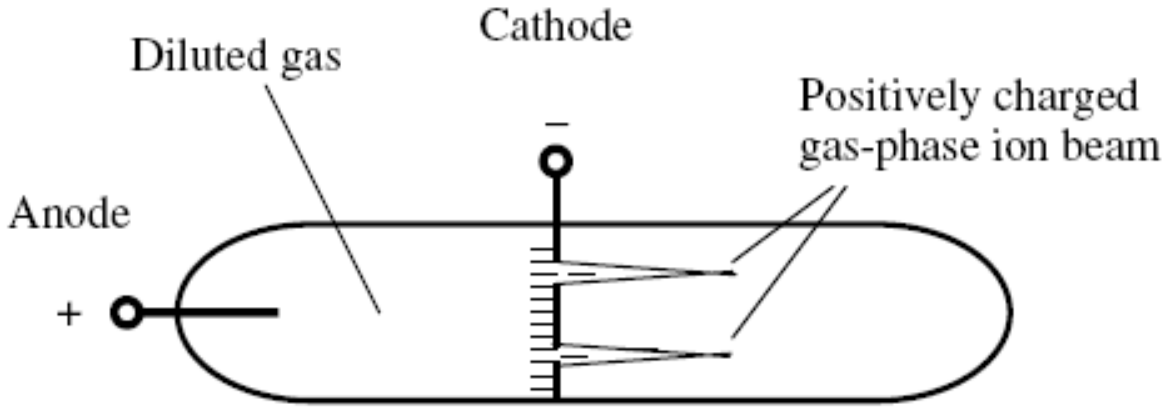

Figure 1.3 *Goldstein's glow discharge tube (1886) for generation of positively charged ions. (C. Brunnée, Int. J. Mass. Spectrom. Ion Proc. 76, 125 (1987). Reproduced by permission of Elsevier.)*

First fluorescent lamp and ion source.

Wien 1902: Wien filter

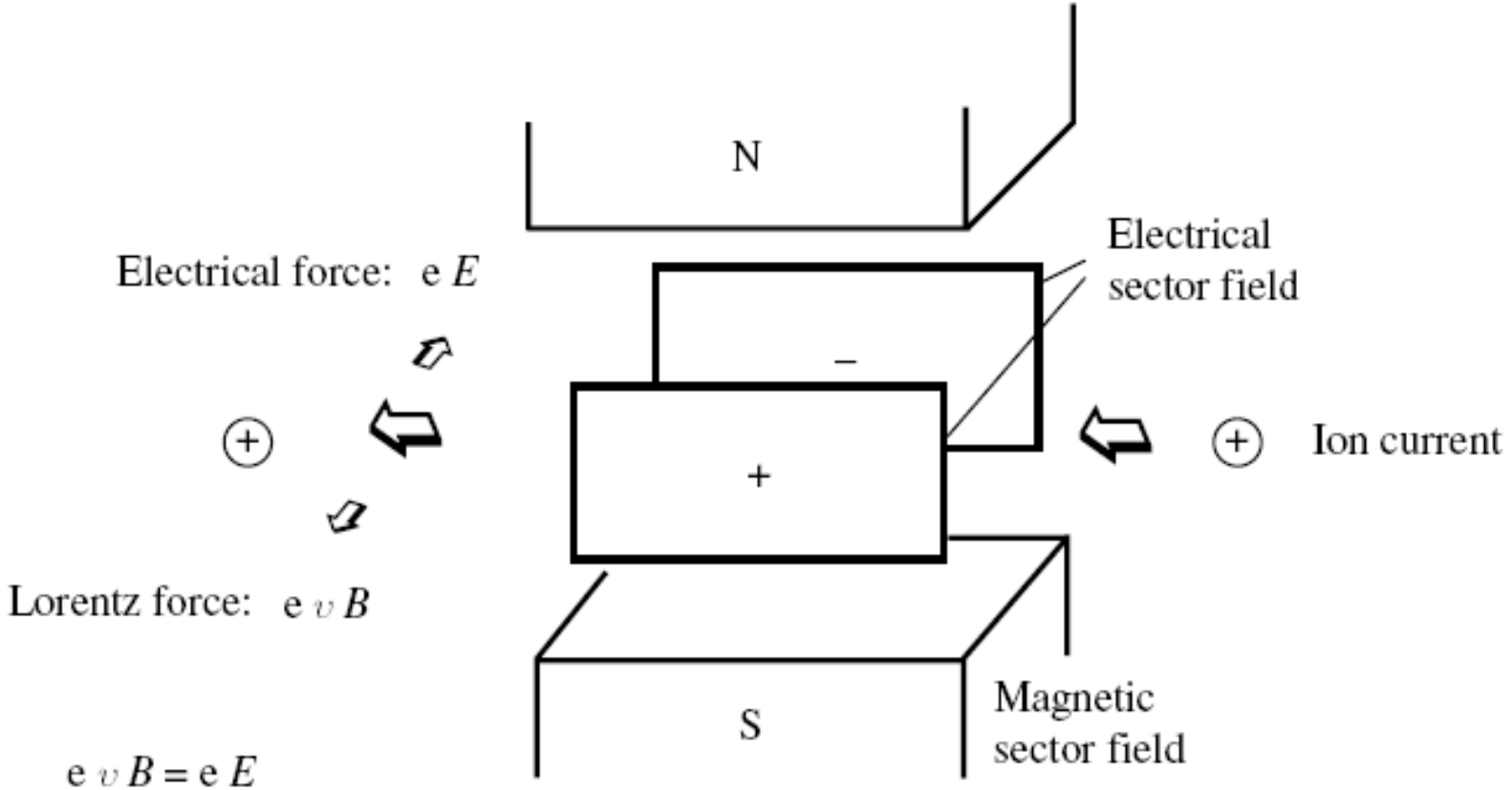

Electric field perpendicular to magnetic field

Figure 1.4 *Schematic of a Wien velocity filter with EB configuration: combination of electric (E) and magnetic (B) field (Wien,1898). (C. Brunnée, Int. J. Mass. Spectrom. Ion Proc. 76, 125 (1987). Reproduced by permission of Elsevier.)*

Wien: Nobel price in physics 1911 for discovery that "Kanalstrahlen" carry positive charge

Thomson 1910: parabola mass spectrograph

Electric field parallel to magnetic field

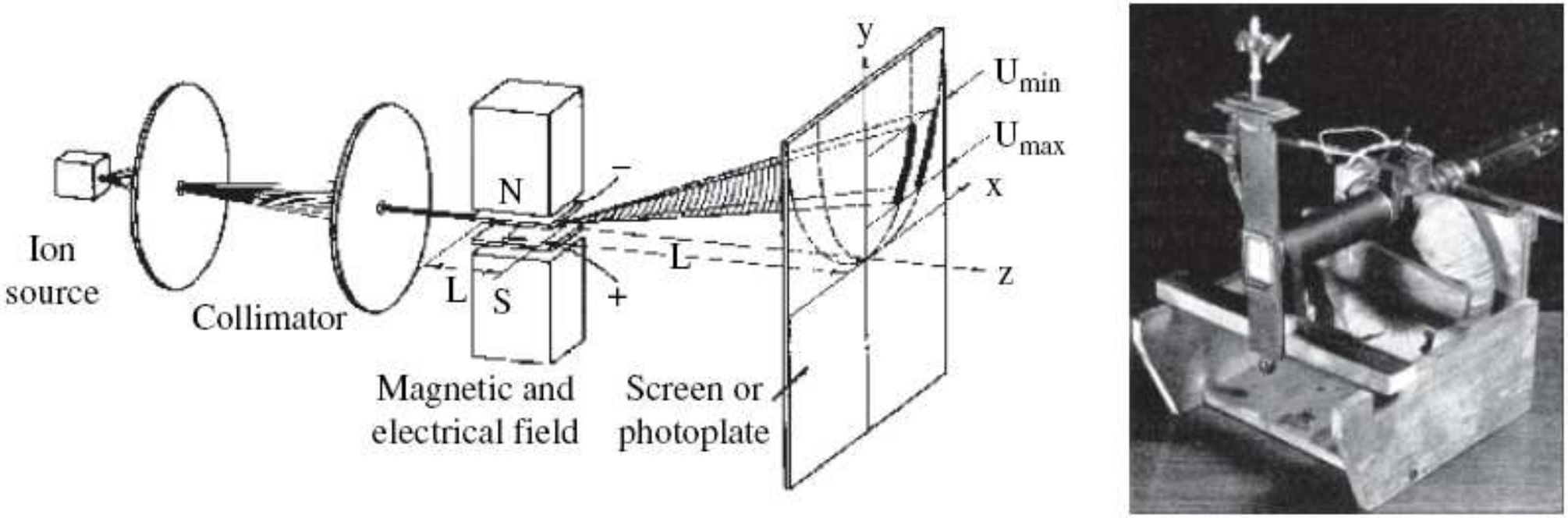

Figure 1.5 *Parabola mass spectrograph constructed by J. J. Thomson (1910) with a discharge tube as ion source, a superimposed electrical field and a magnetic field oriented parallel to it for ion separation, and a photoplate for ion detection. (H. Kienitz (ed.), Massenspektrometrie (1968), Verlag Chemie, Weinheim. Reproduced by permission of Wiley-VCH.)*

Neon consists of two isotopes with mass 20 and 22

Thomson 1913: mass spectrum of neon

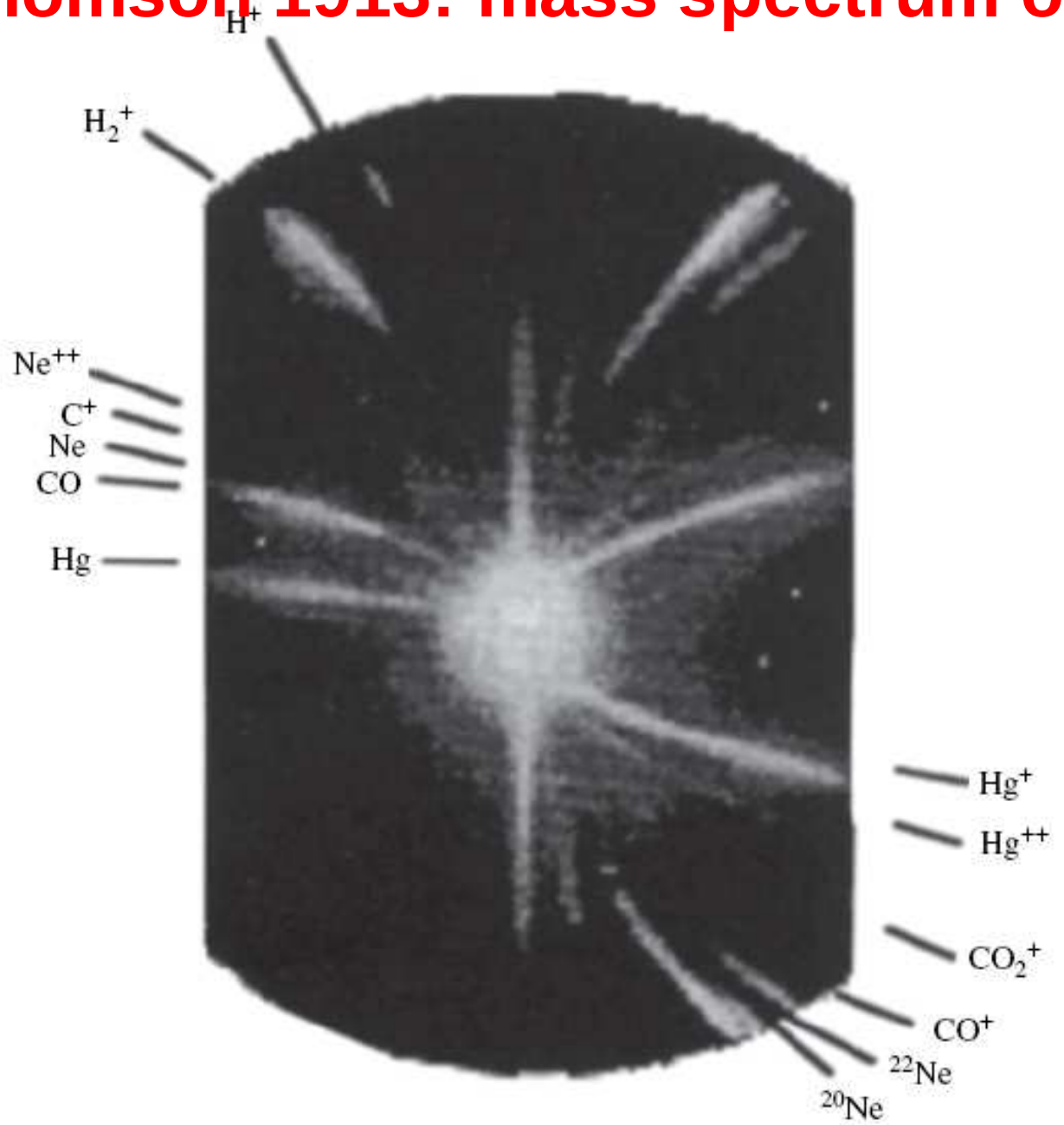

Figure 1.6 *Mass spectrum of neon with masses 20 and 22 u measured by J.J. Thomson (1913) using his parabola mass spectrograph is shown in Figure 1.5. (H. Kienitz (ed.), Massenspektrometrie (1968), Verlag Chemie, Weinheim. Reproduced by permission of Wiley-VCH.)*

Parabola spectrograph

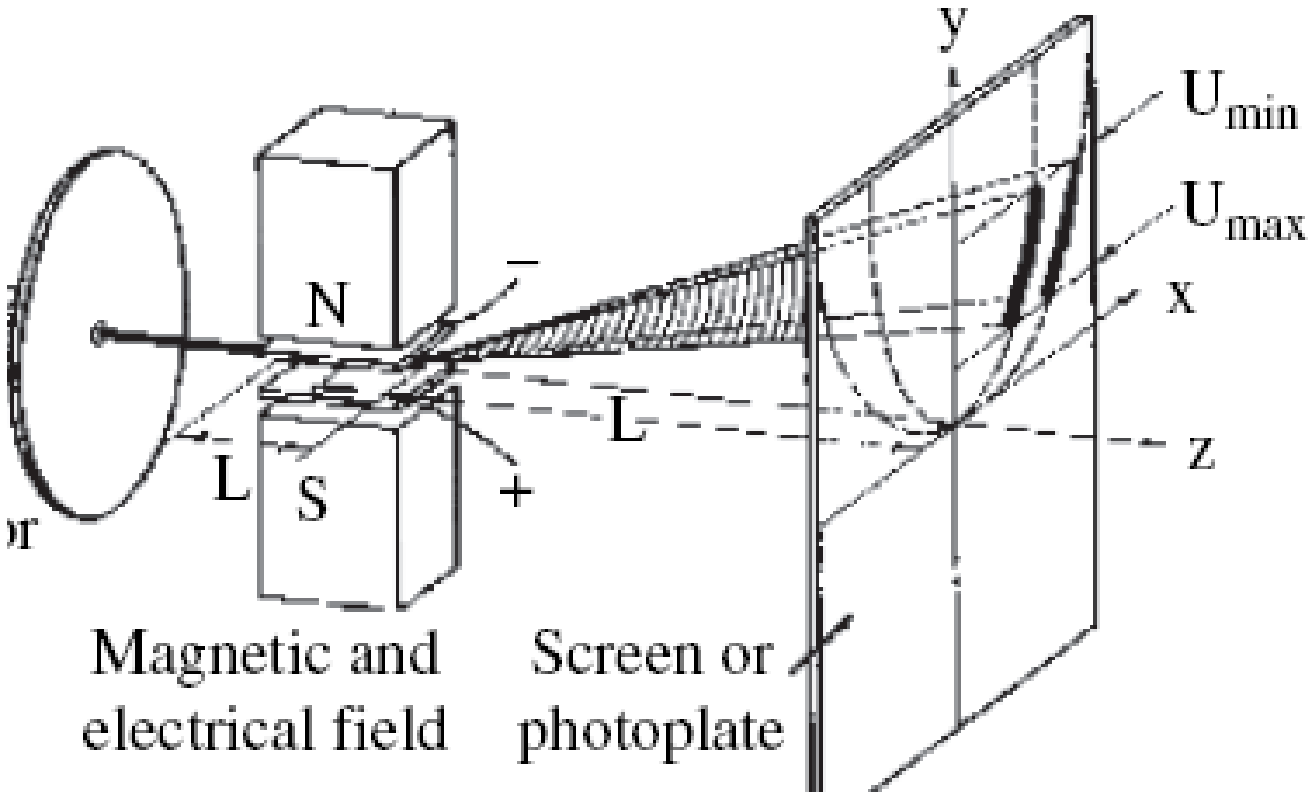

transit time through field: $t = L/v$

vertical displacement: $y = \frac{1}{2}\, U/d\; q/m\; (L/v)^2$

horizontal displacement: $x = \frac{1}{2}\, B\; q/m\; L^2/v$

$y = k\; m/q\; x^2$; $k = 2\; U/(d\; B^2\; L^2)$

The LOHENGRIN fission fragment separator

Angular focusing in x and y direction.

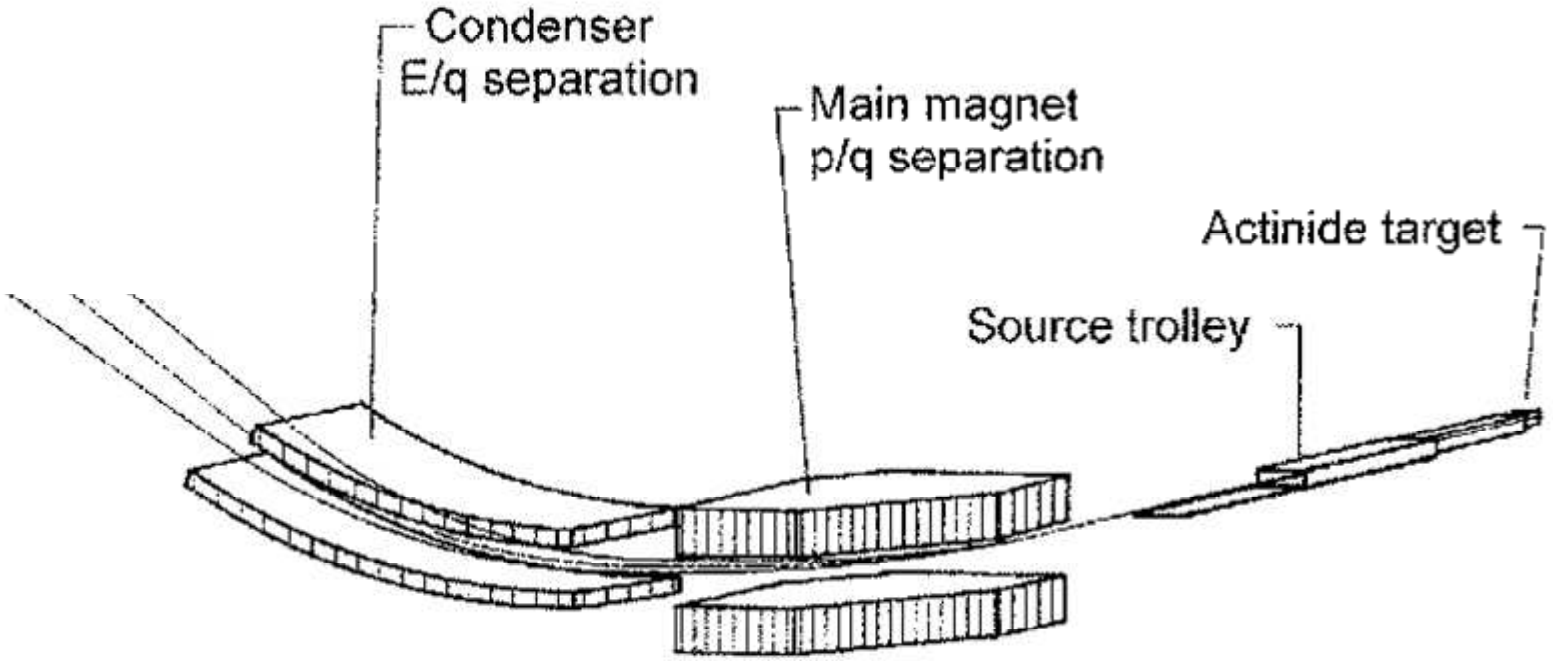

$$m\,v^2 / r_{el} = q\,E \qquad m\,v^2 / r_{magn} = q\,v\,B$$

$$E_{kin} / q = E / 2\,r_{el} \qquad m\,v / q = B\,r_{magn}$$

Animation!

Aston 1919: velocity focusing spectrograph

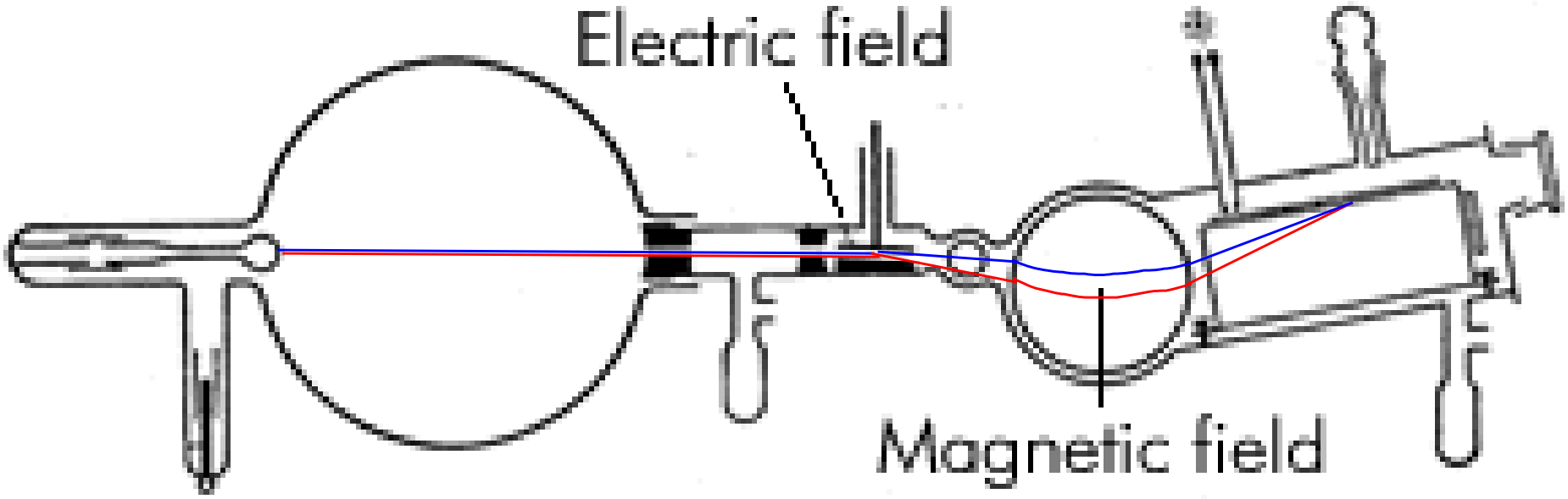

Aston's design for the mass spectrograph.

Aston: velocity focusing gives factor 10 improvement in mass resolution ($\Delta m/m = 1/130$)

Noble prize in chemistry 1922 for the discovery that elements may have isotopes of different mass (^{20}Ne, ^{21}Ne and ^{22}Ne).

Dempster 1918: 180 degree spectrometer

- electron bombardment ion source for monoenergetic ions
- 180 degree magnetic field provides angular focusing
- scan of magnetic field to measure mass spectra

1920: discovery of isotopes in Mg, Li, K, Ca, Zn

$$q/m = 2\,U / (B^2\,r^2)$$

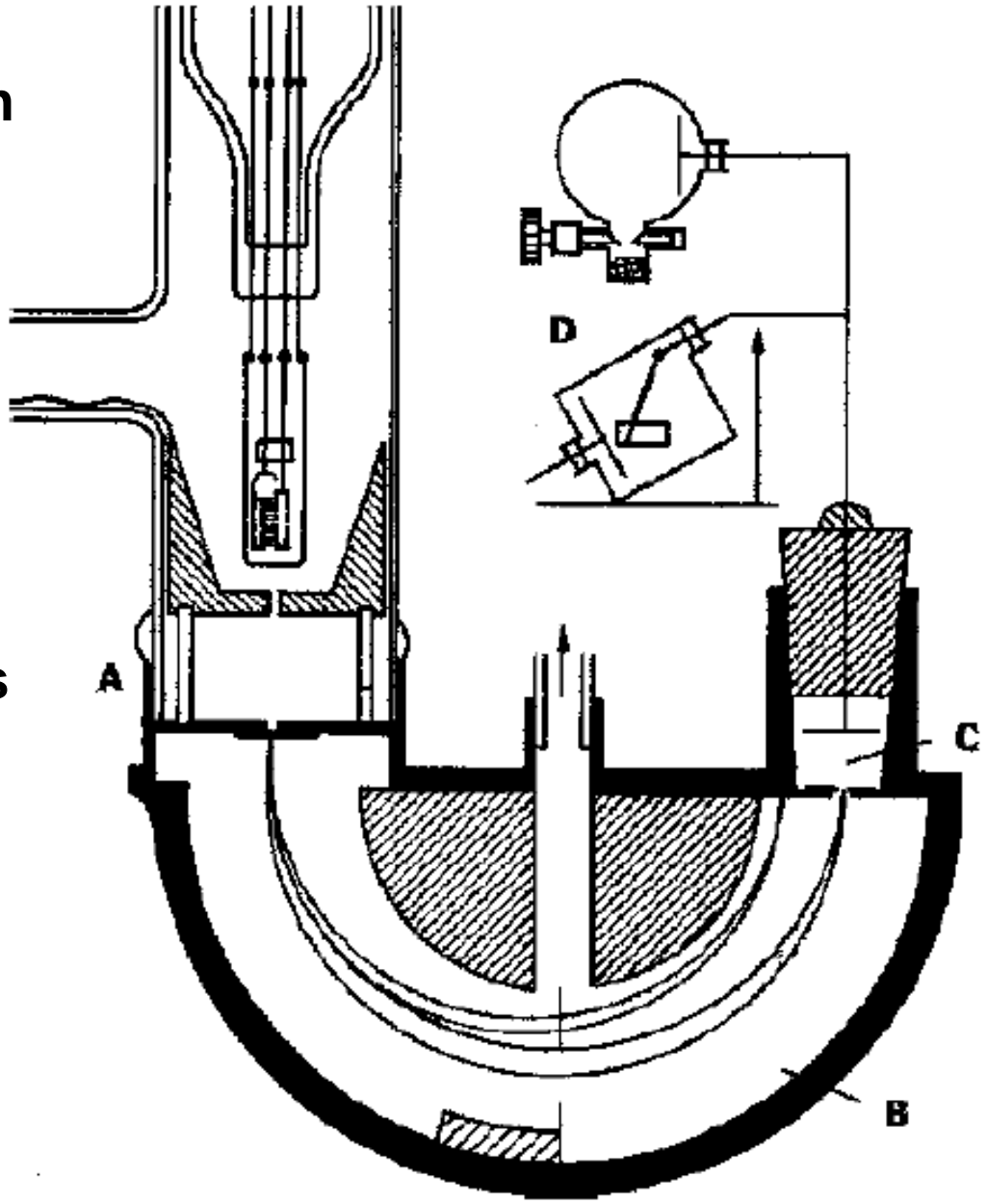

Figure 1.7 Mass spectrometer from A.J. Dempster (1918). A – ion source; B – electromagnet; C – Faraday cup; D – electrometer. (H. Kienitz (ed.), Massenspektrometrie (1968), Verlag Chemie, Weinheim. Reproduced by permission of Wiley-VCH.)

Calutron 1942: electromagnetic isotope separation

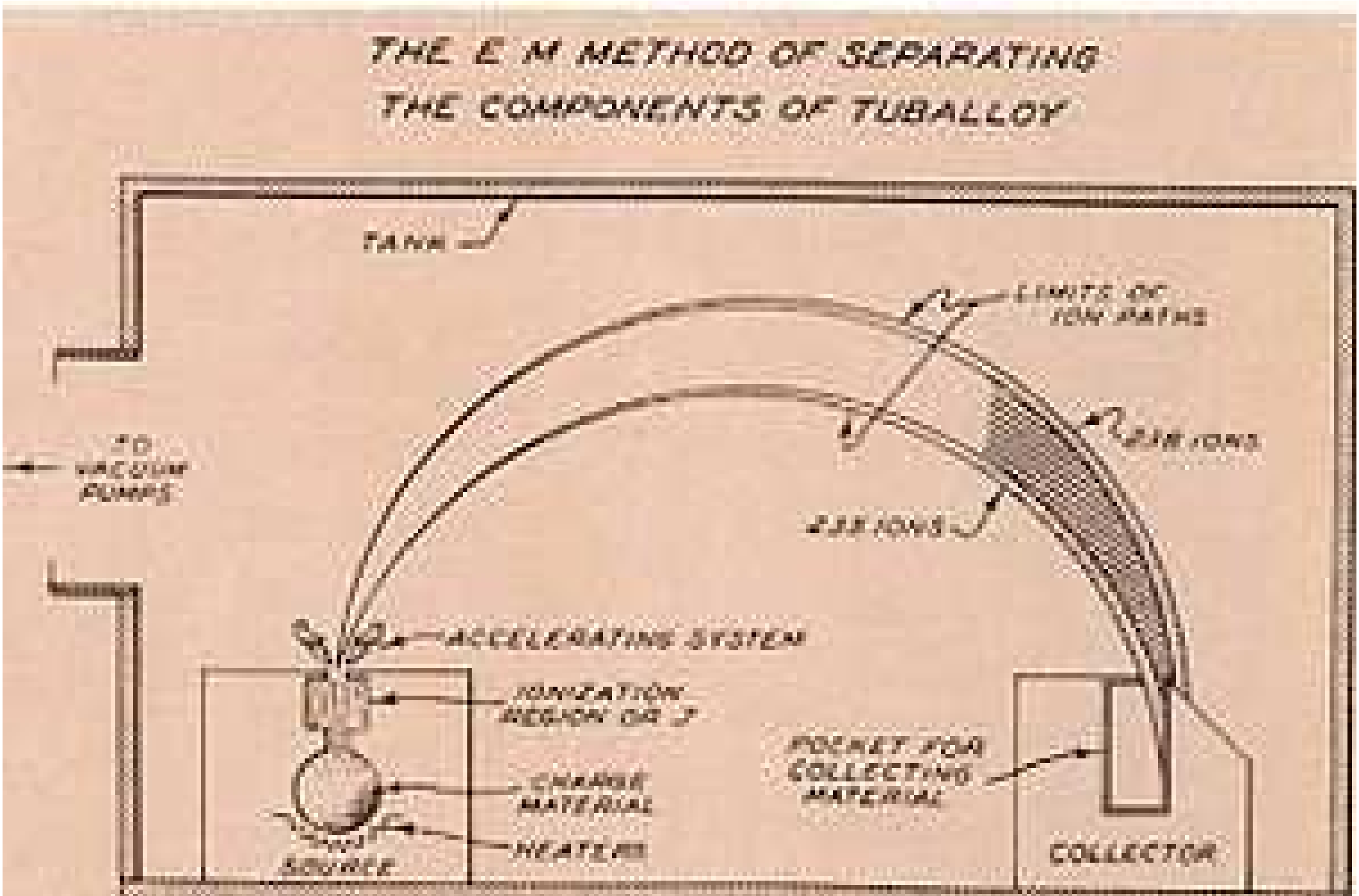

Large scale electromagnetic isotope separation

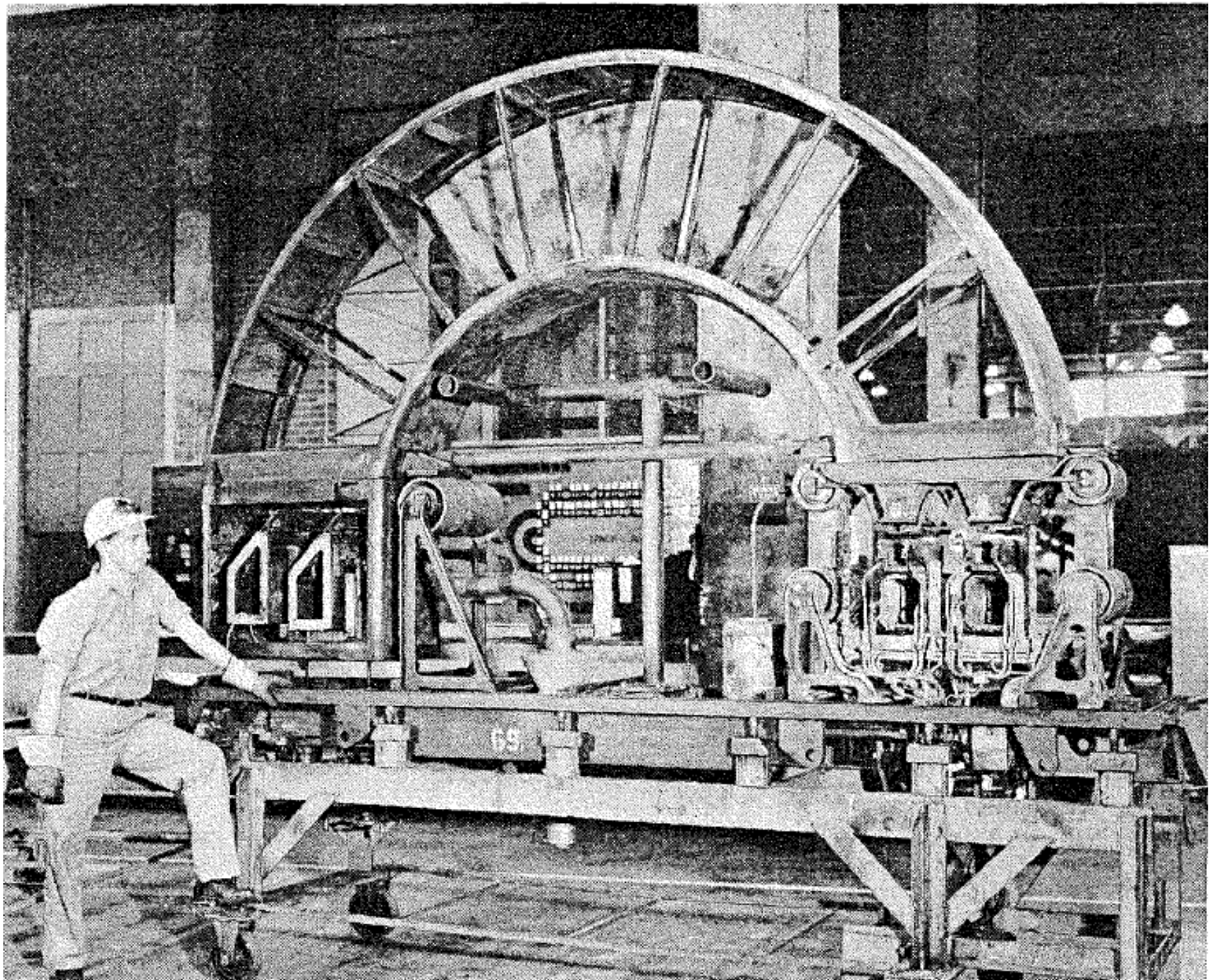

Collector plates of a Calutron

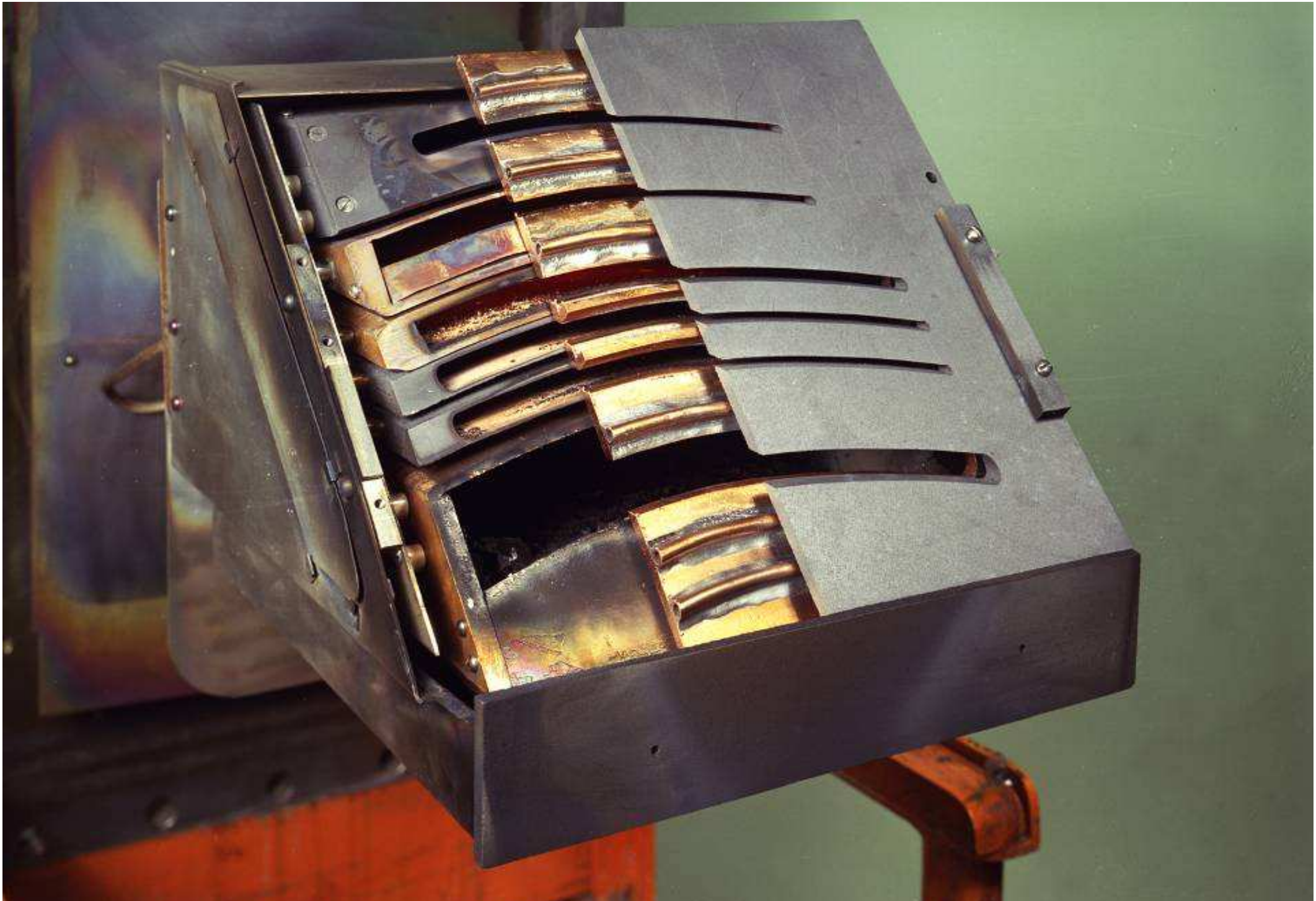

1945: large scale electromagnetic isotope separation

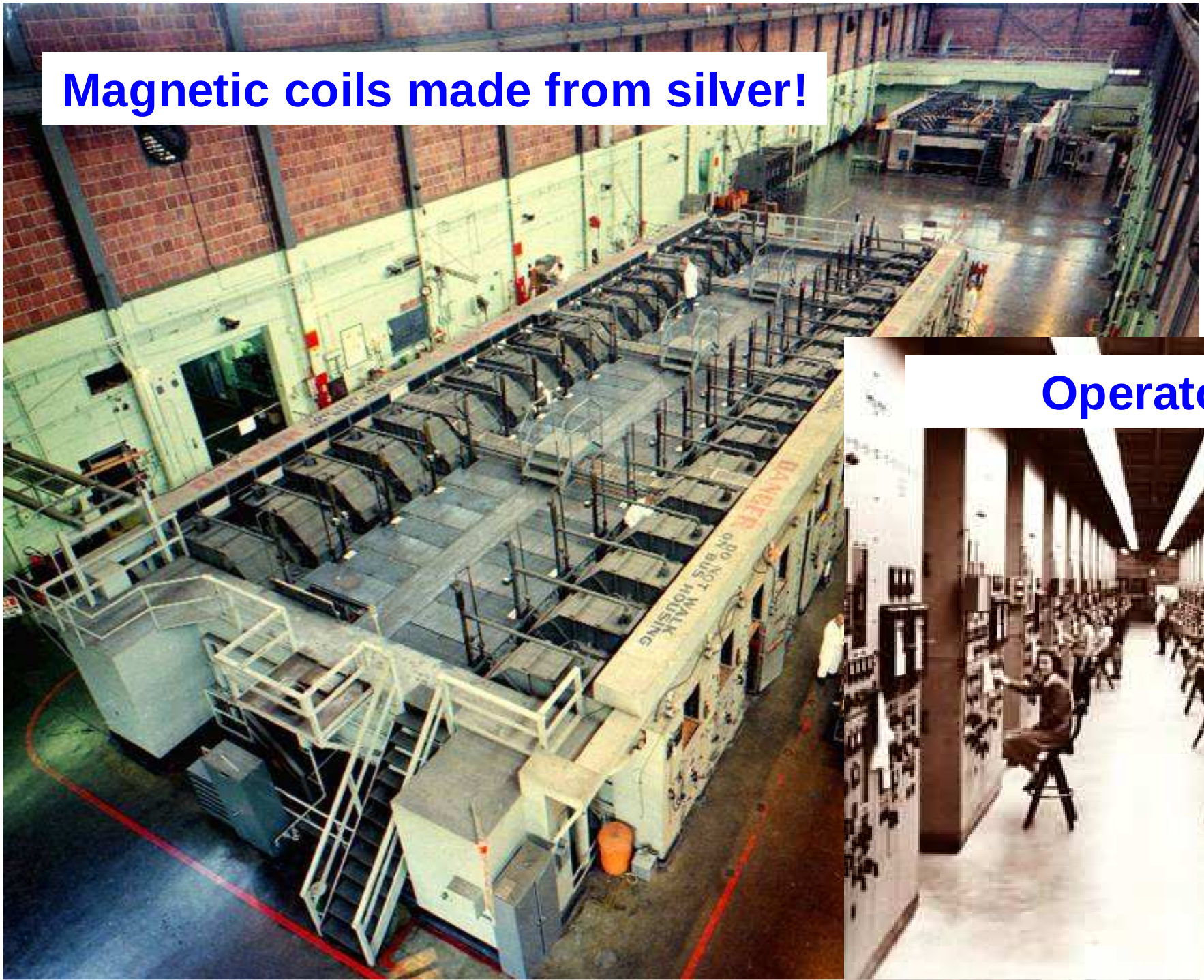

1945: “Impact” of electromagnetic isotope separation

Hiroshima: 60 kg of isotopically enriched ^{235}U

Aston 1925: improved mass spectrograph

Improved version gives mass resolution: $\Delta m/m = 1/600$

Accuracy of mass determination: 10^{-4}

Used to study deviations of atomic masses m from A.

Introduced: "packing fraction" = m/A – 1

Systematic investigation of nuclear binding energies

Carbon isotopes

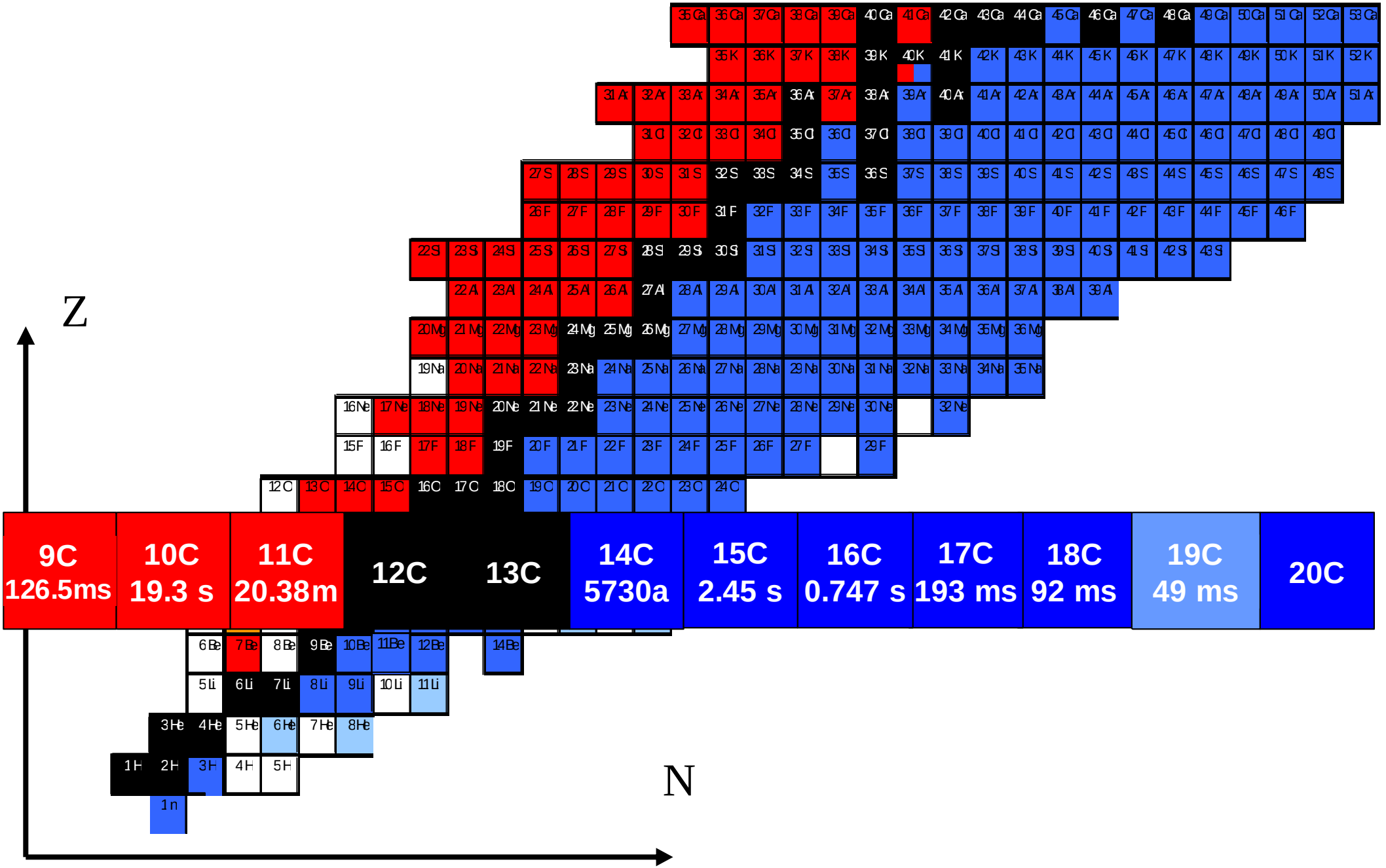

Chart of the nuclides

Ca. 3000 isotopes known, thereof less than 10% are stable

>3000 additional isotopes are expected to exist!

Production of radioisotopes via nuclear reactions!

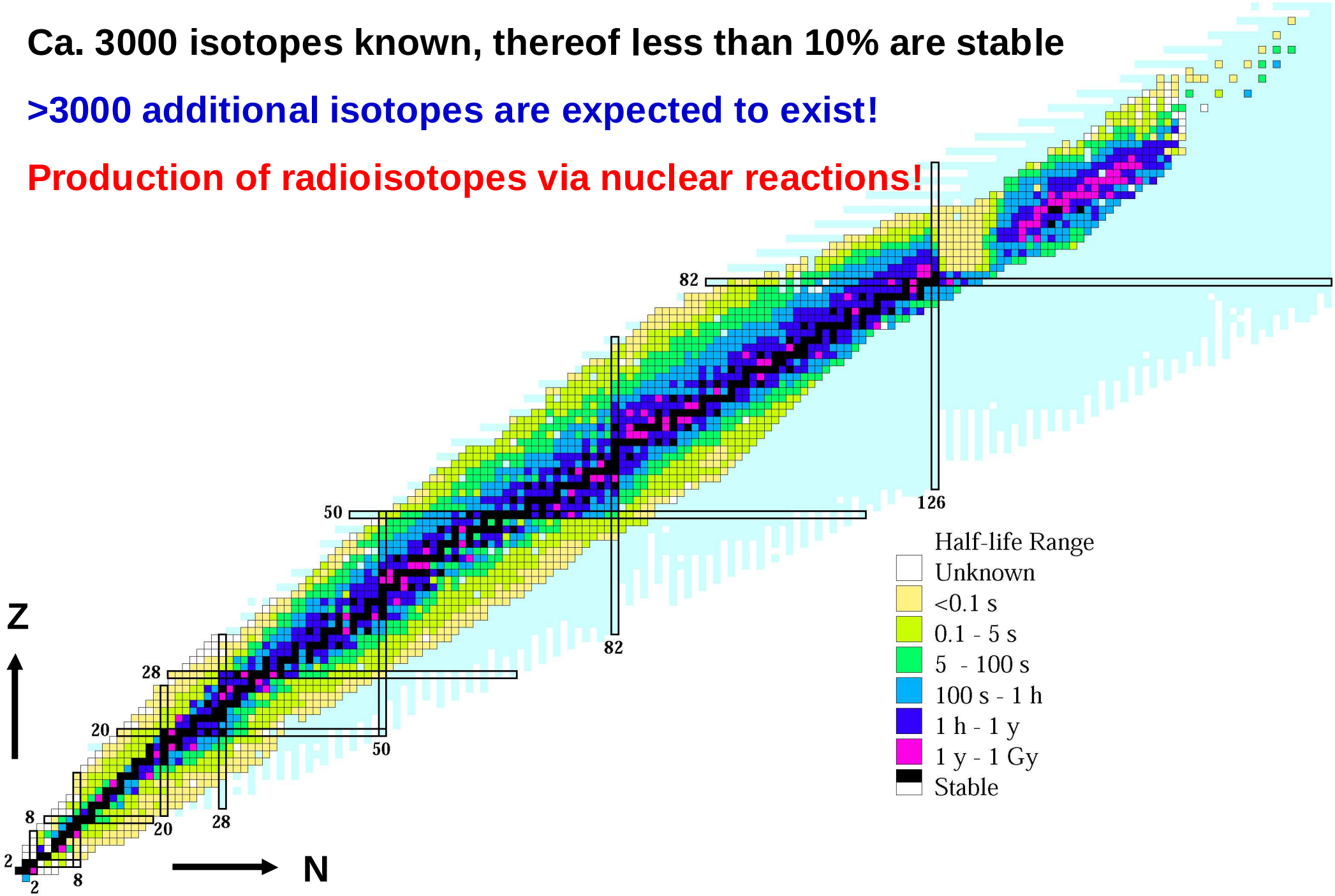

Why “ion beams”?

Production:

high radiation environment

primary beam

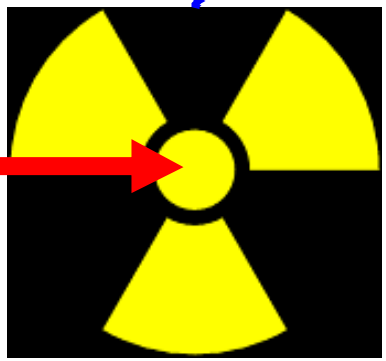

target

Detection:

low radiation background

Transport methods:

- carry (“SRAFAP”)
- drive (*G.T. Seaborg and W.D. Loveland, The Elements beyond Uranium, John Wiley & Sons, 1990*)
- transport shuttle with pressurized air
- transport in gas-jet
- pump through vacuum system
- send as ion beam

Irradiations of targets

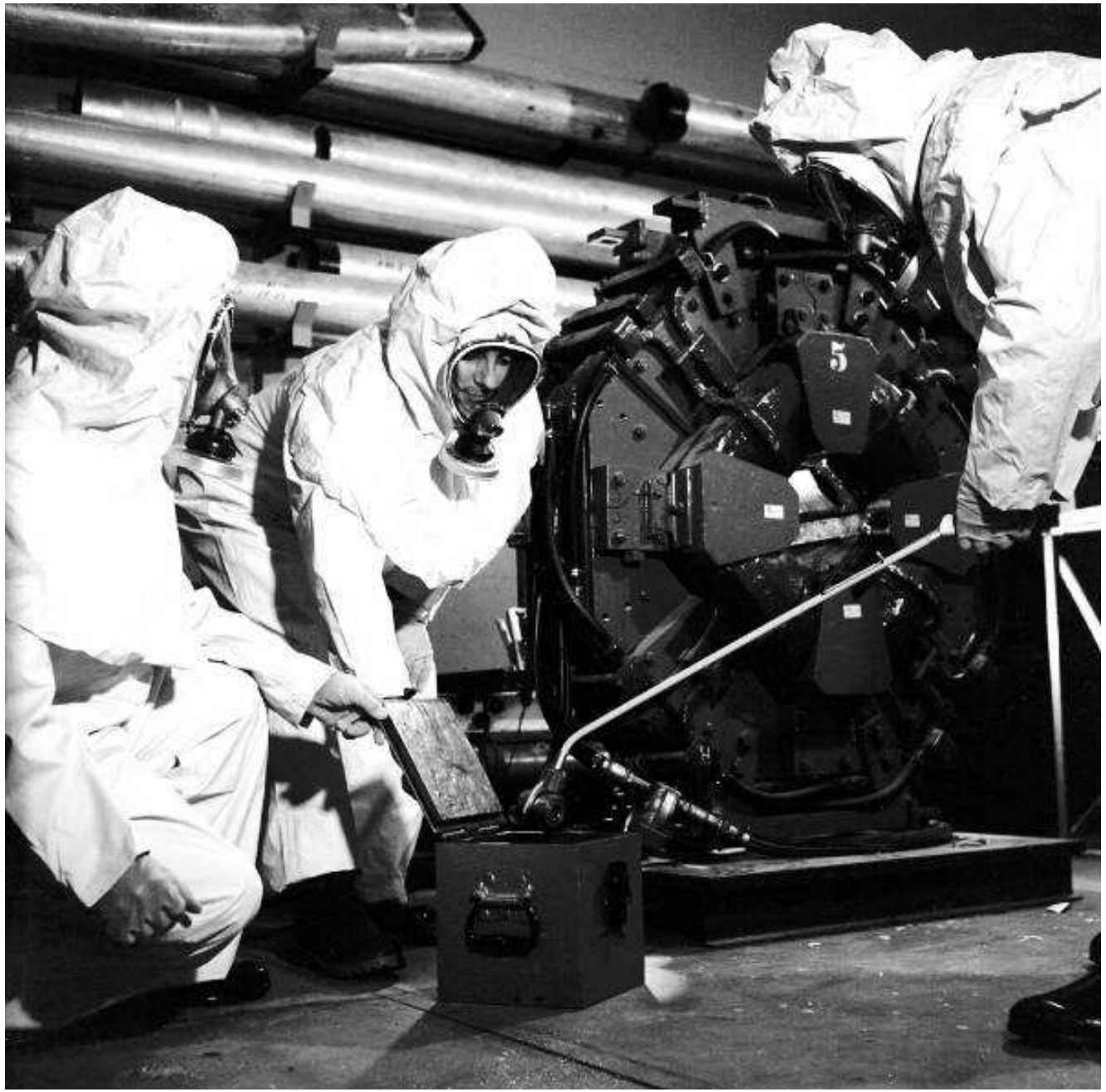

Off-line mass separator

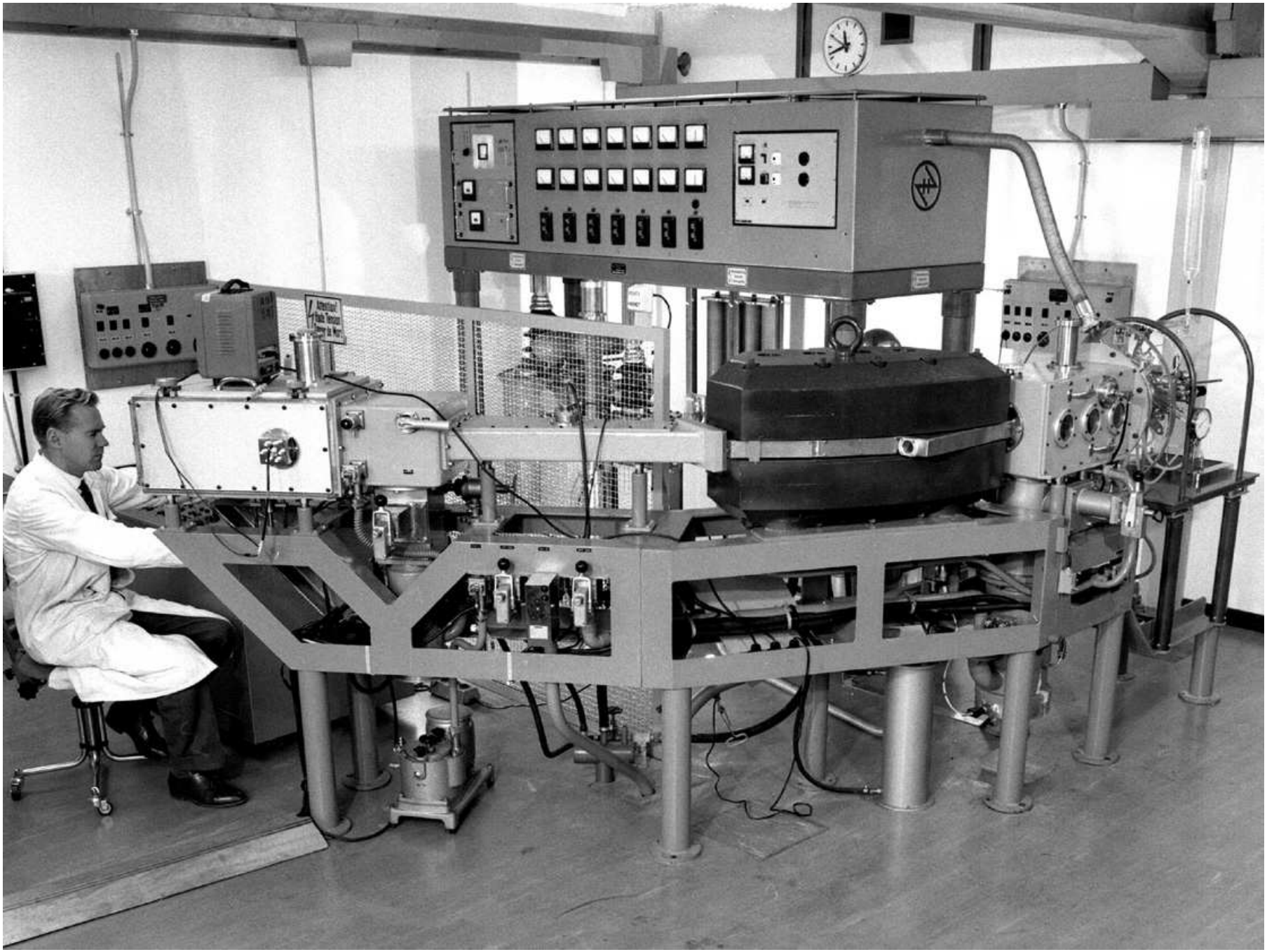

1951: first ISOL experiment at Niels Bohr Institute

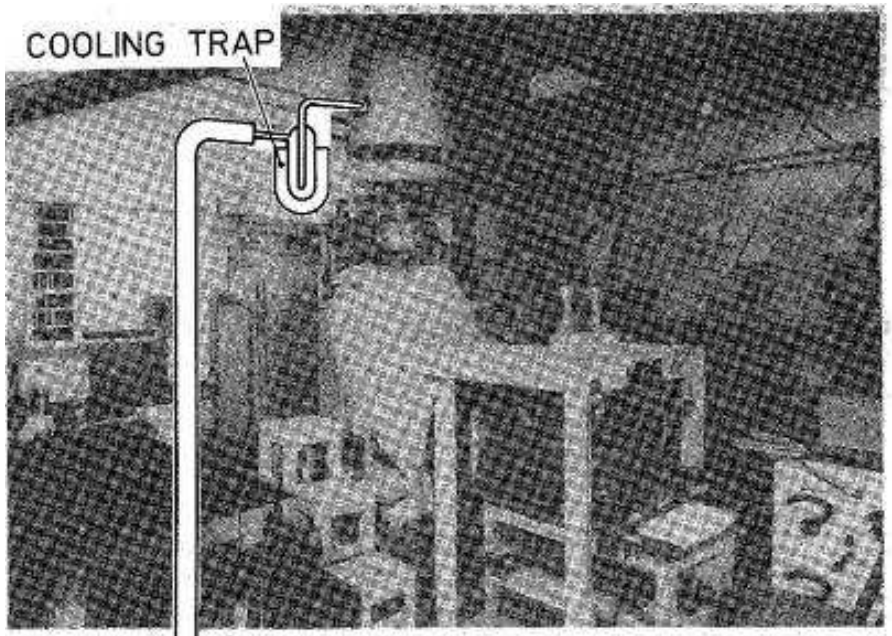

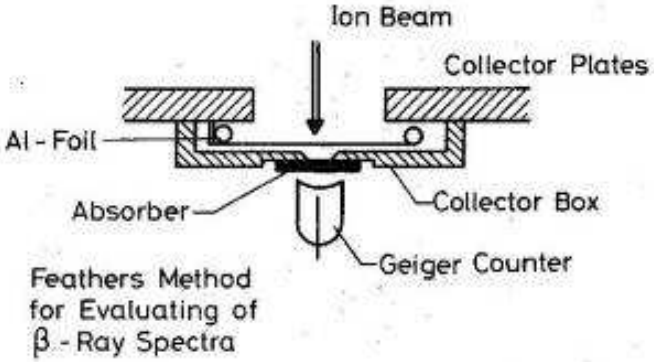

ISOL beams of $^{89\text{-}93}$Kr

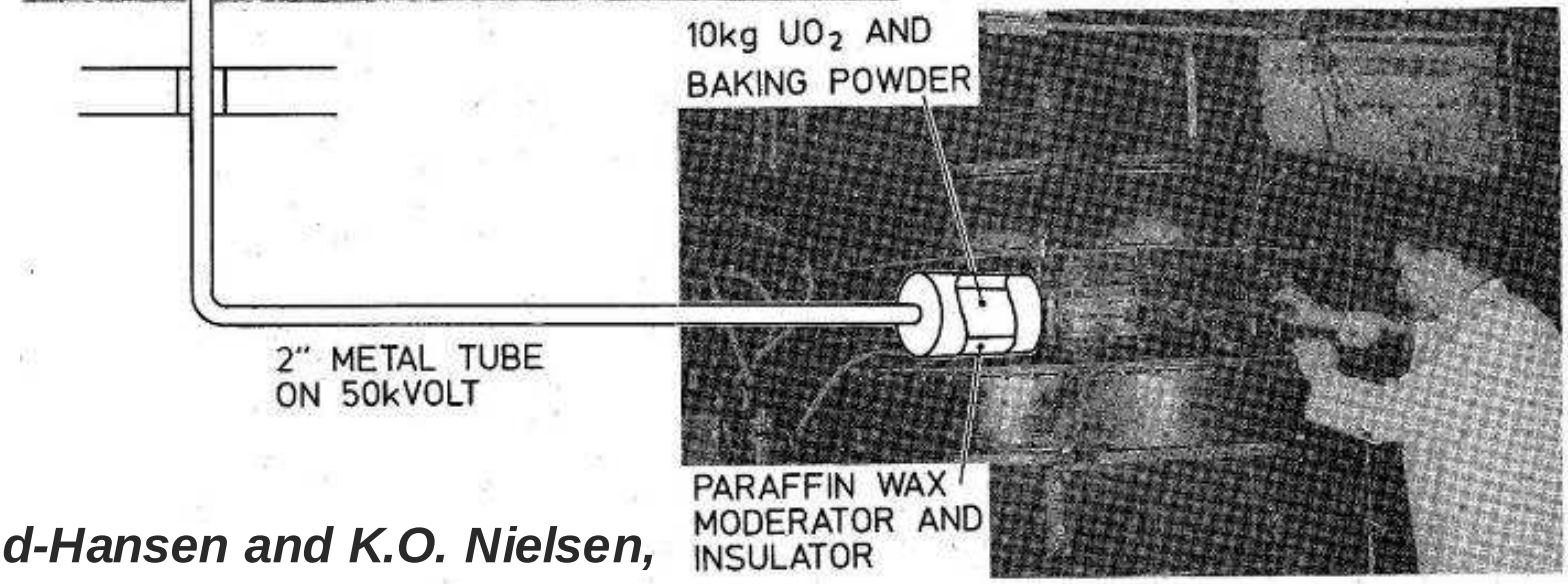

O. Kofoed-Hansen and K.O. Nielsen,

Mat. Fys. Medd. Dan. Vid. Selsk. 26, Nr. 7 (1951).

*I*sotope *S*eparation *O*n-*L*ine

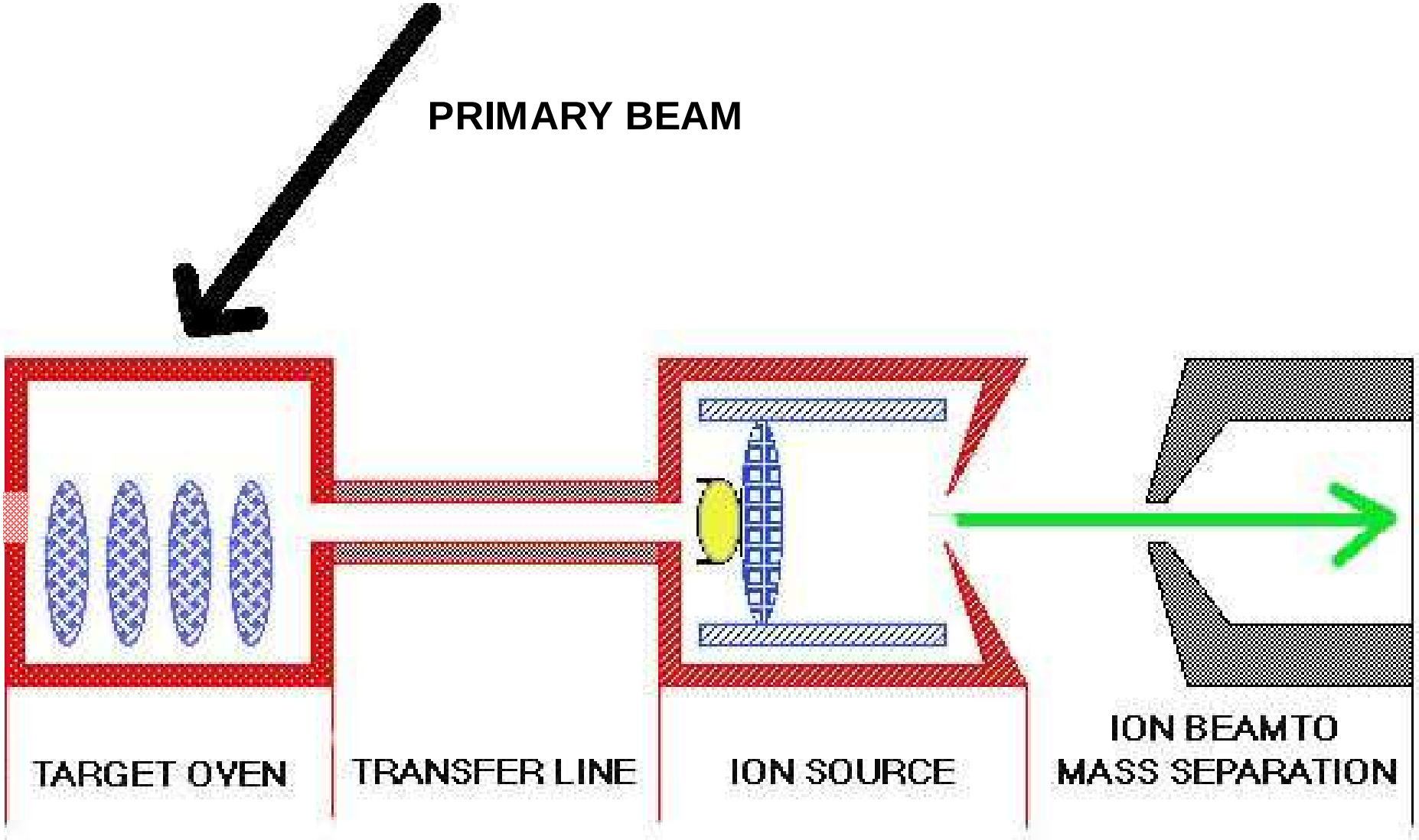

Isotope selection

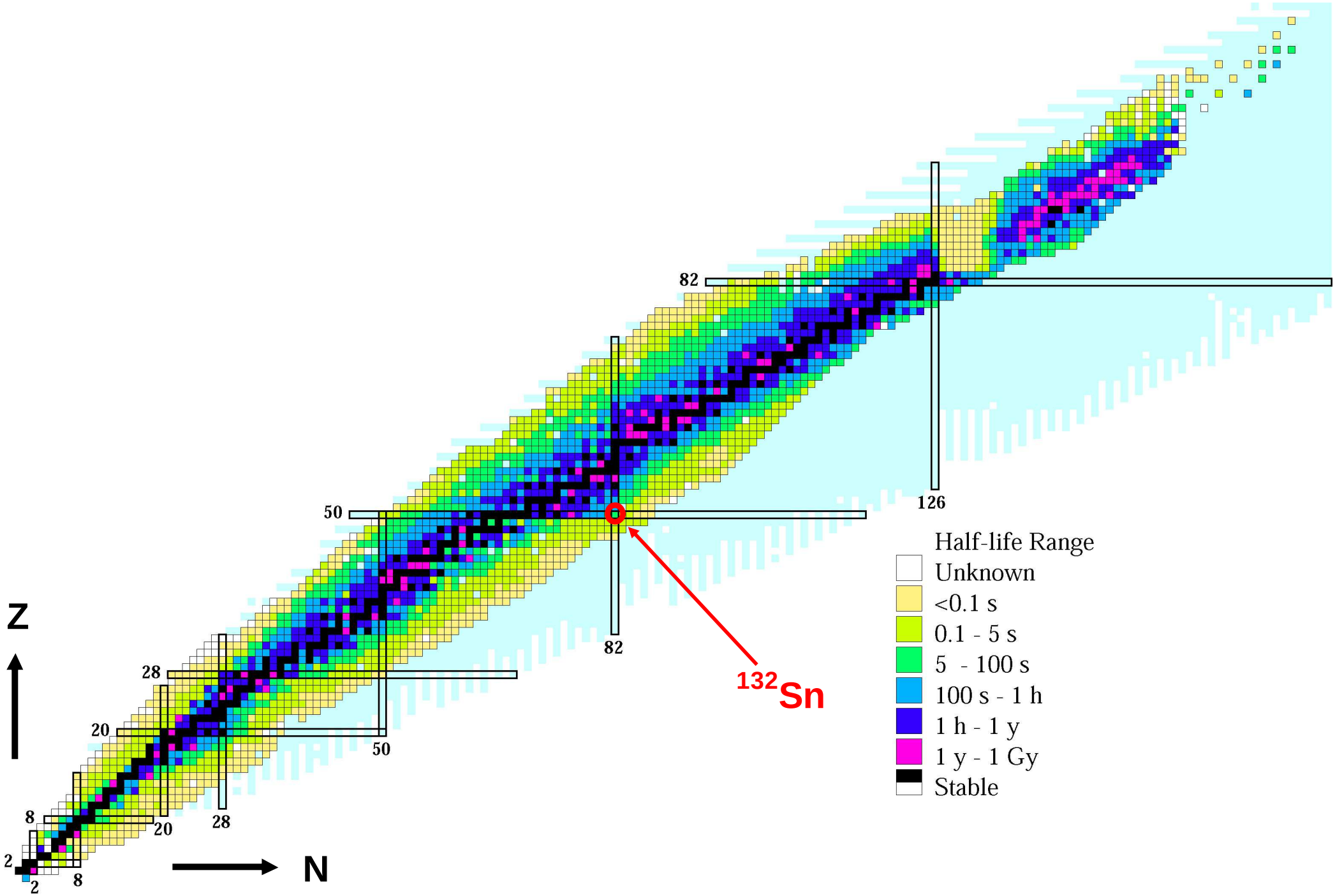

Isotope selection with ISOL method

- Ionization to q = 1+
- Acceleration to 60 keV
- Mass selection by magnetic deflection
- $B\rho = p/q \propto \sqrt{A}$

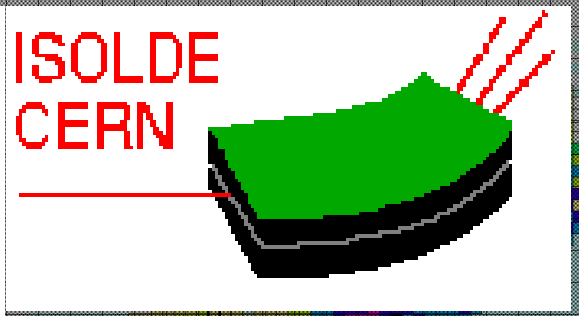

Z selection by chemically selective step

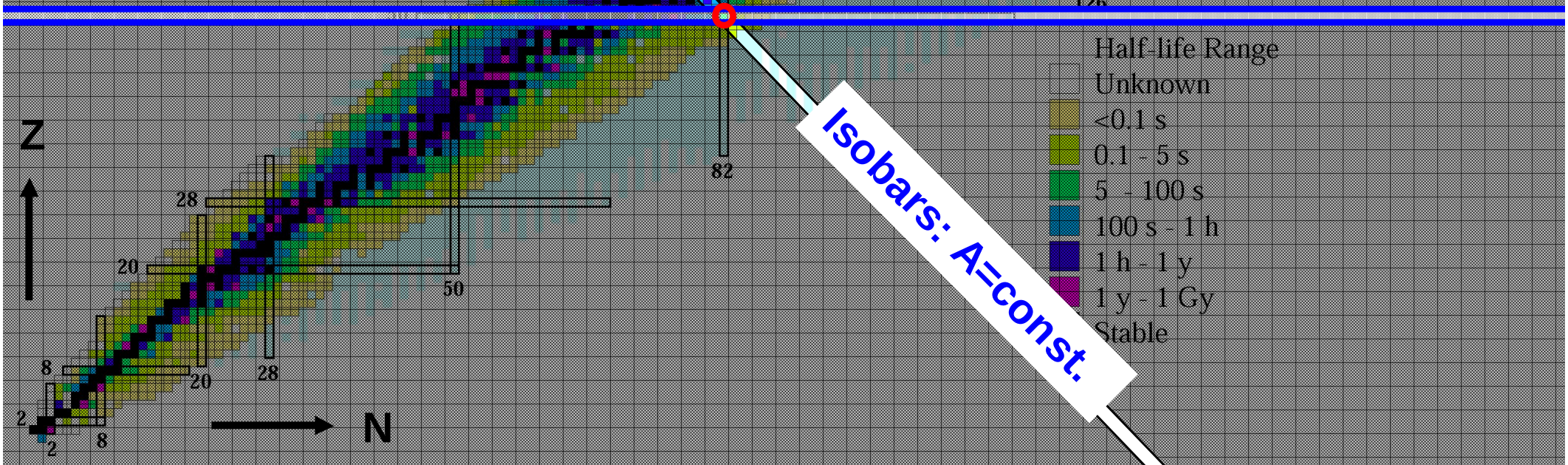

The challenge of the extremes!

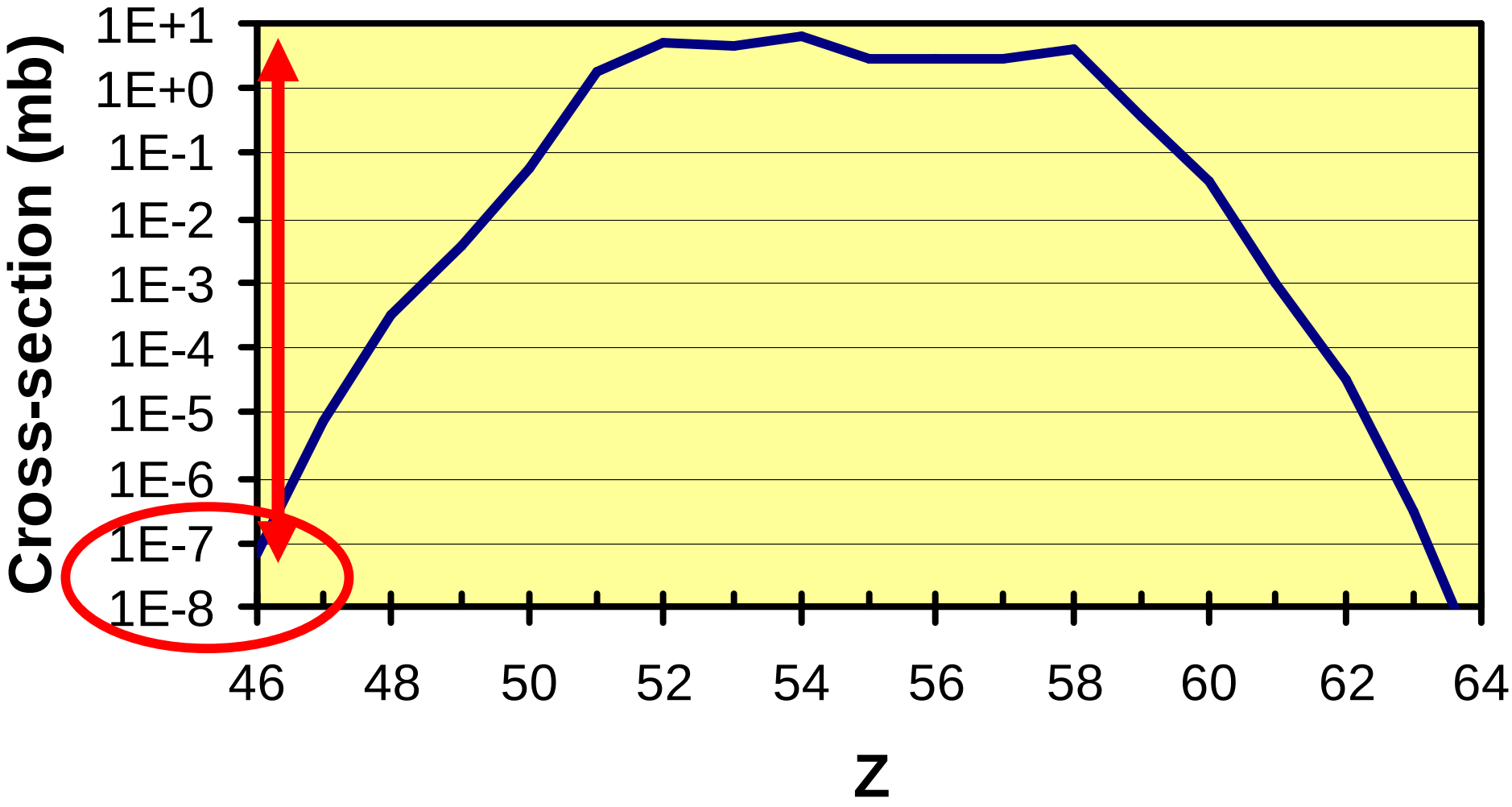

1. low cross-sections ⇒ optimize efficiency
2. enormous production of isobars ⇒ optimize selectivity
3. short half-lives ⇒ optimize rapidity

Optimize event rate

All steps of the separation chain need to be optimized!

$$r = \underbrace{\Phi \cdot \sigma \cdot N}_{\text{In-target production}} \cdot \underbrace{\varepsilon_{target} \cdot \varepsilon_{source} \cdot \varepsilon_{transp} \cdot \varepsilon_{det}}_{\text{Efficiency}}$$

Optimize RIB intensity

All steps of the separation chain need to be optimized!

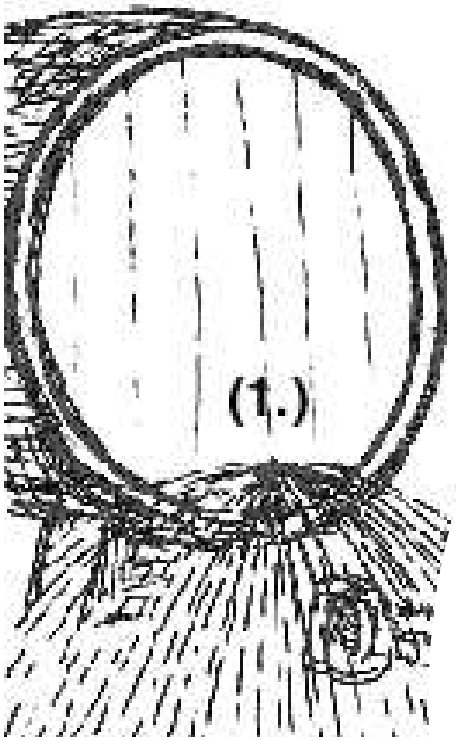

$$r = \Phi \cdot \sigma \cdot N \cdot \varepsilon_{target} \cdot \varepsilon_{source} \cdot \varepsilon_{transp} \cdot \varepsilon_{det}$$

powerful accelerator

$\Rightarrow$ **accelerator technology**

Optimize RIB intensity

All steps of the separation chain need to be optimized!

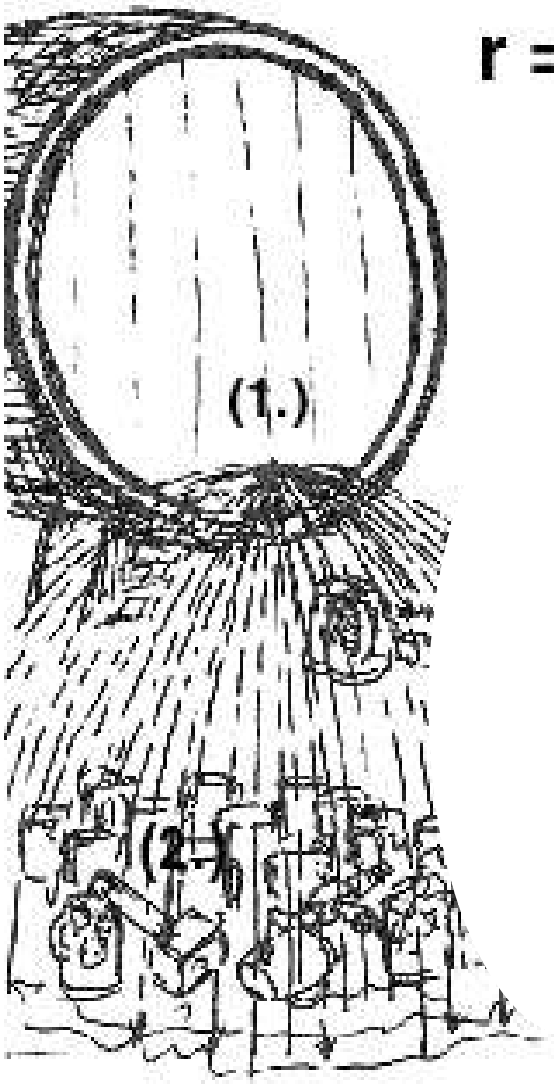

$$r = \Phi \cdot \sigma \cdot N \cdot \varepsilon_{target} \cdot \varepsilon_{source} \cdot \varepsilon_{transp} \cdot \varepsilon_{det}$$

high production cross-sections

$\Rightarrow$ **nuclear physics**

Optimize RIB intensity

All steps of the separation chain need to be optimized!

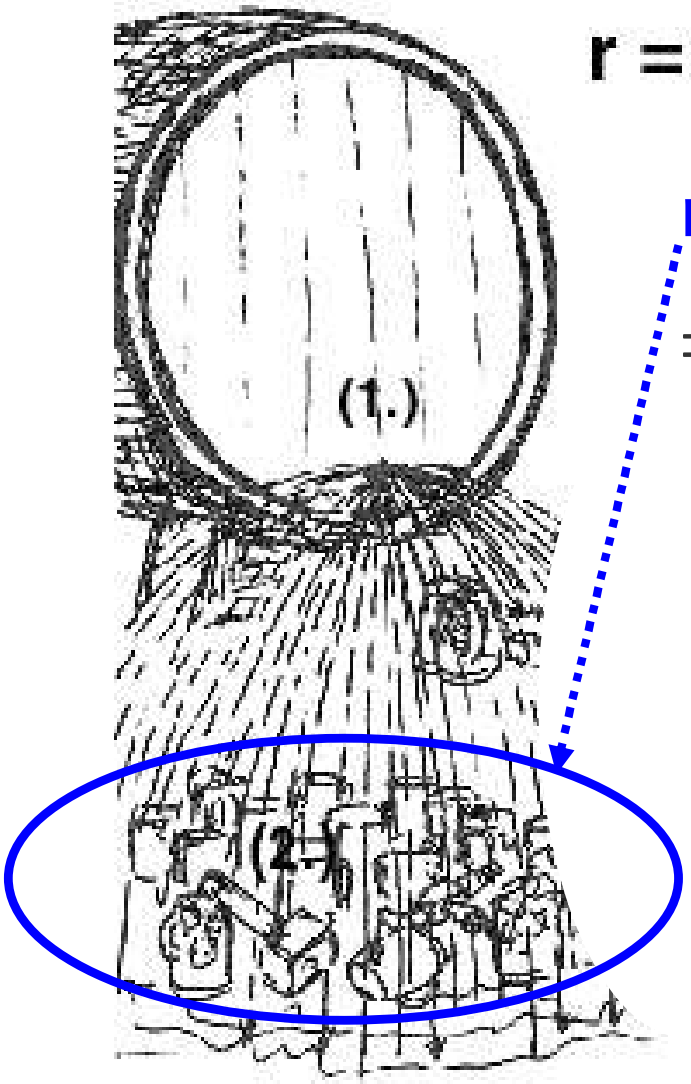

$$r = \Phi \cdot \sigma \cdot N \cdot \varepsilon_{target} \cdot \varepsilon_{source} \cdot \varepsilon_{transp} \cdot \varepsilon_{det}$$

reliable “thick” targets

$\Rightarrow$ materials science

Optimize RIB intensity

All steps of the separation chain need to be optimized!

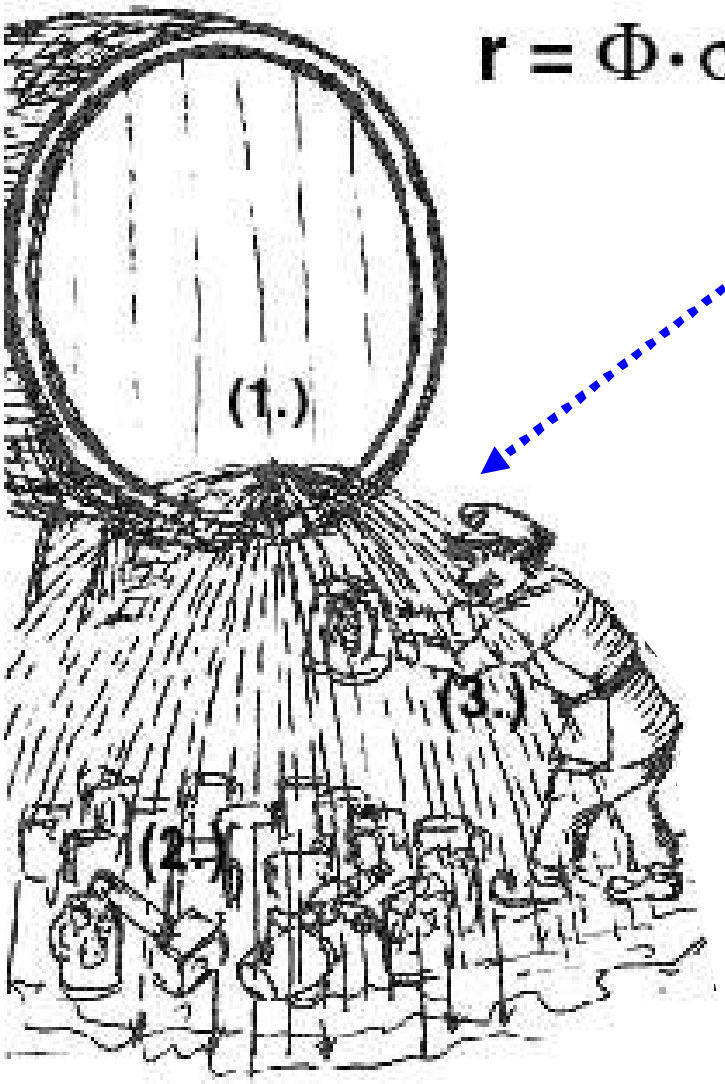

$$r = \Phi \cdot \sigma \cdot N \cdot \varepsilon_{target} \cdot \varepsilon_{source} \cdot \varepsilon_{transp} \cdot \varepsilon_{det}$$

Extraction efficiency from target determined by:

- **bulk diffusion**

⇒ **solid state physics**

- **surface desorption**

⇒ **surface chemistry**

- **effusion**

⇒ **gas phase chemistry**

strongly element dependent!

Optimize RIB intensity

All steps of the separation chain need to be optimized!

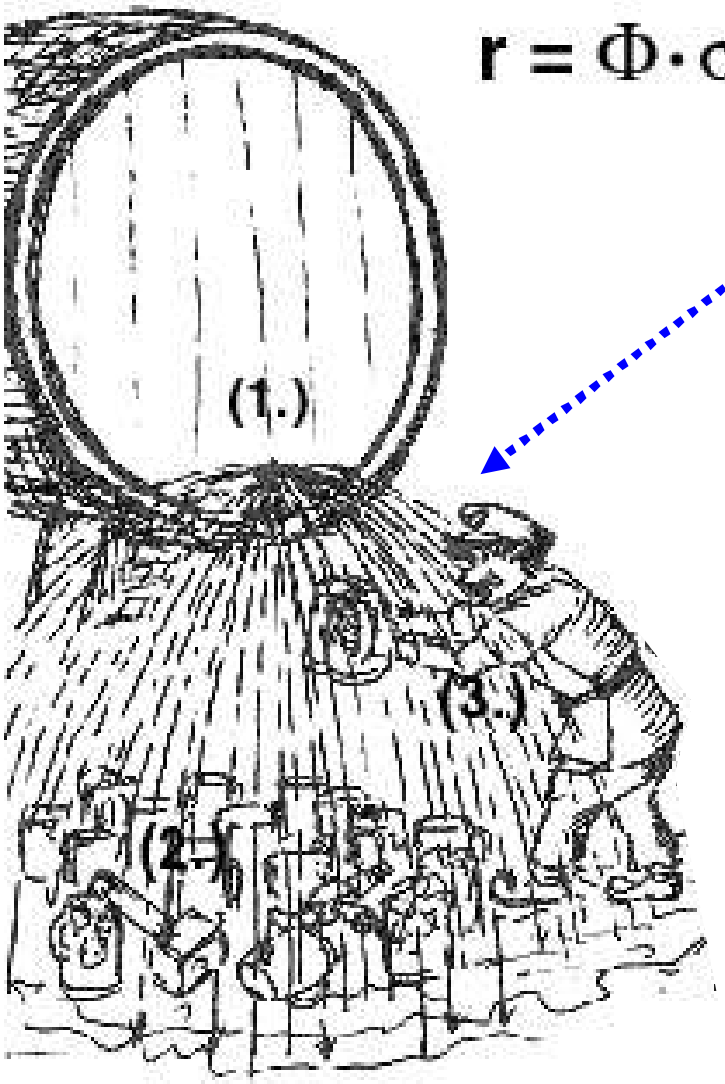

$$r = \Phi \cdot \sigma \cdot N \cdot \varepsilon_{target} \cdot \varepsilon_{source} \cdot \varepsilon_{transp} \cdot \varepsilon_{det}$$

high ionization and extraction efficiency

$\Rightarrow$ ion source technology

Optimize RIB intensity

All steps of the separation chain need to be optimized!

$$r = \Phi \cdot \sigma \cdot N \cdot \varepsilon_{target} \cdot \varepsilon_{source} \cdot \varepsilon_{transp} \cdot \varepsilon_{det}$$

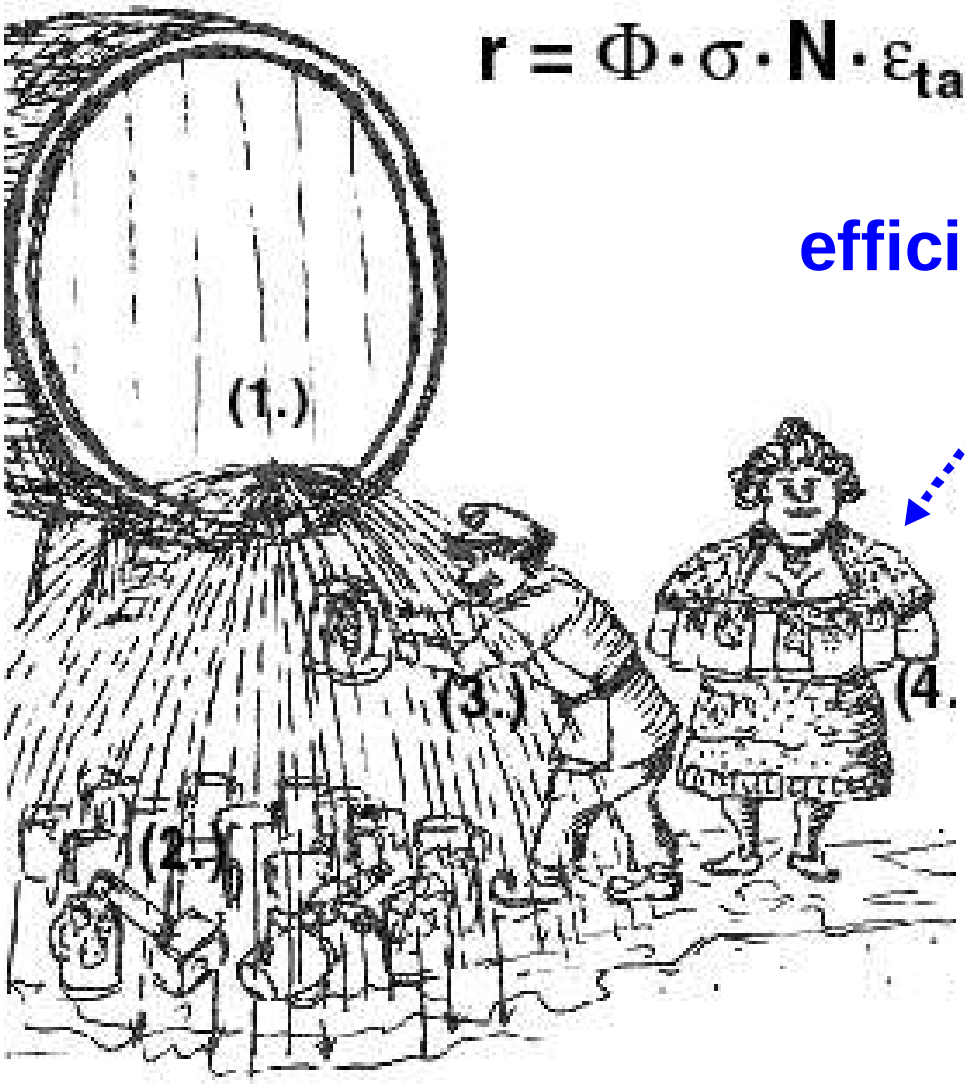

efficient transport of RIB

$\Rightarrow$ ion optics

Optimize RIB intensity

All steps of the separation chain need to be optimized!

$$r = \Phi \cdot \sigma \cdot N \cdot \underbrace{\varepsilon_{target} \cdot \varepsilon_{source} \cdot \varepsilon_{transp}} \cdot \varepsilon_{det}$$

Mind the decay losses during delays

$\Rightarrow$ efficiency strongly half-life dependent

$\Rightarrow$ rapid extraction required!

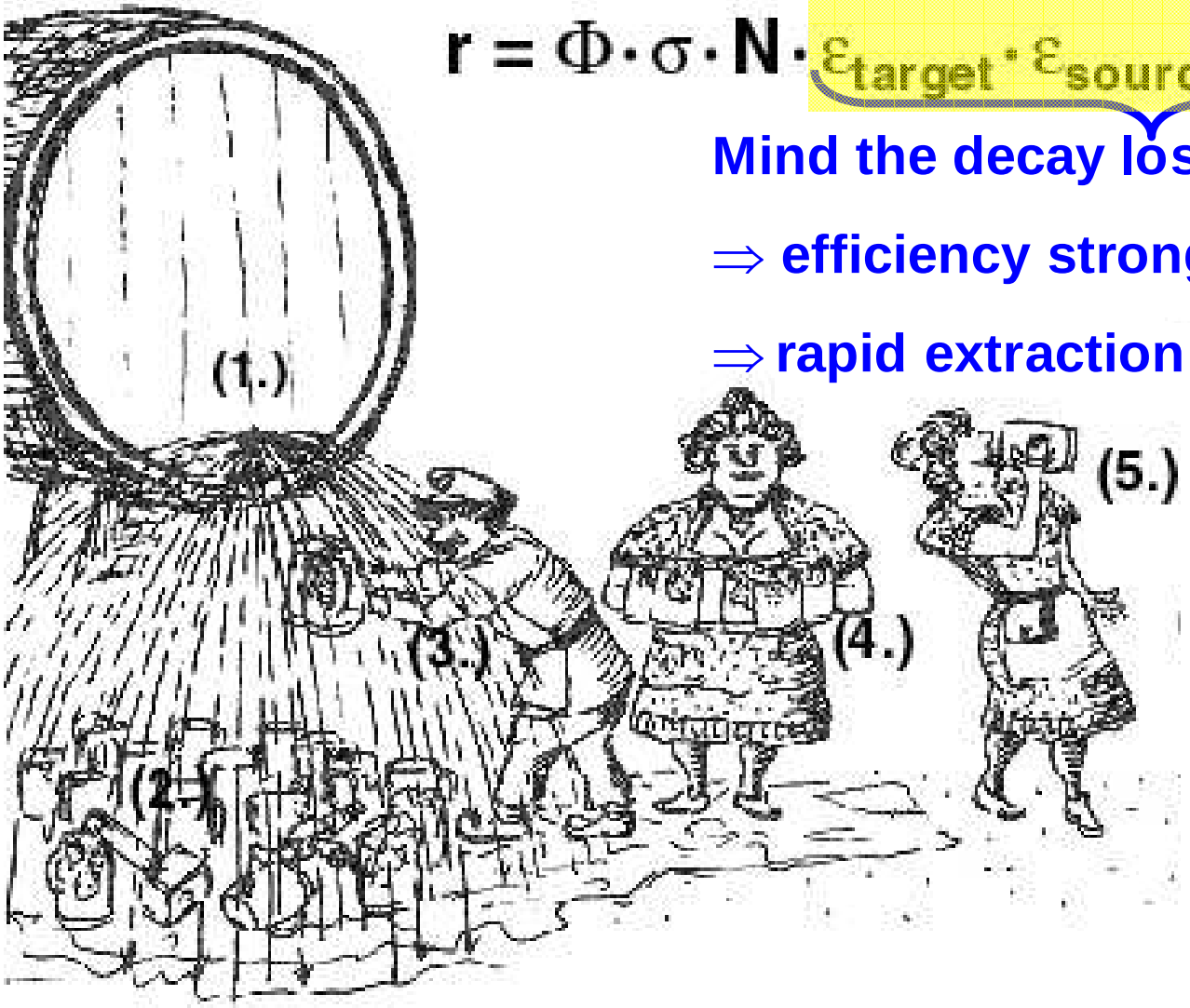

Optimize RIB intensity

All steps of the separation chain need to be optimized!

$$r = \Phi \cdot \sigma \cdot N \cdot \varepsilon_{target} \cdot \varepsilon_{source} \cdot \varepsilon_{transp} \cdot \varepsilon_{det}$$

Detection efficiency

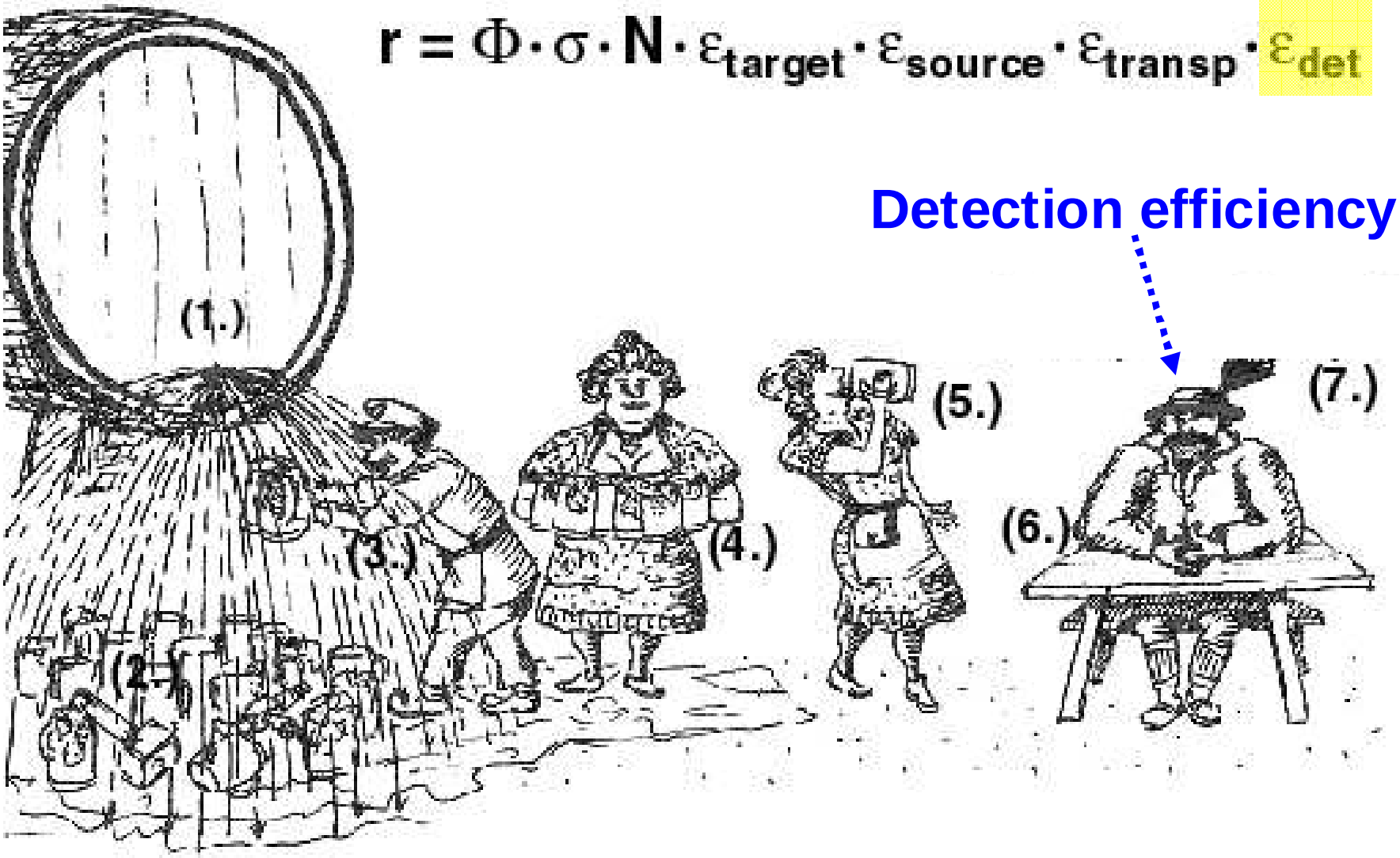

Optimize RIB intensity and purity

All steps of the separation chain need to be optimized!

$$r = \Phi \cdot \sigma \cdot N \cdot \varepsilon_{target} \cdot \varepsilon_{source} \cdot \varepsilon_{transp} \cdot \varepsilon_{det}$$

Selective separation required for exotic isotopes!

⇒ chemistry

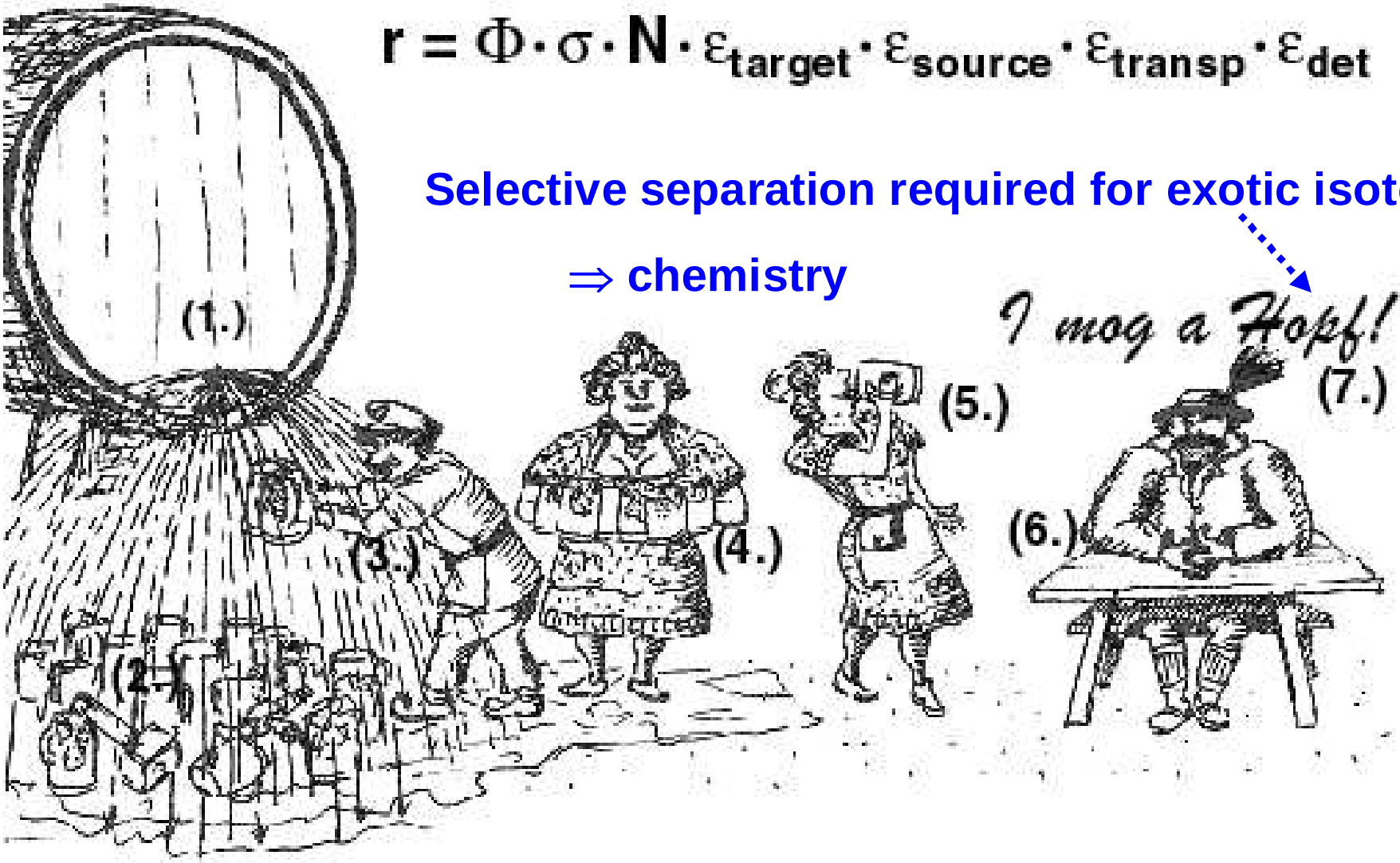

Optimize RIB intensity

Factors are highly correlated and isotope dependent!

$$r = \Phi \cdot \sigma \cdot N \cdot \varepsilon_{target} \cdot \varepsilon_{source} \cdot \varepsilon_{transp} \cdot \varepsilon_{det}$$

Individual optimisation!

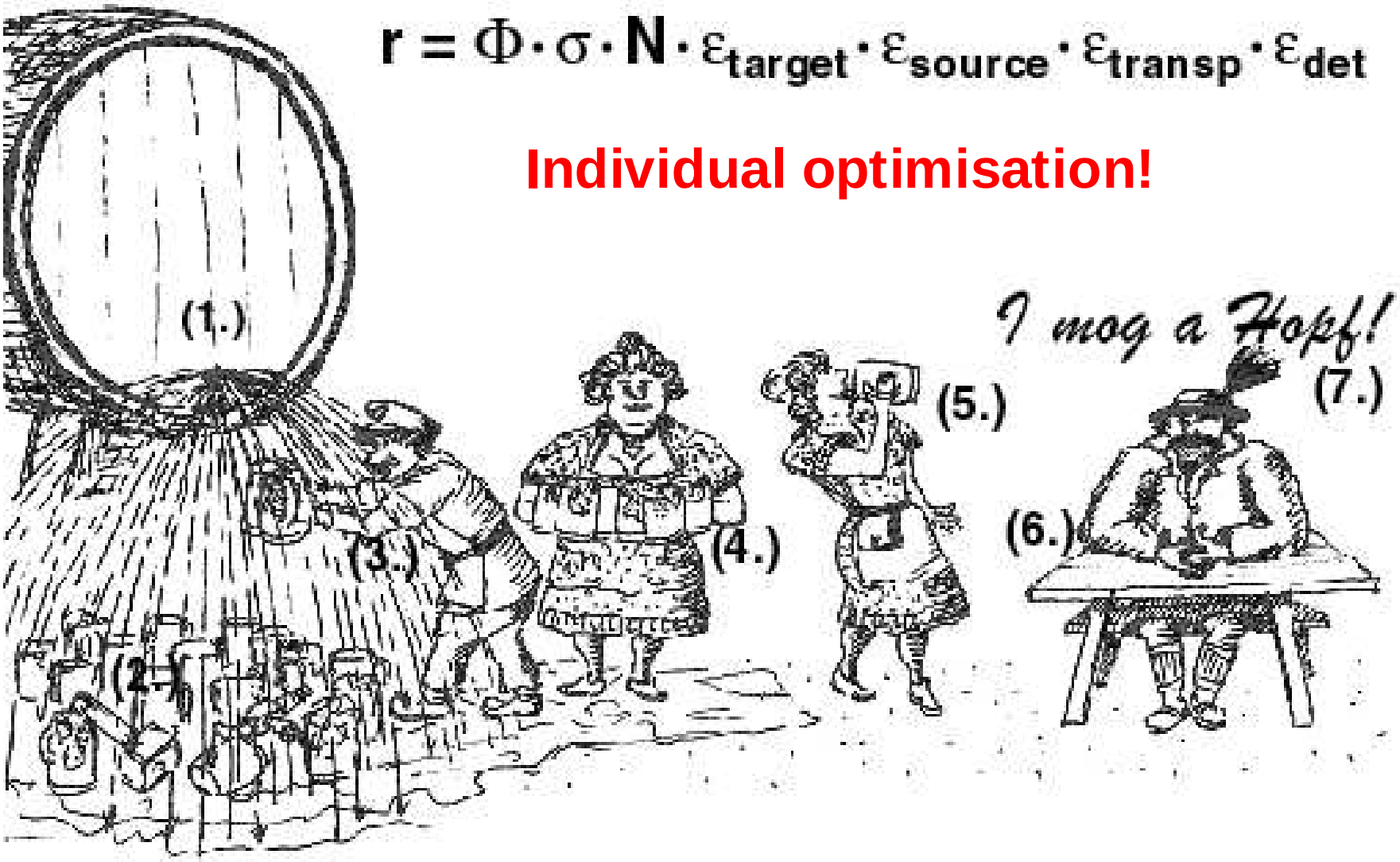

U.K., Prog. Part. Nucl. Phys. 46 (2001) 411.

Particle accelerators

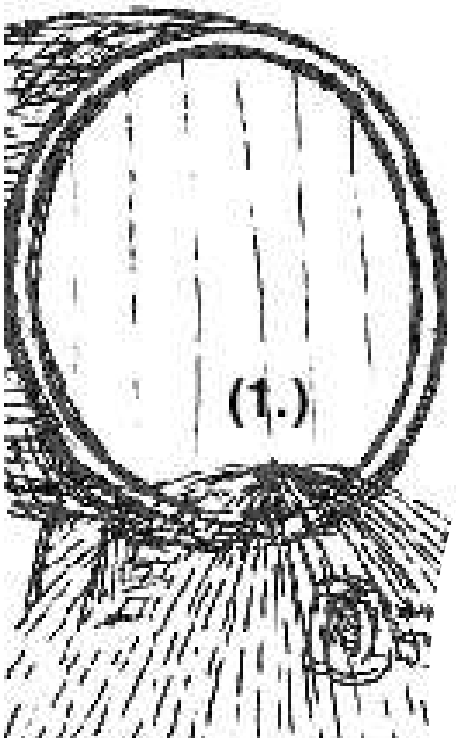

$$r = \Phi \cdot \sigma \cdot N \cdot \varepsilon_{target} \cdot \varepsilon_{source} \cdot \varepsilon_{transp} \cdot \varepsilon_{det}$$

CERN synchrocyclotron 1957-1990

600 MeV p

up to 4 μA

910 MeV ^{3}He

1 GeV ^{12}C

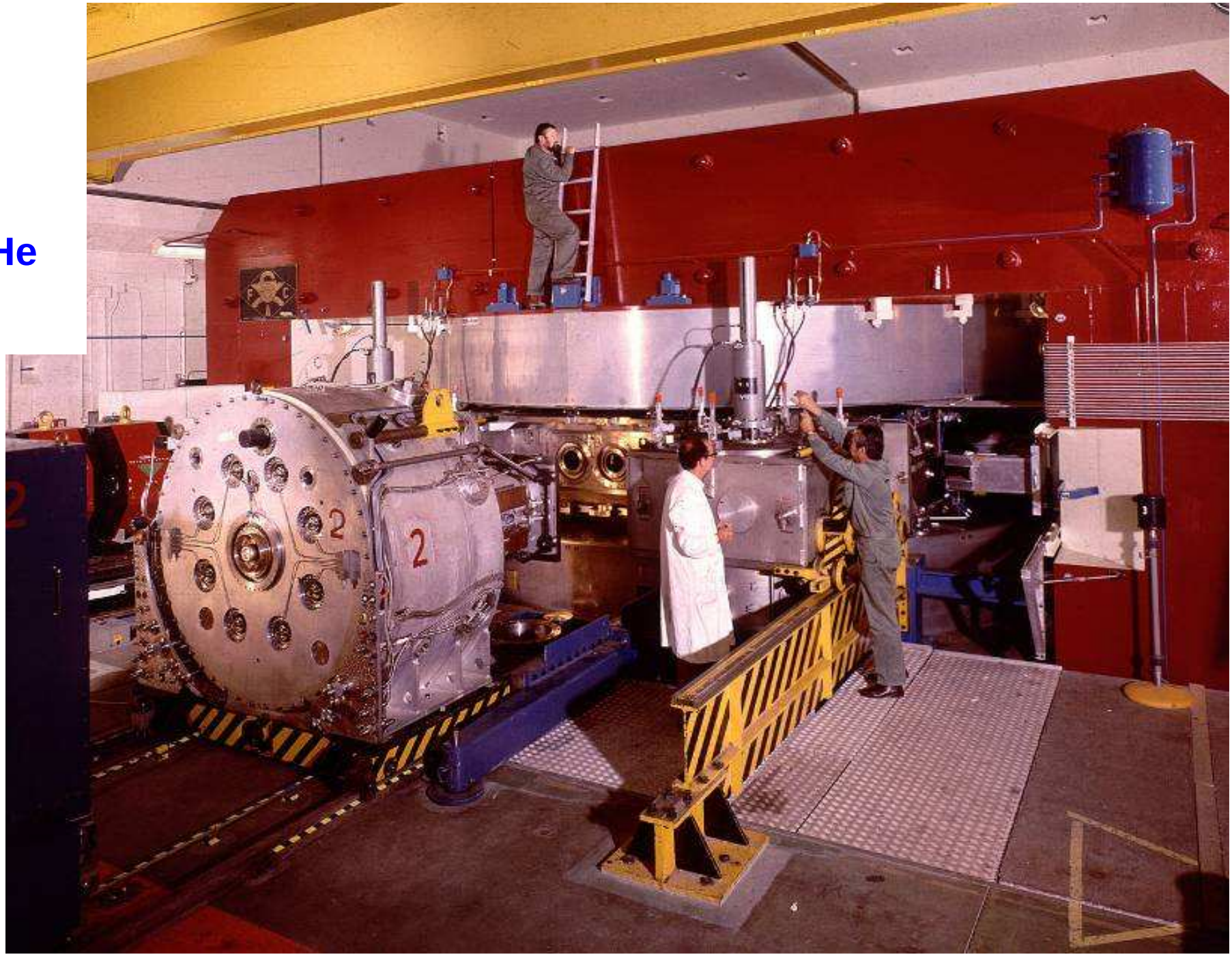

CERN accelerator structure

CERN-PS Booster Synchrotrons

E_p = 1.4 GeV

$3 \cdot 10^{13}$ protons/pulse = 5 μC

$I_{average}$ = 4 μA

$p_{average}$ = 6 kW

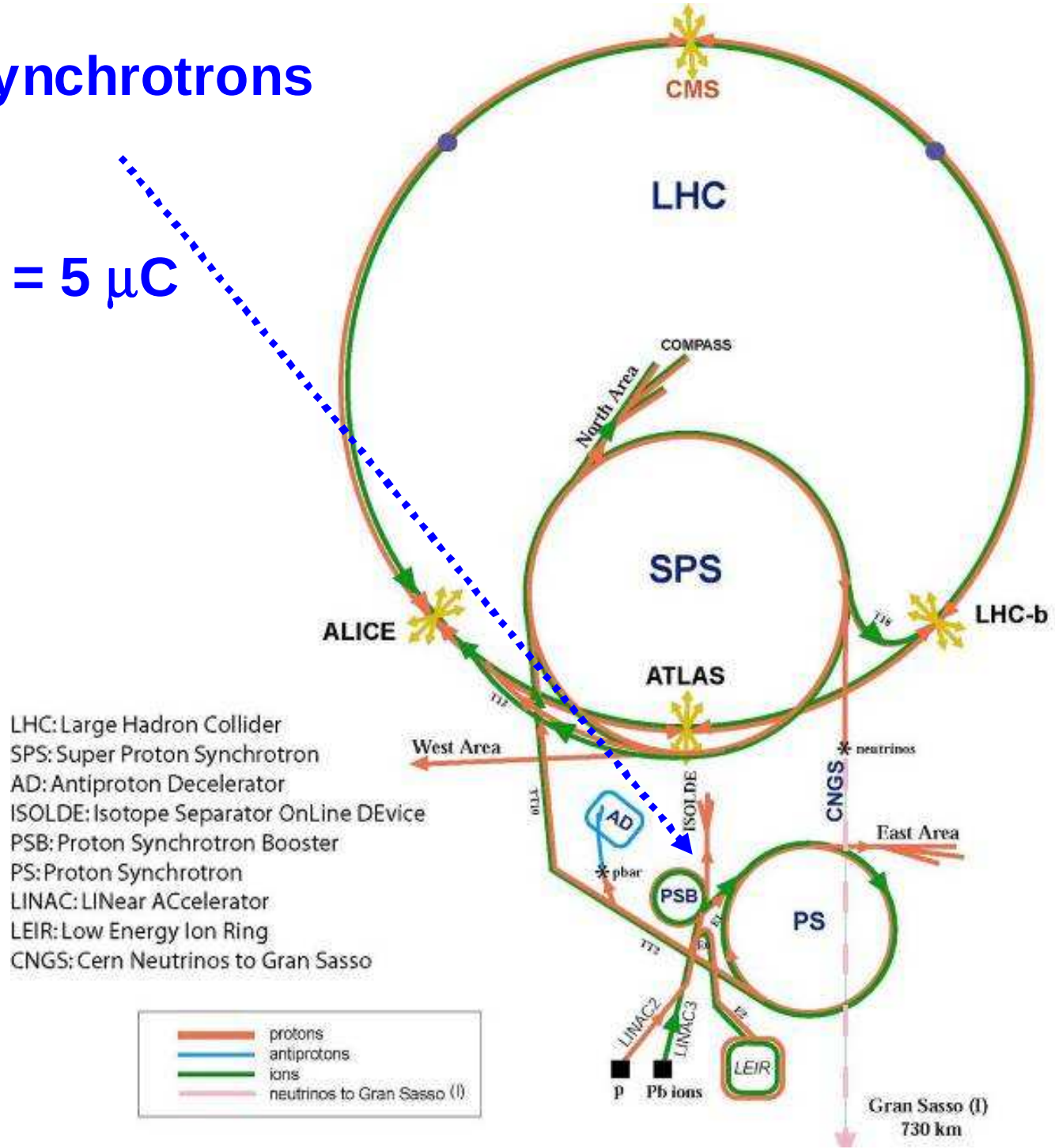

Nuclear reactions

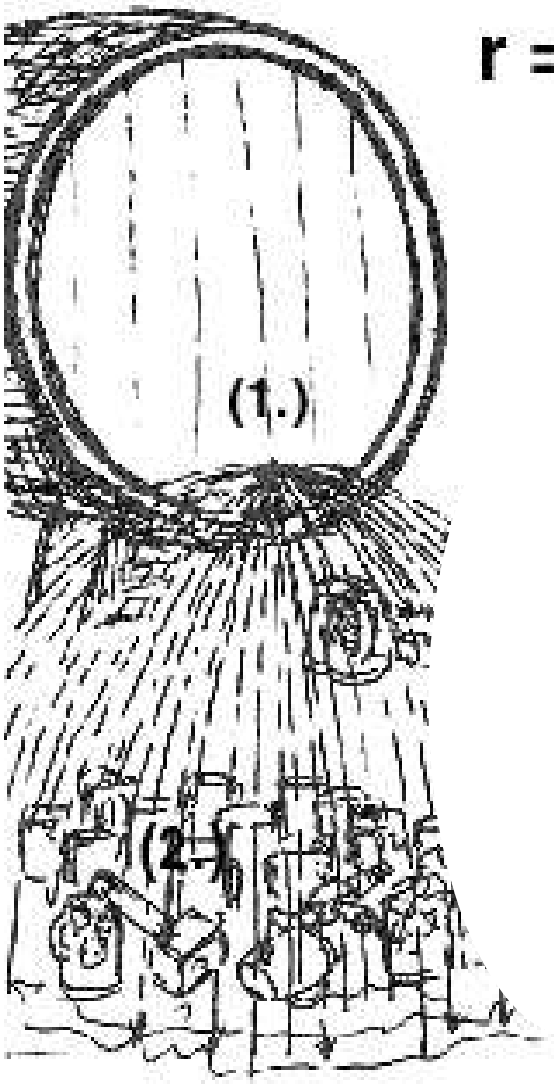

$$r = \Phi \cdot \sigma \cdot N \cdot \varepsilon_{target} \cdot \varepsilon_{source} \cdot \varepsilon_{transp} \cdot \varepsilon_{det}$$

Direct reactions

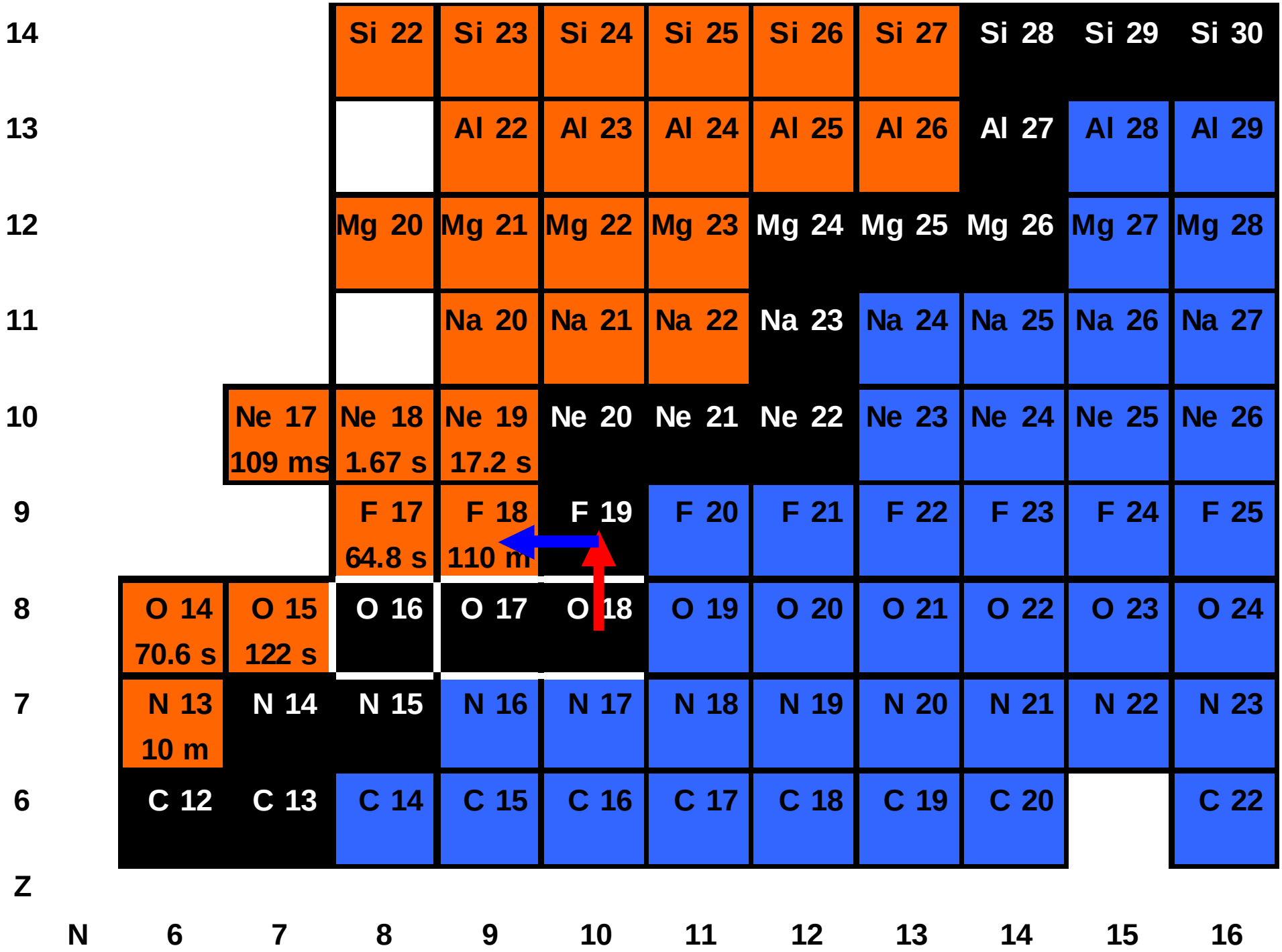

$^{18}O(p,n)^{18}F$ cross-sections

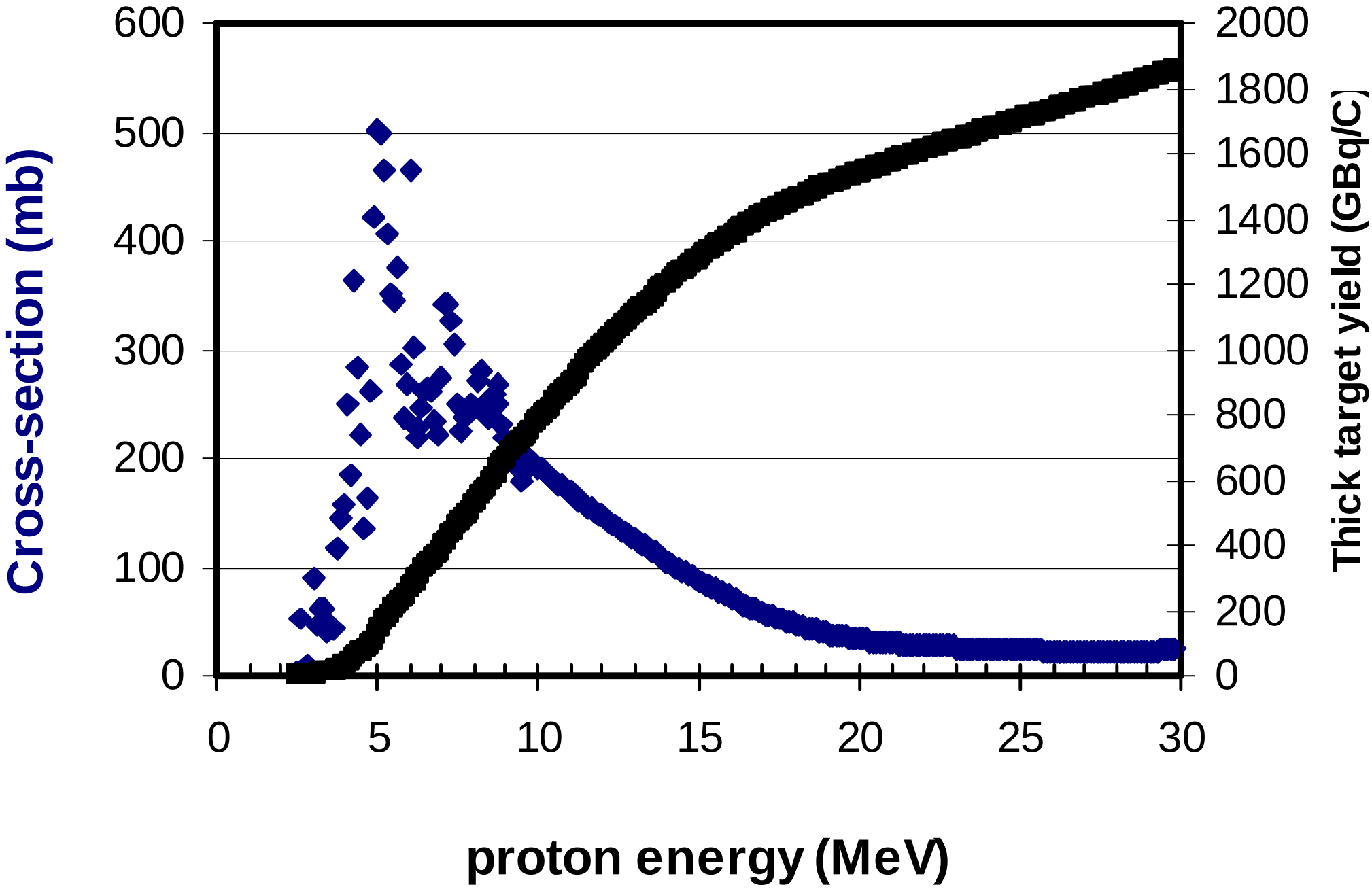

Nuclear reactions

1. Direct reactions

- (p,n), (^{3}He,n), (α,n), (n,α),...
- high cross-sections, products relatively close to stability
- driver beams from (low-cost) cyclotrons

Fusion-evaporation

$^{58}Ni(^{58}Ni,2n)^{114}Ba$

$^{58}Ni(^{58}Ni,\alpha 2n)^{110}Xe$

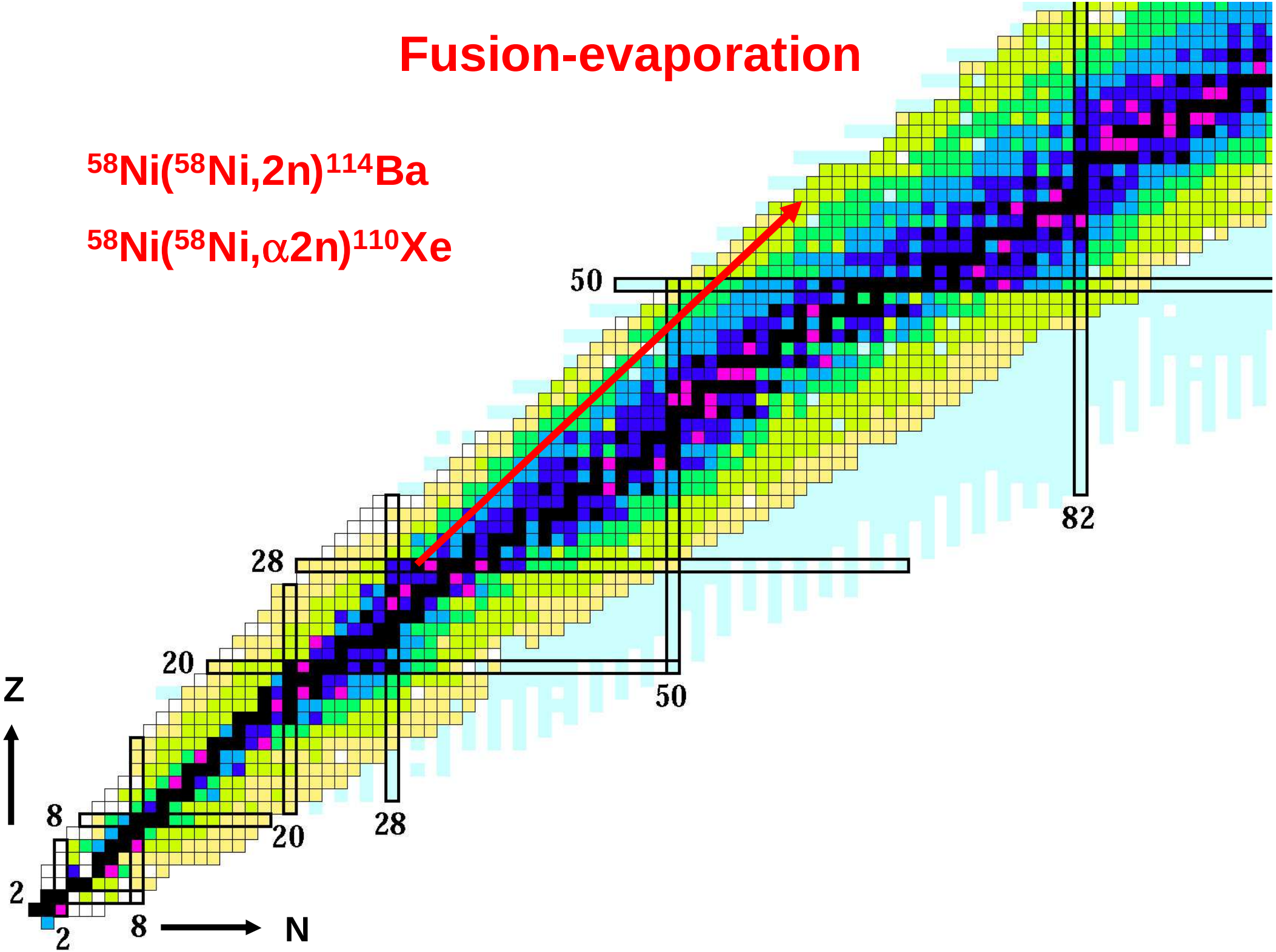

Nuclear reactions

1. Direct reactions

- (p,n), (^{3}He,n), (α,n), (n,α),...
- high cross-sections, products relatively close to stability
- driver beams from (low-cost) cyclotrons

2. Heavy-ion fusion-evaporation

- produces neutron-deficient heavier isotopes
- small energy window in vicinity of Coulomb barrier (some MeV/nucl.)
- requires heavy ion beams $\Rightarrow$ bigger cyclotrons or LINACs

Multinucleon transfer reactions

$^{186}W(^{64}Ni,X)^{184}Lu$

K. Krumbholz et al., Z. Phys. A352 (1995) 1.

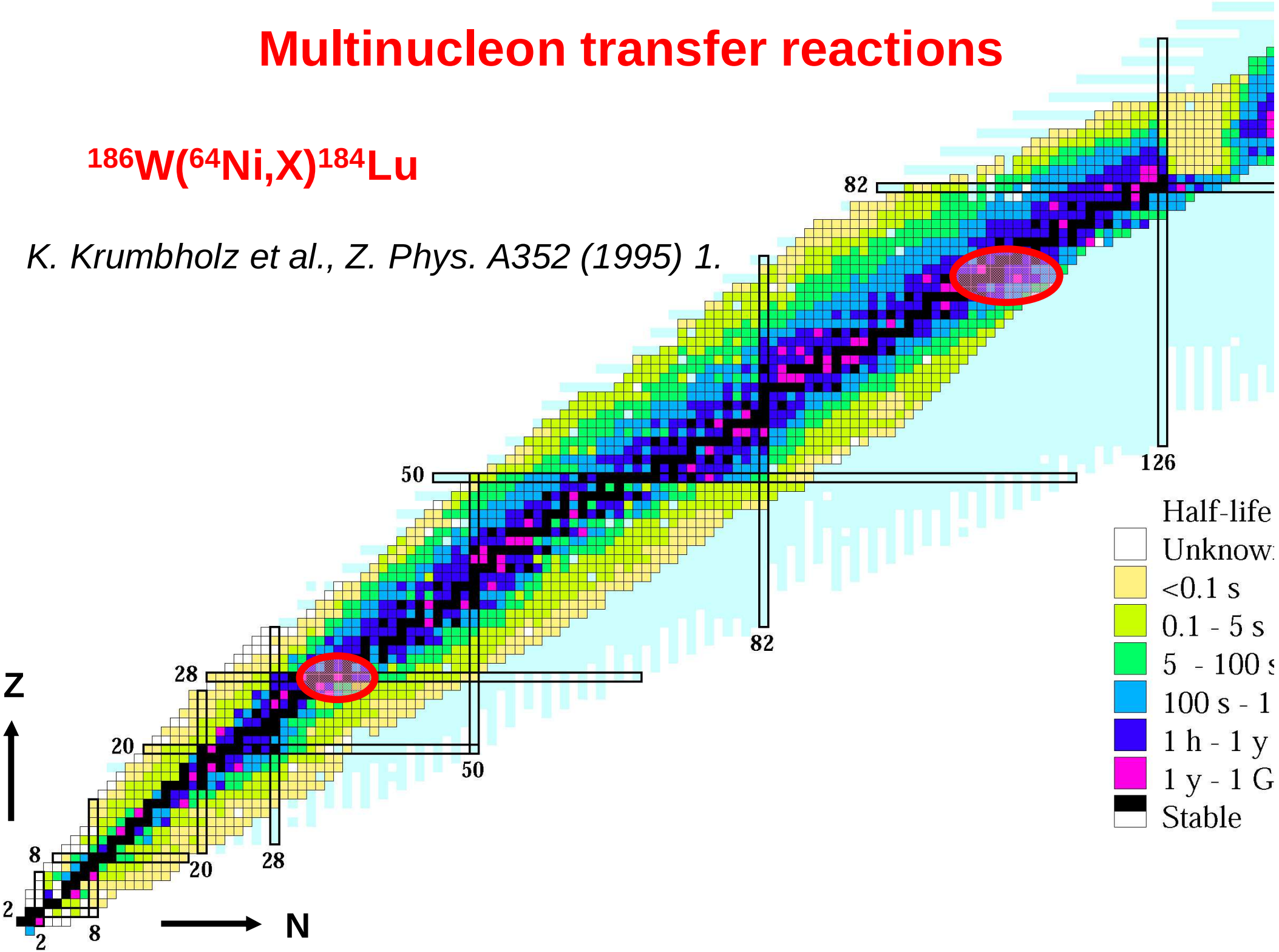

Nuclear reactions

1. Direct reactions
- high cross-sections, products relatively close to stability
- driver beams from (low-cost) cyclotrons

2. Heavy-ion fusion-evaporation
- produces neutron-deficient heavier isotopes
- small energy window in vicinity of Coulomb barrier (some MeV/nucleon)
- requires heavy ion beams $\Rightarrow$ bigger cyclotrons or LINACs

3. Deep inelastic collisions (multi-nucleon transfer)
- products close to target, mass-flow towards stability
- light to heavy ion beams (tens of MeV/nucleon)
- only method to reach neutron-rich isotopes with $N_{product} > N_{target} + 1$

4. Spallation
- intranuclear cascade heats nucleus
- evaporation of preferentially neutrons $\Rightarrow$ neutron-deficient products
- high cross-sections for products close to target
- requires protons of >100 MeV $\Rightarrow$ big p cyclotron, synchrotron or LINAC

Spallation + Fragmentation + Fission

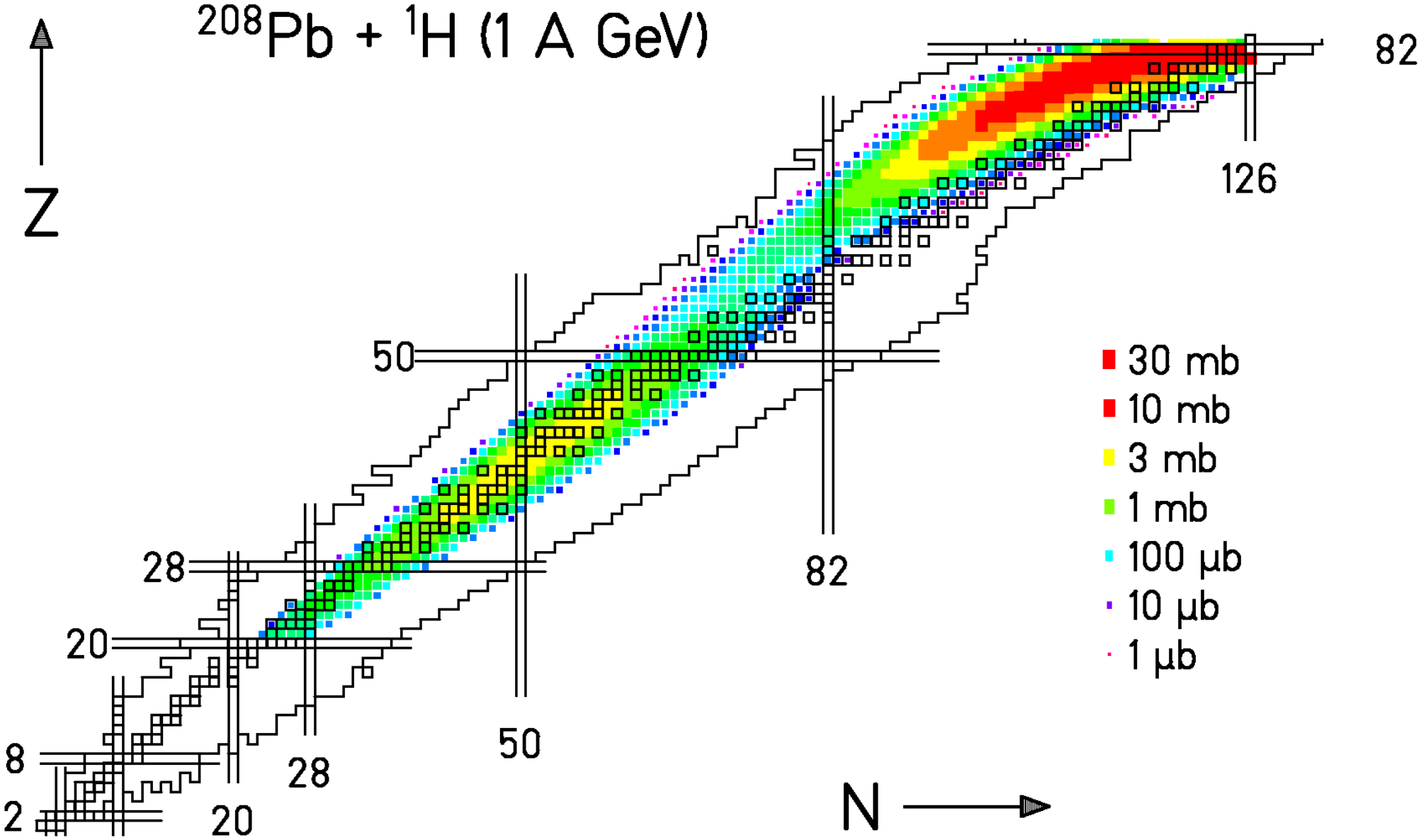

T. Enqvist et al., Nucl. Phys. A686 (2001) 481.

Nuclear reactions

5. Fragmentation

- many cross-sections show little energy dependence in the region 40-2000 MeV/nucleon
- target fragmentation needs e.g. high energy protons (see spallation)
- projectile fragmentation needs high energy heavy ions

$\Rightarrow$ huge cyclotron, synchrotron or LINAC

High energy nuclear reactions

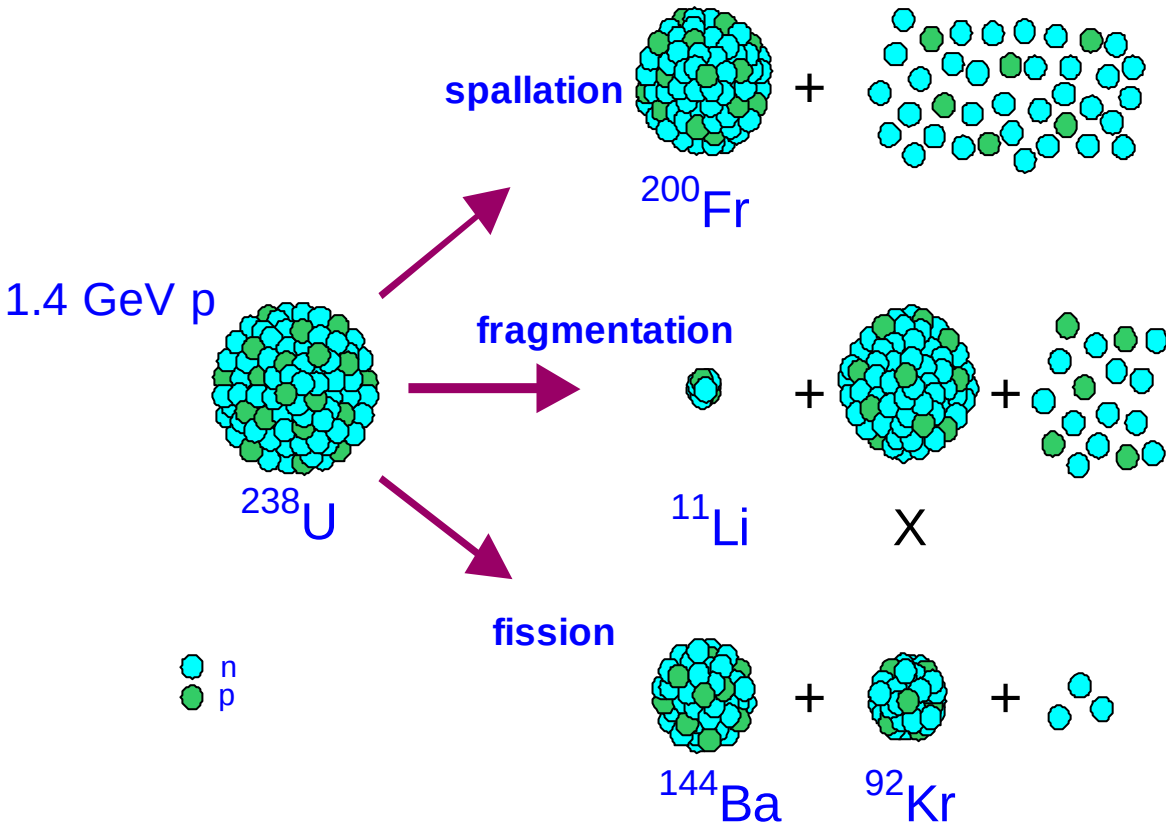

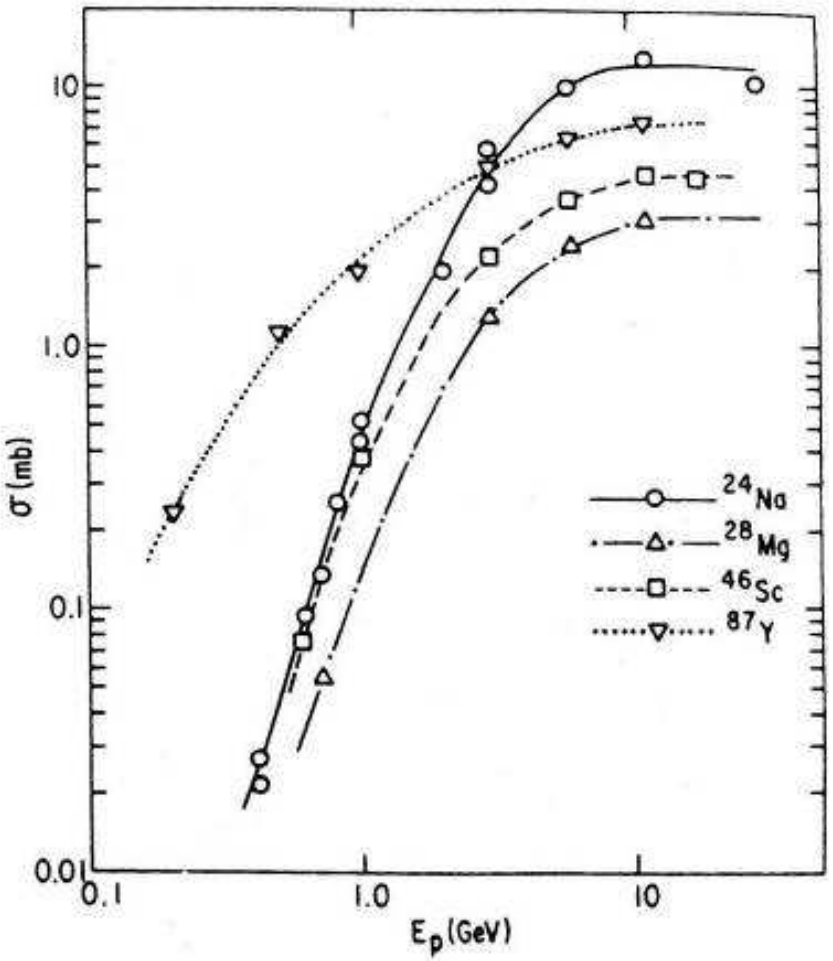

$\sigma_i = 44.9\ A^{0.7}$ mb

R. Silberberg and C.H. Tsao, Phys. Rep. 191 (1990) 351.

Low-energy fission

UCD: unchanged charge distribution

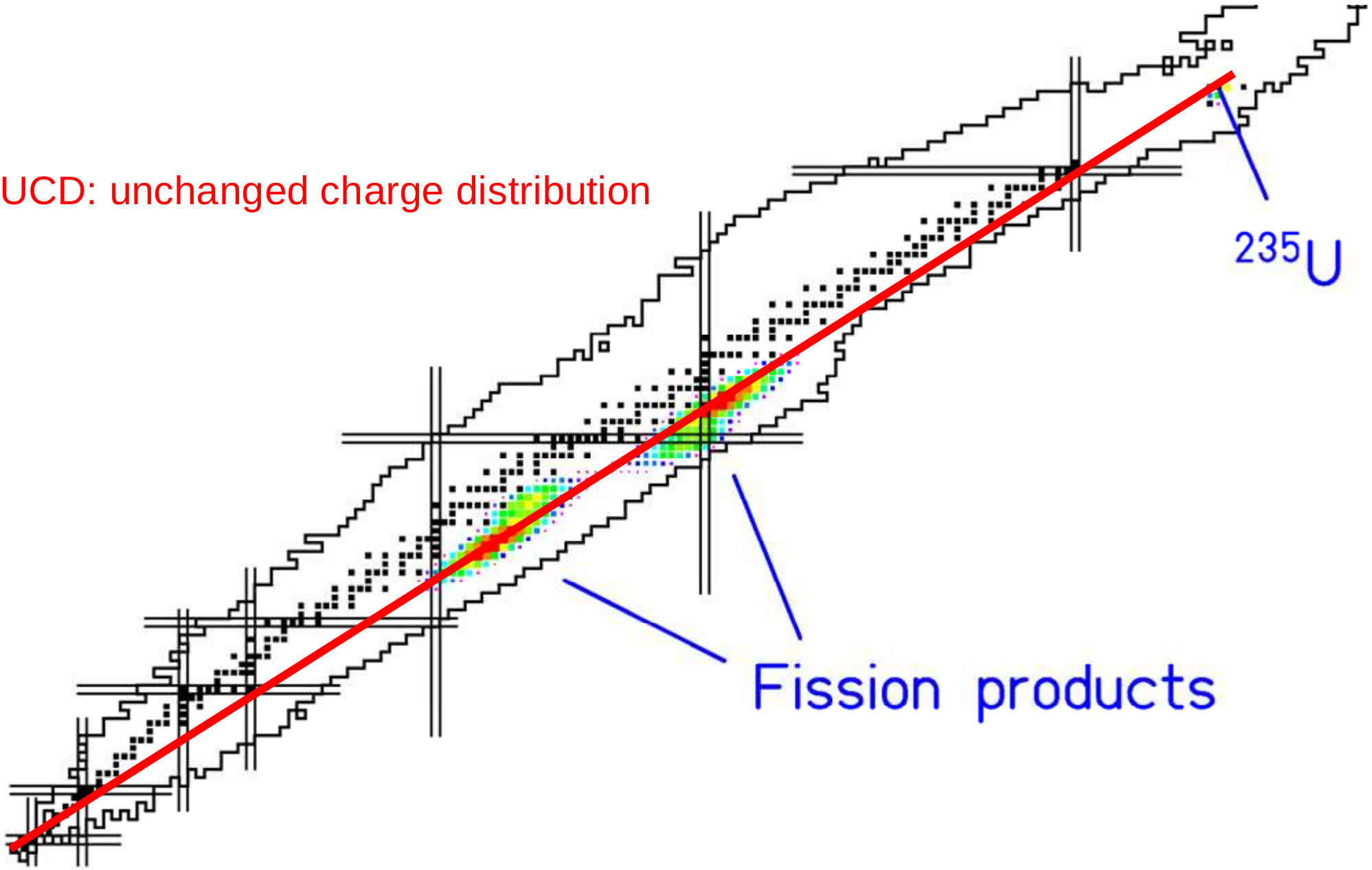

“Low-energy” fission (^{238}U(γ,f) from 50 MeV e$^-$)

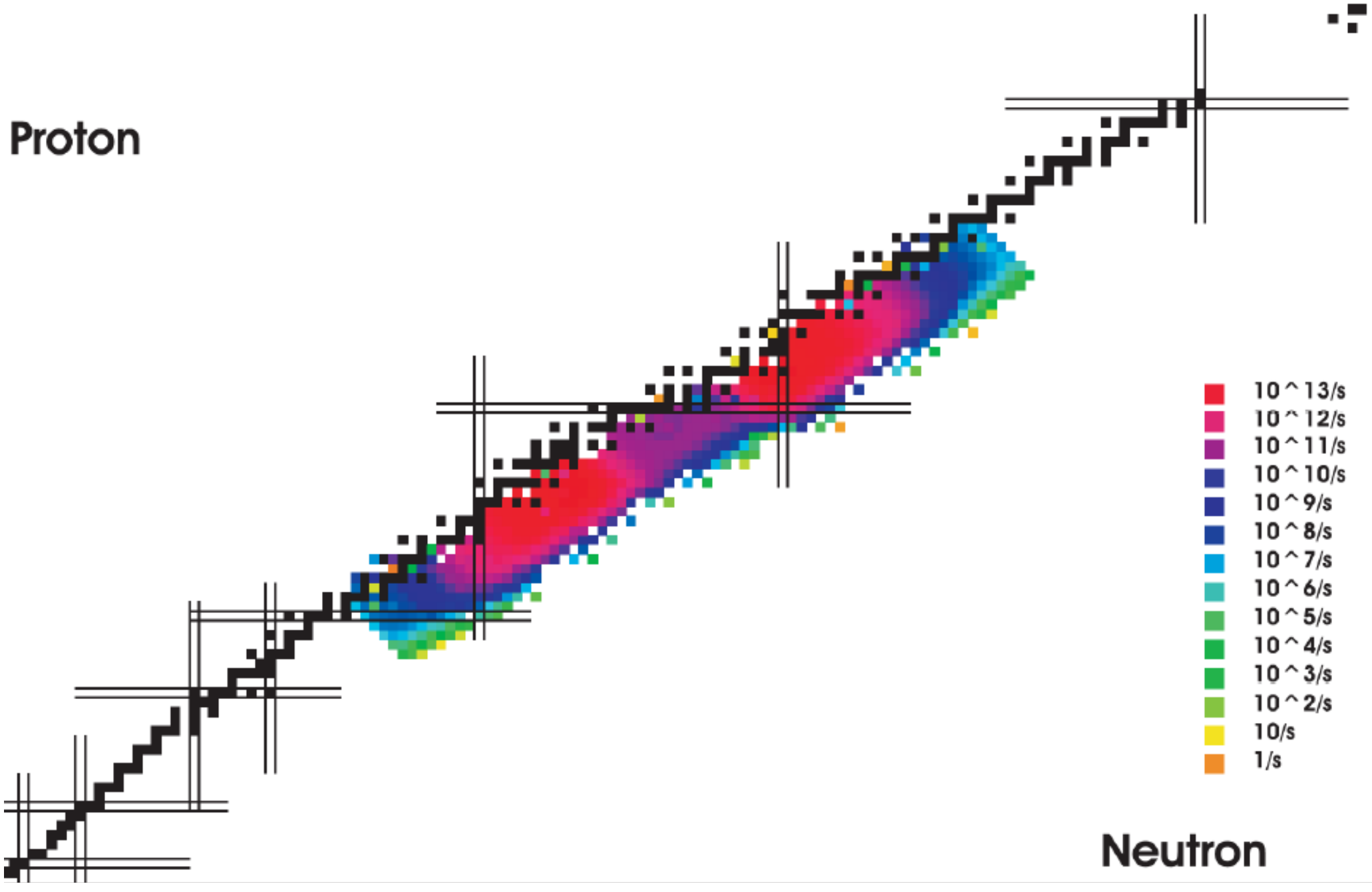

High-energy fission (500 MeV p on ^{238}U)

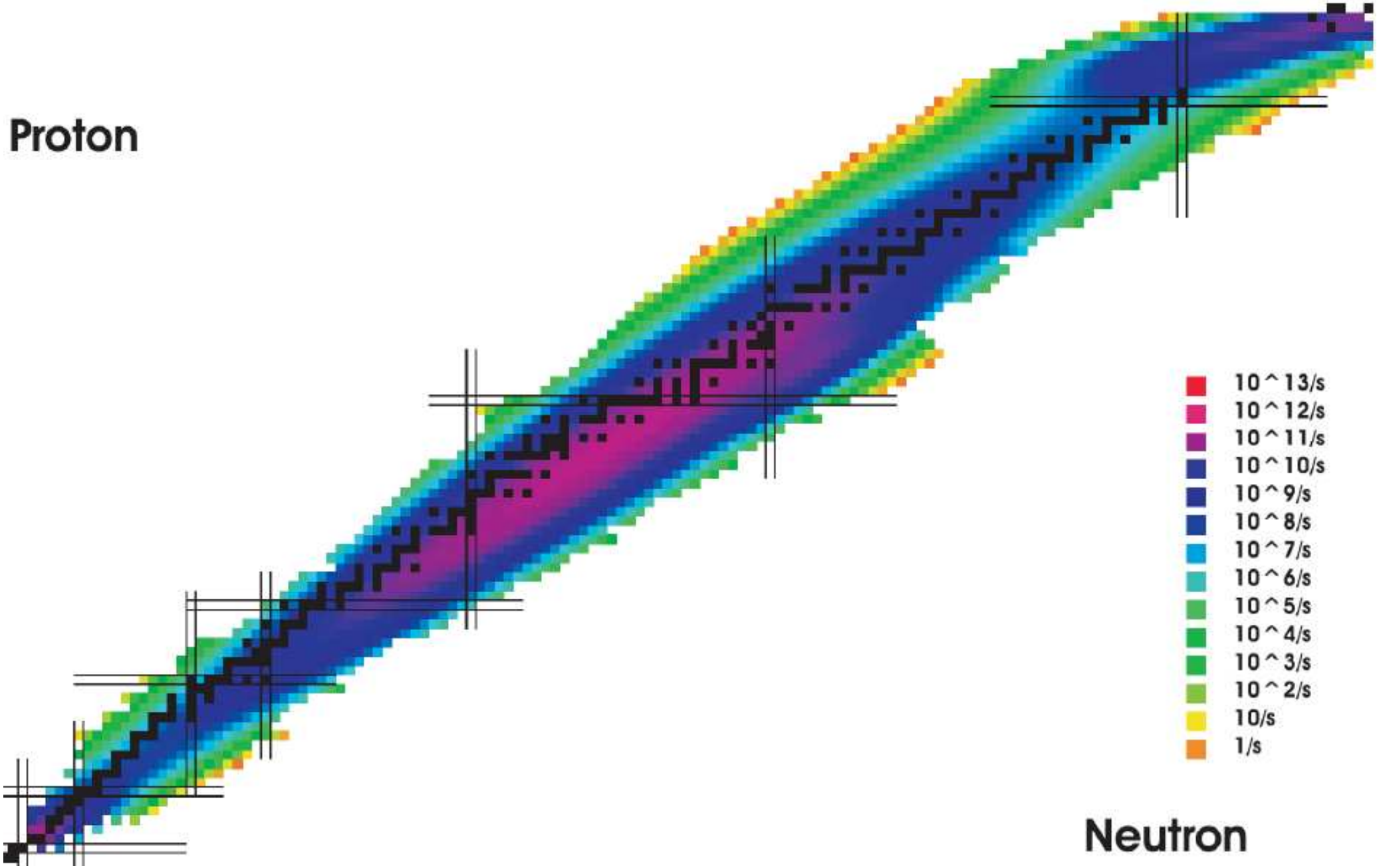

Rubidium cross-sections

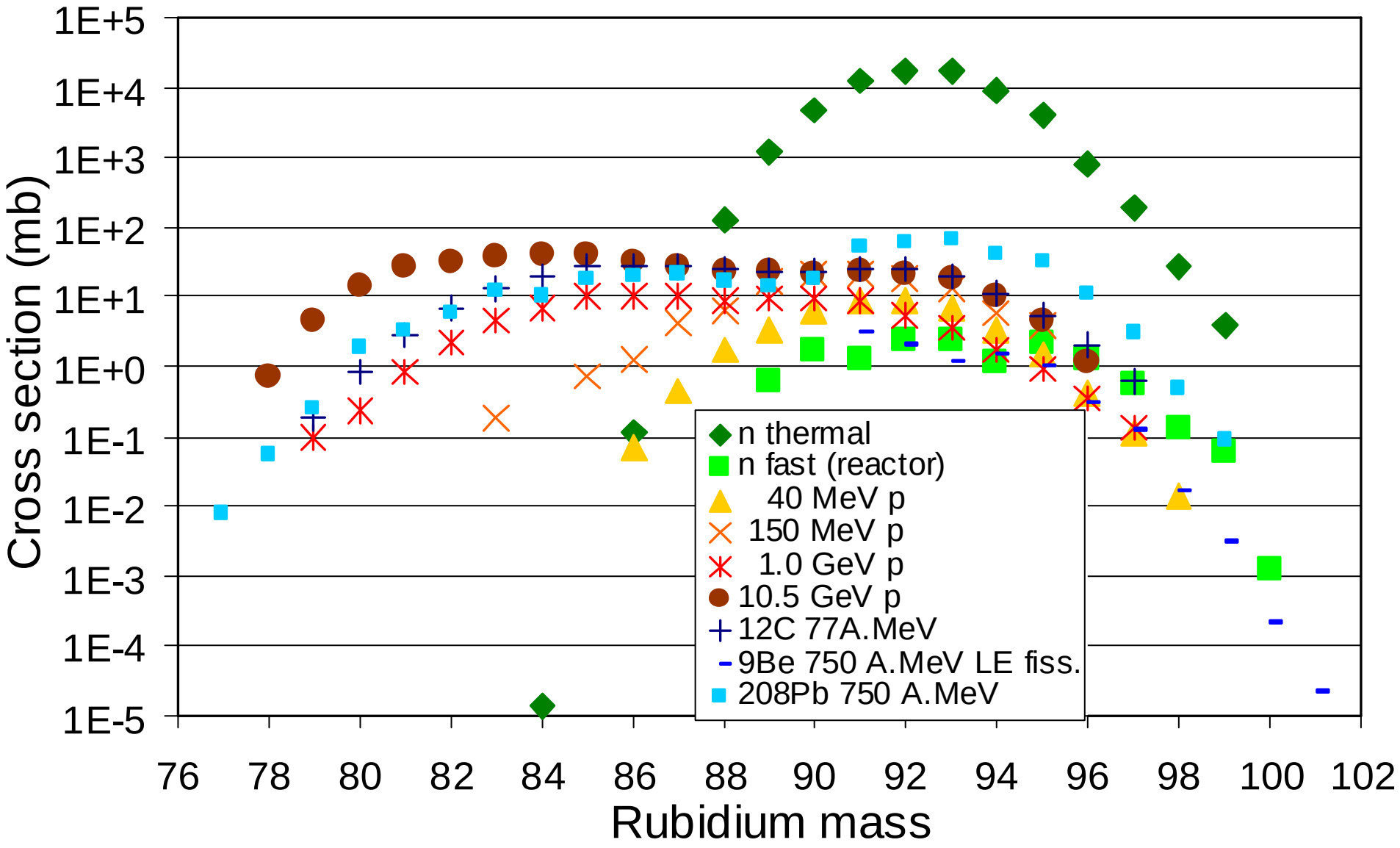

Nuclear reactions

5. Fragmentation

- many cross-sections show little energy dependence in the region
  40-2000 MeV/nucleon
- target fragmentation needs high energy protons (see spallation)
- projectile fragmentation needs high energy heavy ions
  $\Rightarrow$ huge cyclotron, synchrotron or LINAC

6. Fission

- induced by: “time” (**spontaneous**), **neutrons**, **photons**, **protons**, **heavy ions**, antiprotons, pions, post fusion-evaporation, beta-decay/EC
- highest cross-sections for thermal neutrons
- with increasing excitation energy symmetric and far asymmetric fission is favored, but the products get in average less neutron-rich!
- driver accelerators: reactors, medium-energy (some MeV to tens MeV) deuterons from cyclotron or LINAC, microtron or LINAC for electron beams,…

Radioactive ion beam facilities for fission products

Previous, presently operating and future RIB facilities using fission:

^{252}Cf(sf)	CARIBU
^{235}U(n_{th},f)	OSTIS, OSIRIS, LOHENGRIN, TRIGA-SPEC, CARR-ISOL, PIAFE, MAFF, PIK-ISOL
^{238}U(p,f)	ISOLDE, IRIS, LISOL, JYFL, HRIBF, TRIAC, ISAC-II, SPES
W(p,xn..) > ^{238}U(n,f)	ISOLDE, IRIS, ISAC-II, EURISOL
^{12}C(d,n) > ^{238}U(n,f)	PARRNe, SPIRAL-II
^{2}H(d,n) > ^{238}U(n,f)	SPIRAL-II
^{9}Be(d,n) > ^{238}U(n,f)	PARRNe
^{7}Li(d,n) > ^{238}U(n,f)	FRIB
W(e^-,γ) > ^{238}U(γ,f)	ALTO, DRIBS, HRIBF upgrade, ISAC upgrade
^{1}H, ^{9}Be..^{208}Pb(^{238}U,f)	GSI-FRS, RIKEN, FRIB, FAIR

ISOL facilities using fission

Facility	Location	Target		Driver beam			Fiss. rate
			g/cm2	Type	MeV	uA	per s
TRIGA-SPEC	Uni Mainz, D	249Cf	3E-4	(n,f)	3E-8	"0.03"	2E+08
CARIBU	Argonne, US	252Cf	nr	sf	nr	nr	1E+09
ALTO	Orsay, F	238U	40	(g,f)	50	10	8E+10
TRIAC	Tokai, JP	238U	1	(p,f)	36	3	1E+11
IGISOL	Jyväskylä, FIN	238U	0.12	(p,f)	30	10	1E+11
HRIBF	Oak Ridge, US	238U	2.1	(p,f)	42	10	4E+11
ISOLDE	CERN, CH	238U	50	(p,f)	1400	2	2E+12
CARR-ISOL	Beijing, CN	235U	3E-2	(n,f)	3E-8	"32"	7E+12
SPES	Legnaro, I	238U	2.5	(p,f)	40	200	1E+13
ISAC2	Vancouver, CAN	238U	(40)	(g,f)	50	10000	5E+13
SPIRAL2	Caen, F	238U	(40)	d>(n,f)	40	5000	<1E14

ALTO @ IPN Orsay

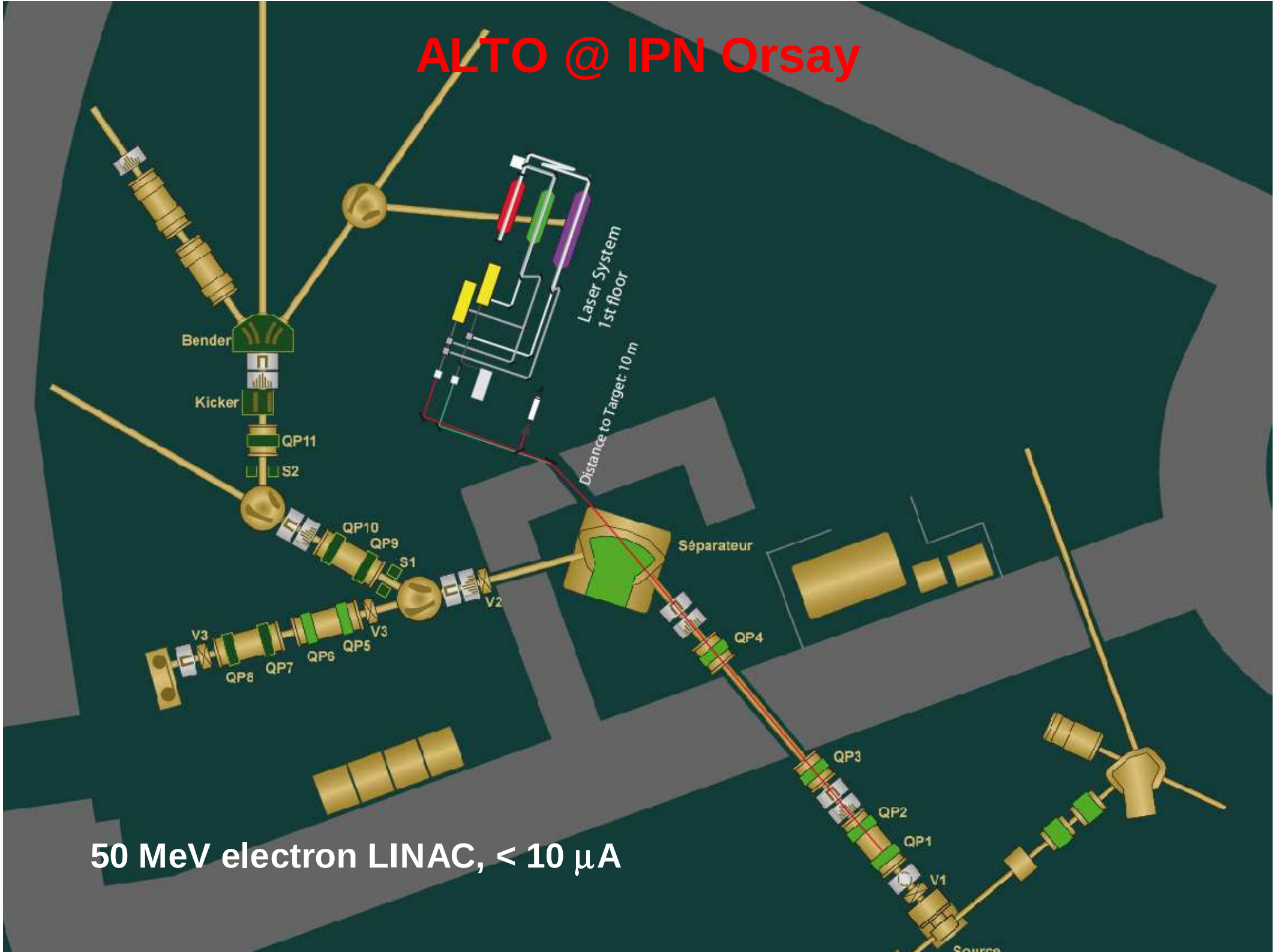

50 MeV electron LINAC, < 10 μA

ISAC @ TRIUMF (fission upgrade)

- 50 MeV, 10 mA electron LINAC
- <100 kW till 2015, 500 kW till 2020
- aim 4.6E13 fissions/s with liquid Hg converter

- but also 500 MeV protons with maximum 10 μA on UC_x

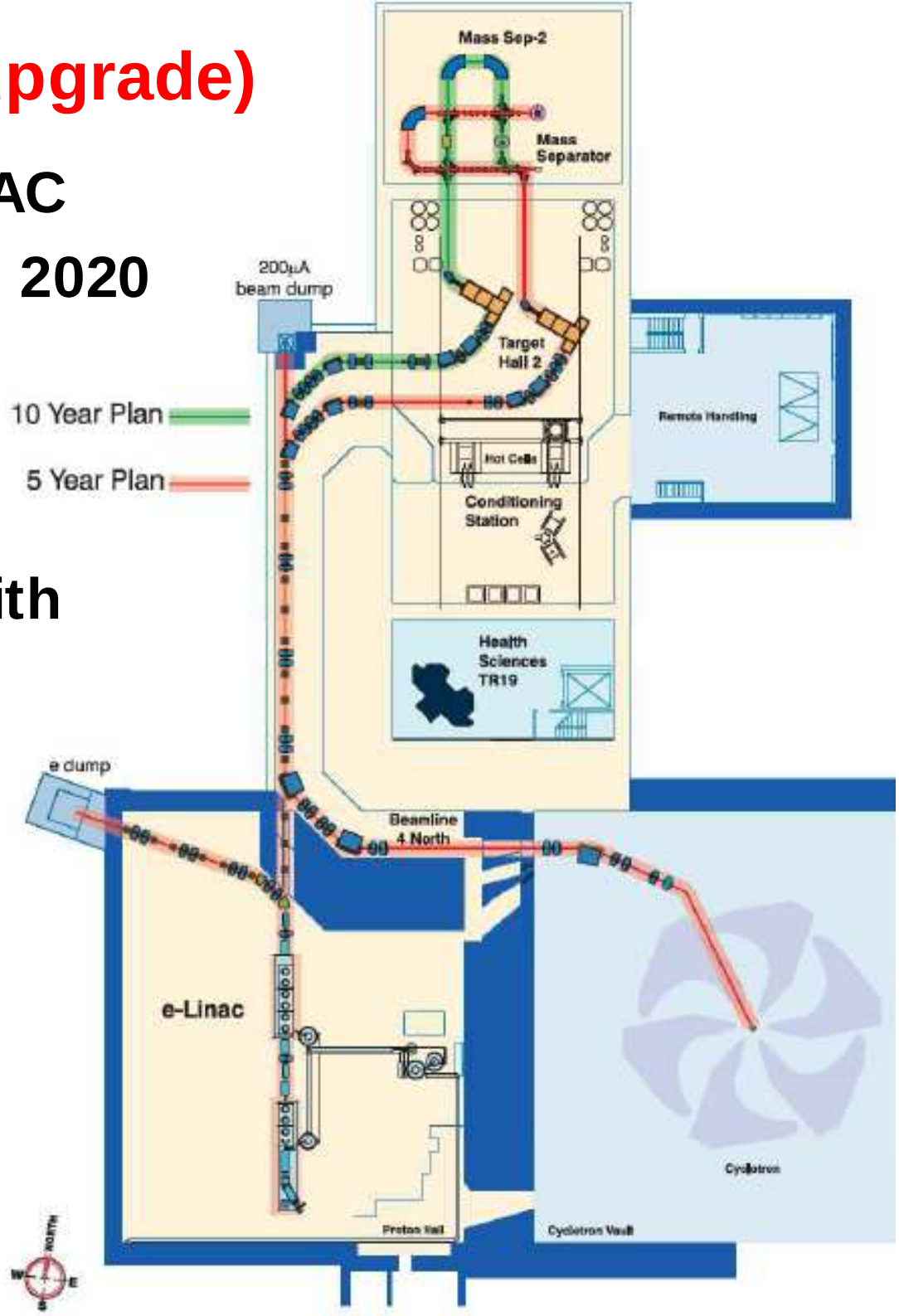

SPIRAL2 facility at GANIL

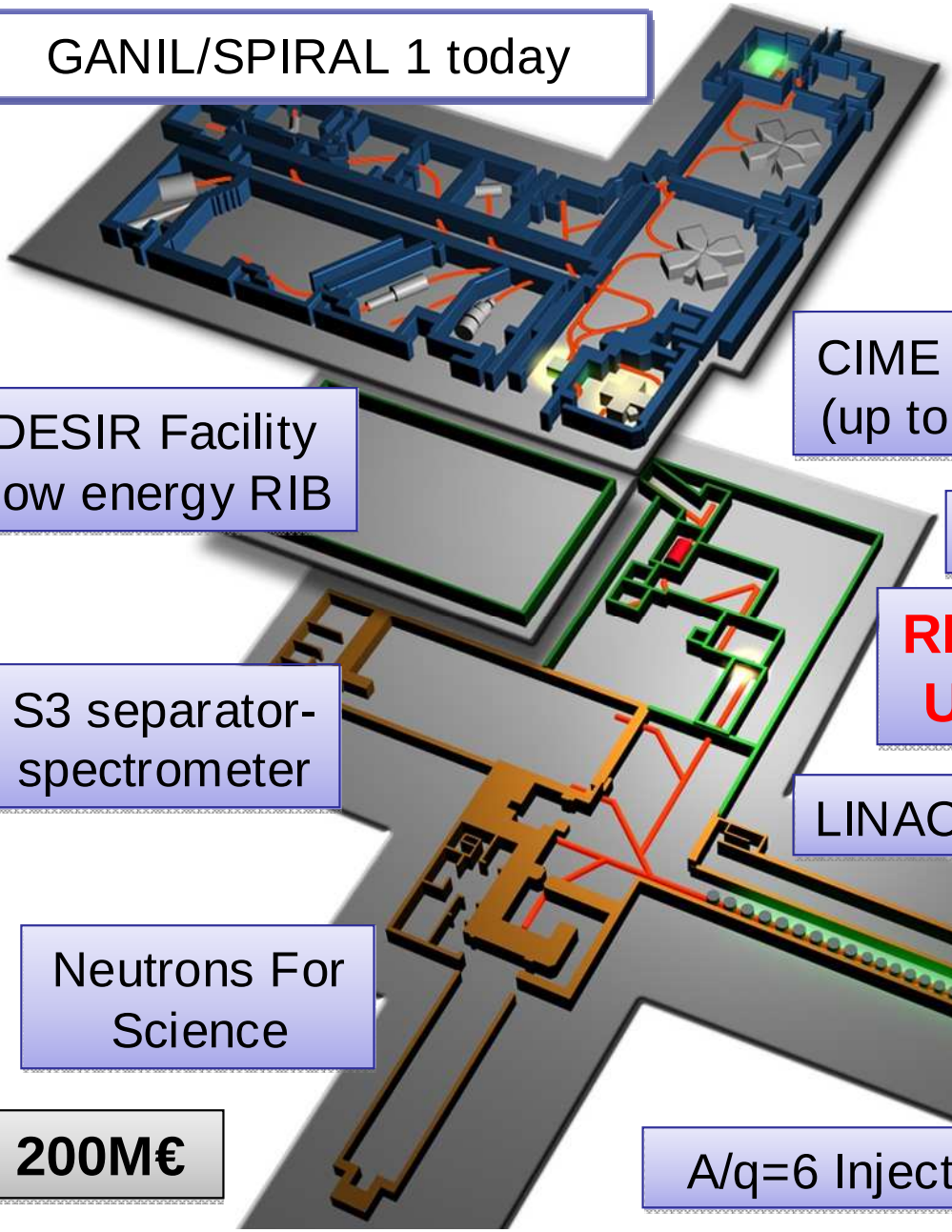

GANIL/SPIRAL 1 today

SP2 Beam time: 44 weeks/y
GANIL Beam time: 35 weeks/y
ISOL RIB Beams: 28-33 weeks/y
GANIL+SP 2 Users: 700-800/y

CIME cyclotron RIB at 1-20 AMeV (up to 9 AMeV for fiss. fragments)

DESIR Facility low energy RIB

HRS+RFQ Cooler

RIB Production Cave Up to 10^{14} fiss./sec.

S3 separator-spectrometer

LINAC: 33MeV p, 40 MeV d, 14.5 A MeV HI

Neutrons For Science

A/q=3 HI source Up to 1mA

Cost: 200M€

A/q=6 Injector option

A/q=2 source p, d, ^{3,4}He 5mA

SPIRAL2 RIB production module

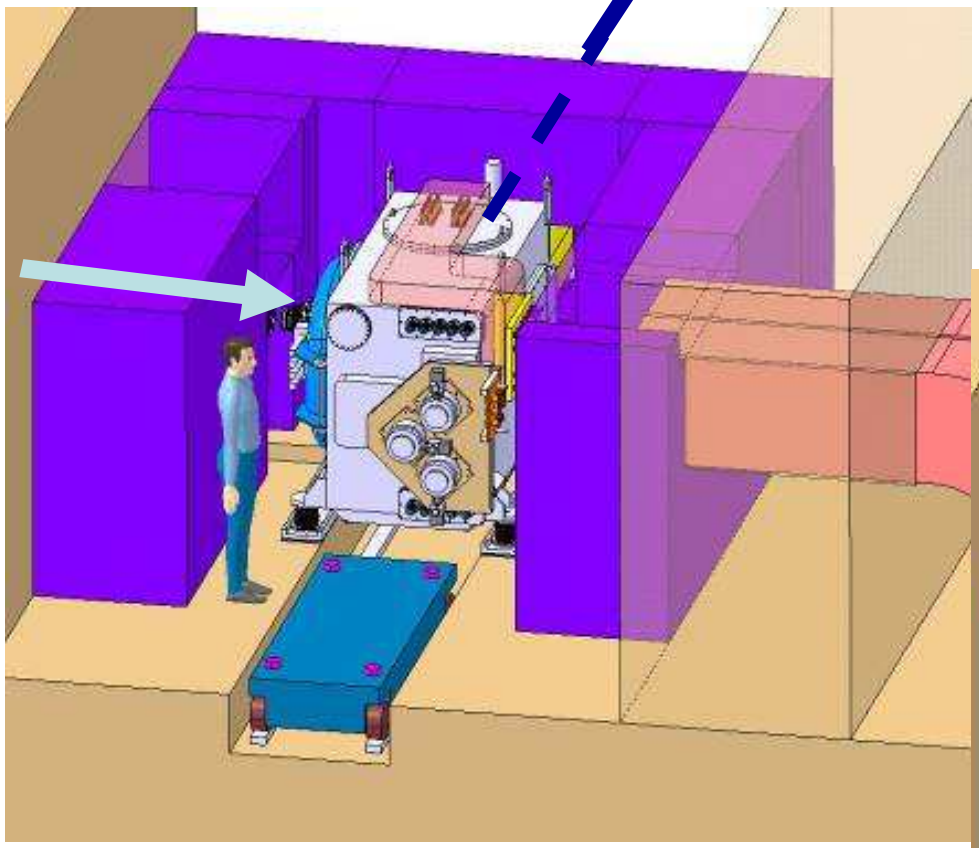

RIB

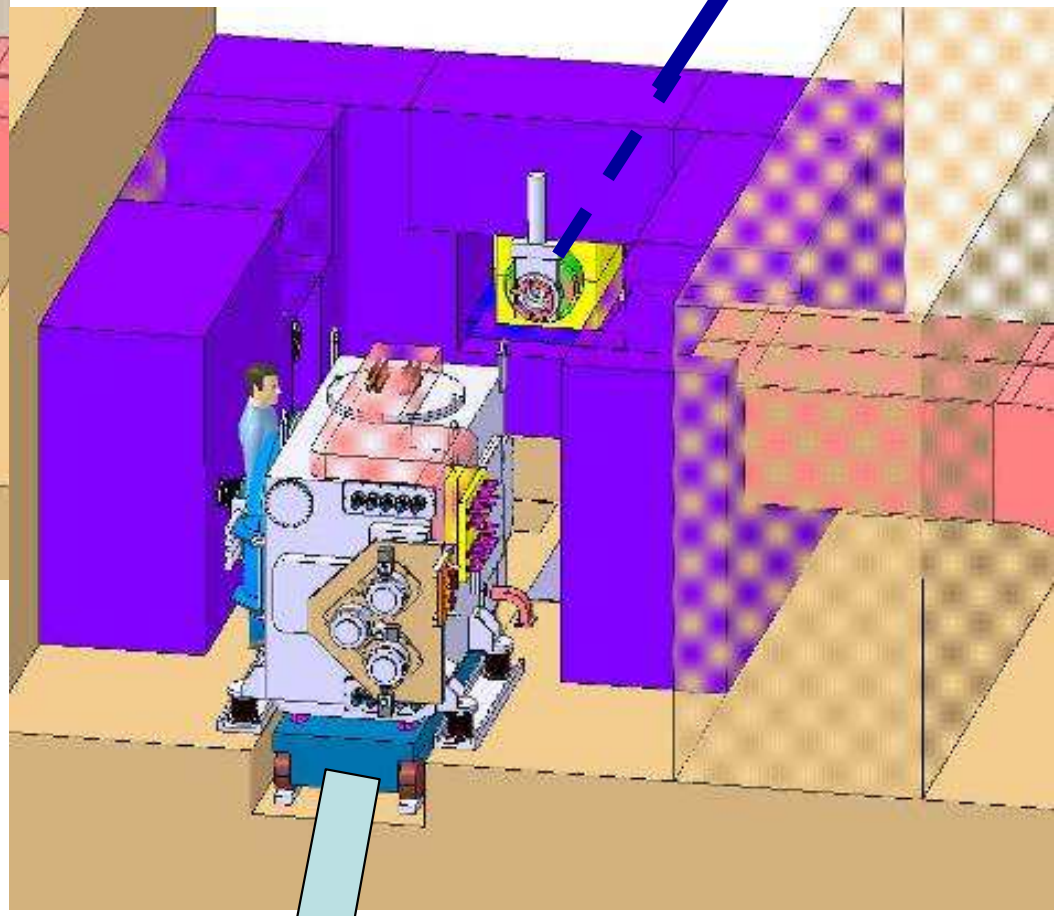

Maintenance and Storage cells

EURISOL

1-2.2 GeV, multi-MW proton driver

Several direct target stations (ca. 100 kW)

One Hg spallation + fission target station (>1 MW, i.e. 1E15 fissions/s)

Multiple user operation in parallel

Low-energy beam area

Post-acceleration with
LINAC up to ca. 10 A.MeV

Post-acceleration to
ca. 100 A.MeV
with LINAC or cyclotron

Fragmentation of
post-accelerated RIBs

Commissioning: > 2020?

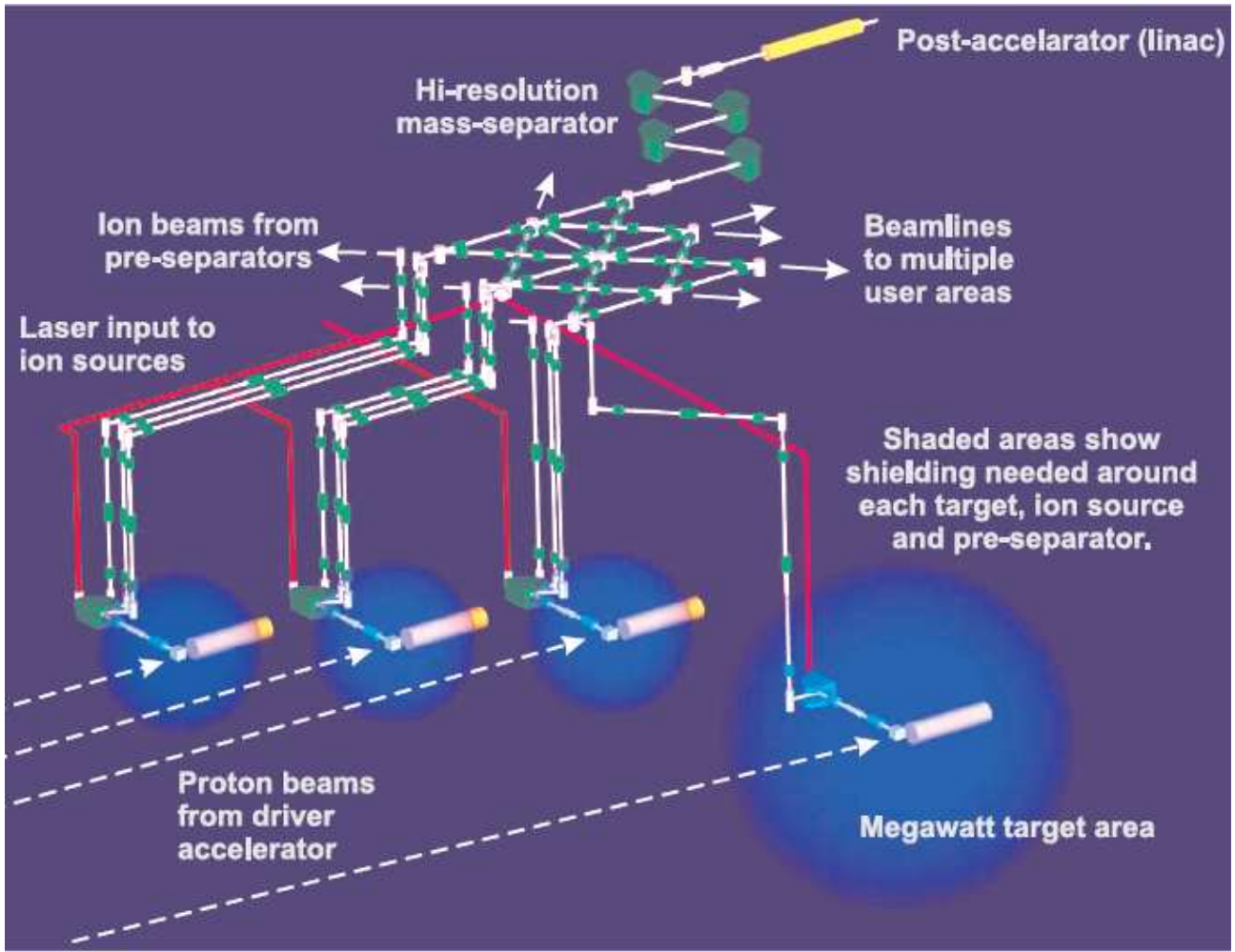

IGISOL method

$X^{n+} + He^0 \rightarrow X^{(n-1)+} + He^+$ or

$X^{n+} + Ar^0 \rightarrow X^{(n-1)+} + Ar^+$

rapid reduction of ionic charge state to 2+ or 1+ by charge exchange reactions with buffer gas

IP(He)=24.6 eV, IP(Ar)=15.8 eV

~~$X^+ + He^0 \rightarrow X^0 + He^+$~~ or

~~$X^+ + Ar^0 \rightarrow X^0 + Ar^+$~~

remains in 1+ or 2+ charge state until charge exchange reaction with impurity molecule (O_2, N_2,...) occurs

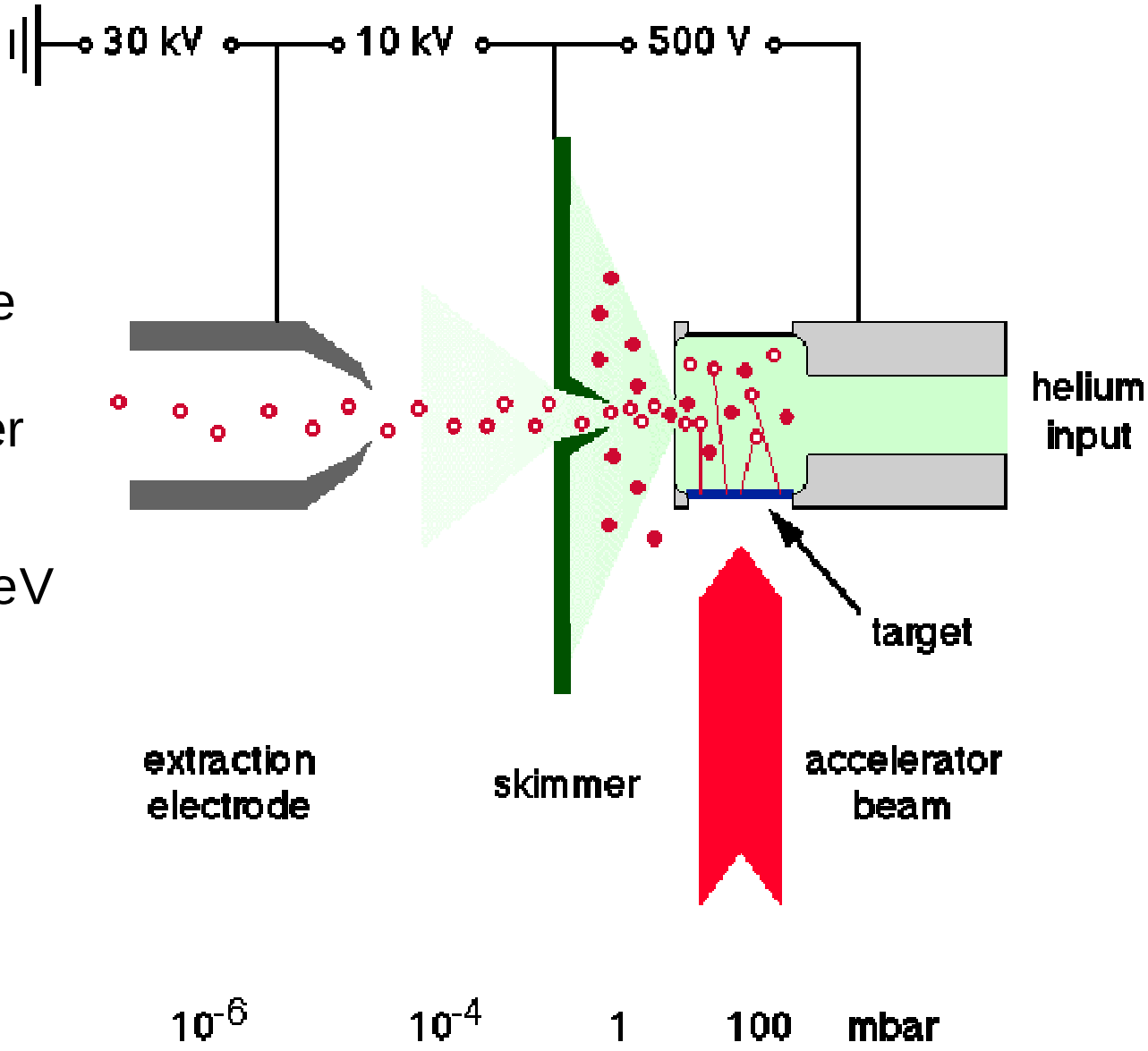

Volatility of the elements

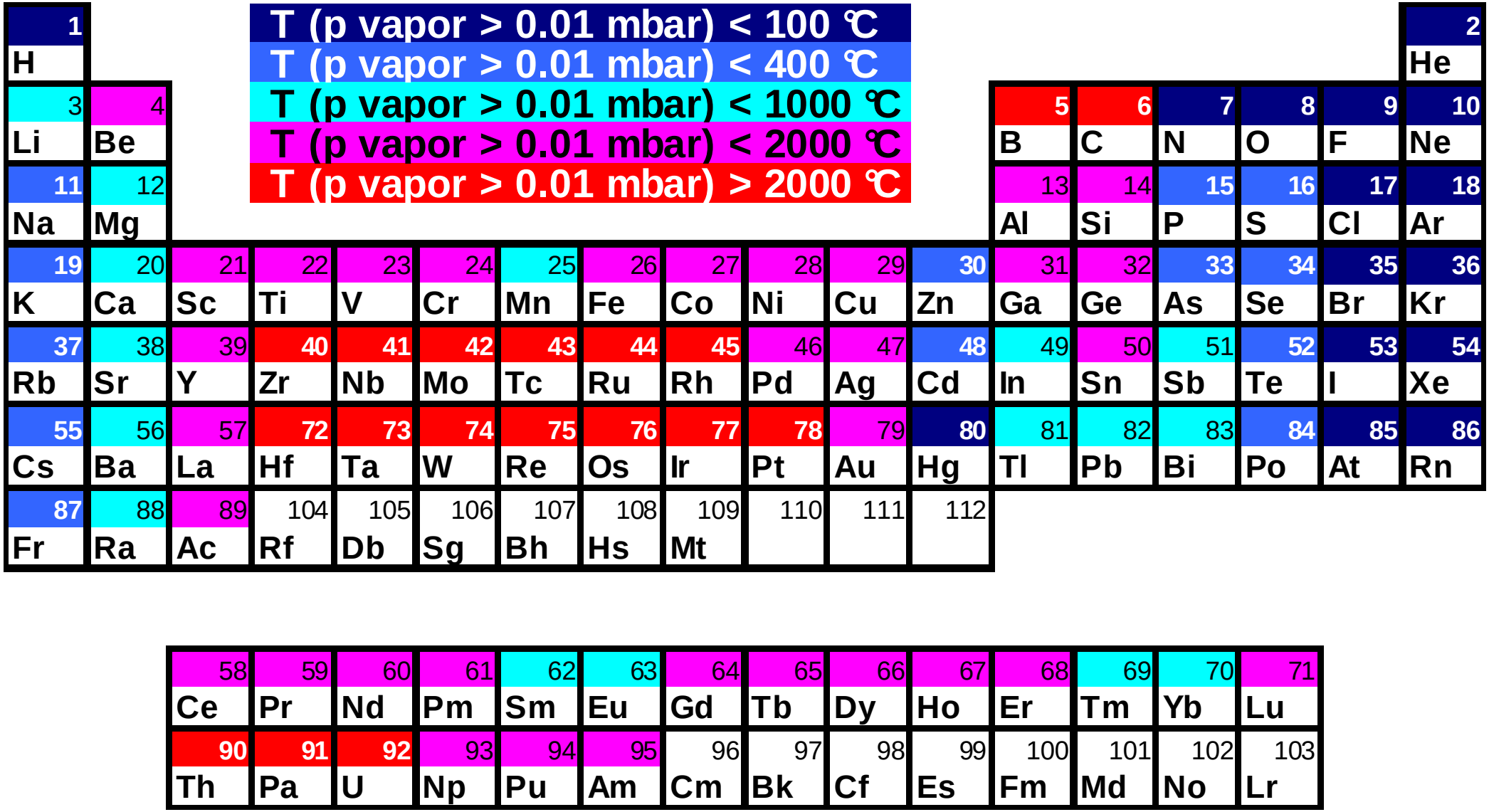

The IGISOL facility at JYFL

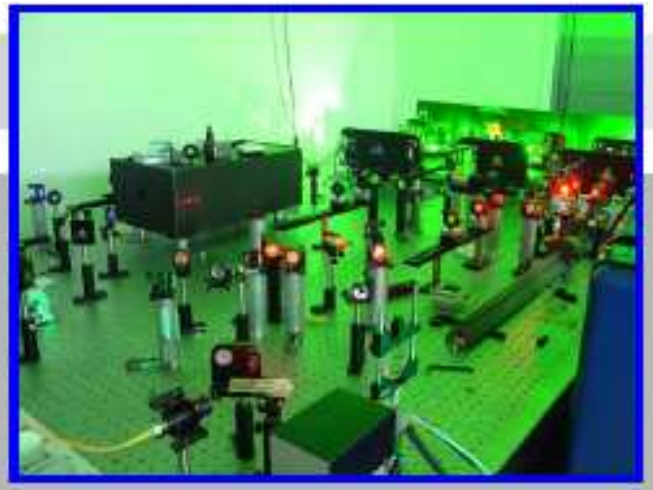

Laser cabin

Collinear laser spectroscopy

Mass & decay spectroscopy

Ion guide & laser ion source (trap)

RFQ cooler & buncher – optical manipulation

LISOL

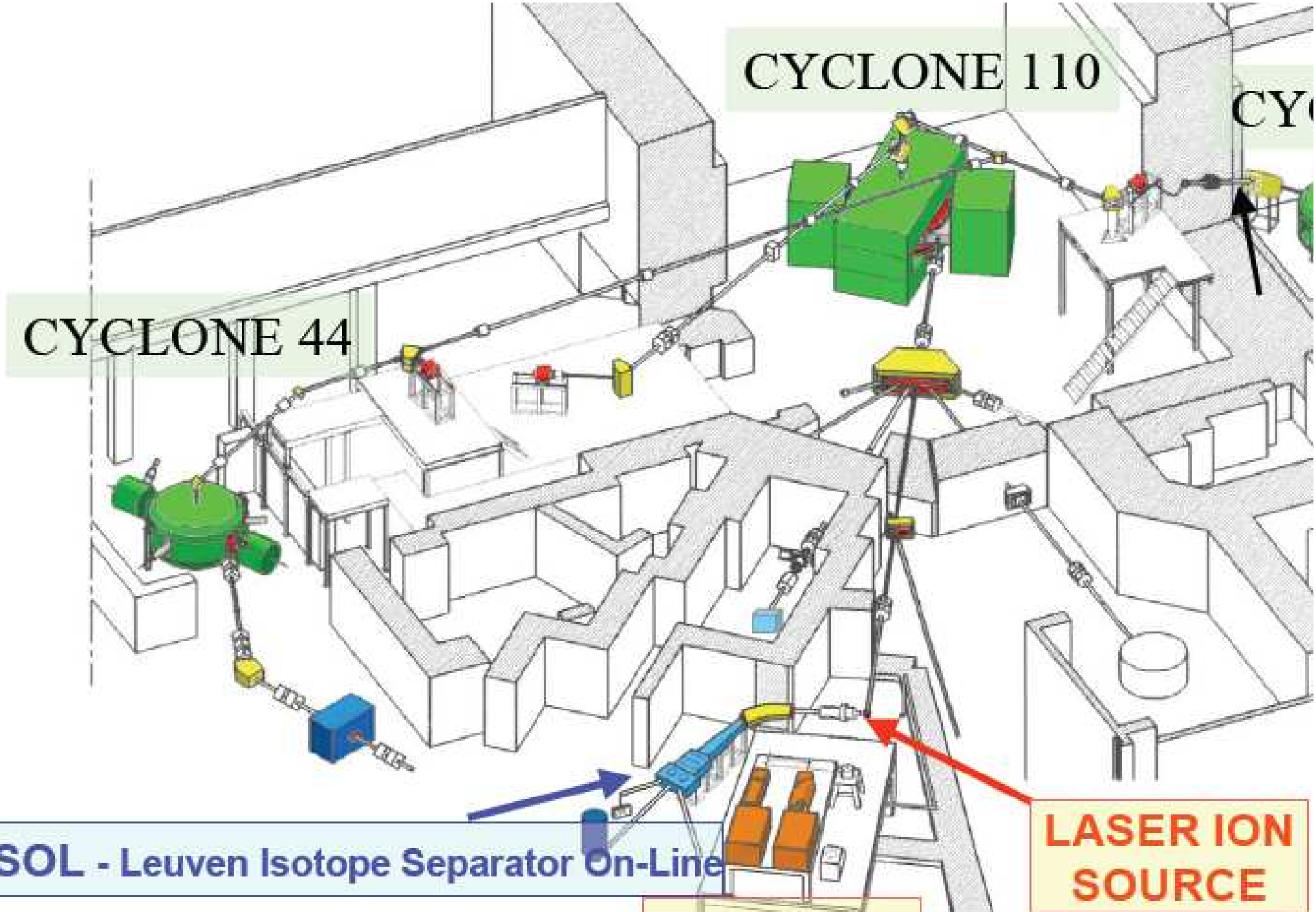
CYCLONE 110
CYCLONE 44
LISOL - Leuven Isotope Separator On-Line
LASER ION SOURCE

CARIBU: Radioactive Beams from ^{252}Cf(sf)

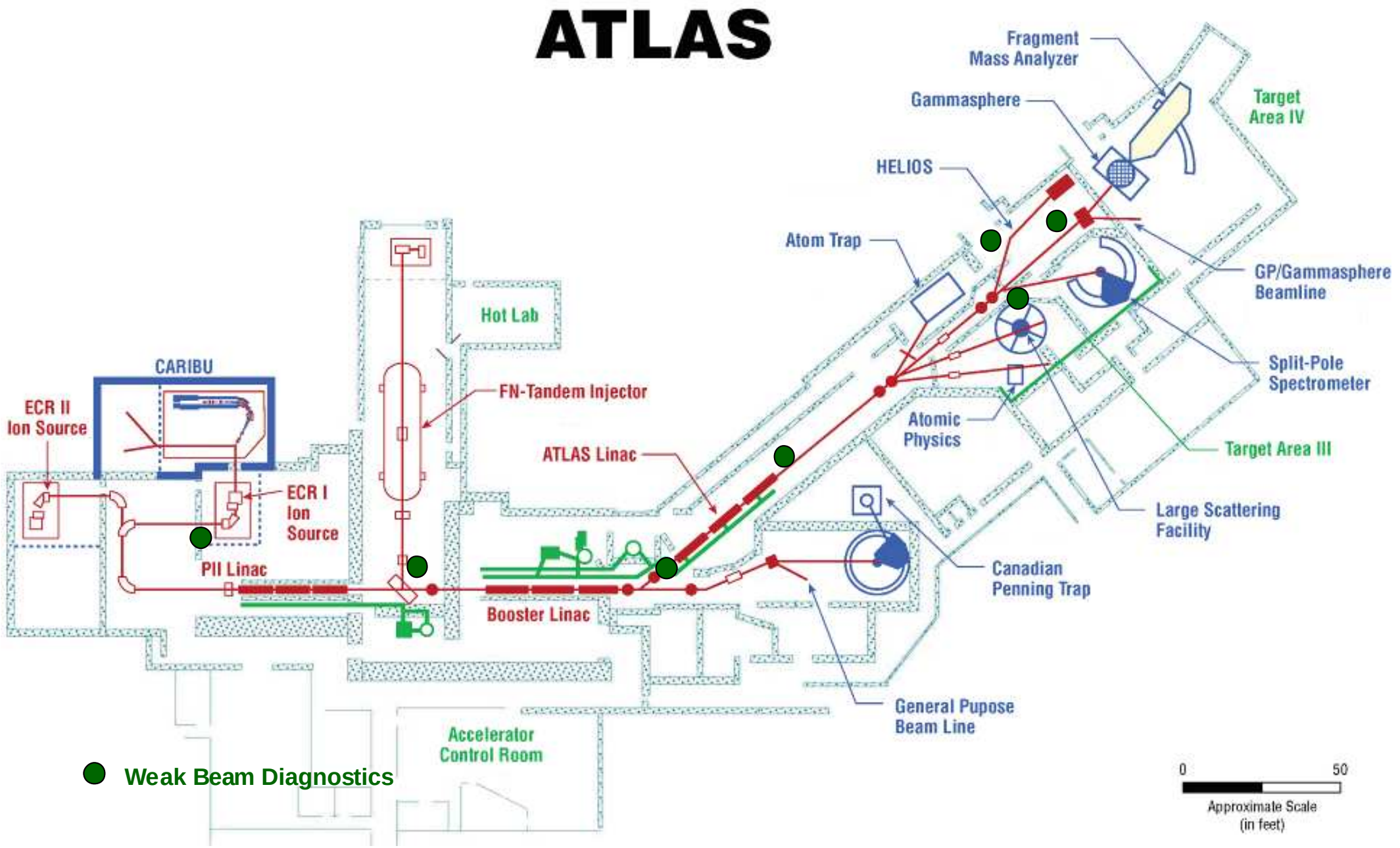

1 Ci ^{252}Cf source (1E9 fiss./s) expected end of 2009

TRIGA-SPEC at Mainz reactor

- 0.5 mg ^{235}U or 0.5 mg ^{239}Pu or 0.3 mg ^{249}Cf
- 1.8E11 n./cm^2/s
- 2E8 fiss./s
- start 2009

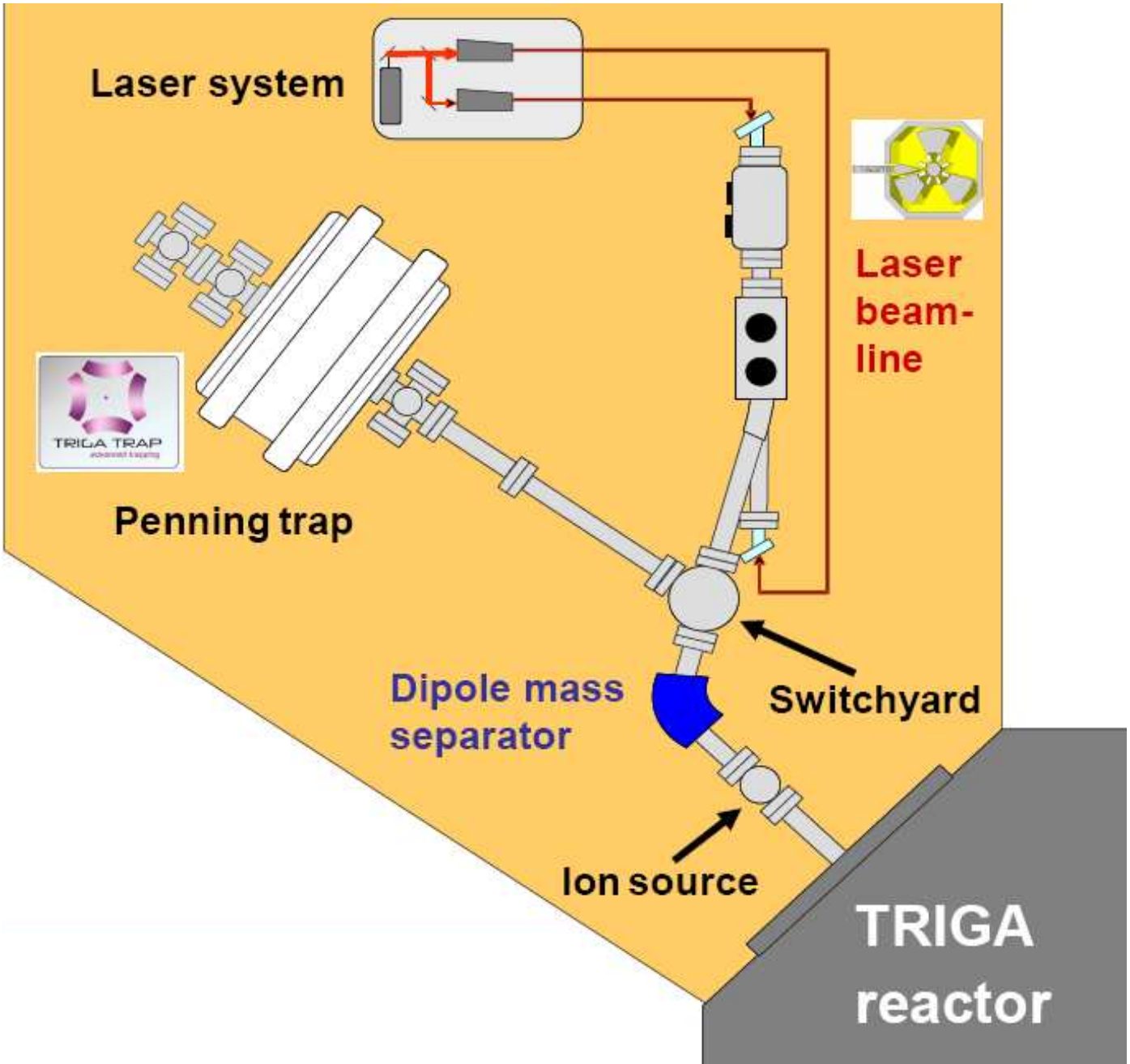

ISOL@CARR

- 60 MW China Advanced Research Reactor (CARR).
- Expected start of operation in 2009.
- gas-jet ISOL system
- 25 mg ^{235}U (90%) in Φ=2E14 n./cm^2/s
- 7E12 fiss./s

Optimize RIB intensity

All steps of the separation chain need to be optimized!

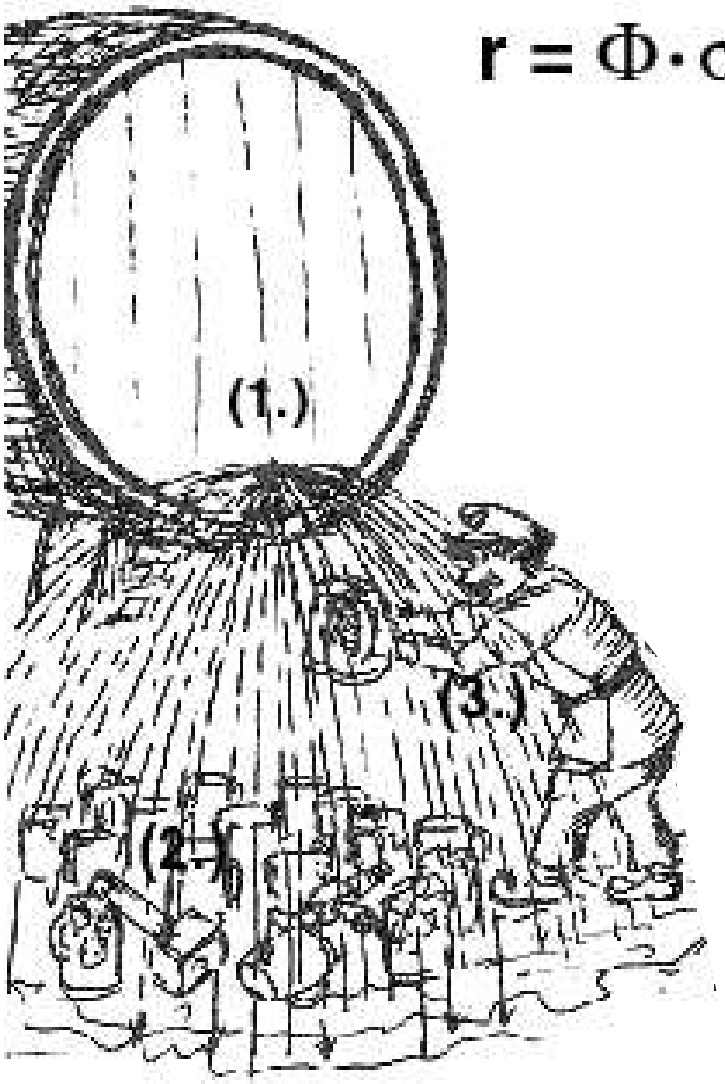

$$r = \Phi \cdot \sigma \cdot N \cdot \varepsilon_{target} \cdot \varepsilon_{source} \cdot \varepsilon_{transp} \cdot \varepsilon_{det}$$

Target (1967)

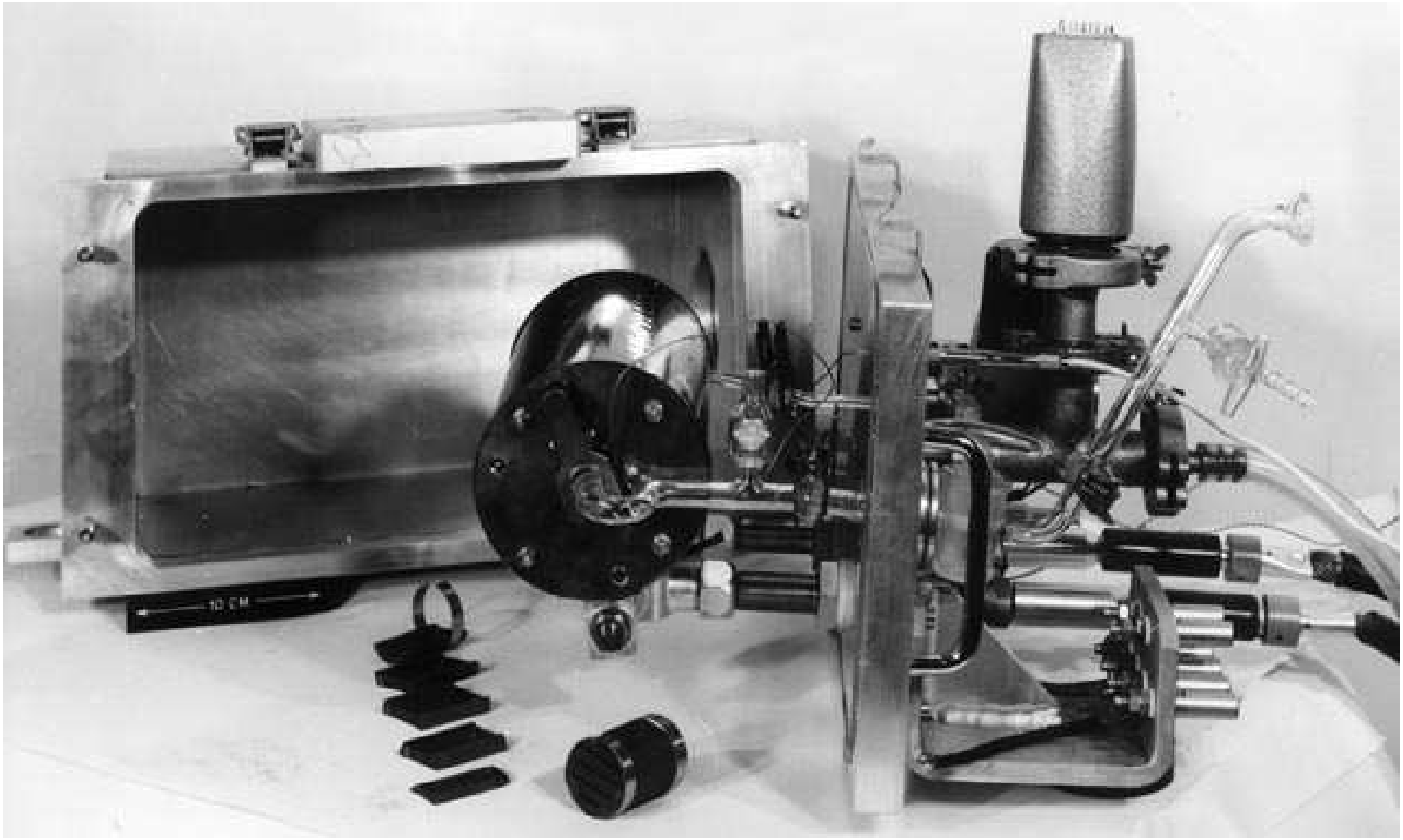

Target and ion source (1968)

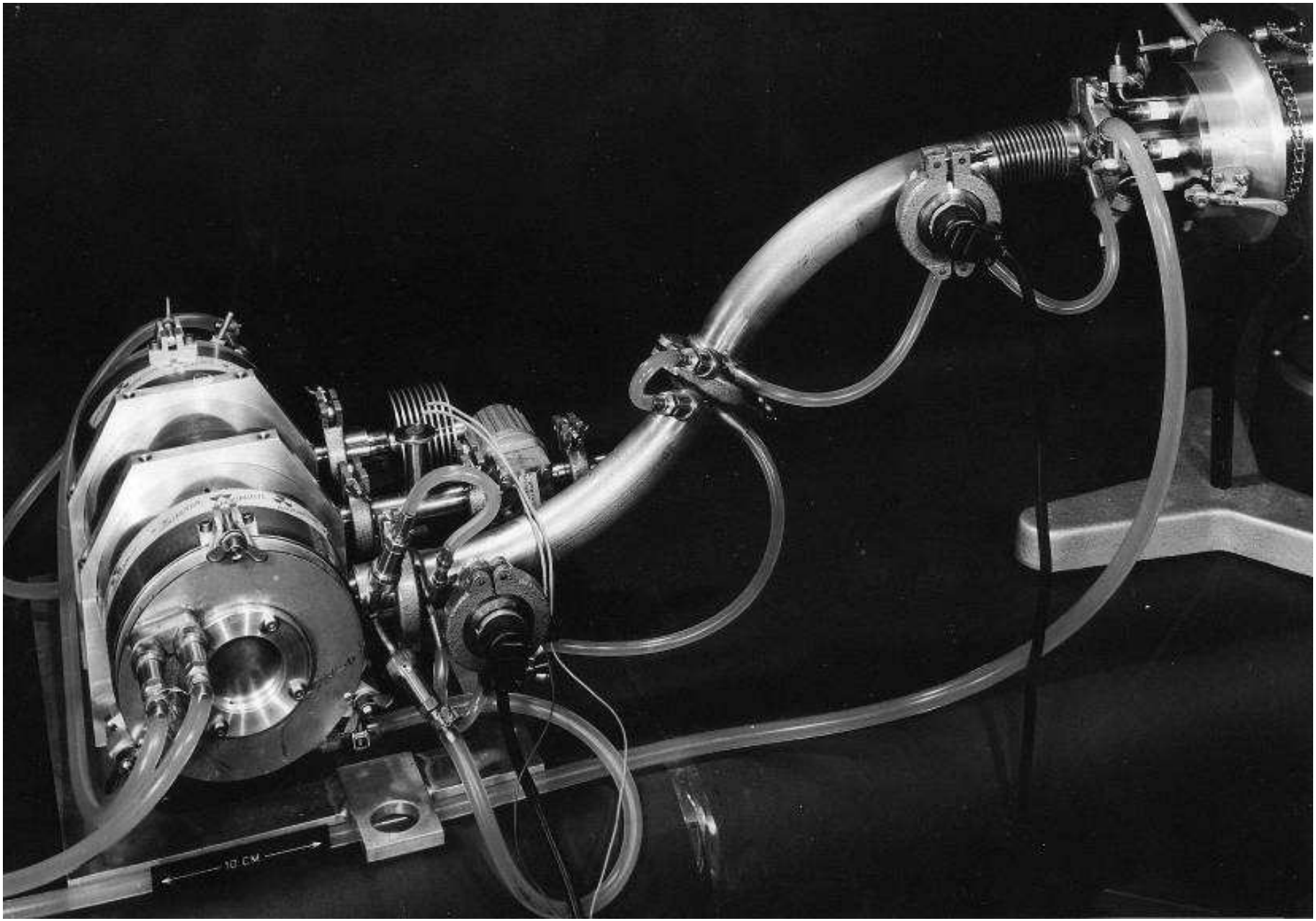

Compact target and ion source (1974)

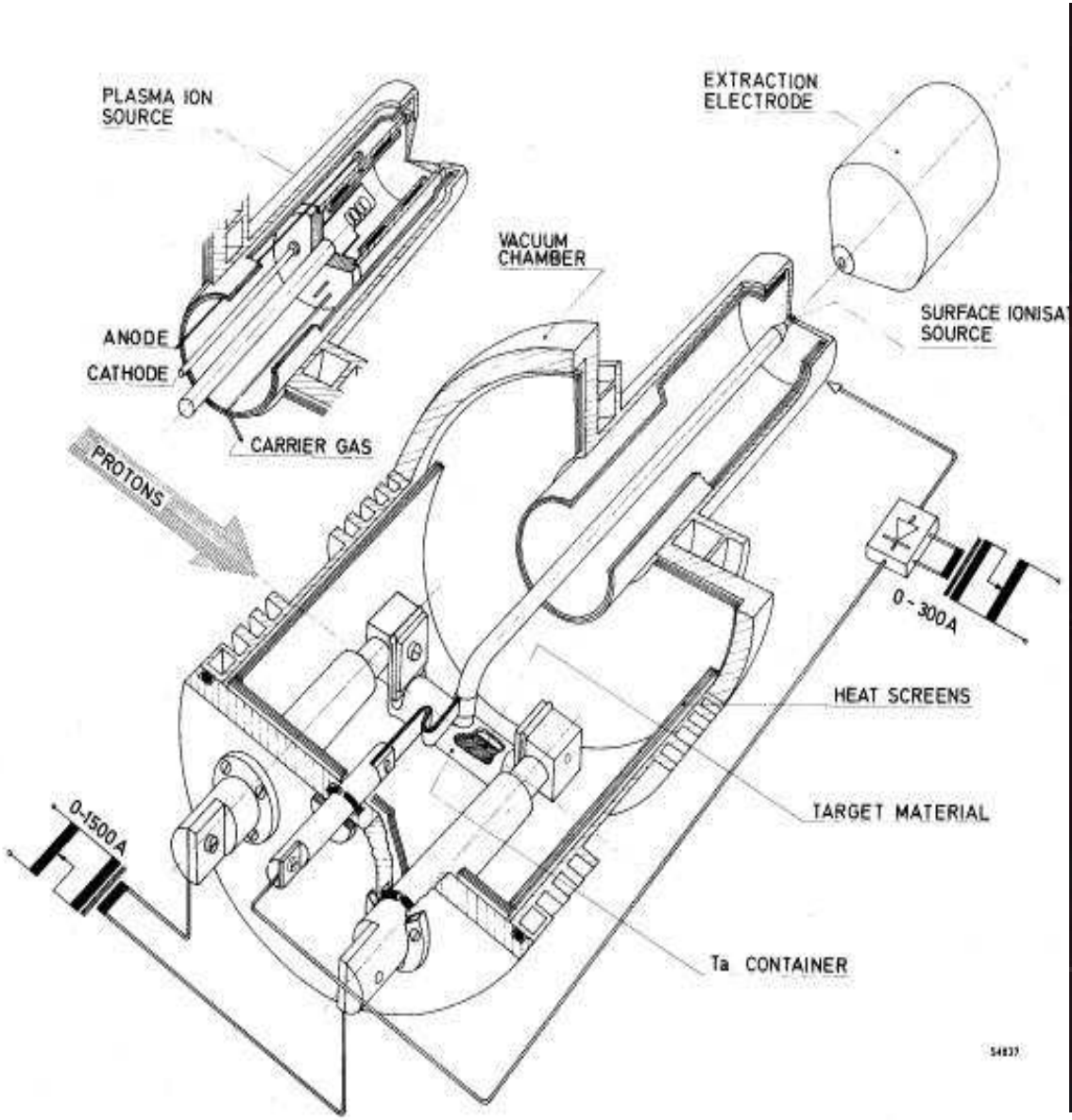

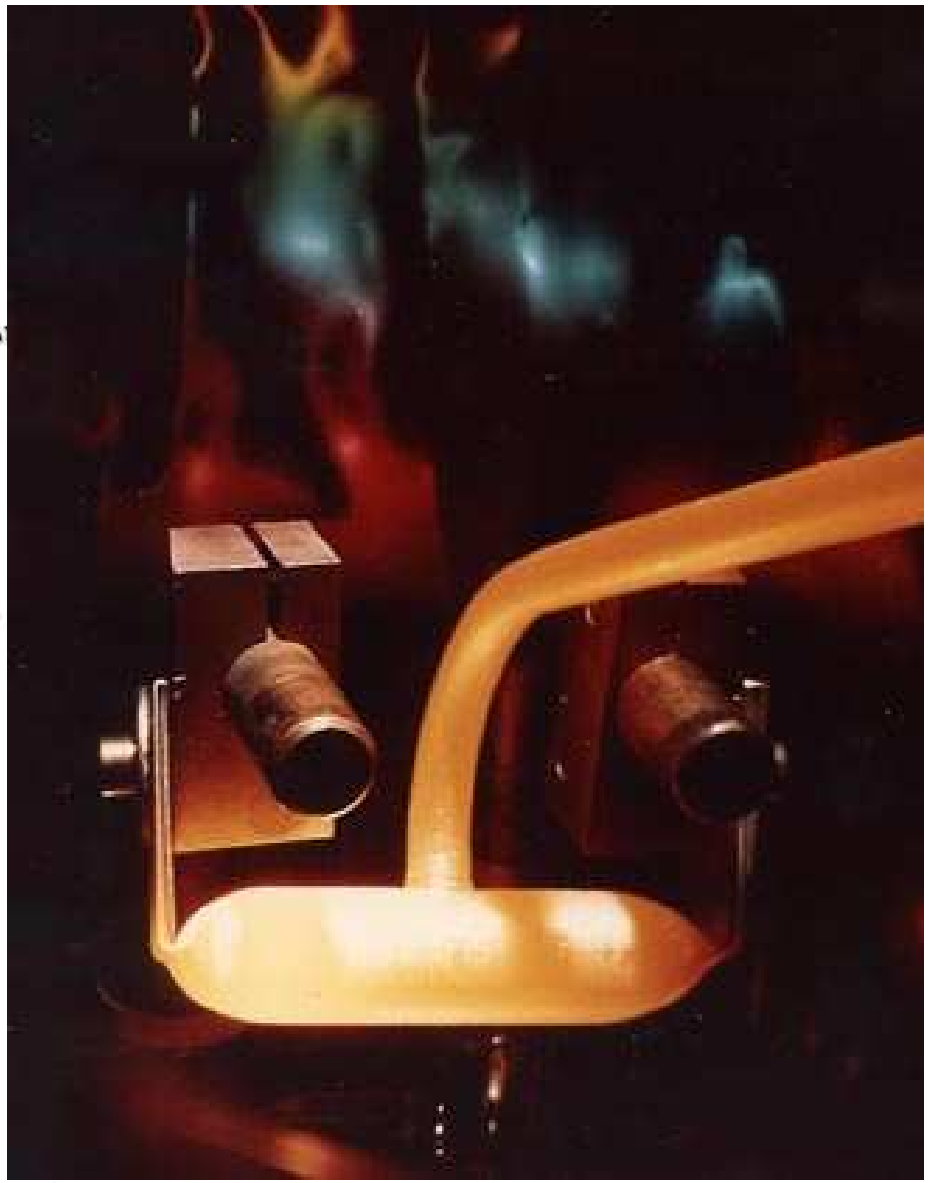

Robot handling

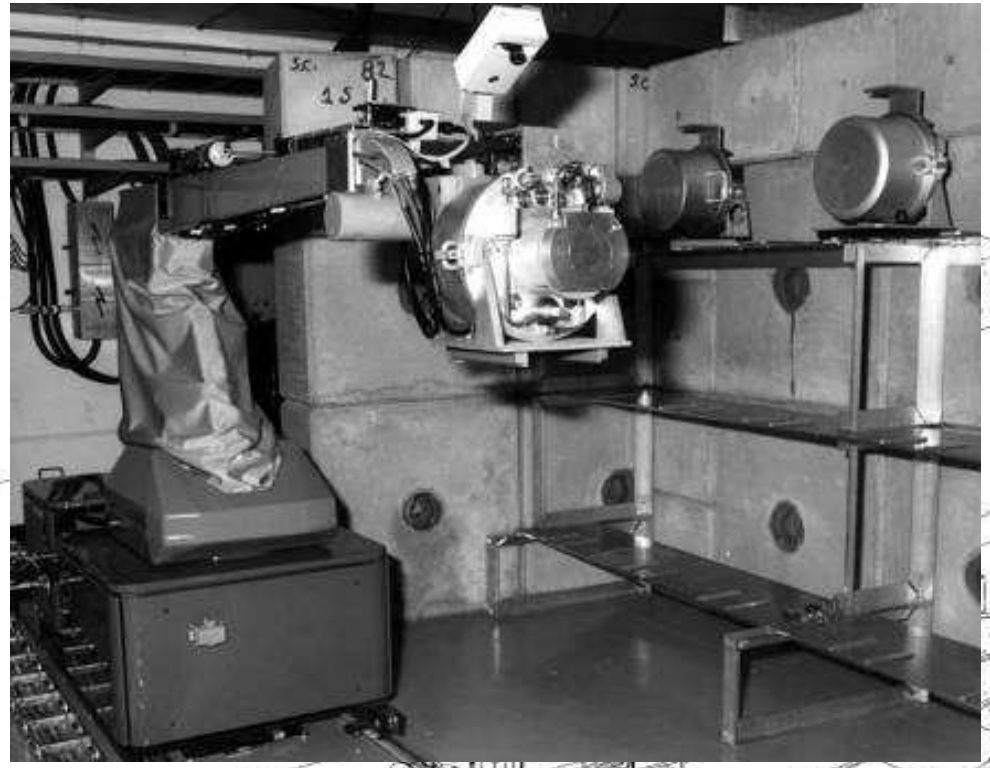

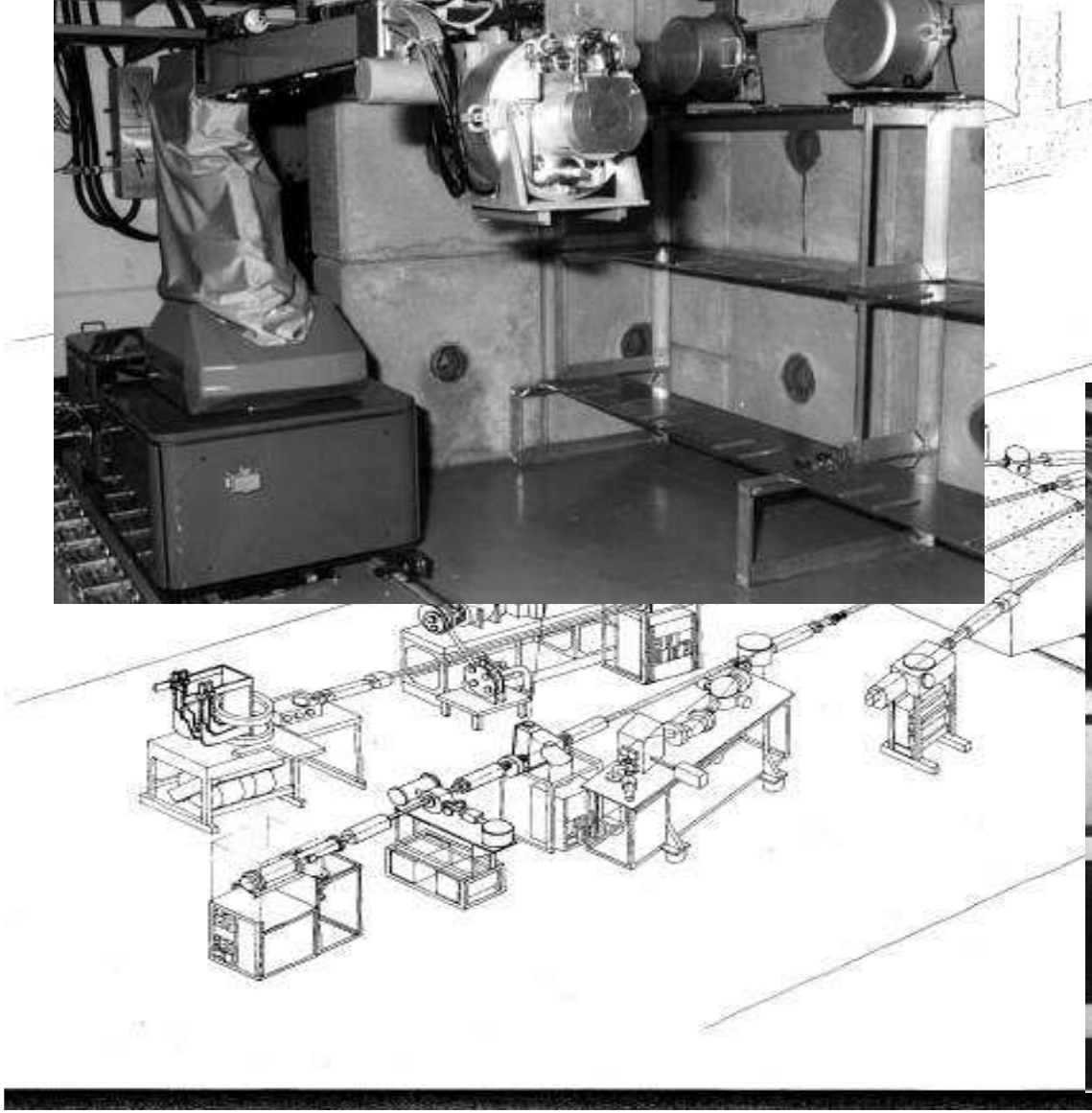

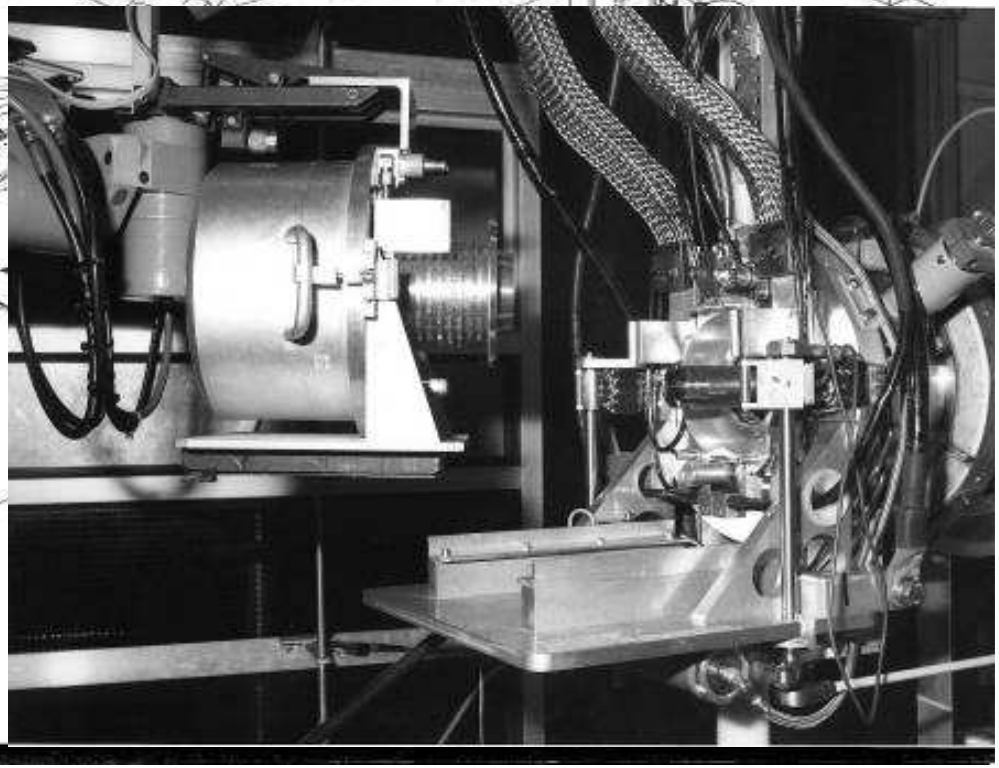

ISOLDE target and ion source unit

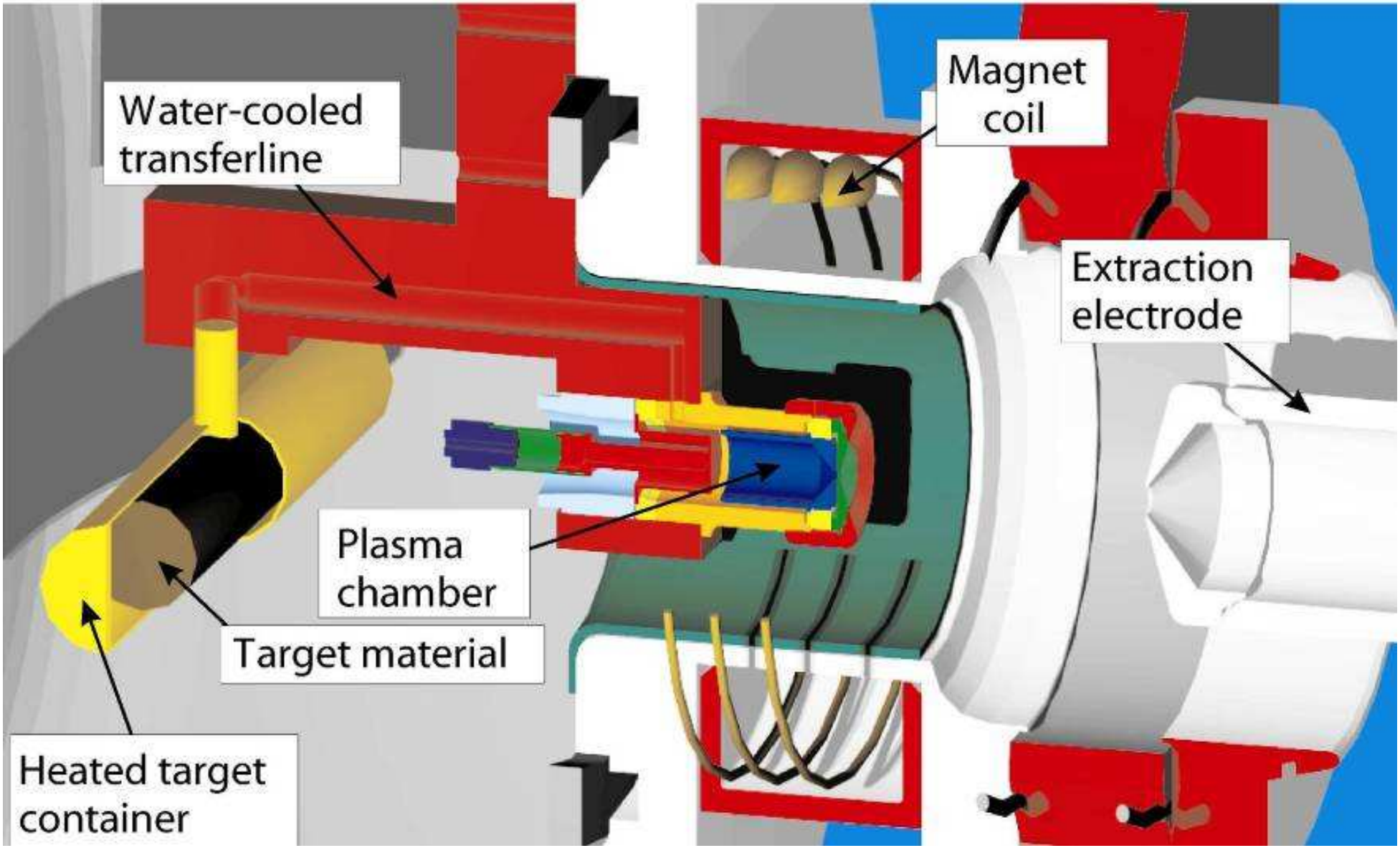

Historical development

Miniaturisation $\Rightarrow$ **faster release**

Standardisation $\Rightarrow$ **easier mass-production**

Remote handling $\Rightarrow$ **higher activities**

SPIRAL target and ion source unit

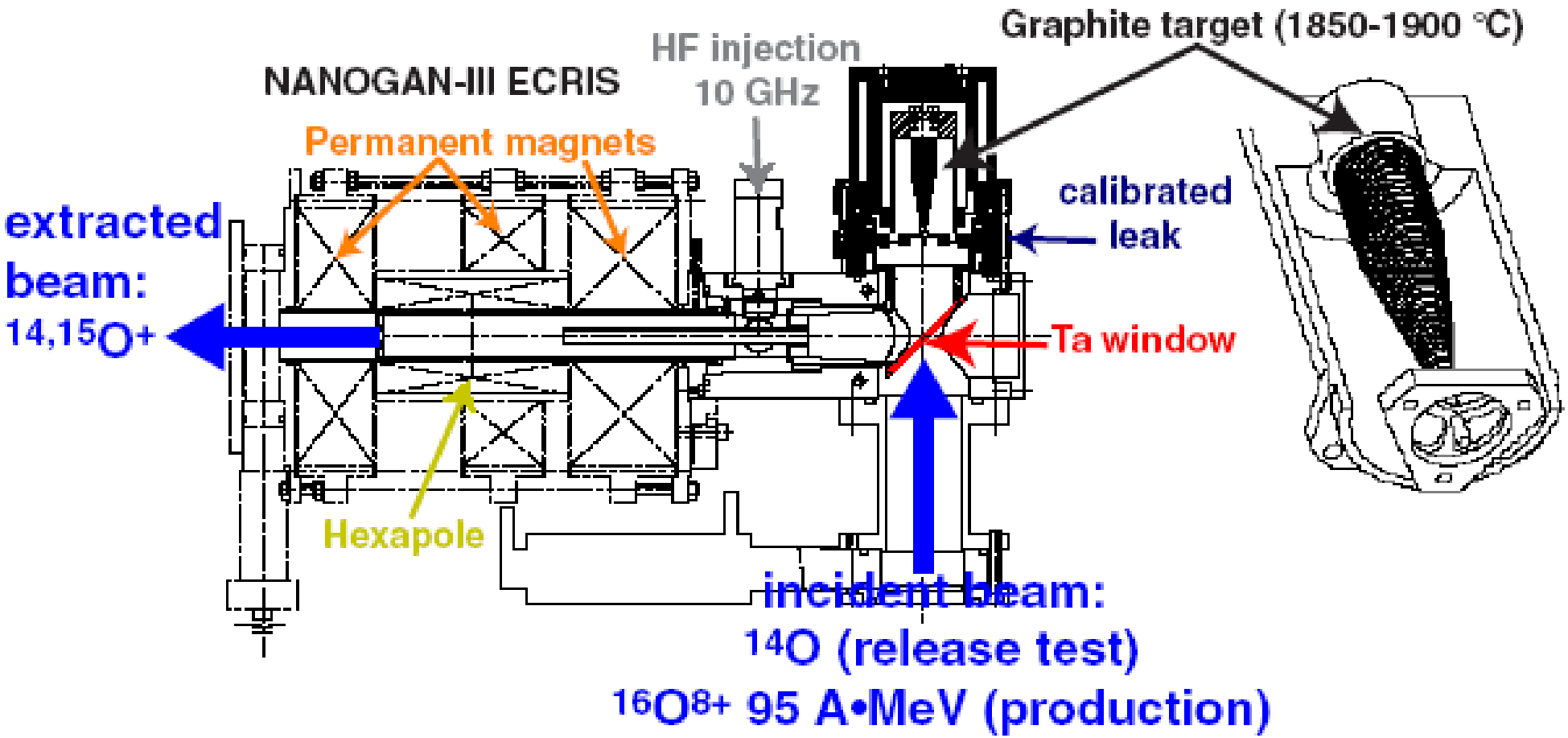

GSI-ISOL target and ion source unit

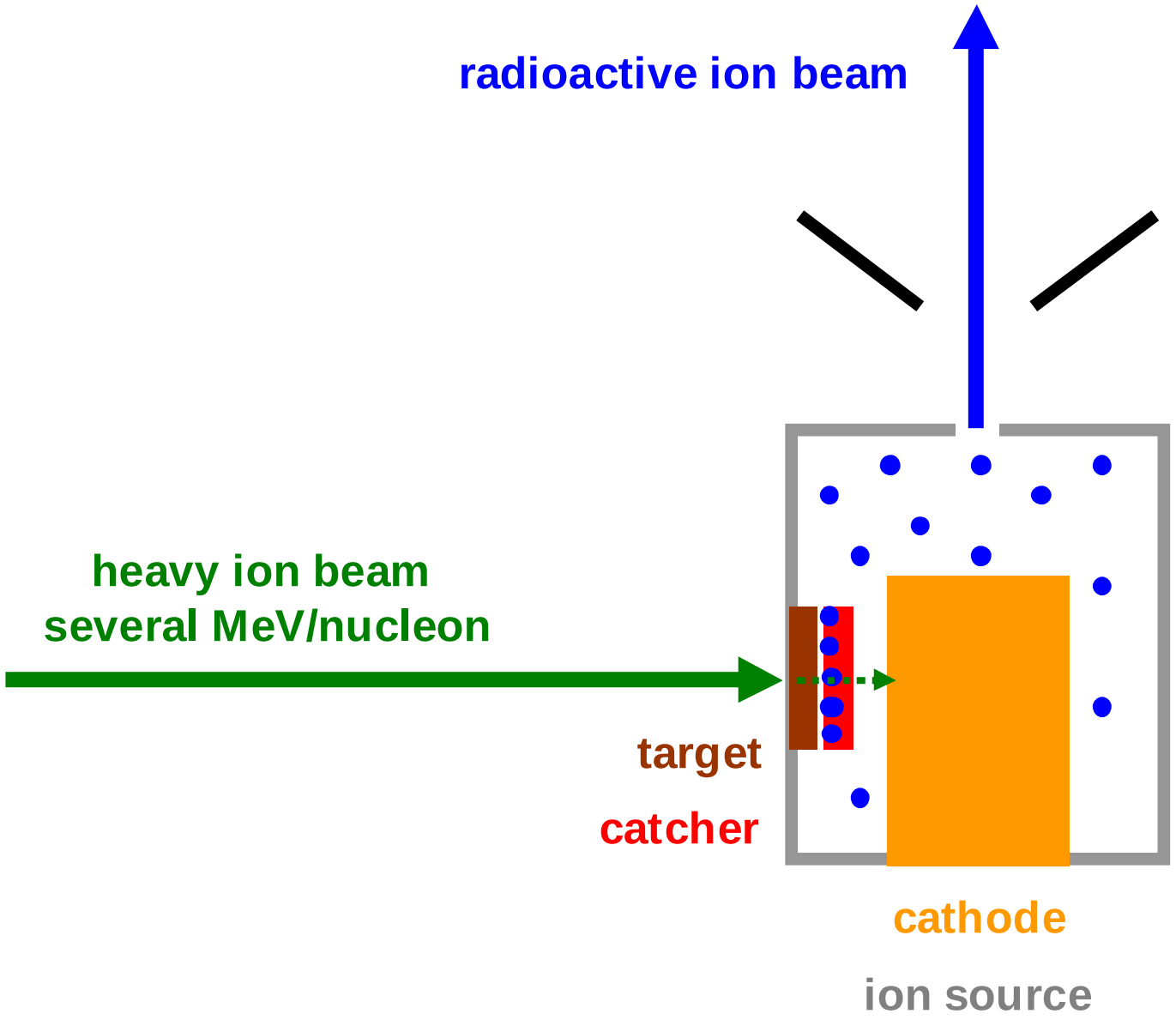

Variants of ISOL facilities

1a **protons on thick (heavy) target**: fragmentation, spallation, fission
ISOLDE-CERN (1.4 GeV), IRIS-PNPI (1 GeV), ISAC-TRIUMF (0.5 GeV)

1b **direct reactions in thick target**
CRC Louvain-la-Neuve, HRIBF Oak Ridge, TRIAC Tokai

1c **fission in thick target**
OSIRIS (Studsvik), HRIBF Oak Ridge, TRIAC Tokai, SPIRAL2 (GANIL)

2 **projectile fragmentation in thick (carbon) target**
SPIRAL (GANIL), DRIBS (Dubna), EXCYT (LNS Catania)

3 **fusion-evap. or multinucleon transfer in thin target plus solid catcher**
GSI-ISOL, UNIRIB (ORNL), DOLIS (Daresbury), LISOL (Leuven),
IMP Lanzhou, MASHA (Dubna), SPIRAL2 (GANIL)

4 **fusion-evap., direct reaction or fission in thin target plus gas catcher (Ion Guide ISOL = IGISOL)**
IGISOL (Jyväskylä), LISOL (Leuven), …

5 **liquid helium catcher**
JYFL Jyväskylä, KVI Groningen

The life cycle of an ISOLDE target

SICMI
41313

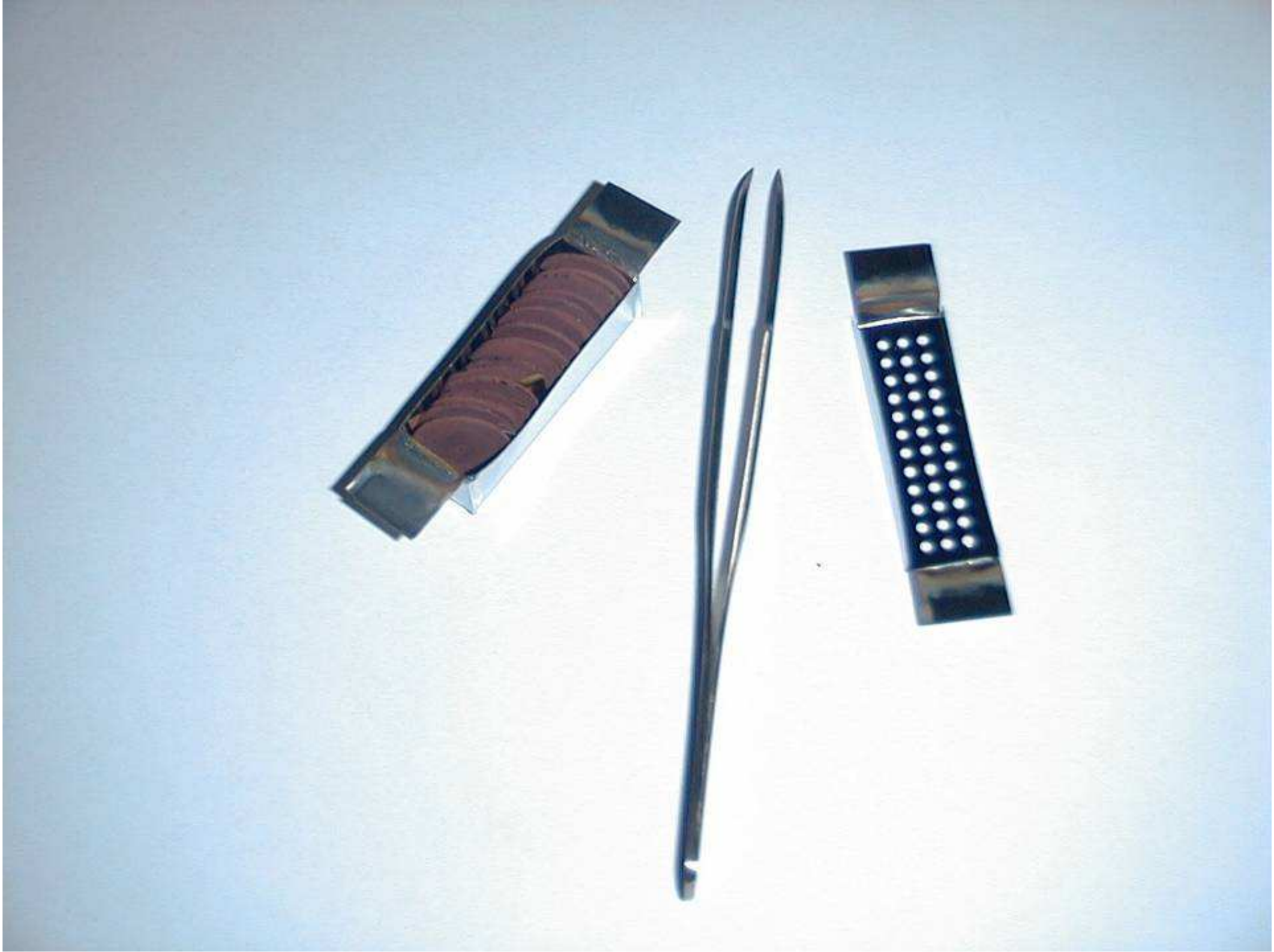

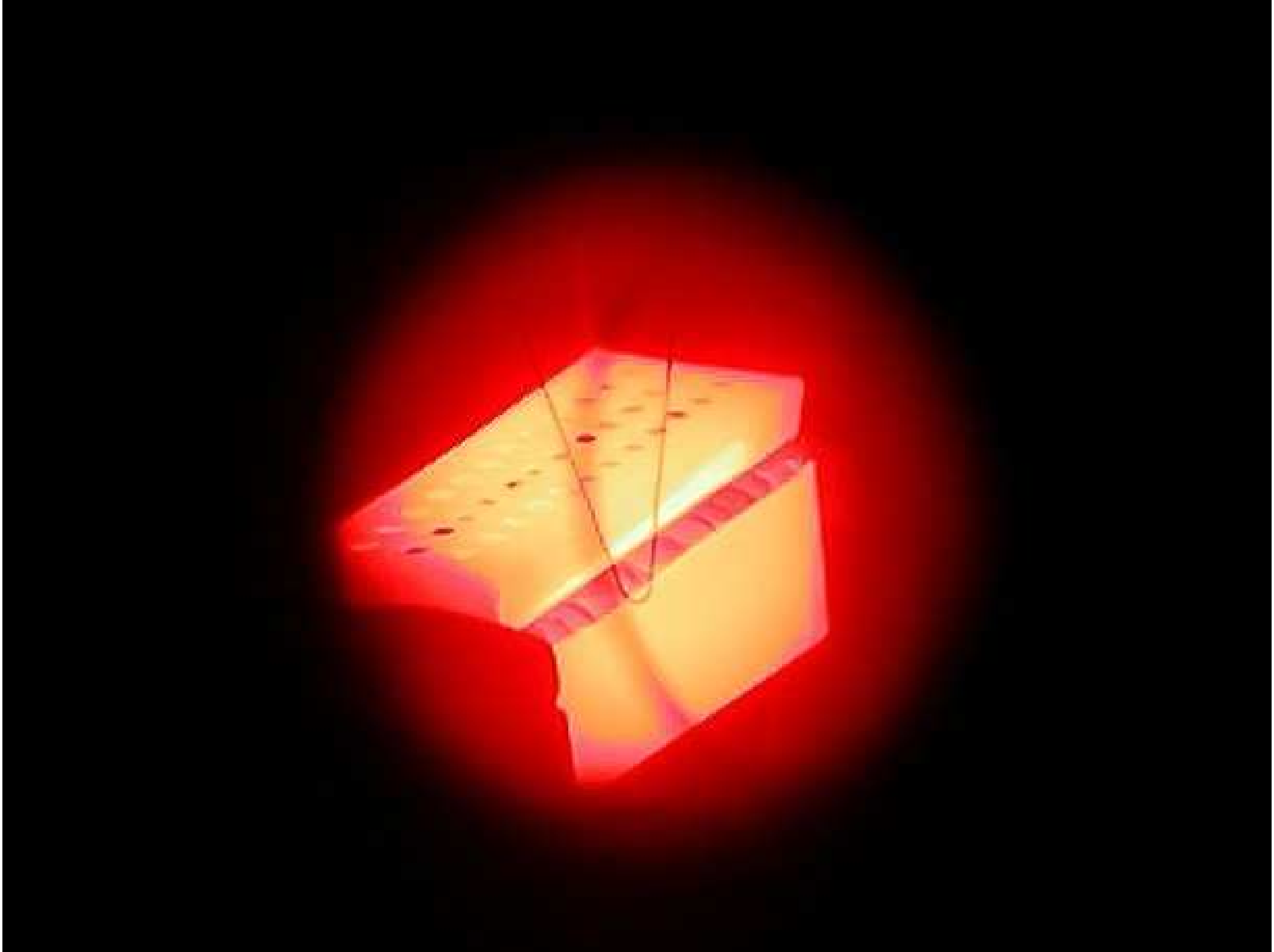

HB
0

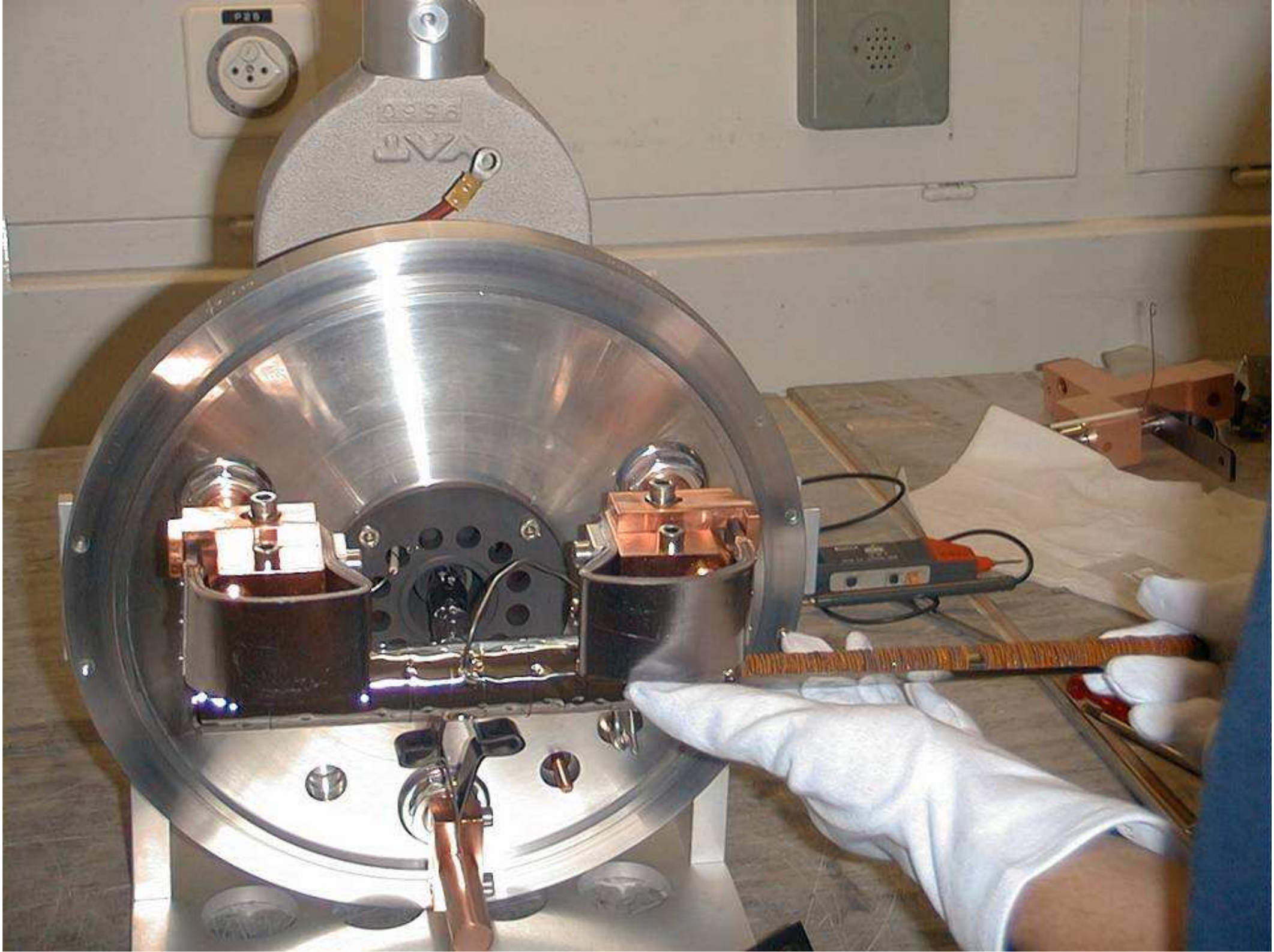

EUR D'URGENCE
GENCY STOP
RADIATION
contamination of
U+Th (inside)

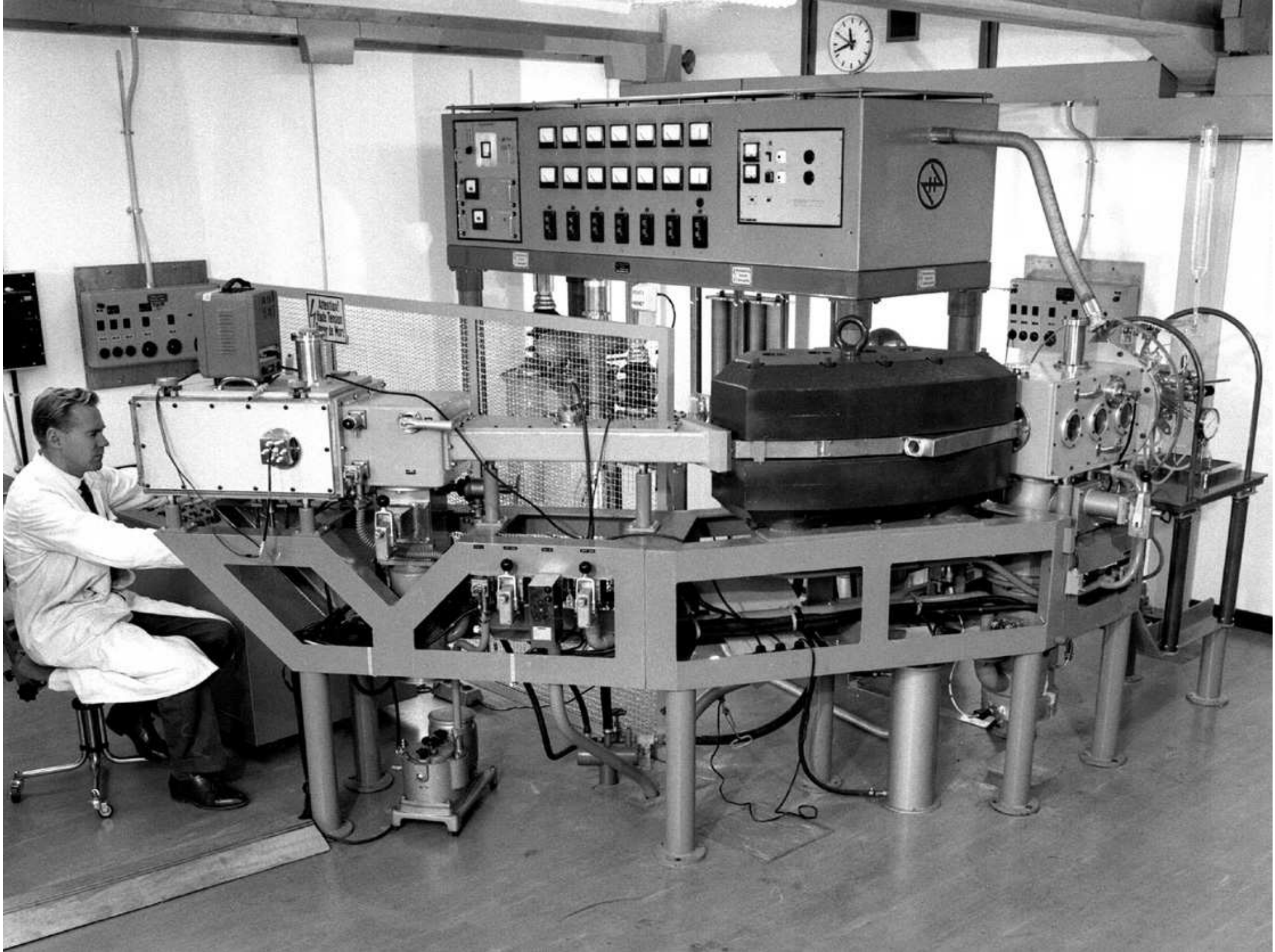

ISOLDE front-ends

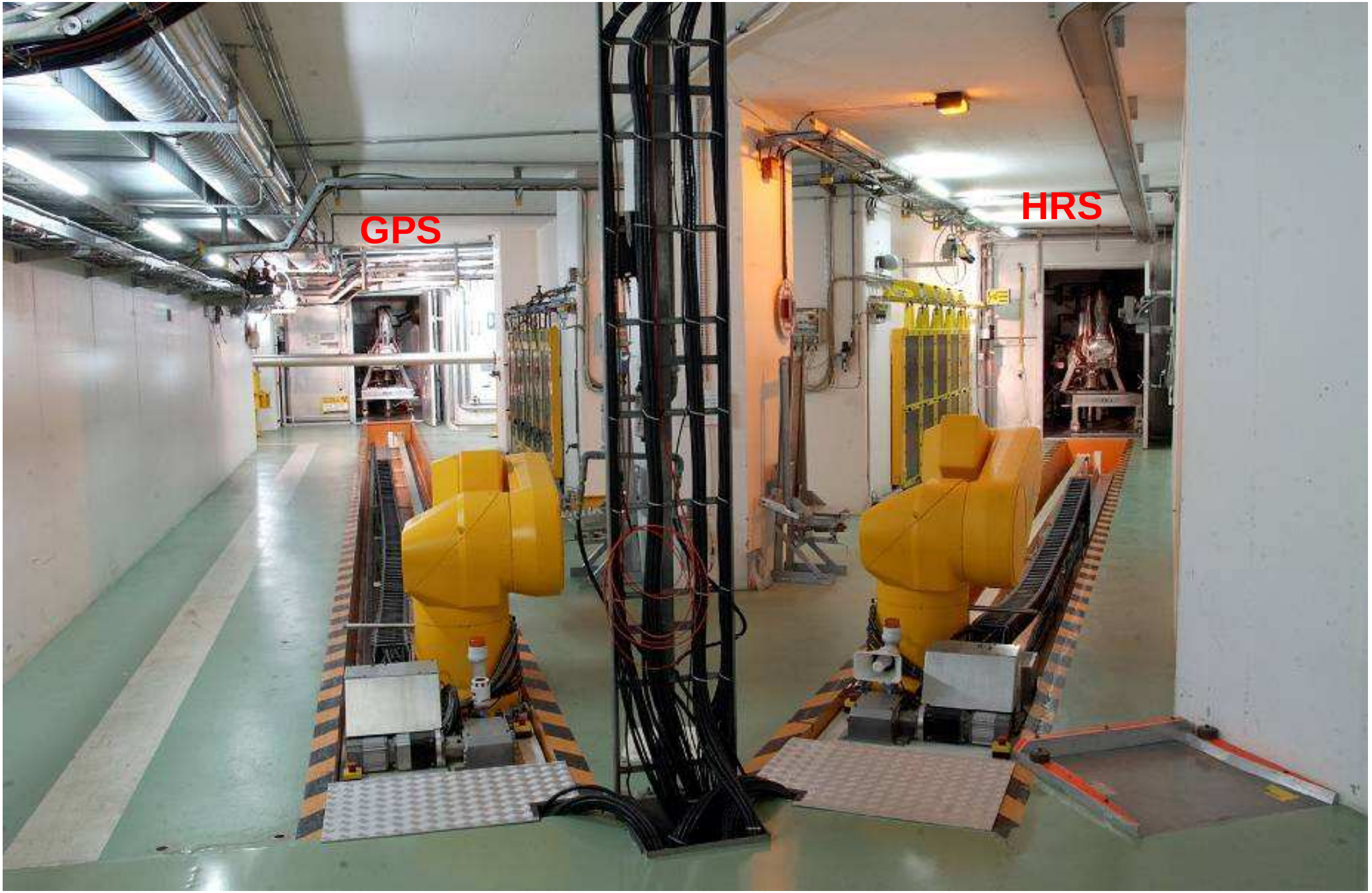

ISOLDE CERN

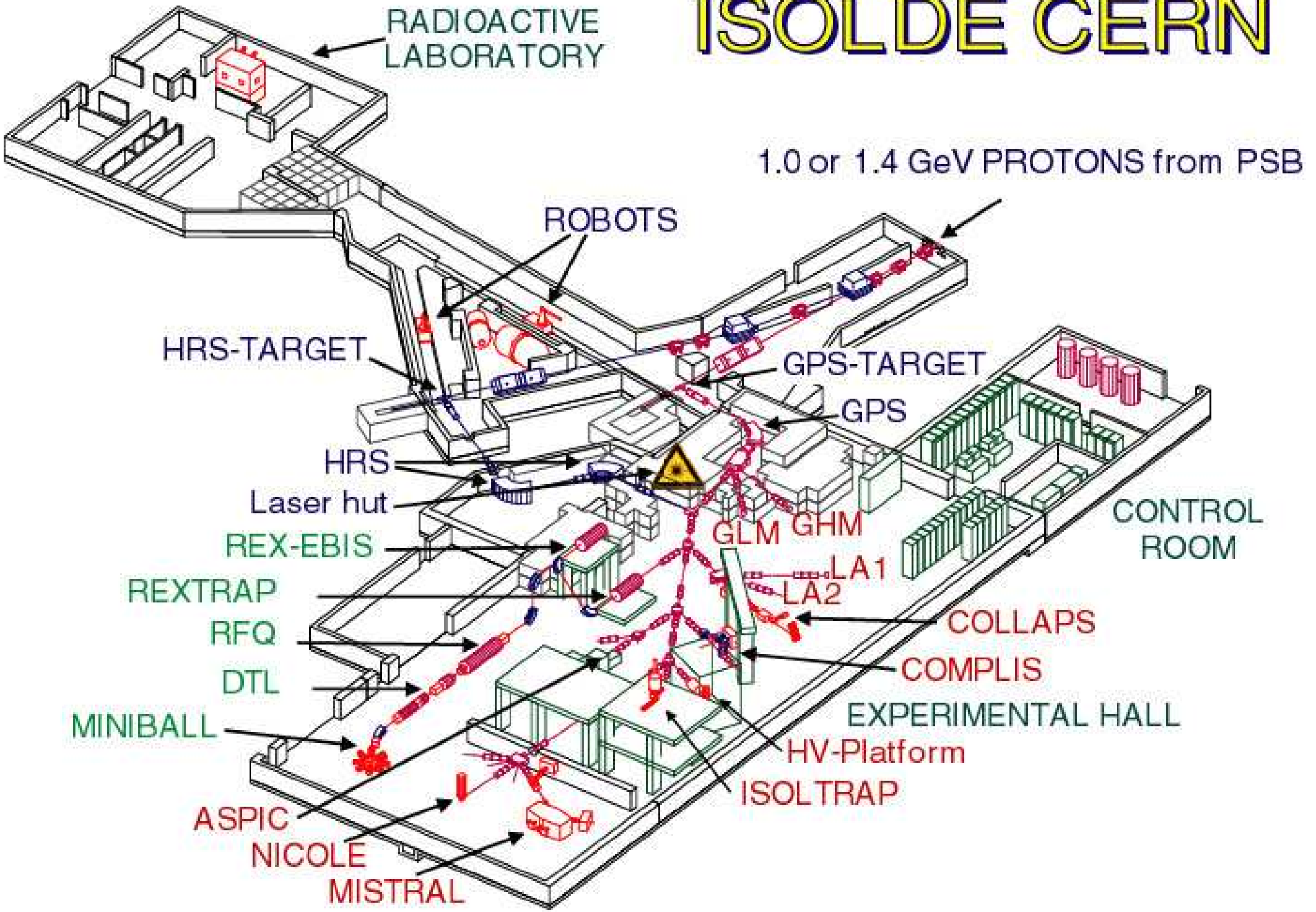
RADIOACTIVE LABORATORY
1.0 or 1.4 GeV PROTONS from PSB
ROBOTS
HRS-TARGET
GPS-TARGET
GPS
HRS
Laser hut
REX-EBIS
REXTRAP
RFQ
DTL
MINIBALL
ASPIC
NICOLE
MISTRAL
GLM
GHM
LA1
LA2
COLLAPS
COMPLIS
HV-Platform
ISOLTRAP
CONTROL ROOM
EXPERIMENTAL HALL

Postmortem examination of used targets

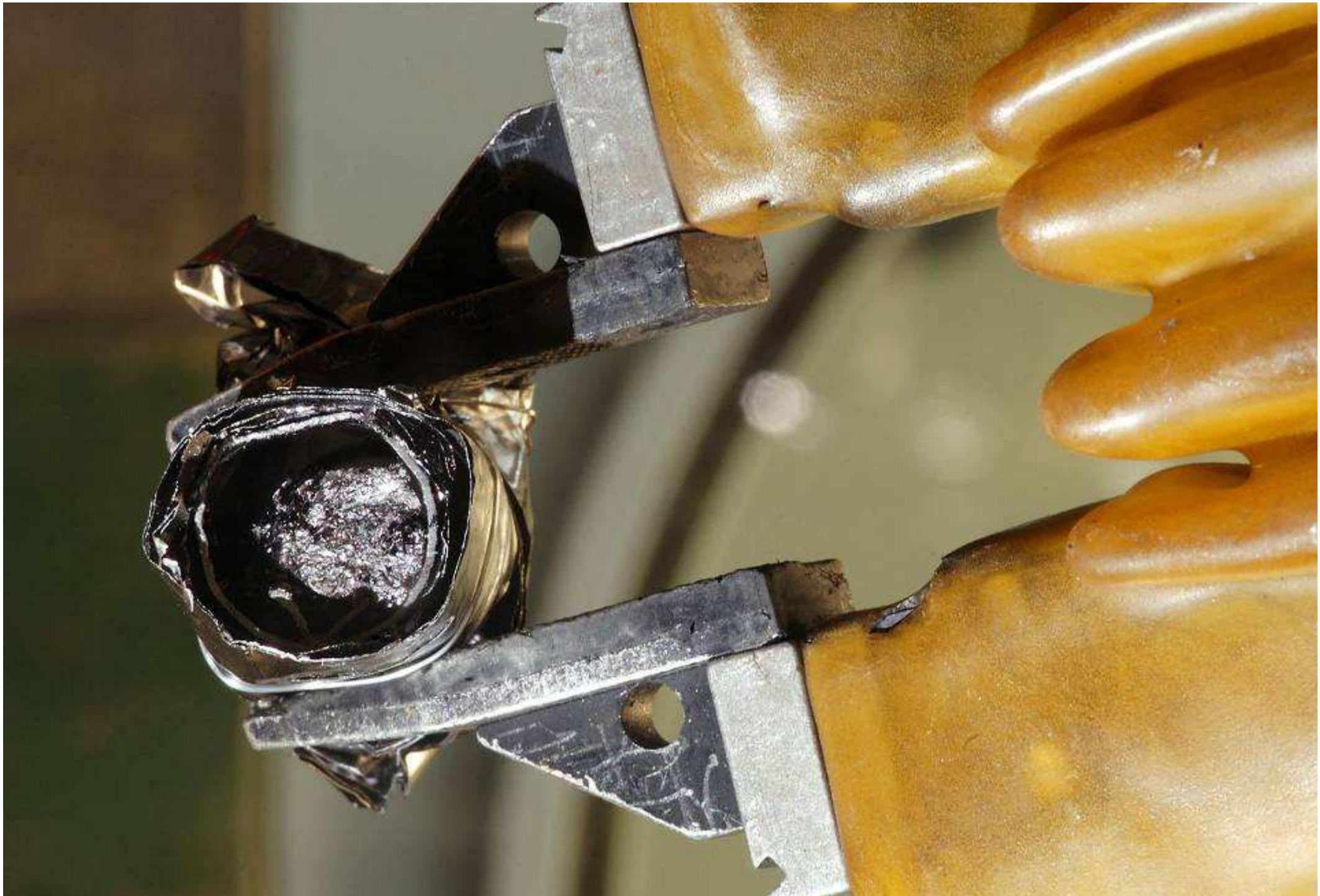

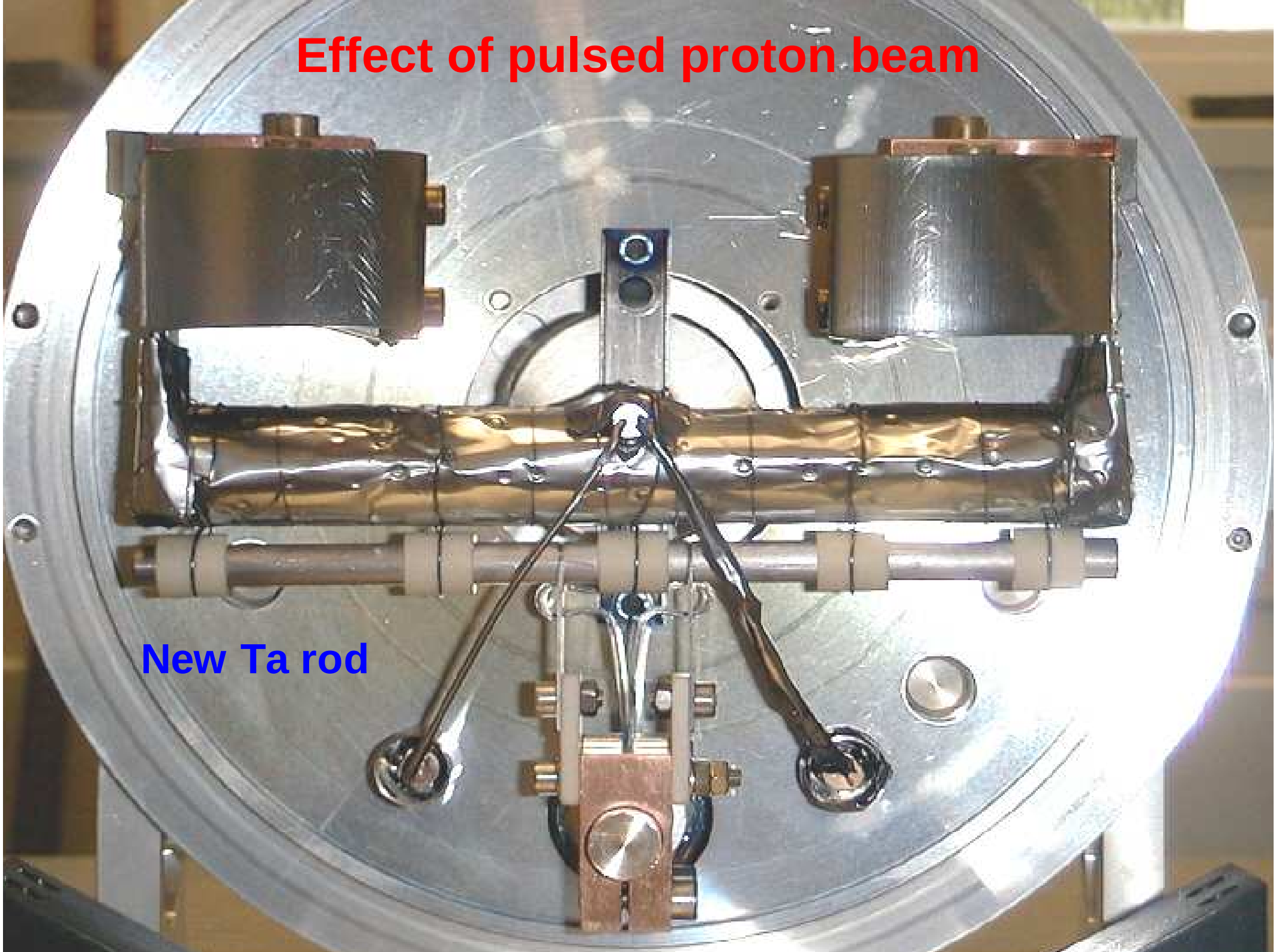
Effect of pulsed proton beam
New Ta rod

Effect of pulsed proton beam

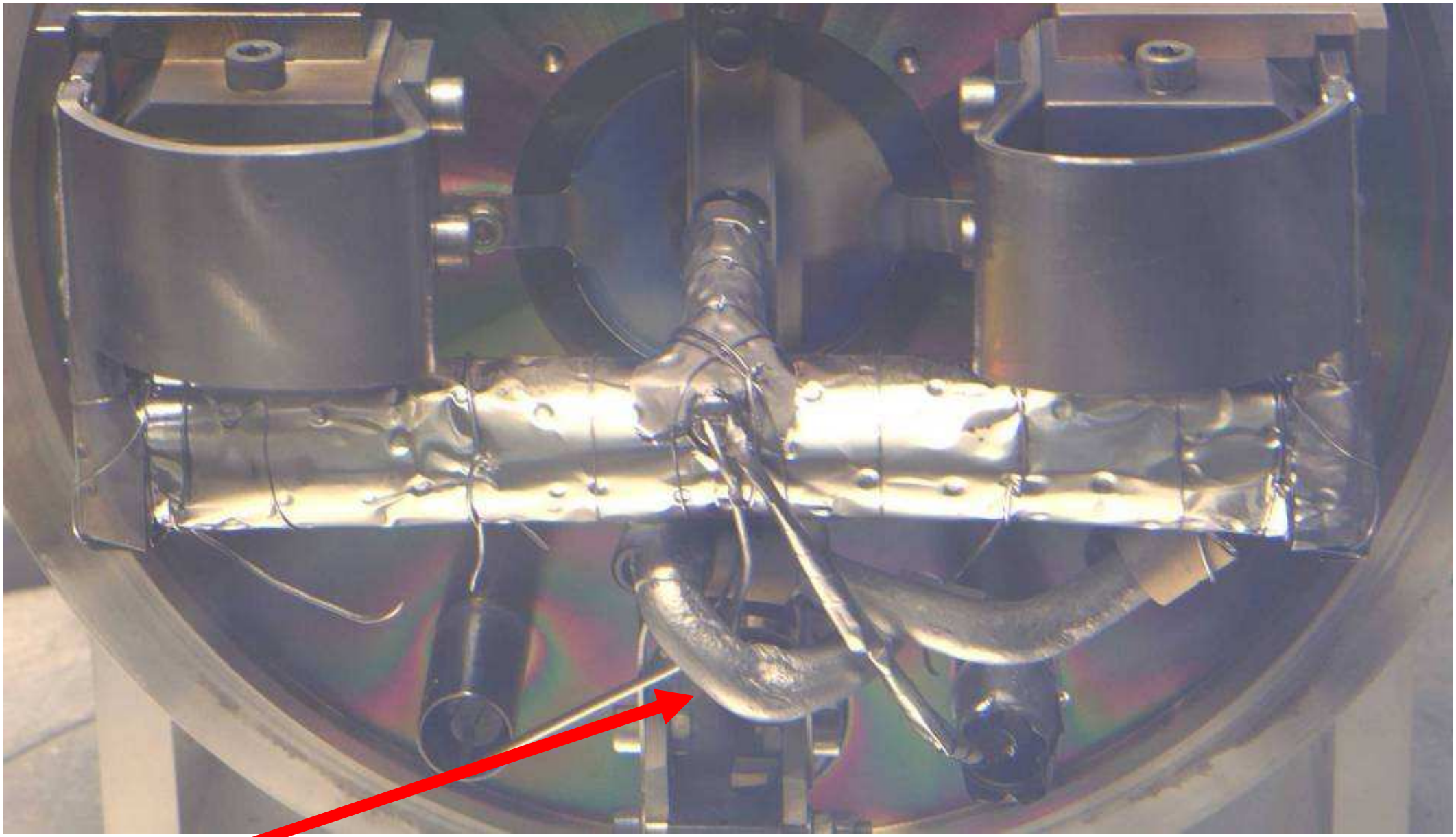

Ta rod after irradiation with ca. 200000 proton pulses (1 Coulomb)

ISOL targets

Target materials:

1. **molten metals:** Ge, Sn, La, Pb, Bi, U,...
2. **solid metals:** Ti, Zr, Nb, Mo, Ta, W, Th,...
3. **carbides:** Al_4C_3, SiC, VC, ZrC, LaC_x, ThC_x, UC_x,...
4. **oxides:** MgO, Al_2O_3, CaO, TiO_x, ZrO_2, CeO_x, ThO_2,...
5. **others:** graphite, borides, silicides, sulfides, zeolithes,...

Target dimensions:

target container: 20 cm long, 2 cm diameter

target thickness 2—200 g/cm^2, 10—100% of bulk density

micro-dimensions of foils, fibers or pressed powder: 1—30 μm

U.K. for the ISOLDE Collaboration, Radiochimica Acta 89 (2001) 749.

Diffusion characteristics

Bad diffusion hosts (narrow and/or stiff crystal lattice):

Re, diamond, SiC,...

Good diffusion hosts (wide crystal lattice):

Ti, Zr, Hf (fcc metals), Nb, Ta, graphite,

polycrystalline oxides (in particular fibers!)

Characteristic diffusion length:

$d = (2\ n\ D\ t)^{1/2}$ **n=1 (foil), n=2 (fiber), n=3 (sphere)**

Maximize D and minimize diffusion path:

$\Rightarrow$ **thin metal foils (2 μm ... 30 μm)**

$\Rightarrow$ **fine powders (μm)**

$\Rightarrow$ **thin fibers (some μm)**

Effusion: random walk release

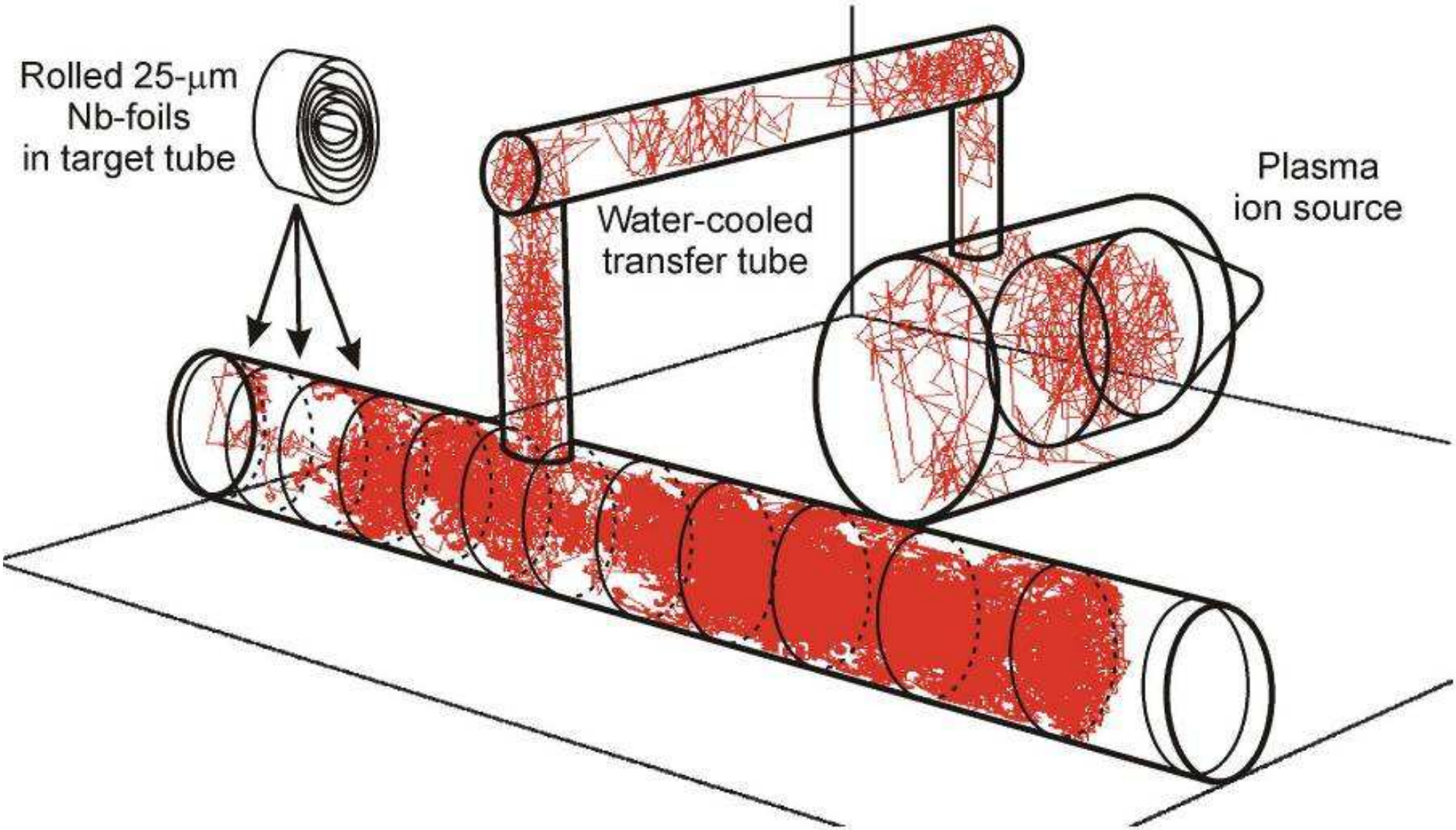

Optimize RIB intensity

All steps of the separation chain need to be optimized!

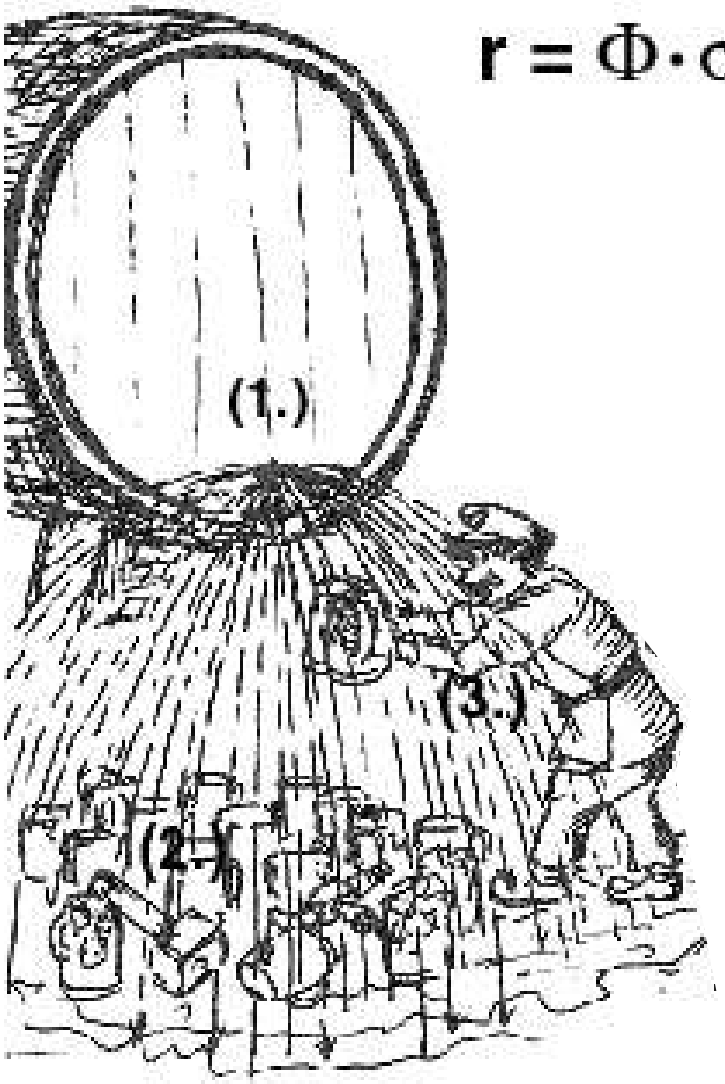

$$r = \Phi \cdot \sigma \cdot N \cdot \varepsilon_{target} \cdot \varepsilon_{source} \cdot \varepsilon_{transp} \cdot \varepsilon_{det}$$

The first ionization energy of the elements

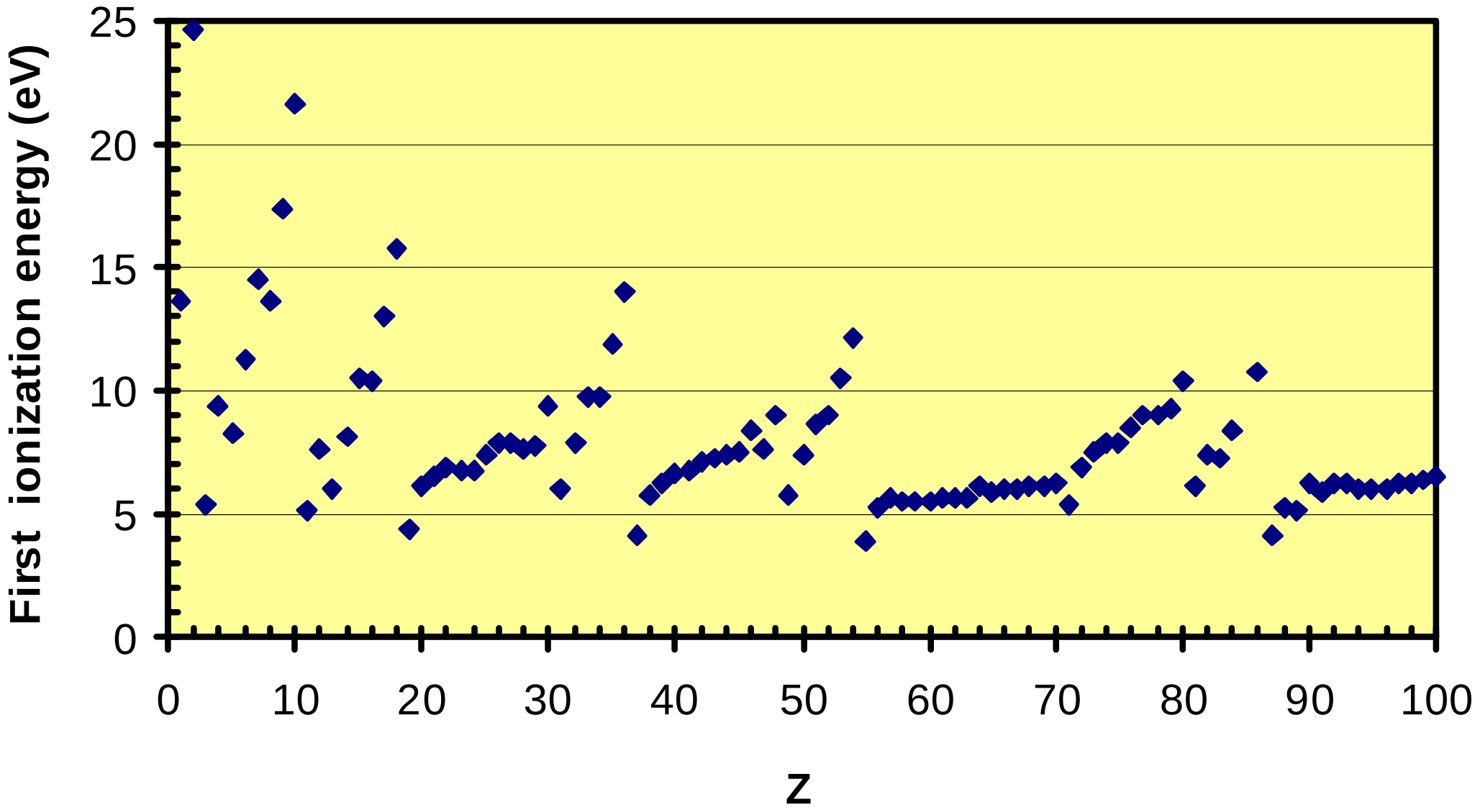

Positive surface ionization source

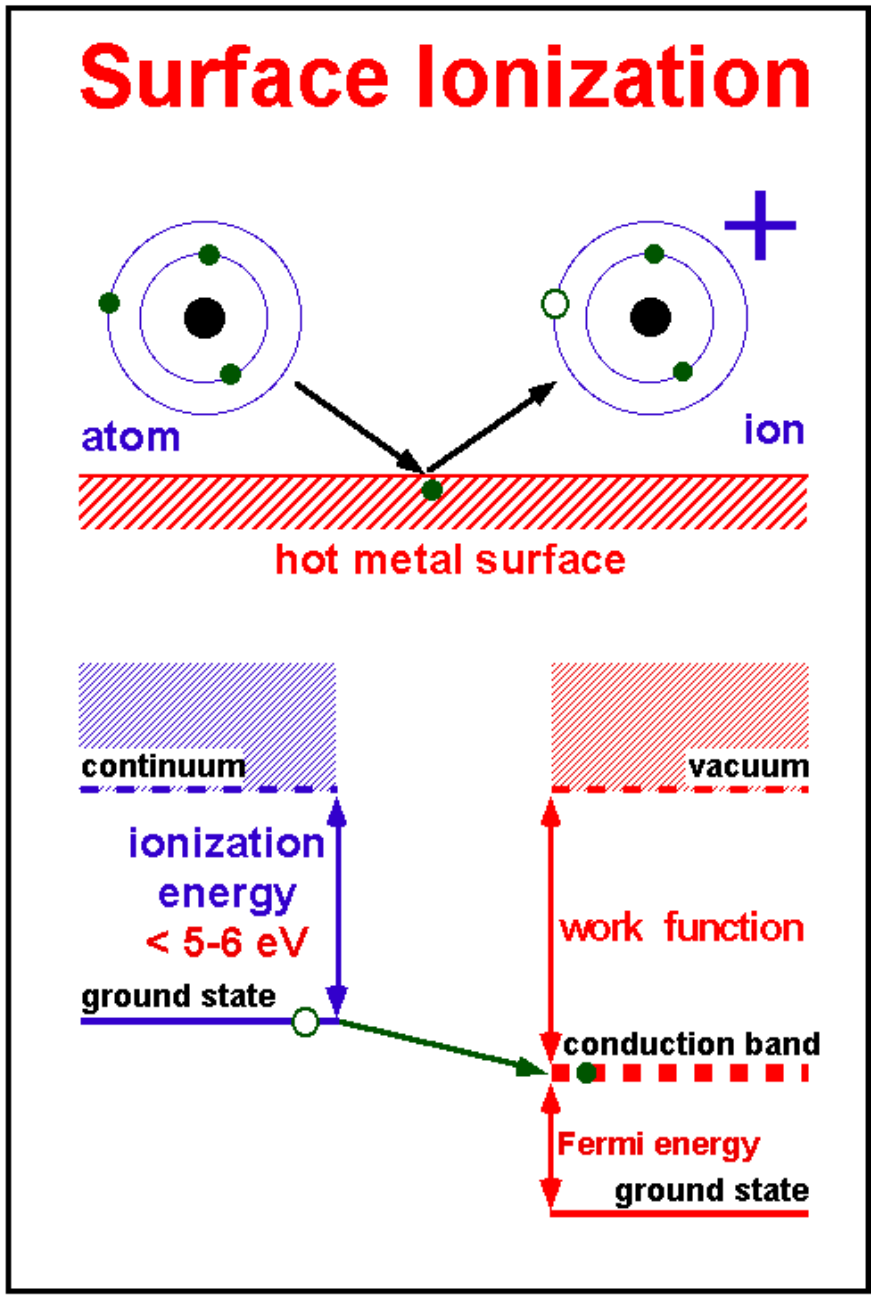

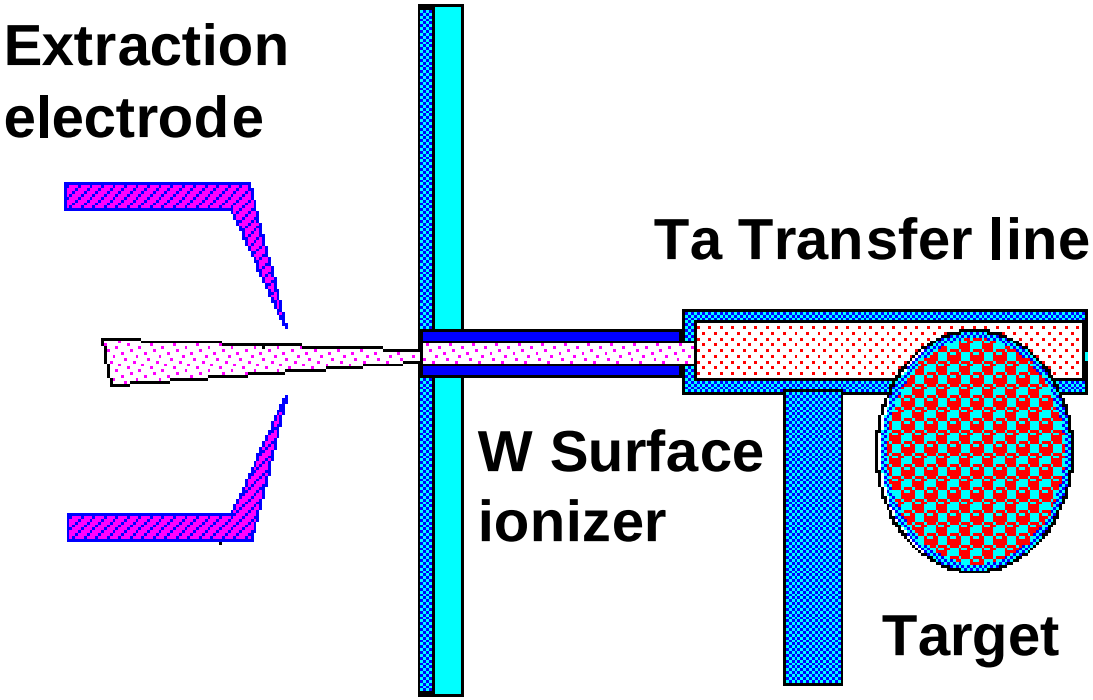

$$\alpha_s = g_+/g_0 \exp(-(IP - \Phi)/kT))$$

$$\varepsilon_s = \alpha_s / (1 + \alpha_s)$$

Saha-Langmuir equation

ε_s	surface ionization efficiency
Φ	work function of surface
IP	ionization potential of atom
g=2J+1	stat. factor (g_0=2, g_+=1 for alkalis)

Surface ionization versus thermal ionization

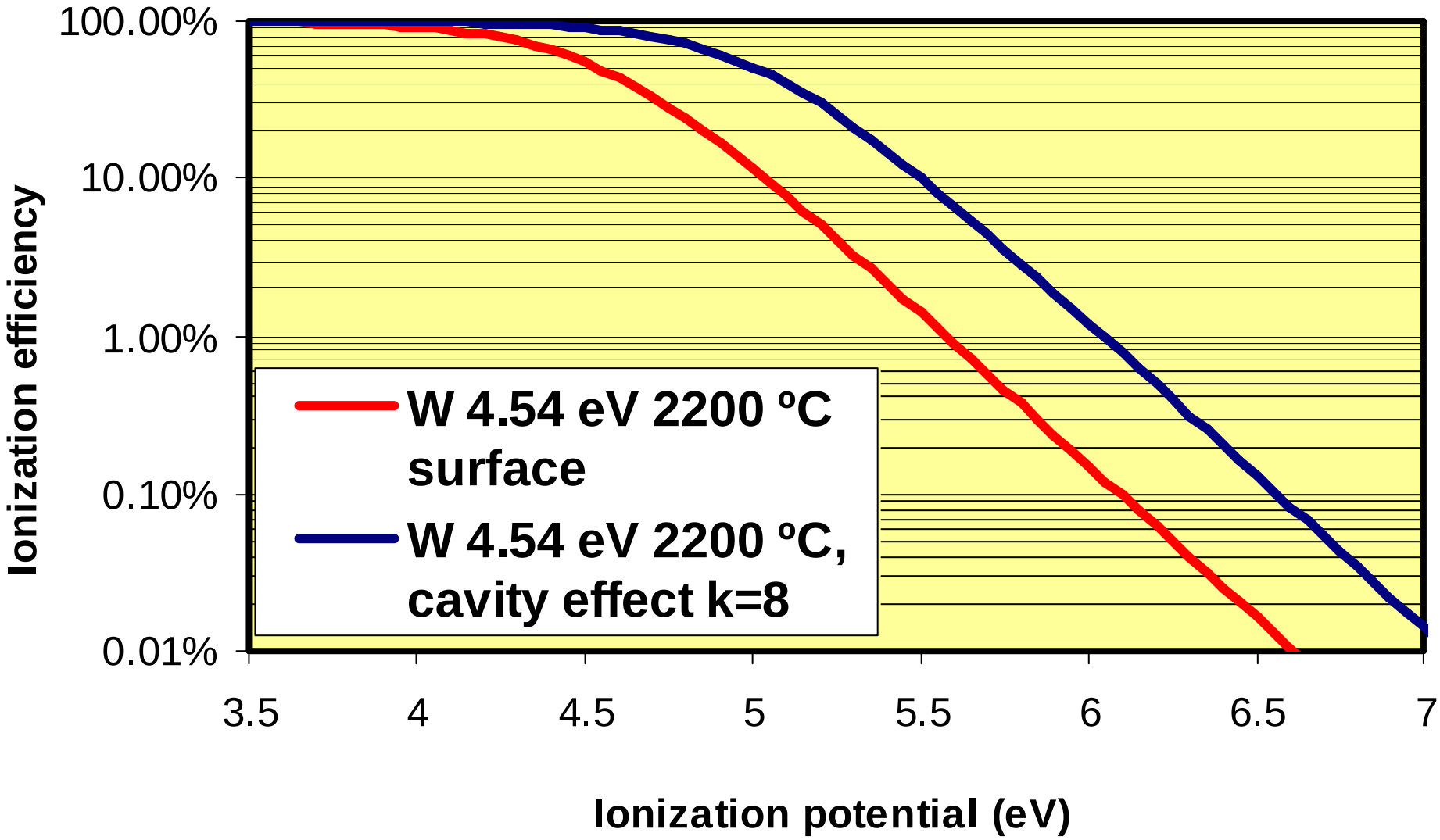

$$\varepsilon_{th} = 1/(1 + g_0/g_+/k \exp((IP - \Phi)/kT))$$

Thermal ionization efficiency in realistic ionizer cavity

R. Kirchner, Nucl. Instr. Meth. A292 (1987) 204.

Thermal ionization efficiency in realistic cavity

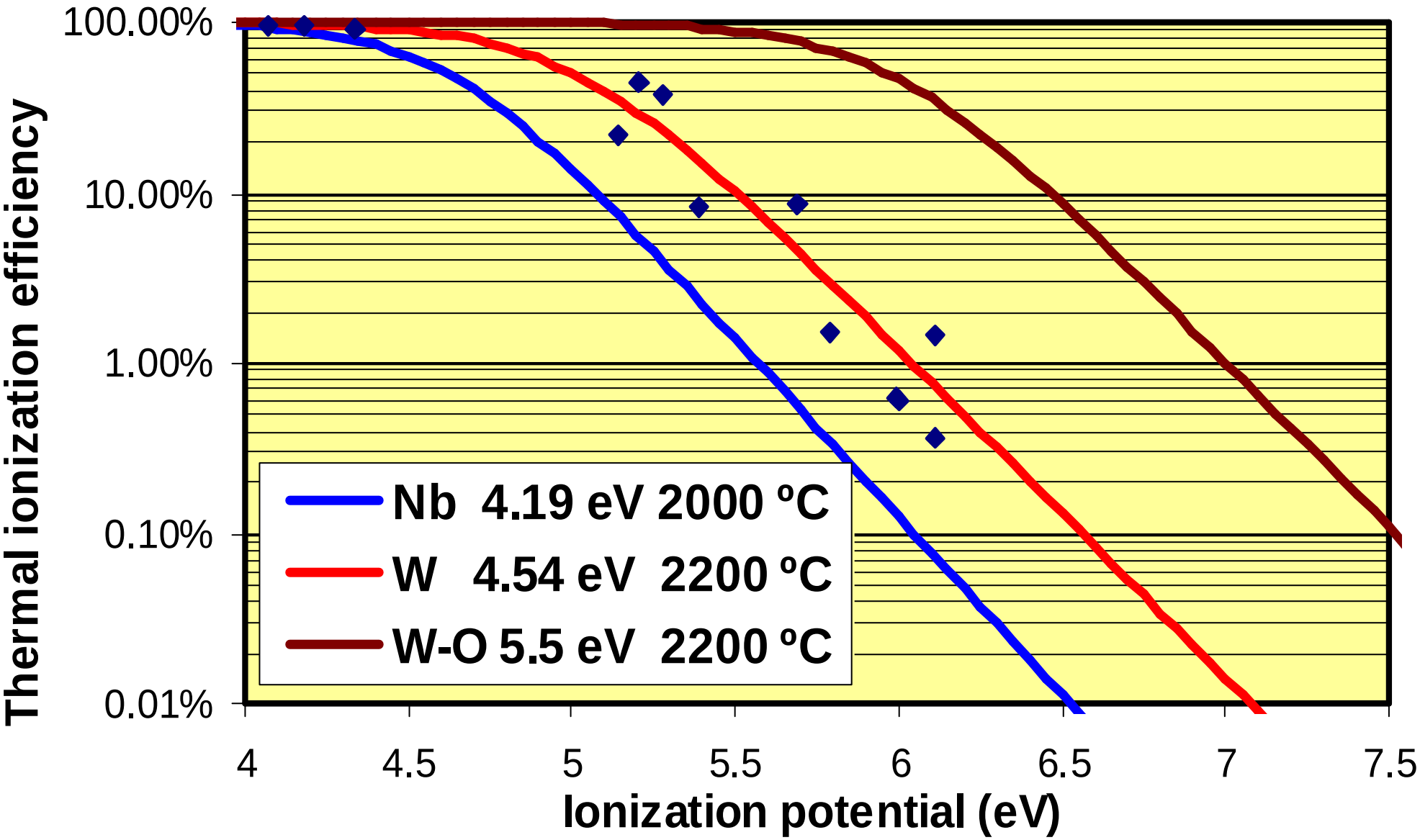

Watch out for surface contaminations!

Ionization potentials of the elements

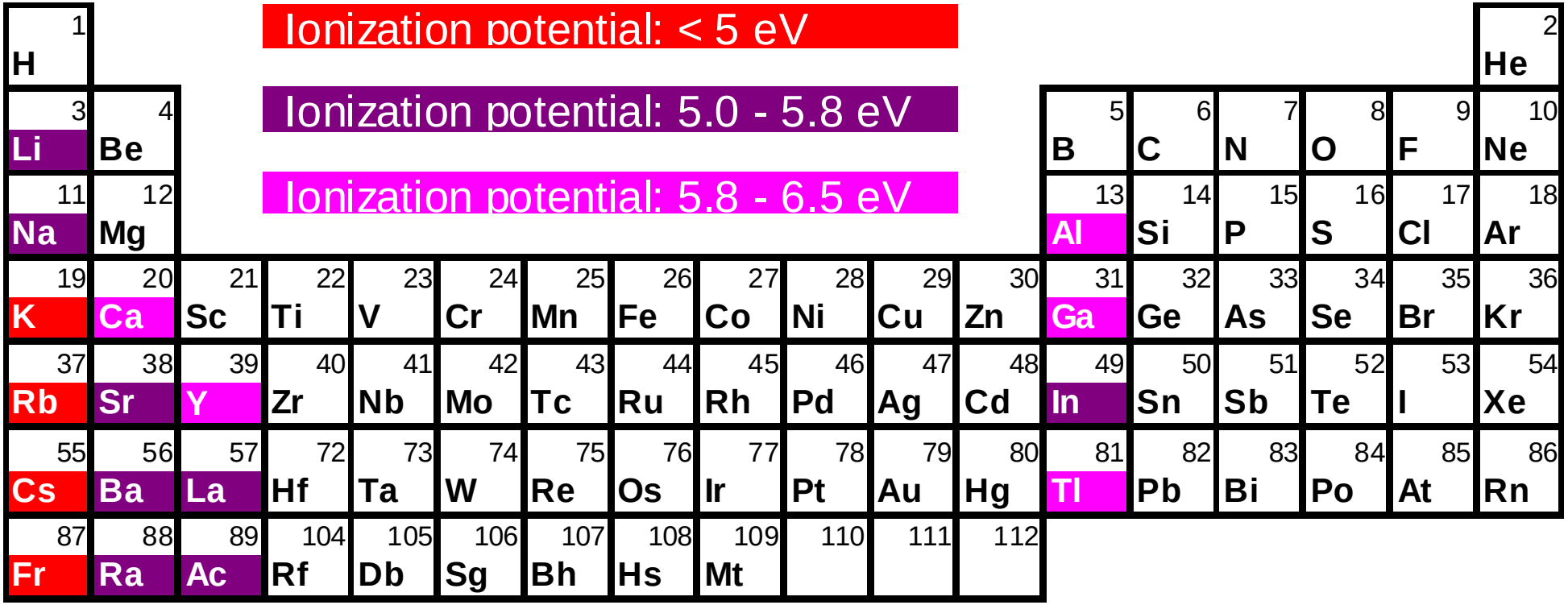

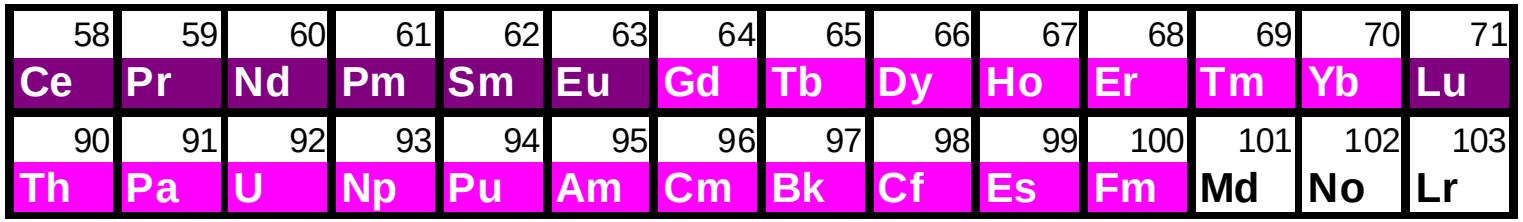

Ingredients of a plasma ion source

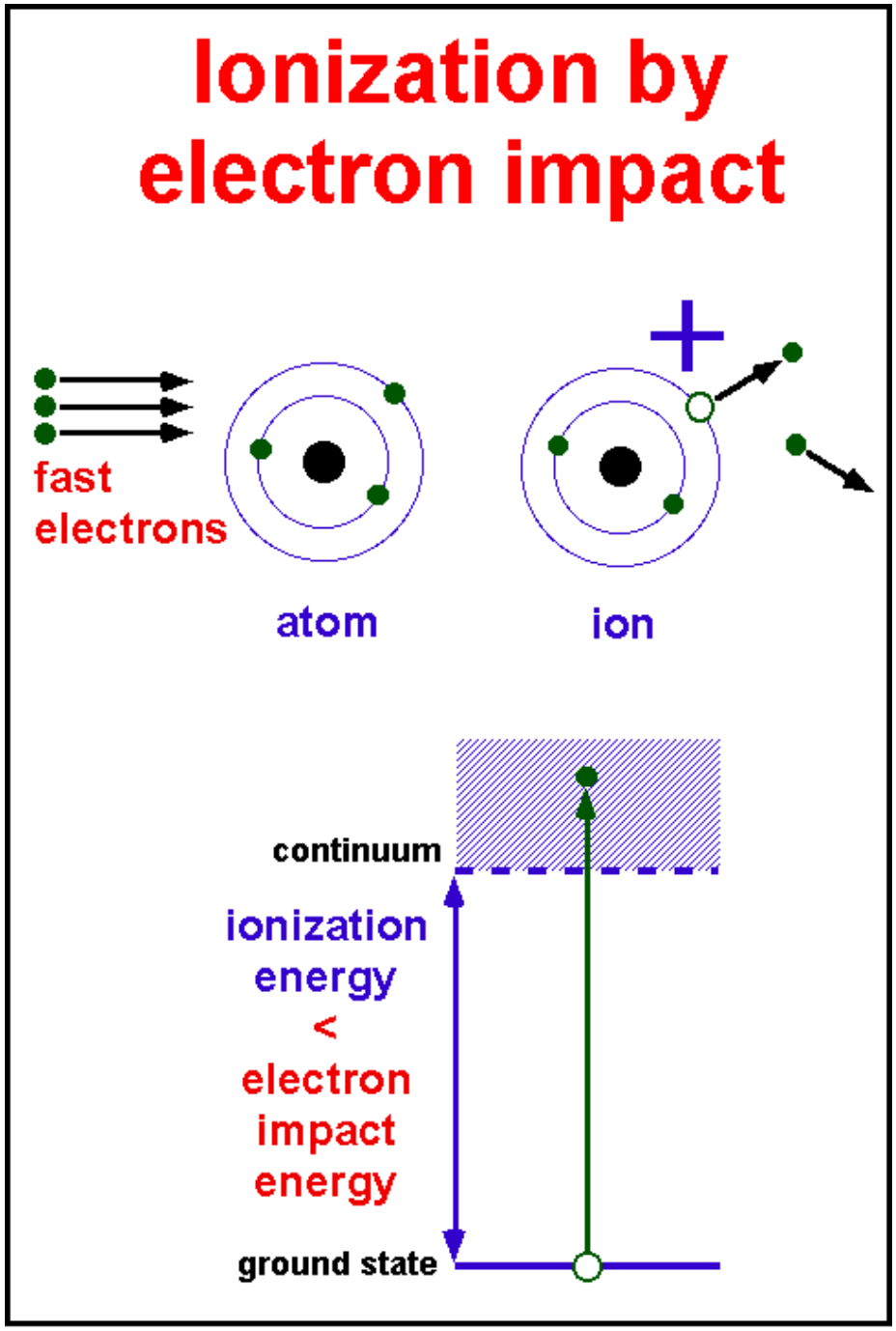

- Fast electrons:
  - A) Thermionic emission + accelerating field
  - B) RF heating
- Atom confinement: plasma chamber
- Electron "recycling": magnetic field
- Ion extraction system

$I[A] = A^* T[K]^2 \exp(-\Phi[eV]/kT[K])$

$A^* = 120\ A\ cm^{-2}\ K^{-2}$

$\nu_{cyc}[GHz] = 28\ B[T]$

$r[mm] = 0.35\ E_e[eV]^{1/2}/B[T]$

Ionization and neutralization

$X^0 + e^- \rightarrow X^+ + 2\ e^-$, $Q = -\ IP_1$

$X^0 + e^- \rightarrow X^{2+} + 3\ e^-$, $Q = -\ (IP_1 + IP_2)$

$X^0 + e^- \rightarrow X^{3+} + 4\ e^-$, $Q = -\ (IP_1 + IP_2 + IP_3)$

$X^+ + e^- \rightarrow X^{2+} + 2\ e^-$, $Q = -\ IP_2$

$X^+ + e^- \rightarrow X^0$, $Q = IP_1$ **Neutralization**

$X^0 + Y^+ \rightarrow X^+ + Y^0$, $Q = IP_Y - IP_X$ **Charge exchange**

Electron impact ionization cross-sections

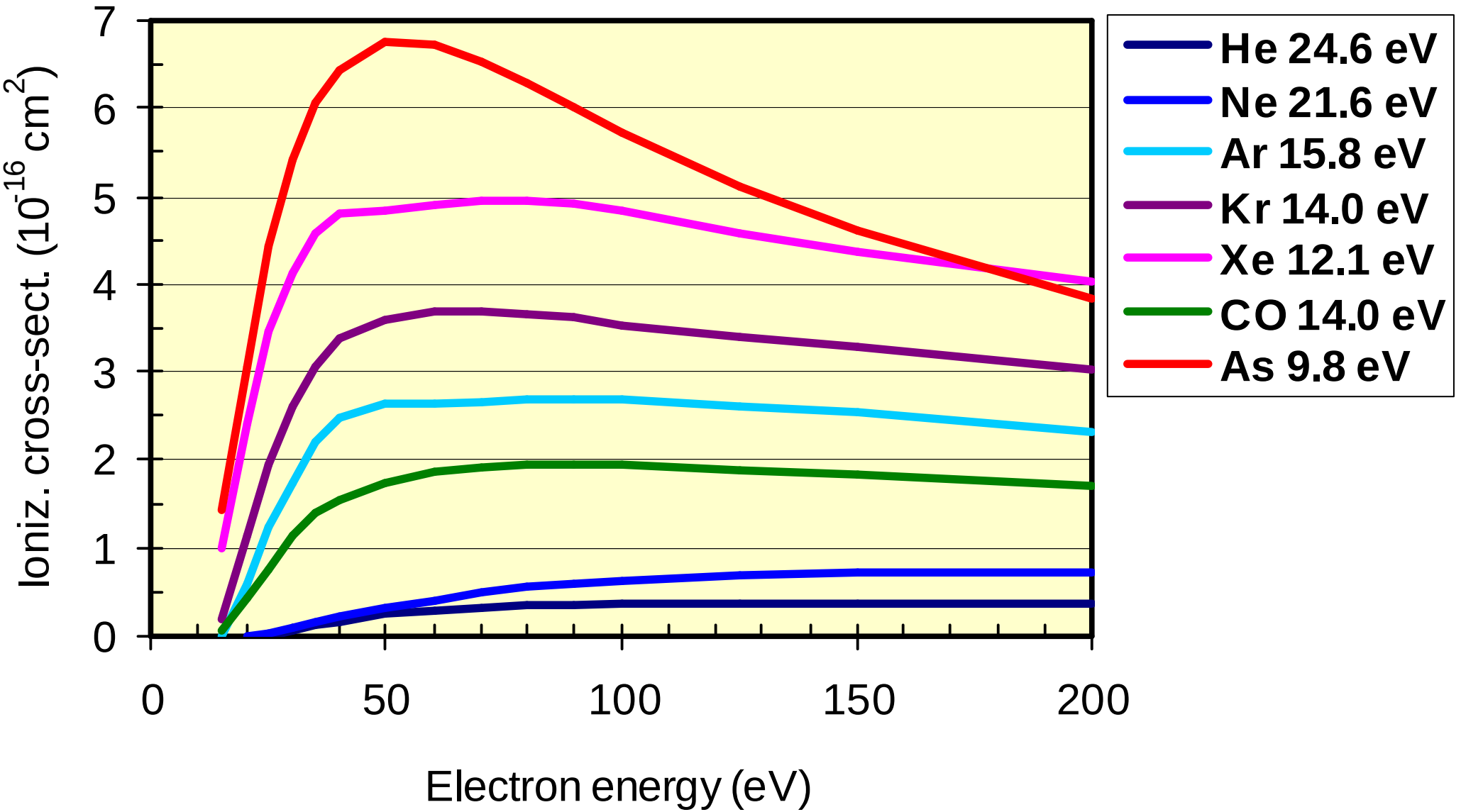

Forced Electron Beam Ion Arc Discharge (FEBIAD)

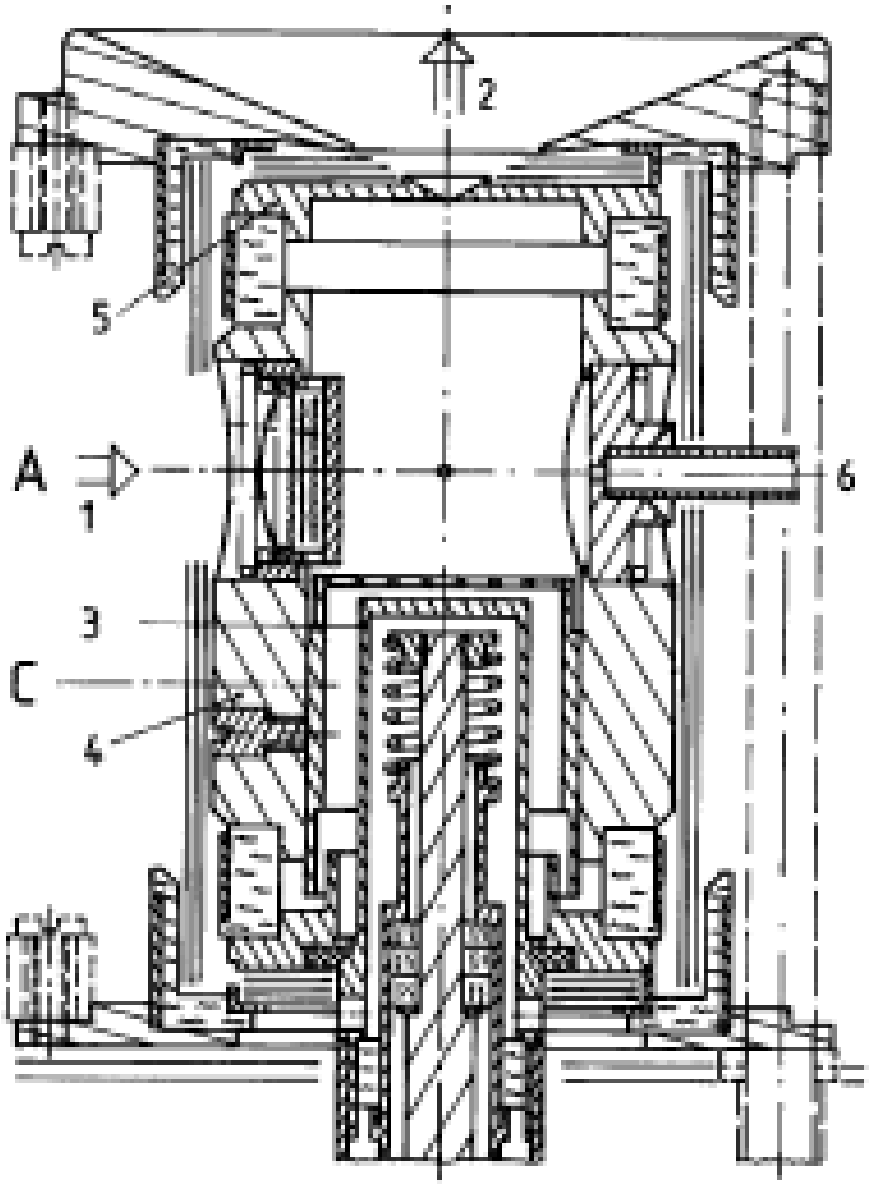

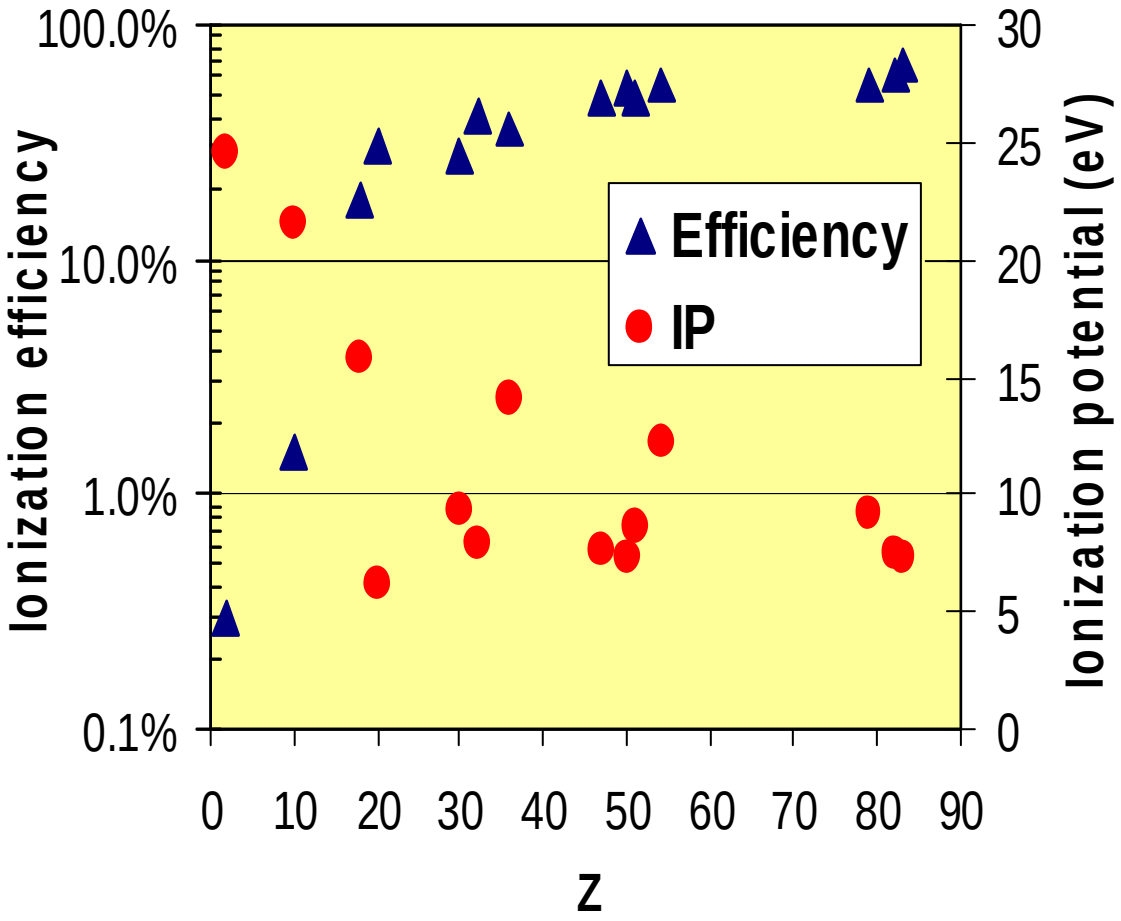

FEBIAD ion sources are excellent for heavier elements!

R. Kirchner, Rev. Sci. Instr. 67 (1996) 928.

ISOLDE “FEBIAD”

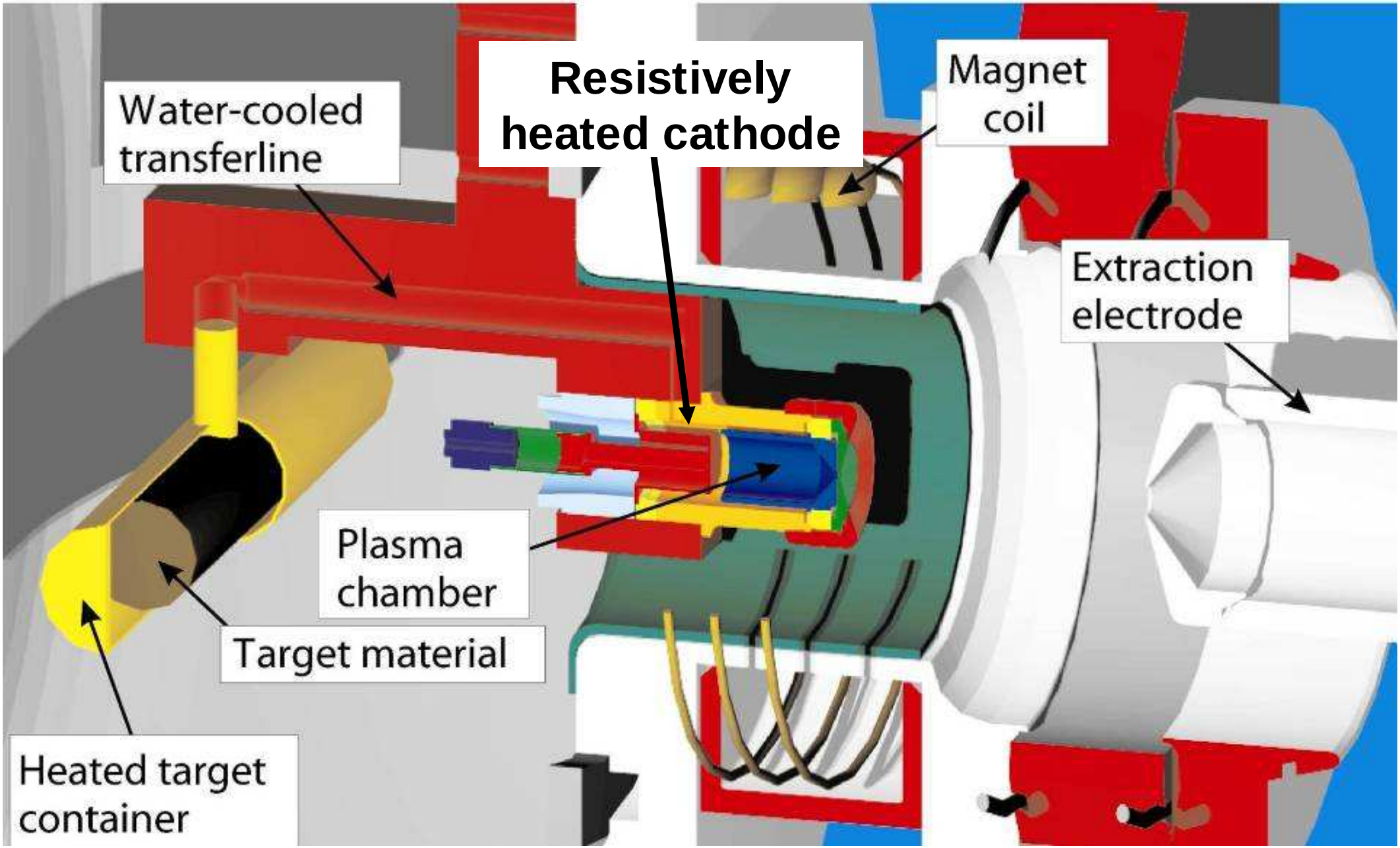

2001: $^{94\text{-}99}$Kr decay studied at ISOLDE

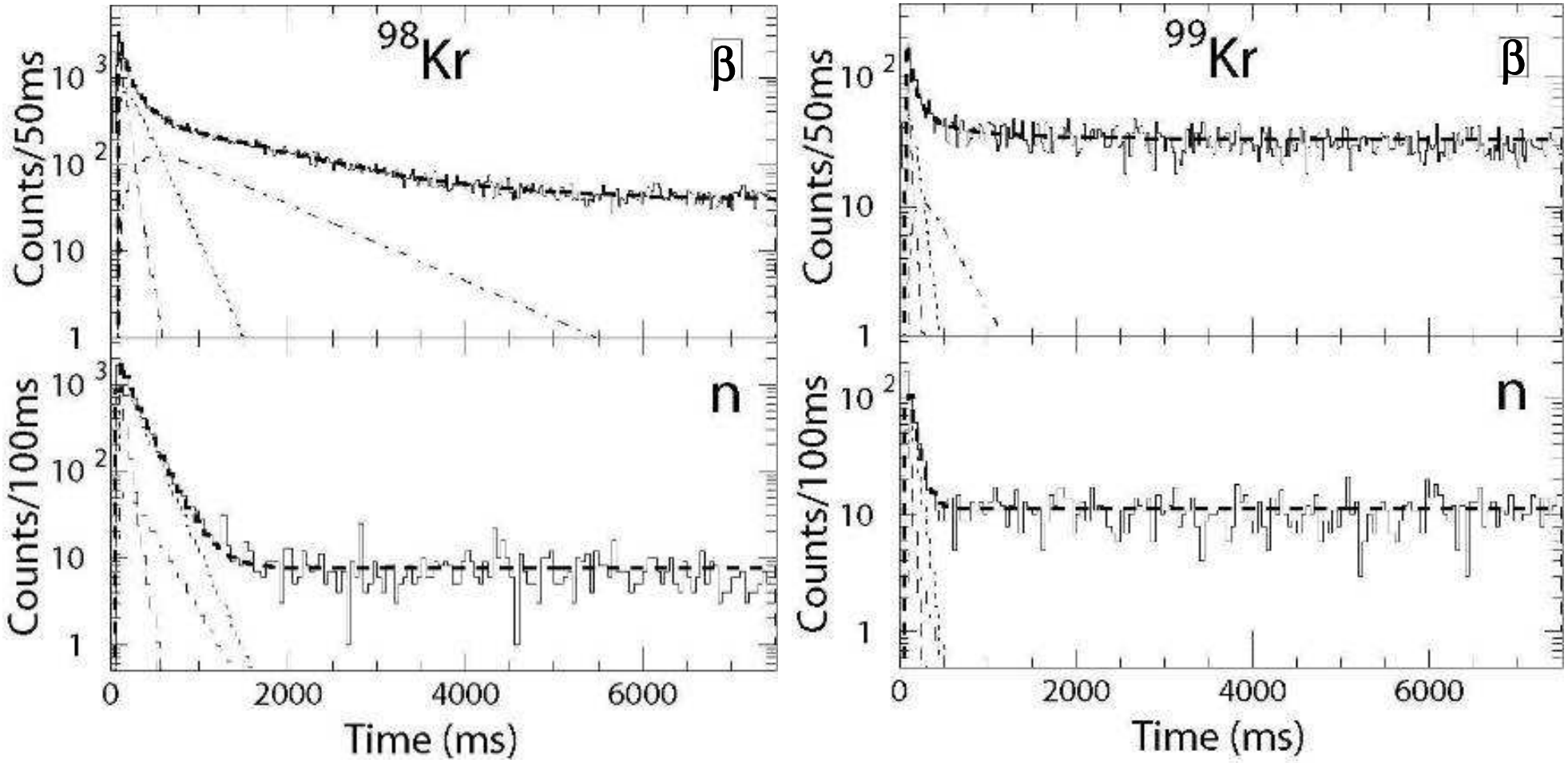

U.C. Bergmann et al., Nucl. Phys. A 714 (2003) 21.

Volatility of the elements

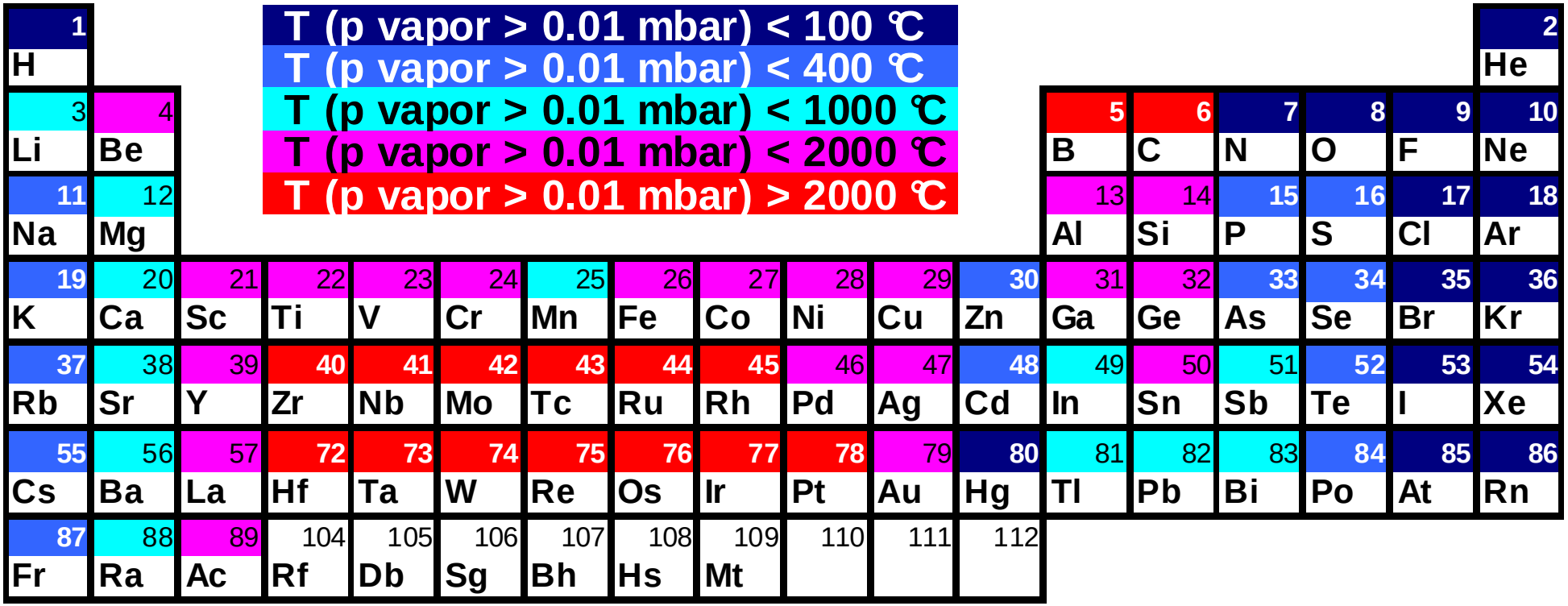

Electron Cyclotron Resonance Ion Source (ECRIS)

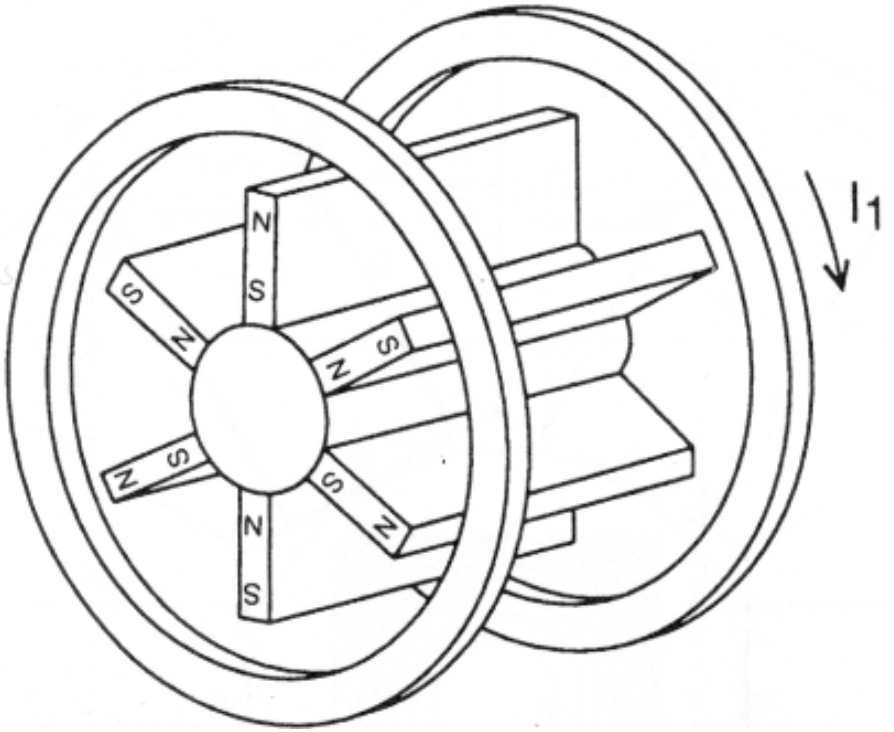

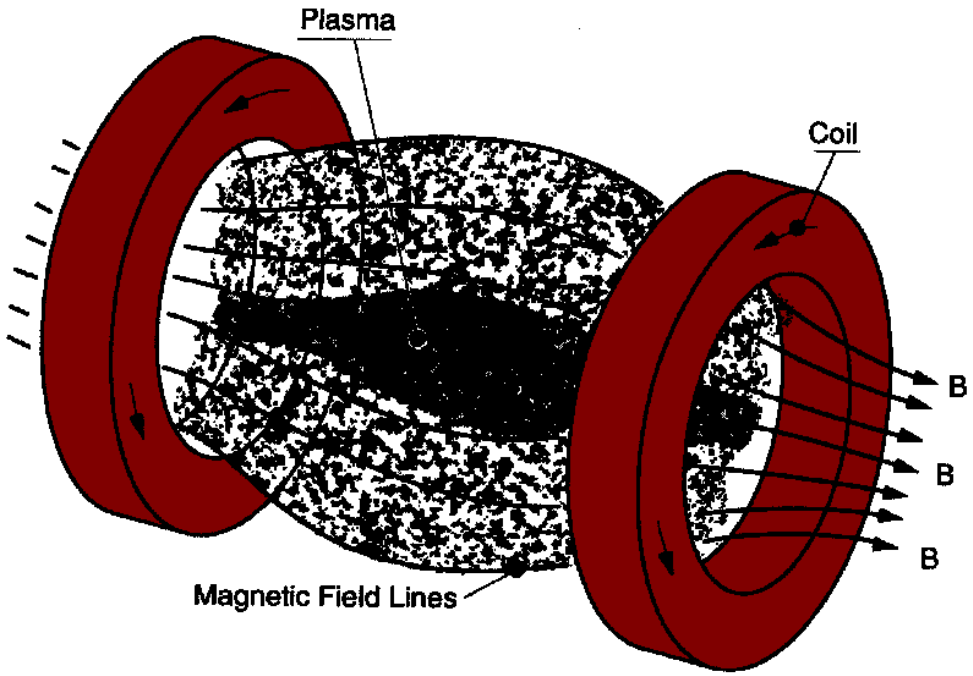

radial plasma confinement by magnetic multipole field

longitudinal plasma confinement by magnetic bottle effect (1+ ECRIS)
or minimum B configuration (n+ ECRIS)

plasma heating by RF (typically 2.45 – 30 GHz)

good efficiency for light elements (20% He^+, 50% C^+, O^+, Ar^+, 90% Xe^+)

R. Geller, Electron Cyclotron Resonance Ion Sources and ECR Plasmas, IOP, Bristol, 1996.

Laser Ionization

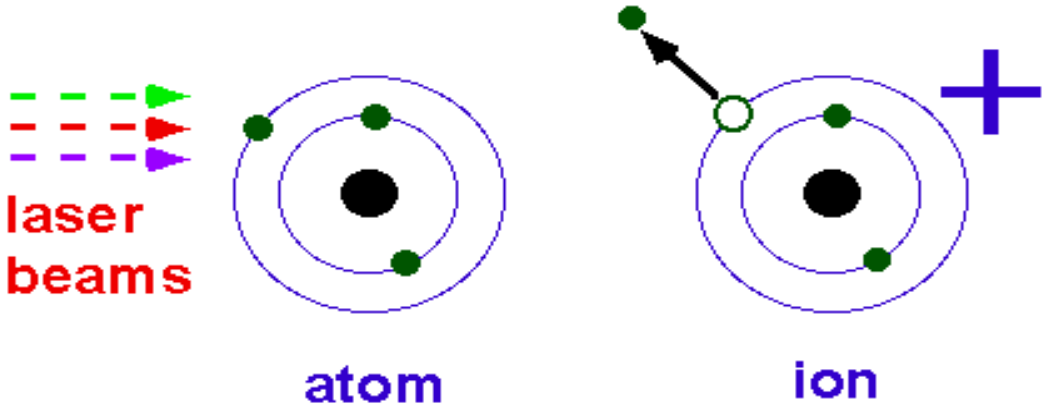

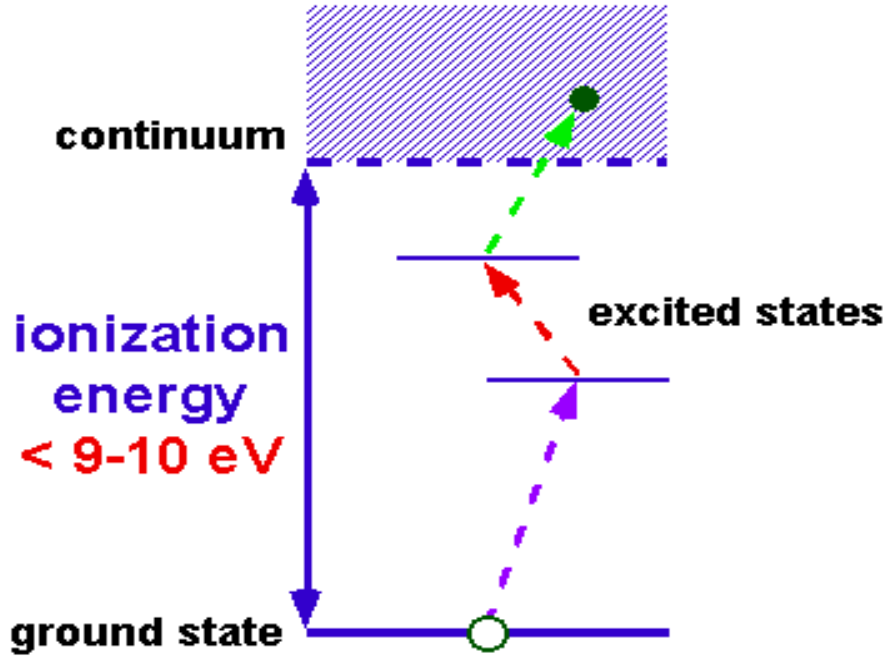

Resonance Ionization Laser Ion Source

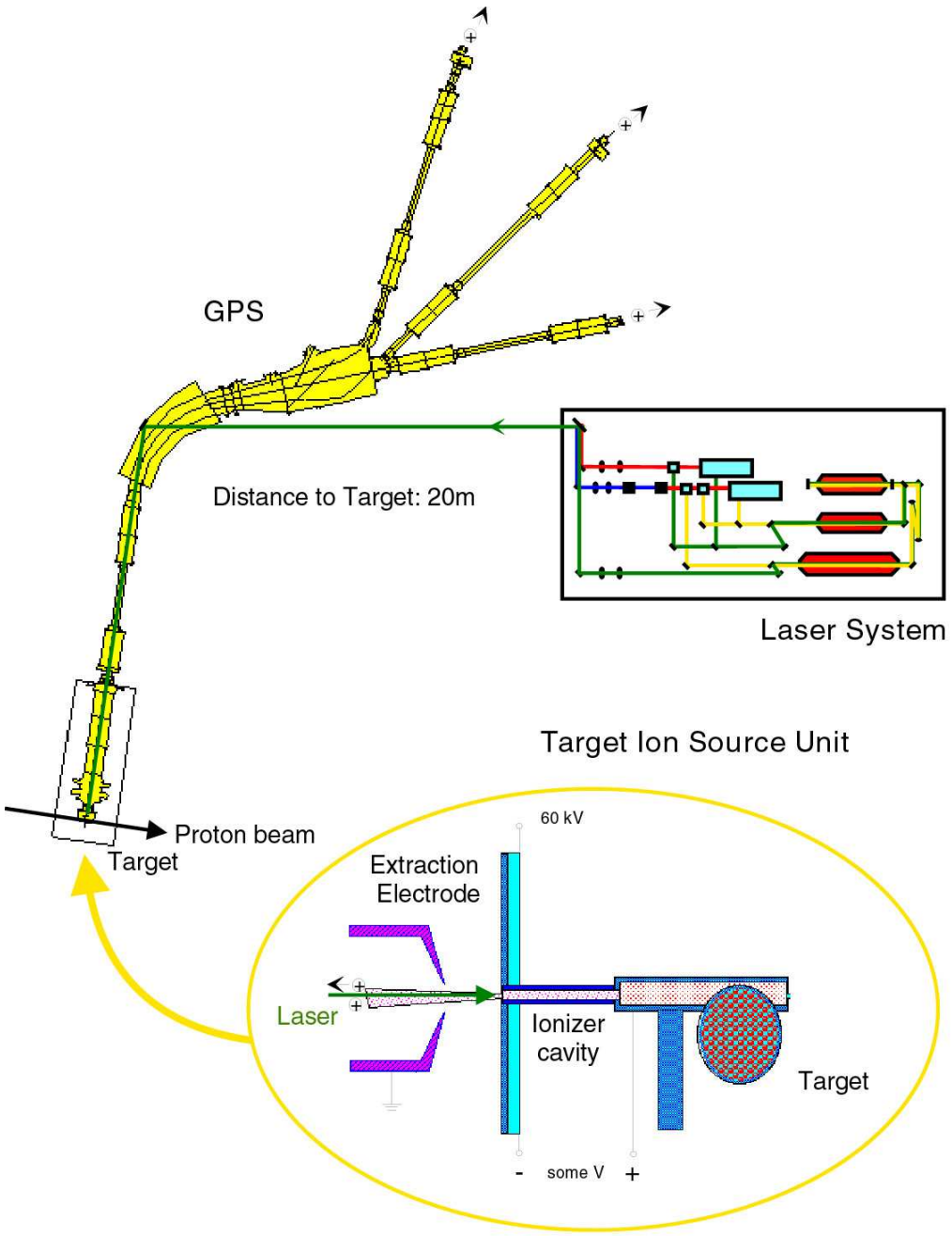

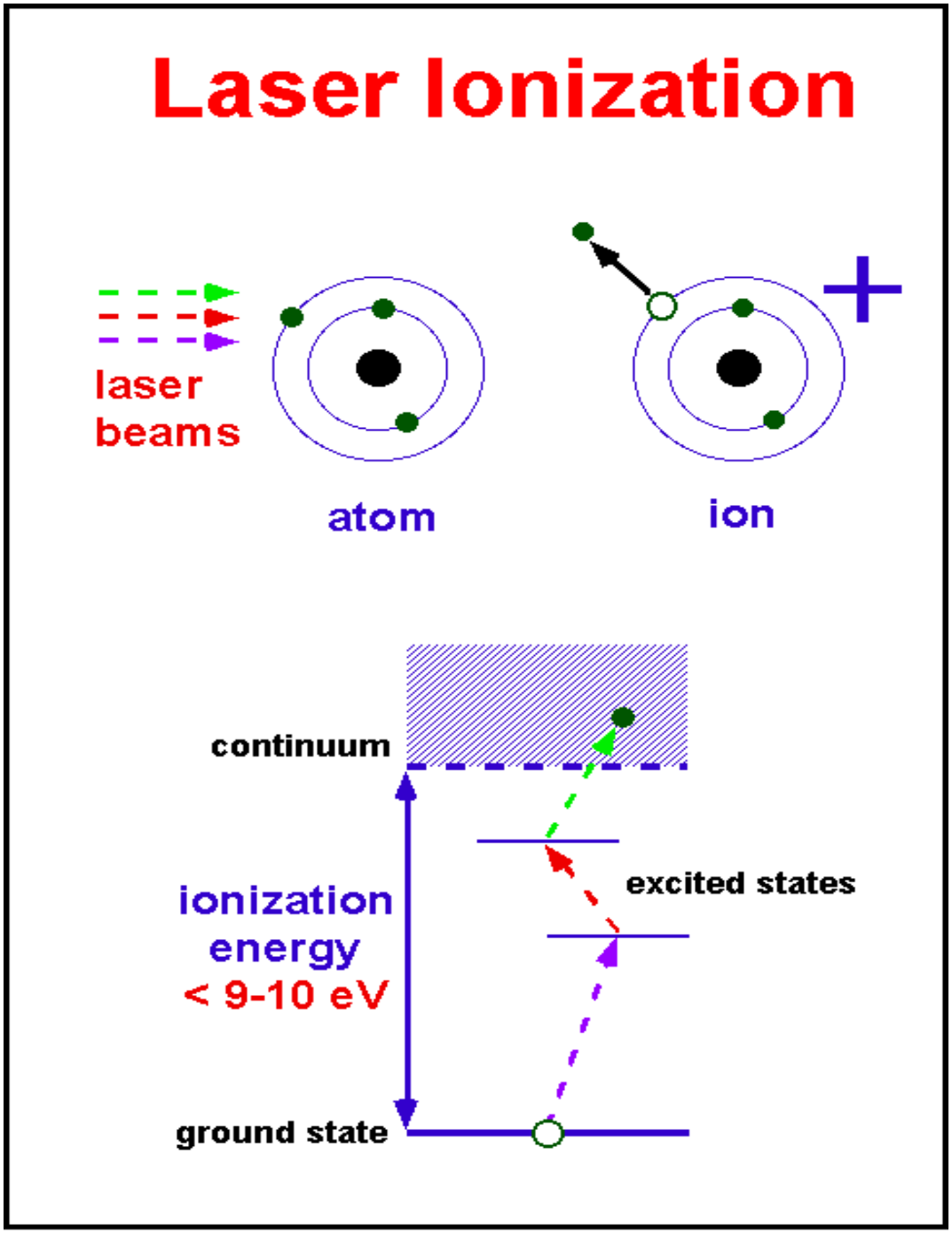

Ionization of Cu

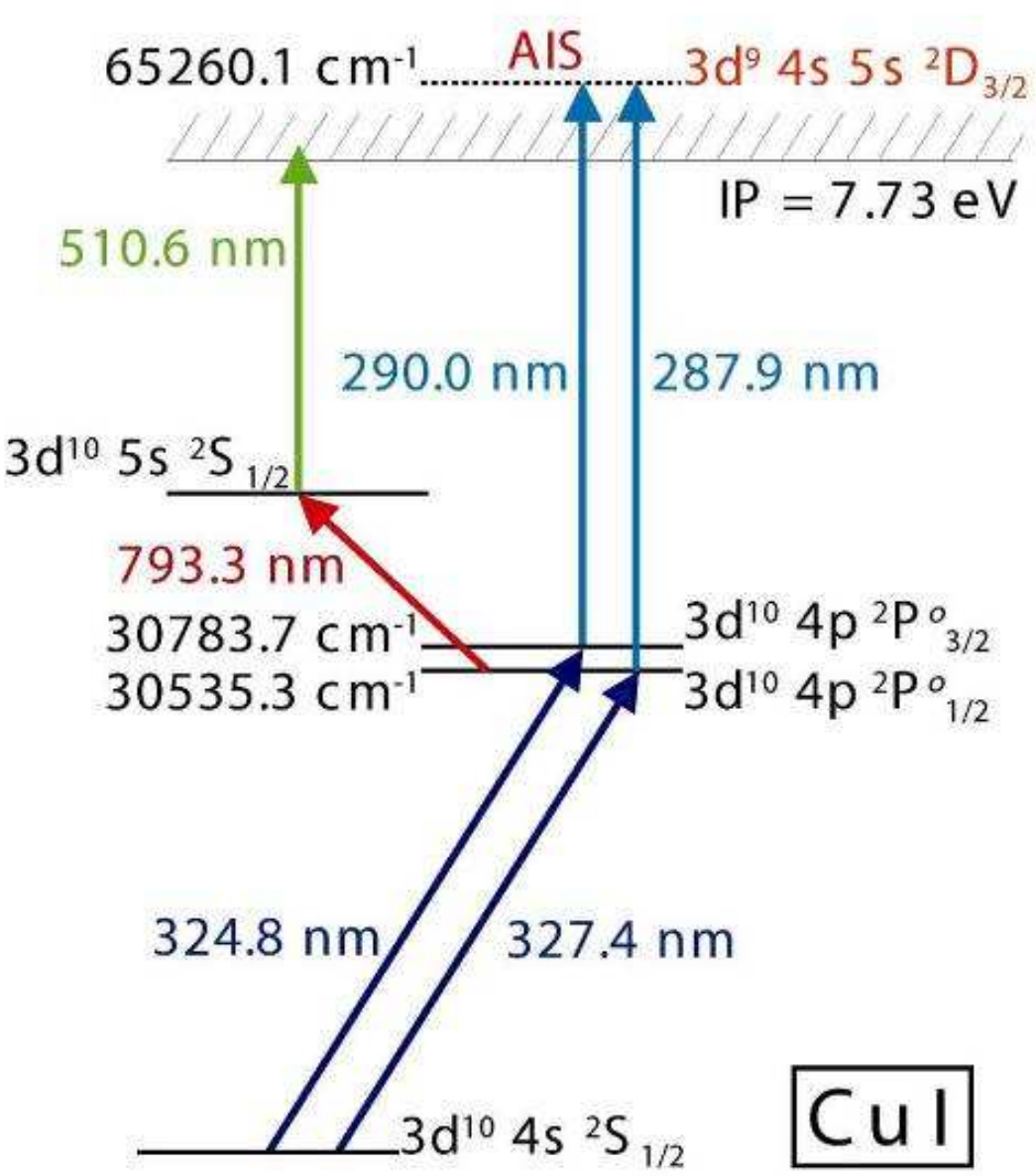

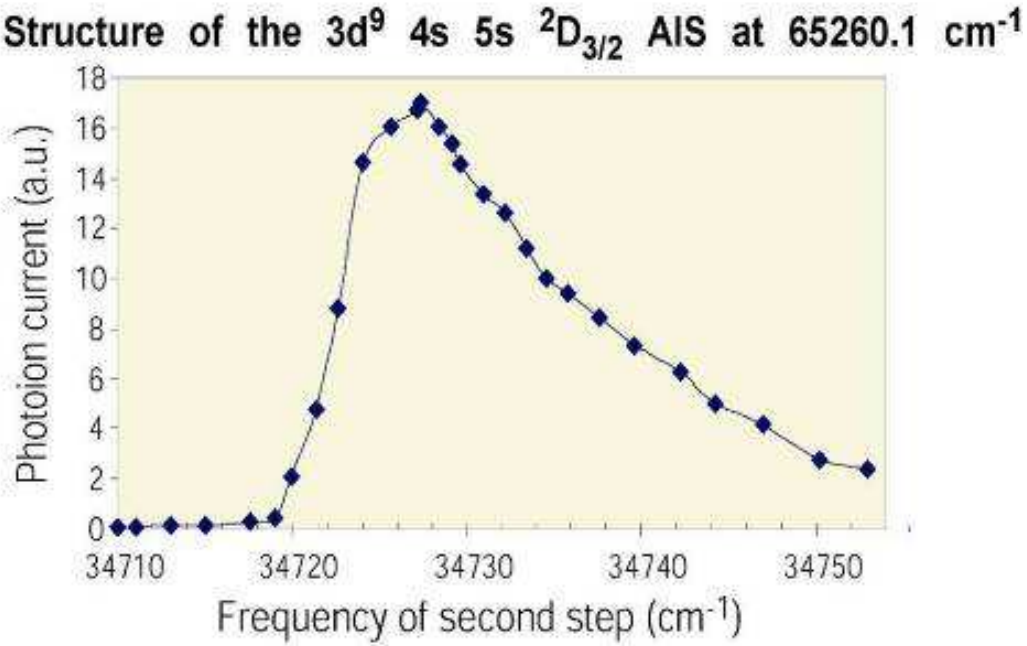

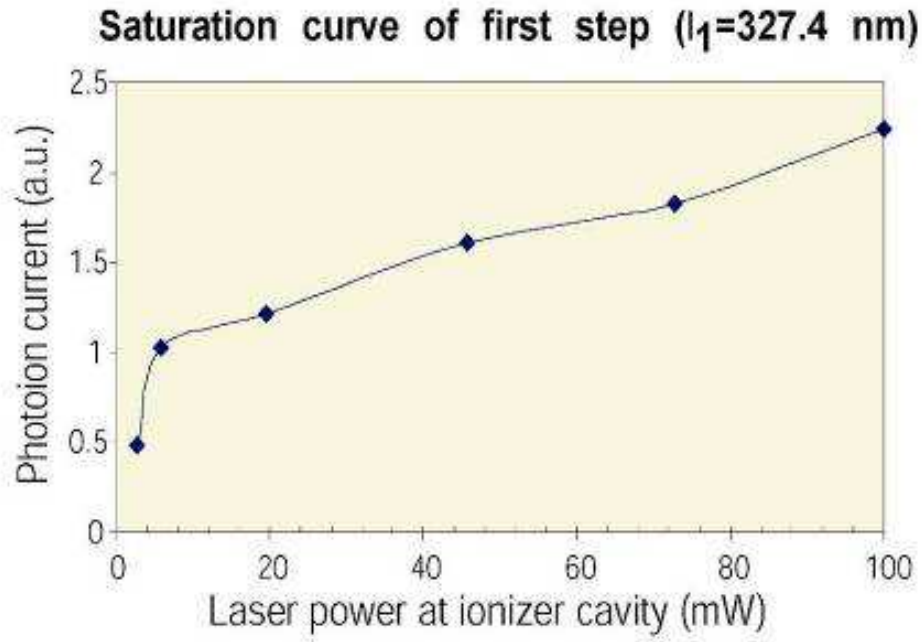

The laser system

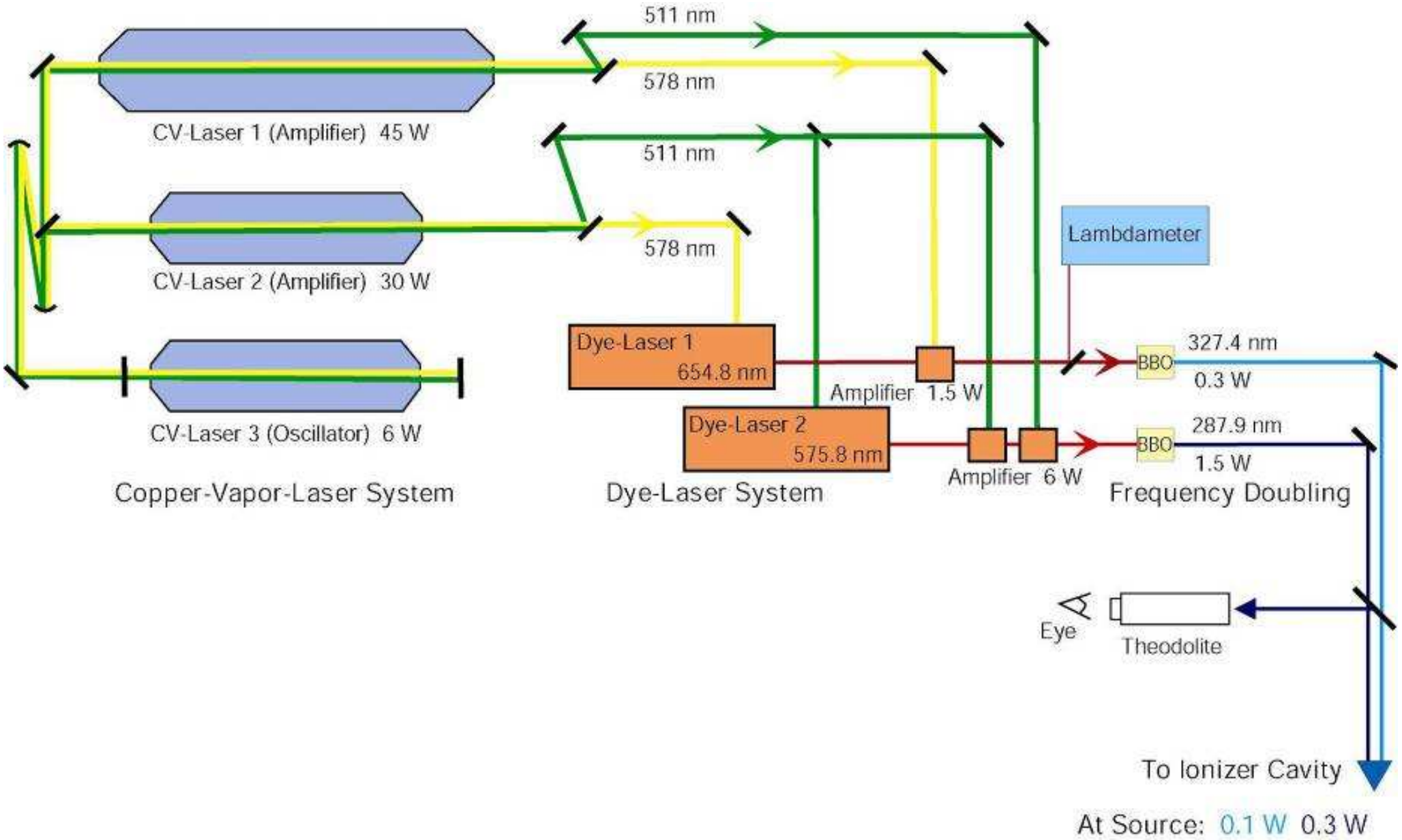

ISOL versus In-flight separation

- ^{76}Ge fragmentation at A1200 fragment separator (MSU)
- Ge detectors (80% and 120%) in close geometry
- 24 h data taking for ^{73}Cu

M. Huhta et al., Phys. Rev. C58 (1998) 3187.

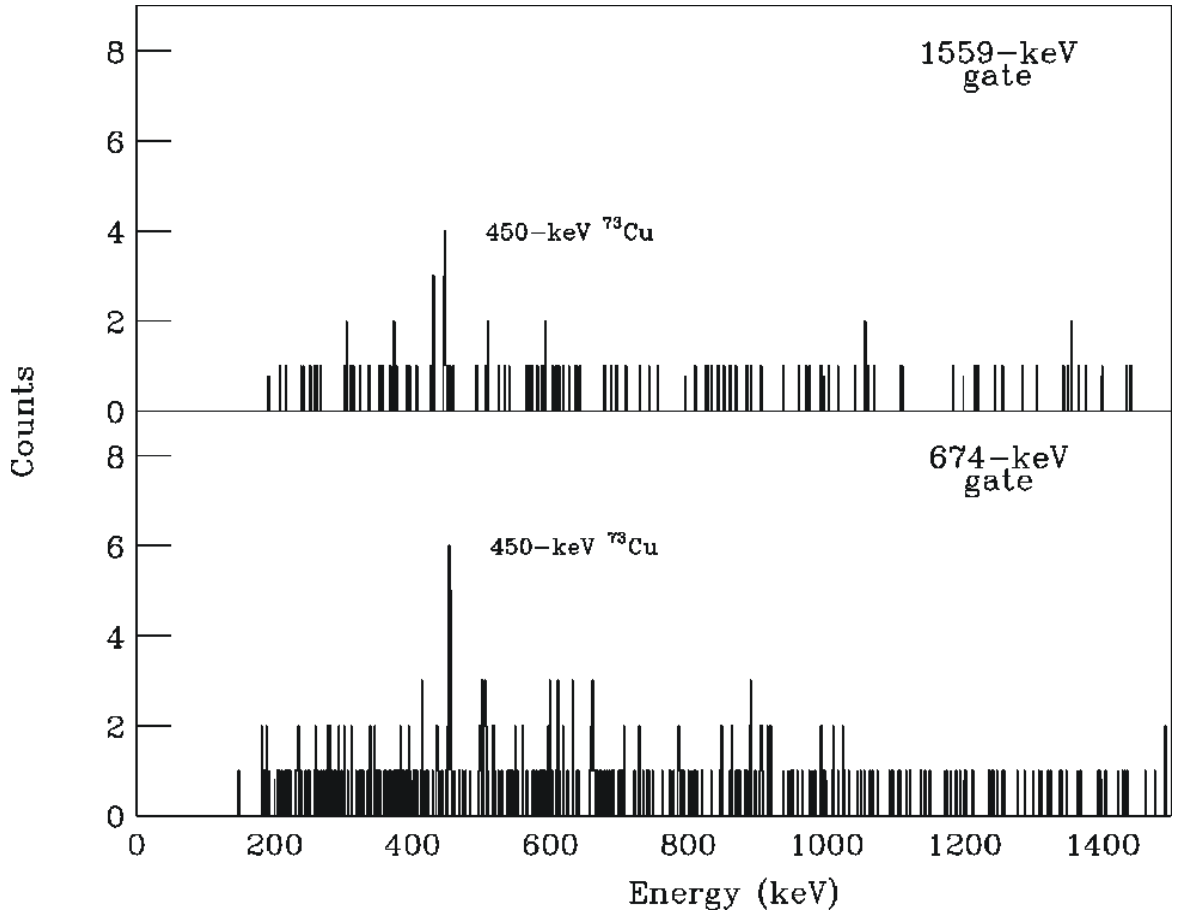

ISOL versus In-flight separation

- **ISOLDE: 50 g/cm^2 UC$_x$/graphite target plus RILIS**
- **Ge detectors (75% and 64%) in close geometry**
- **20 min data taking for ^{73}Cu**

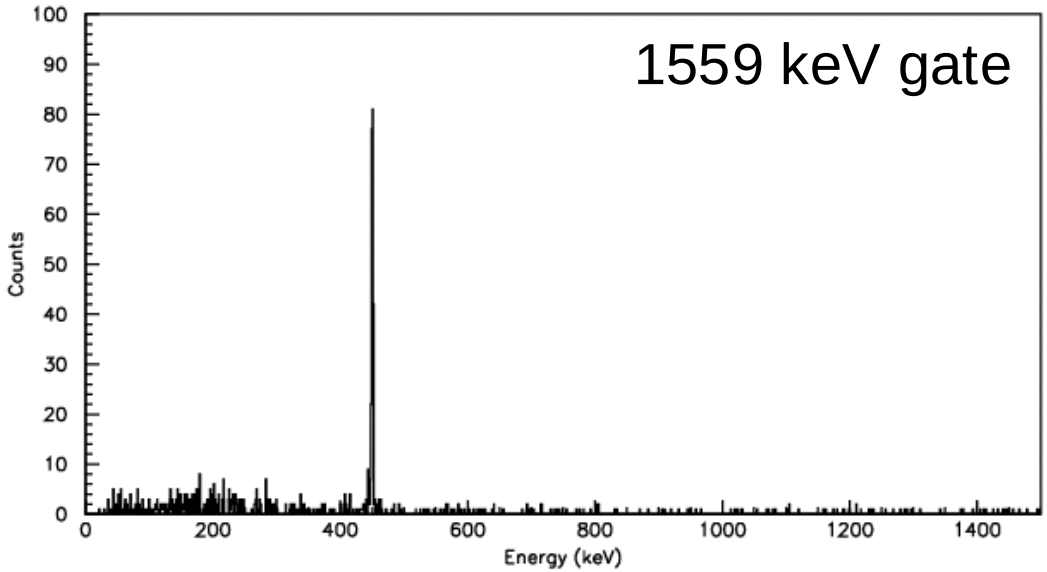

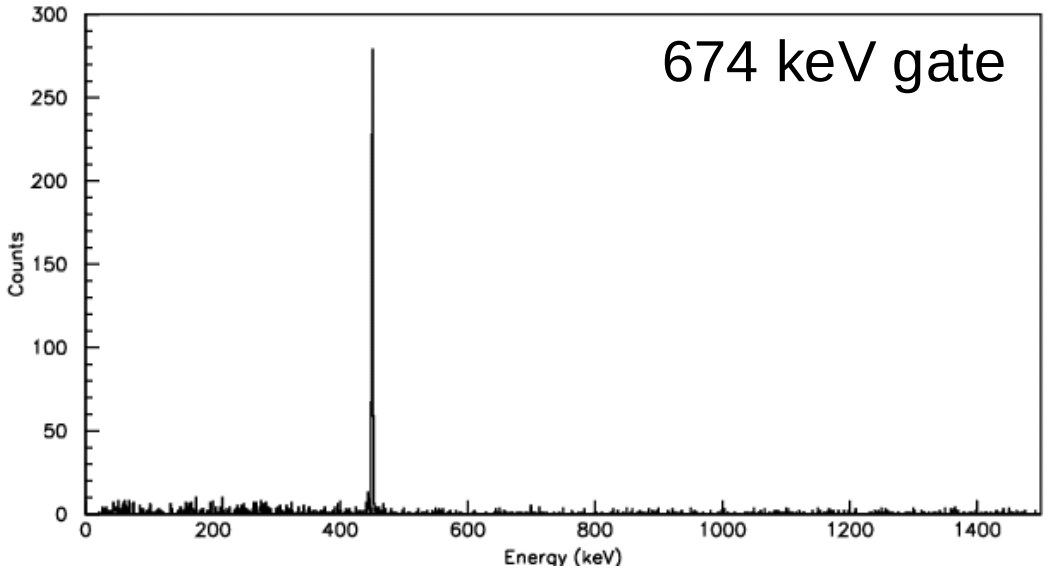

Neutron-rich Mn isotopes from UC_x/graphite target

M. Hannawald et al., Phys. Rev. Lett. 82 (1999) 1391.

^{67}Cu for nuclear solid state physics

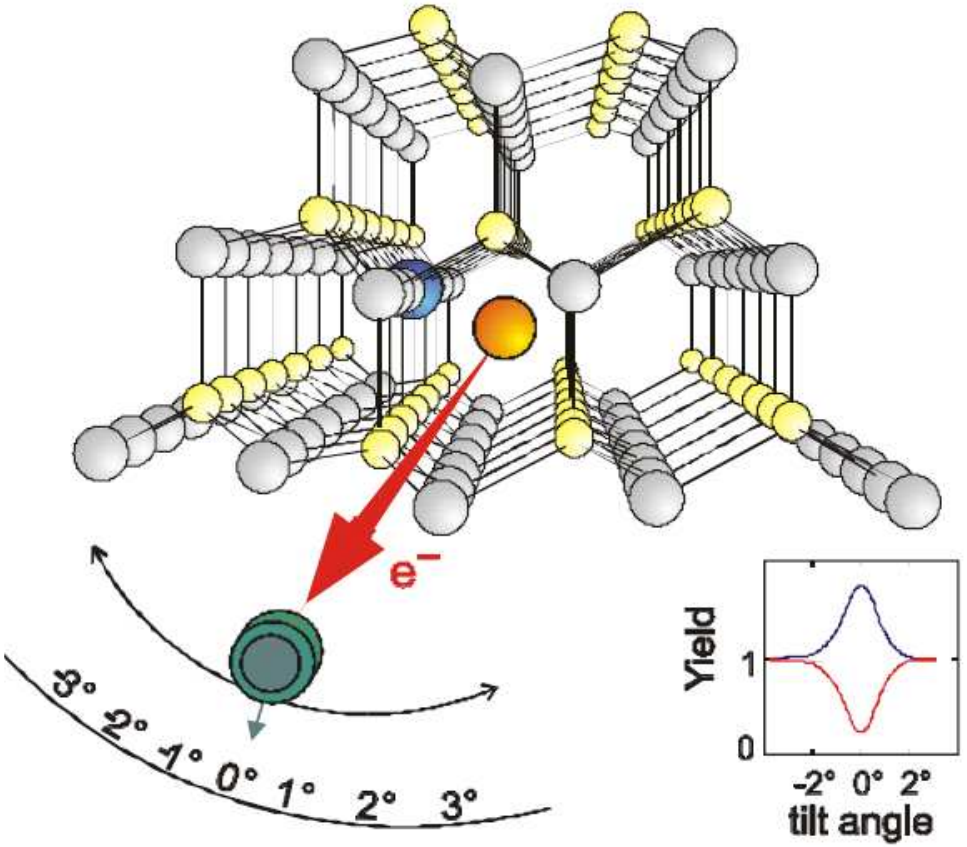

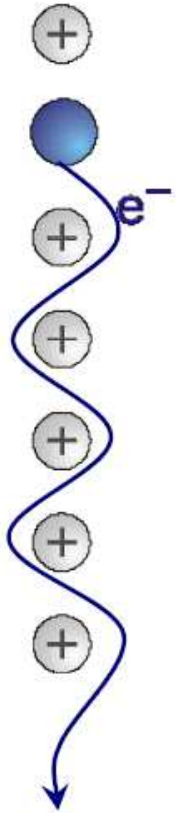

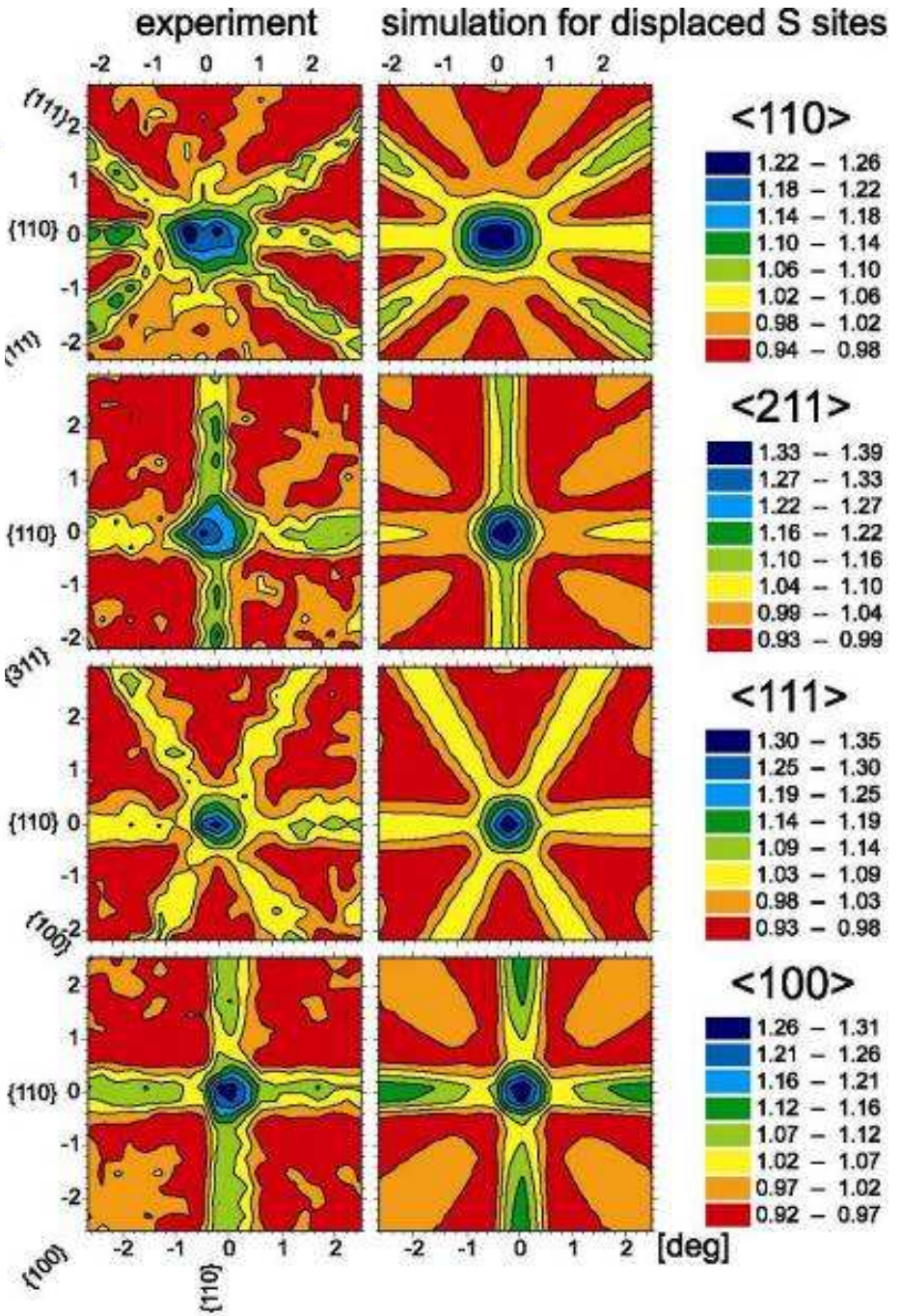

- **Lattice location of Cu in Si studied by emission channeling**
- **5 samples with each 5 min implantation of ^{67}Cu (ca. 100 ppm doping)**

U. Wahl et al., Phys. Rev. Lett. 84 (2000) 1495.

RILIS Laser setup

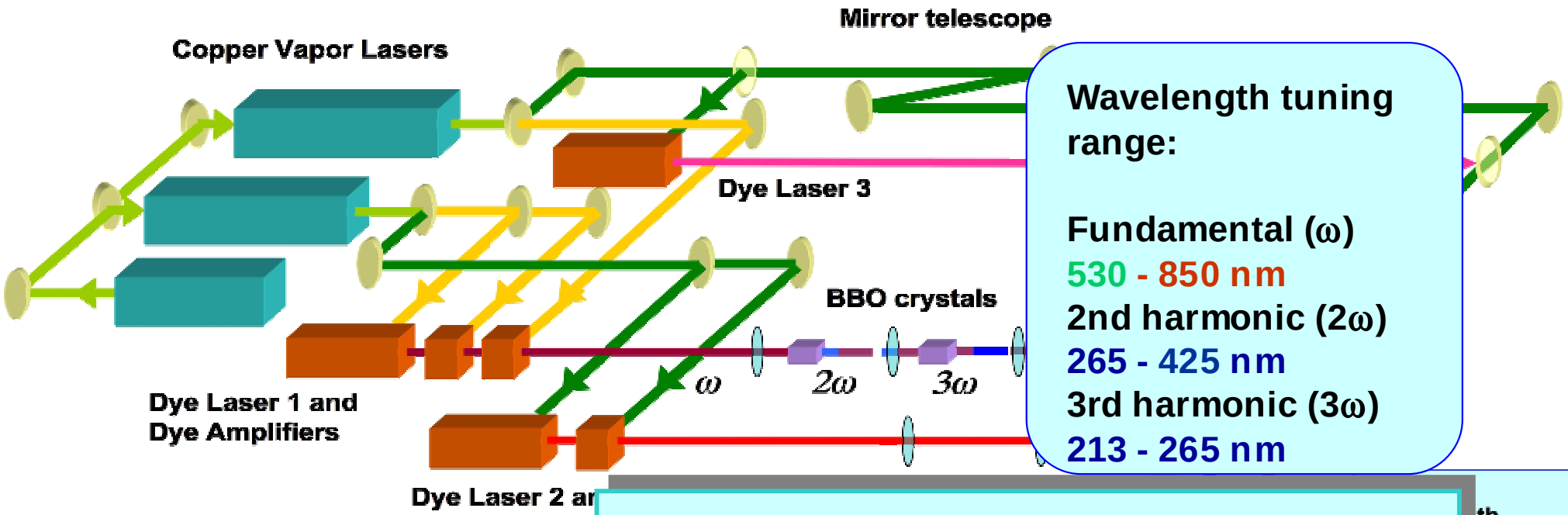

Wavelength tuning range:

Fundamental (ω)
530 - 850 nm
2nd harmonic (2ω)
265 - 425 nm
3rd harmonic (3ω)
213 - 265 nm

Lasers: f_{rep} = 11.000 Hz, t_{pulse} = 15 ns

3 Copper Vapor Tubes - $P_{Cu}^{total} \leq 80\ W$

2-3 Dye Lasers with Amplifiers - $P_{dye} \leq 8\ W$

Nonlinear Crystals BBO - $P_{2\omega} \leq 2\ W$

$P_{3\omega} \leq 0.2\ W$

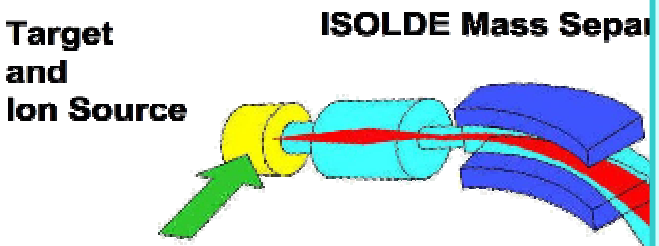

Proton Beam

0.6 GeV, 1 GeV, 1.4 GeV,
$3 \cdot 10^{13}$ pps
2.4 ms pulse length
1.2 s period

Elements ionized with CVL pumped dye lasers

elements ionized with ISOLDE RILIS

tested ionization scheme

possible ionization scheme (untested)

1 H																	2 He
3 Li	4 Be											5 B	6 C	7 N	8 O	9 F	10 Ne
11 Na	12 Mg											13 Al	14 Si	15 P	16 S	17 Cl	18 Ar
19 K	20 Ca	21 Sc	22 Ti	23 V	24 Cr	25 Mn	26 Fe	27 Co	28 Ni	29 Cu	30 Zn	31 Ga	32 Ge	33 As	34 Se	35 Br	36 Kr
37 Rb	38 Sr	39 Y	40 Zr	41 Nb	42 Mo	43 Tc	44 Ru	45 Rh	46 Pd	47 Ag	48 Cd	49 In	50 Sn	51 Sb	52 Te	53 I	54 Xe
55 Cs	56 Ba	57 La	72 Hf	73 Ta	74 W	75 Re	76 Os	77 Ir	78 Pt	79 Au	80 Hg	81 Tl	82 Pb	83 Bi	84 Po	85 At	86 Rn
87 Fr	88 Ra	89 Ac	104 Rf	105 Db	106 Sg	107 Bh	108 Hs	109 Mt	110	111	112						

58 Ce	59 Pr	60 Nd	61 Pm	62 Sm	63 Eu	64 Gd	65 Tb	66 Dy	67 Ho	68 Er	69 Tm	70 Yb	71 Lu
90 Th	91 Pa	92 U	93 Np	94 Pu	95 Am	96 Cm	97 Bk	98 Cf	99 Es	100 Fm	101 Md	102 No	103 Lr

Isomer separation

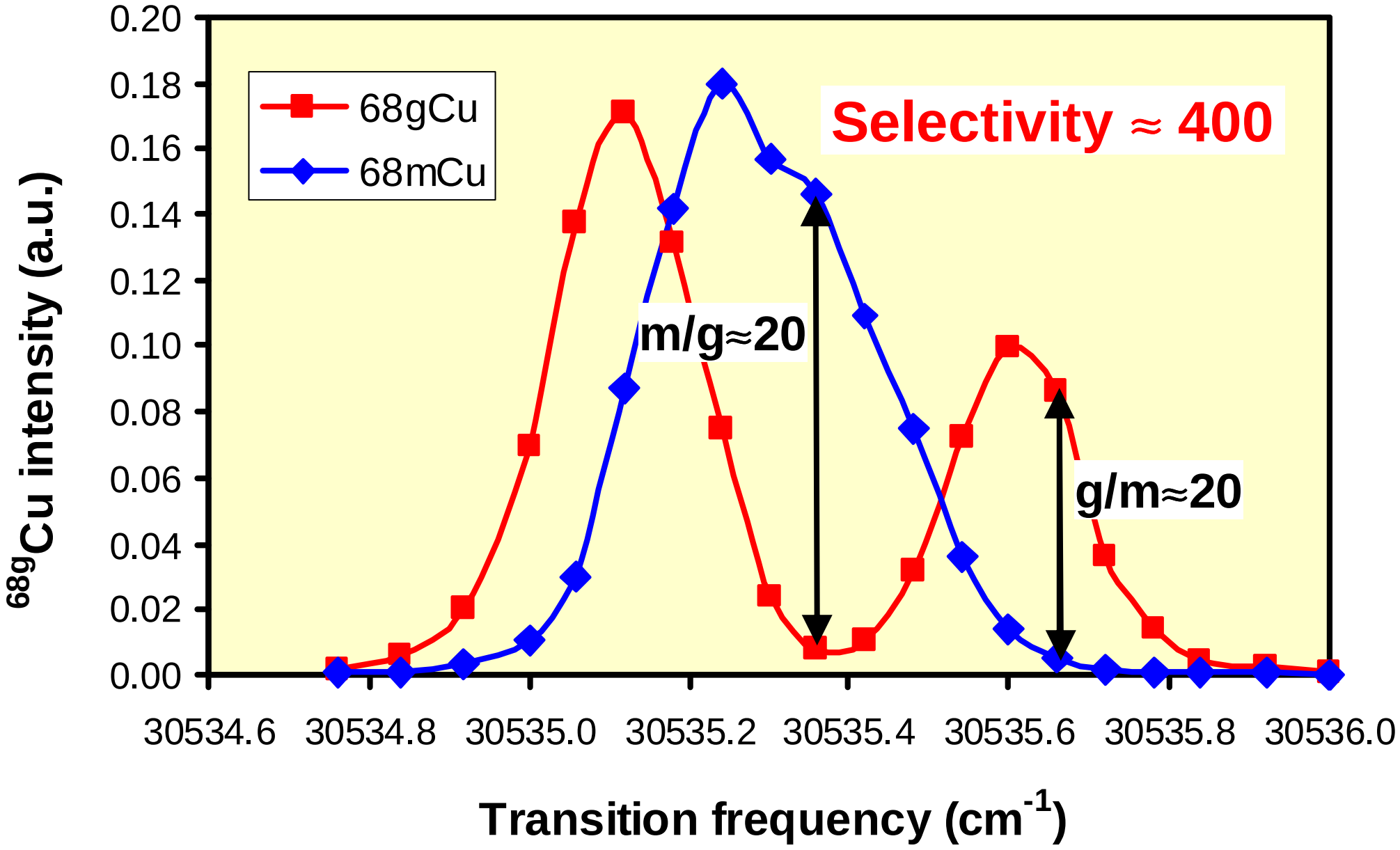

U.K. et al., Hyperfine Interactions 127 (2000) 417.

Mass measurements with Penning traps

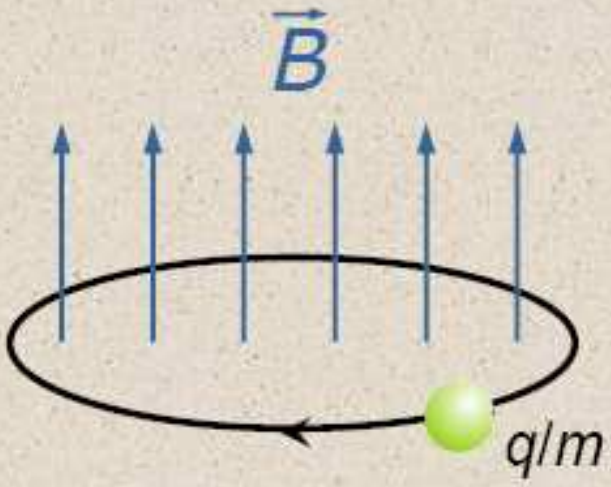

Cyclotron frequency: $f_c = \frac{1}{2\pi} \cdot \frac{q}{m} \cdot B$

PENNING trap

- Strong homogeneous magnetic field
- Weak electric 3D quadrupole field

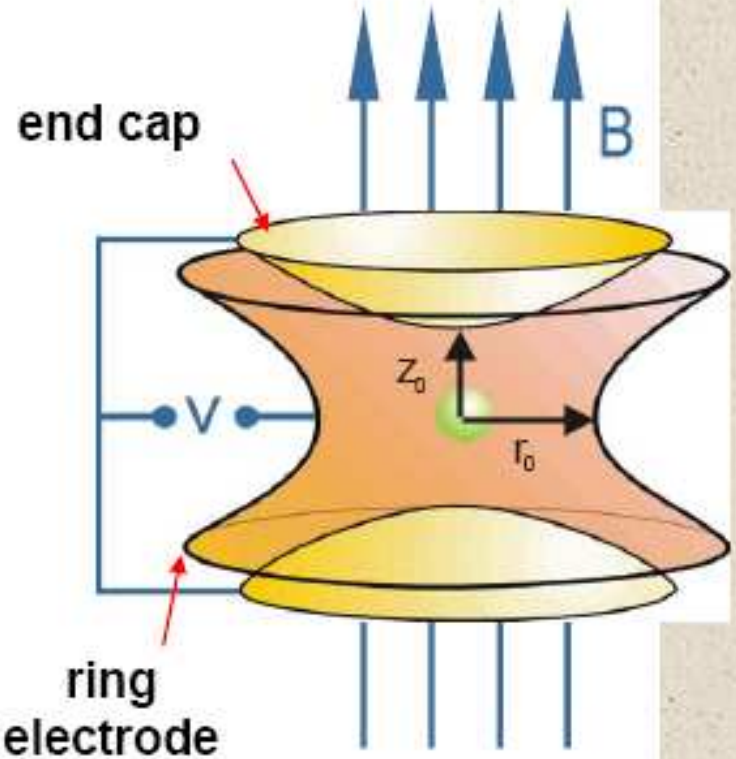

$$\omega_+ + \omega_- = \omega_c = \frac{q}{m} B$$

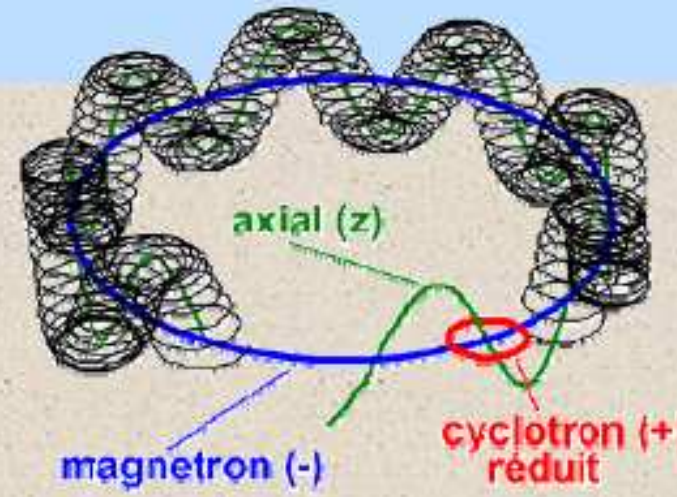

Resonance frequency measurement via TOF method

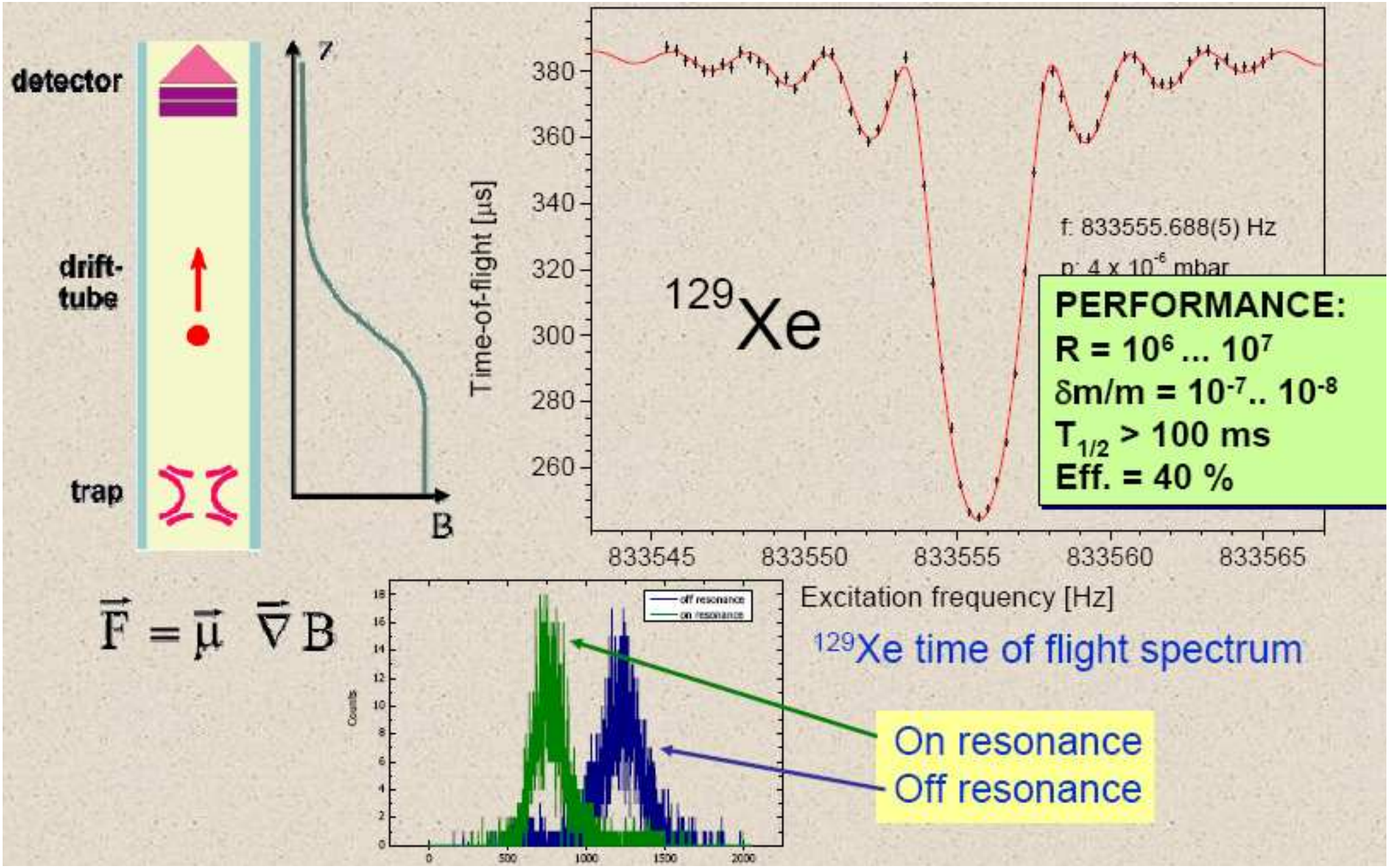

M. König et al., Int. J. Mass Spectr. Ion Proc. 142 (1995) 95.

Mass measurements with ISOLTRAP

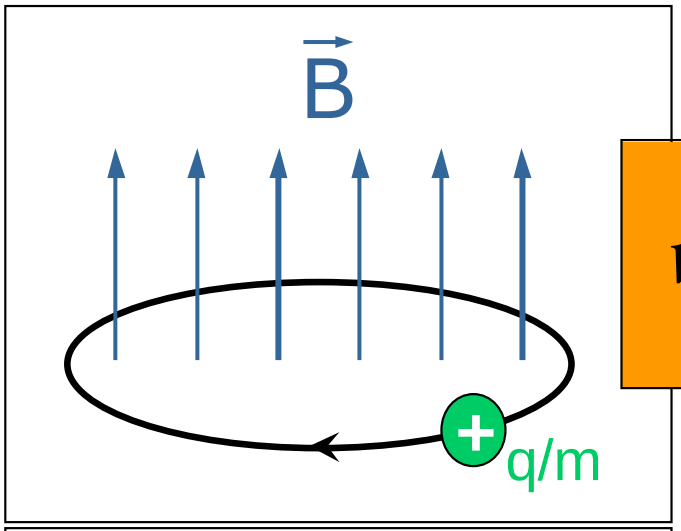

$$\nu_c = \frac{1}{2\pi}\frac{q}{m}B$$

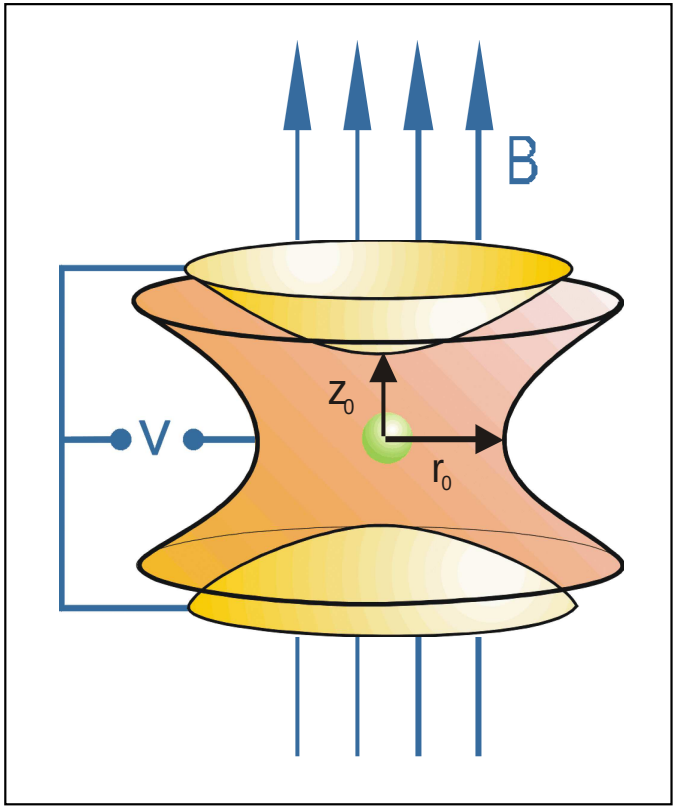

determination of cyclotron frequency ($R = 10^7$)

removal of contaminant ions ($R = 10^5$)

Bunching of the continuous beam

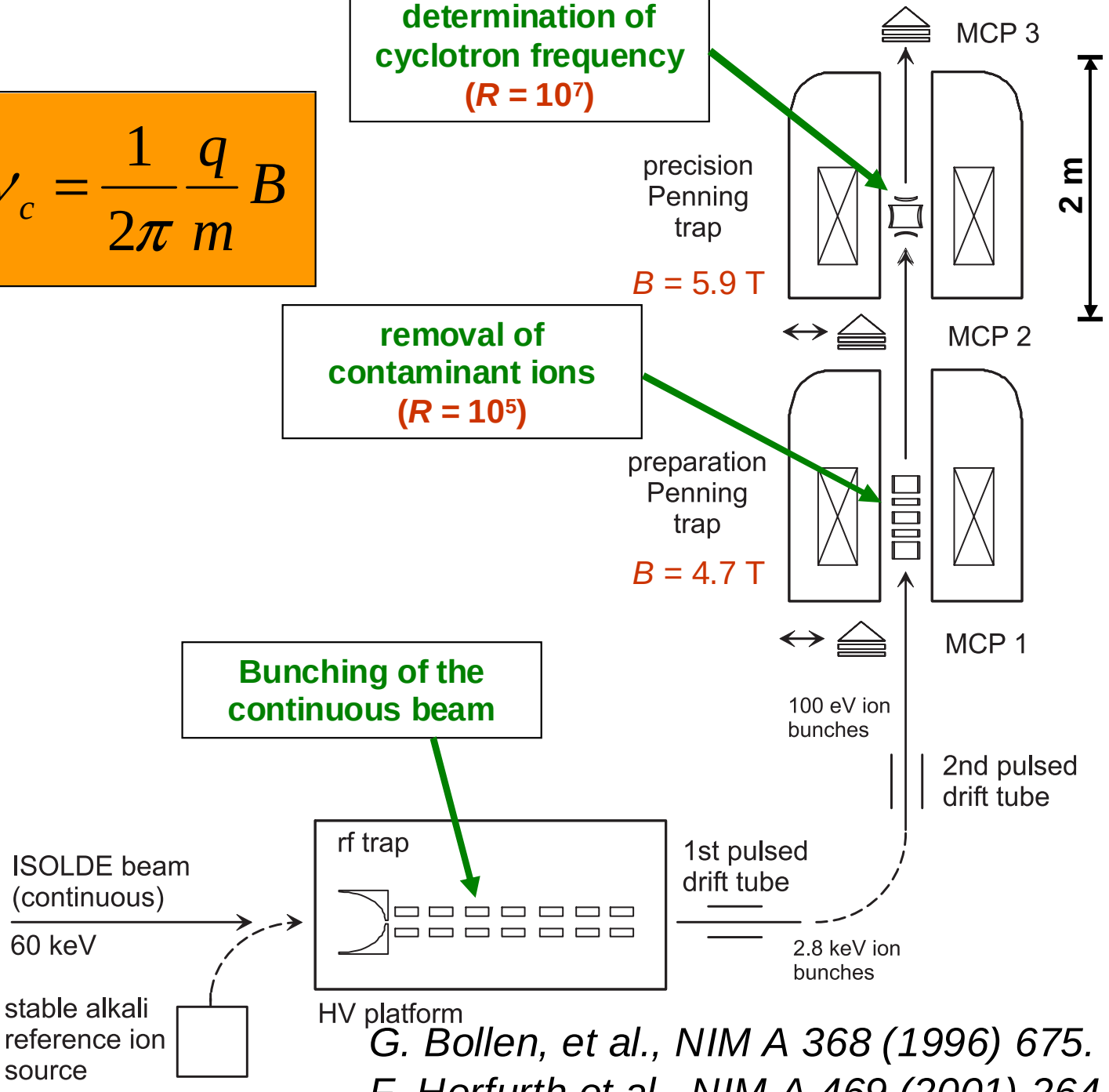

G. Bollen, et al., NIM A 368 (1996) 675.
F. Herfurth et al., NIM A 469 (2001) 264.

Solving the ^{70}Cu mass puzzle

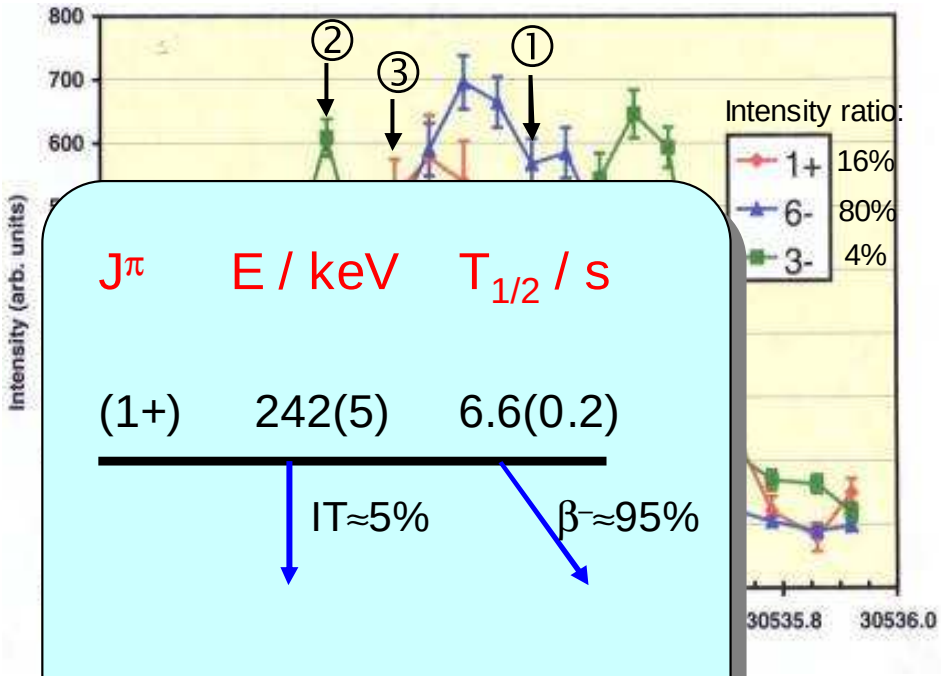

J^π E / keV $T_{1/2}$ / s

(1+) 242(5) 6.6(0.2)

IT≈5% β^-≈95%

(3-) 101(5) 33(2)

IT≈50% β^-≈50%

(6-) 0 44.5(0.2)

β^-=100%

ω_c

s state

nt!

state

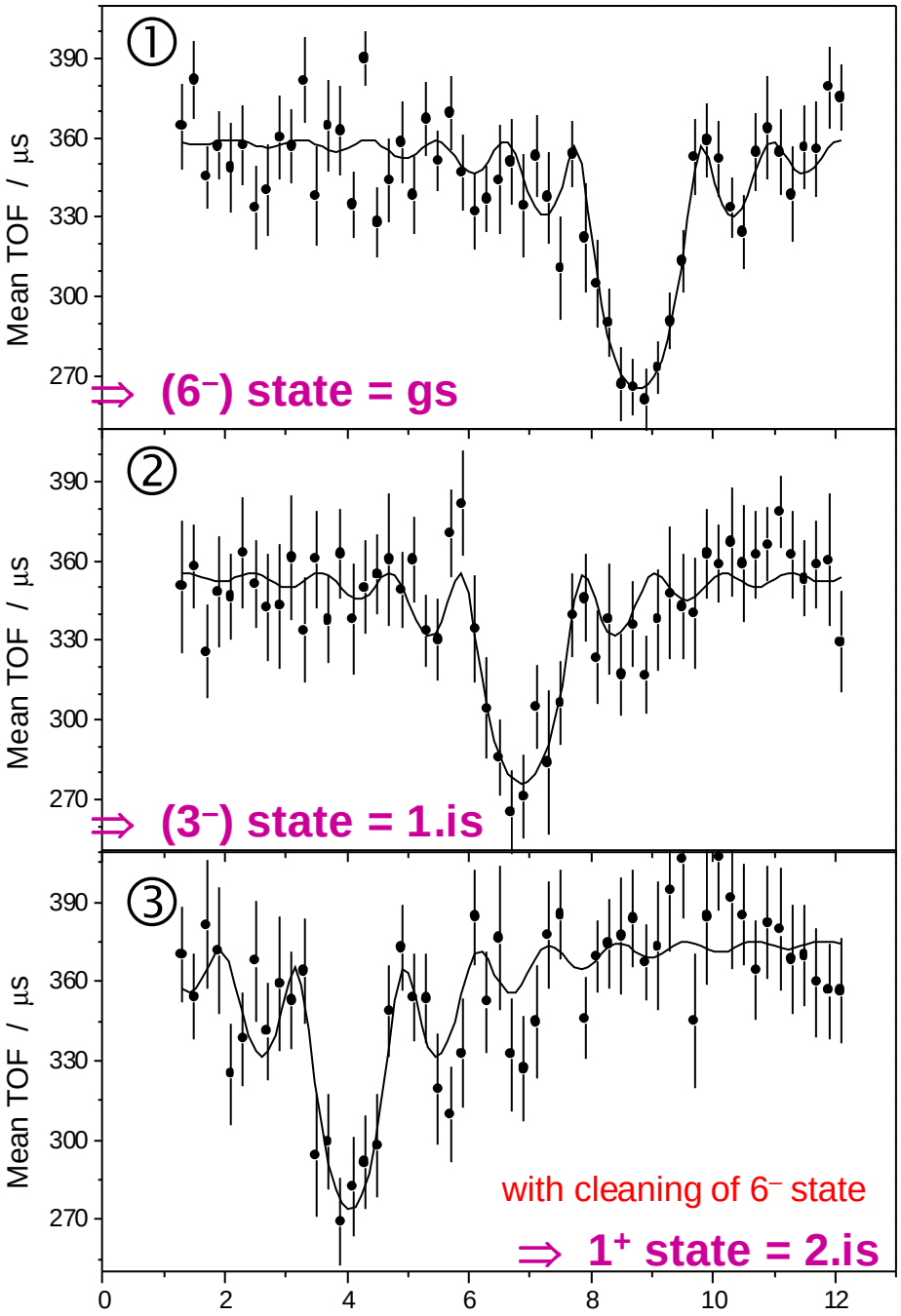

J. Van Roosbroeck et al., Phys. Rev. Lett. 92 (2004) 112501.

CERN accelerator structure

CERN-PS Booster Synchrotrons

E_p = 1.4 GeV

$3 \cdot 10^{13}$ protons/pulse = 5 μC

$I_{average}$ = 4 μA

$p_{average}$ = 6 kW

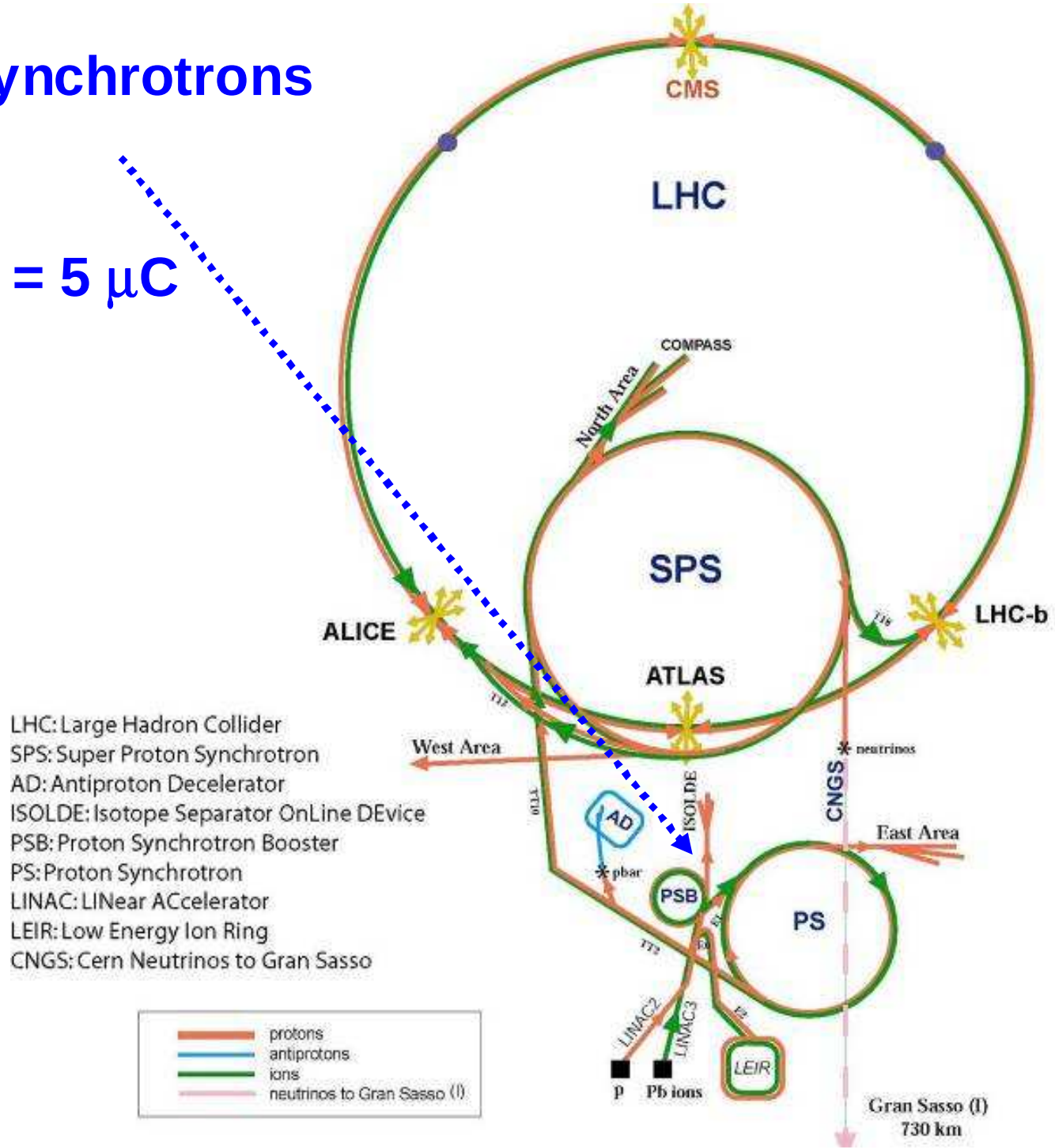

Antiproton traps at CERN

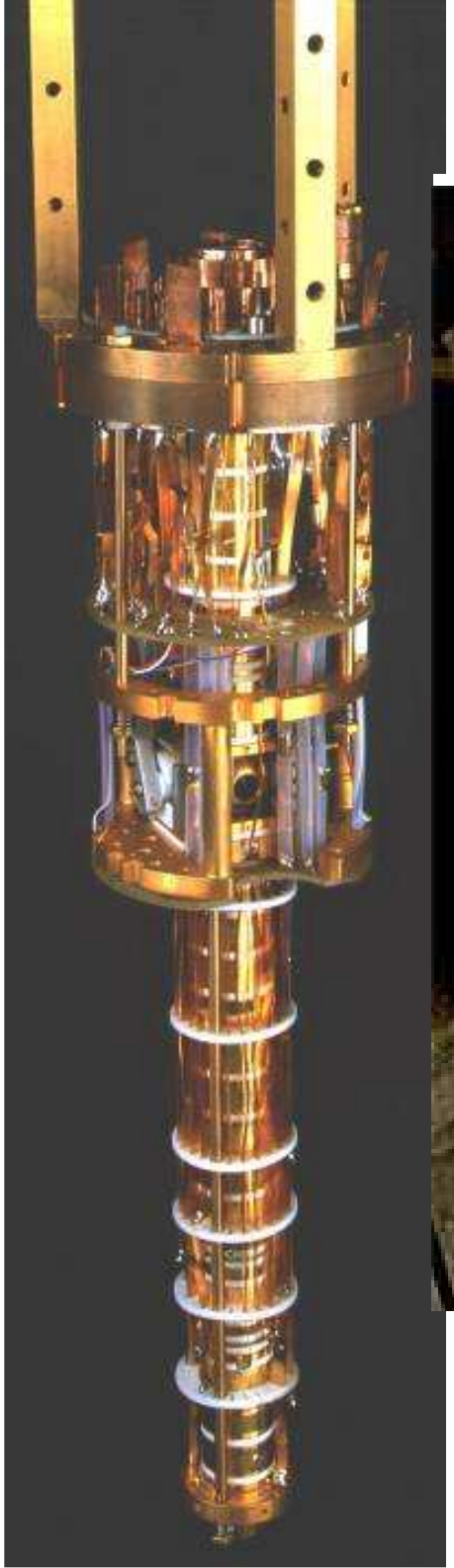

G. Gabrielse et al., Phys. Rev. Lett. 100 (2008) 113001.

M. Amoretti et al., Phys. Lett. B 583 (2004) 59.

D. Brown, R. Howard et al., "Angels and Demons" (2009).

Measurement of magnetic moments

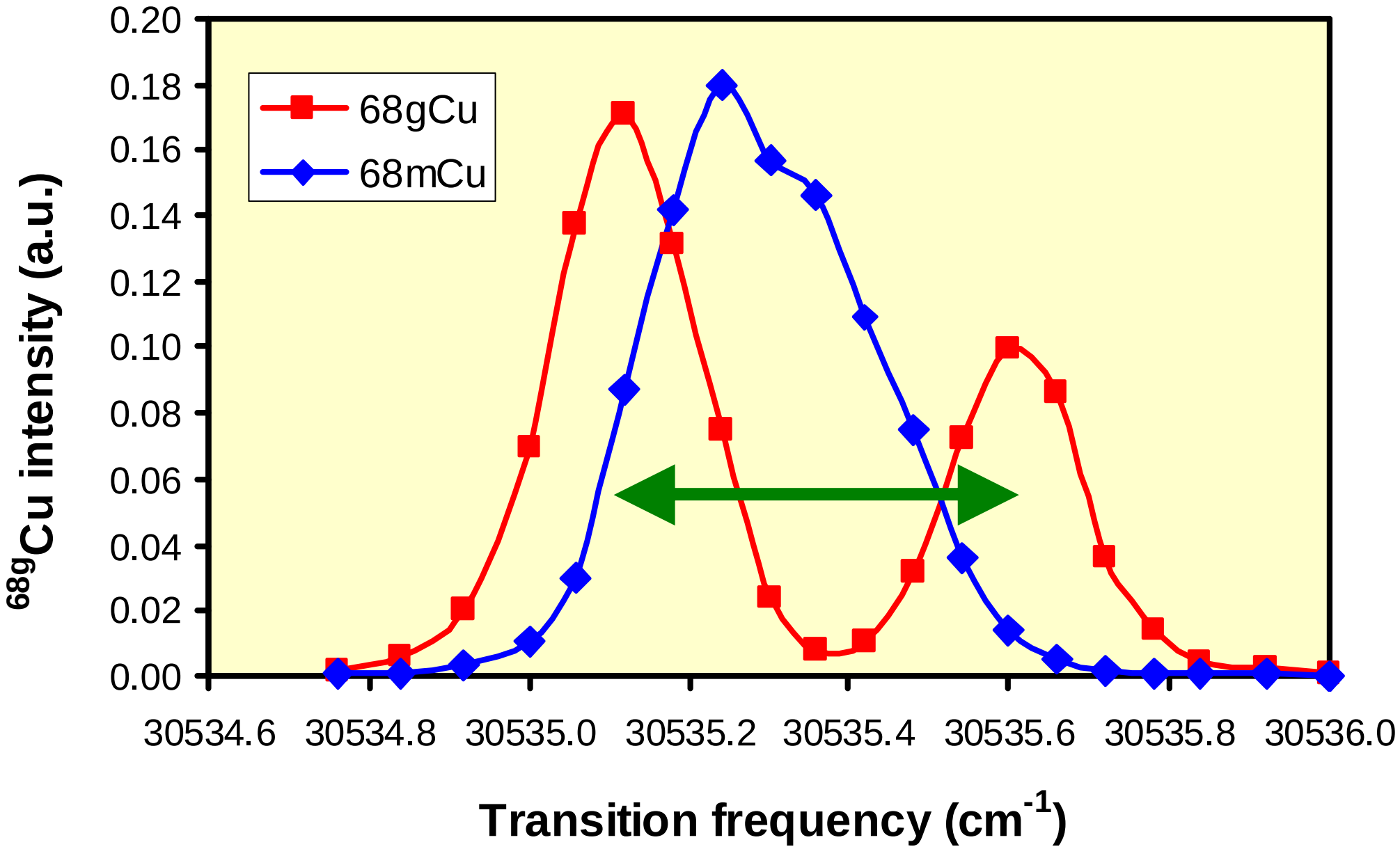

hyperfine splitting proportional to g-factor

Nuclear properties from laser spectroscopy

Hyperfine splitting in electronic transitions:

$$\Delta E_{HFS} = \frac{A}{2} * K + \frac{B}{4} * \frac{\frac{3}{2} K(K+1) - 2I(I+1)J(J+1)}{I(2I-1)J(2J-1)}$$

$$K = \frac{F(F+1) - J(J+1) - I(I+1)}{J(J+1)(2l+1)}$$

$$A = \frac{\mu \cdot H_e(0)}{IJ} \quad \Rightarrow \textbf{magnetic dipole moment} \qquad \mu \ (J > 0)$$

$$B = \frac{eQ_s}{\left|\frac{d\Phi}{dr}(0)\right|} \quad \Rightarrow \textbf{electric quadrupole moment} \quad Q \ (J > 1/2)$$

Isotope shift between two nuclei:

$$\delta\nu_{IS}^{A,A'} = (K_{NMS} + K_{SMS}) * \frac{M_{A'} - M_A}{M_{A'} M_A} + F_{el.} * \delta\left\langle r^2 \right\rangle^{A'A}$$

$\Rightarrow$ **nuclear charge radii** $\delta\langle r^2\rangle^{AA'}$

Atomic vapor laser isotope separation (AVLIS)

large scale application of resonant laser ionization!

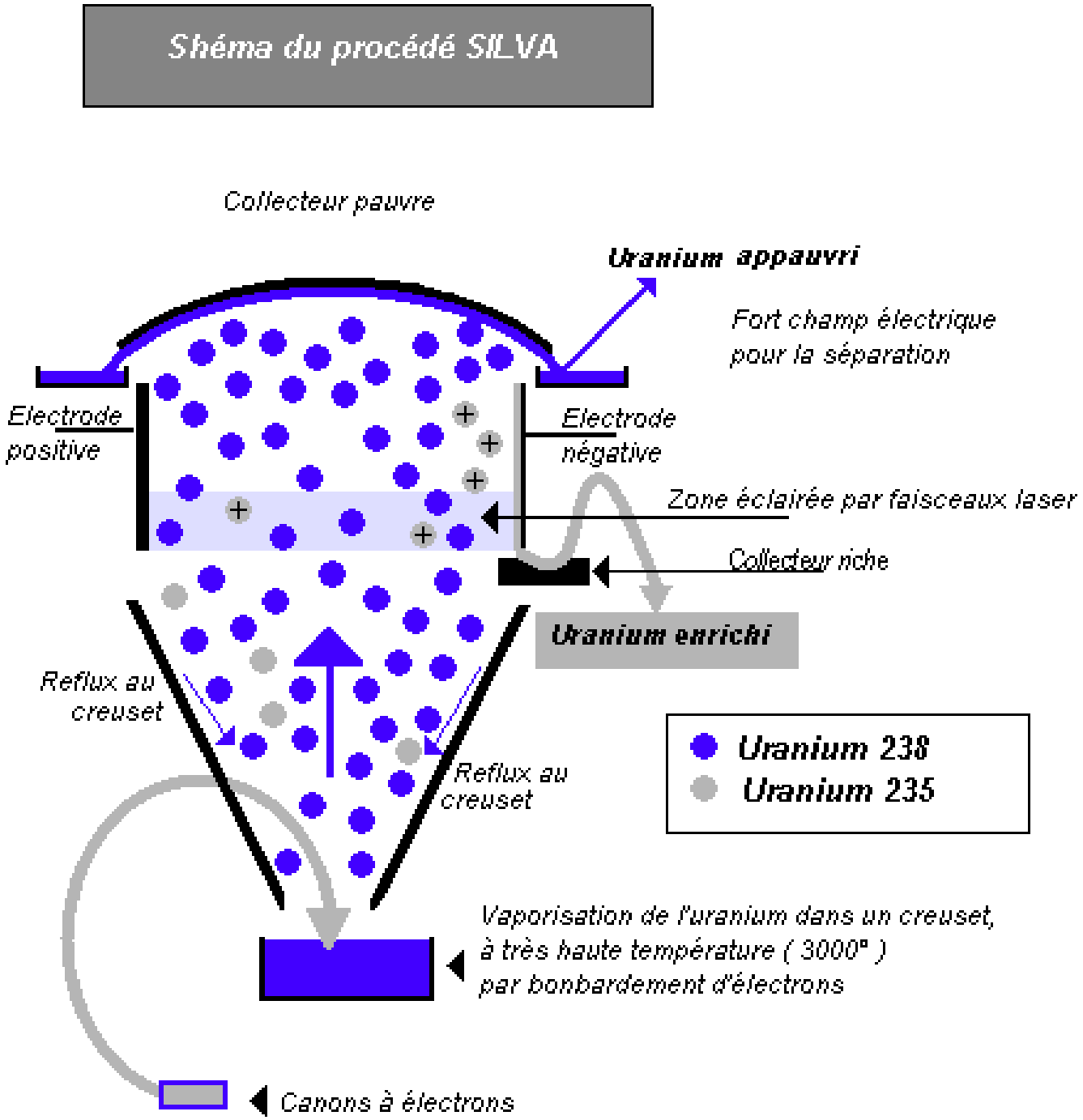

Surface ionized background

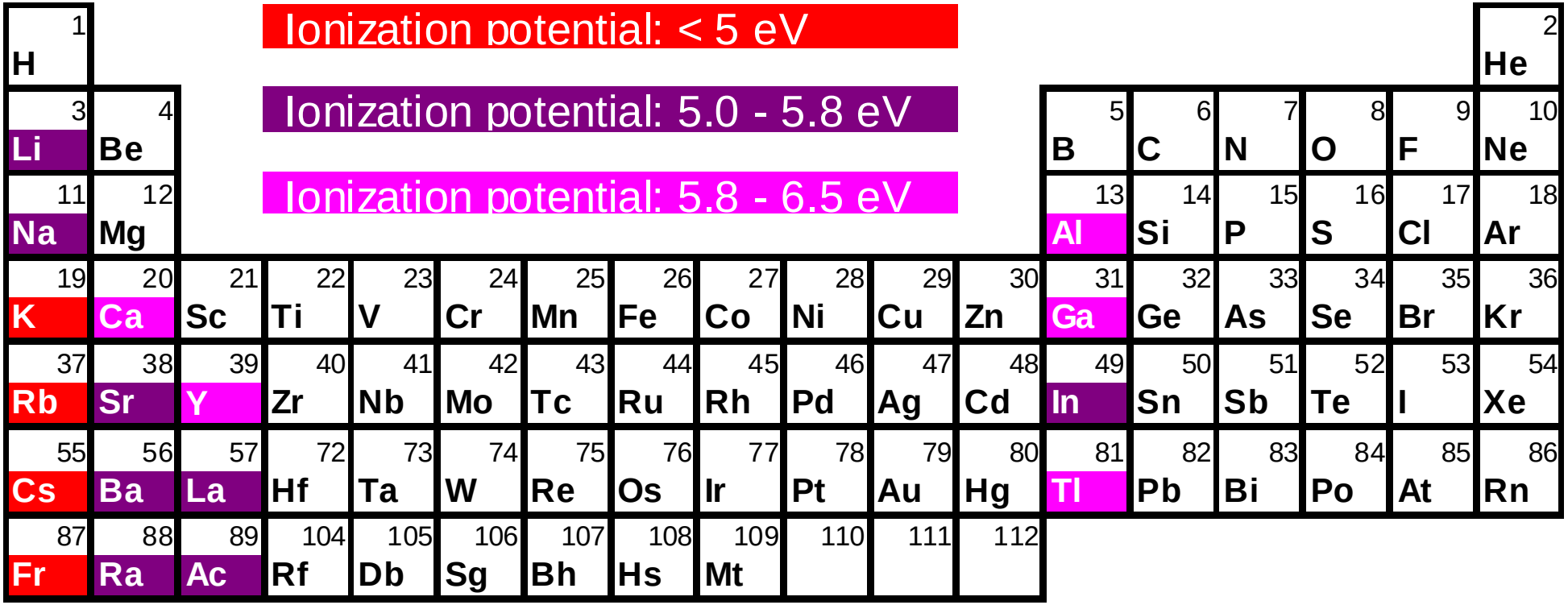

ISOLDE beams around N=50

^{81}Rb background is 150000 times more abundant than ^{81}Zn!

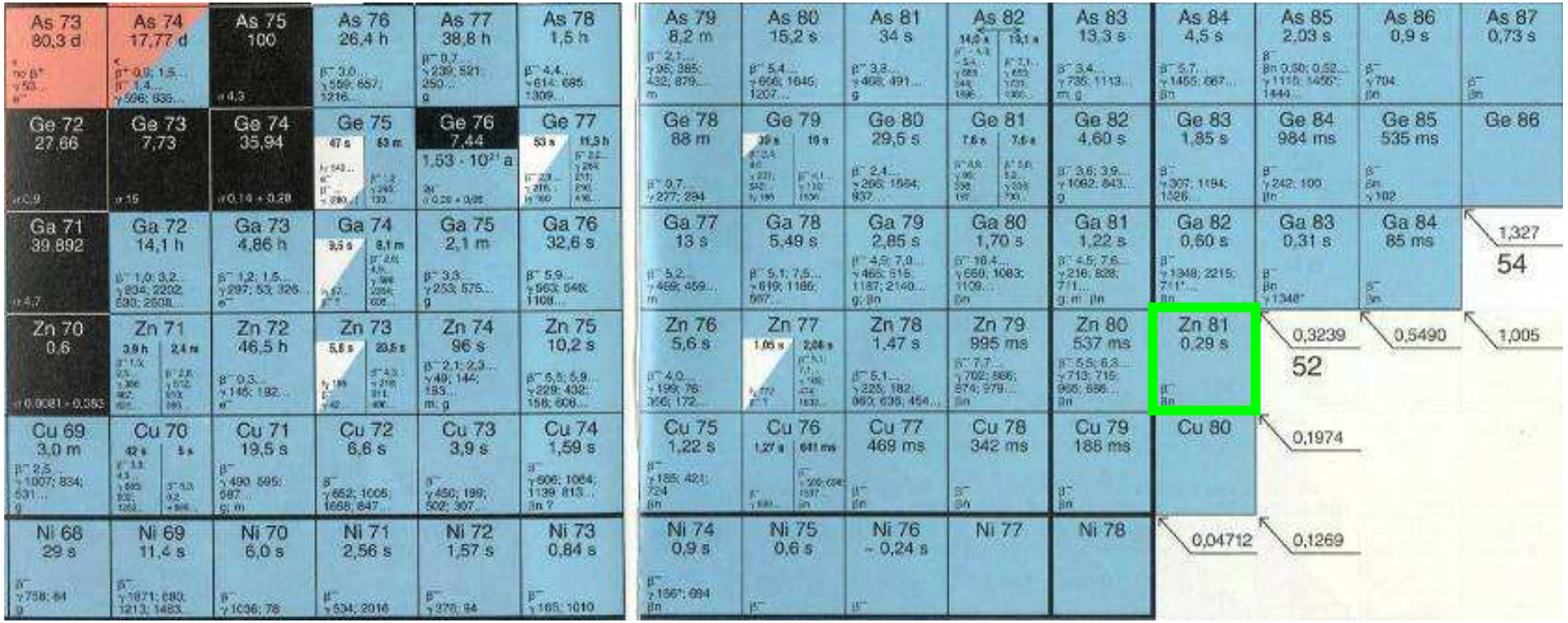

Rubidium cross-sections

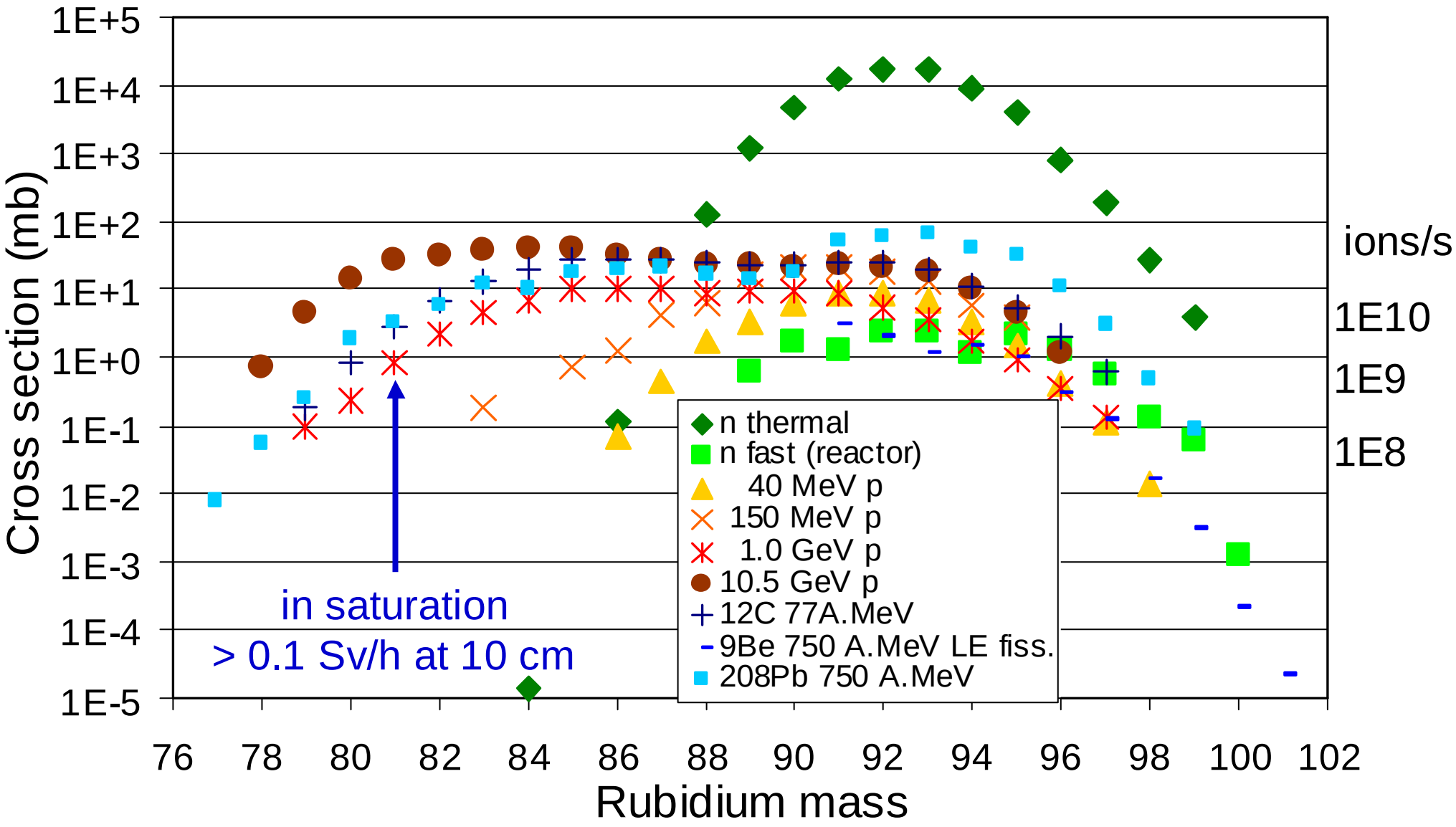

better use neutron-induced fission!

Neutron “converter” geometry

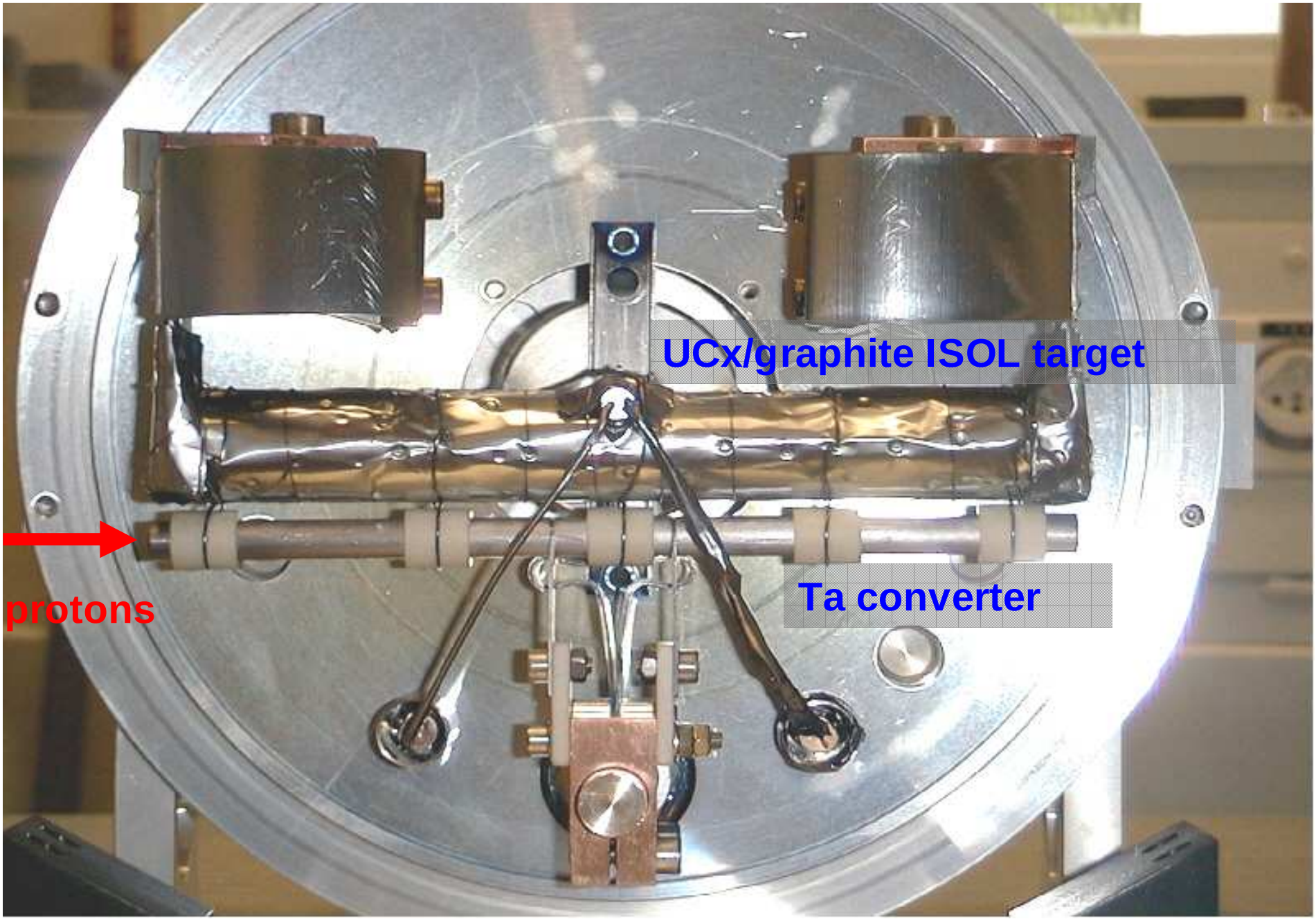

Ga & Rb suppression with the “neutron converter”

proton beam on **target**

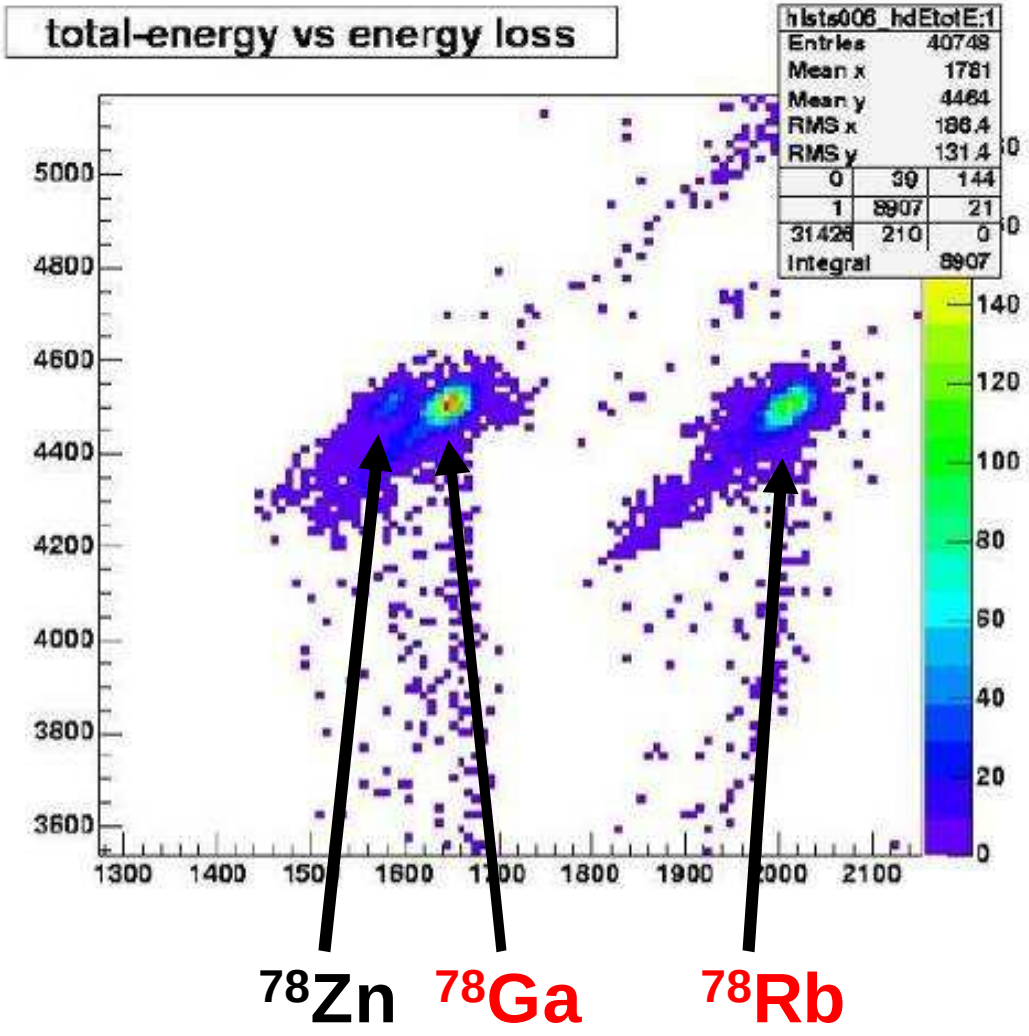

proton beam on **converter**

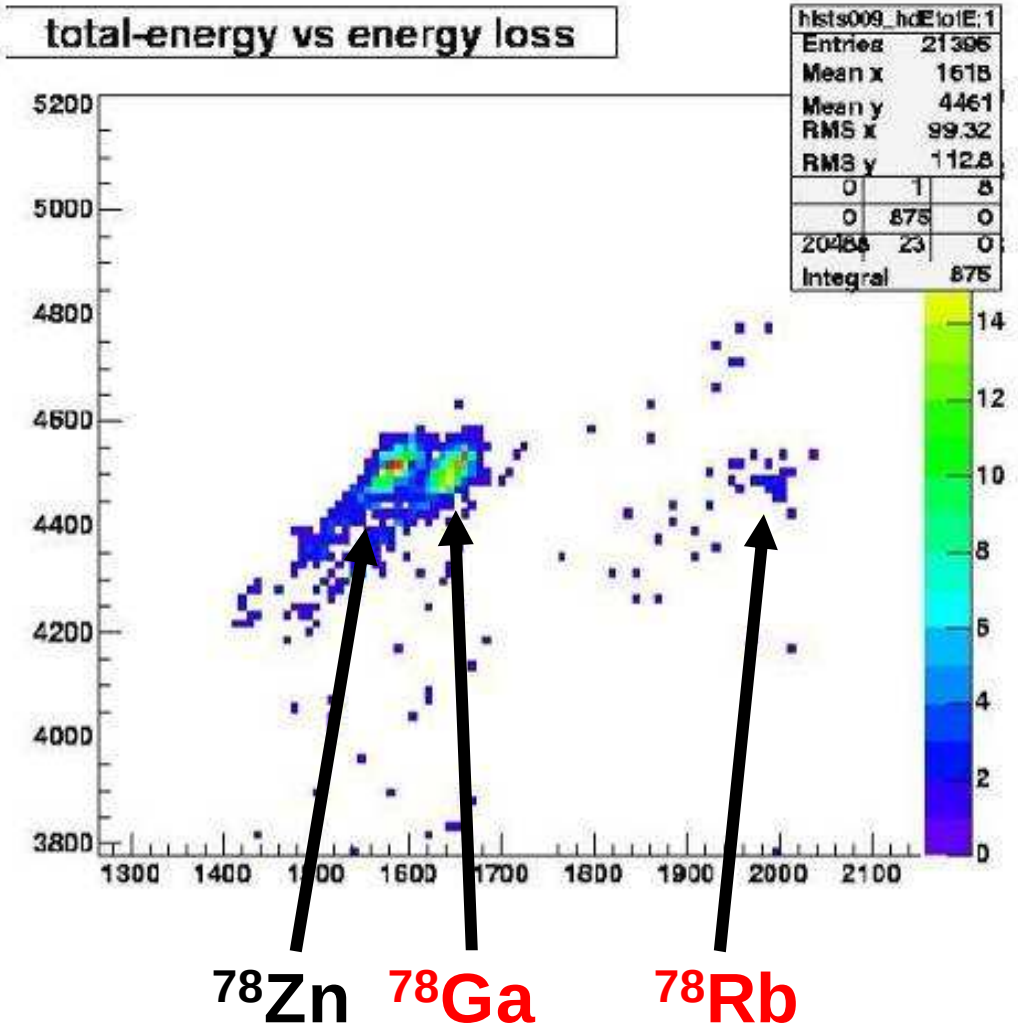

U.K., Eur. Phys. J. A15 (2002) 255.

U.K. et al., AIP Conf. Proc. 798 (2005) 315.

ISOLDE thermochromatography set-up

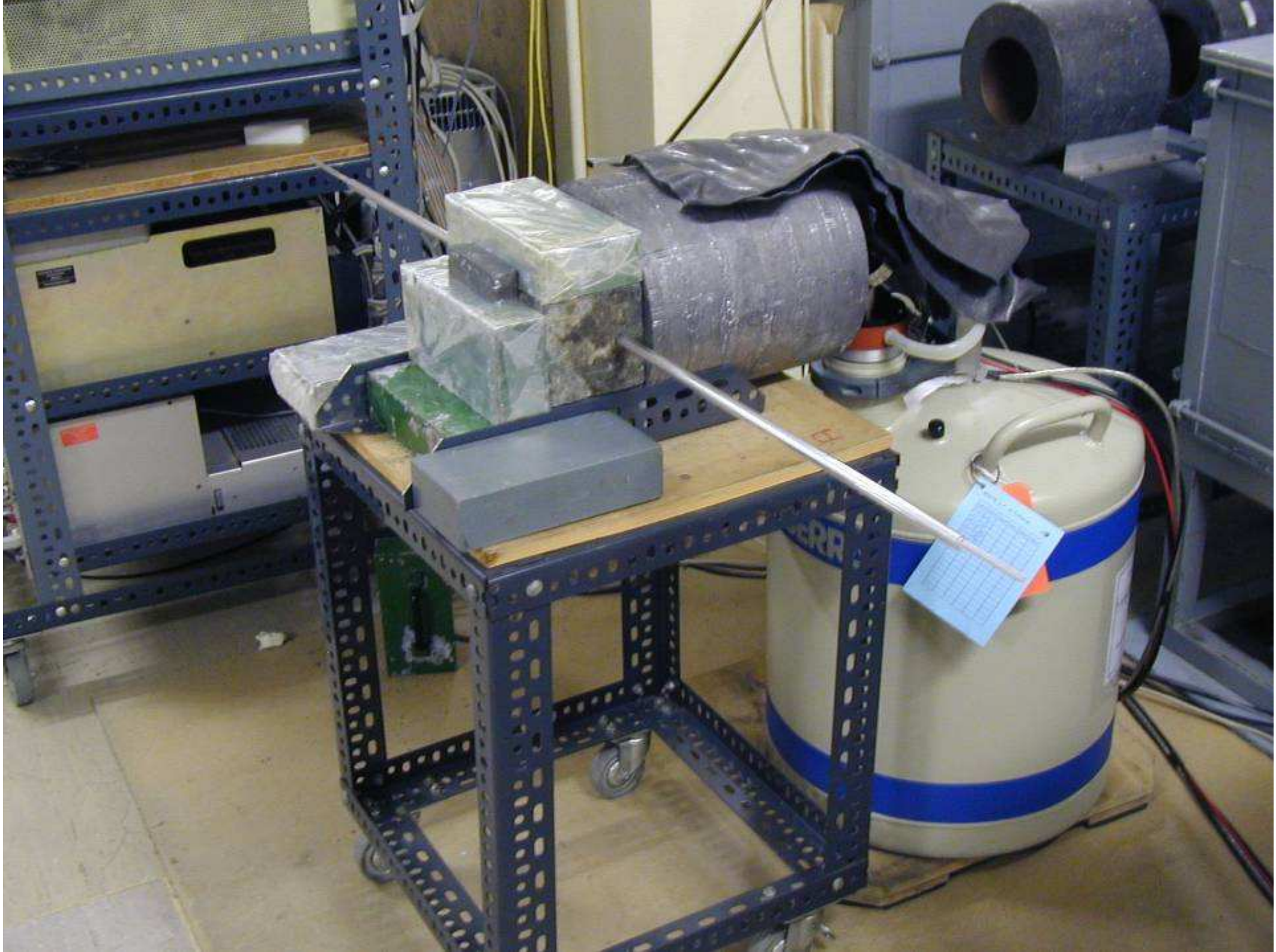

Zn/Rb discrimination on quartz surface!

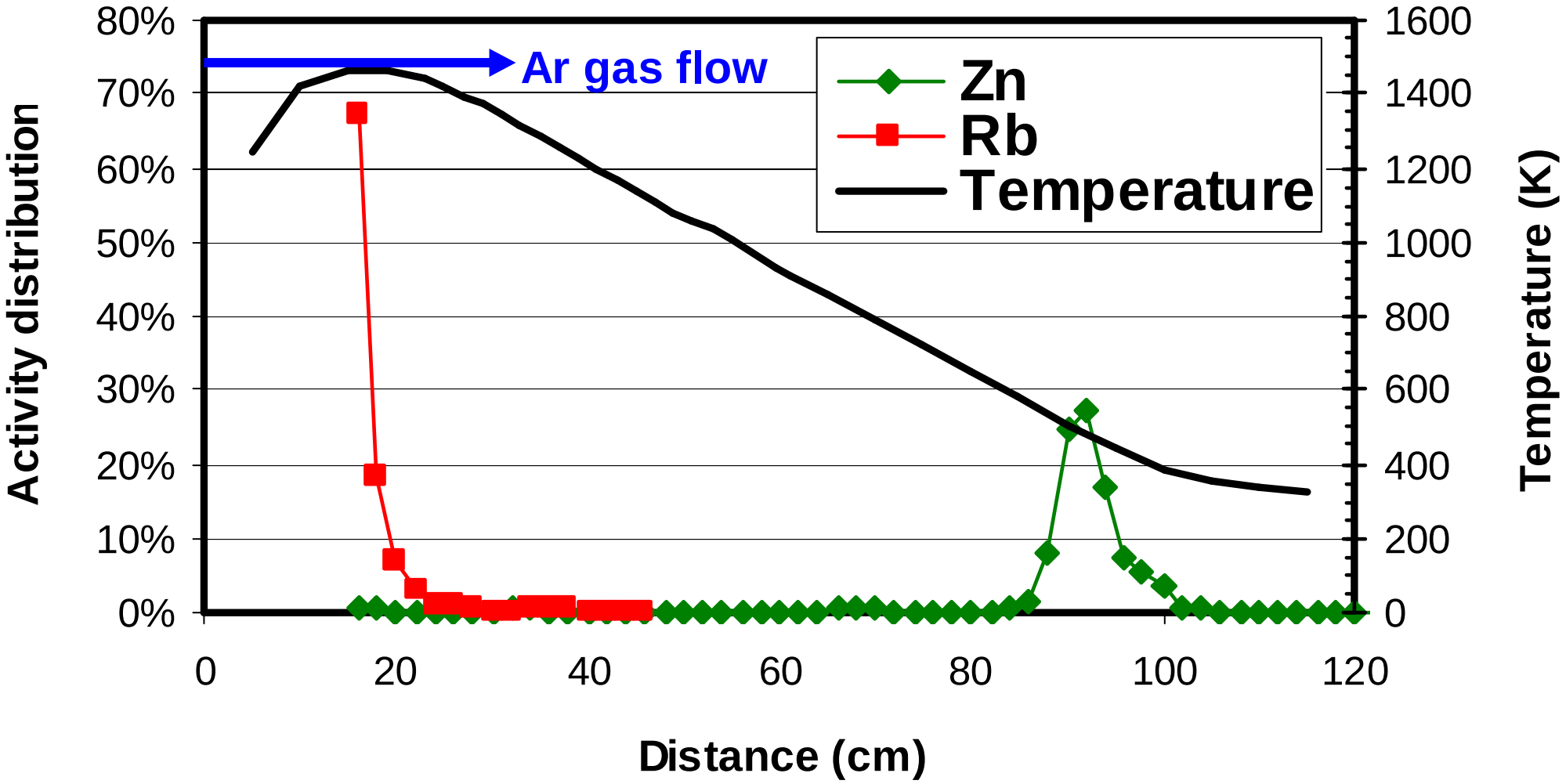

Combination of neutron converter and quartz transfer line provides ^{81}Zn/^{81}Rb selectivity gain of 100000!

U.K. et al., Nucl. Instr. Meth. B266 (2008) 4229.

Zn/Rb discrimination on quartz surface!

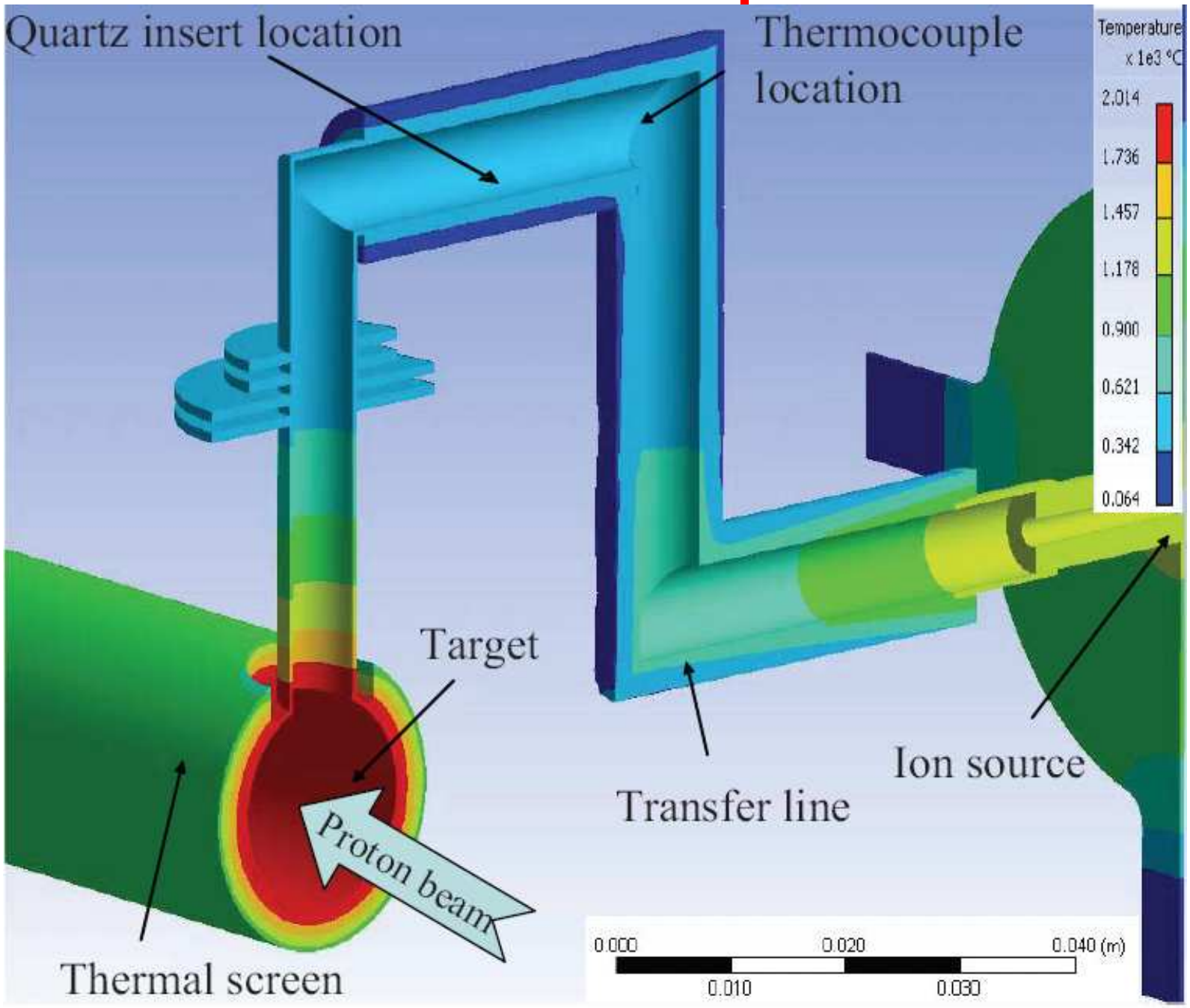

E. Boucquerel et al., Nucl. Instr. Meth. B266 (2008) 4298.

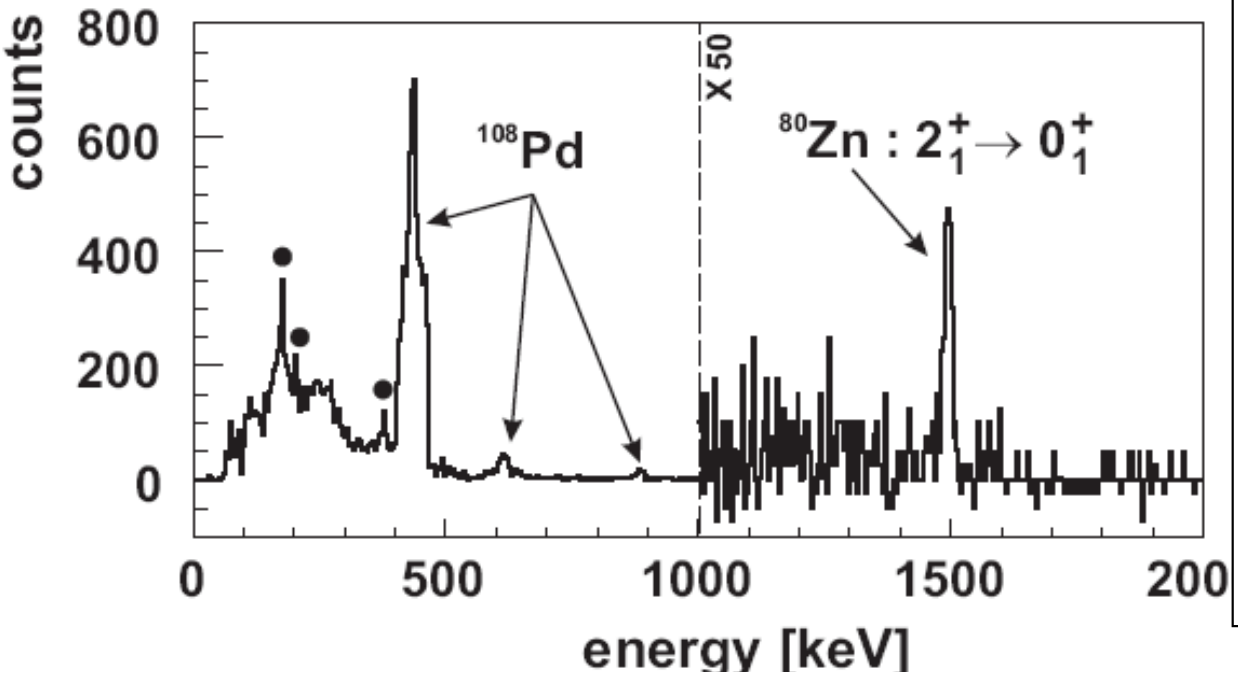

J. Van de Walle et al., Phys. Rev. Lett. 99 (2007) 142501.

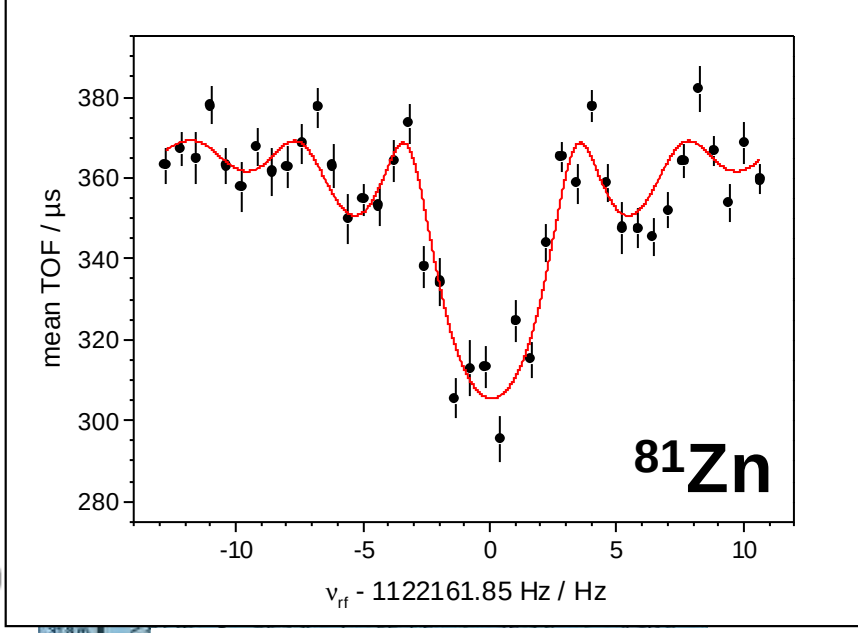

S. Baruah et al., Phys. Rev. Lett. 101 (2008) 262501.

REX performs Coulex measurement of ^{80}Zn observing its 2^+ state

ISOLTRAP performs direct mass measurement of r-process nucleus!

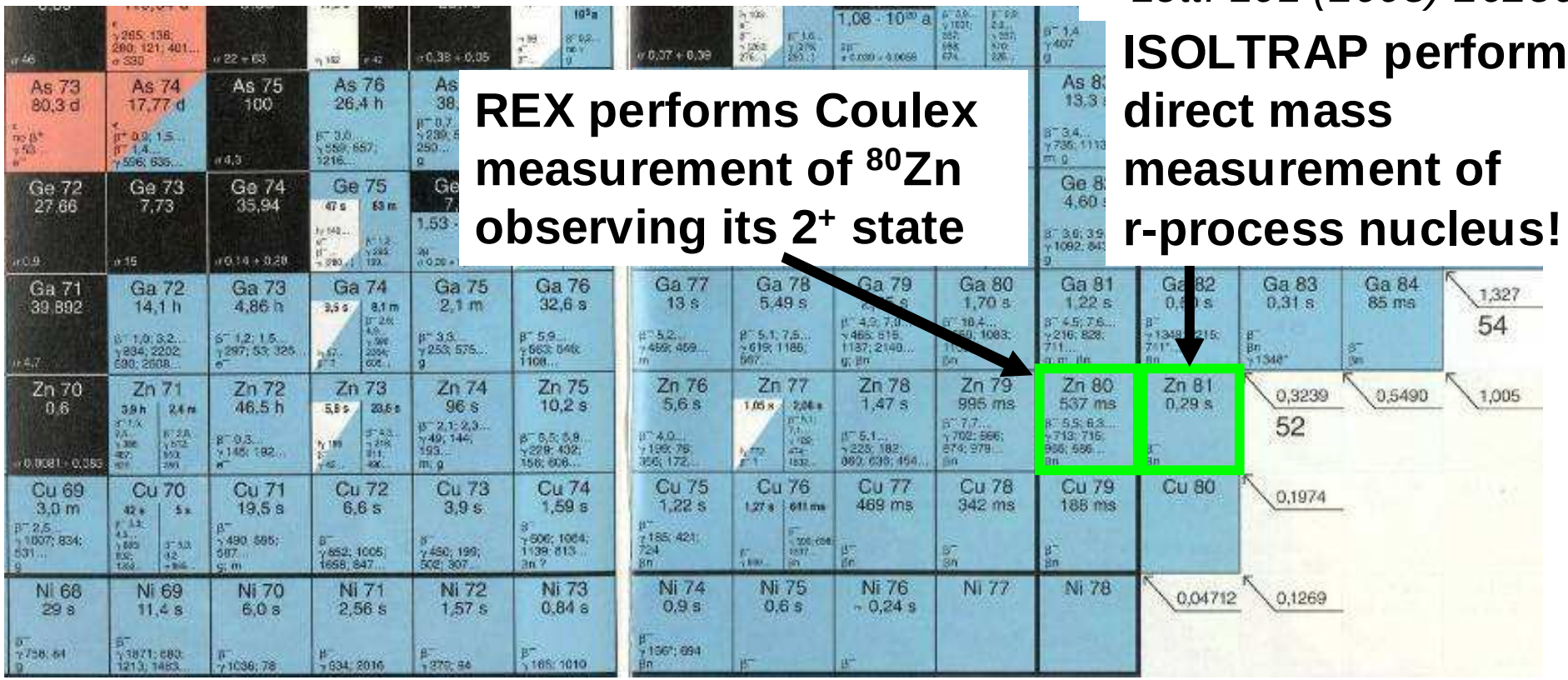

Experimental access to *r*-process nuclides

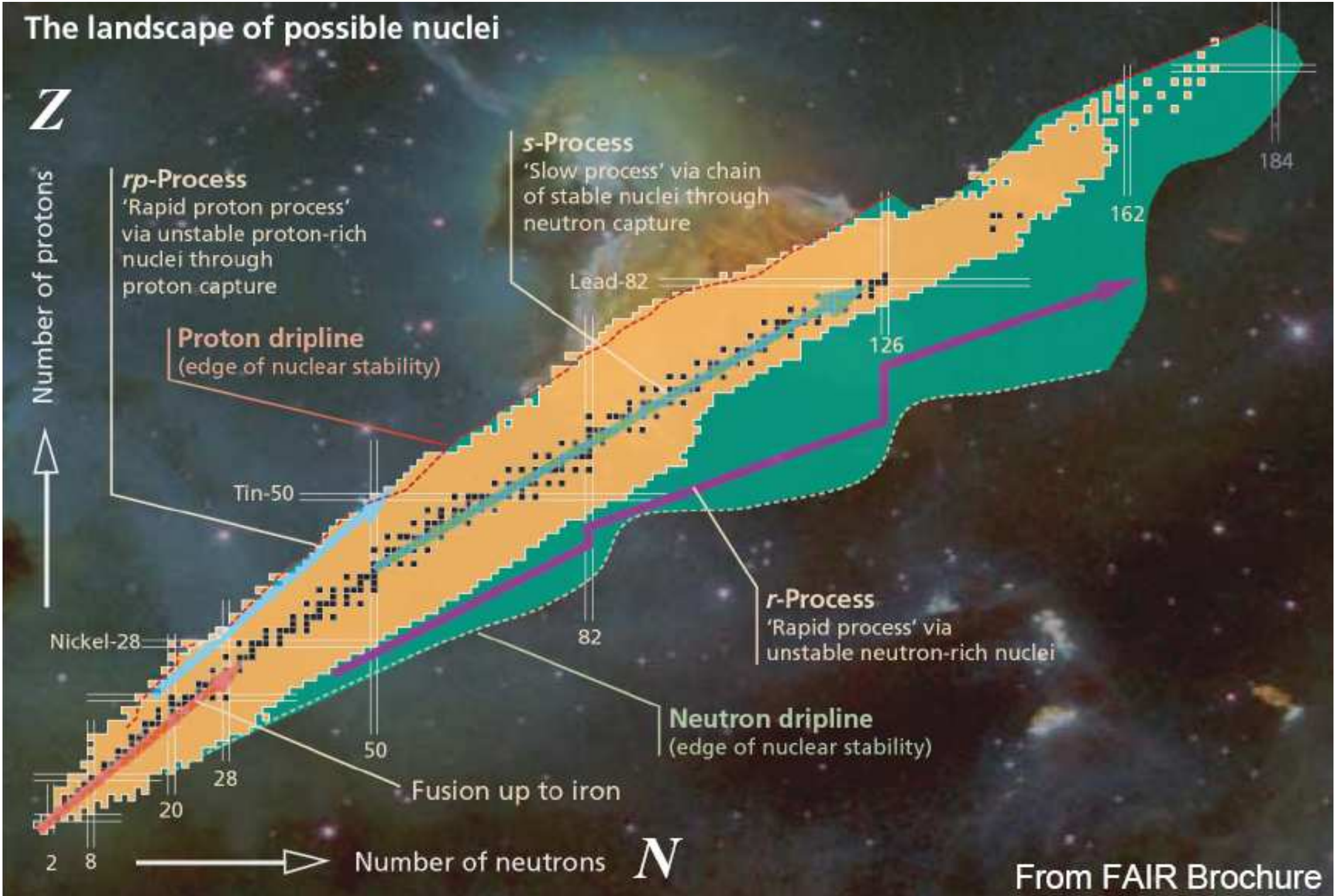

Elements ionizable with CVL pumped dye lasers

elements ionized with ISOLDE RILIS

tested ionization scheme

possible ionization scheme (untested)

refractory elements

1 H																	2 He
3 Li	4 Be											5 B	6 C	7 N	8 O	9 F	10 Ne
11 Na	12 Mg											13 Al	14 Si	15 P	16 S	17 Cl	18 Ar
19 K	20 Ca	21 Sc	22 Ti	23 V	24 Cr	25 Mn	26 Fe	27 Co	28 Ni	29 Cu	30 Zn	31 Ga	32 Ge	33 As	34 Se	35 Br	36 Kr
37 Rb	38 Sr	39 Y	40 Zr	41 Nb	42 Mo	43 Tc	44 Ru	45 Rh	46 Pd	47 Ag	48 Cd	49 In	50 Sn	51 Sb	52 Te	53 I	54 Xe
55 Cs	56 Ba	57 La	72 Hf	73 Ta	74 W	75 Re	76 Os	77 Ir	78 Pt	79 Au	80 Hg	81 Tl	82 Pb	83 Bi	84 Po	85 At	86 Rn
87 Fr	88 Ra	89 Ac	104 Rf	105 Db	106 Sg	107 Bh	108 Hs	109 Mt	110	111	112						

58 Ce	59 Pr	60 Nd	61 Pm	62 Sm	63 Eu	64 Gd	65 Tb	66 Dy	67 Ho	68 Er	69 Tm	70 Yb	71 Lu
90 Th	91 Pa	92 U	93 Np	94 Pu	95 Am	96 Cm	97 Bk	98 Cf	99 Es	100 Fm	101 Md	102 No	103 Lr

Hf beams at ISOLDE

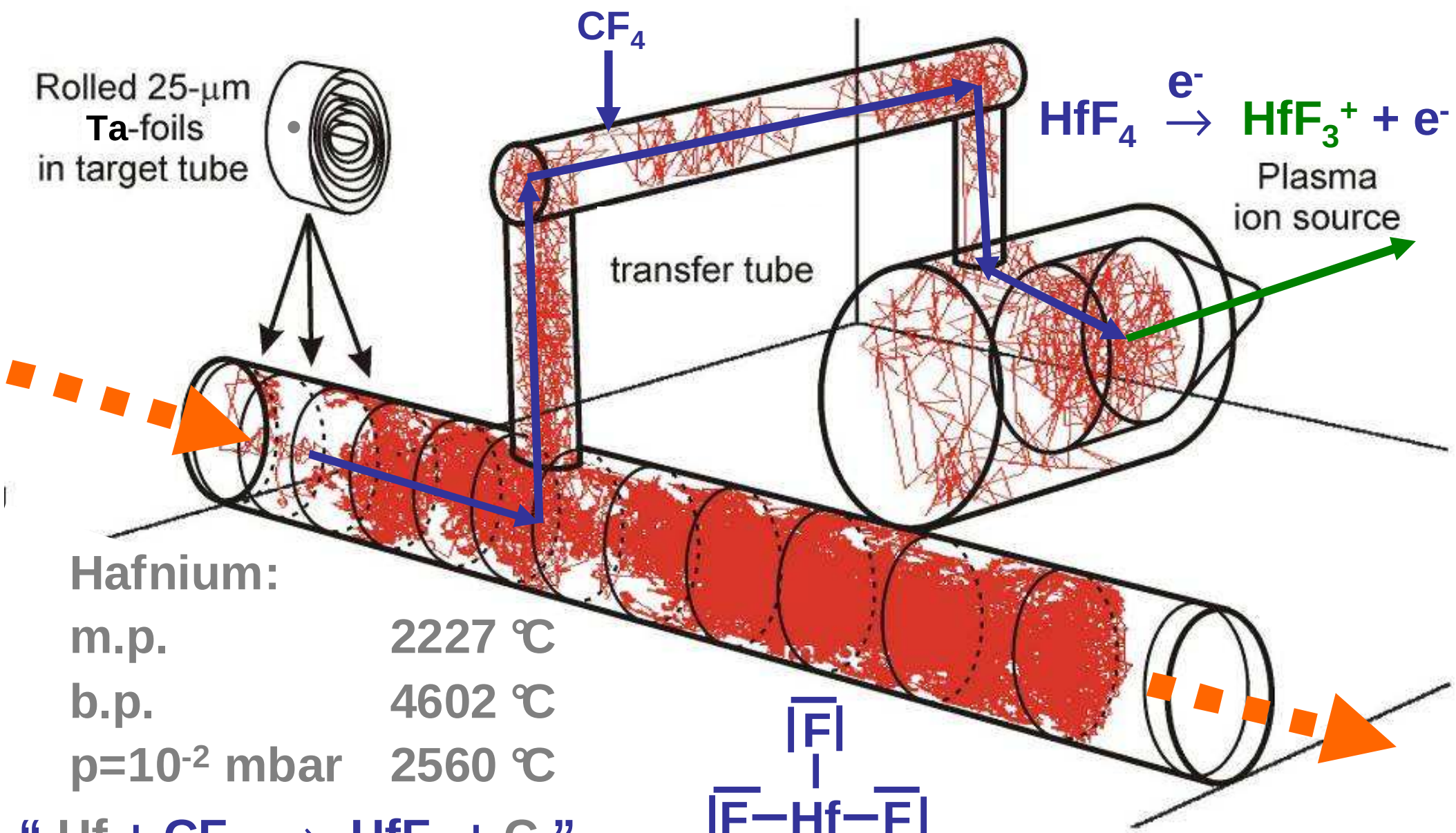

Hafnium:

m.p.	2227 ℃
b.p.	4602 ℃
p=10^{-2} mbar	2560 ℃

“ Hf + CF_4 → HfF_4 + C ”

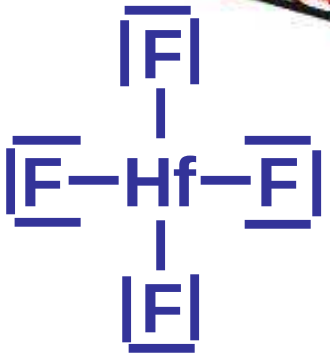

HfF_4: p=10^{-2} mbar ca. 1200 ℃

Ta/W foil target + MK5 + CF_4

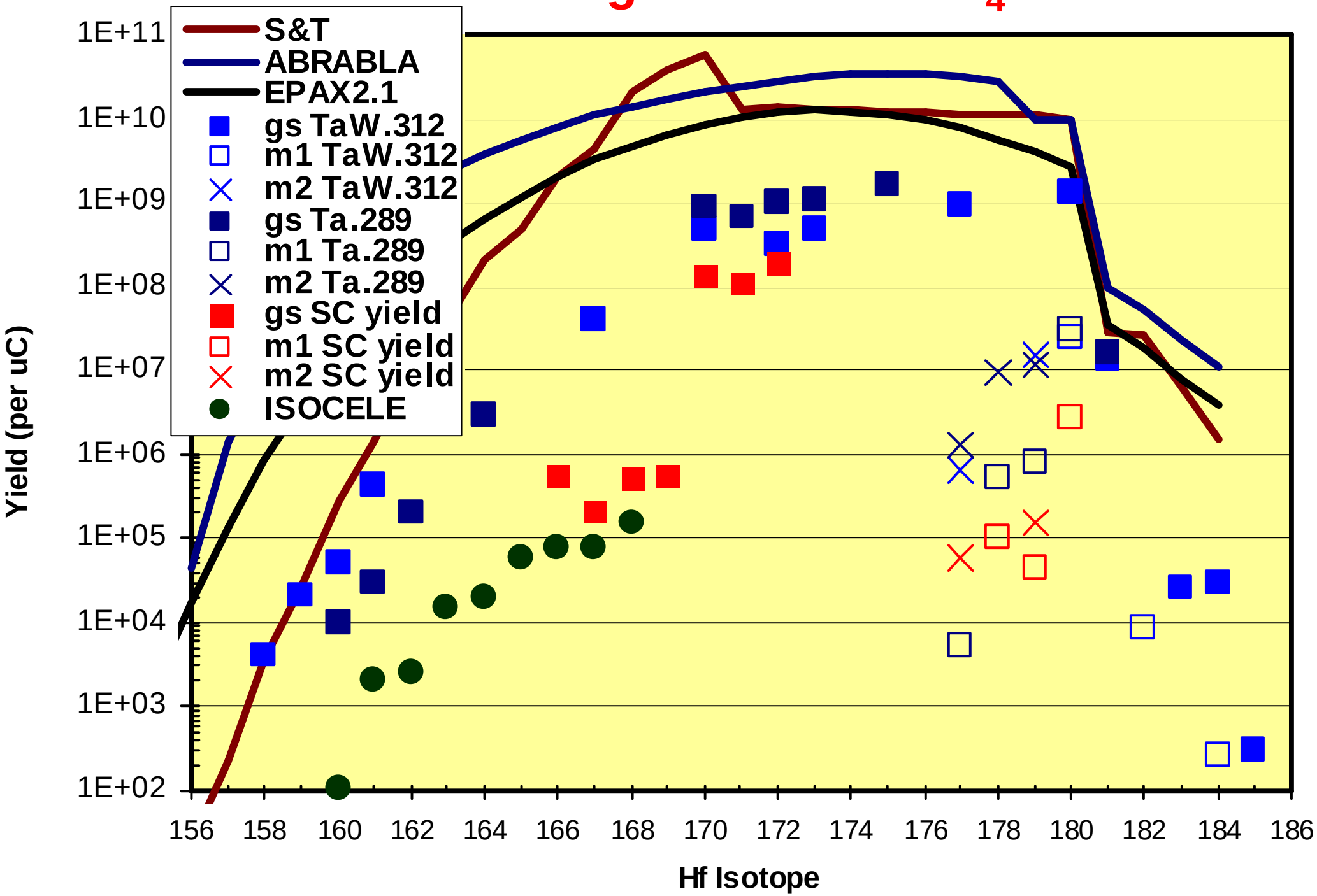

U.K. et al., Eur. Phys. J. Spec. Topics 150 (2007) 293.

Neutron-rich hafnium beams

Overview of molecular ISOL beams

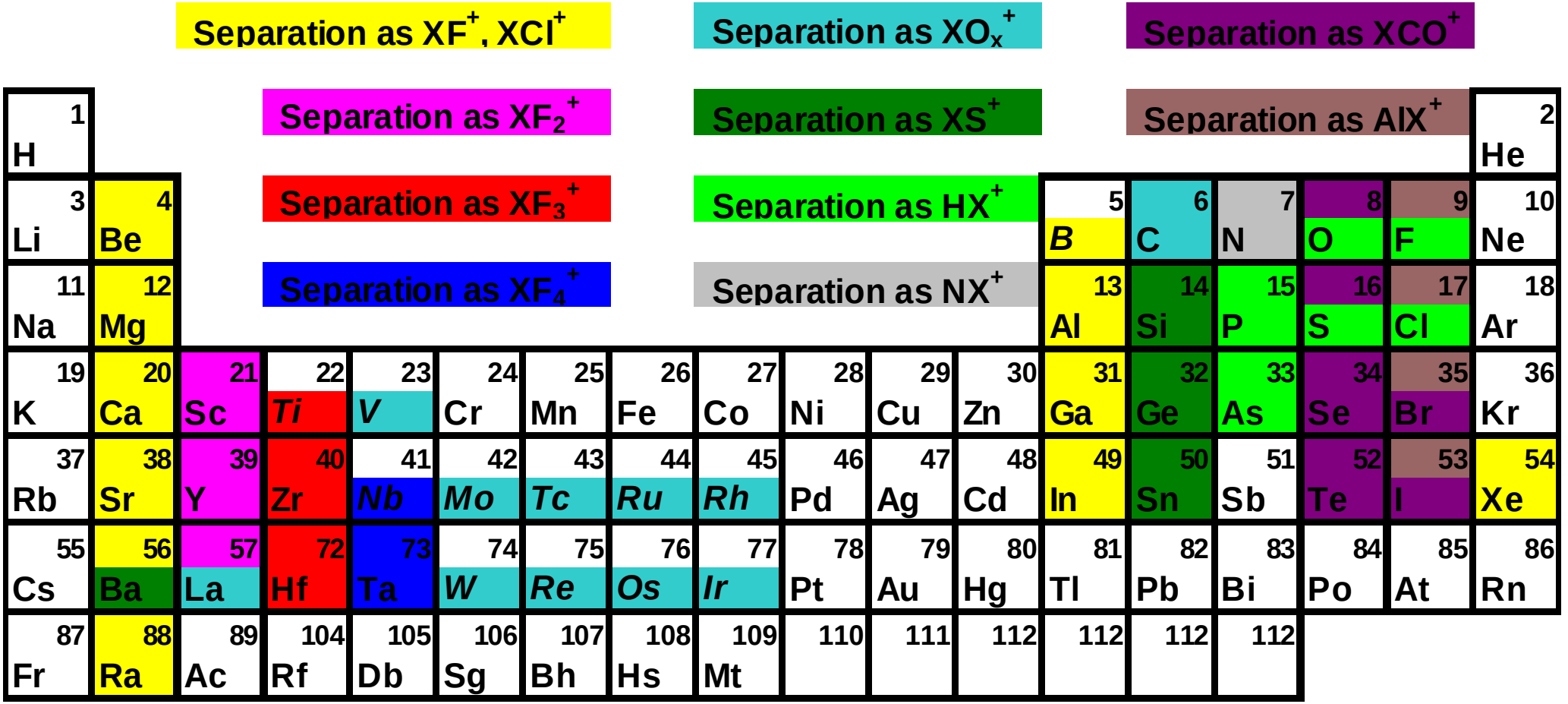

U.K. et al., Nucl. Instr. Meth. B266 (2008) 4229.

General Purpose Separator (GPS)

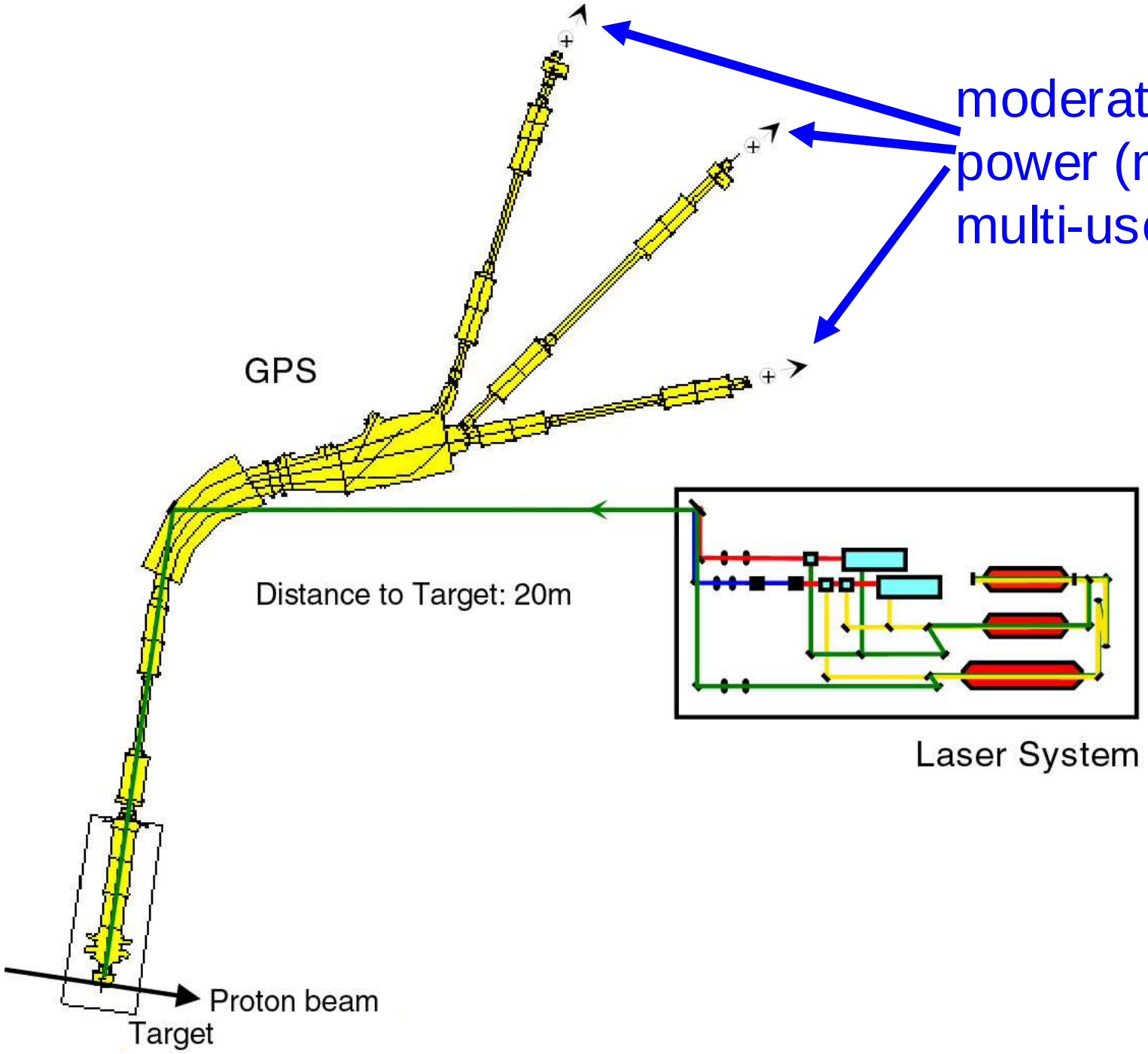

moderate mass resolving power ($m/\Delta m \approx 1000$), but multi-user capability!

Francium beams

Francium

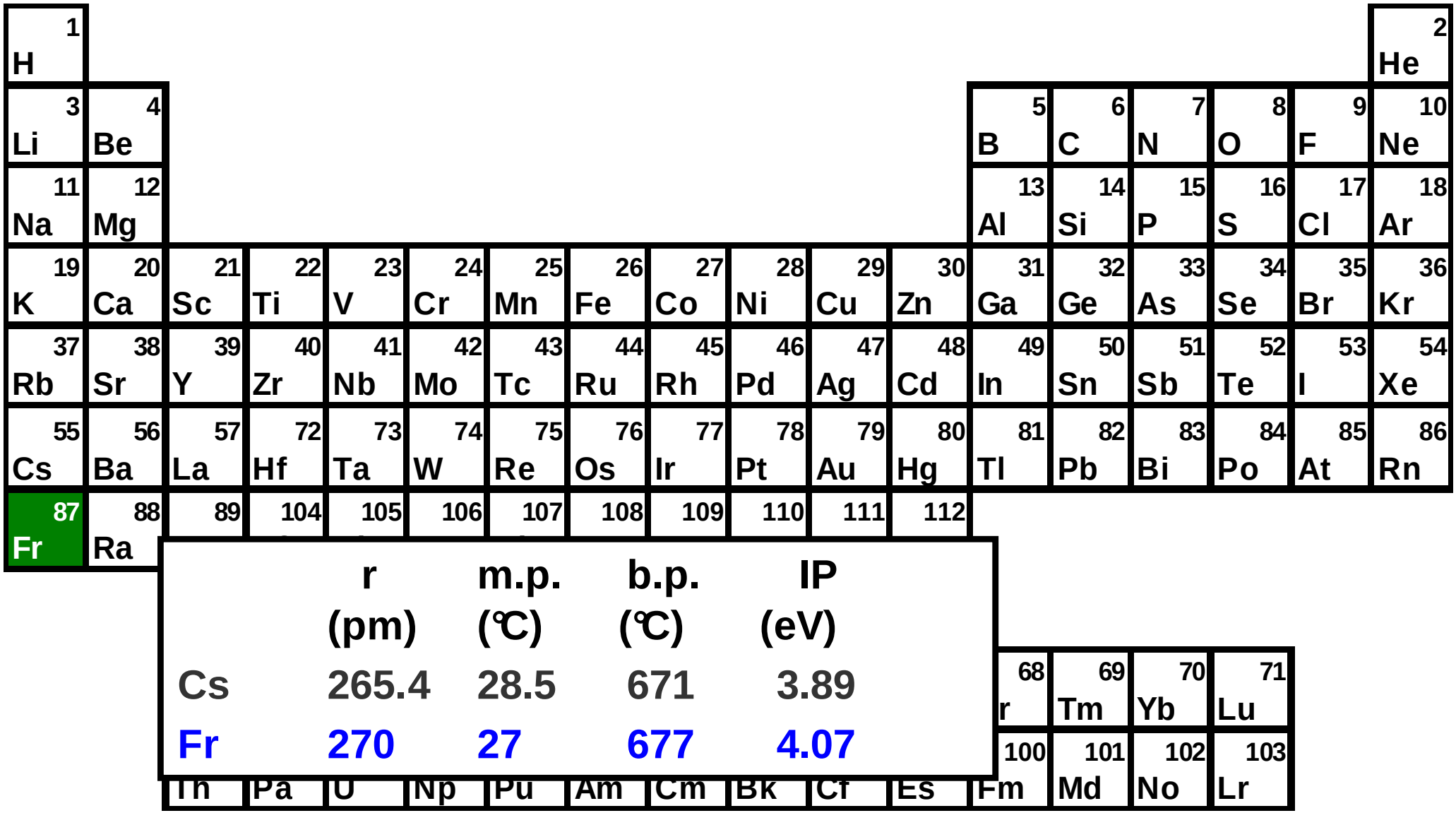
1 H
2 He
3 Li
4 Be
5 B
6 C
7 N
8 O
9 F
10 Ne
11 Na
12 Mg
13 Al
14 Si
15 P
16 S
17 Cl
18 Ar
19 K
20 Ca
21 Sc
22 Ti
23 V
24 Cr
25 Mn
26 Fe
27 Co
28 Ni
29 Cu
30 Zn
31 Ga
32 Ge
33 As
34 Se
35 Br
36 Kr
37 Rb
38 Sr
39 Y
40 Zr
41 Nb
42 Mo
43 Tc
44 Ru
45 Rh
46 Pd
47 Ag
48 Cd
49 In
50 Sn
51 Sb
52 Te
53 I
54 Xe
55 Cs
56 Ba
57 La
72 Hf
73 Ta
74 W
75 Re
76 Os
77 Ir
78 Pt
79 Au
80 Hg
81 Tl
82 Pb
83 Bi
84 Po
85 At
86 Rn
87 Fr
88 Ra
89
104
105
106
107
108
109
110
111
112
r
m.p.
b.p.
IP
(pm)
(℃)
(℃)
(eV)
Cs
265.4
28.5
671
3.89
Fr
270
27
677
4.07
68 r
69 Tm
70 Yb
71 Lu
100 Fm
101 Md
102 No
103 Lr
Th
Pa
U
Np
Pu
Am
Cm
Bk
Cf
Es

Positive surface ionization source

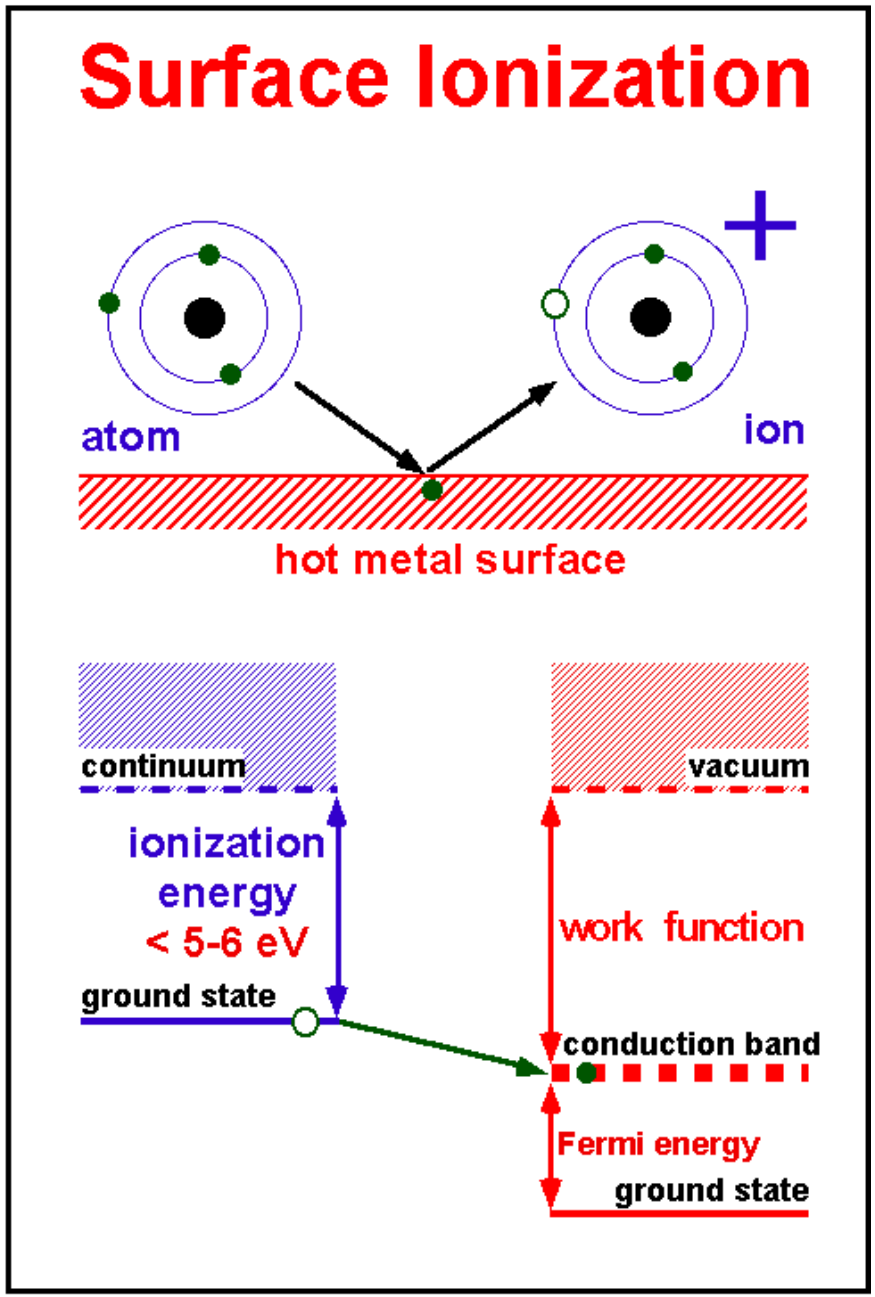

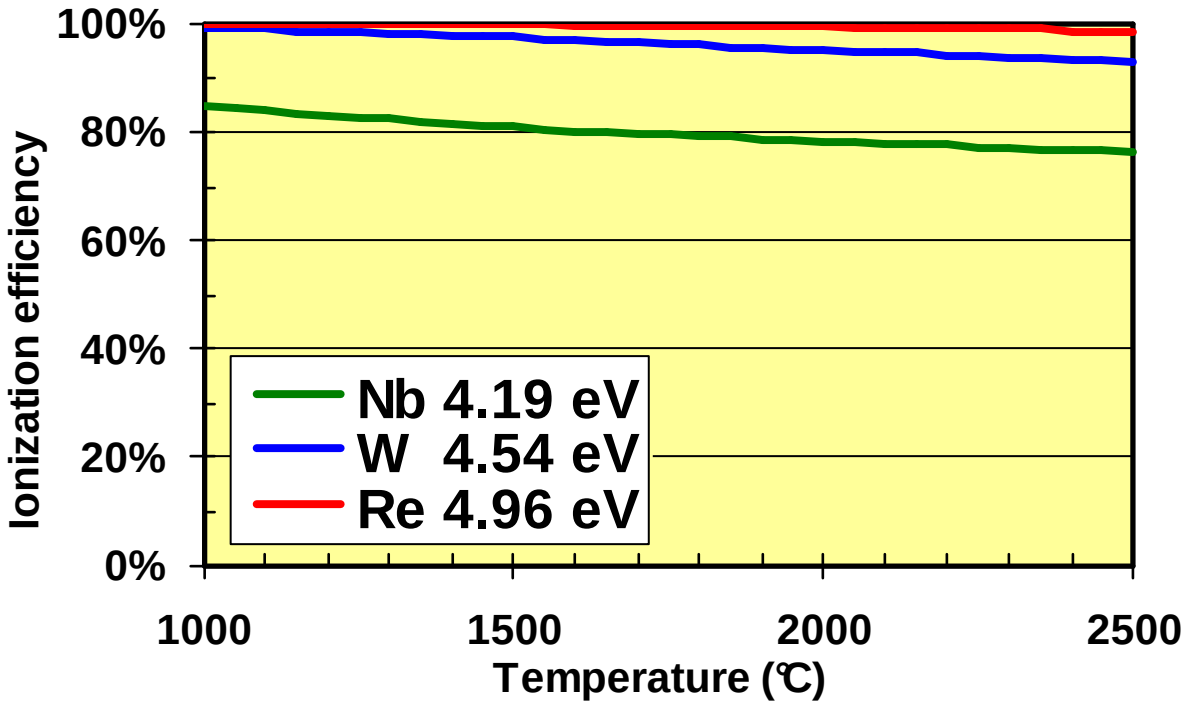

$$\alpha_s = g_+/g_0 \exp(-(IP - \Phi)/kT))$$

$$\varepsilon_s = \alpha_s / (1 + \alpha_s)$$

Saha-Langmuir equation

ε_s	surface ionization efficiency
Φ	work function of surface
IP	ionization potential of atom
g=2J+1	stat. factor (g_0=2, g_+=1 for alkalis)

Francium beam intensities

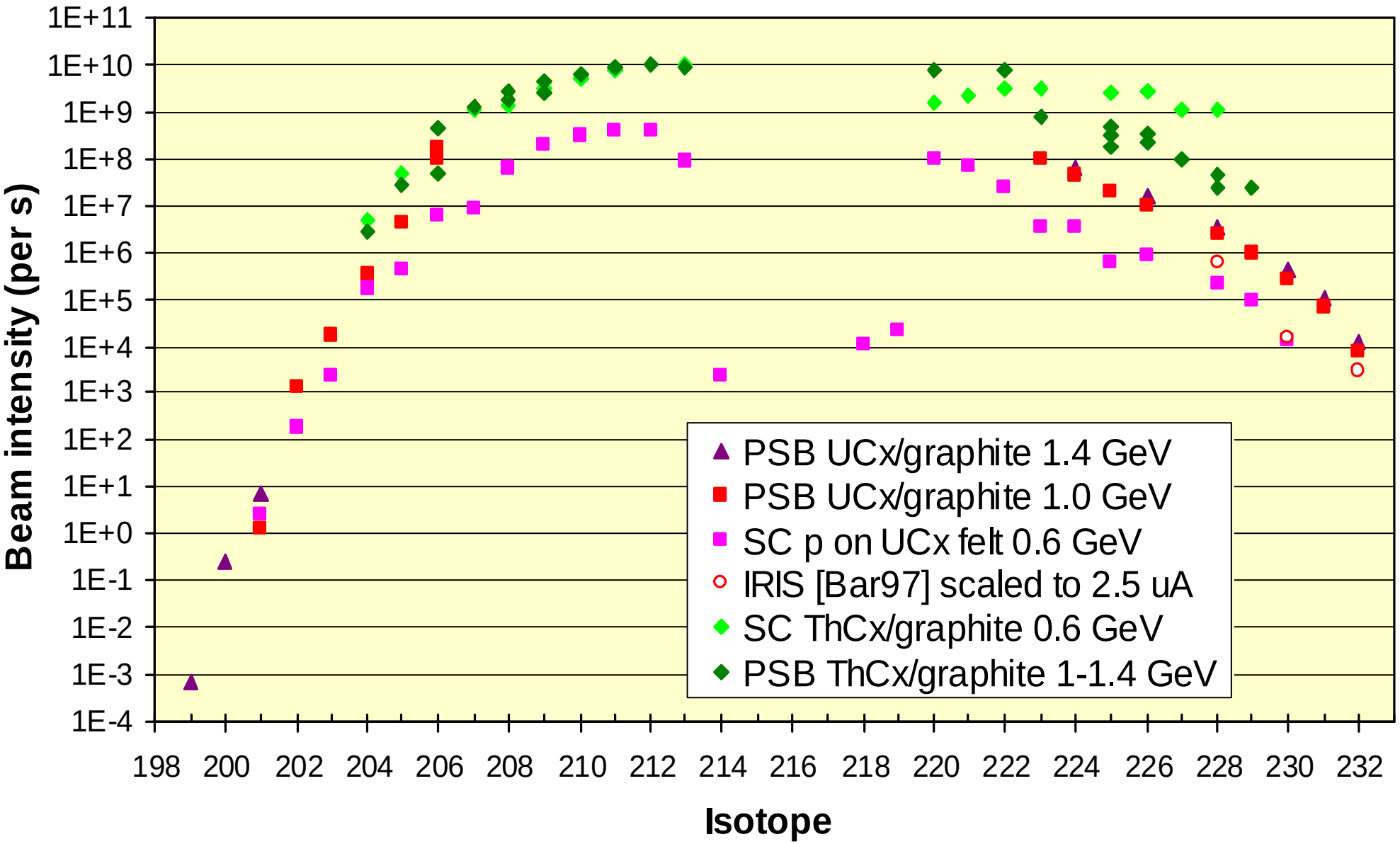

Mass separation

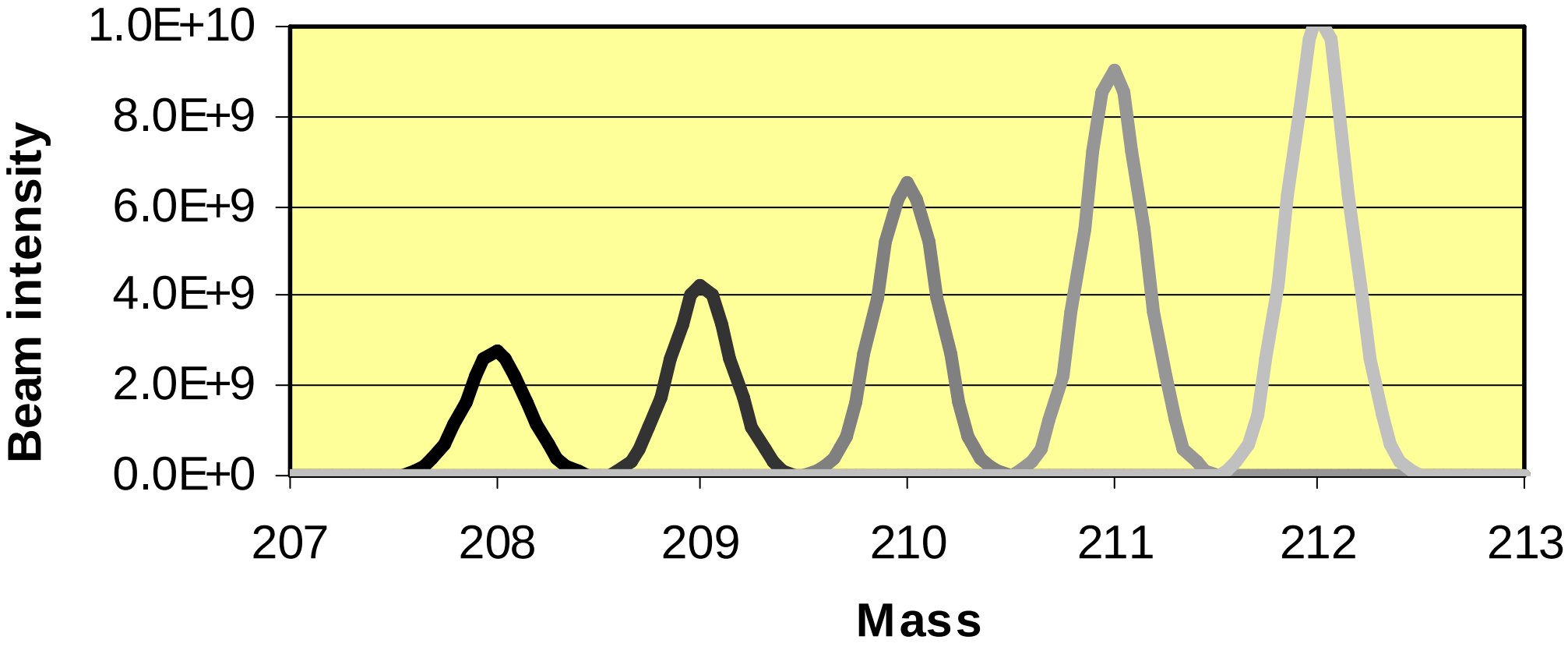

Mass separation

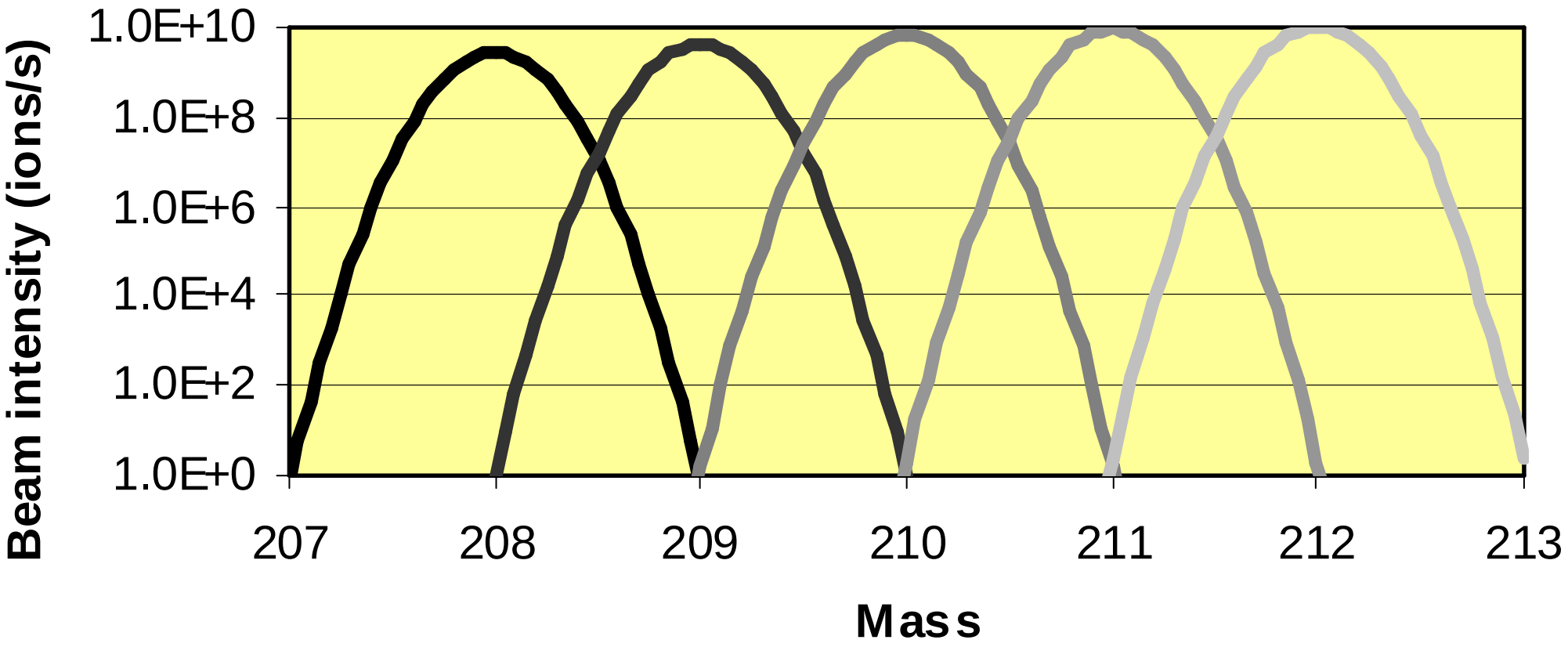

General Purpose Separator (GPS)

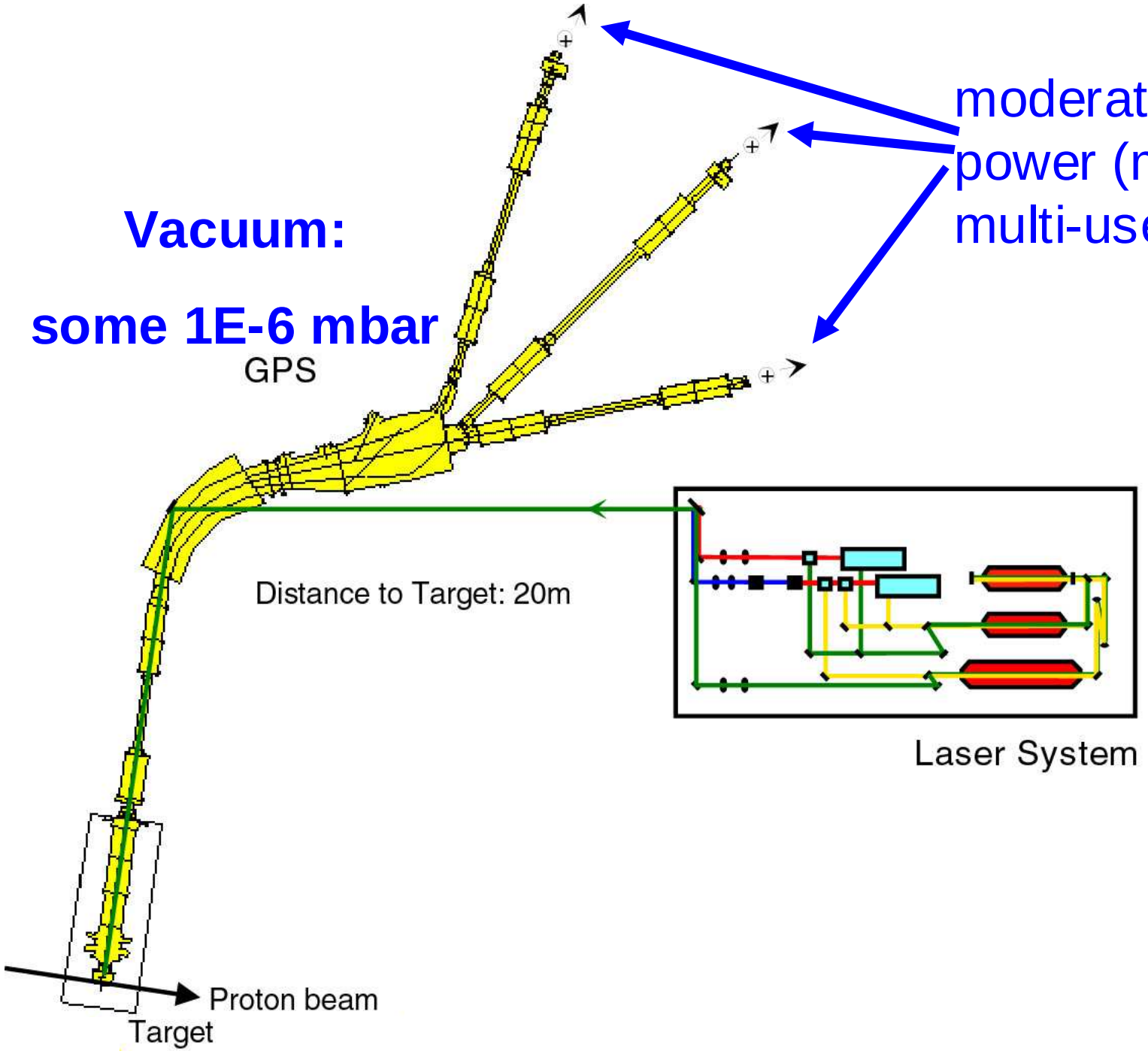

Mass separation

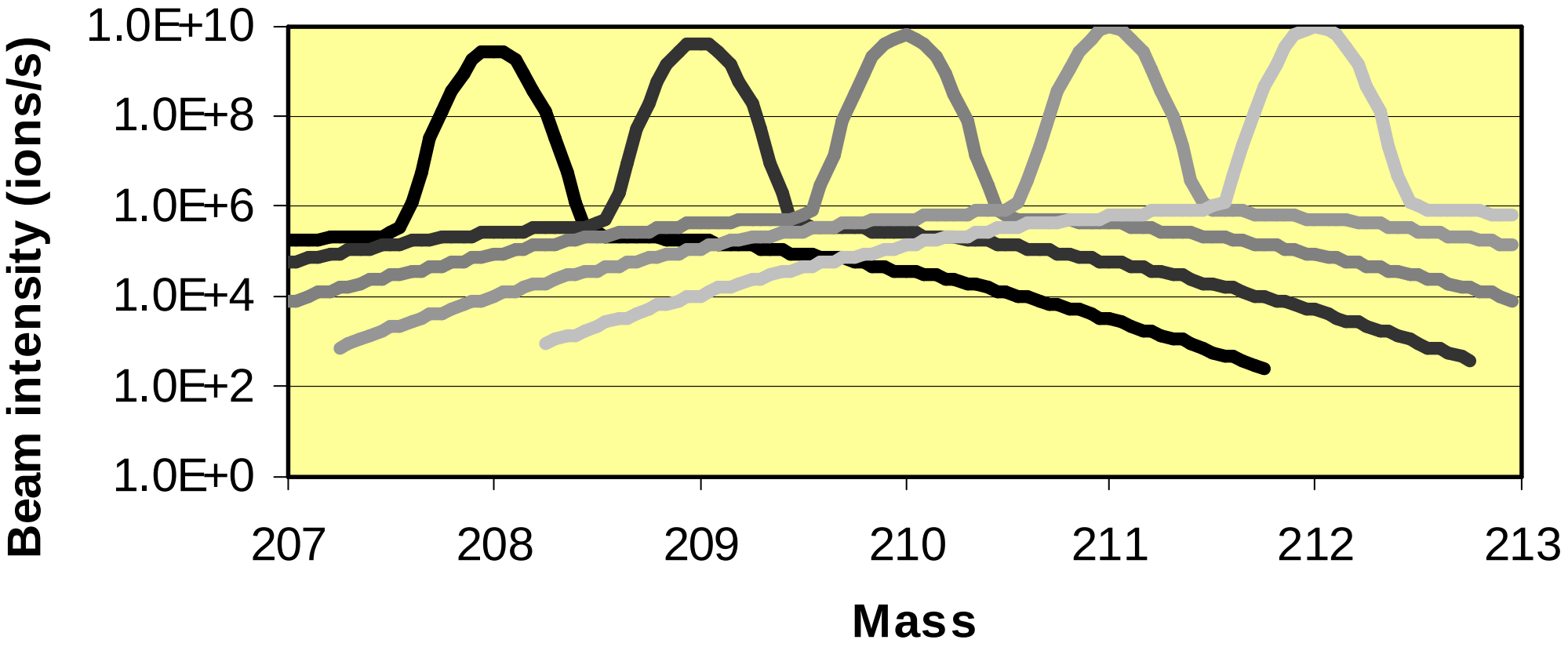

Mass separation

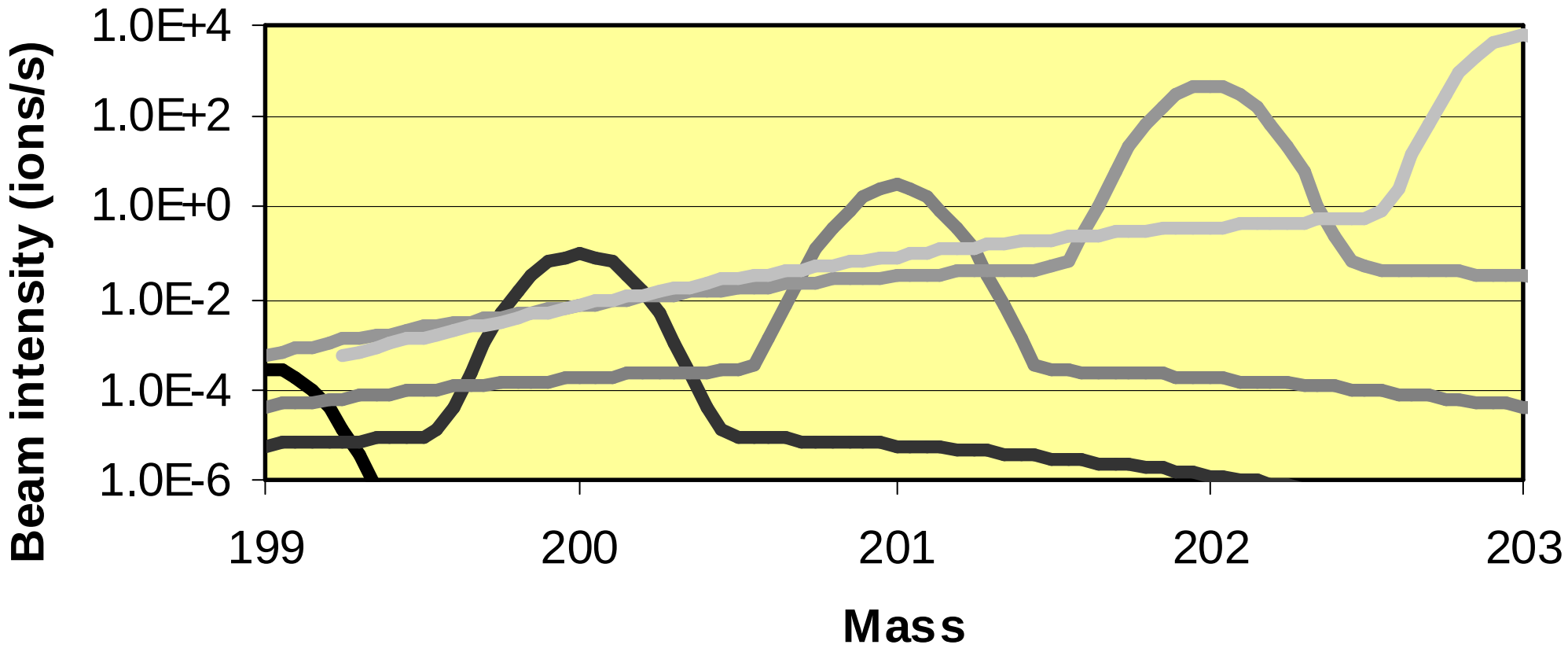

High Resolution Separator (HRS)

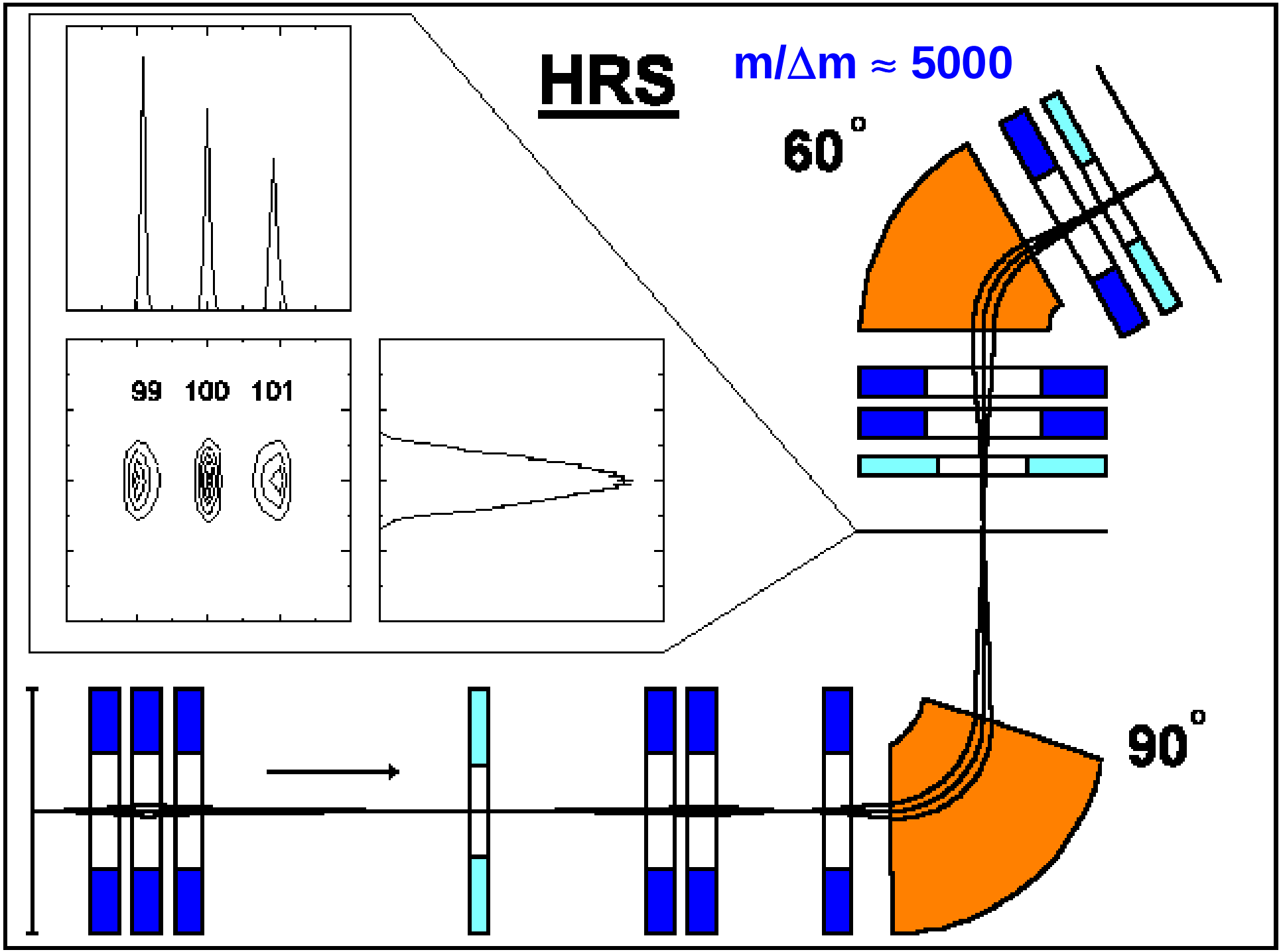

Mass separation

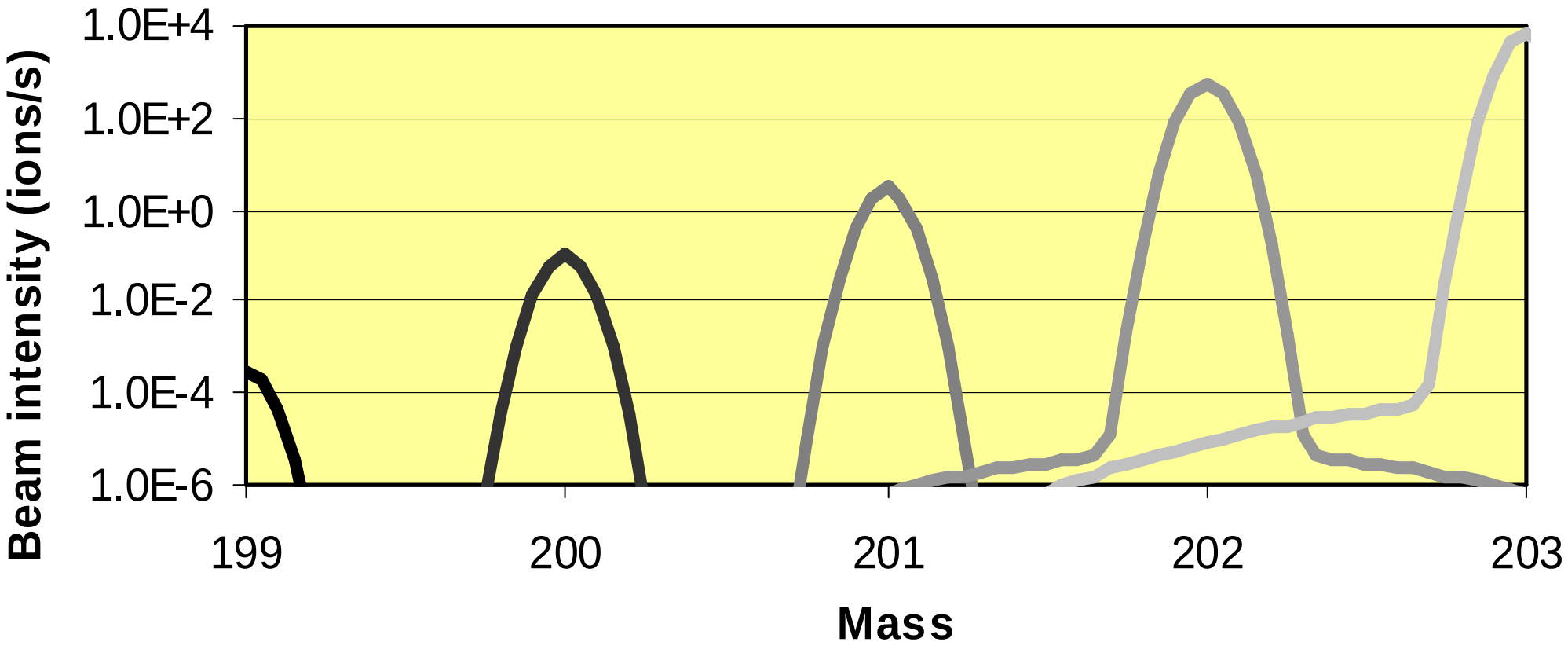

A=200 alpha energy spectrum

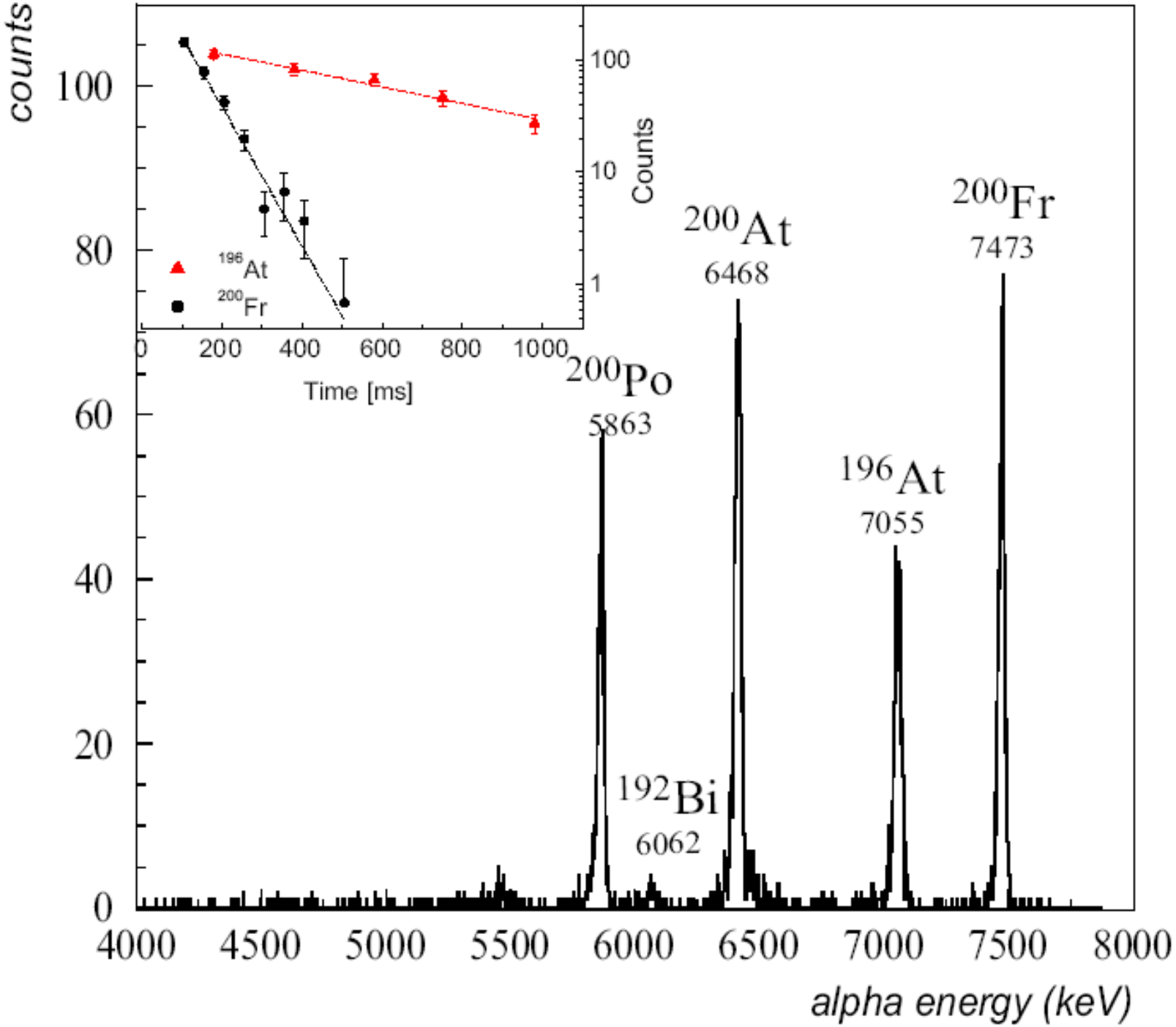

Beam transport

electrostatic beam transport is mass-independent (E=60 keV),
but has space charge limit for high beam intensities (>10 μA)
⇒ high current beams need magnetic beam transport

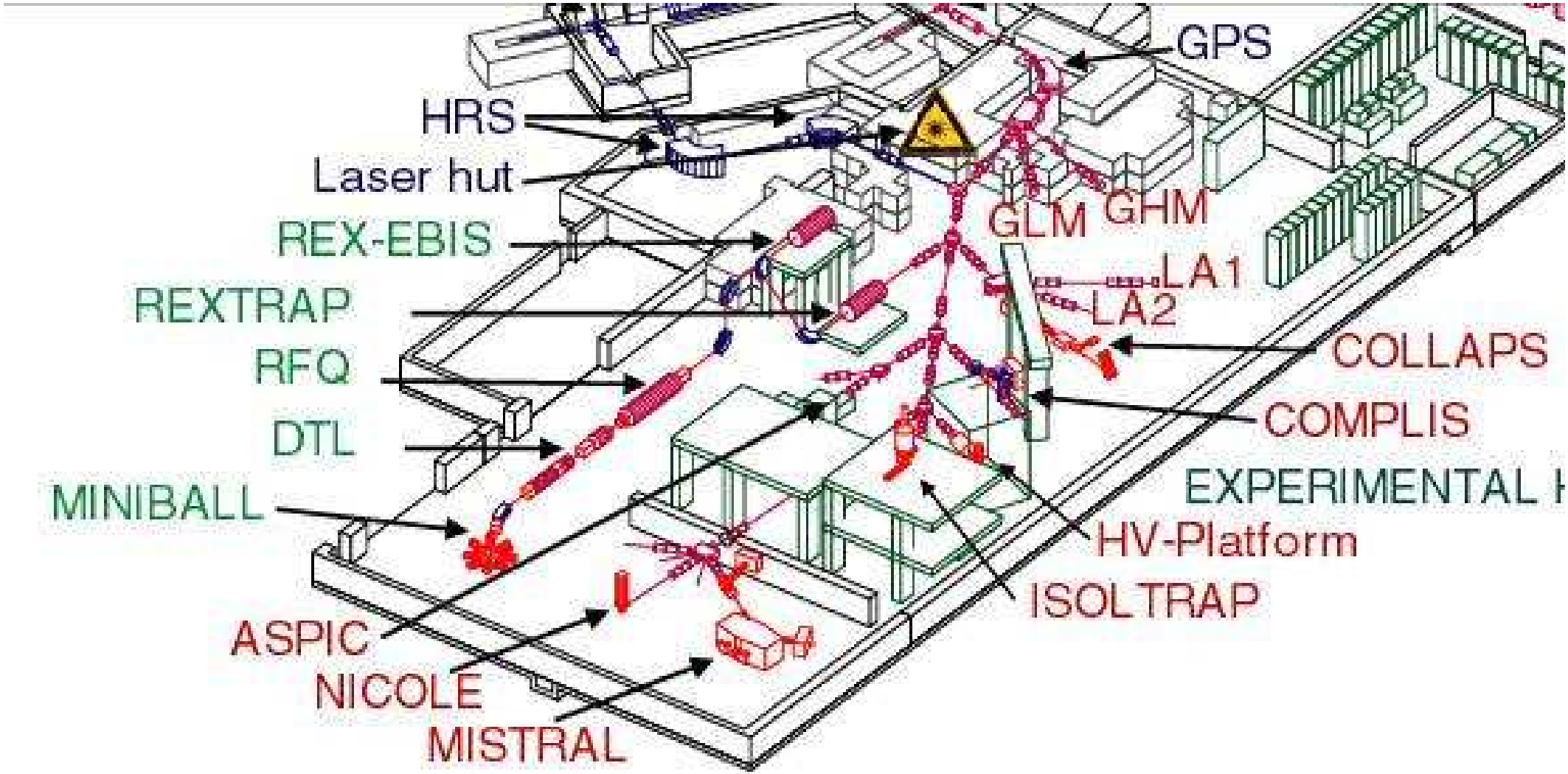

ISOLDE CERN

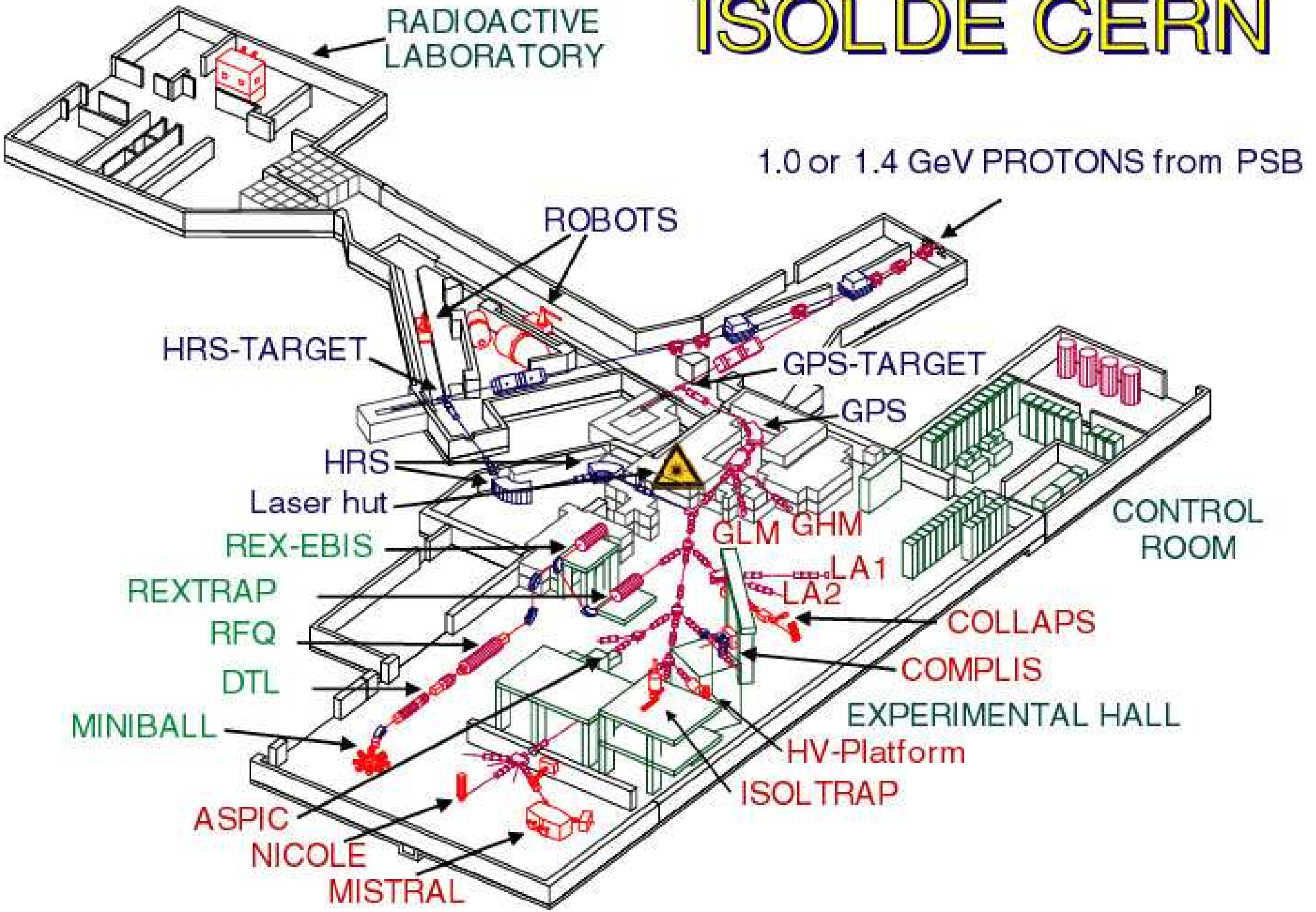
RADIOACTIVE LABORATORY
1.0 or 1.4 GeV PROTONS from PSB
ROBOTS
HRS-TARGET
GPS-TARGET
GPS
HRS
Laser hut
REX-EBIS
REXTRAP
RFQ
DTL
MINIBALL
ASPIC
NICOLE
MISTRAL
GLM
GHM
LA1
LA2
COLLAPS
COMPLIS
HV-Platform
ISOLTRAP
CONTROL ROOM
EXPERIMENTAL HALL

Applications

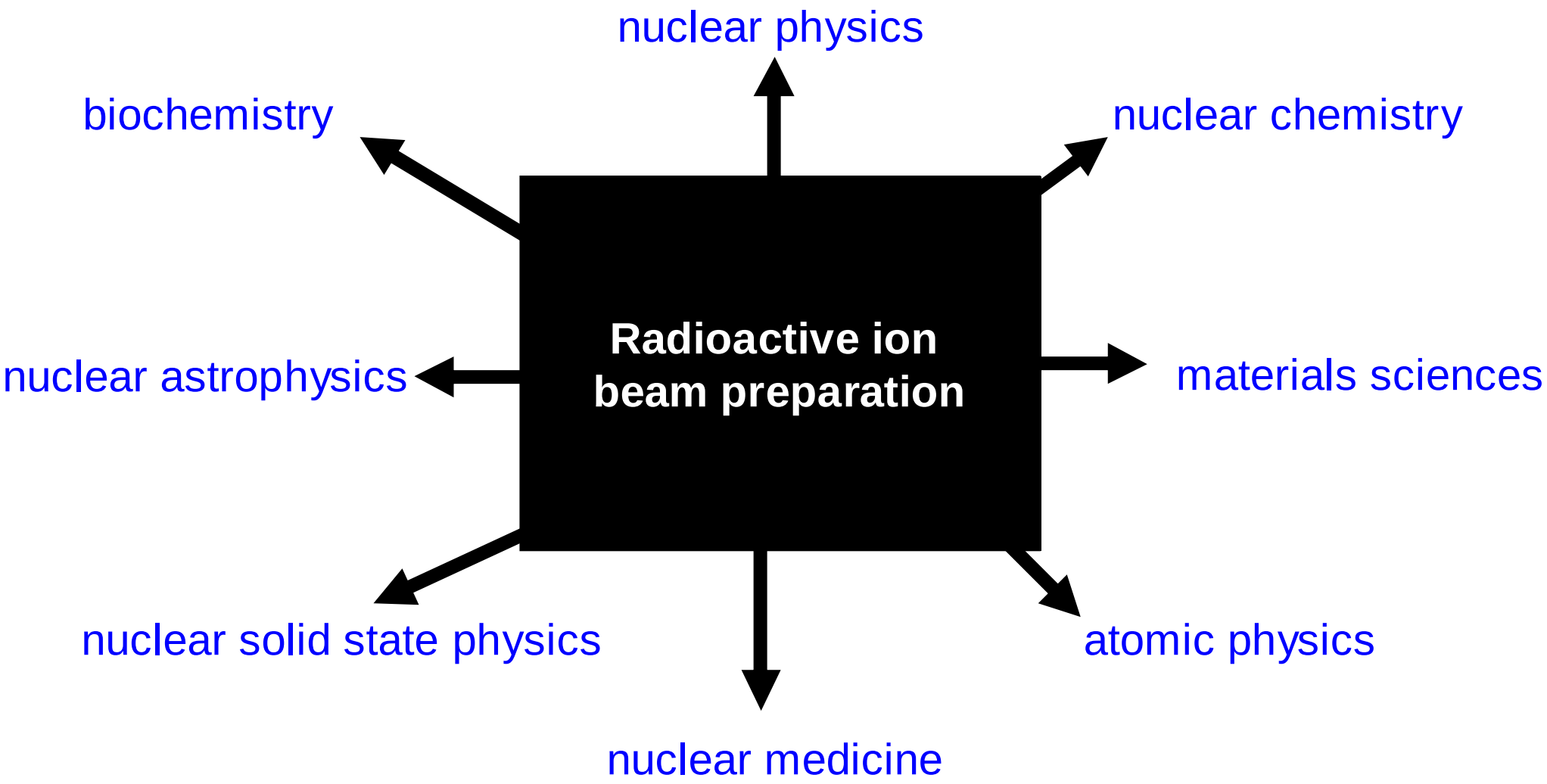

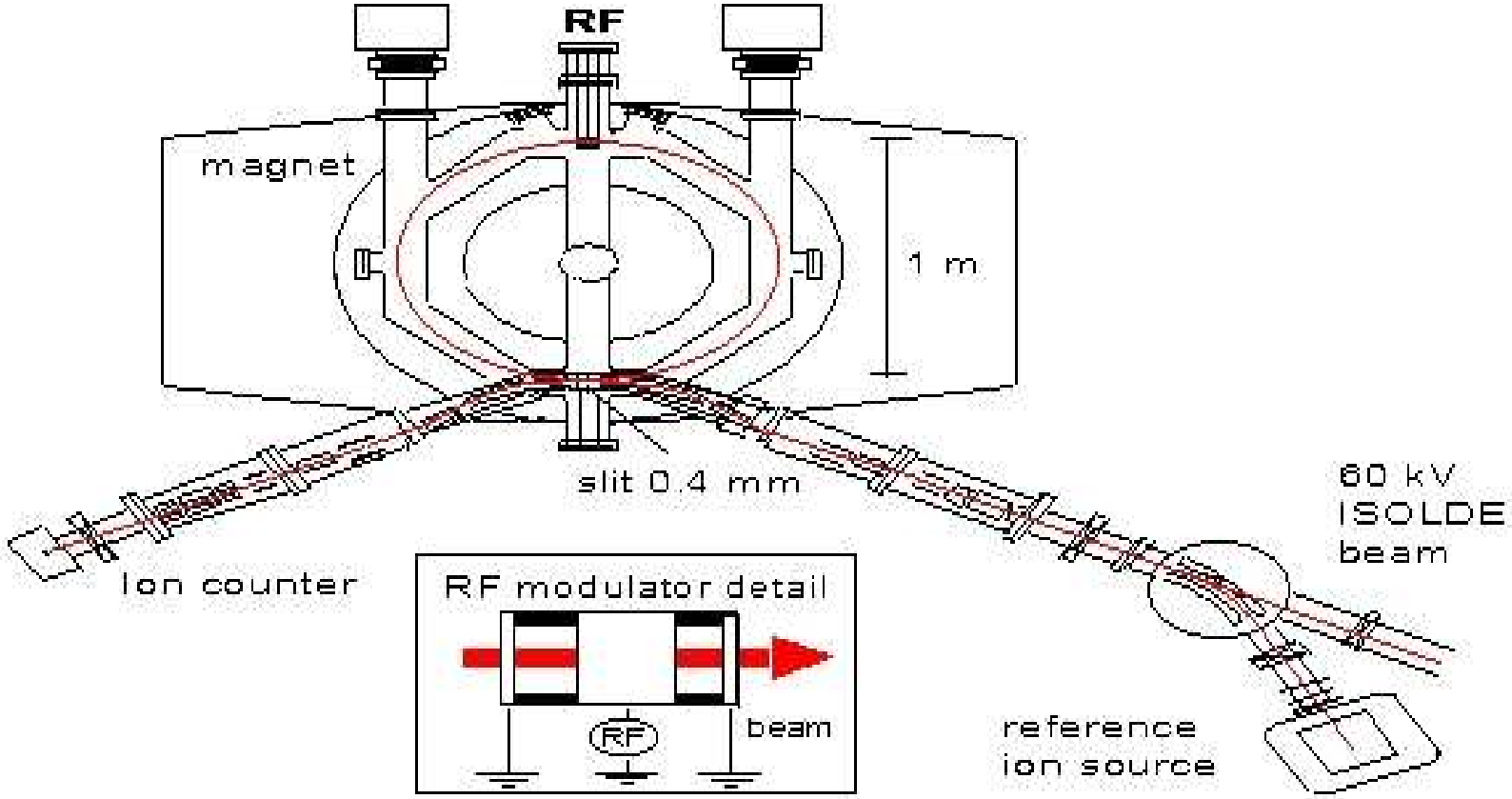

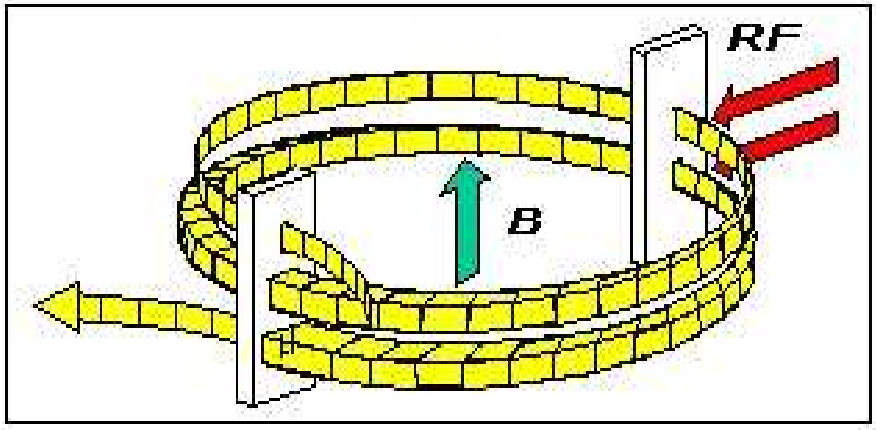

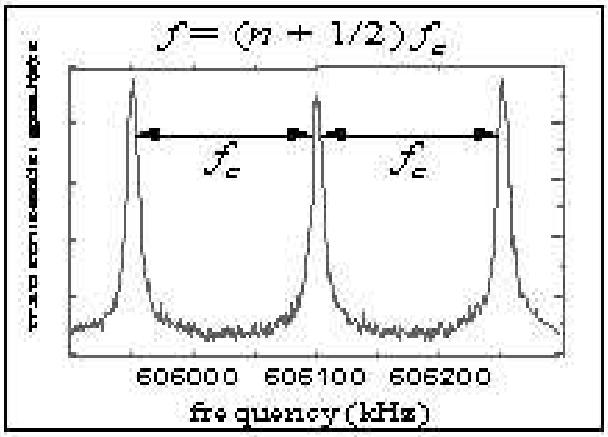

M. de Saint Simon et al., Phys. Scr. T59 (1995) 406.

Mass measurement of ^{11}Li ($T_{1/2}$ = 9 ms)

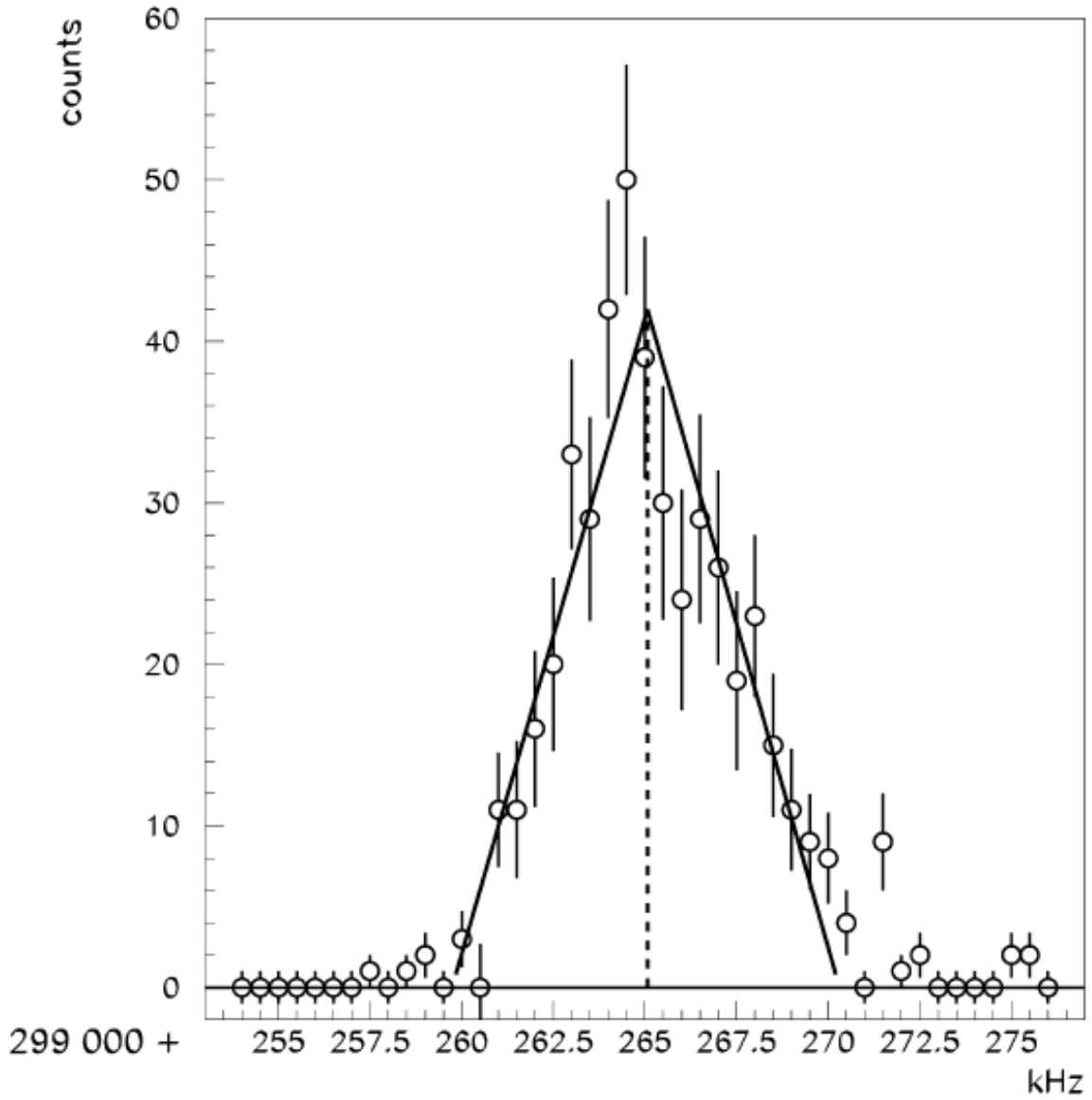

Fig. 2. Example of accumulated transmission peak for ^{11}Li. The center position (299 265 kHz) corresponds to the 917th harmonic of the cyclotron frequency. With a *RF* power of 100 W, a mass resolving power of $\frac{\Delta M}{M} \sim 57\,000$ was achieved.

C. Bachelet et al., Phys. Rev. Lett. 100 (2008) 182501.

Retardation spectrometer

- electrostatic energy measurement
- charged particles move against electrostatic potential; transmission measured as function of repulsive potential
- analyzes only the energy component perpendicular to the analyzer
- total energy measurement requires perfectly parallel beam

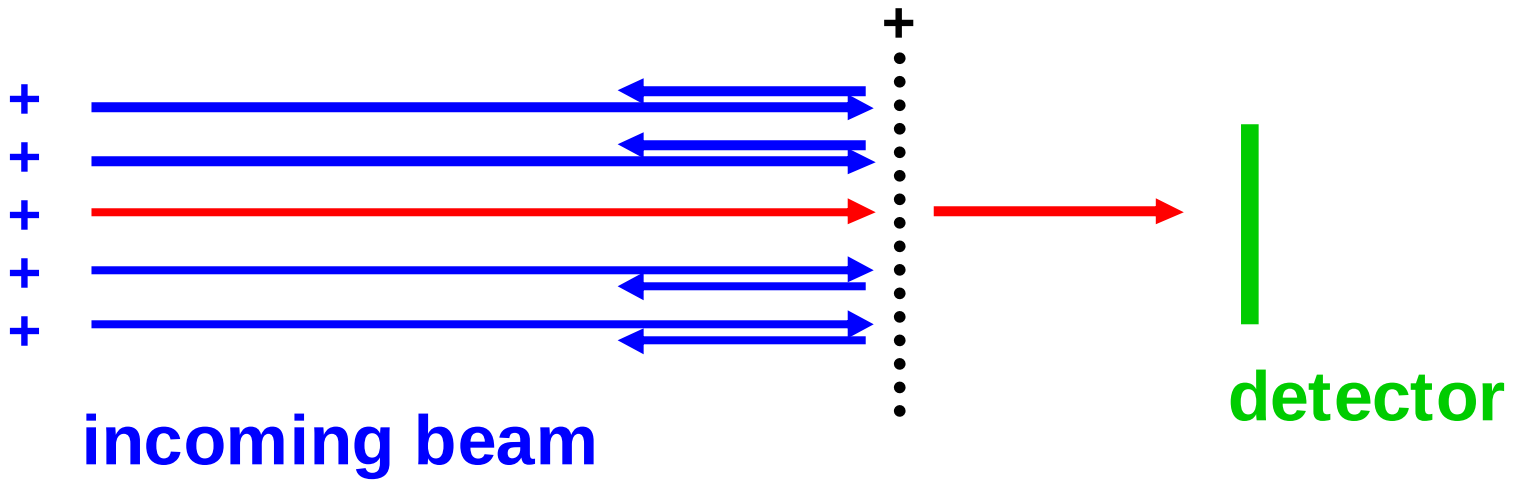

Examples of MAC-E retardation spectrometer

1. **WITCH at ISOLDE: weak interaction studies via recoil detection after EC/β^+ decay**
2. **ASPECT at ILL: precision spectroscopy of angular correlation between neutron spin and decay protons**
3. **KATRIN in Karlsruhe: precision measurement of beta endpoint in tritium decay for neutrino mass determination**

ß-decay and neutrino mass

model independent neutrino mass from ß-decay kinematics

$$\frac{\mathrm{d}\Gamma_i}{\mathrm{d}E} = C\,p\,(E+m_e)\,(E_0-E)\,\sqrt{(E_0-E)^2-m_i^2}\,F(E)\,\theta(E_0-E-m_i)$$

$$C = G_F^2\frac{m_e^5}{2\,\pi^3}\,\cos^2\theta_C\,|M|^2$$

experimental observable is m_ν^2

E_0 = 18.6 keV
$T_{1/2}$ = 12.3 y

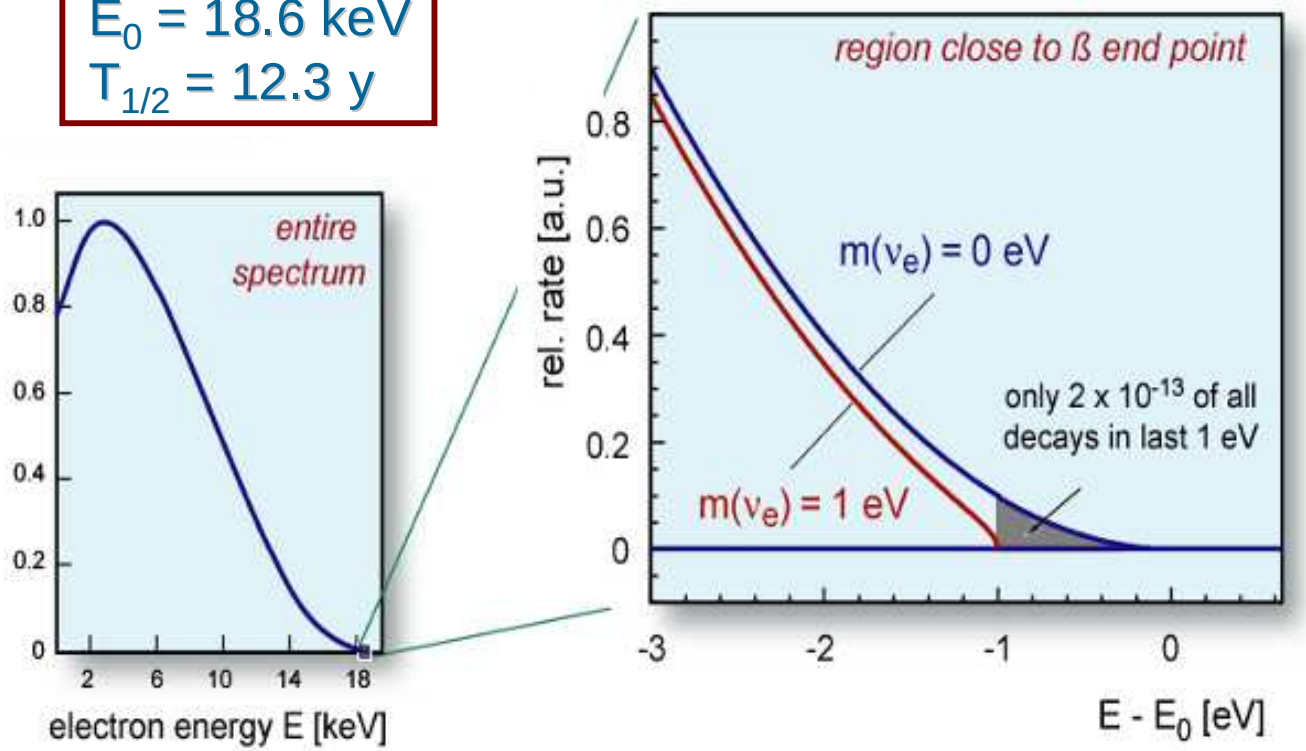

ß-source requirements :

- high ß-decay rate (short $t_{1/2}$)
- low ß-endpoint energy E_0
- superallowed ß-transition
- few inelastic scatters of ß's

ß-detection requirements :

- high resolution (ΔE< few eV)
- large solid angle (ΔΩ ~ 2π)
- low background

Electrostatic filter with Magnetic Adiabatic Collimation

MAC-E-Technique

adiabatic guiding of ß-particles along the magnetic field lines

inhomogen. B-Feld: stray field of 2 super-conducting magnets

B_{max} = 3 - 6 T

B_{min} < 1 mT

very large solid angle !

$\Delta\Omega \sim 2\pi$

$$\vec{F} = (\vec{\mu} \cdot \vec{\nabla})\,\vec{B} + q\,\vec{E}$$

$$\mu = E_{\perp} / B = \text{const}$$

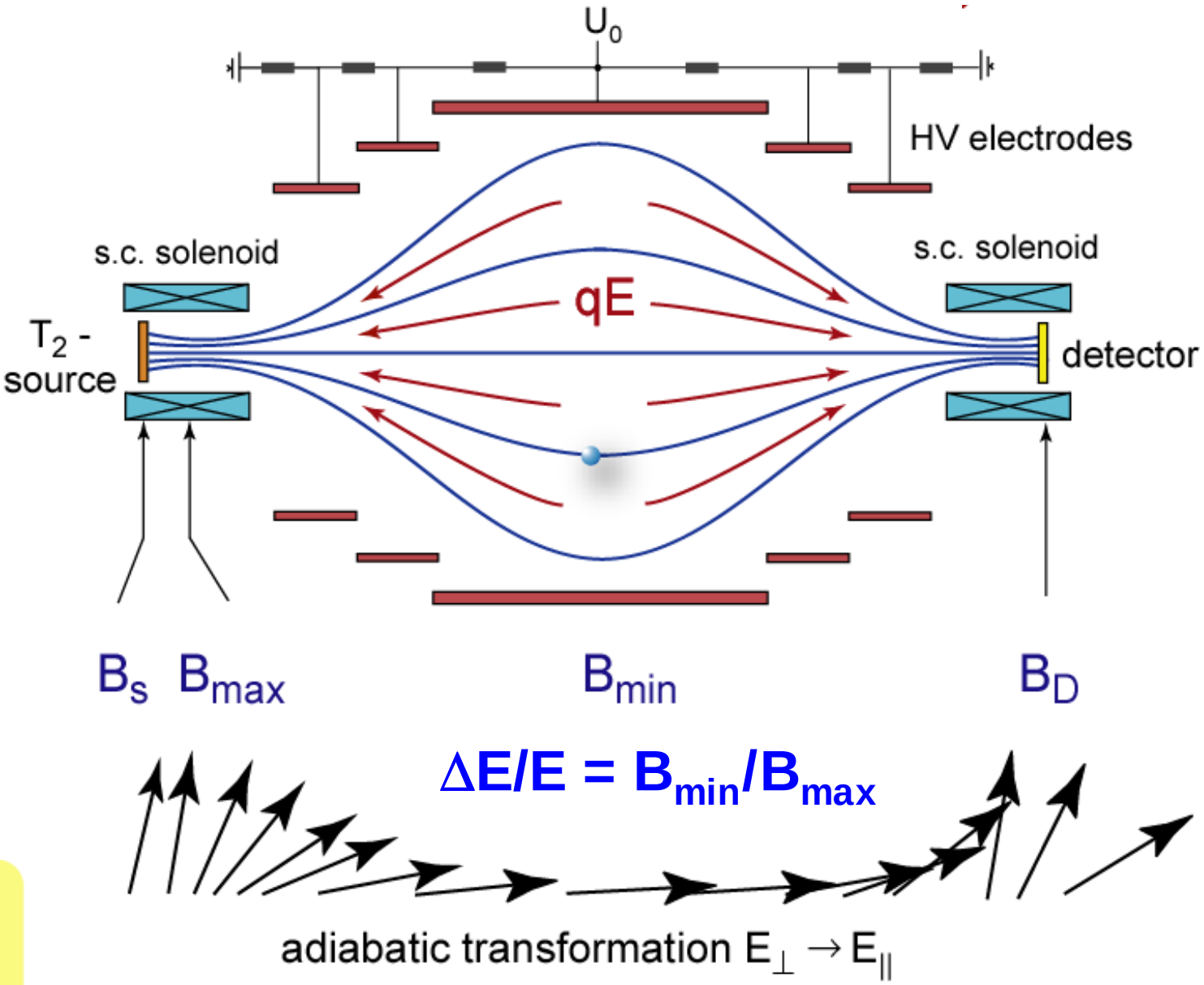

A. Picard et al., Nucl. Instr. Meth. B63 (1992) 345.

KATRIN experiment

Karlsruhe **Tri**tium **N**eutrino Experiment

at Forschungszentrum Karlsruhe
unique facility for closed T_2 cycle:
Tritium Laboratory Karlsruhe

40 g ^{3}H per day

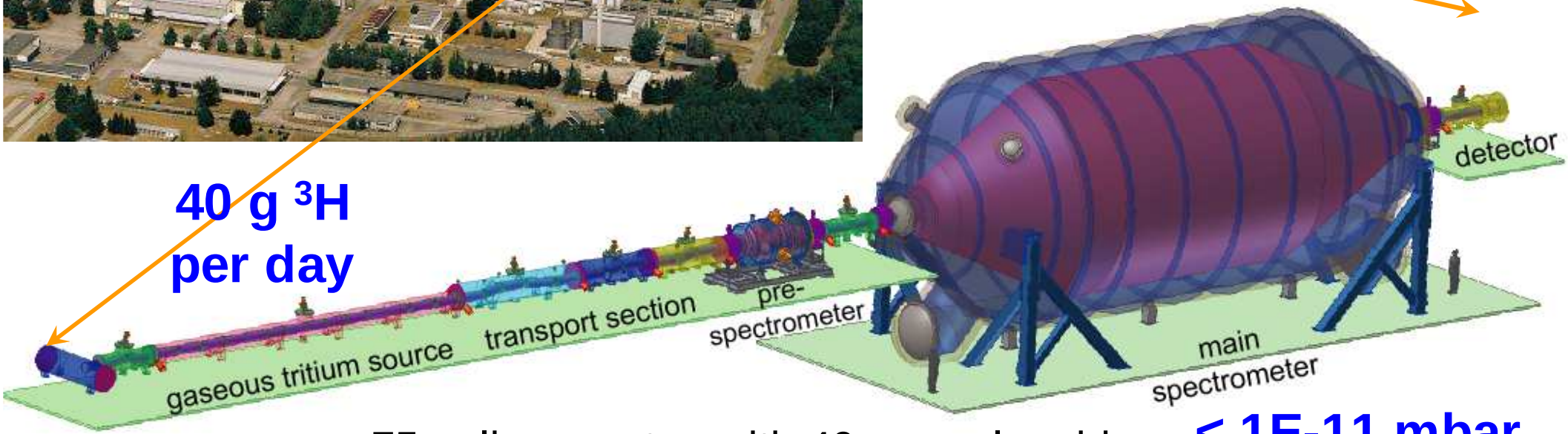

~ 75 m linear setup with 40 s.c. solenoids

< 1E-11 mbar
< 1E-20 mbar ^{3}H

main spectrometer – design

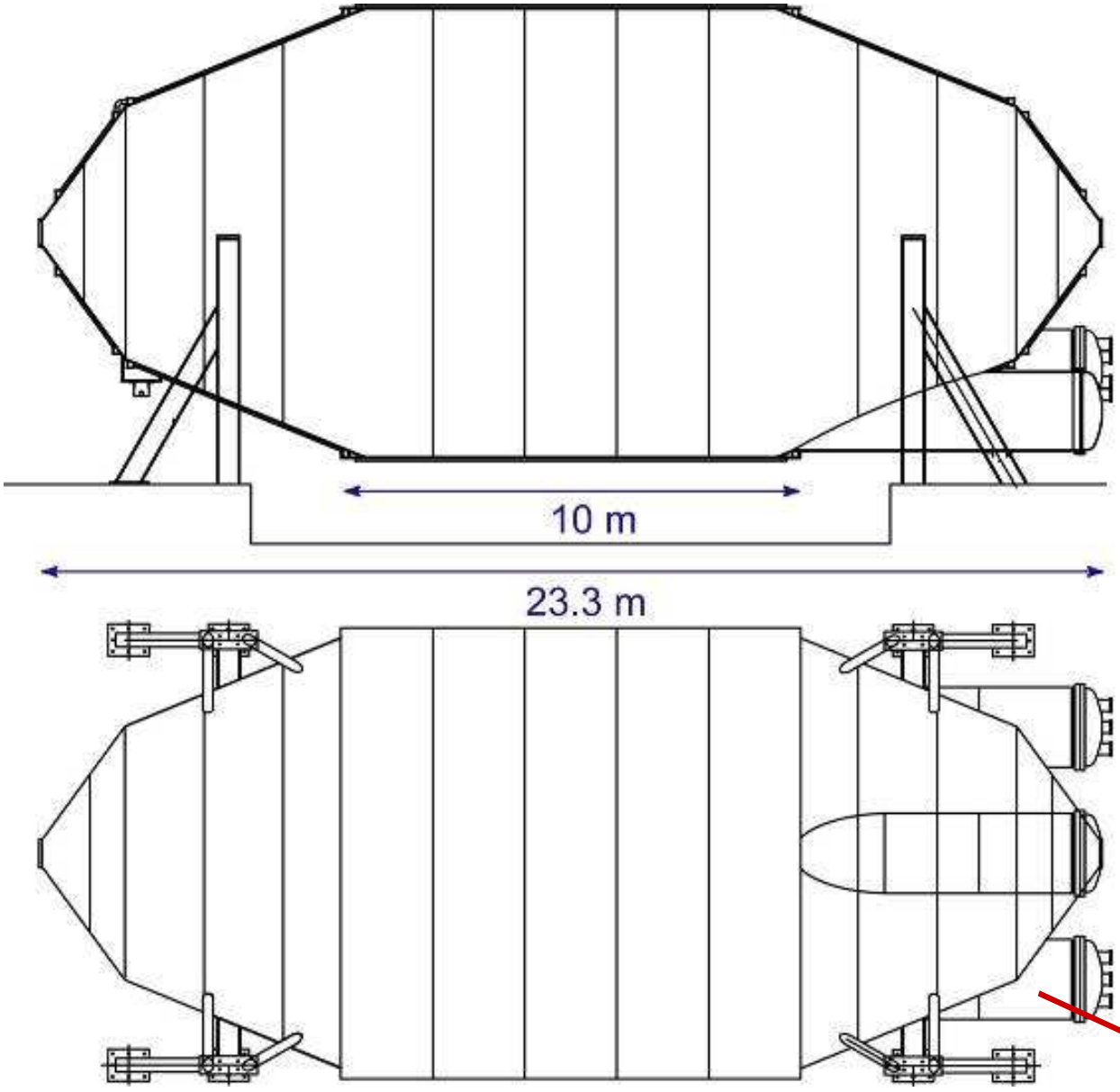

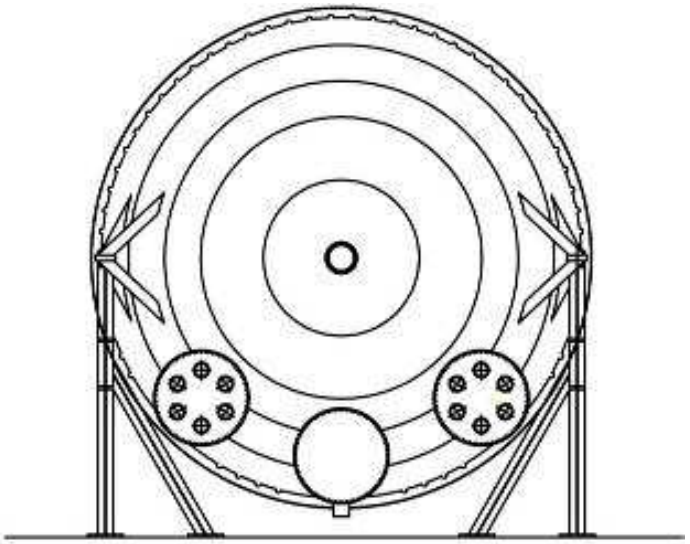

design parameters:

volume:	1258 m^3
surface:	605 m^2
thickness:	32 mm
material	1.4429
weight:	192 t

pumping port
for getters

UNITED KINGDOM
IRELAND
Belfast
Dublin
Irish Sea
Isle of Man (U.K.)
Leeds
Manchester
Liverpool
Birmingham
Cardiff
London
Celtic Sea
Guernsey (U.K.)
Jersey (U.K.)
Amsterdam
NETH.
Rotterdam
Brussels
Lille
BEL.
Paris
Nantes
Bay of Biscay
FRANCE
Bordeaux
MASSIF CENTRAL
Lyon
Toulouse
Andorra la Vella
ANDORRA
PYRENEES
Marseille
MONACO
Bilbao
Porto
PORTUGAL
Lisbon
Madrid
Zaragoza
Barcelona
SPAIN
Valencia
Sevilla
Gibraltar (U.K.)
Málaga
Strait of Gibraltar
Ceuta (SPAIN)
Alborán Sea
Melilla (SPAIN)
Oran
Rabat
Casablanca
MOROCCO
ALGERIA
Algiers
Tunis
TUNISIA
Balearic Sea
BALEARIC ISLANDS
Mediterranean Sea
Corsica
Sardinia
Cagliari
Ligurian Sea
Florence
Genoa
Turin
Milan
Venice
SAN MARINO
ITALY
Rome
VATICAN CITY
Naples
Palermo
Sicily
Tyrrhenian Sea
Adriatic Sea
Ionian Sea
Valletta
MALTA
Scale 1: 19,500,000
Lambert Conformal Conic Projection, standard parallels 40°N and 56°N
0 300 Kilometers
0 300 Miles
DENMARK
Copenhagen
Malmö
Bornholm
Hamburg
Bremen
Berlin
Leipzig
Essen
Cologne
Bonn
GERMANY
Frankfurt am Main
Luxembourg
LUX.
Stuttgart
Strasbourg
Munich
LIECH.
Zürich
Bern
SWITZ.
Vaduz
Geneva
AUSTRIA
Vienna
Prague
CZECH REPUBLIC
Brno
Bratislava
SLOVAKIA
Budapest
HUNGARY
Kaliningrad
RUSSIA
Gdańsk
Poznań
POLAND
Warsaw
Łódź
Wrocław
Kraków
Vilnius
Minsk
Mahilyow
BELARUS
Hrodna
Homyel'
Brest
Kiev
Rivne
UKRAINE
L'viv
Chernivtsi
Mykolayiv
Chişinău
Iaşi
MOLDOVA
Odes
Cluj-Napoca
ROMANIA
Bucharest
Constanţa
Black Sea
Varna
BULGARIA
Sofia
Istanbul
Bursa
Izmir
Aegean Sea
TURKEY
Thessaloniki
GREECE
Athens
Rhodes
Crete
Ljubljana
SLOVENIA
Zagreb
CROATIA
BOSNIA AND HERZEGOVINA
Belgrade
Serbia
Sarajevo
Montenegro
Podgorica
Skopje
F.Y.R.O.M.
Tirana
ALB.

Applications

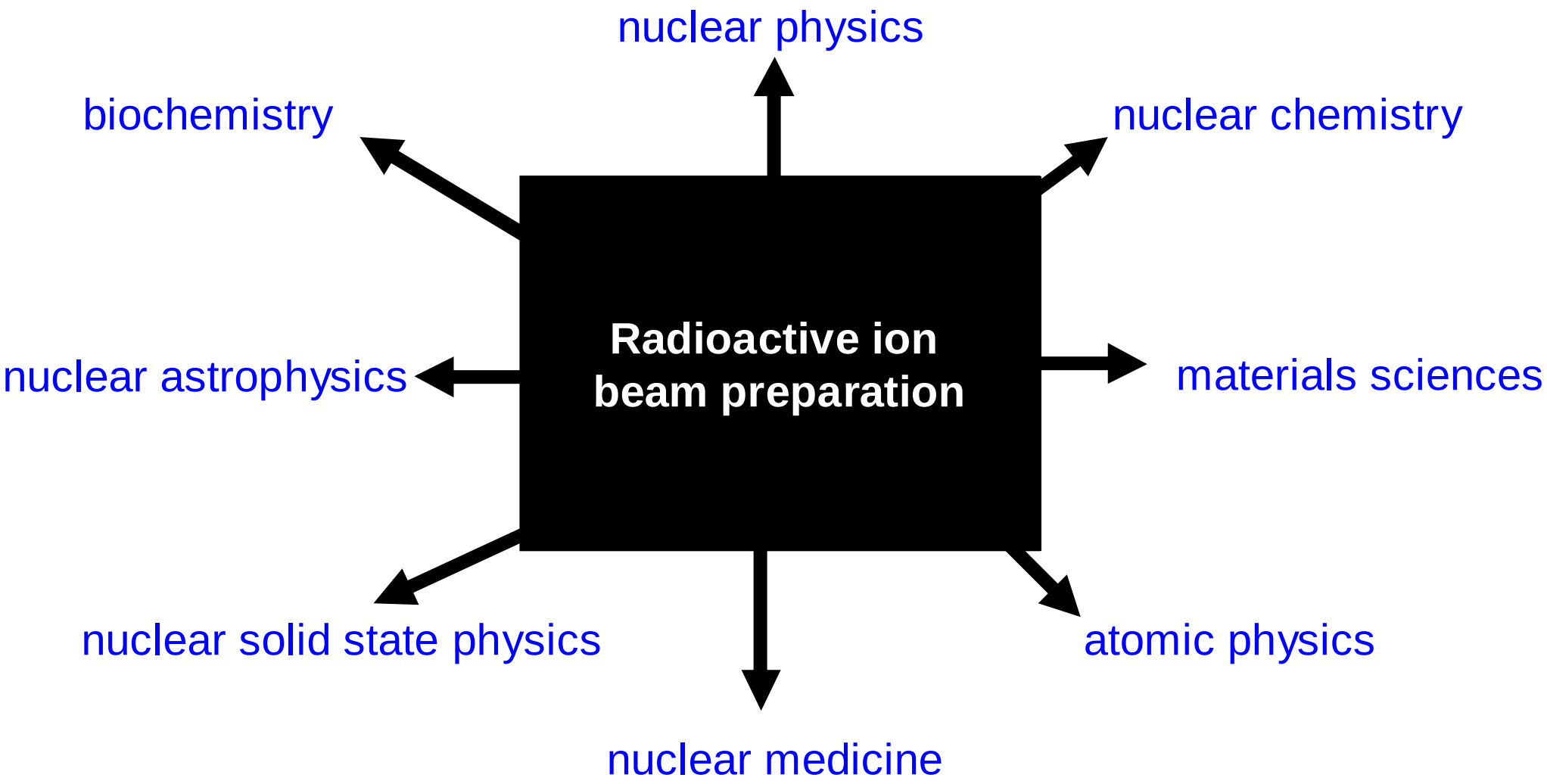

Production of ^{12}C in stars

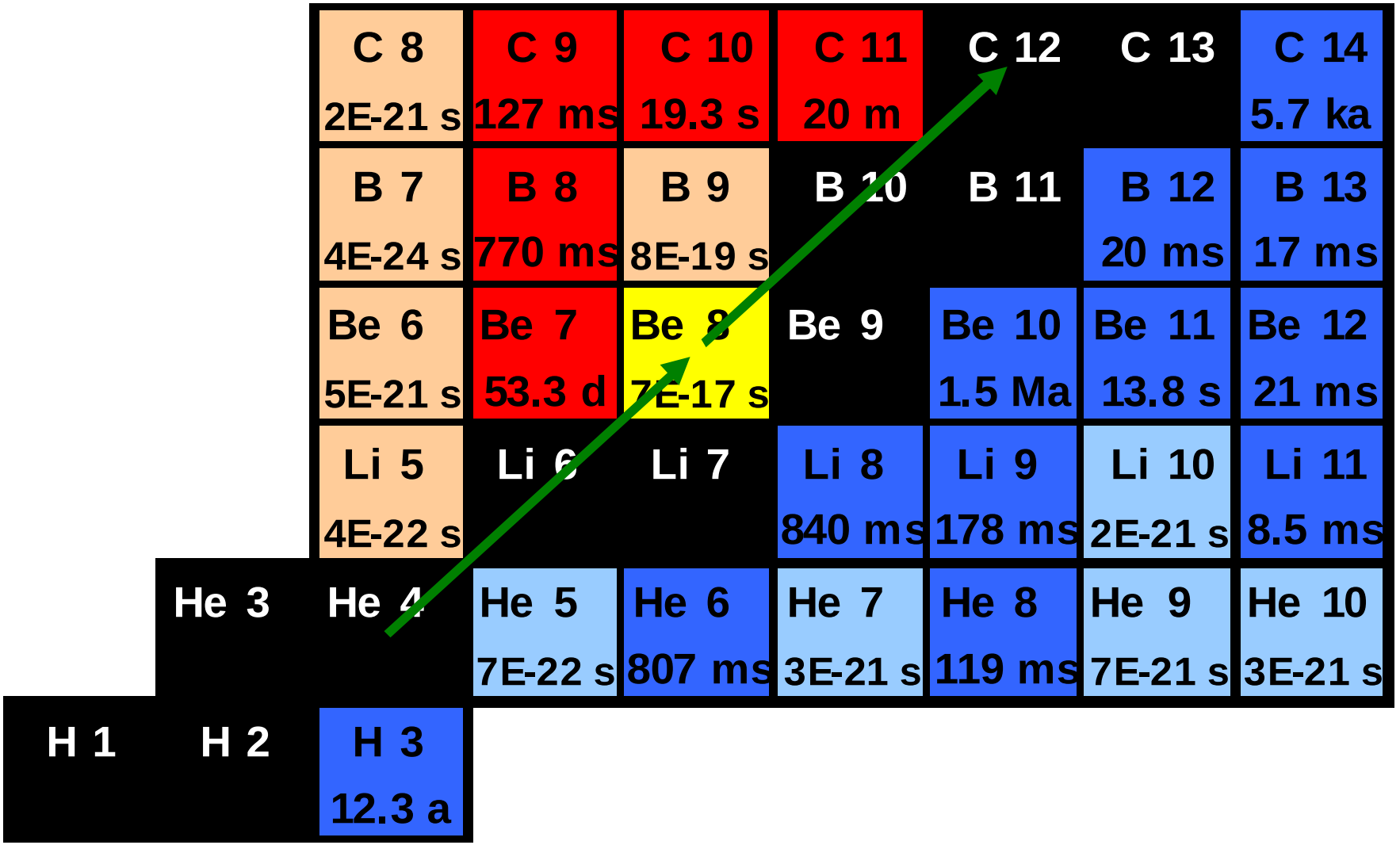

The triple-alpha process: rate

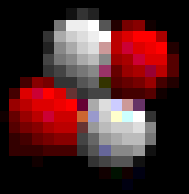

$^{4}_{2}He_{2}$

The triple-alpha process

$$r_{3\alpha} \propto \Gamma_{rad}\, e^{-Q/kT}$$

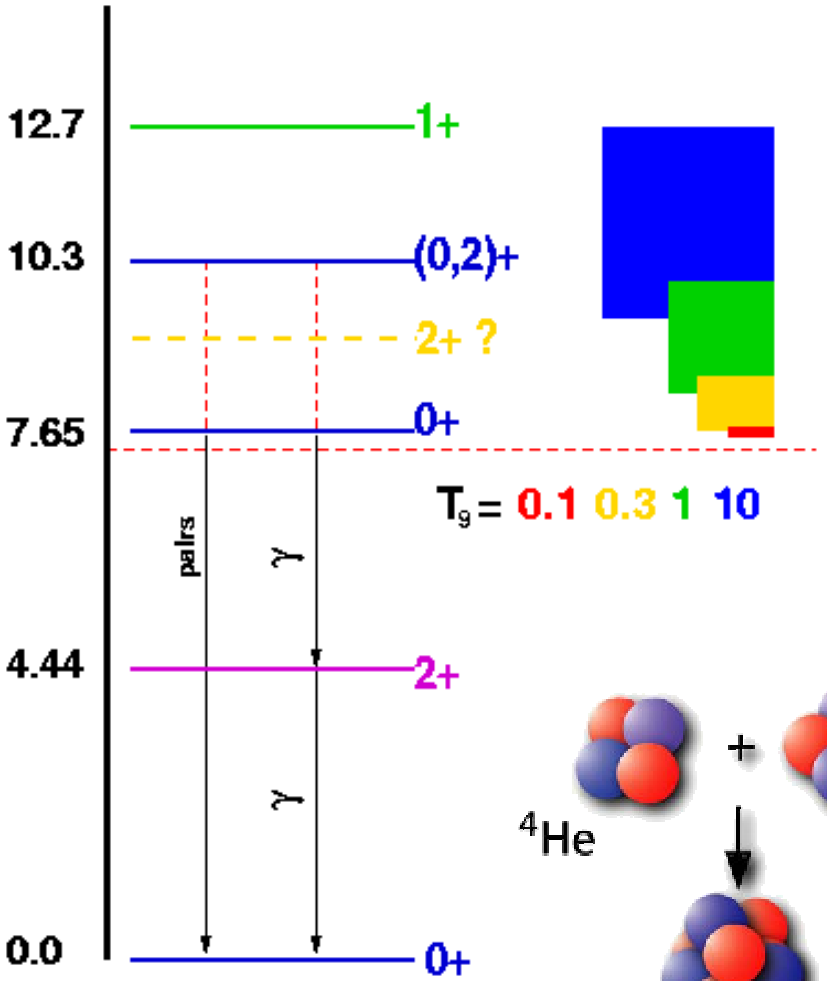

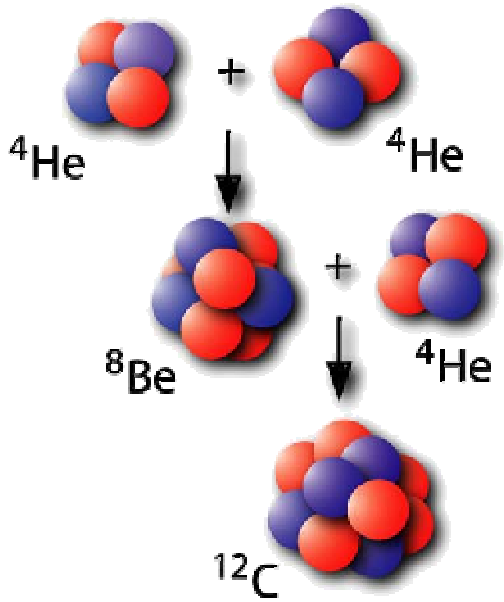

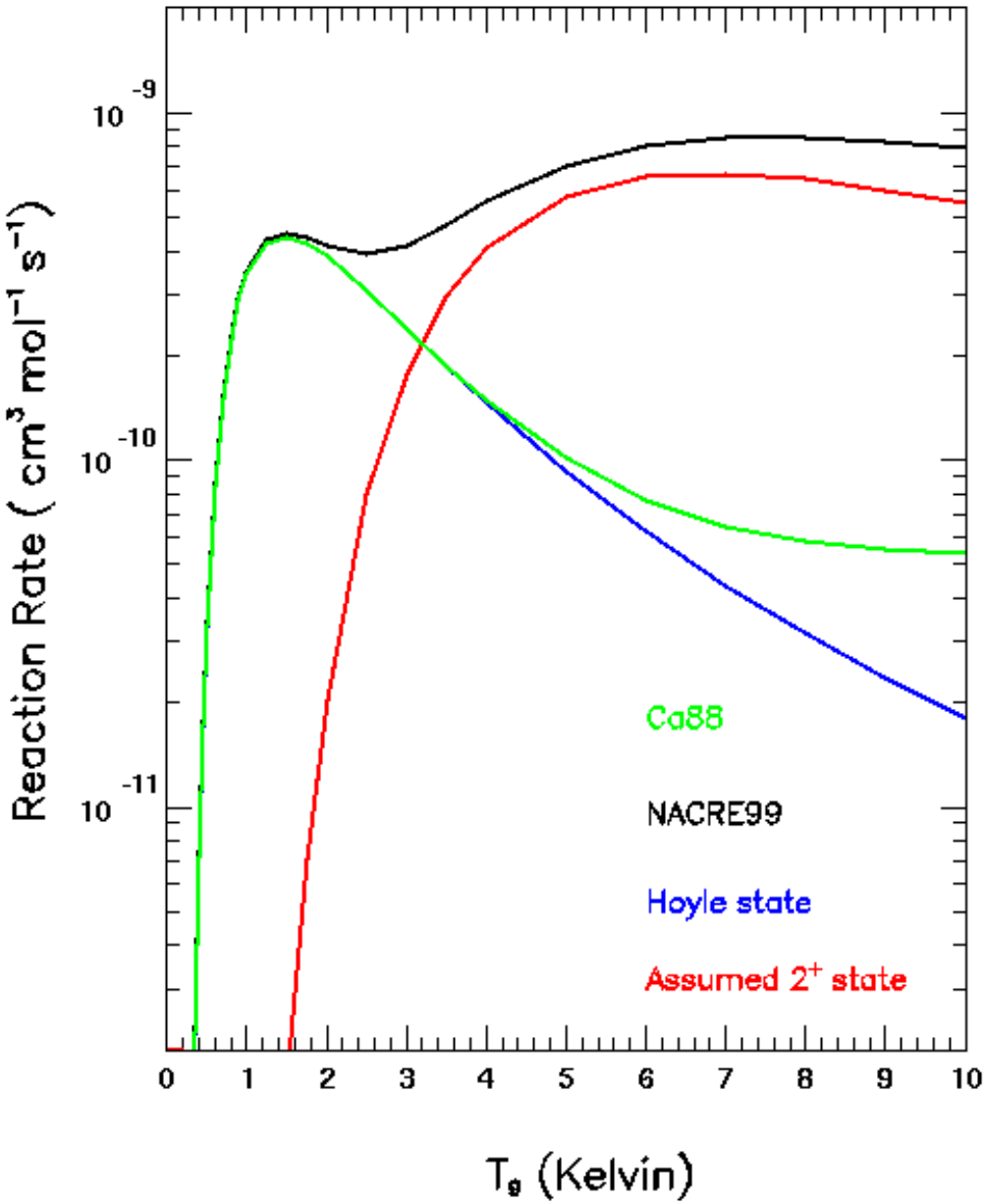

Setup for study of three-body-fusion?

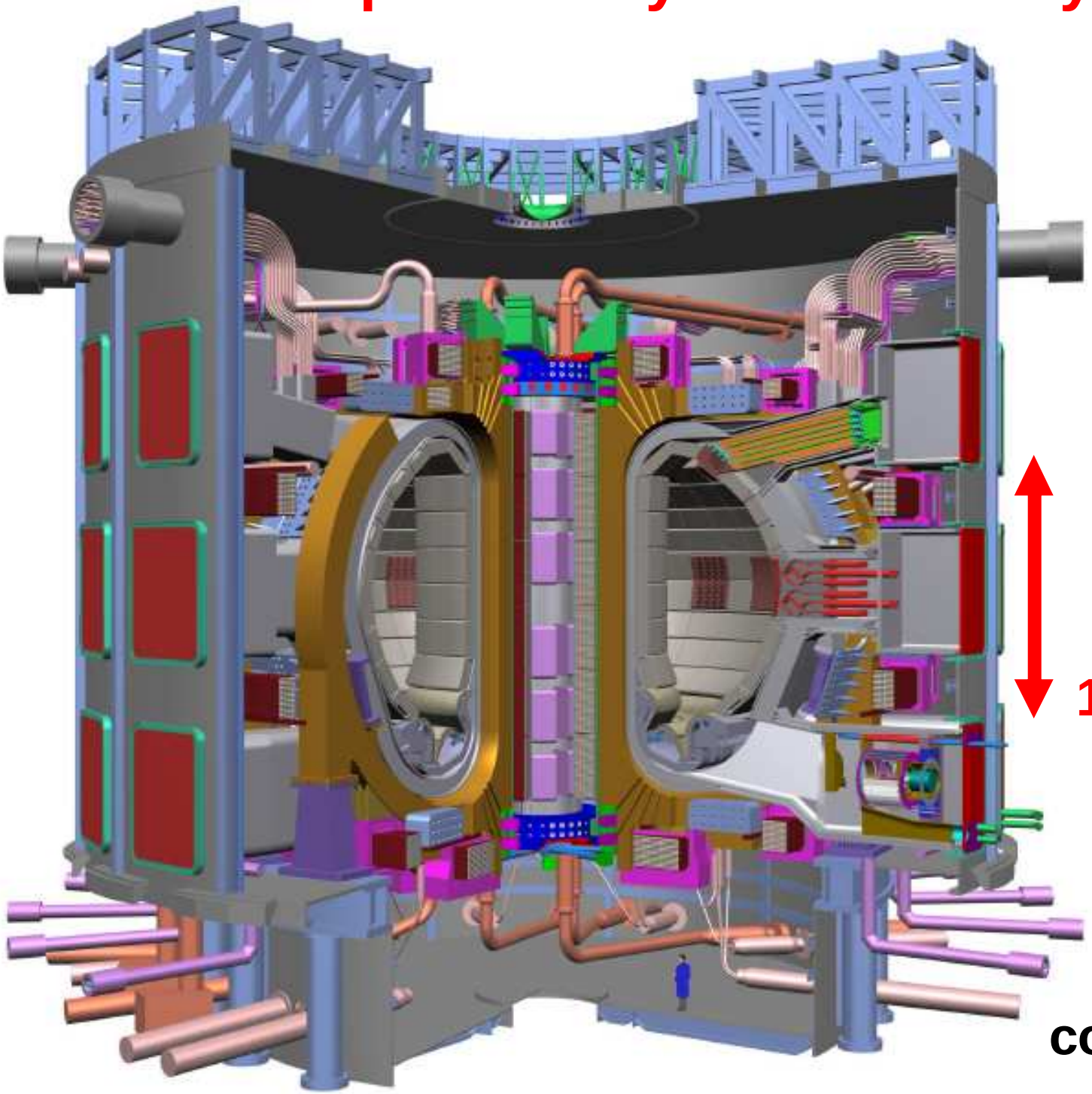

Exercise:

scale from two-body fusion d+t to three-body fusion ^{4}He+^{4}He+^{4}He!

14 m

cost ca. 10^{10} EUR

Setup for study of triple alpha reaction!

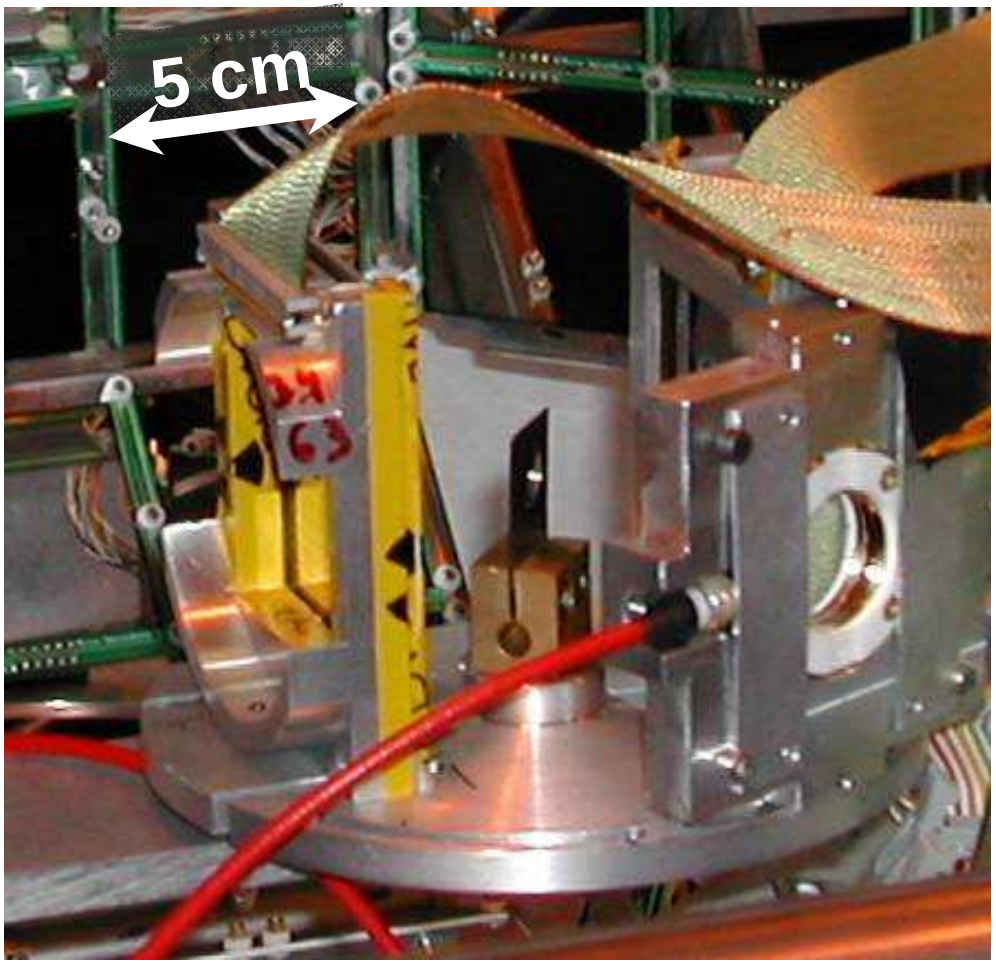

New detector design

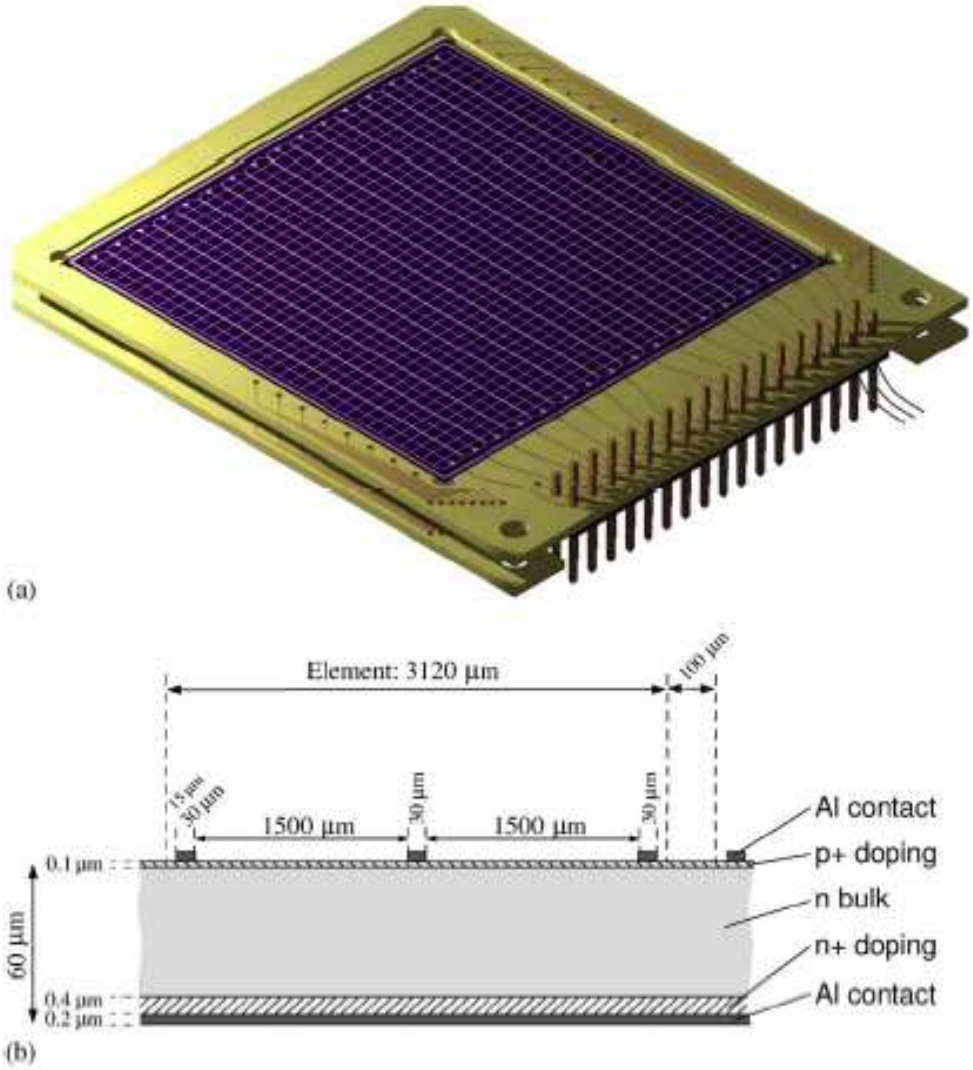

Reduced deadlayer

Inverse reaction: $^{12}B(\beta,3\alpha)$ decay

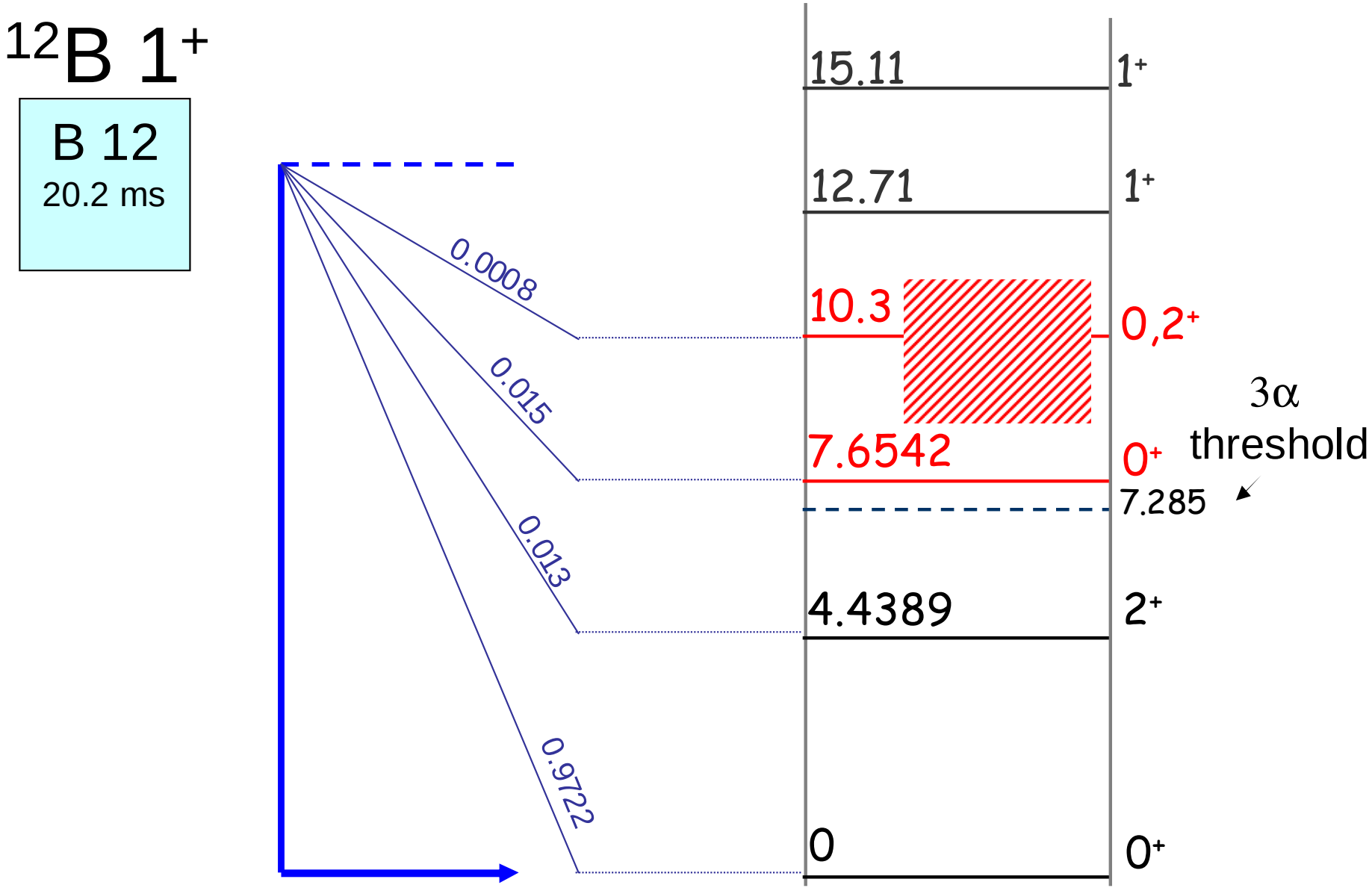

$^{12}C^*$ from the beta-decays of ^{12}N and ^{12}B

β-delayed α-spectrum measured:

- 1950 by Alvarez ^{12}N
- 1957 by Fowler *et al.* ^{12}B
- 1963 by Wilkinson *et al.* $^{12}B/^{12}N$
- 1966 by Schwalm and Povh $^{12}B/^{12}N$
- 1978 by Schwalm and Gergely (unpublished) ^{12}N

How to measure beta-delayed particle emission?

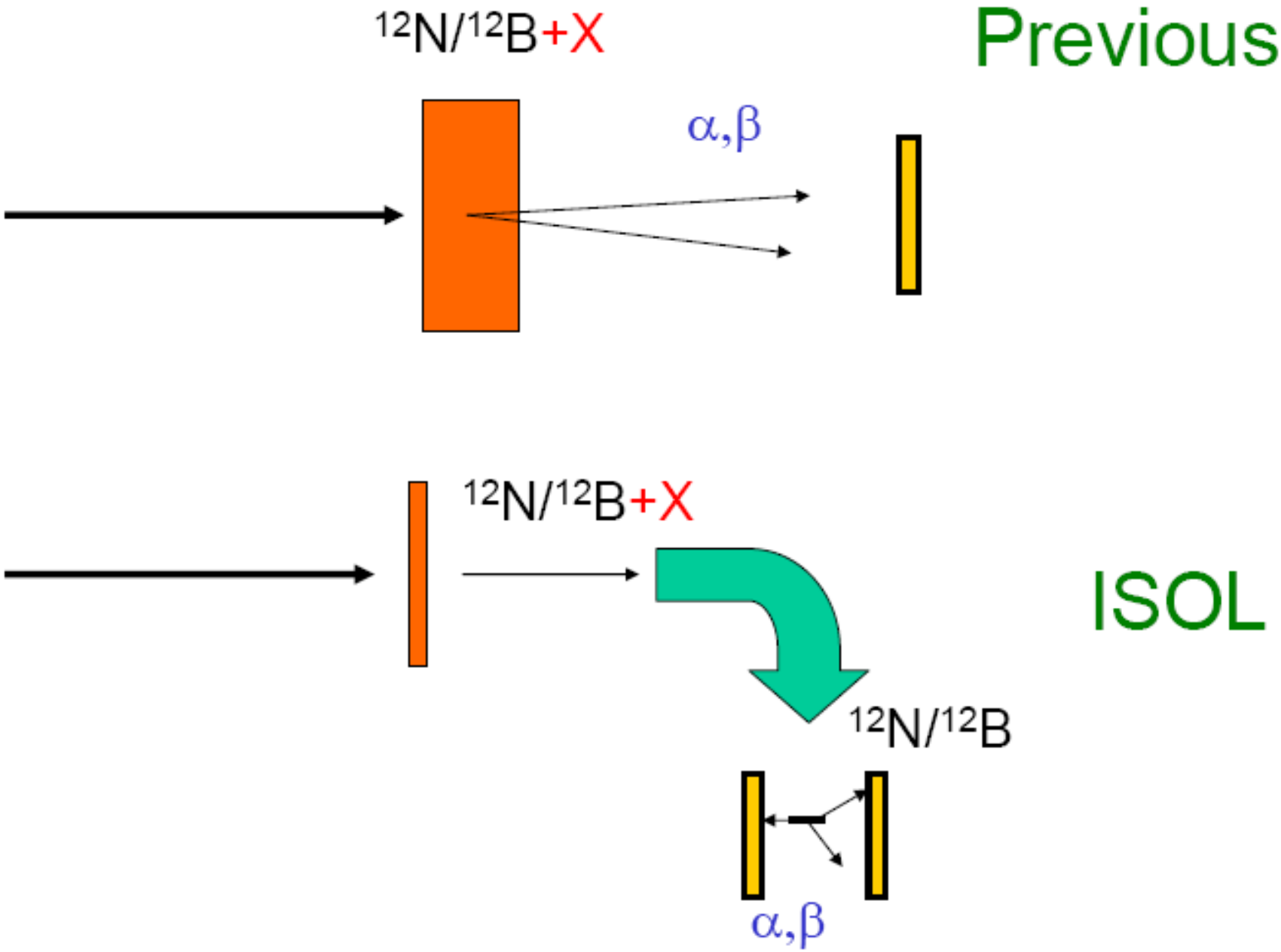

$^{12}Be(\beta^-)^{12}B$ beta decay to $^{12}C^* \rightarrow 2\alpha$ detected

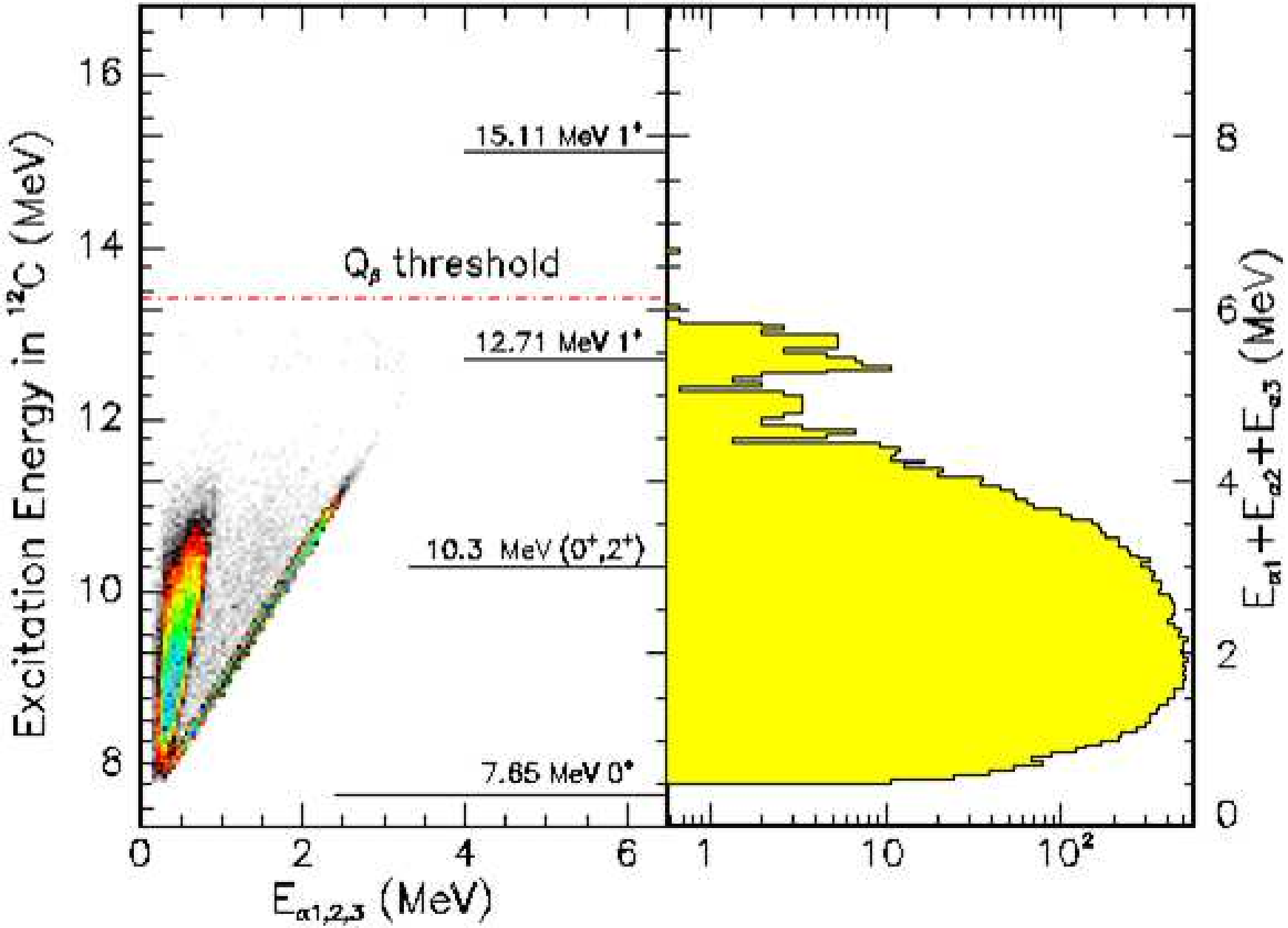

The triple-alpha process: ^{12}B and ^{12}N decays

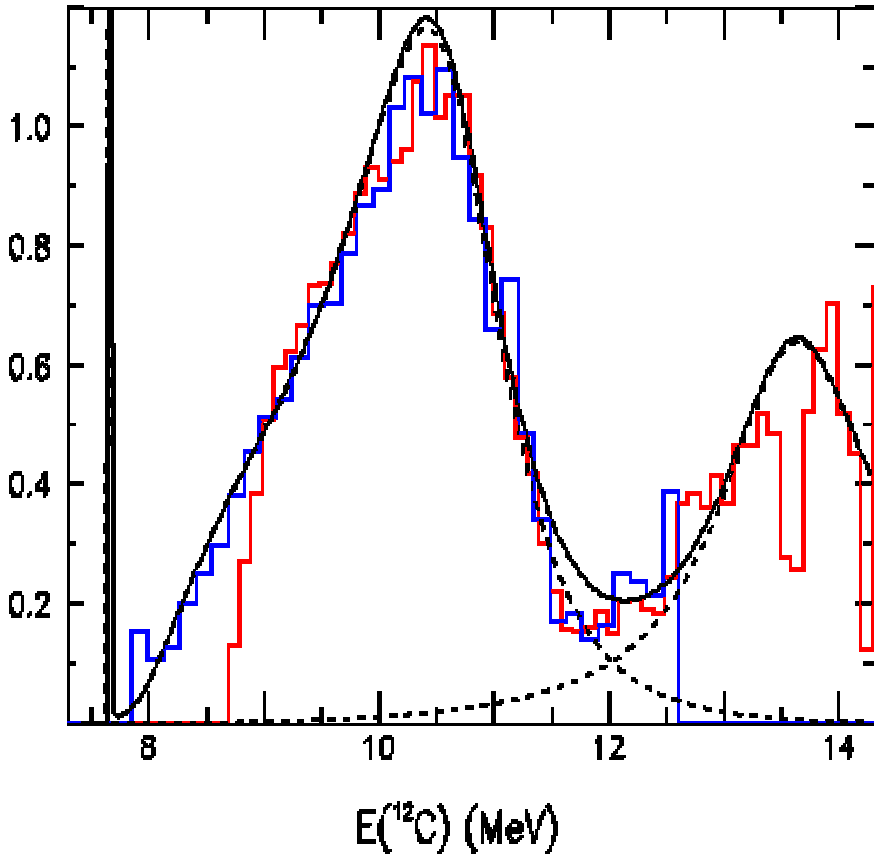

Combined R-matrix fit of ^{12}B and ^{12}N

ISOLDE - JYFL

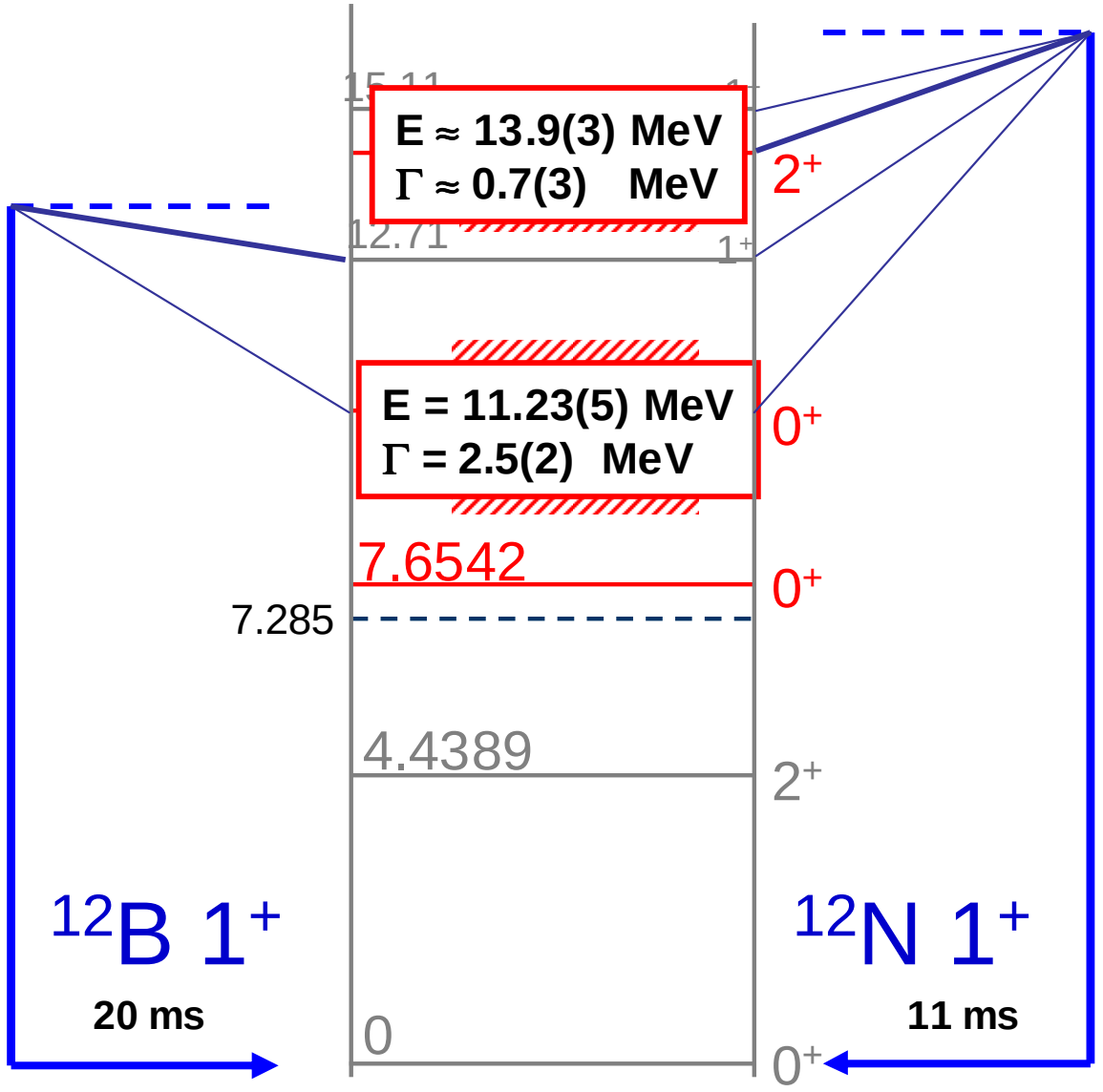

H.O.U. Fynbo et al., Nature 433 (2005) 136.

New rates for the triple-alpha process

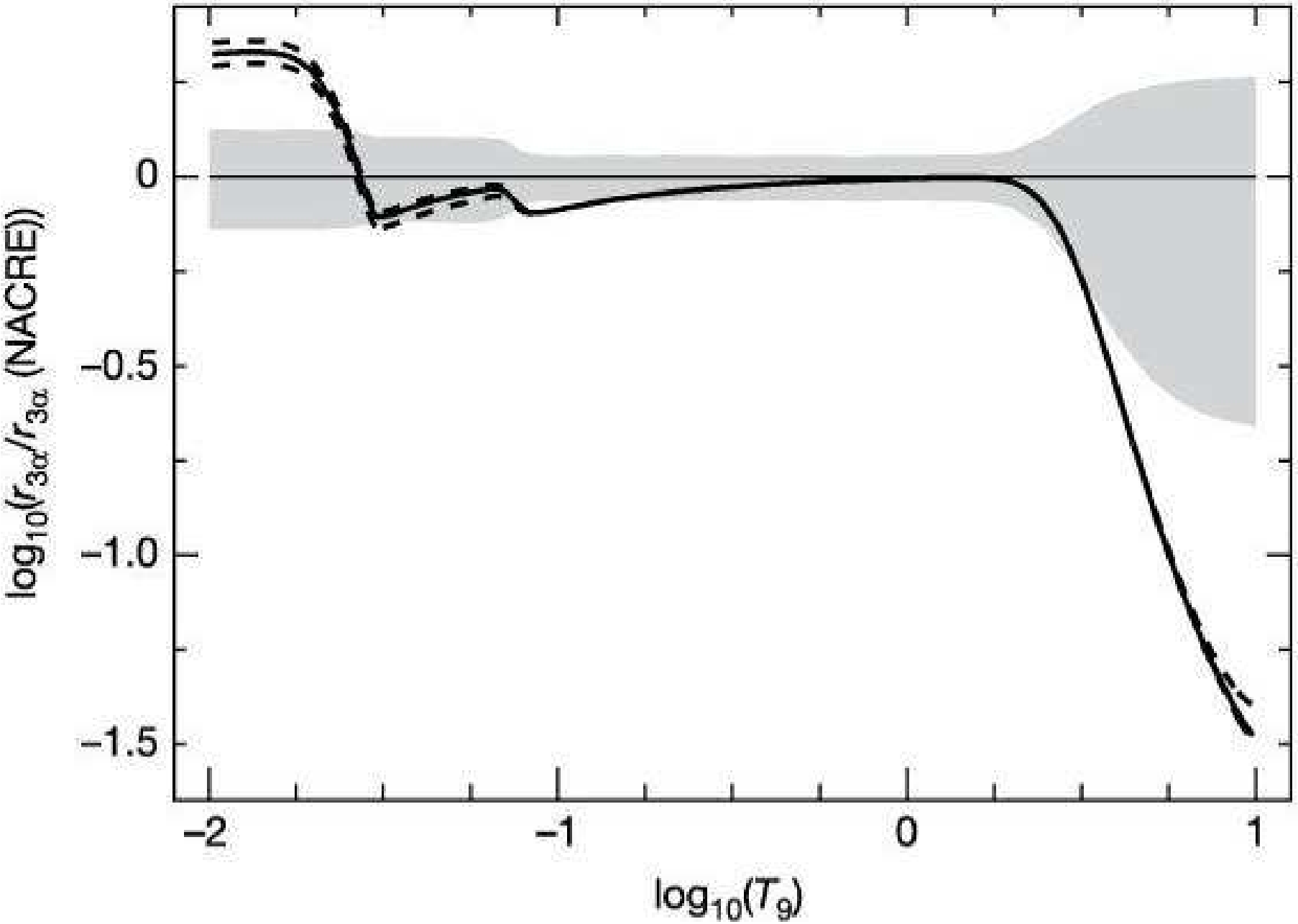

H.O.U. Fynbo et al., Nature 433 (2005) 136.

^{7,10}Be from Paul Scherrer Institute

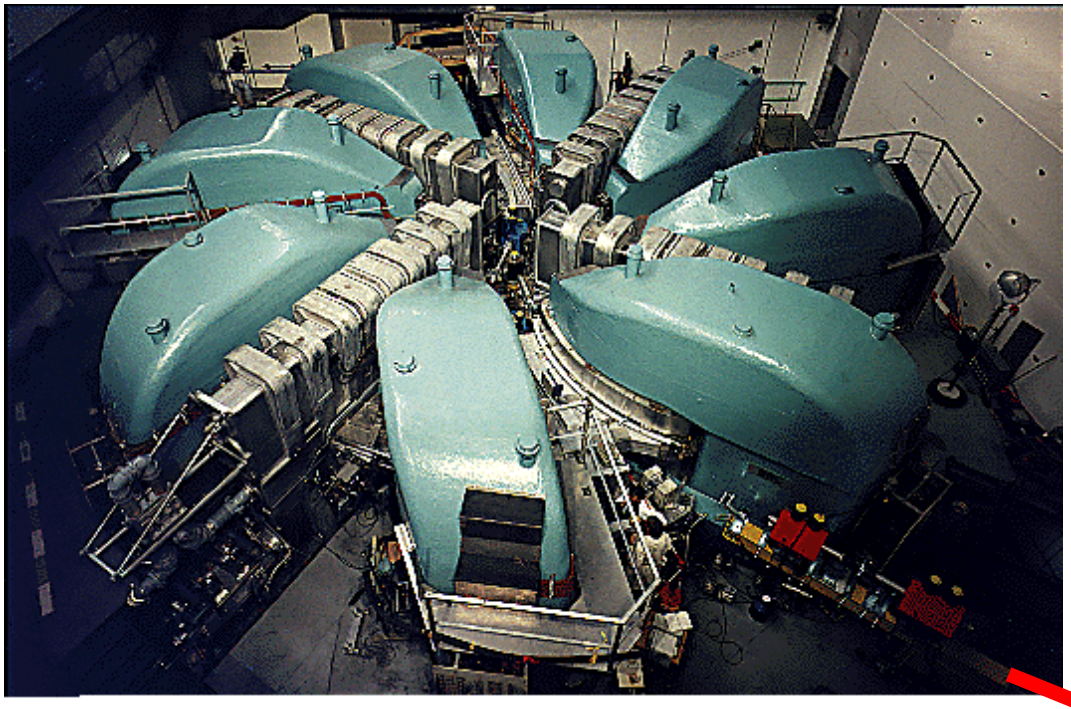

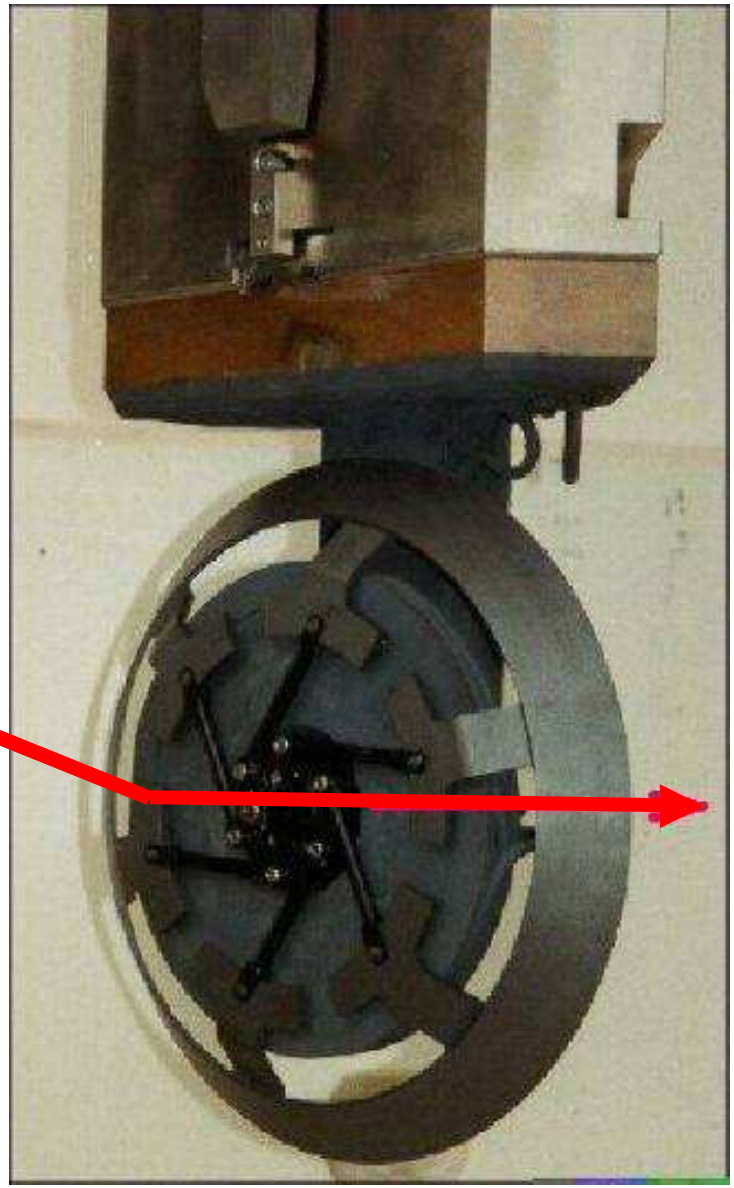

PSI: 2 mA 590 MeV protons onto graphite target for pion production

Spallation products

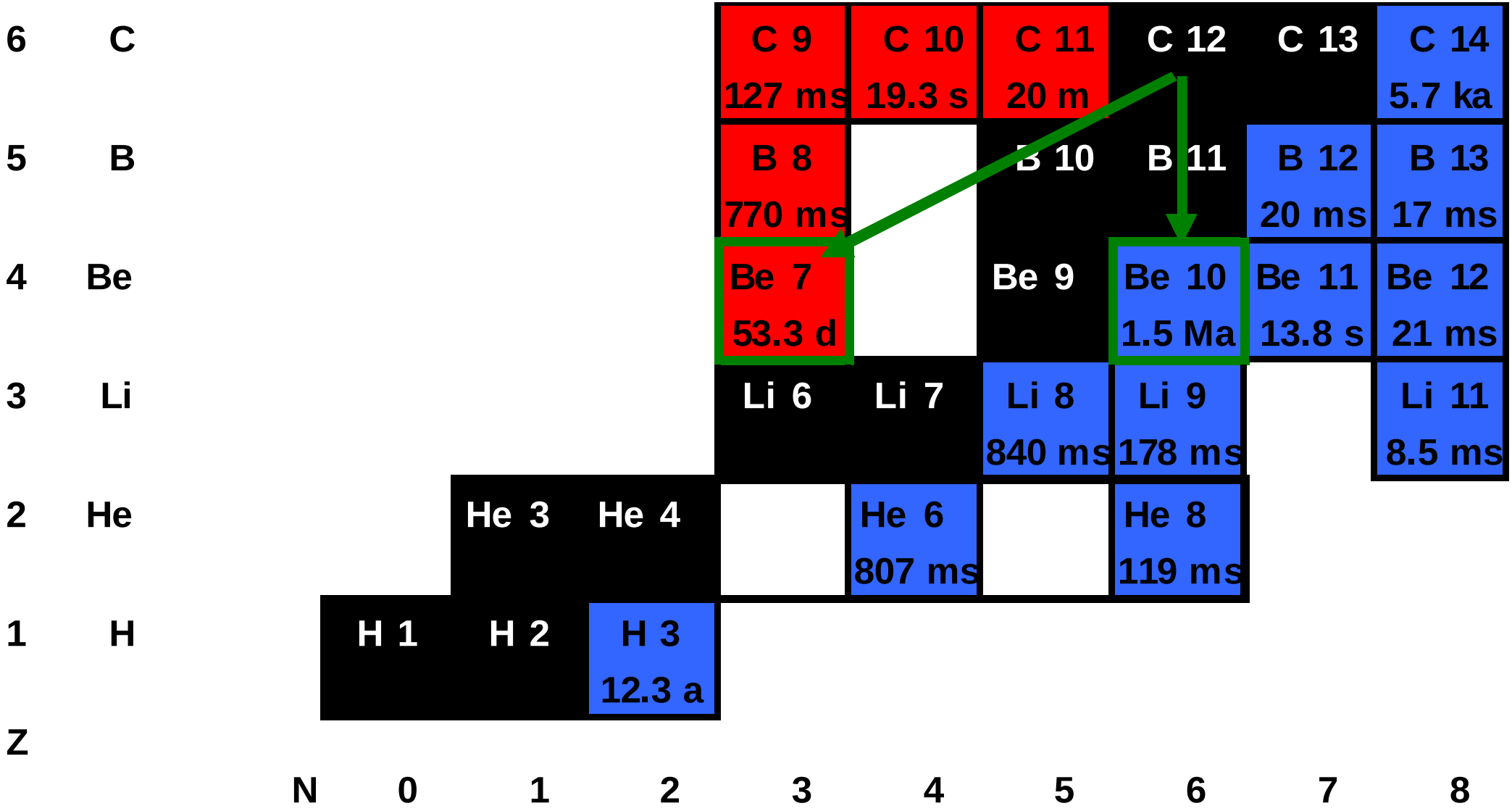

Procedure for off-line produced ^{7}Be beams

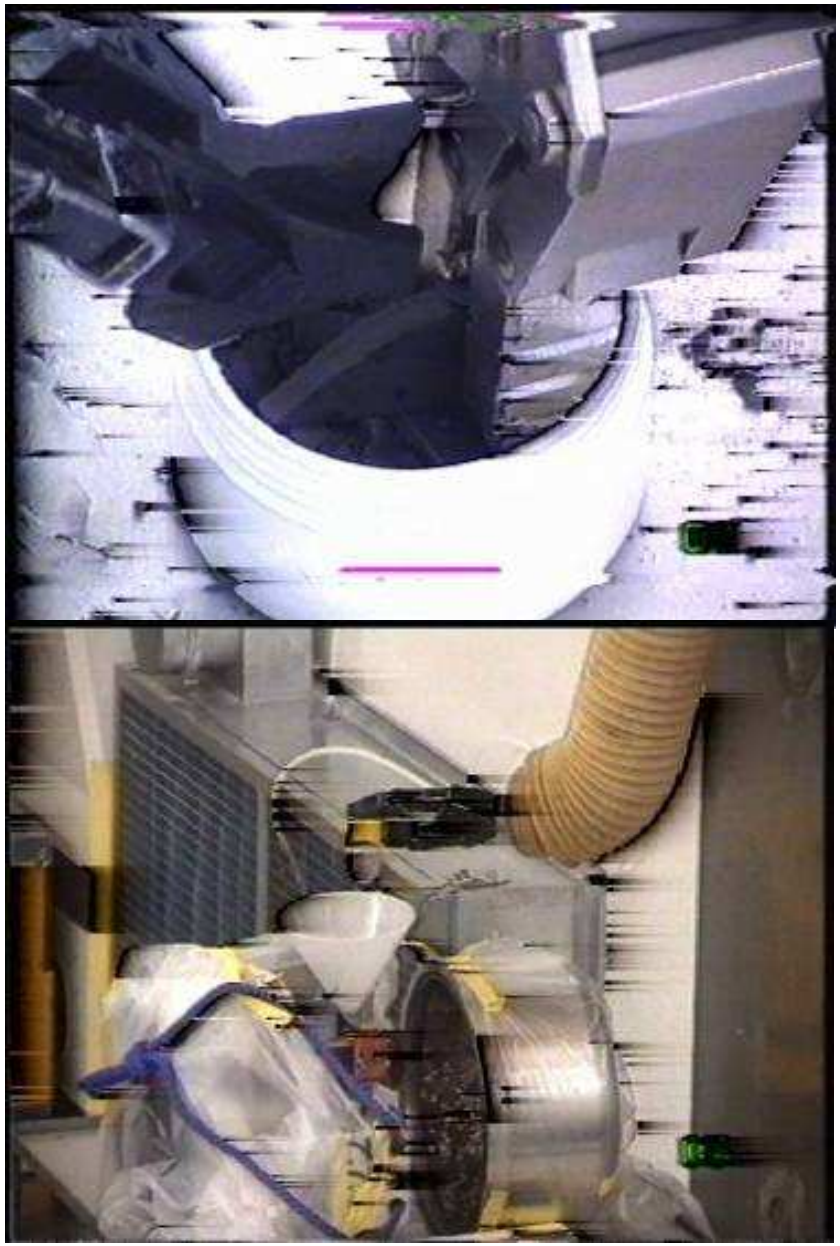

1. Break graphite into pieces
2. Fill ISOLDE target container
3. Put into Pb-shielded container
4. Transport to ISOLDE
5. Heat target container to 1700 ℃
6. Ionize Be with RILIS

RIB with “macroscopic” intensity!

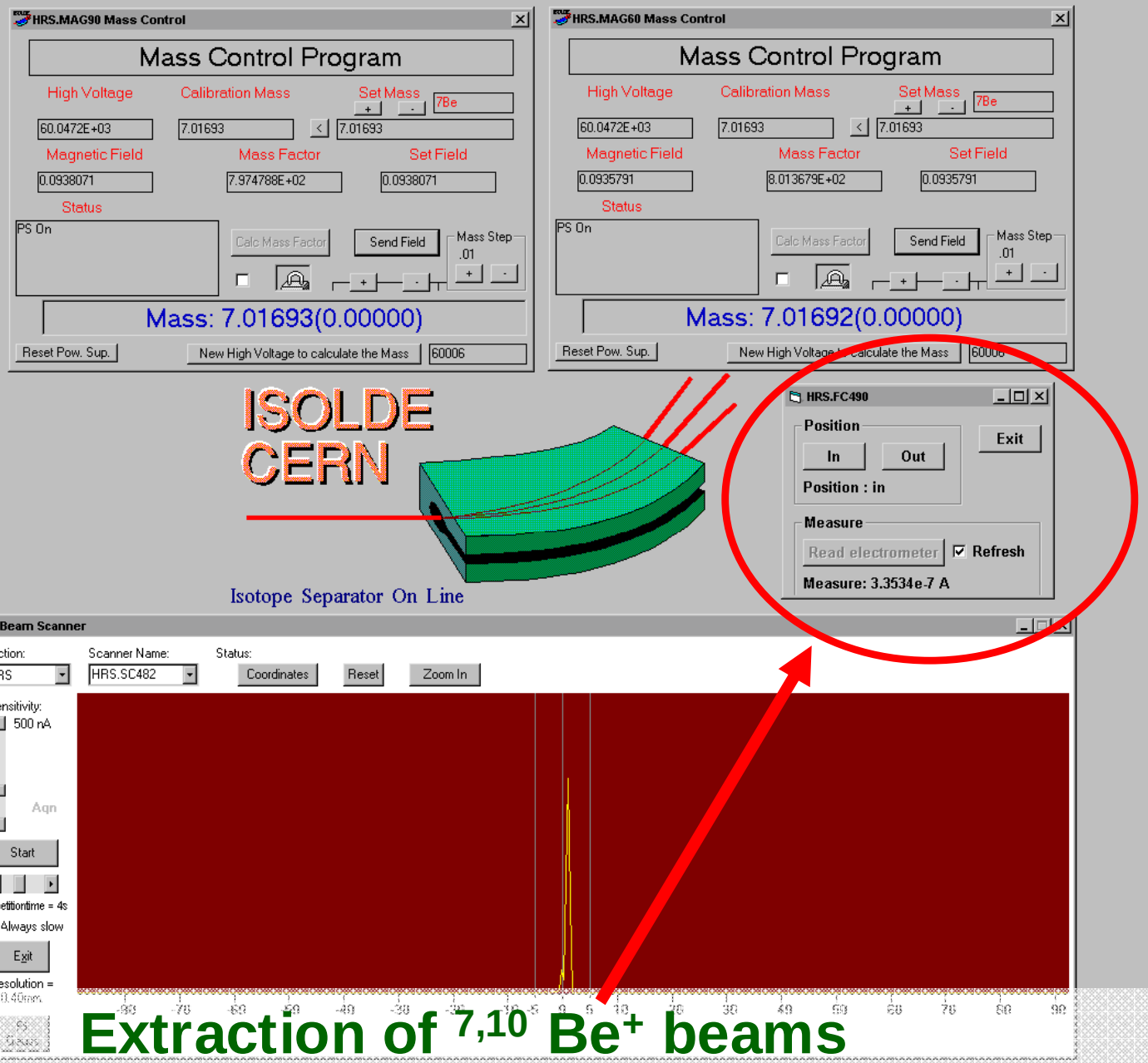

Extraction of $^{7,10}Be^{+}$ beams

with 300 pnA (2E12 ions per s) for many hours!

U.K. et al., Nucl. Instr. Meth. B204 (2003) 343.

Measurement of ^{7}Be(p,γ) with ion-implanted target

^{7}Be target from ISOLDE with 1.2E16 atoms (1.8 GBq)

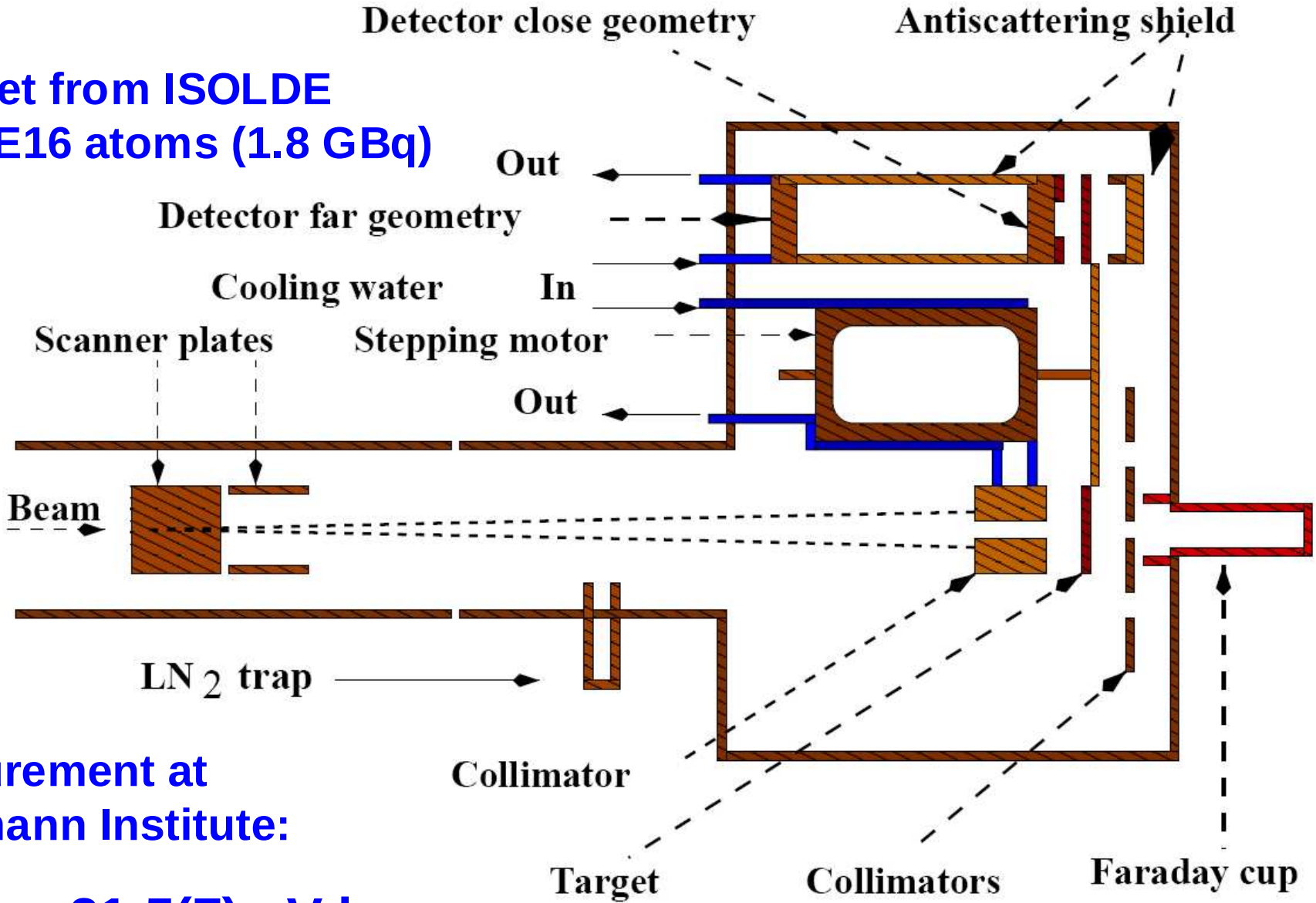

Measurement at Weizmann Institute:

$S_{17}(0) = 21.5(7)$ eV b

L.T. Baby et al., Phys. Rev. Lett. 90 (2003) 022501 & 92 (2004) 029901.

Measurement of $^{7}Be(p,\gamma)$ with ion-implanted target

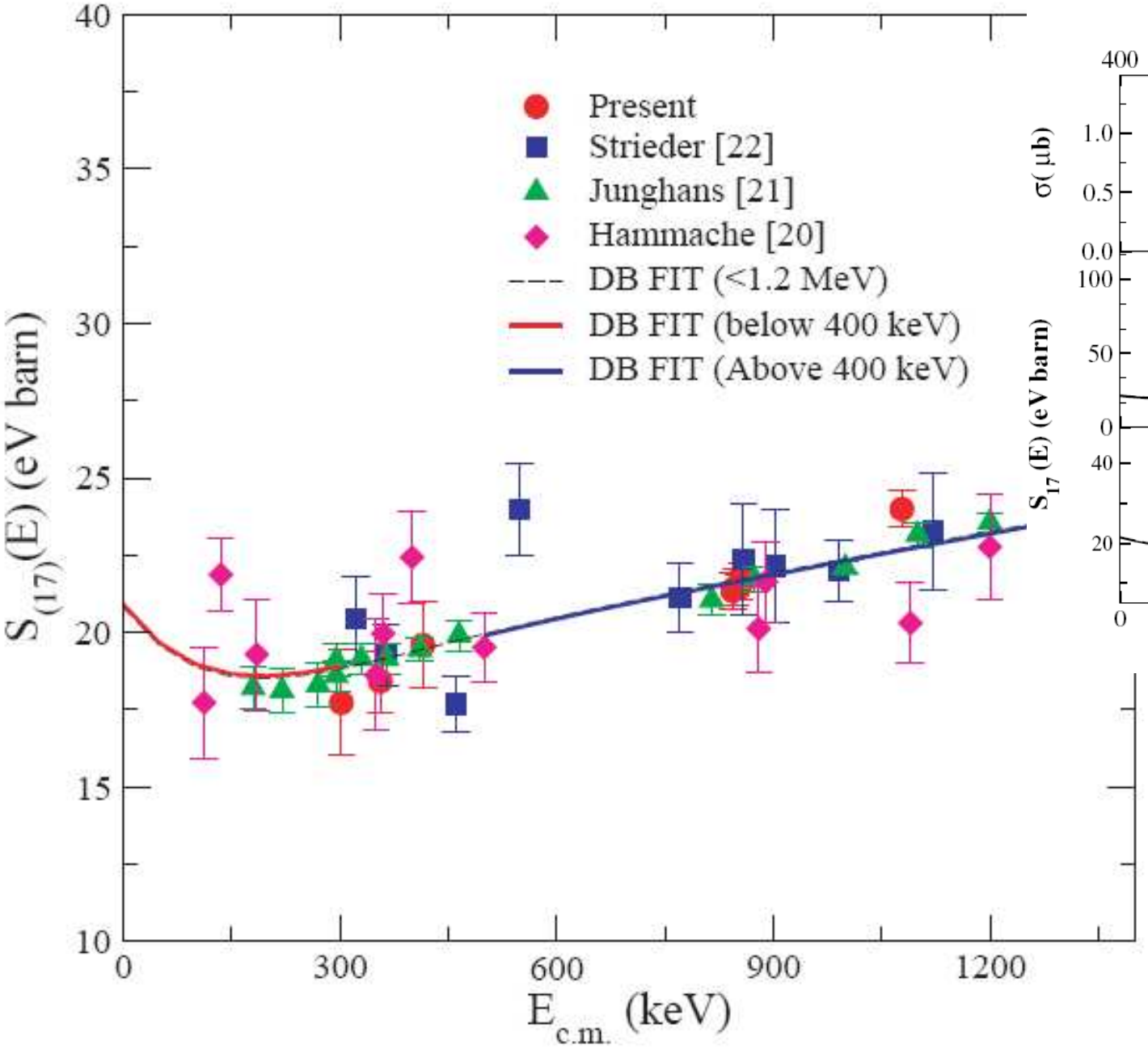

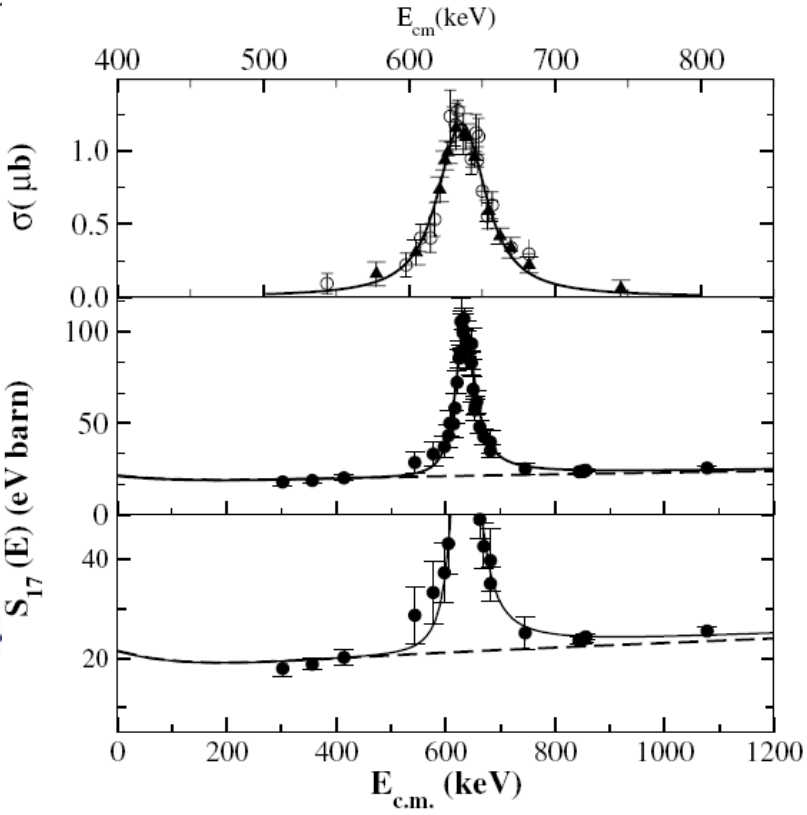

L.T. Baby et al., Phys. Rev. Lett. 90 (2003) 022501 & 92 (2004) 029901.

High sensitivity wear measurements

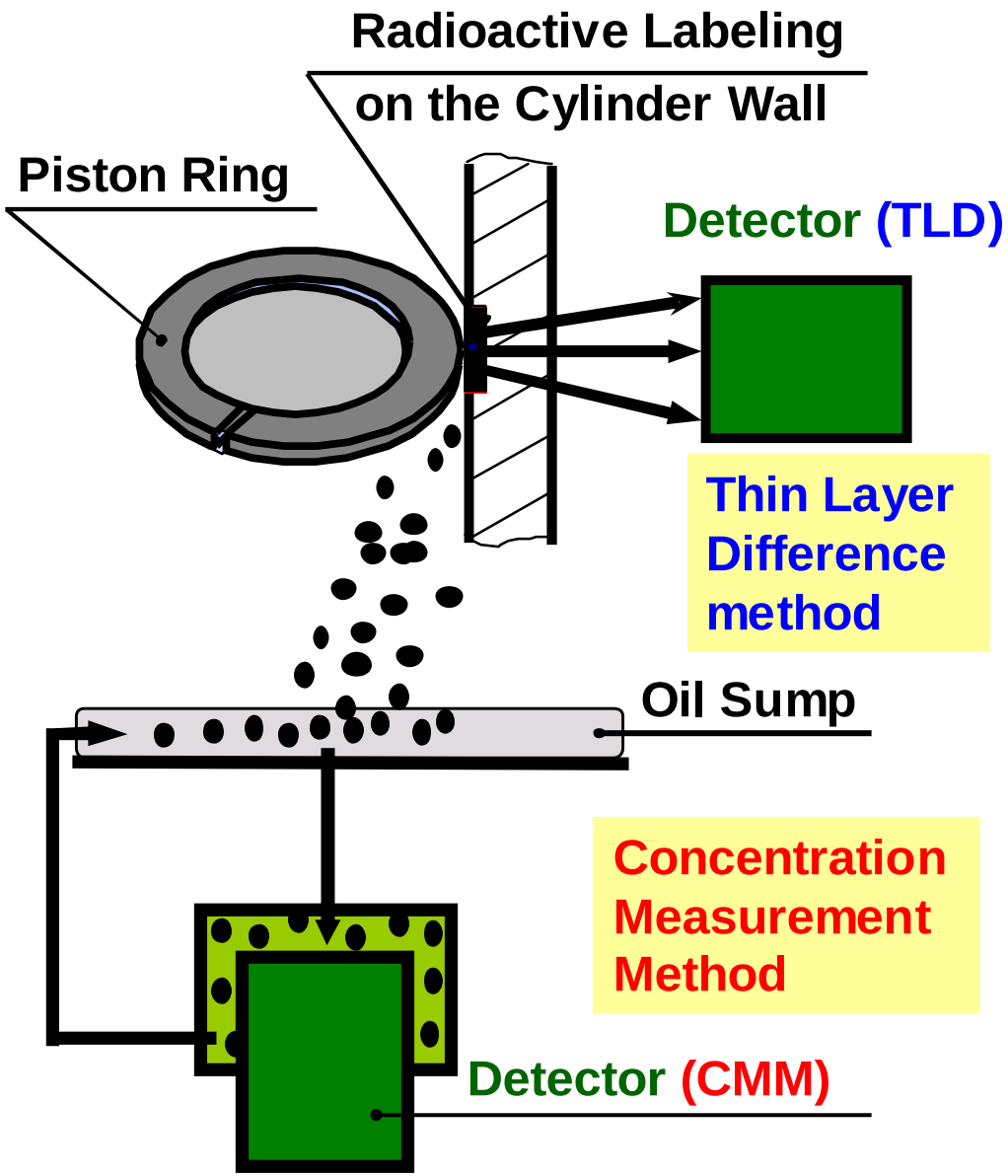

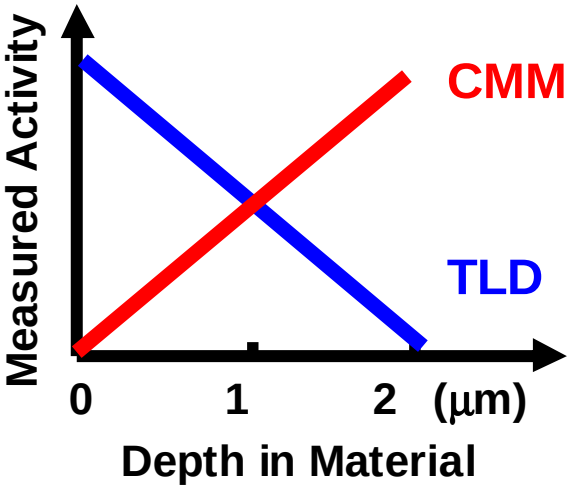

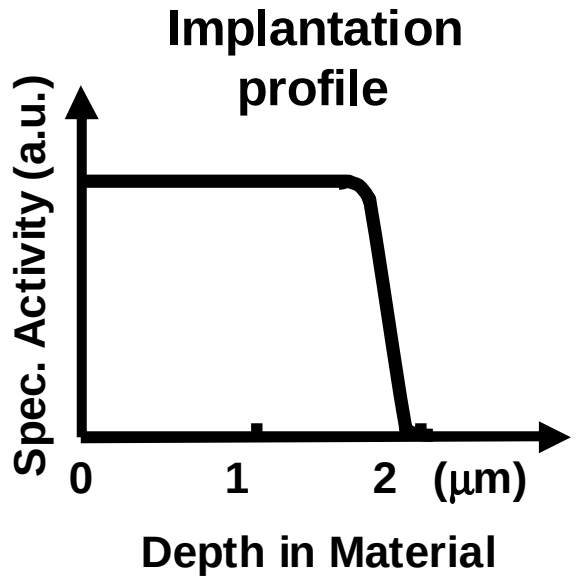

M. Hoffmann et al., Nucl. Instr. Meth. B183 (2001) 419.

P. Fehsenfeld et al., Nucl. Phys. A701 (2002) 235c.

^{7}Be for wear analysis

Material	Density g/cm3	Wear rate μm/10^6 cyc.	Implant. depth in μm at beam energy of: 60 keV	260 keV	1.2 MeV	6 MeV	15 MeV
UHMWPE	0.97	50	0.36	1.1	2.9	13	43
Ti	4.52		0.17	0.56	1.5	6.1	18
CoCrMo	8.28		0.11	0.39	1.1	4.1	12
Alumina	3.1	0.15	0.20	0.59	1.6	6.7	21
Zirconia	5.5		0.15	0.48	1.3	5.3	16

In-vivo use: ≈10^6 cycles/year

Simulator runs: (2-10)•10^6 cycles

Required dose: some pnA per cm^2 (e.g. ball of 22-28 mm diameter)

Cancer

About 1 000 000 new cancer cases per year in EU (15)
58 % local disease, 42 % generalized

45 % cured (5 year survival)

22 % surgery alone
12 % radiation therapy
6 % combination surgery + radiation
5 % chemo-therapy
just beginning of systemic radionuclide therapy

HOW: expose cancer cells or cancer tissue to sufficient radiation doses?

Radioisotopes in therapy = surgery with radiation

	Gamma Knife	ß-Knife	α-Knife	Auger Knife
Isotope	^{60}Co E_γ > 1 MeV	^{131}I, ^{90}Y, ^{153}Sm, ^{166}Ho, Others $E_ß$ 1 – 3 MeV	$^{212, 213}$ Bi, ^{211}At, ^{149}Tb, $^{223, 224}$Ra E_α 4–8 MeV	^{125}I ^{165}Er E_e few eV
Range	Full body penetration	about 1 cm	30 – 80 µm	1 µm
Application	Brain cancer	RIT **Radio-immuno therapy**	Leukemia, lymphoma	future
	Tissue surgery ex vivo	Tissue surgery in vivo	Cell surgery	Molecular surgery

Cancer therapy with alpha emitters

- **half-life**
- **radiotoxicity of daughter isotopes**
- **biokinetics: in-vivo stability of chelating agent, clearance,…**
- **affordable**
- **reliable supply: more than one facility per geographic area**

Isotopes for targeted alpha therapy

^{149}Tb for targeted alpha therapy

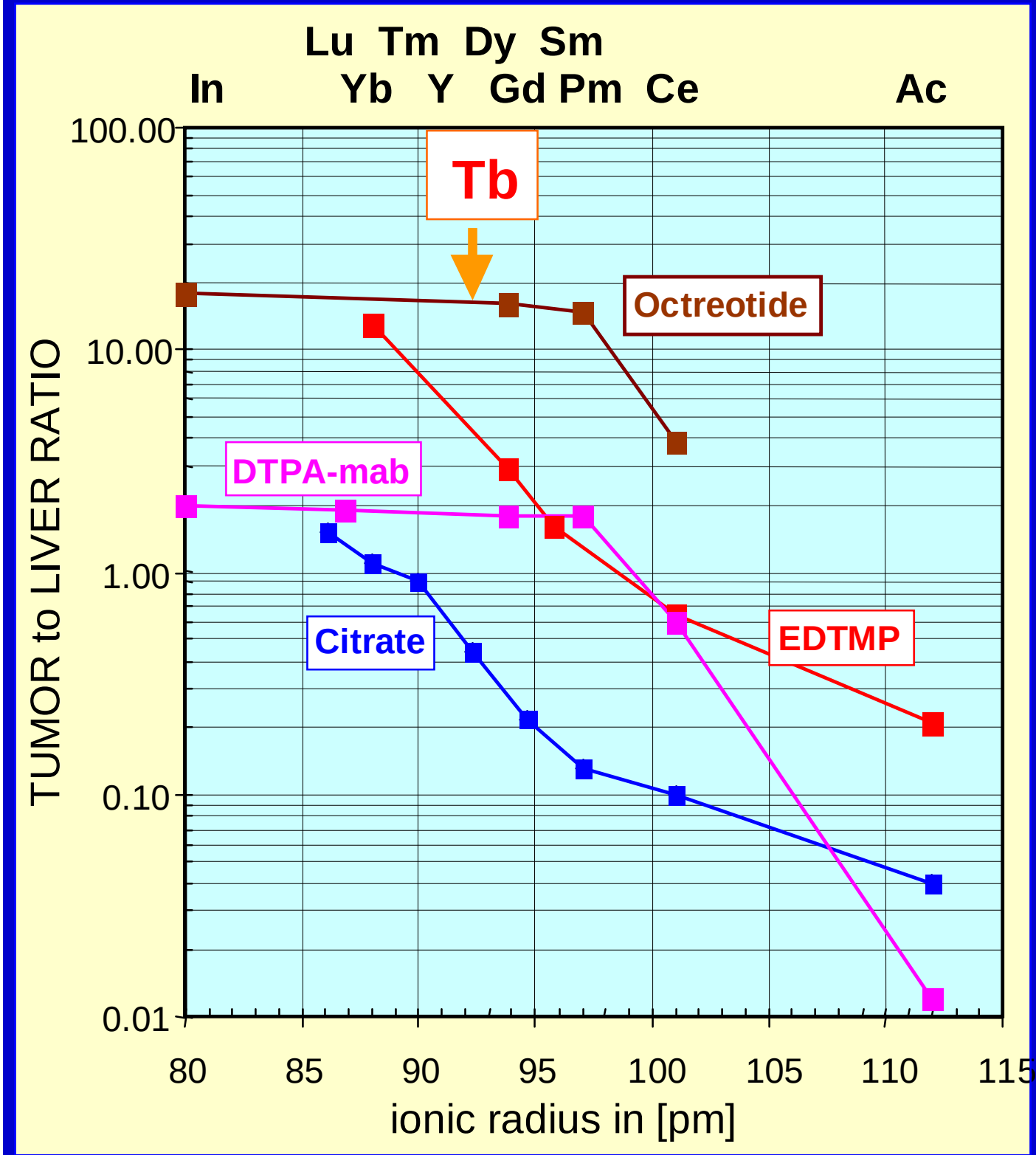

Comparison

of the

bio-distribution

of different

tumor seeking tracers

labeled with

radio-lanthanides, ^{225}Ac and ^{111}In

free chelates:

Citrate

EDTMP

specific tracers:

Octreotide

and

Mab

Linker:

Aminobenzyl-DTPA

G.J.Beyer, Hyperfine Interactions 129 (2000) 529.

Principle of Radio Immuno Therapy

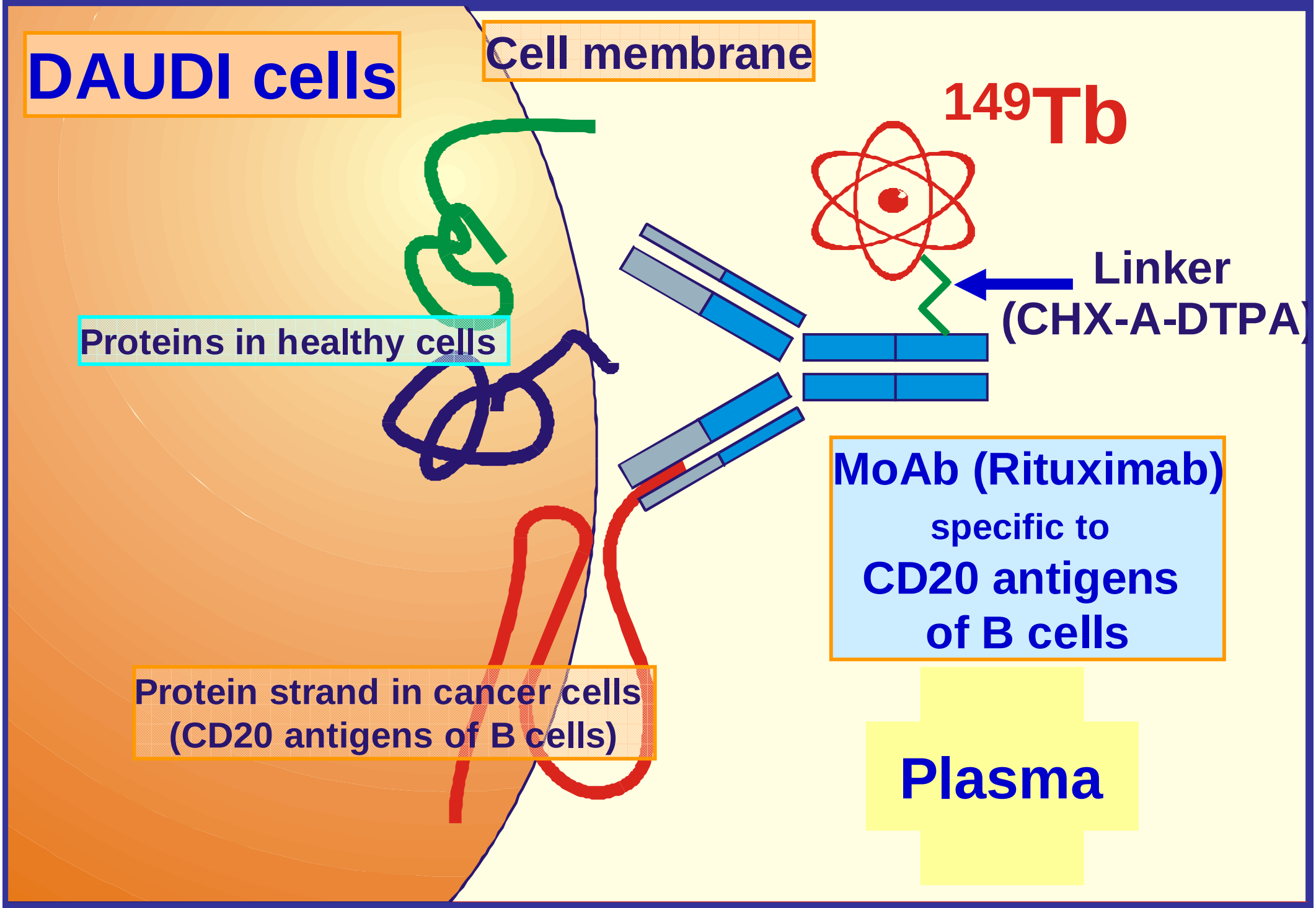

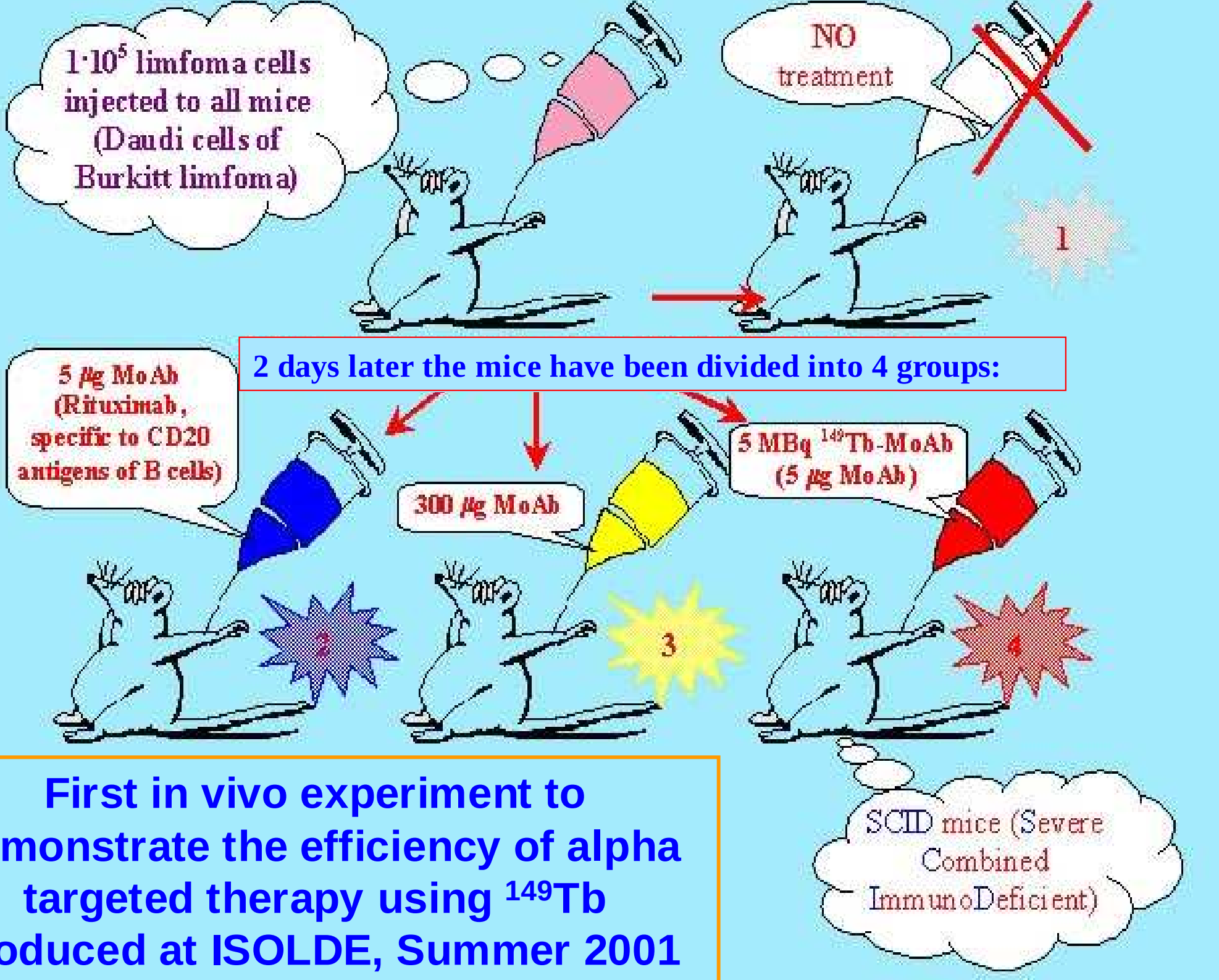

First in vivo experiment to demonstrate the efficiency of alpha targeted therapy using ^{149}Tb produced at ISOLDE, Summer 2001

Survival of SCID mice

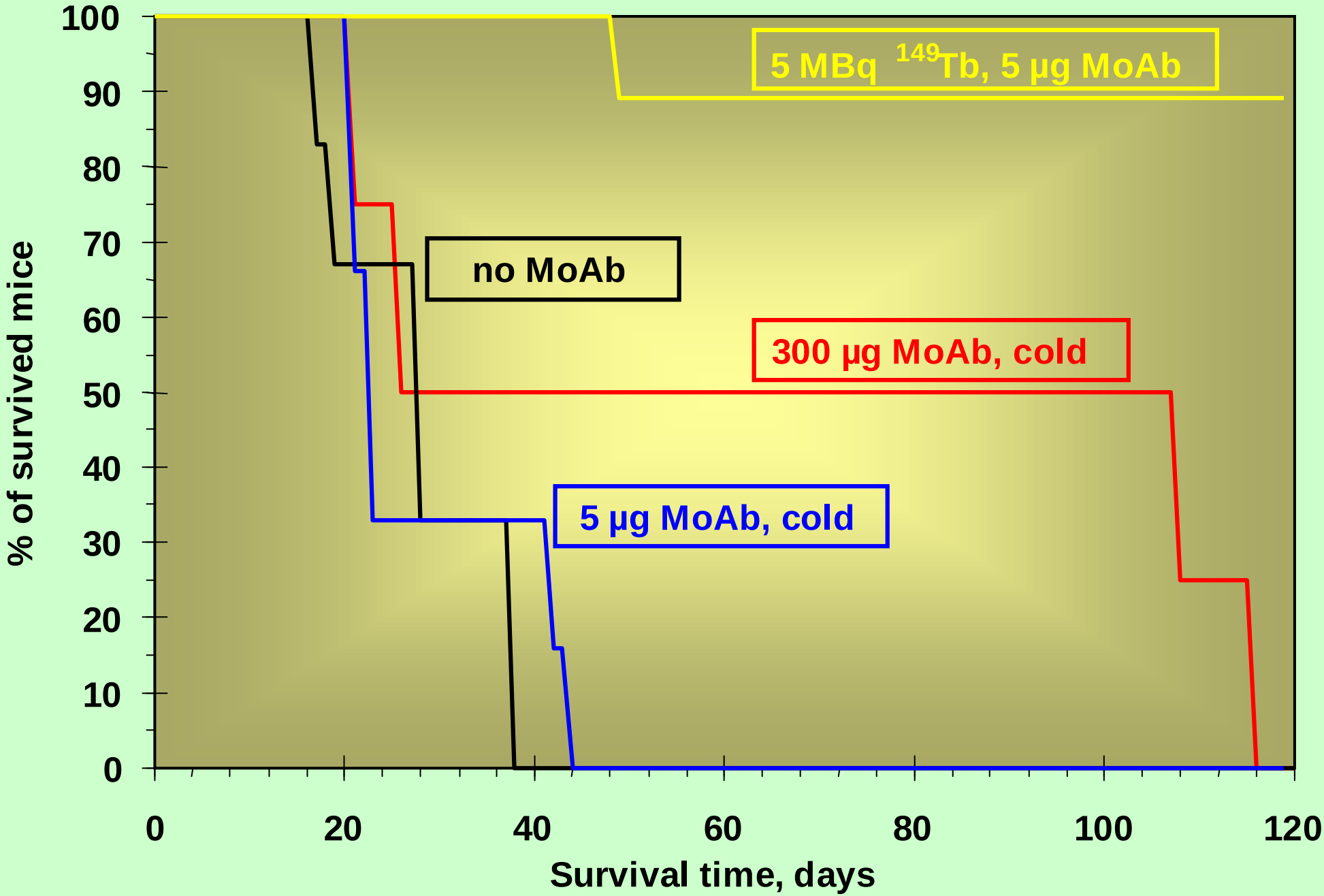

G.J. Beyer et al., Eur. J. Nucl. Med. Molec. Imaging 31 (2004) 547.

103 d p.i.

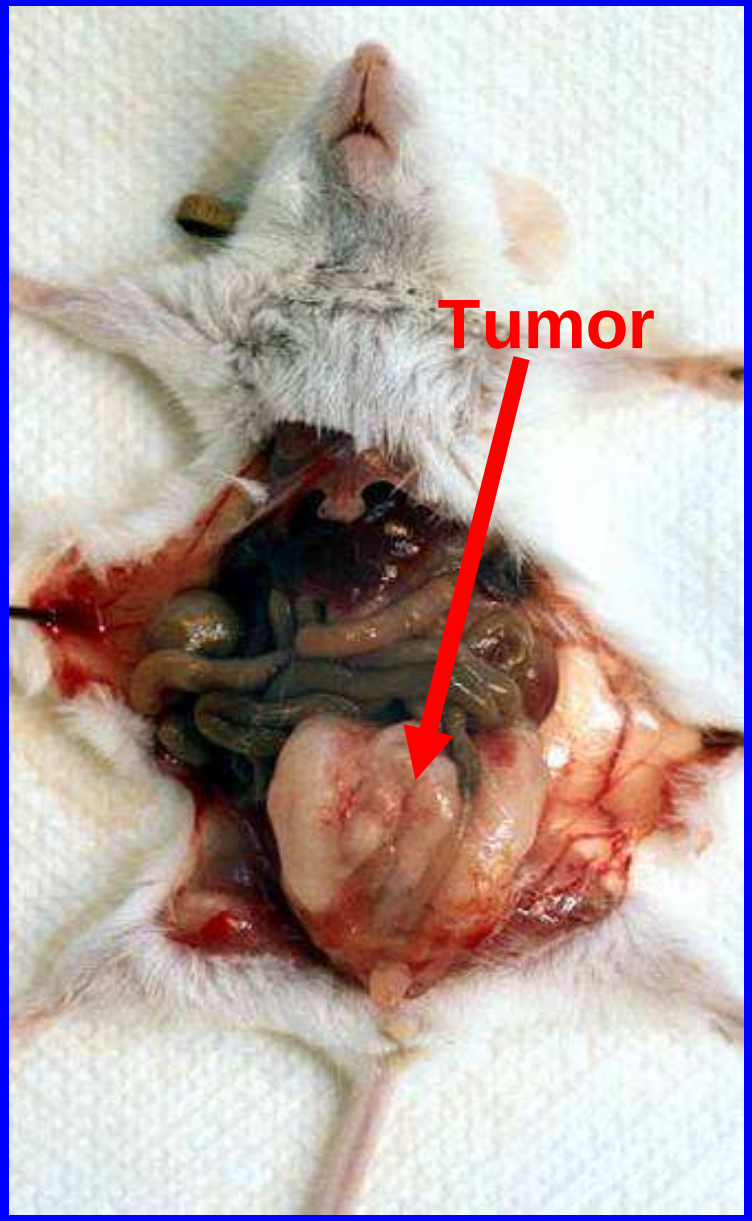

300 µg MoAb cold

108 d p.i.

5 MBq **^{149}Tb-**MoAb (5 µg)

Applications

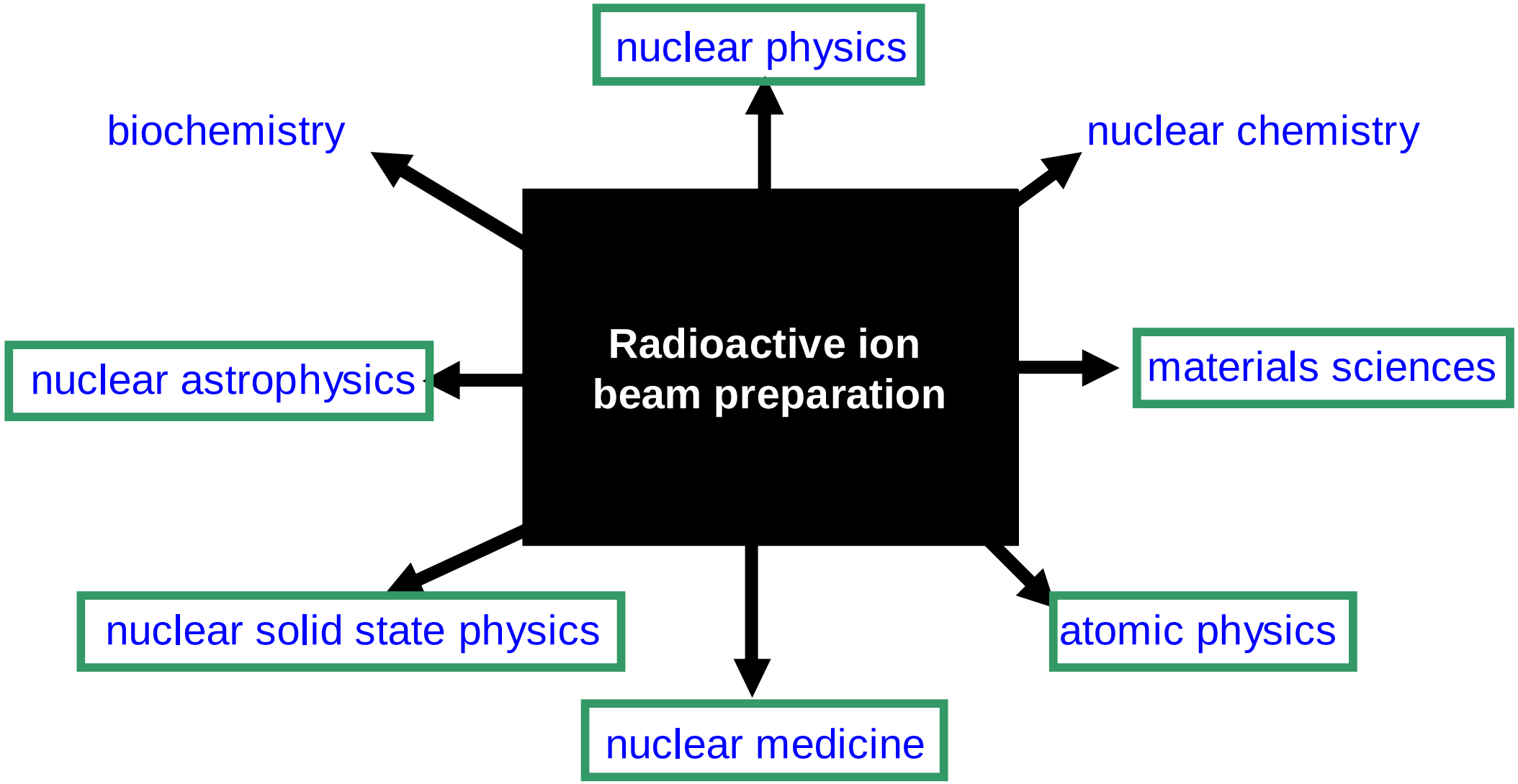

CERN provides physics results even when the LHC does not run!

ISOL beams are not a subfield of nuclear physics but have incredibly many applications across many disciplines

Nuclear chart at ISOLDE

> 600 isotopes available at ISOLDE-SC

> 1100 isotopes produced at ISOLDE till today

> 2000 isotopes in principle feasible with ISOL method

Extension needs target and ion source development!

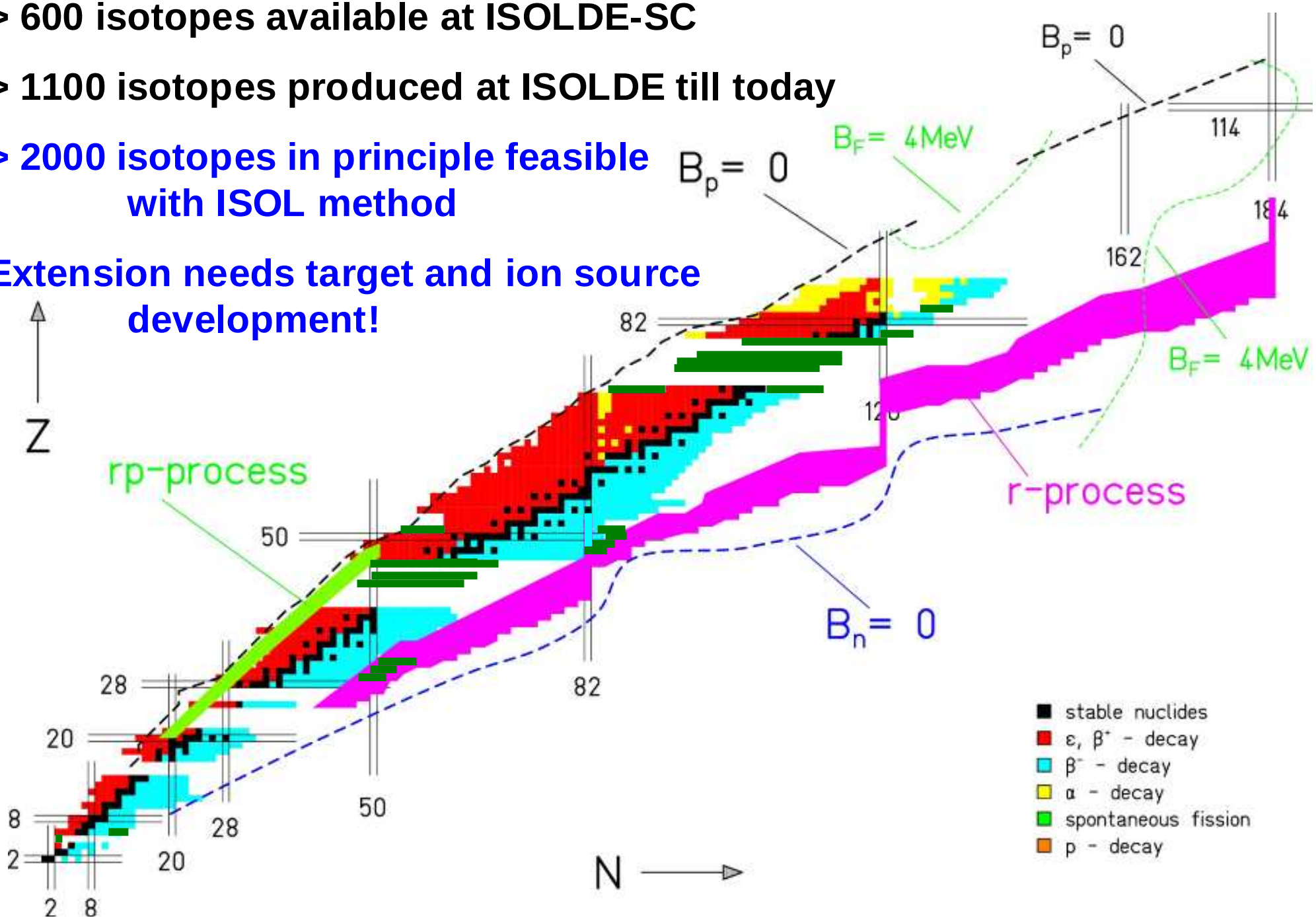

Existing thick-target ISOL beams

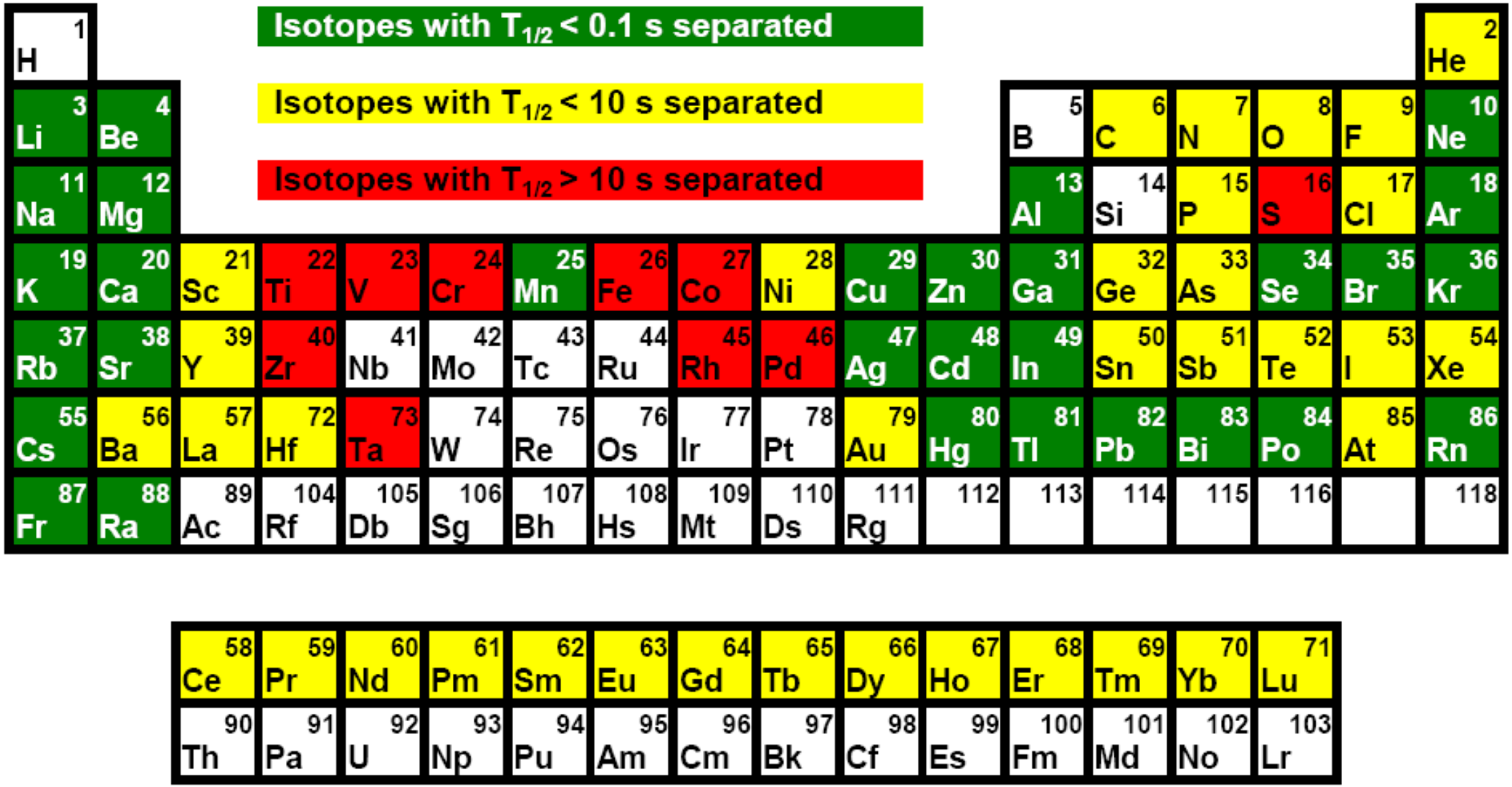

Identification ≠ Separation

- **Identification:**

  The beam composition is determined but not changed.

  e.g. time-of-flight measurement, ΔE measurement,...

- **Separation:**

  Beam contaminations are removed.

  e.g. mass separation, chemical separation,...

- **Unique isotope selection requires the combination of at least two different identification/separation methods.**
- **A higher-fold combination gives improved suppression factors.**

Prism

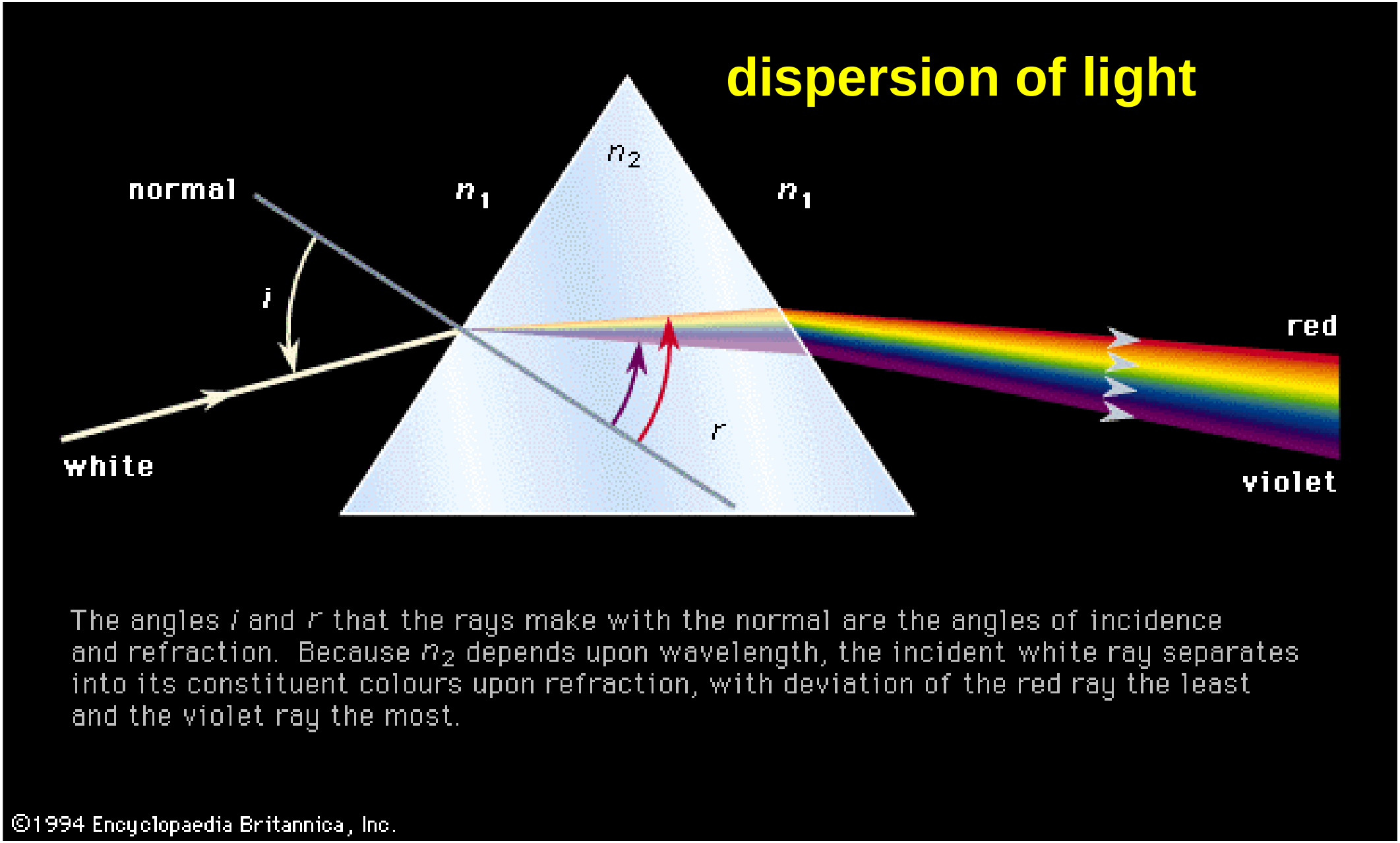
dispersion of light
normal
n_1
n_2
n_1
i
red
white
r
violet
The angles i and r that the rays make with the normal are the angles of incidence and refraction. Because n_2 depends upon wavelength, the incident white ray separates into its constituent colours upon refraction, with deviation of the red ray the least and the violet ray the most.
©1994 Encyclopaedia Britannica, Inc.

Dispersive ion optical elements

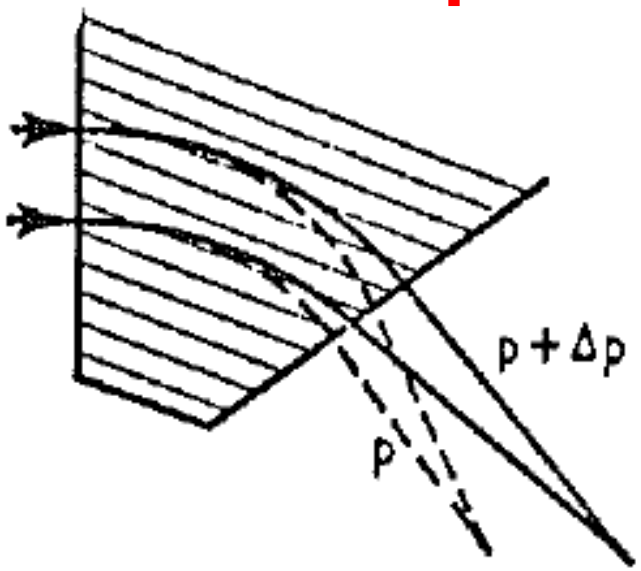

FIG. 5.15 A system with momentum dependent deflection of the central ray, showing lateral displacement due to momentum spread.

- magnets are momentum dispersive
- electrostatic deflectors are energy dispersive
- Wien filters are velocity dispersive

Focusing by tilted entrance/exit of magnetic field

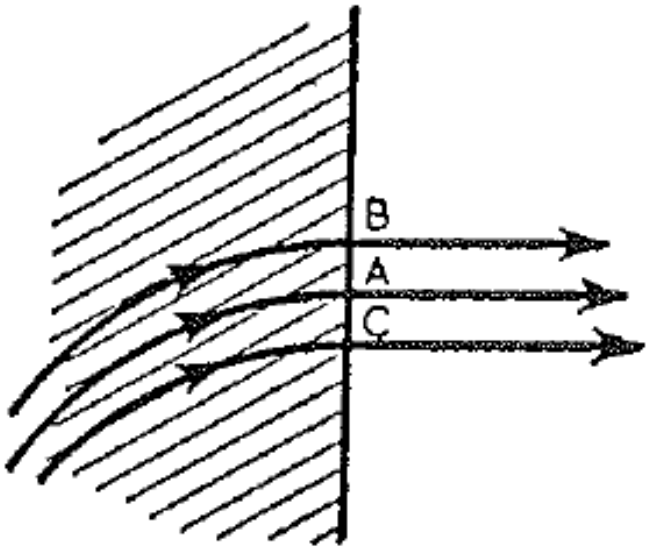

FIG. 5.3 Particles leaving a magnetic field normal to the edge.

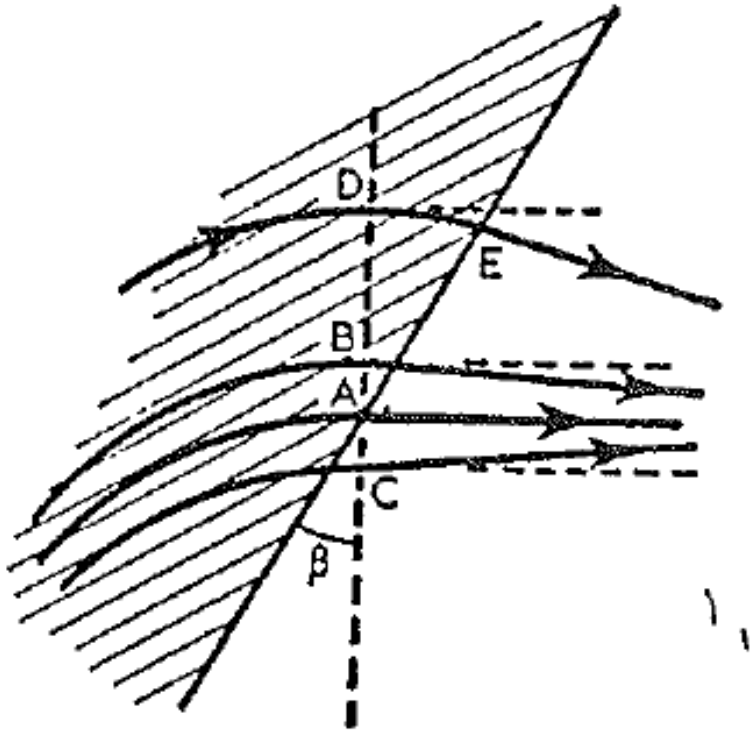

FIG. 5.4 Particles leaving a magnetic field at an angle to the edge. Dotted lines are for normal exit (cf. Fig. 5.3).

horizontal focusing effect

Focusing by tilted entrance/exit of magnetic field

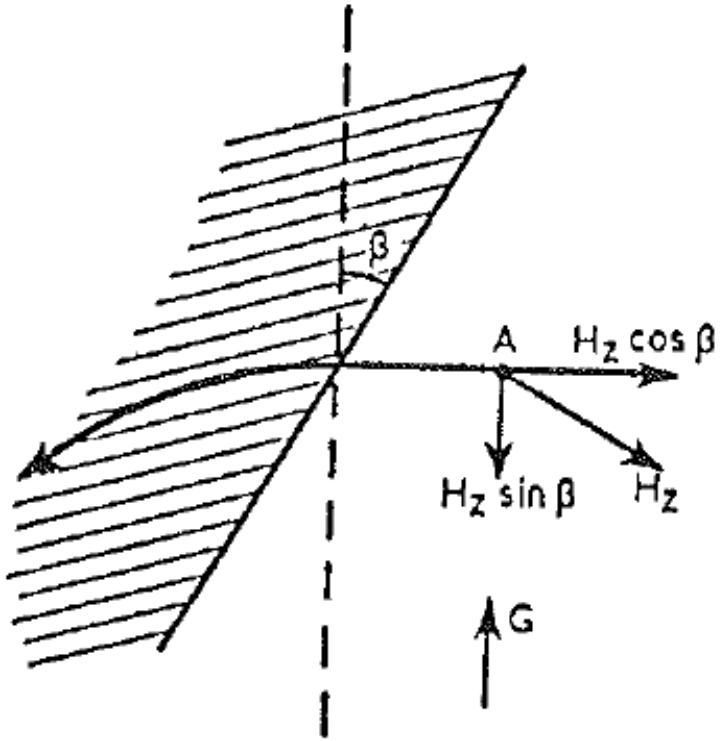

FIG. 5.5 Plan view of a positively charged particle entering a magnetic field directed into the paper. The trajectory makes an angle β with the normal. For view in the direction of arrow G see Fig. 5.6.

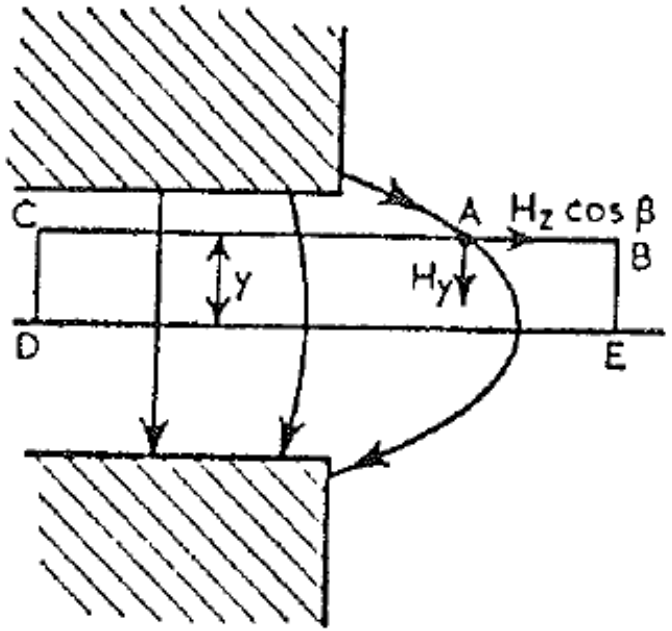

FIG. 5.6 View of Fig. 5.5 in the direction of arrow G. DE is the median plane on which $H_z = 0$.

vertical defocusing effect

Quadrupoles

Electrostatic:

$V = U (x^2 - y^2)/a^2$

$\mathcal{E} = -\,\text{grad}\, V$

$\mathcal{E}_x = -dV/dx = -2U/a^2\, x$

$\mathcal{E}_y = -dV/dy = 2U/a^2\, y$

1. **Force increases proportionally to distance from origin.**

2. **Focusing in x and defocusing in y (or vice versa).**

$\Rightarrow$ **requires quadrupole doublet or triplet to focus in x and y**

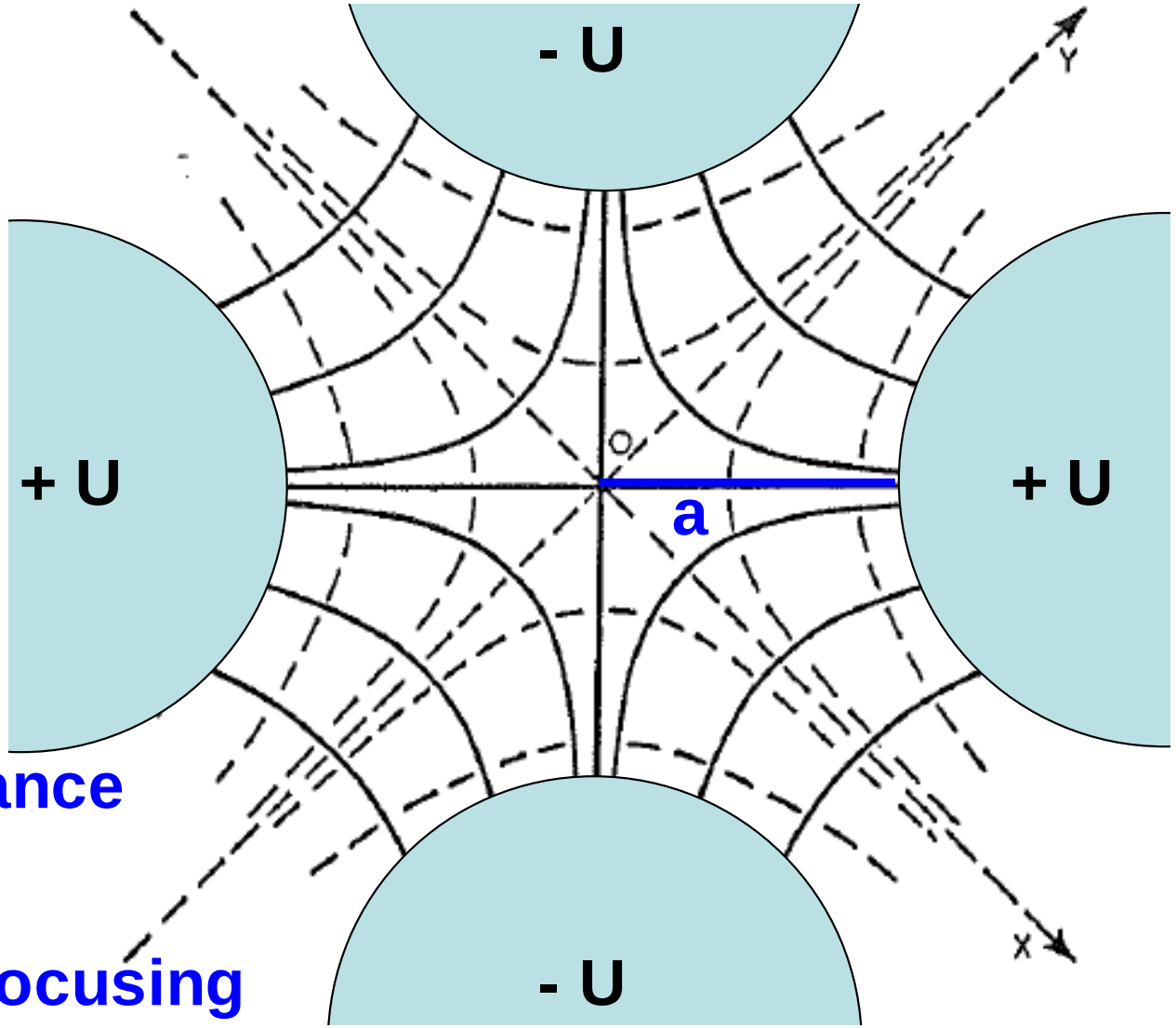

Multipole correction elements

Correction of higher-order effects (aberrations) by hexapole, octupole, etc. fields. Often limited by beam diagnostics!

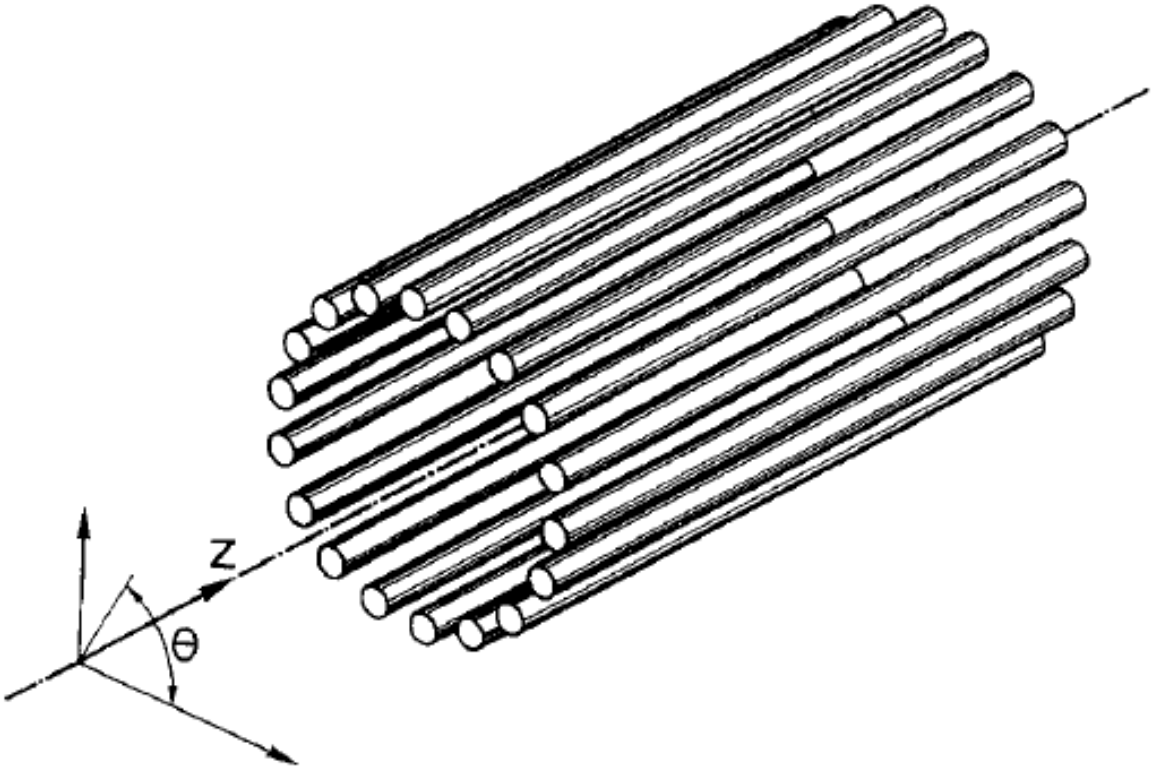

Fig. 1. Squirrel-cage-like electrode arrangement of an electrostatic $2(n+1)$ pole consisting of 18 wires, i.e. a squirrel-cage with $n=8$. In this multipole the potential of each wire is controlled by a separate power supply.

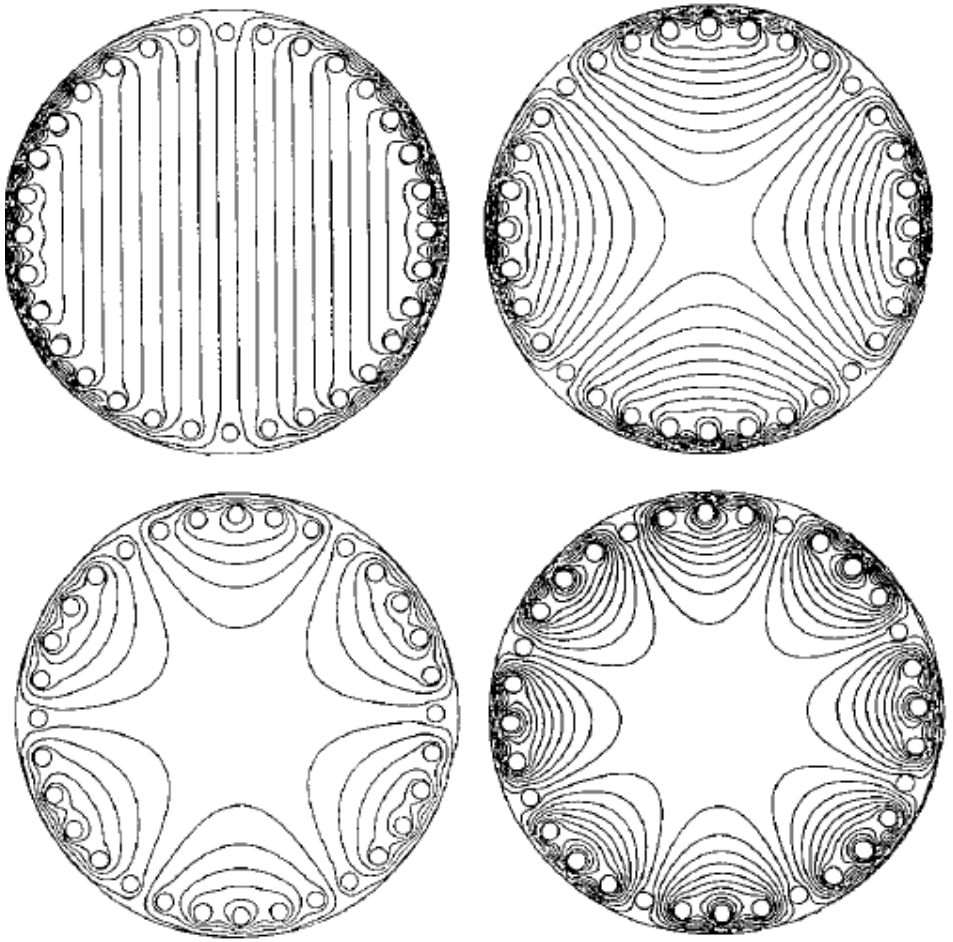

Fig. 3. Calculated potential distributions in a 32-wire squirrel-cage multipole for the cases of dipole ($V_1 \neq 0$), quadrupole ($V_2 \neq 0$), hexapole ($V_3 \neq 0$), octupole ($V_4 \neq 0$) excitations [see eq. (1)] with vanishing $\psi_1, \psi_2, \psi_3, \psi_4, \cdots$.

M. Antl and H. Wollnik, Nucl. Instr. Meth. A274 (1989) 45.

Ion-optical calculations

1. Matrix calculation:

TRANSPORT, COSY-INFINITY, GIOS, GICO, LISE++,…

2. MC simulations/ray tracing:

SIMION, ZGOUBY, RAYTRACE, LISE++, MOCADI,…

Focal plane of LOHENGRIN

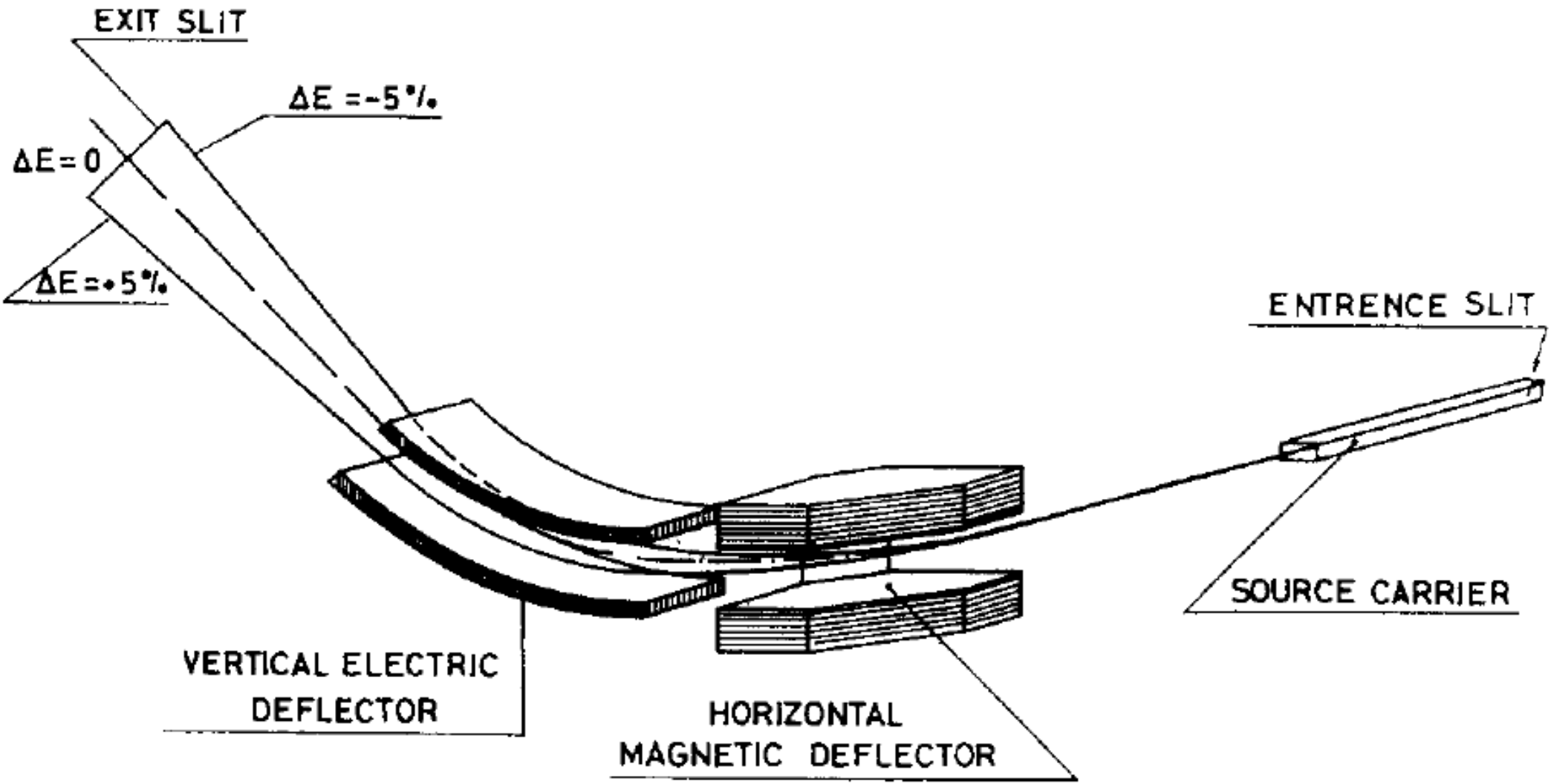

P. Armbruster et al., Nucl. Instr. Meth. 139 (1976) 213.

LOHENGRIN focal plane

Energy dispersion: $\Delta x = D_E \ \Delta E/E$; $D_E = 7.2$ cm/% = 7.2 m

Mass dispersion: $\Delta y = D_m \ \Delta m/m$; $D_m = 3.24$ cm/% = 3.24 m

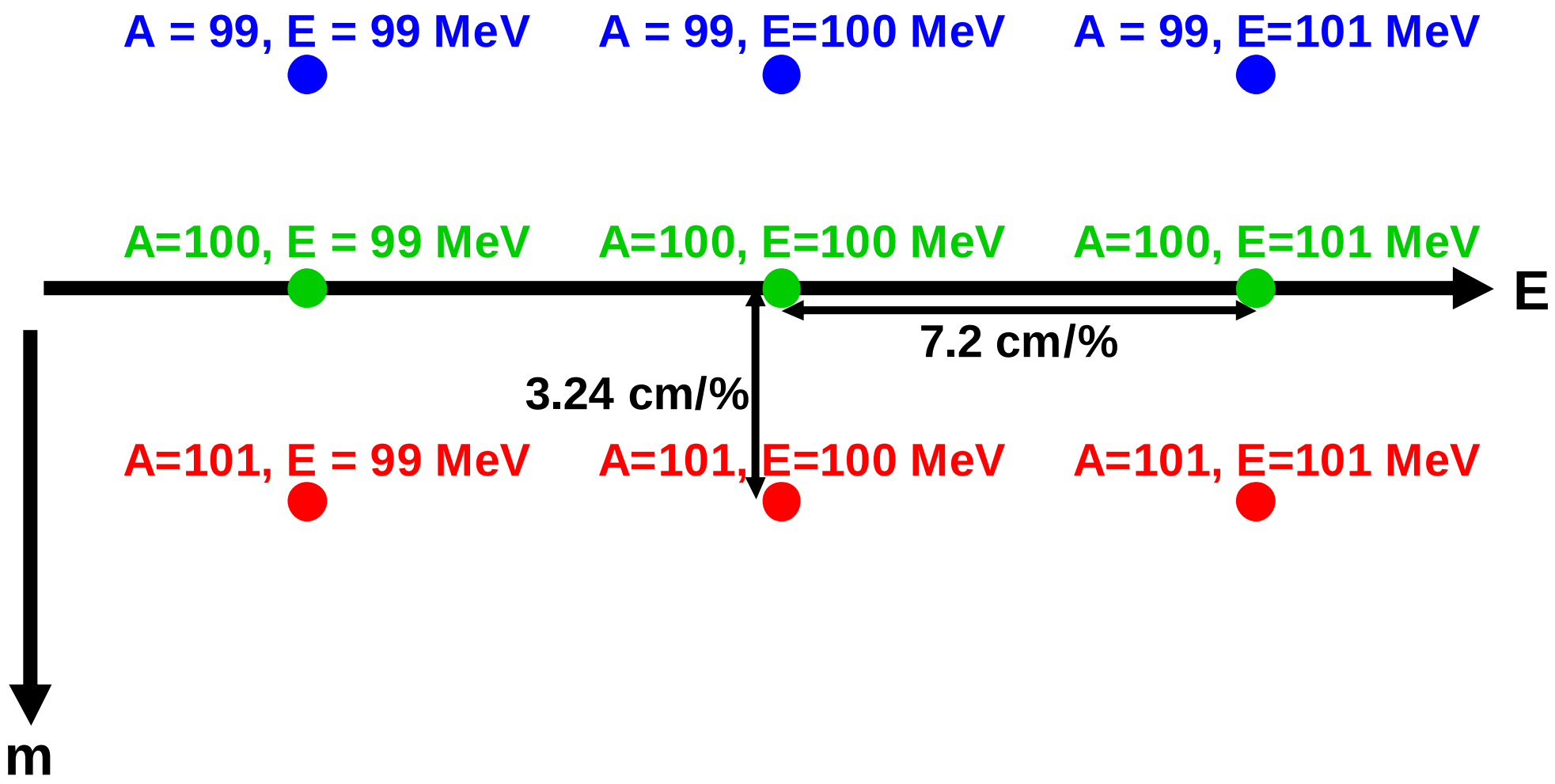

LOHENGRIN energy resolution

Magnification in x: $x_i = M_x\, x_o$

Energy resolution: $R_E = x_i / D_E = M_x \cdot x_o / D_E =$

$= 1.0 \cdot 7.0\ \text{cm} / 7.2\ \text{m} \approx 1/100$

depends on target length!

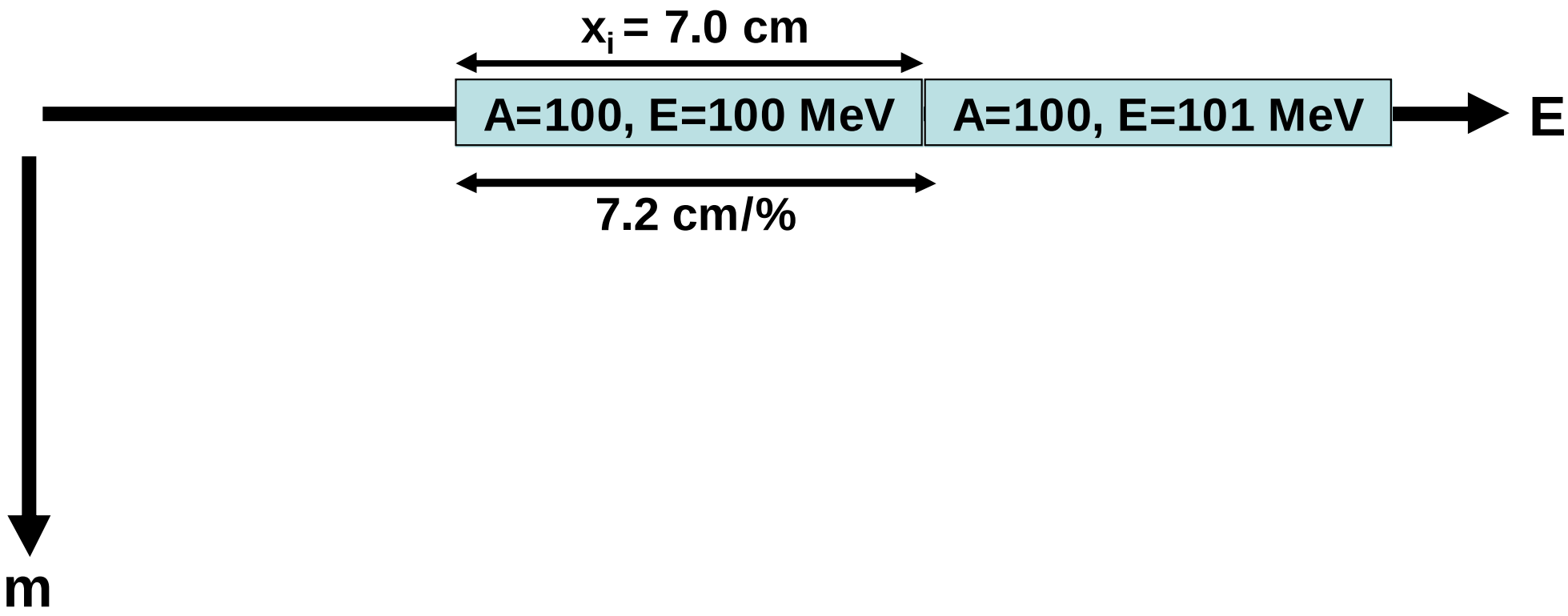

^{7}Be(n,p) spectrum measured at neutron beam

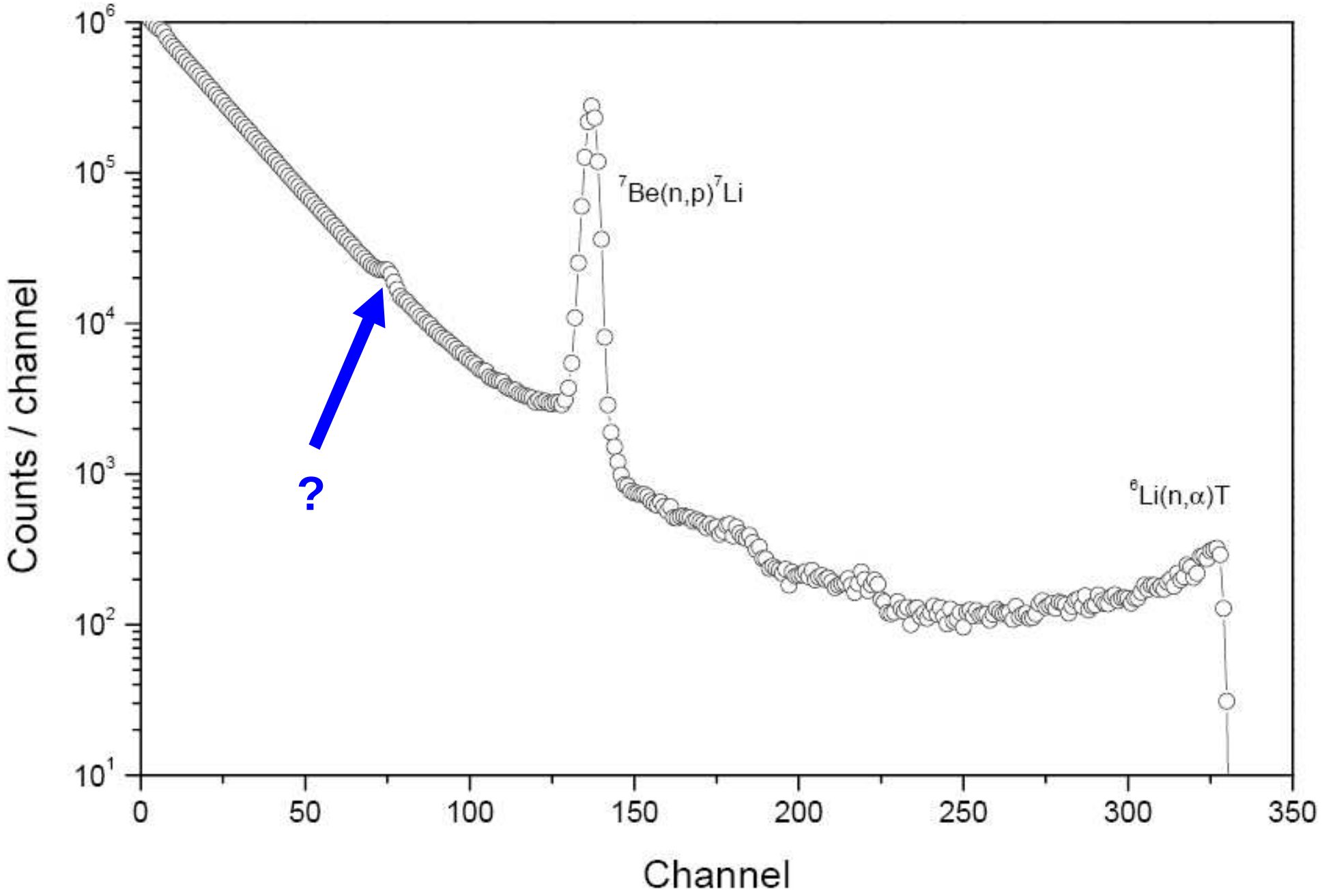

^{7}Be(n,p) measured at LOHENGRIN

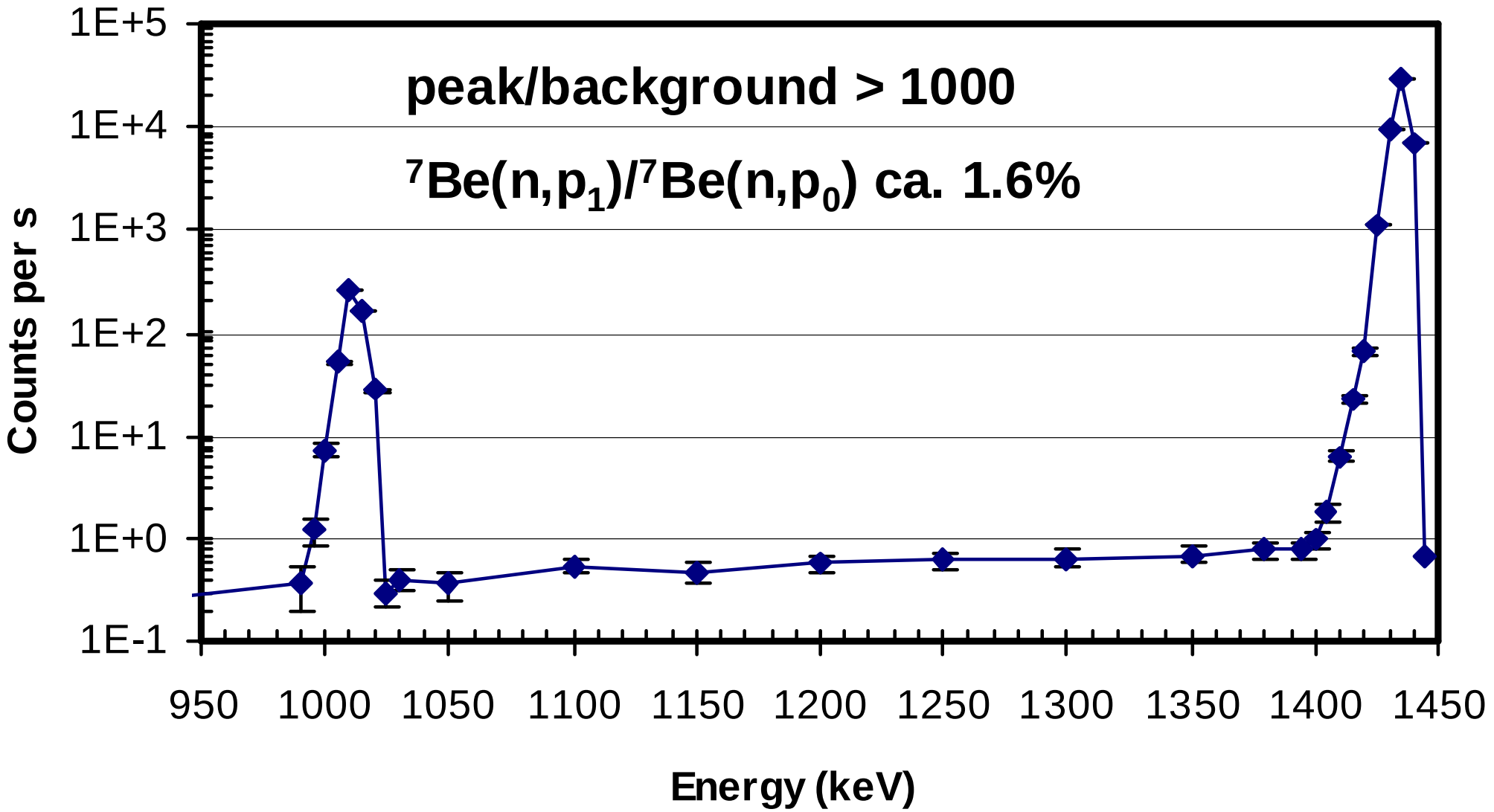

LOHENGRIN mass resolution

Magnification in y: $y_i = M_y\, y_o$

Mass resolution: $R_m = y_i / D_m = M_y \cdot y_o / D_m =$

$= 1.0 \cdot 0.3\ \text{cm} / 3.24\ \text{m} \approx 1/1000$

depends on target width!

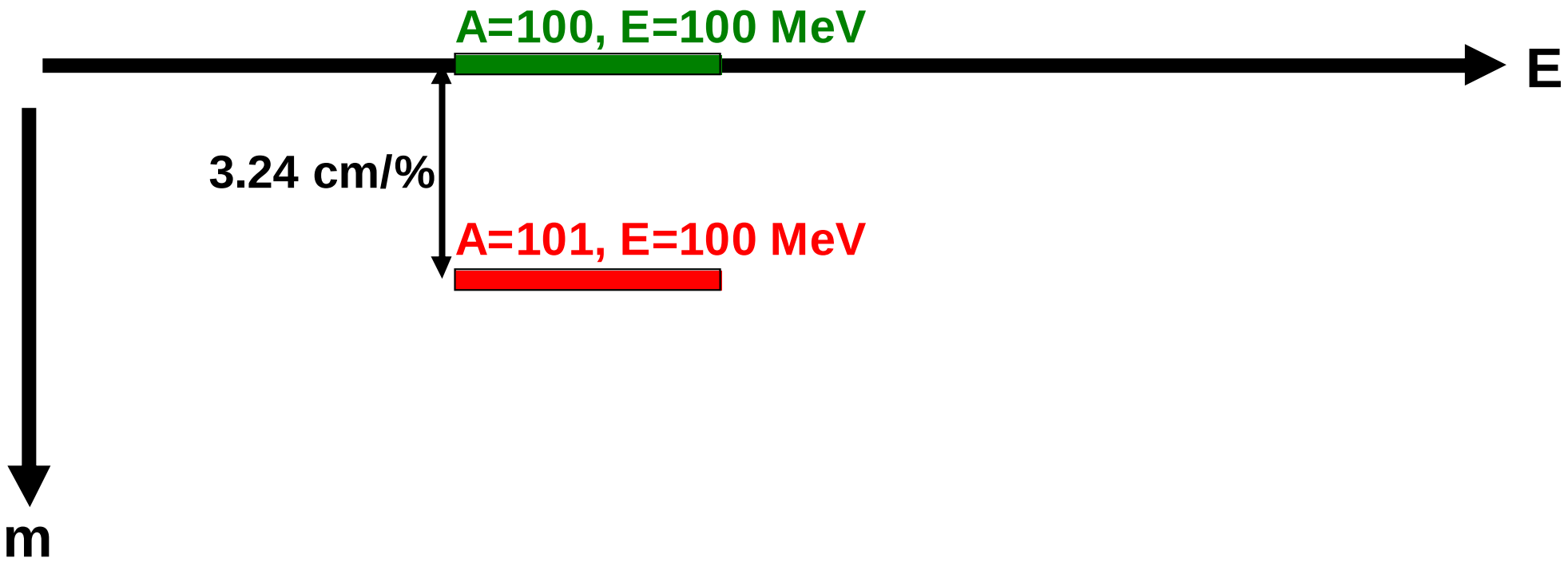

A/q separator

A “mass” separator is in reality an A/q separator and will mix masses with the same A/q and same E/q.

Avoid the use of A/q with (near-)integer ratios!

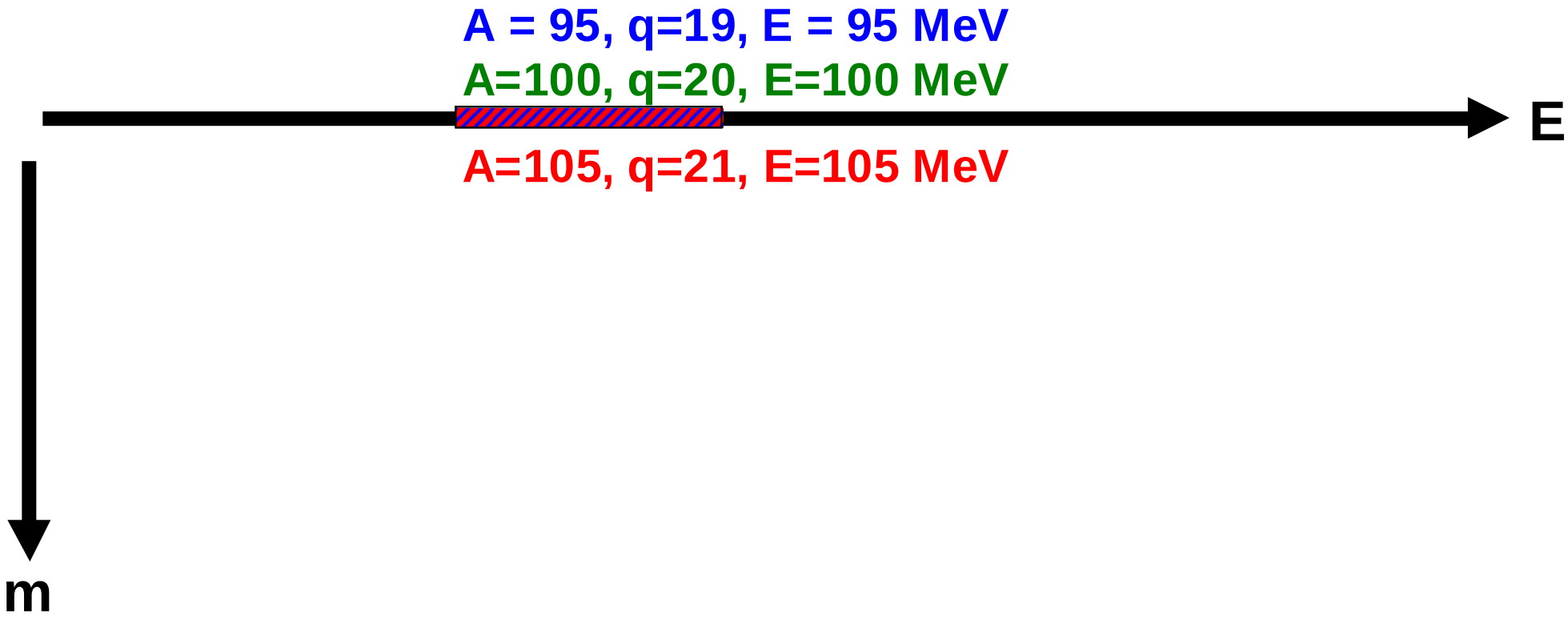

Focal plane of LOHENGRIN

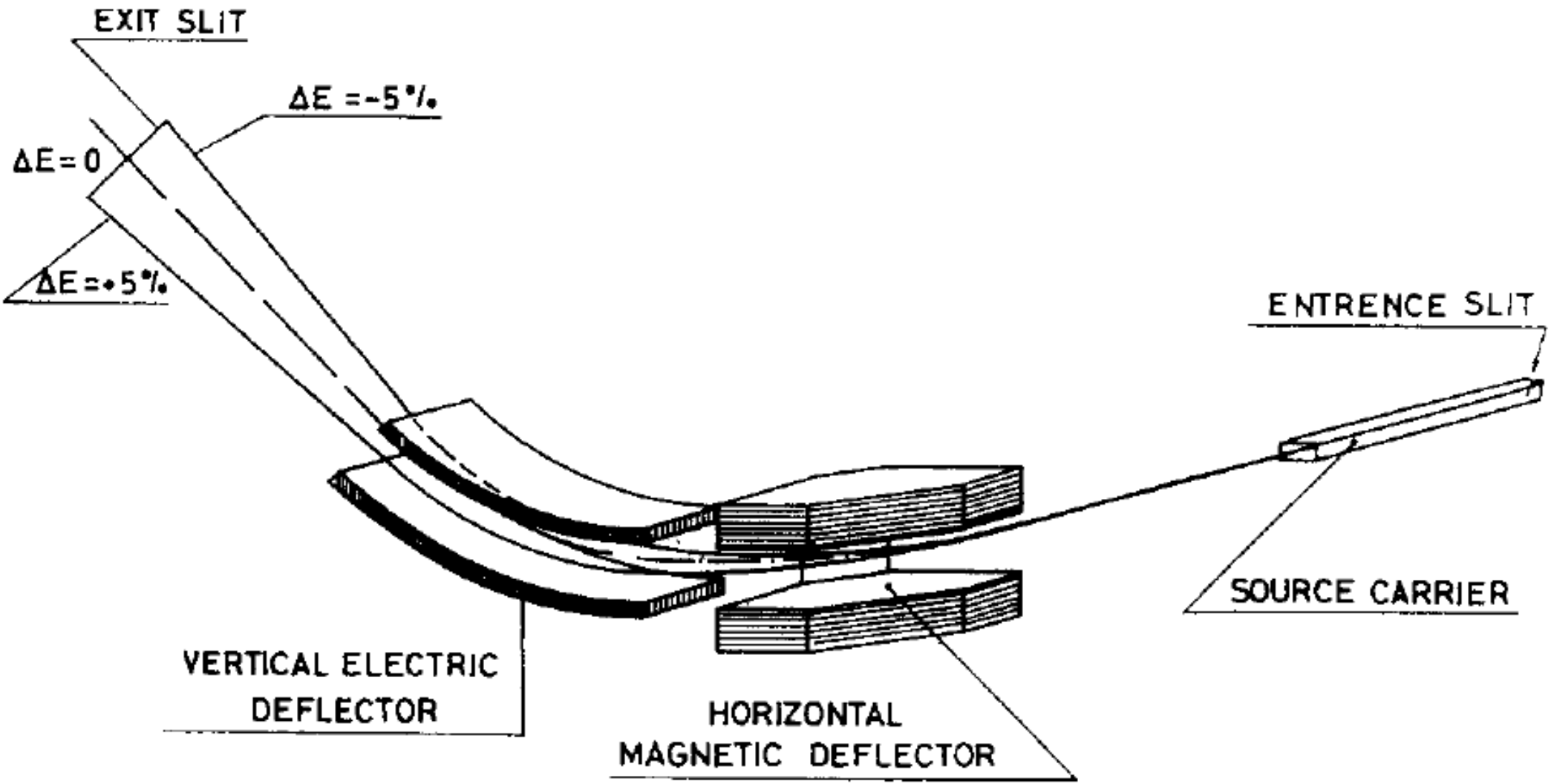

Measured kinetic energy distribution

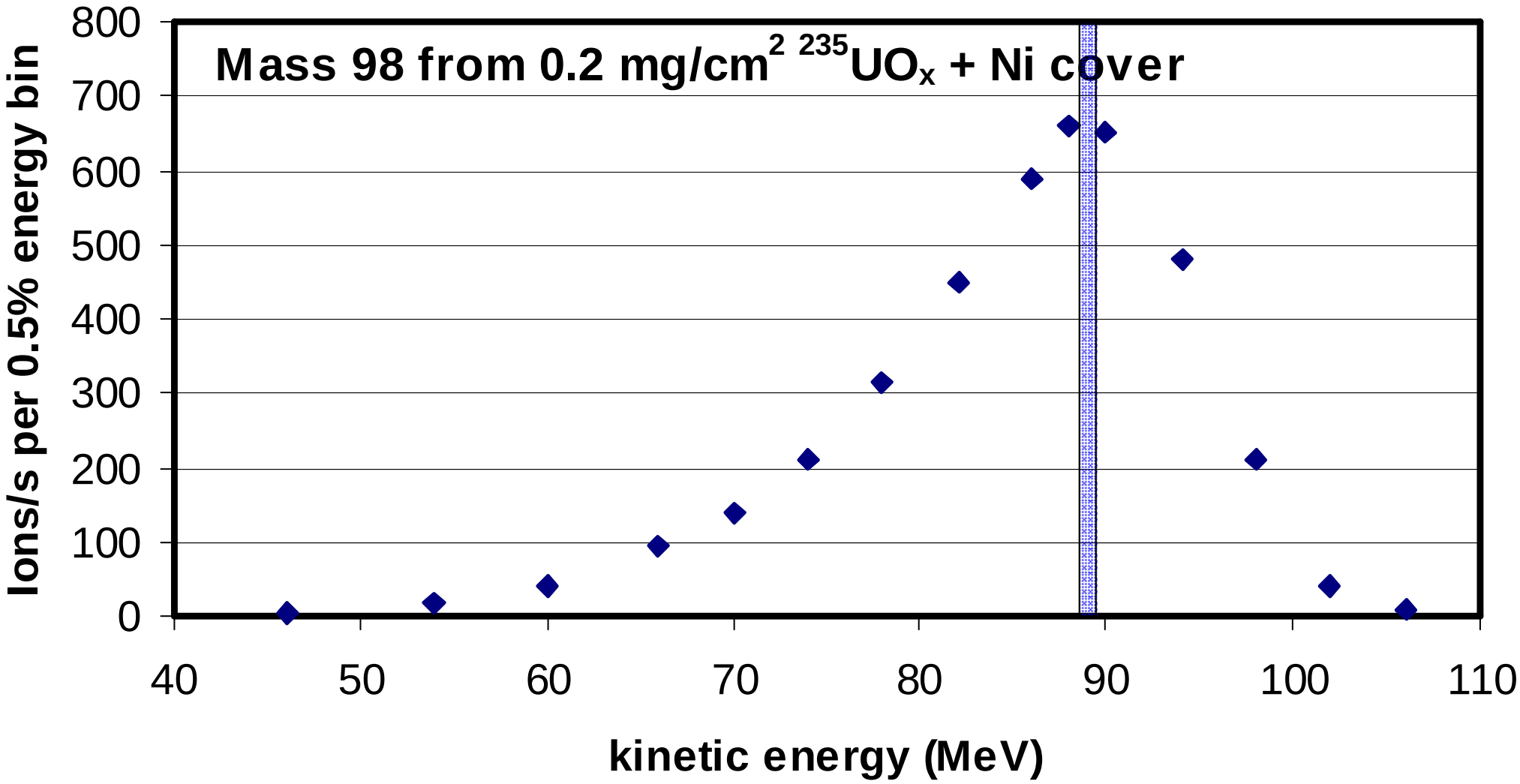

kinetic energy acceptance: $\Delta E/E = 1\%$

Reverse Energy Dispersion magnet

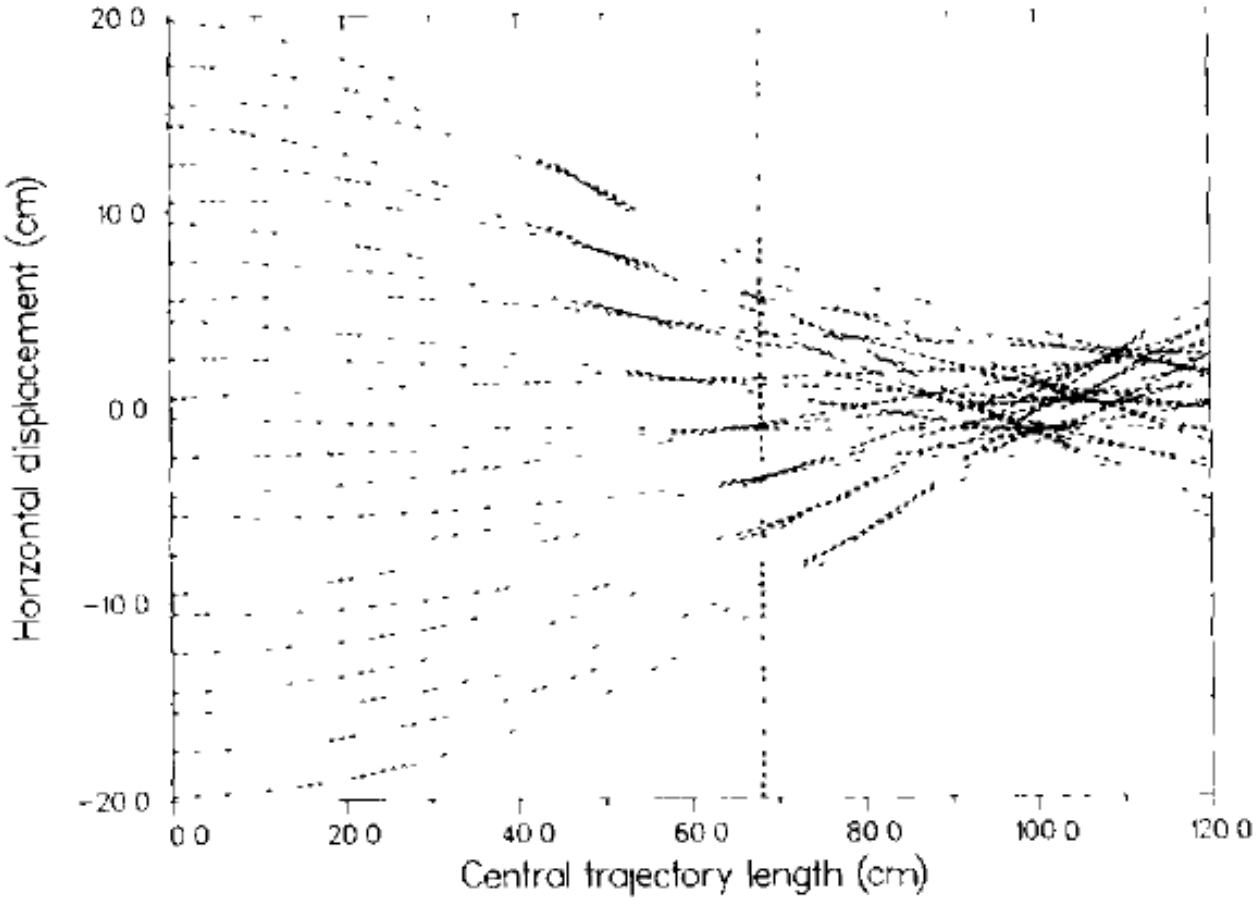

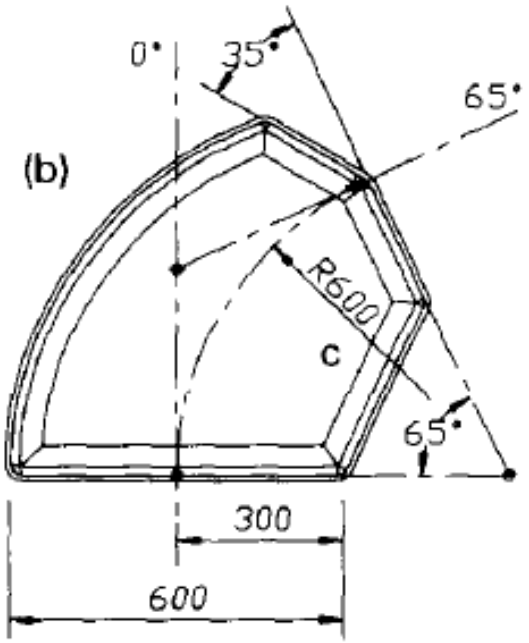

Fig. 5. Horizontal displacement with respect to the central trajectory of a beam arising from a 5×70 mm^2 target vs the central trajectory length. The vertical dashed and dotted lines show respectively the extent of the pole pieces and the focal position.

G. Fioni et al., Nucl. Instr. Meth. A332 (2003) 175.

LOHENGRIN Setup

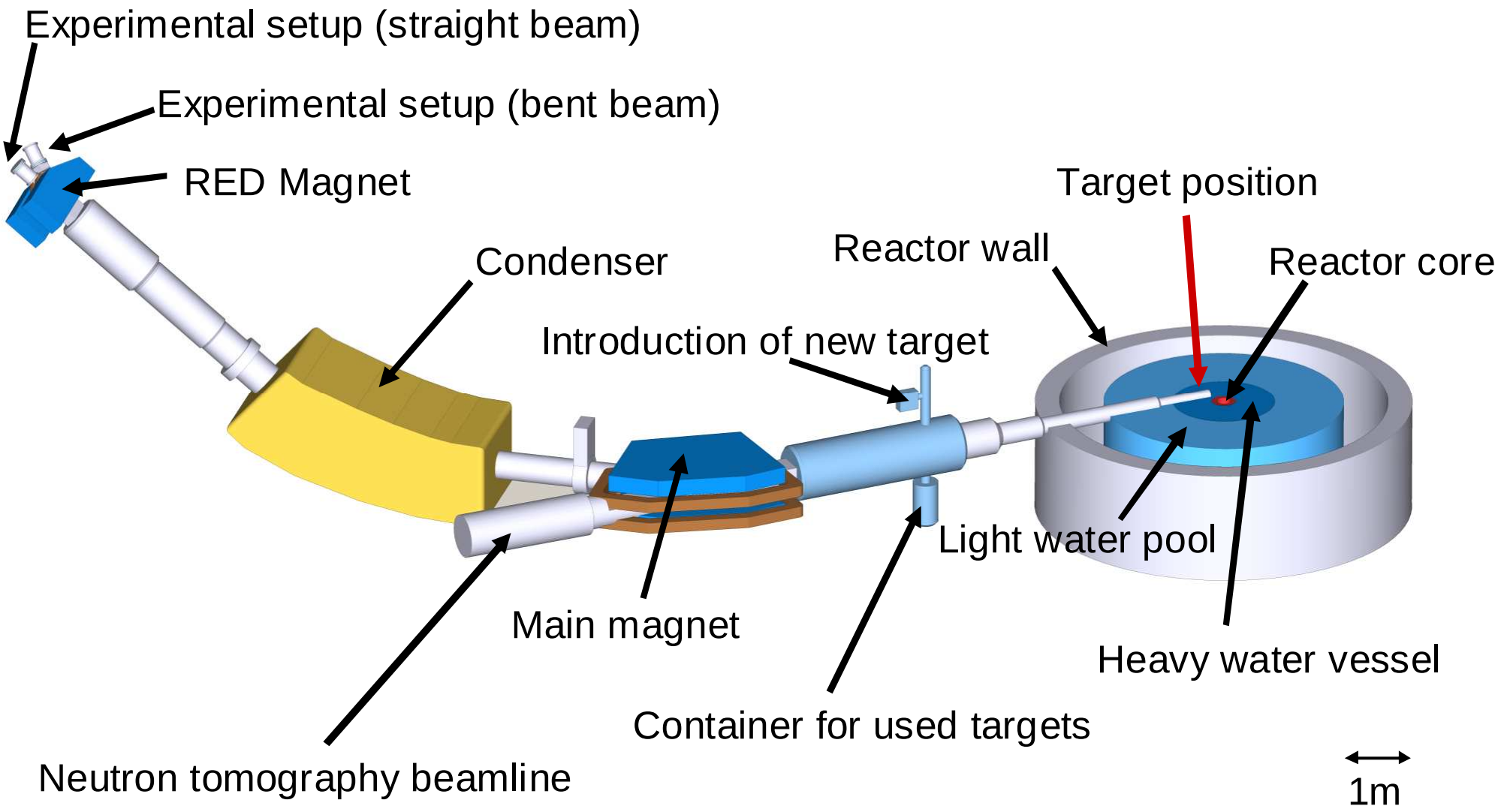

Measured kinetic energy distribution

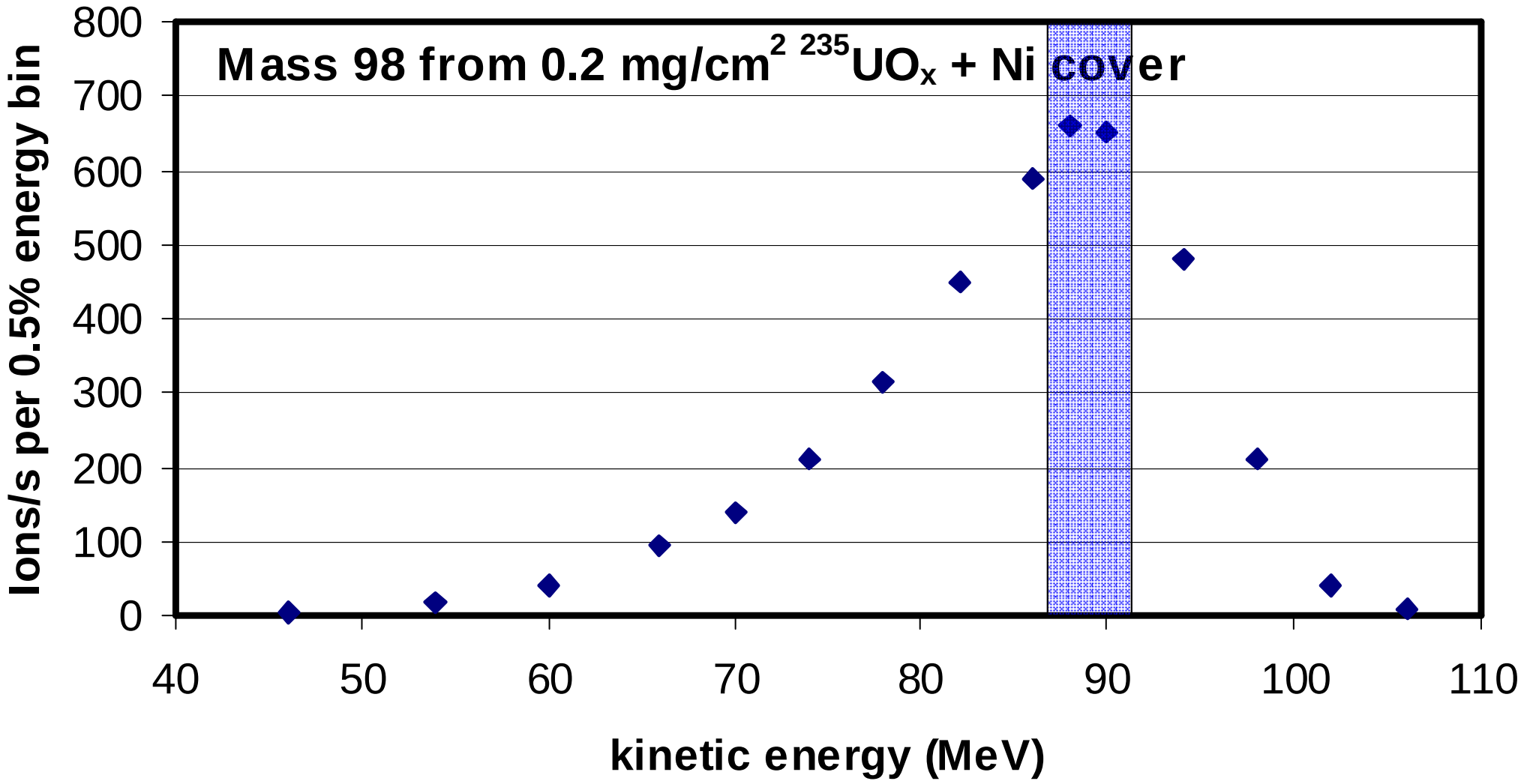

kinetic energy acceptance: $\Delta E/E = 5\%$

$\Rightarrow$ 10-60% transmission (low for thick spectroscopy targets)

Detection of rare ternary particles

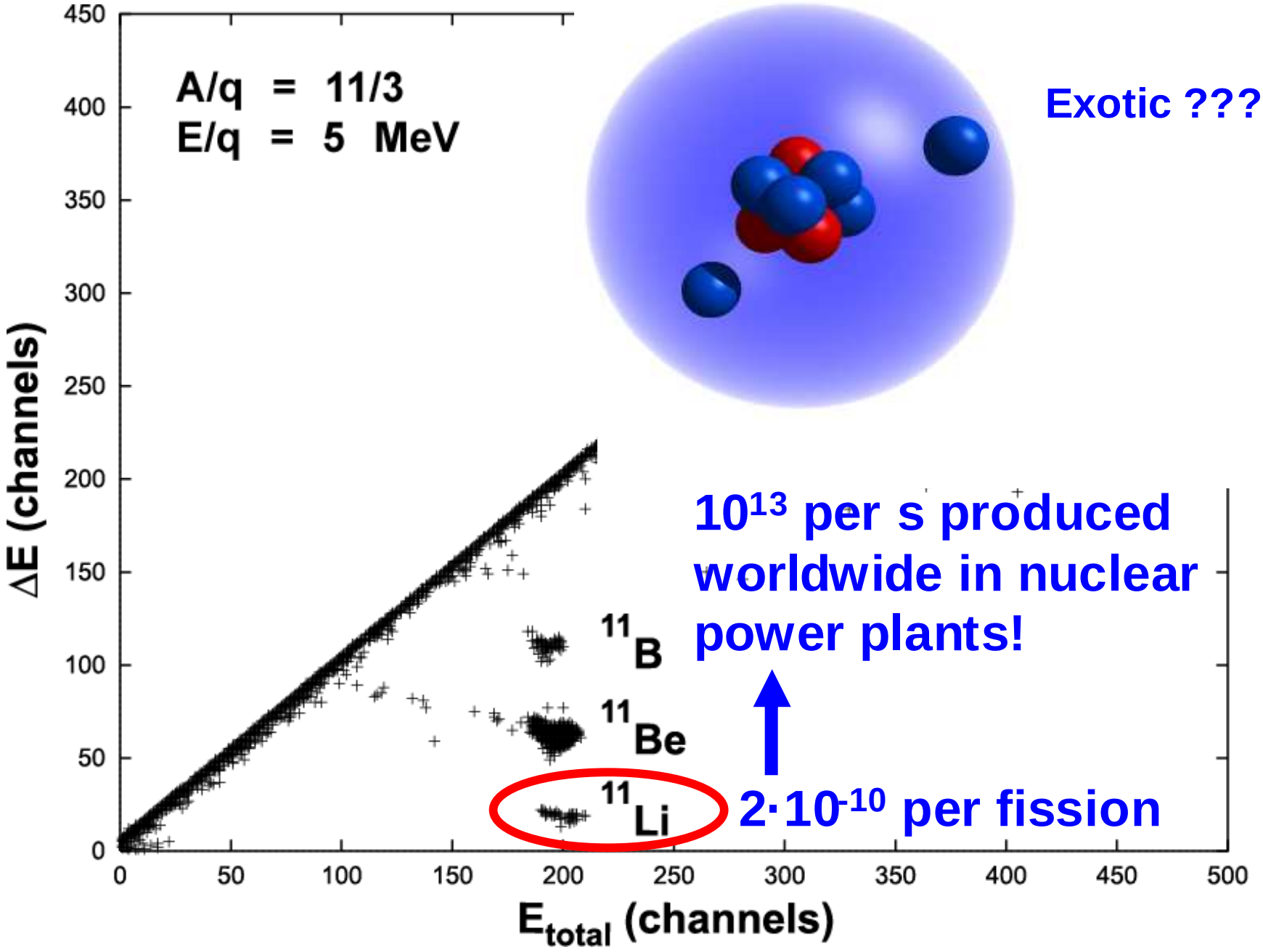

Exotic ???

10^{13} per s produced worldwide in nuclear power plants!

$2 \cdot 10^{-10}$ per fission

Gamma decay of 7.6 μs ^{98}Y isomer

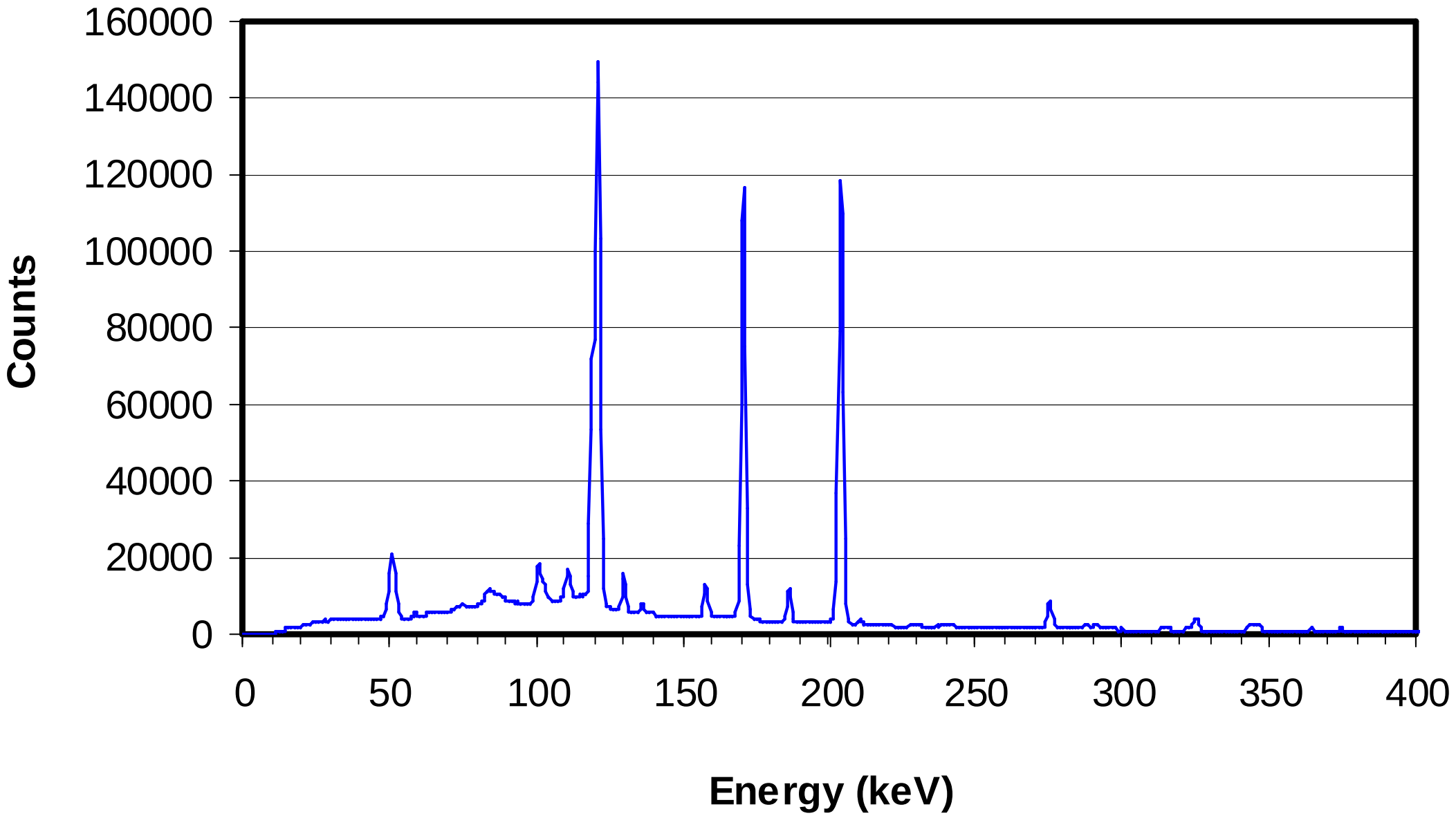

17^- isomer at 6.6 MeV in ^{98}Zr

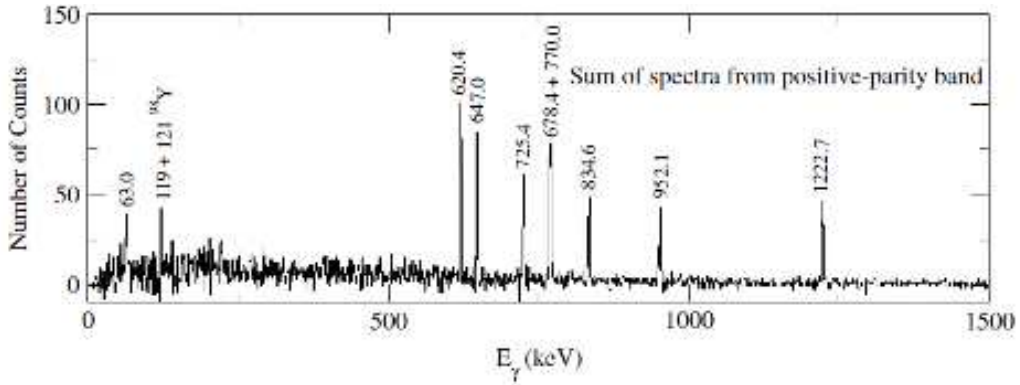

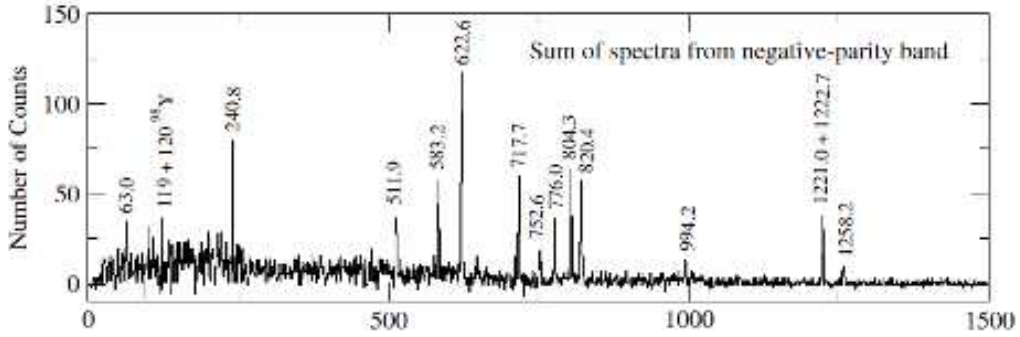

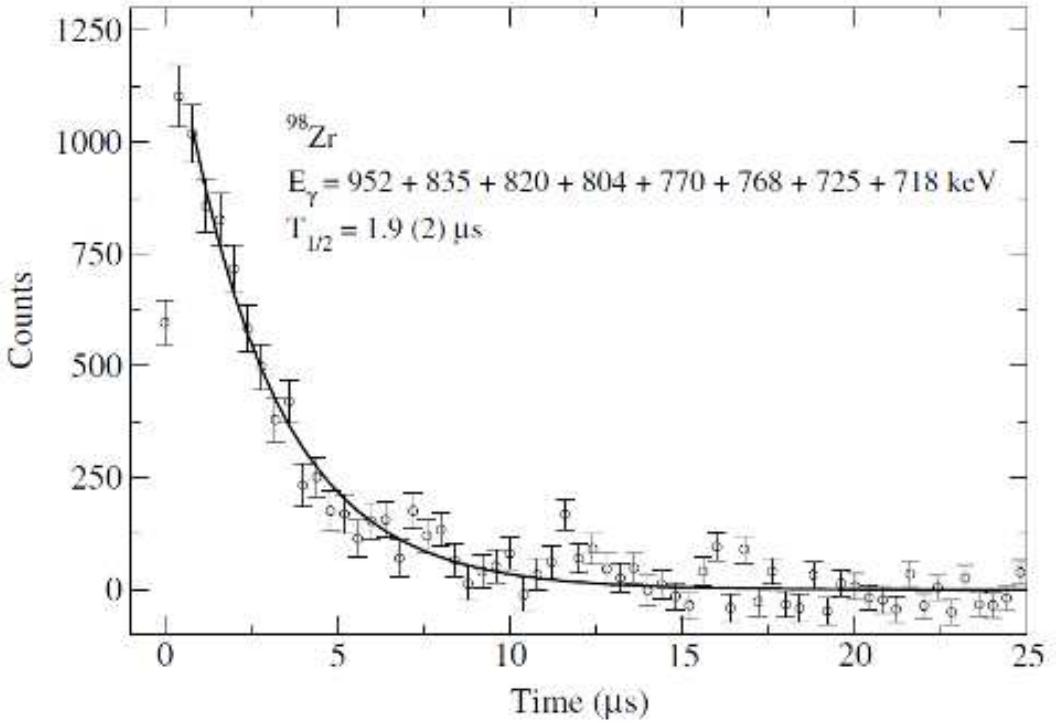

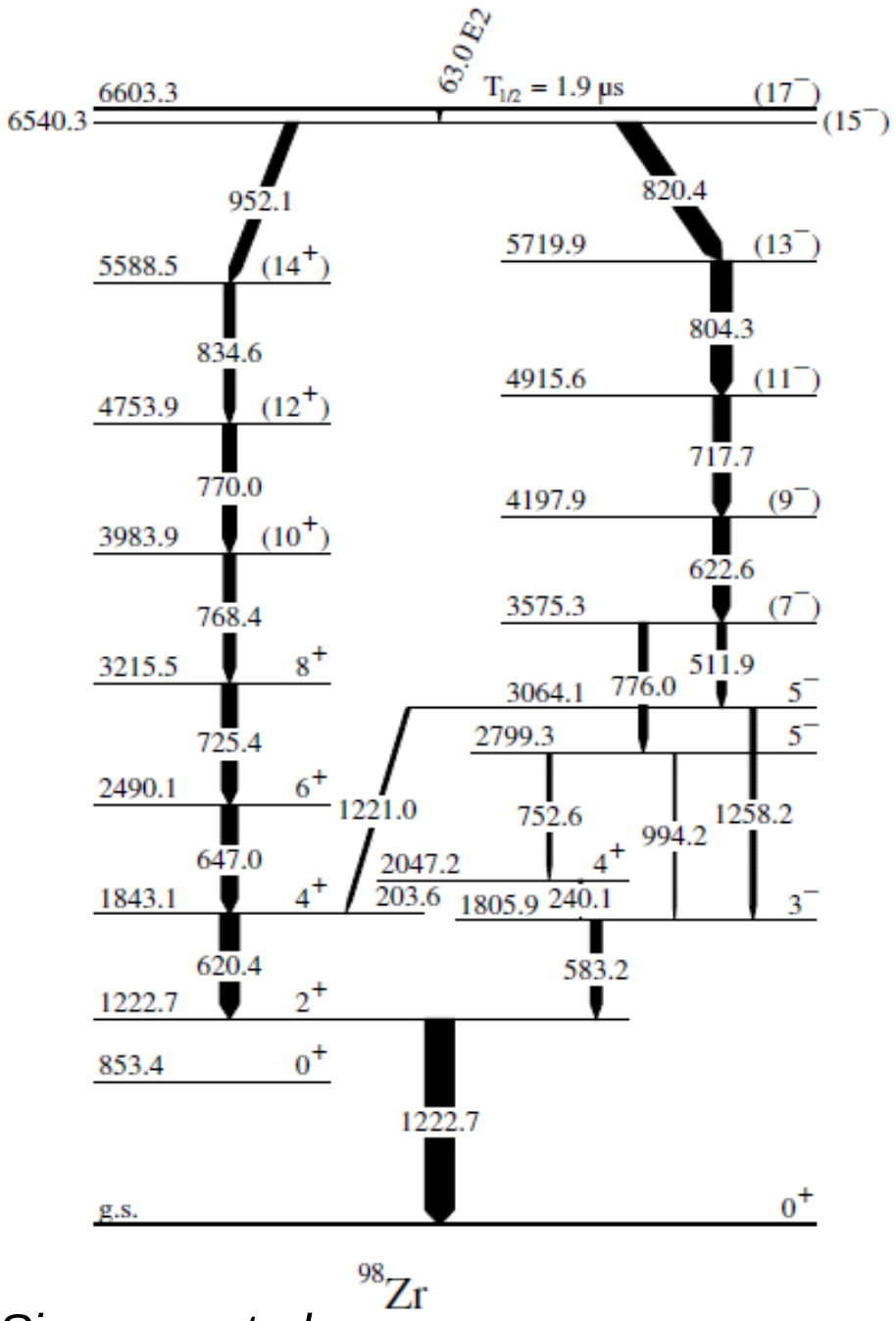

G. Simpson et al.,
Phys. Rev. C 74 (2006) 064308.

Existing thick-target ISOL beams

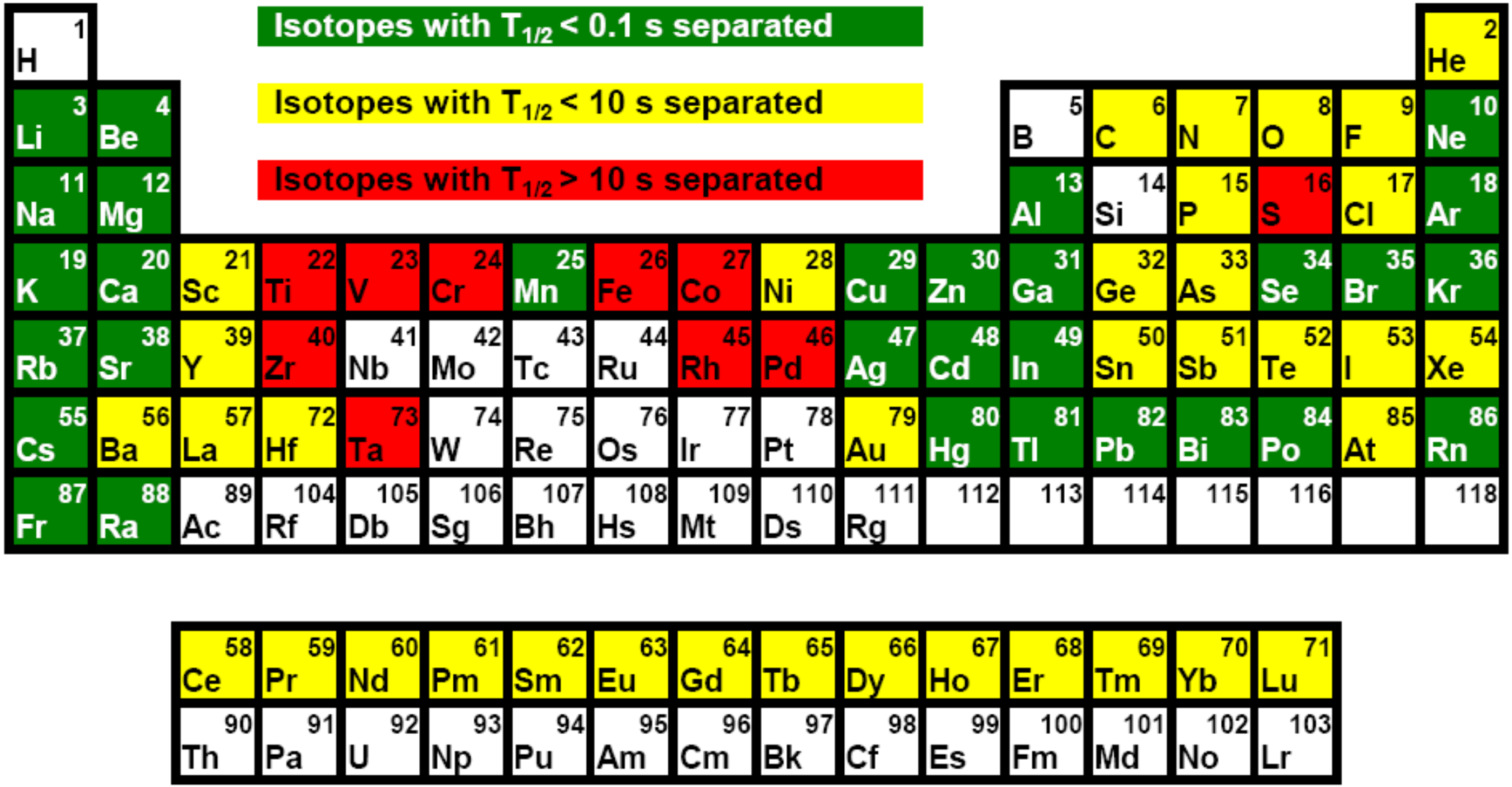

The LOHENGRIN fission fragment separator

mass-separated fission fragments,

up to 10^5 per second, $T_{1/2} \geq$ microsec.

$\Delta A/A$ = 3E-4 – 3E-3

$\Delta E/E$ = 1E-3 – 1E-2

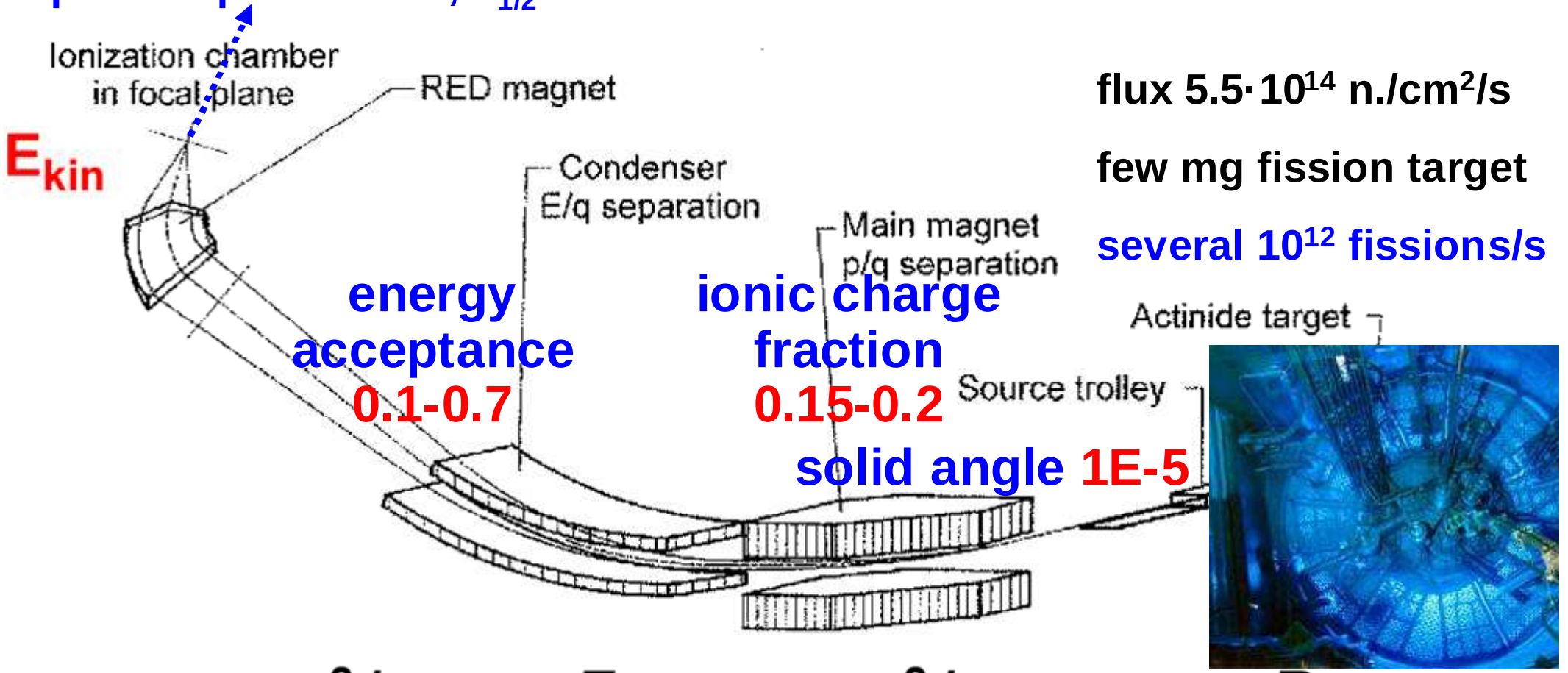

flux 5.5·10^{14} n./cm^2/s

few mg fission target

several 10^{12} fissions/s

$$m\,v^2 / r_{el} = q\,E \qquad E_{kin} / q = E / 2\,r_{el}$$

$$m\,v^2 / r_{magn} = q\,v\,B \qquad m\,v / q = B\,r_{magn}$$

Ionic charge separation

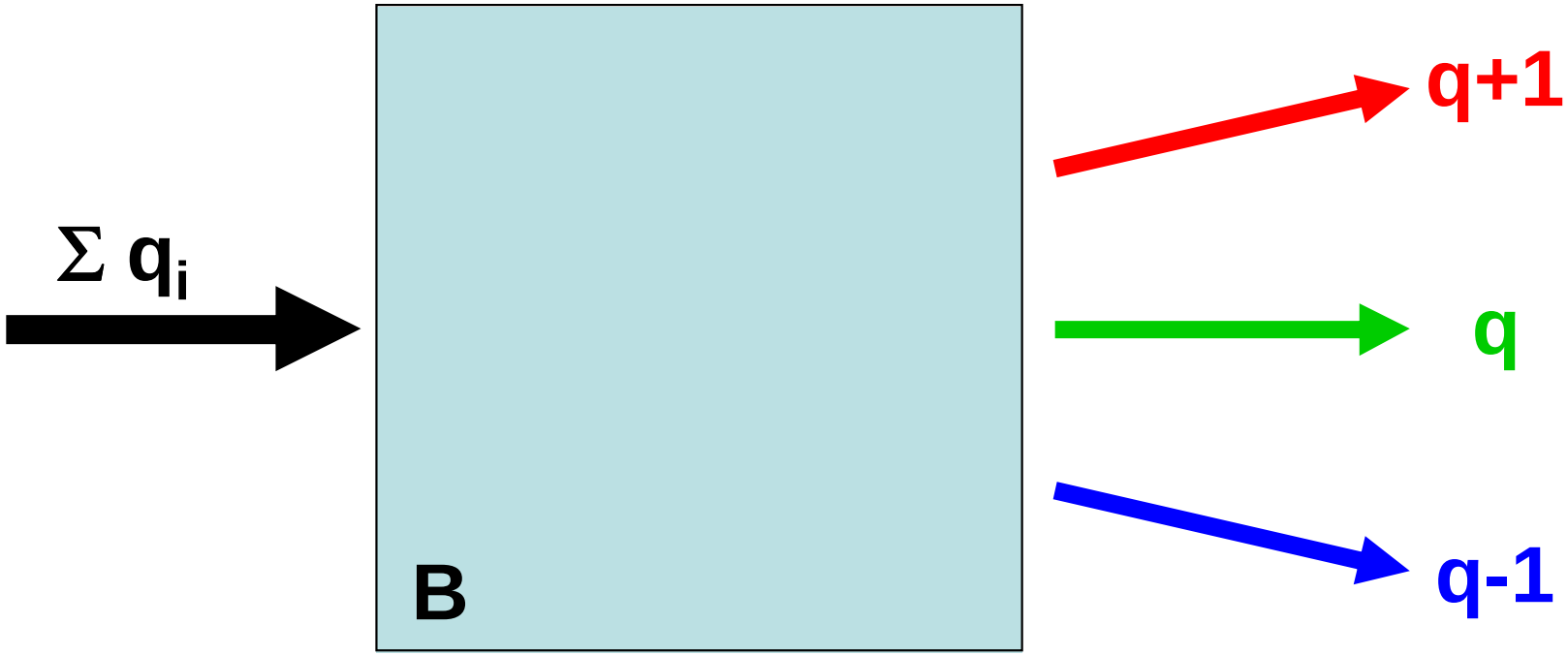

Ionic charge state distribution

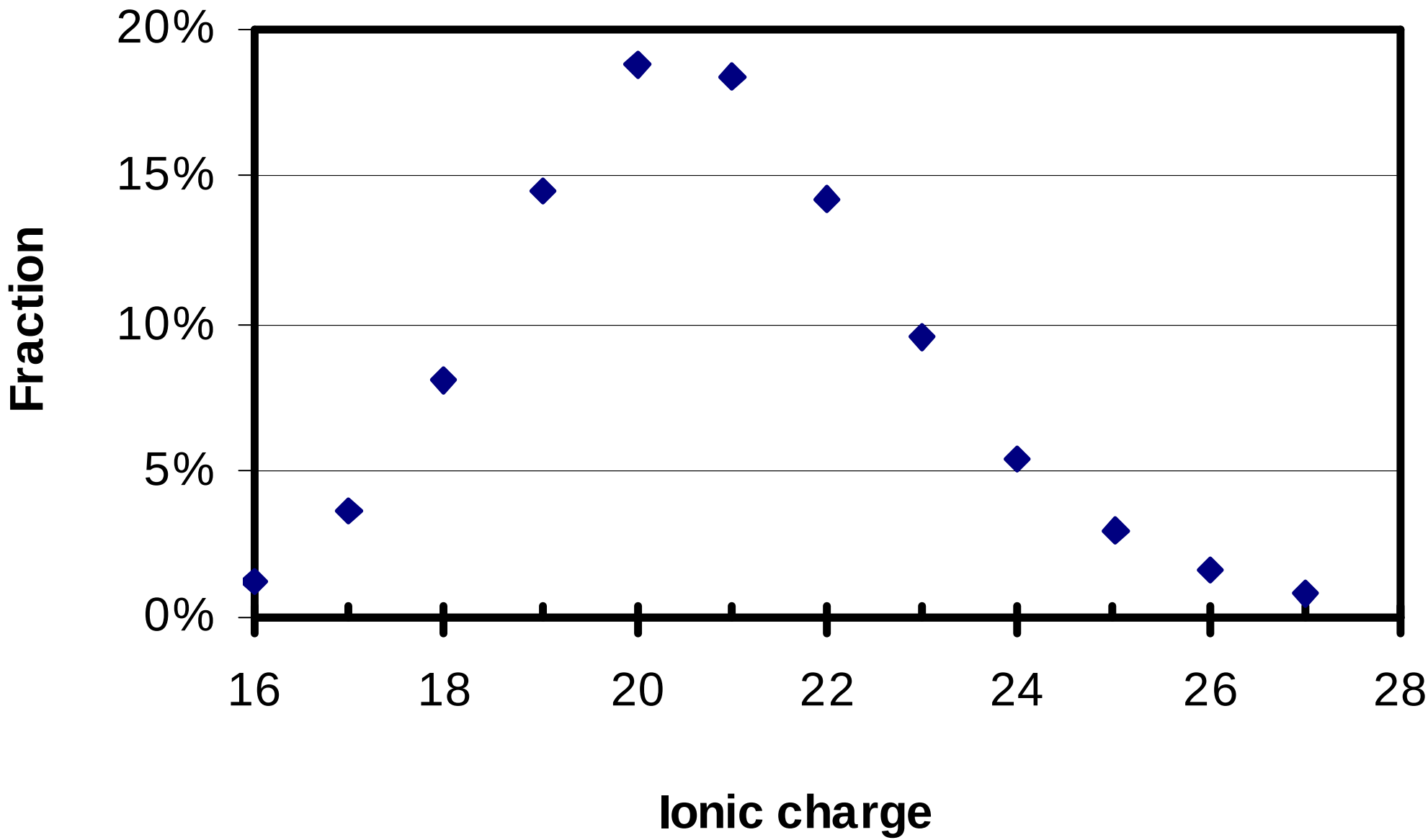

Ionic charge separation

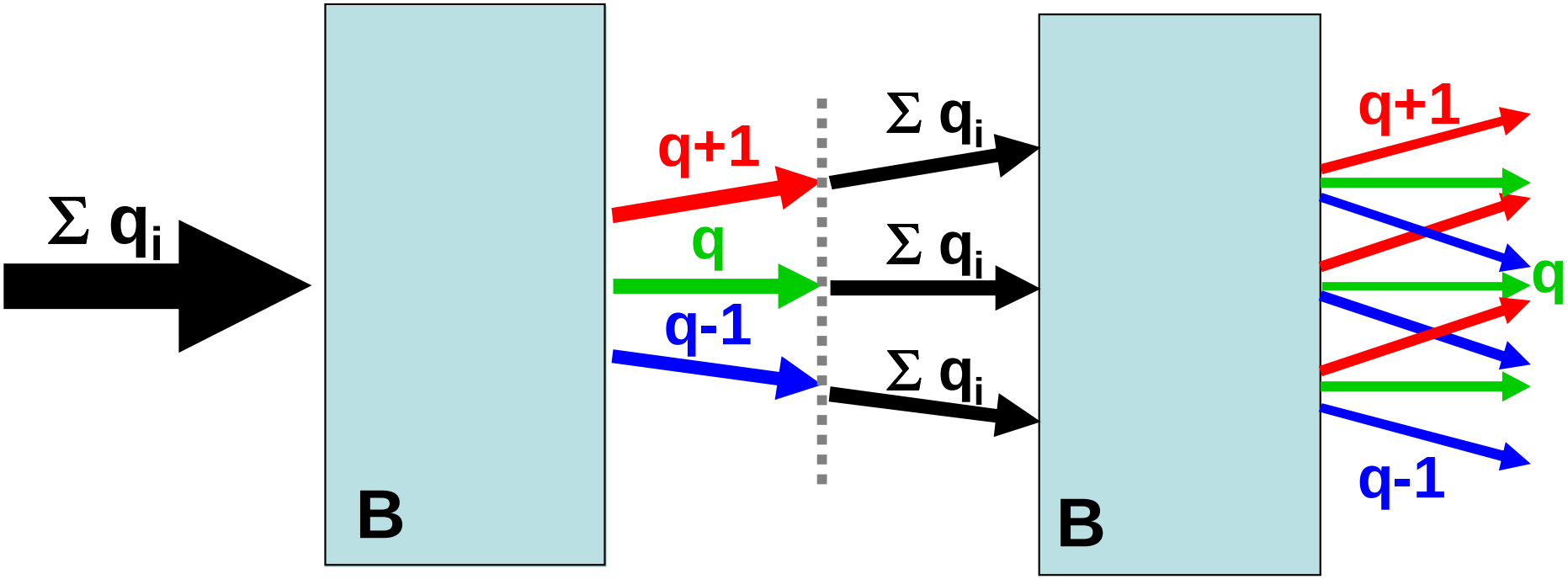

Ionic charge separation

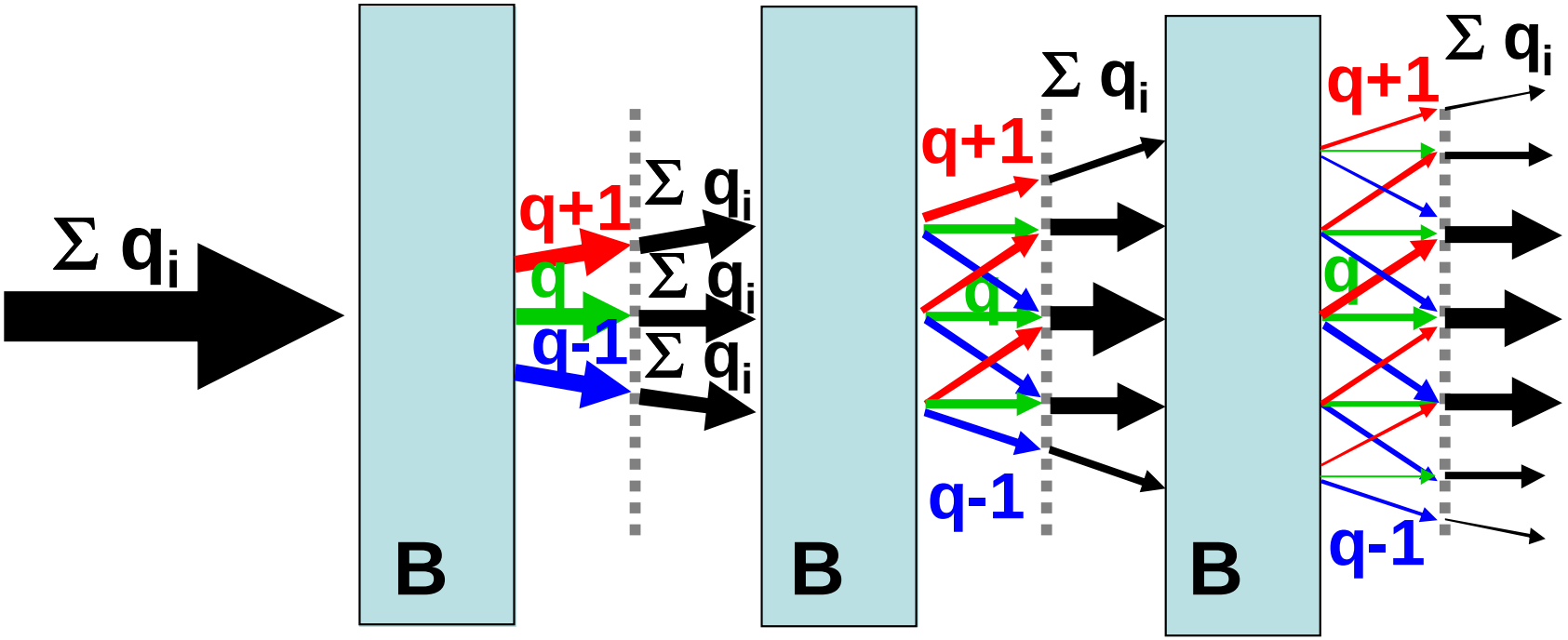

Separation with gas-filled magnet

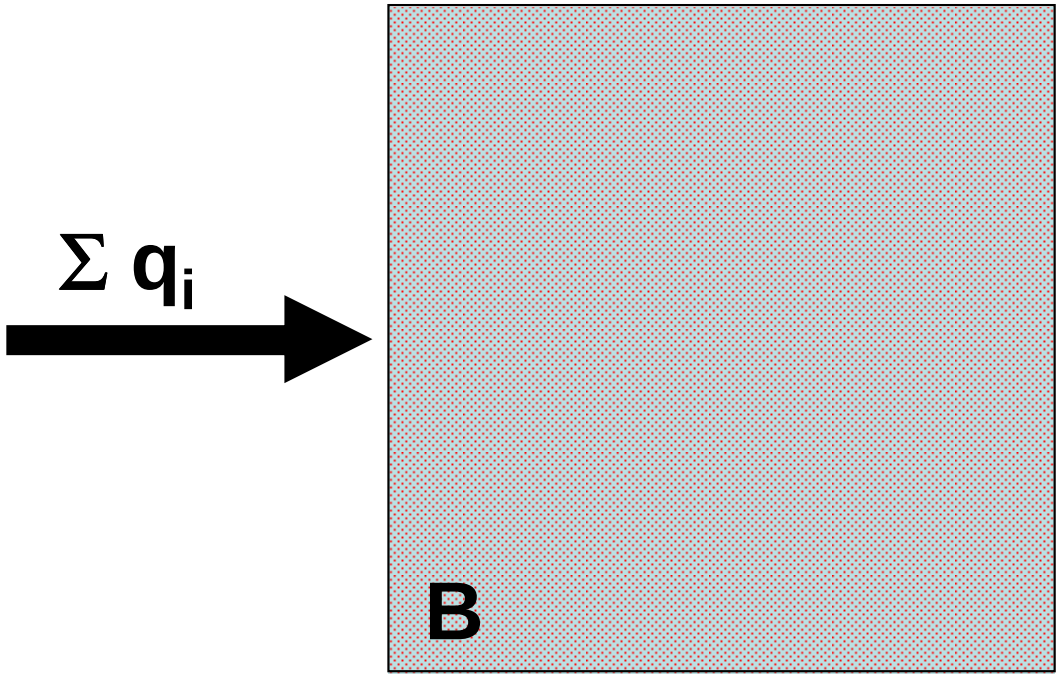

He or N_2 at few mbar

$$q_{average} = v/v_{Bohr}\, Z^{\alpha}$$

$$\alpha_{theo} = 1/3 \text{ (Bohr)}$$

$$\alpha_{exp} = 0.33 - 0.7$$

Isotope selection with gas-filled separators

- **Gas collisions give average q = fkt(Z,v) ∝ $Z^{1/3}$ v/v_{Bohr}**
- **p/q selection by magnetic deflection**
- **Bρ ∝ $A/Z^{1/3}$ (*A. Ghiorso et al., Nucl. Instr. Meth. A269 (1988) 192*)**

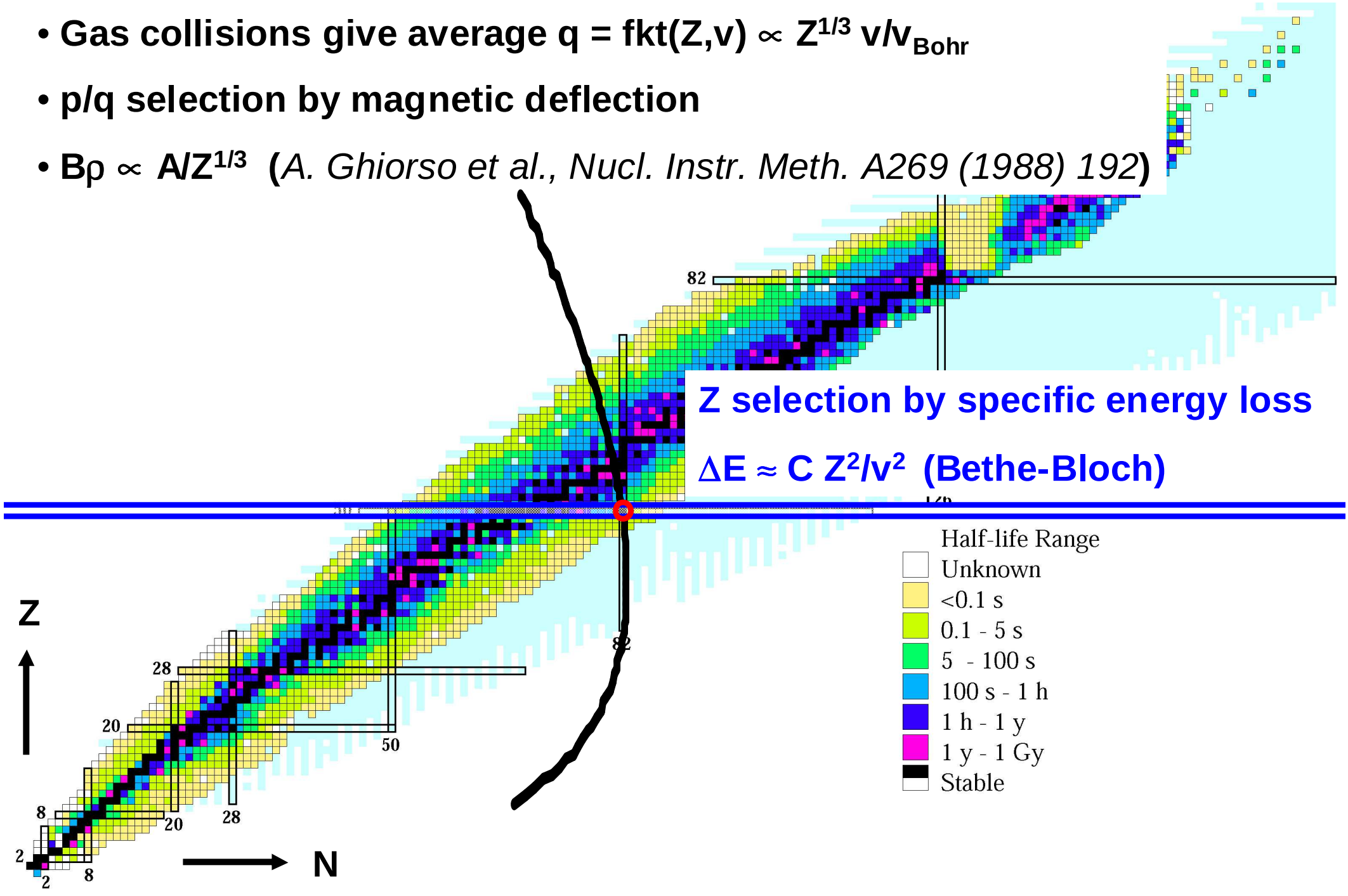

Multistep-Separation in Accelerator Mass Spectrometry

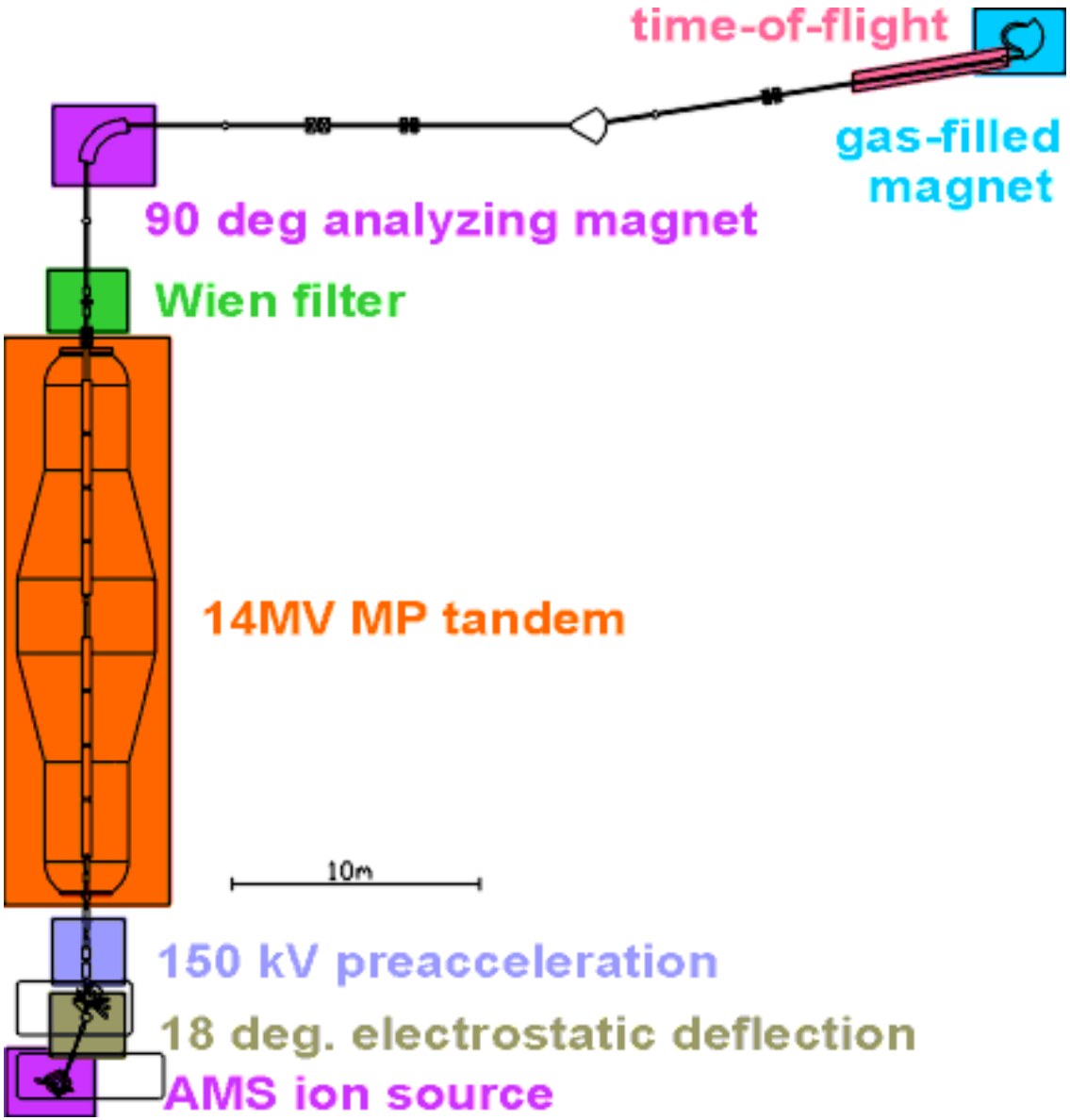

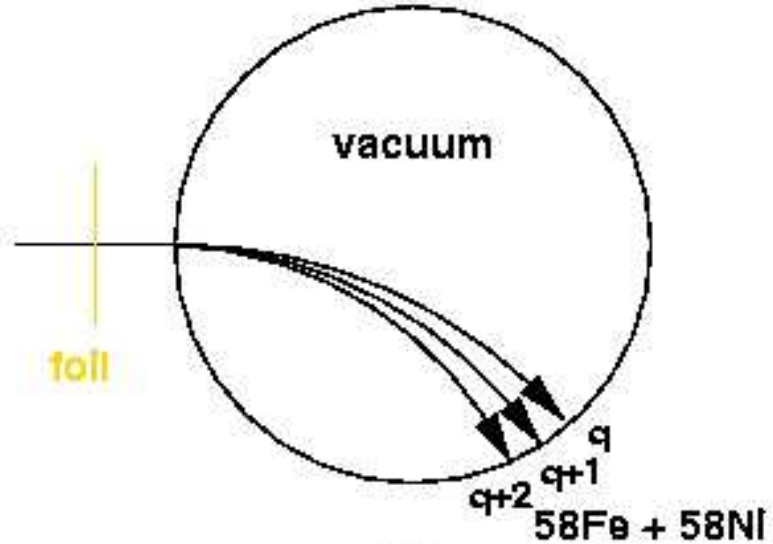

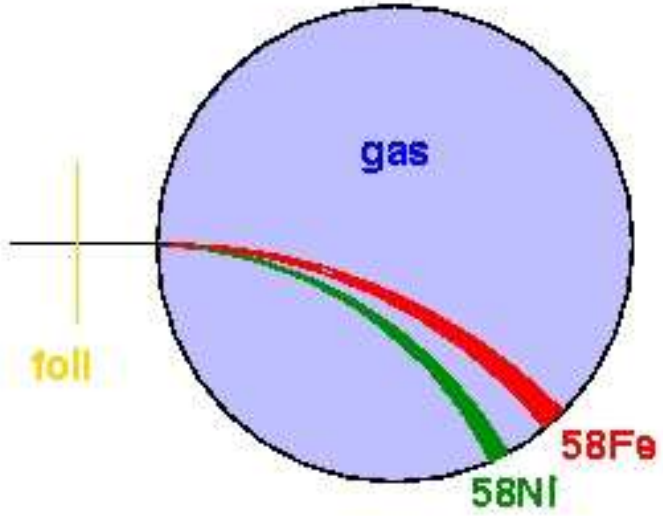

10^{-15} sensitivity!

From ISOL beams to RIBs with higher energies

ISOL beams

- **have well-defined energy ($\Delta E/E \approx 1eV/60$ keV)**
- **have usually small emittance (e.g. 10 π mm mrad), i.e. limited opening angle**
- **have often well-defined ionic charge q=1**
- **Z selection is performed before the mass separator**

Recoils or fragments of nuclear reactions:

- **have large energy spread**
- **large angular spread**
- **different ionic charge states**
- **depending on nuclear reaction different Z**

Fusion-evaporation

$^{58}Ni(^{58}Ni,2n)^{114}Ba$

$^{58}Ni(^{58}Ni,\alpha 2n)^{110}Xe$

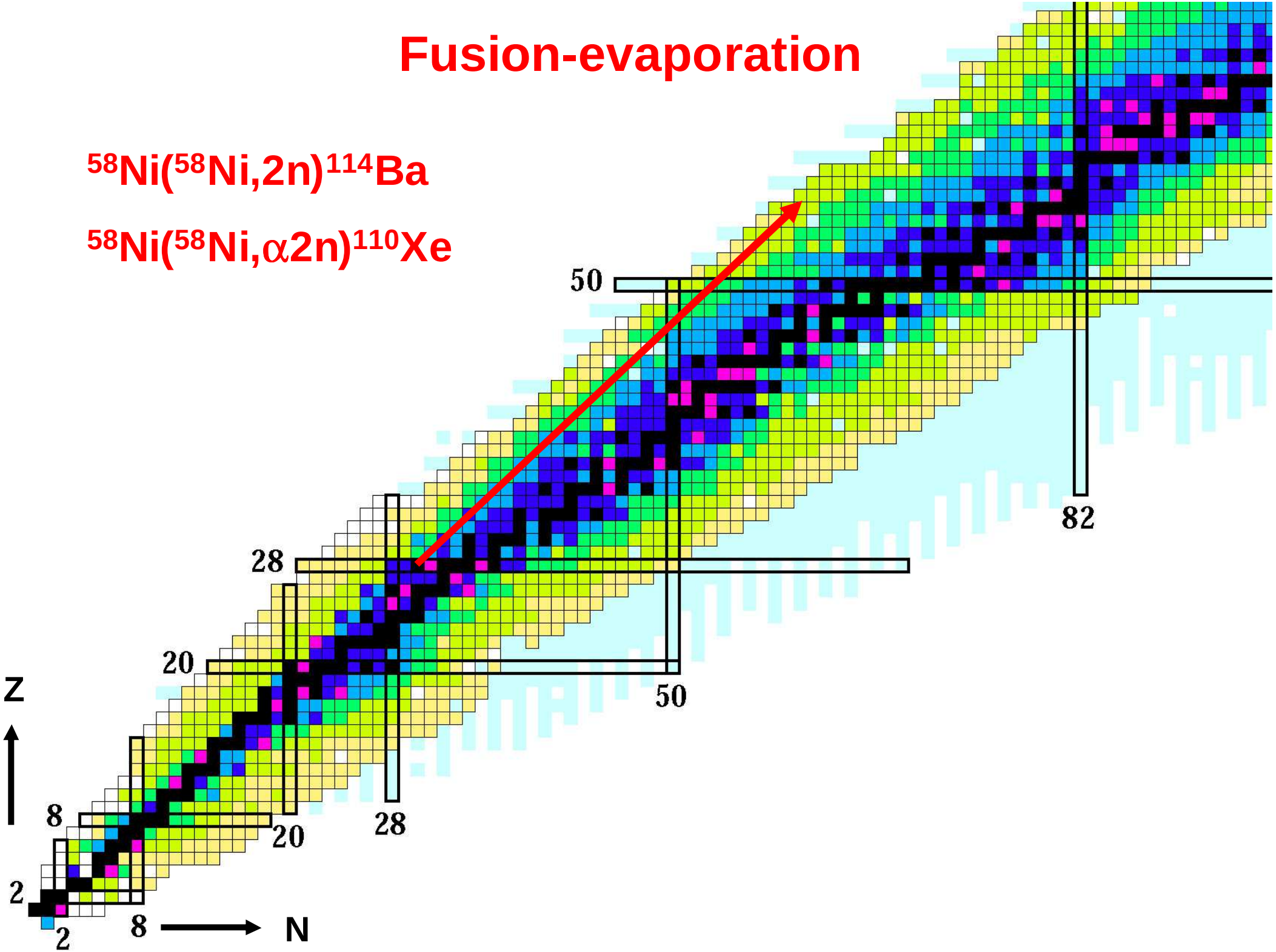

Multinucleon transfer reactions

$^{186}W(^{64}Ni,X)^{184}Lu$

K. Krumbholz et al.,

Z. Phys. A352 (1995) 1.

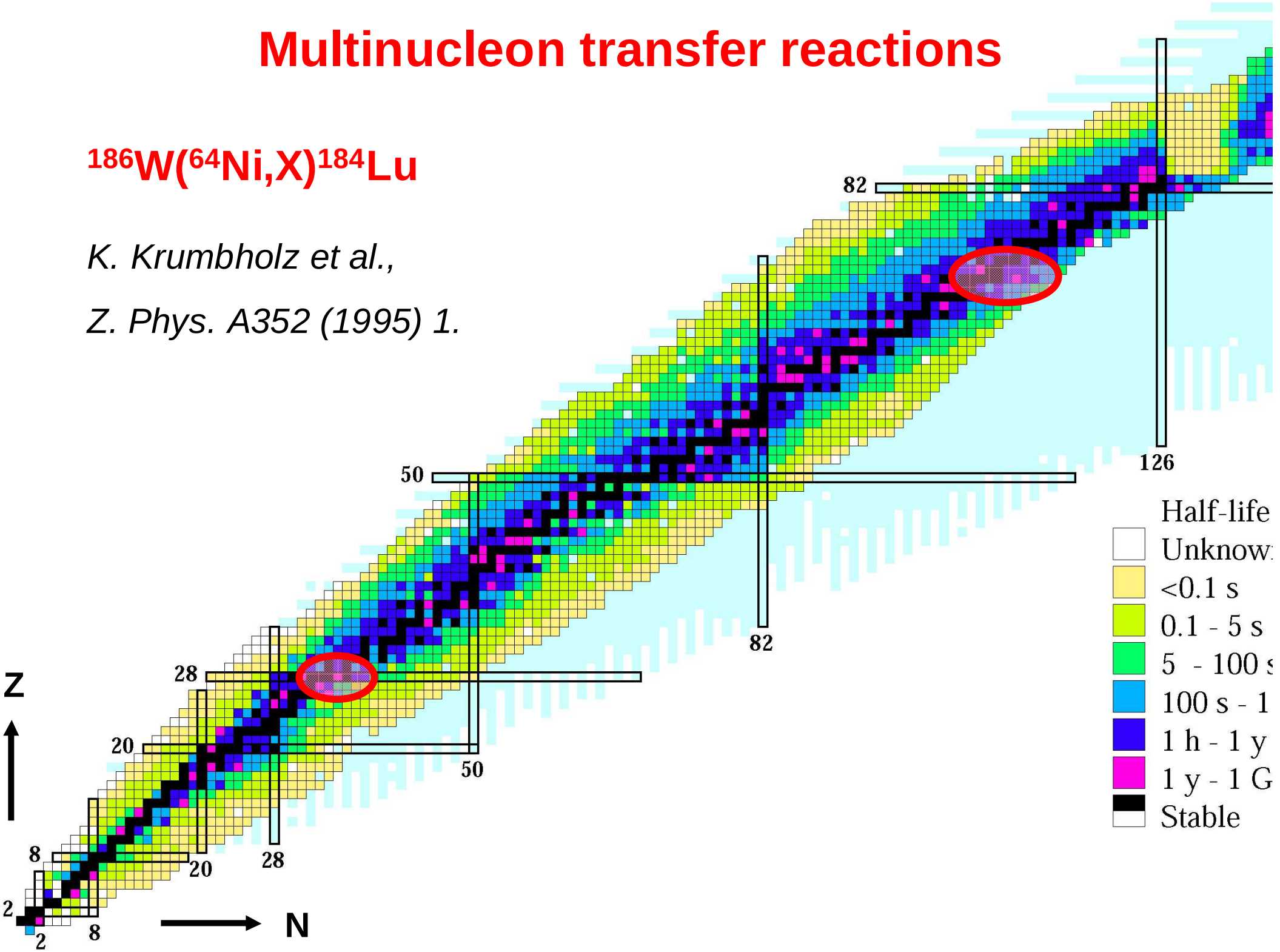

Requirements for in-flight separators

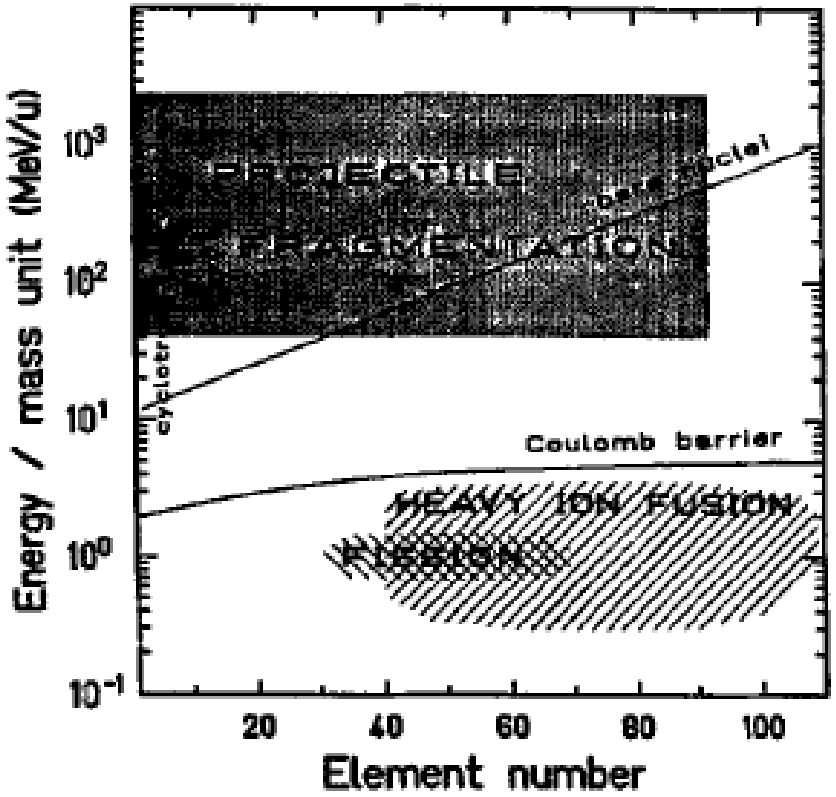

Fig. 2. Domains of kinetic energies of the reaction products from various nuclear reactions.

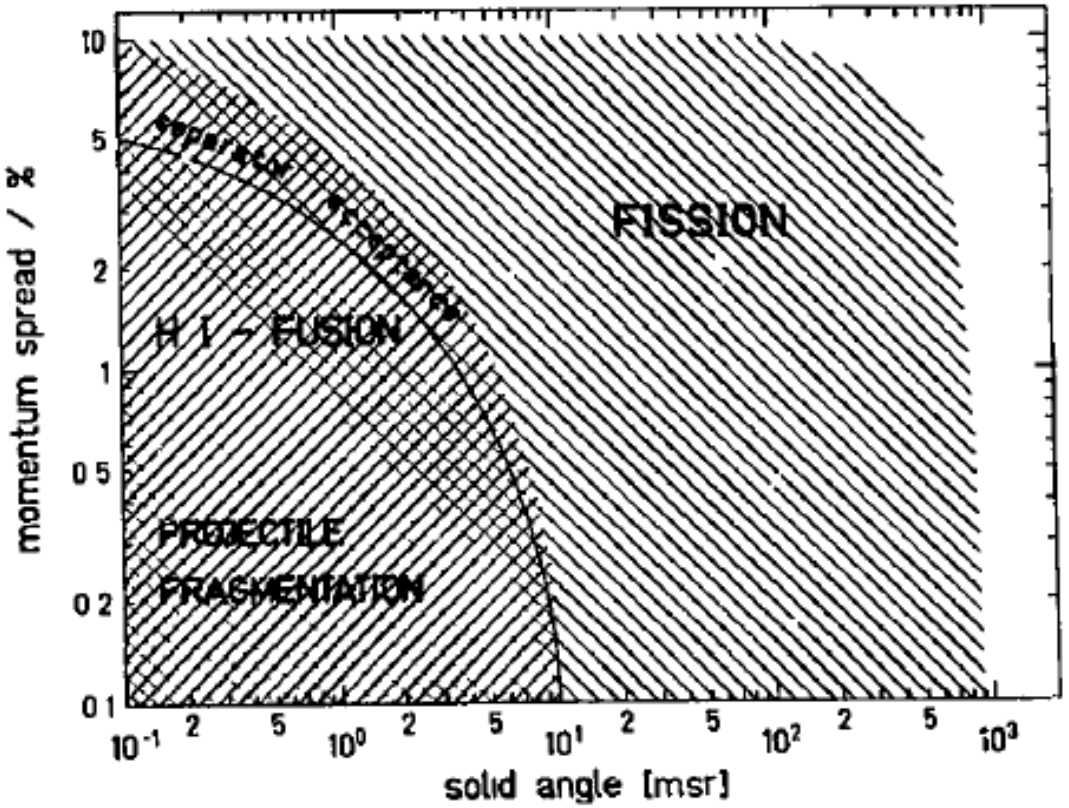

Fig. 3. Solid angle and momentum spread of the reaction products compared to the acceptances of spectrometers.

G. Münzenberg, Nucl. Instr. Meth. B70 (1992) 265.

Recoil separators

- **separate the products of a nuclear reaction (recoils) from the projectile beam**
- **early dumping of unwanted beam**
- **optionally also A/q separation of reaction products**
- **usually kinetic energies up to 10 MeV/nucleon**
- **mass dispersion achieved by combination of magnetic dipoles, electric dipoles or Wien filter**
- **usually additional quadrupoles for focusing**

SHIP at GSI Darmstadt

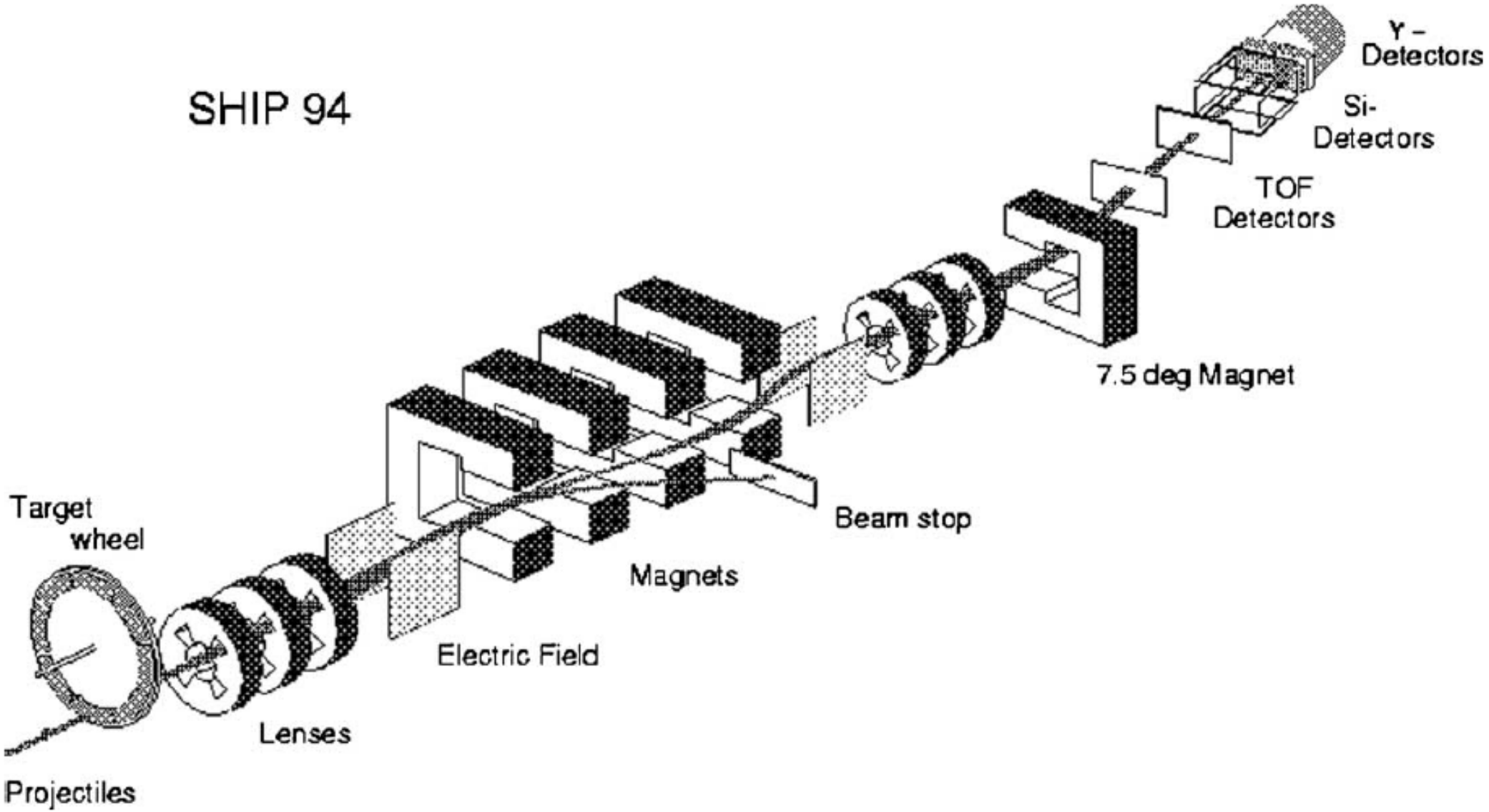

G. Münzenberg et al., Nucl. Instr. Meth. 141 (1979) 65.

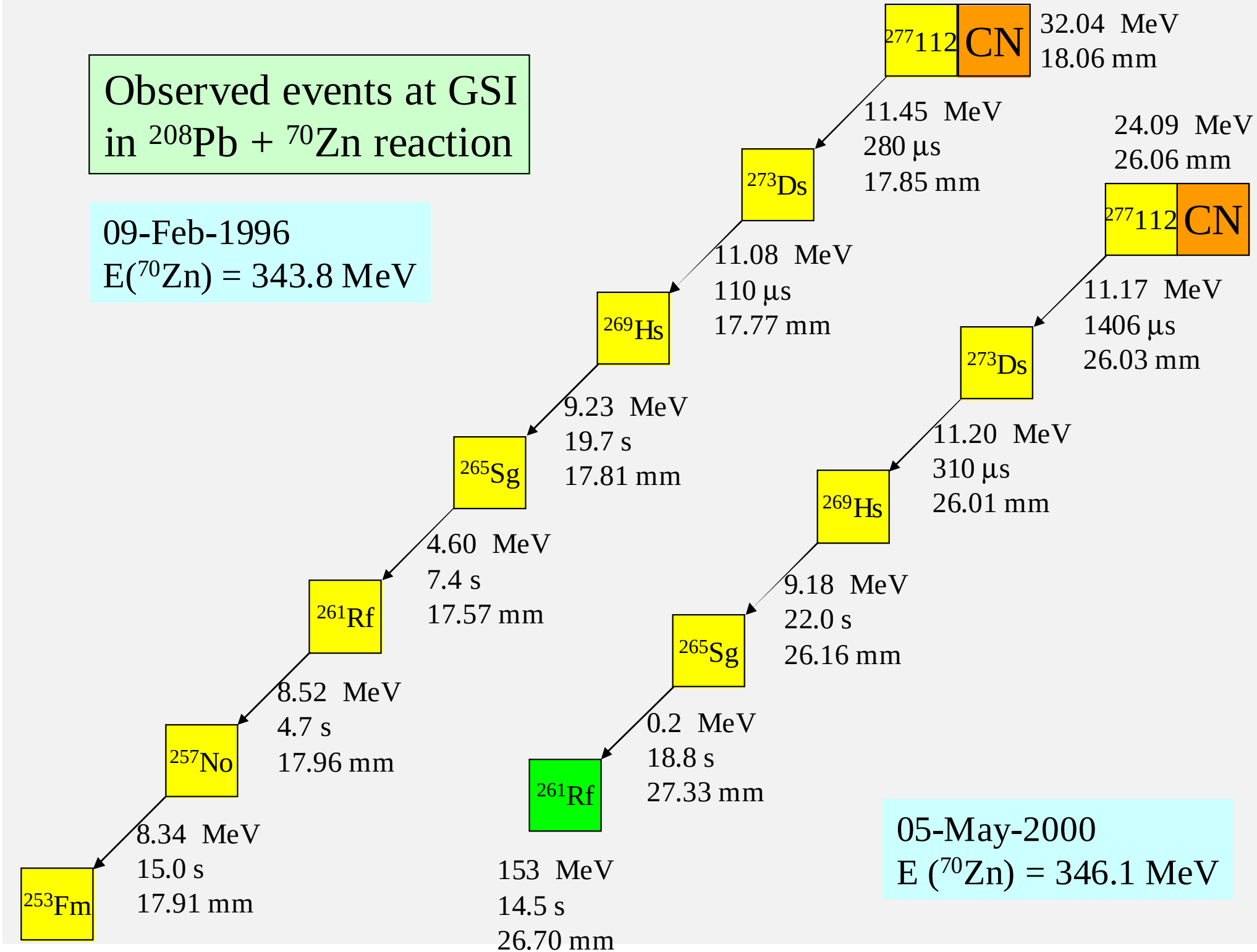
Observed events at GSI
in ^{208}Pb + ^{70}Zn reaction
09-Feb-1996
E(^{70}Zn) = 343.8 MeV
^{277}112 CN
32.04 MeV
18.06 mm
11.45 MeV
280 µs
17.85 mm
^{273}Ds
11.08 MeV
110 µs
17.77 mm
^{269}Hs
9.23 MeV
19.7 s
17.81 mm
^{265}Sg
4.60 MeV
7.4 s
17.57 mm
^{261}Rf
8.52 MeV
4.7 s
17.96 mm
^{257}No
8.34 MeV
15.0 s
17.91 mm
^{253}Fm
24.09 MeV
26.06 mm
^{277}112 CN
11.17 MeV
1406 µs
26.03 mm
^{273}Ds
11.20 MeV
310 µs
26.01 mm
^{269}Hs
9.18 MeV
22.0 s
26.16 mm
^{265}Sg
0.2 MeV
18.8 s
27.33 mm
^{261}Rf
153 MeV
14.5 s
26.70 mm
05-May-2000
E (^{70}Zn) = 346.1 MeV

VASSILISSA

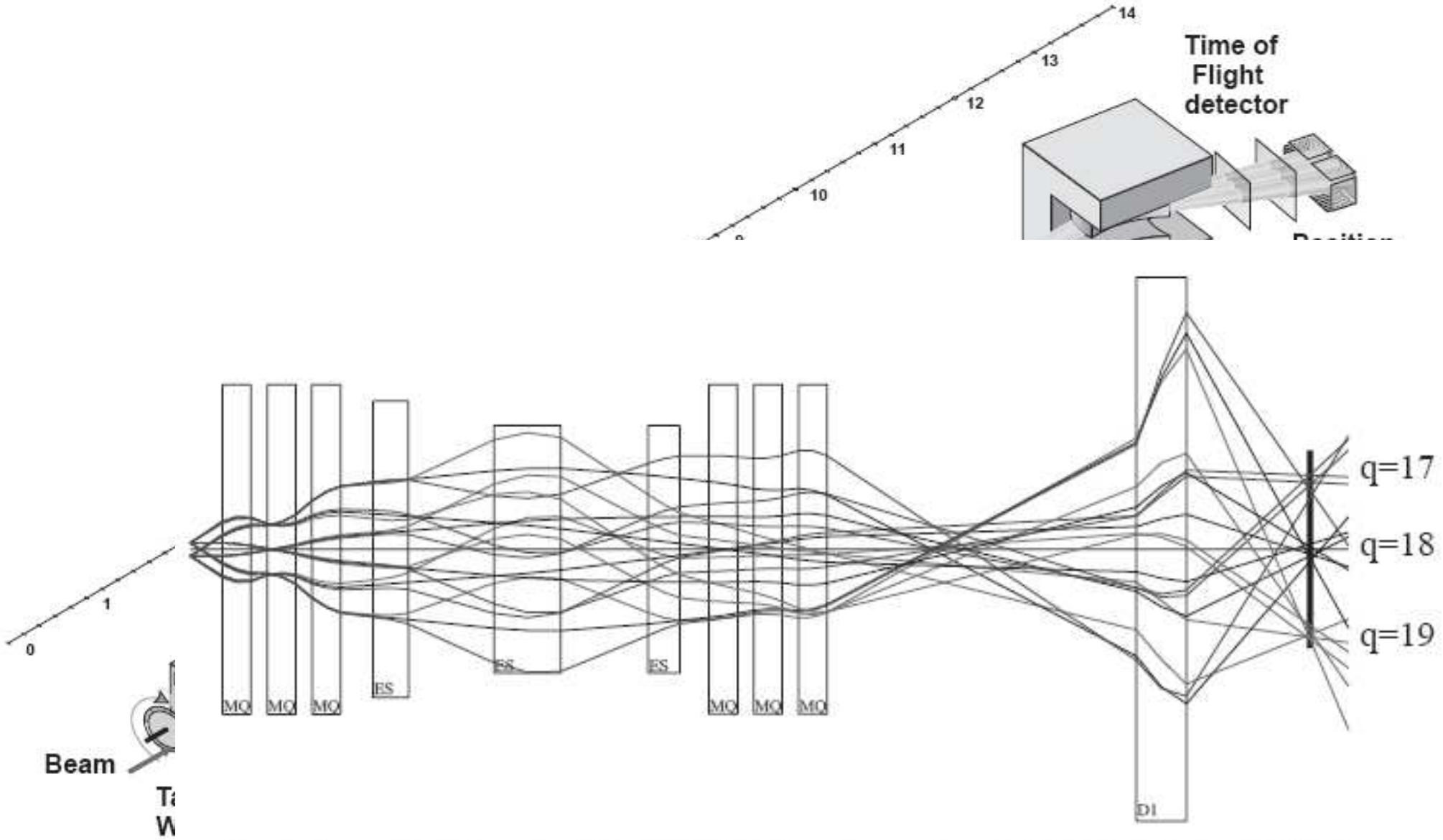

Fig. 5. Ion-optical elements of the VASSILISSA and computer-simulated trajectories of ^{198}Po ions.

A.G. Popeko et al., Nucl. Instr. Meth. A510 (2003) 371.

DGFRS: Dubna Gas-Filled Recoil Separator

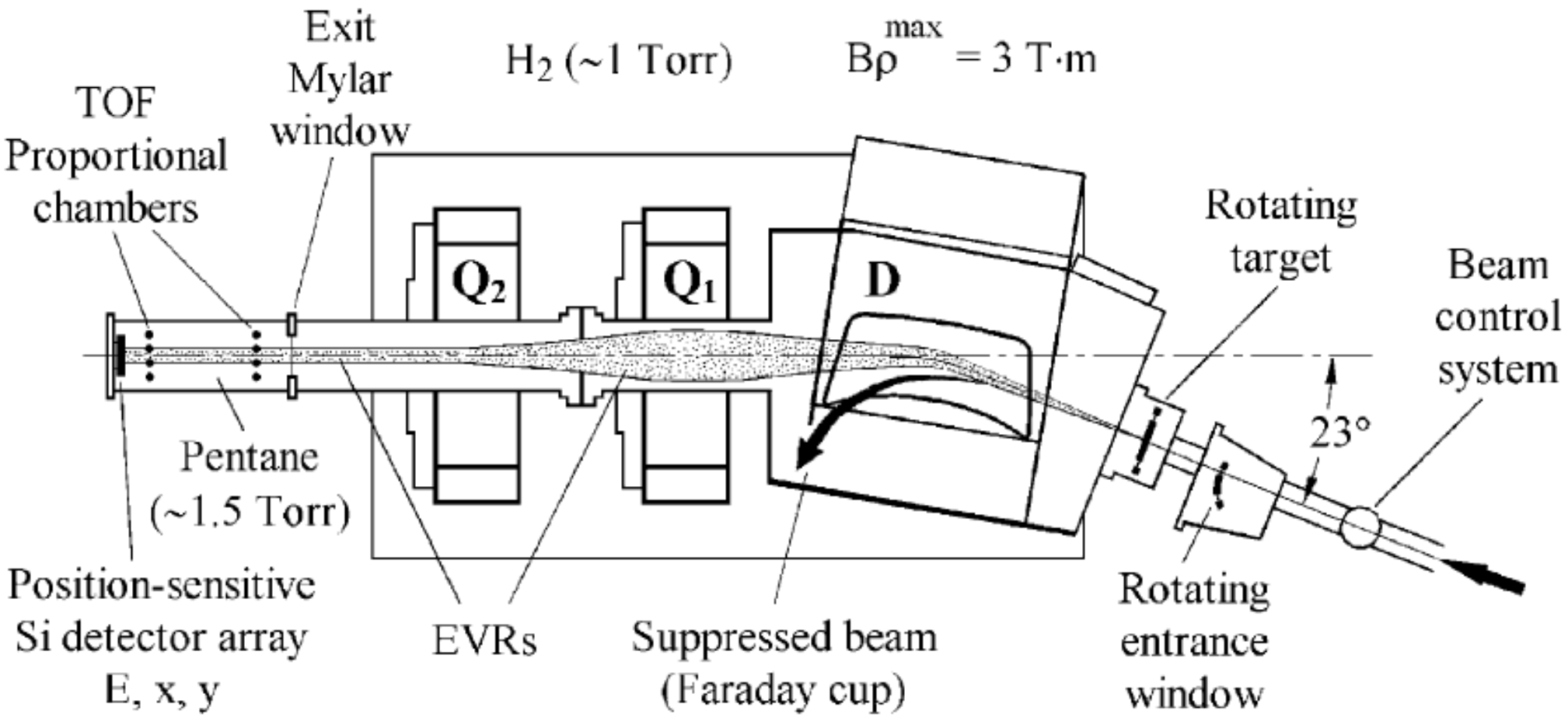

K. Subotic et al., Nucl. Instr. Meth. A481 (2002) 71.

RIKEN Gas-filled Recoil Separator GARIS

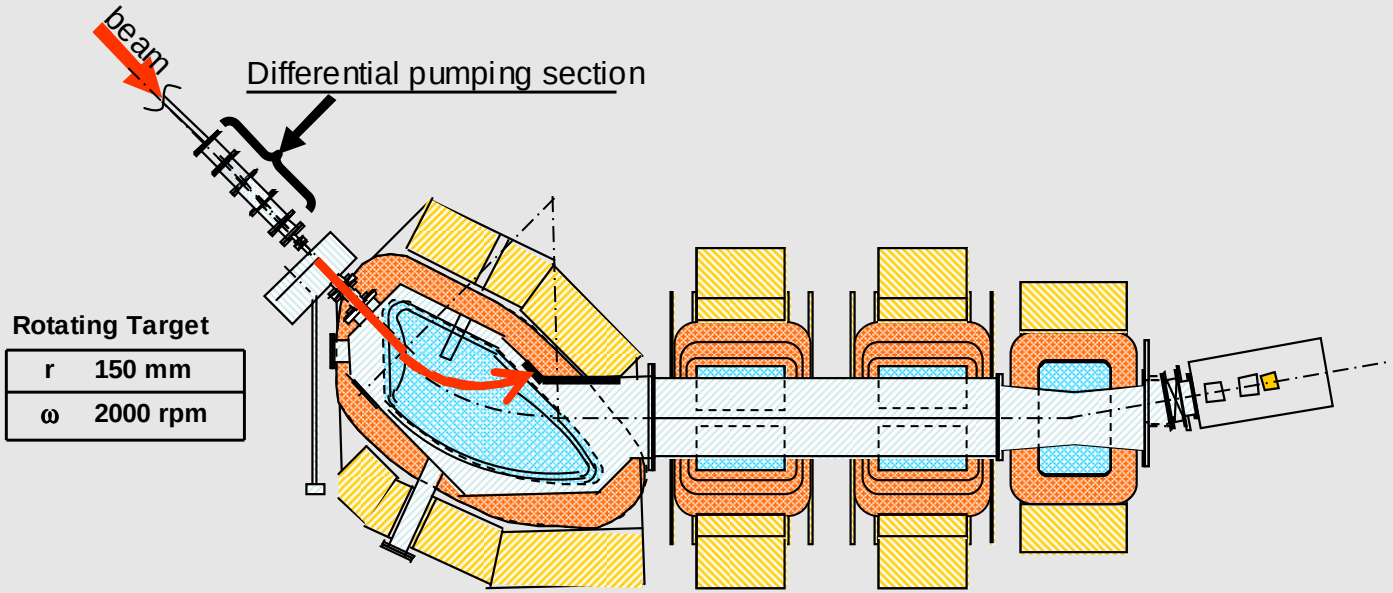

Rotating Target

r	150 mm
ω	2000 rpm

D1 Q1 Q2 D2

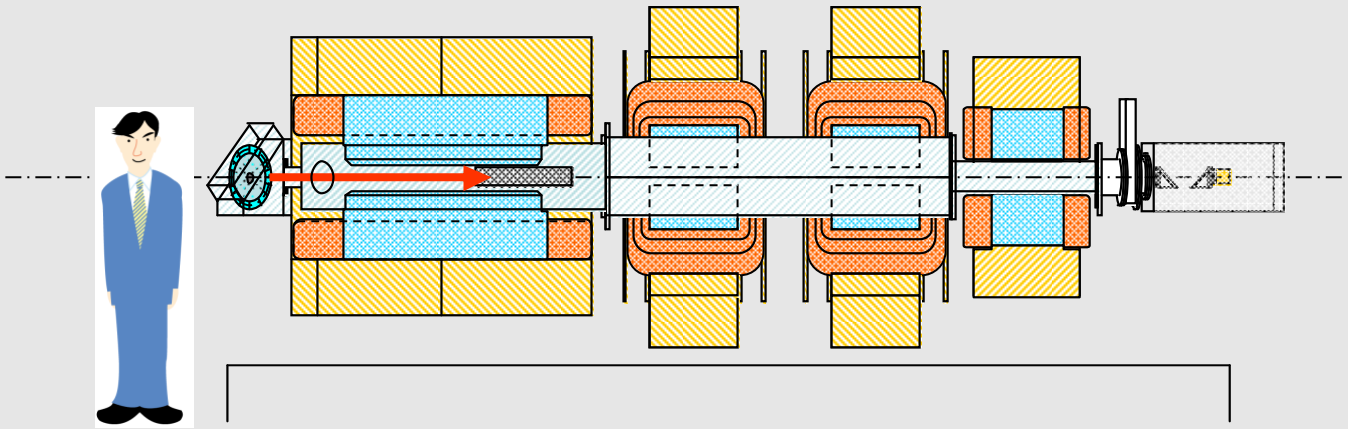

D1

Bending angle	45 degree
Pole gap	150 mm
Radius of central ray	1200 mm
Maximum field	1.54 T

Q1, Q2

Pole length	500 mm
Bore radius	150 mm
Maximum field gradient	5.2 T/m

D2

Bending angle	10 degree
Pole gap	160 mm
Pole length	400 mm
Maximum Field	1.04 T

Magnification	X	-0.76
	Y	-1.99
Dispersion		0.97 cm/%
Total length		5760 mm
Acceptance	Δθ	±68 mrad
	Δϕ	±57 mrad
	ΔΩ	12.2 msr

upper end of nuclear chart 2007

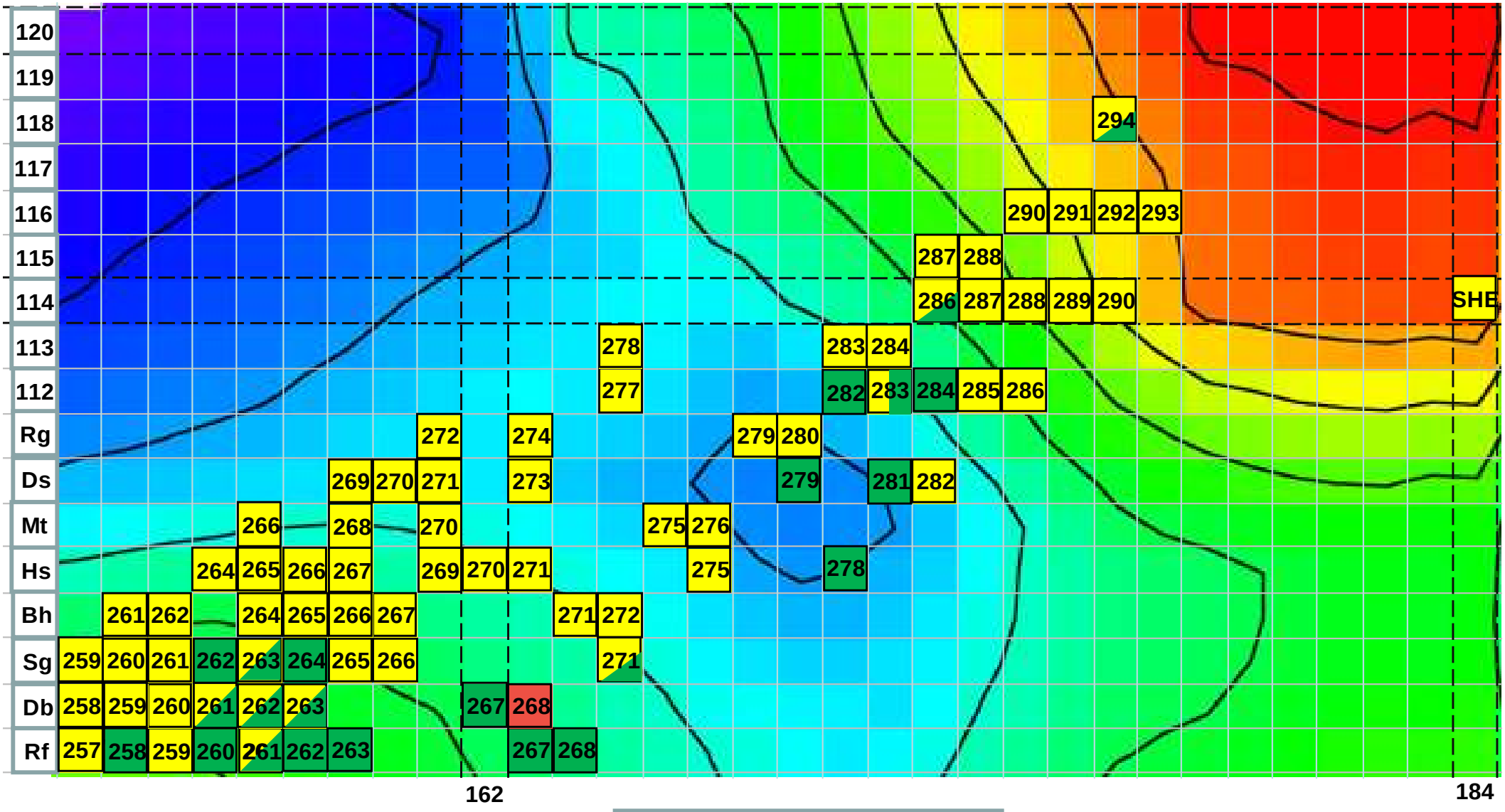

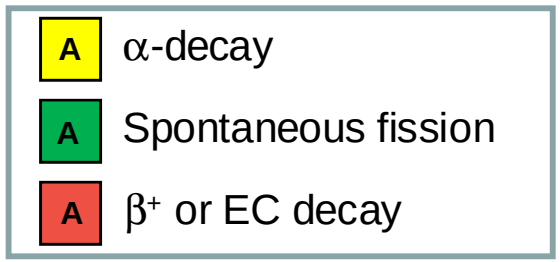

GANIL/SPIRAL1/SPIRAL2 facility

GANIL/SPIRAL 1 today

SP2 Beam time: 44 weeks/y
GANIL Beam time: 35 weeks/y
ISOL RIB Beams: 28-33 weeks/y
GANIL+SP 2 Users: 700-800/y

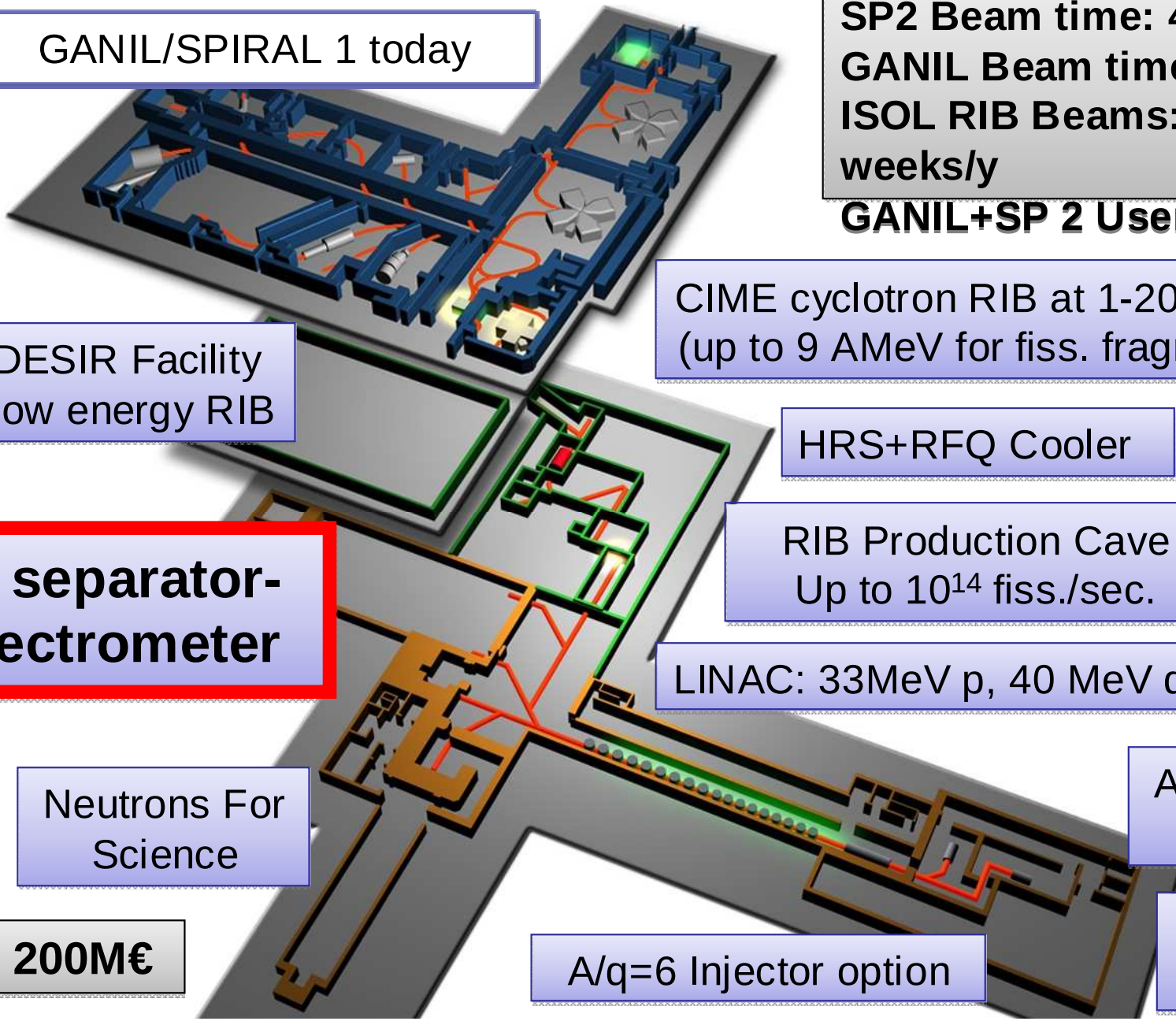

CIME cyclotron RIB at 1-20 AMeV
(up to 9 AMeV for fiss. fragments)

DESIR Facility
low energy RIB

HRS+RFQ Cooler

S3 separator-spectrometer

RIB Production Cave
Up to 10^{14} fiss./sec.

LINAC: 33MeV p, 40 MeV d, 14.5 A MeV HI

Neutrons For Science

A/q=3 HI source
Up to 1mA

Cost: 200M€

A/q=6 Injector option

A/q=2 source
p, d, ^{3,4}He 5mA

S3 at SPIRAL2, GANIL, Caen

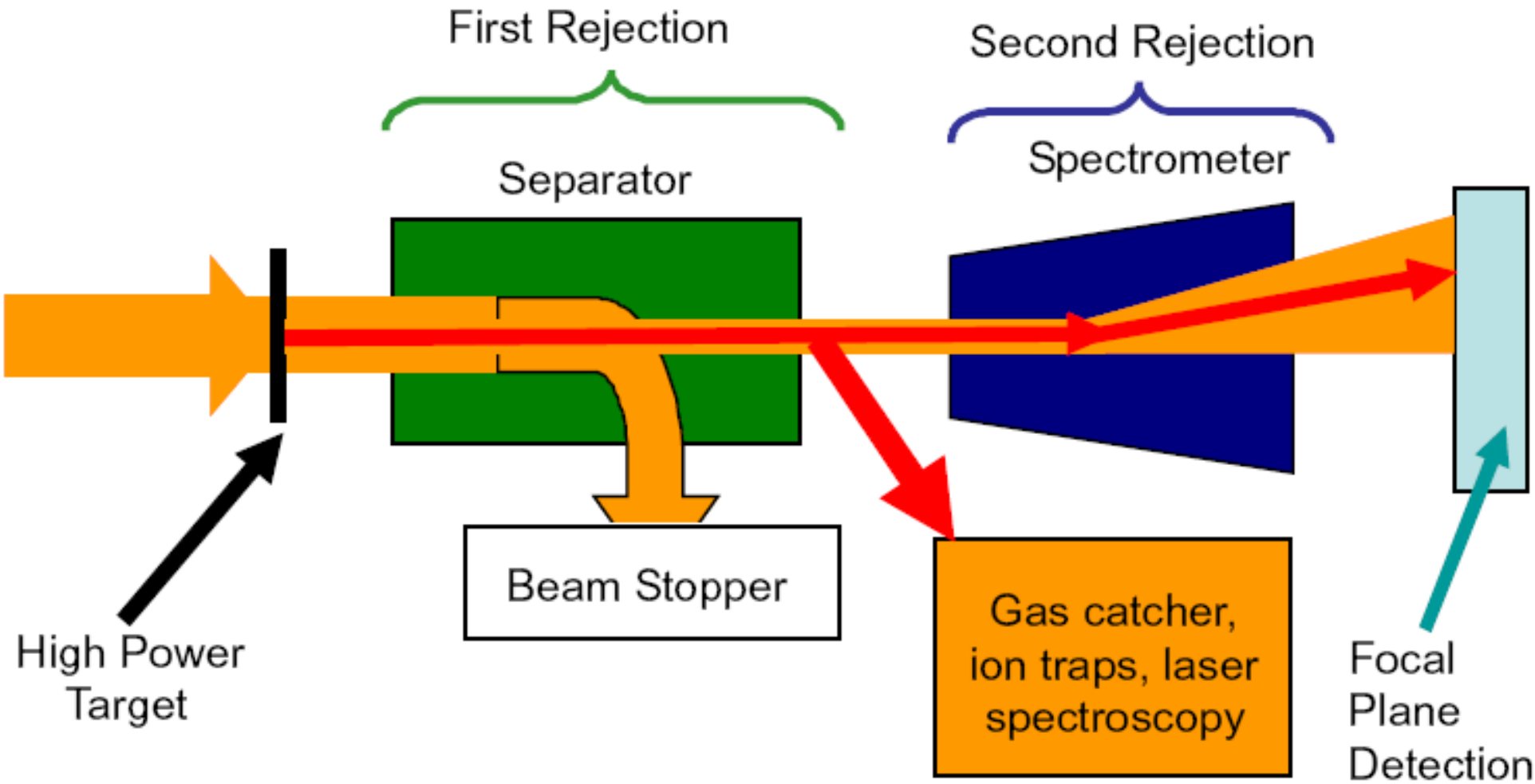

Fig. 1. Schematic idea for S^3 showing the two stage separator.

S3 at SPIRAL2, GANIL, Caen

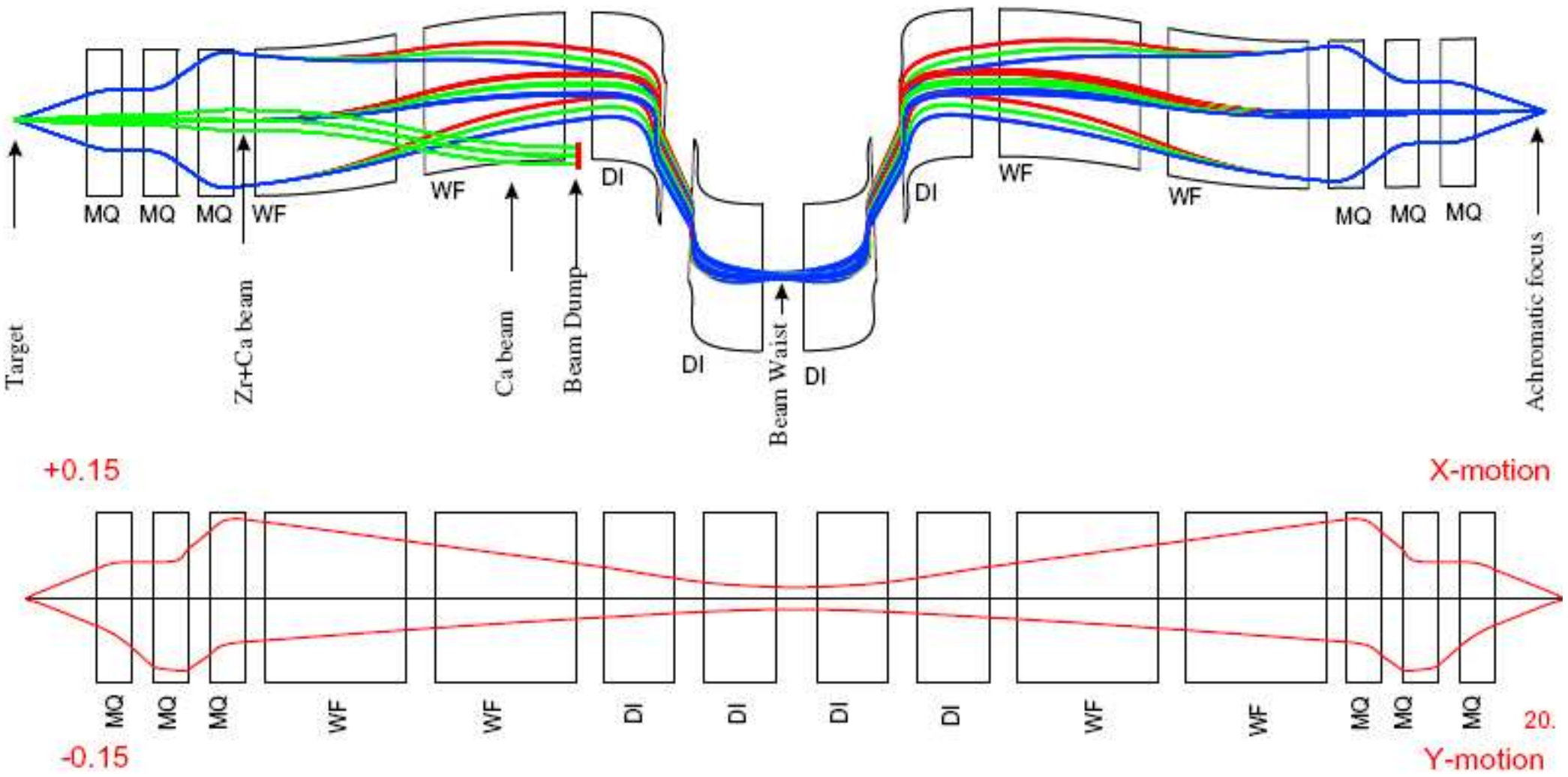

A. Drouart et al., Nucl. Instr. Meth. B266(2008) 4162.

VAMOS at GANIL

Very wide acceptance ⇒ trajectory reconstruction for aberration correction

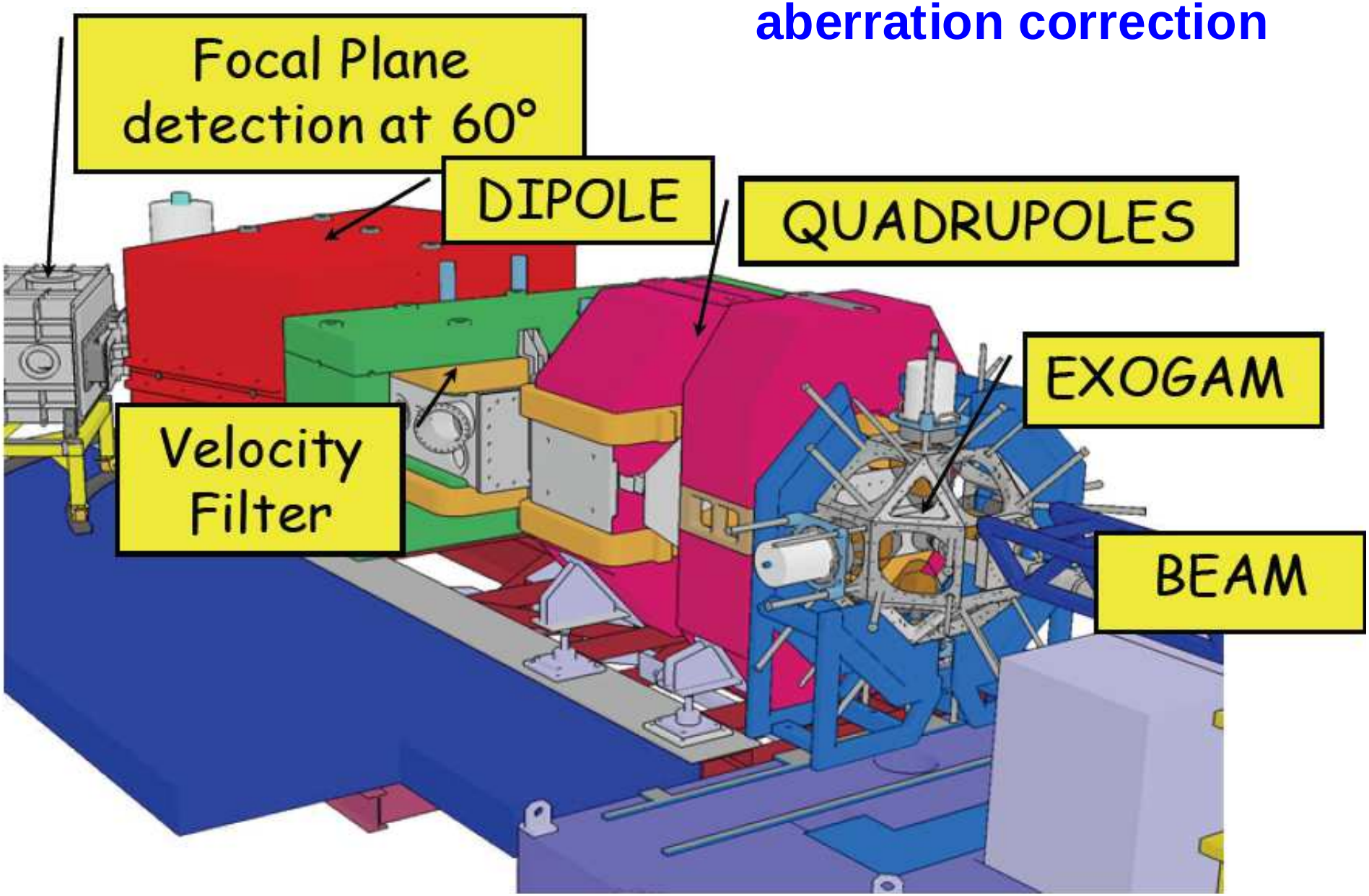

H. Savajols for the VAMOS Collaboration, Nucl. Instr. Meth. B204 (2003) 146.

DRAGON

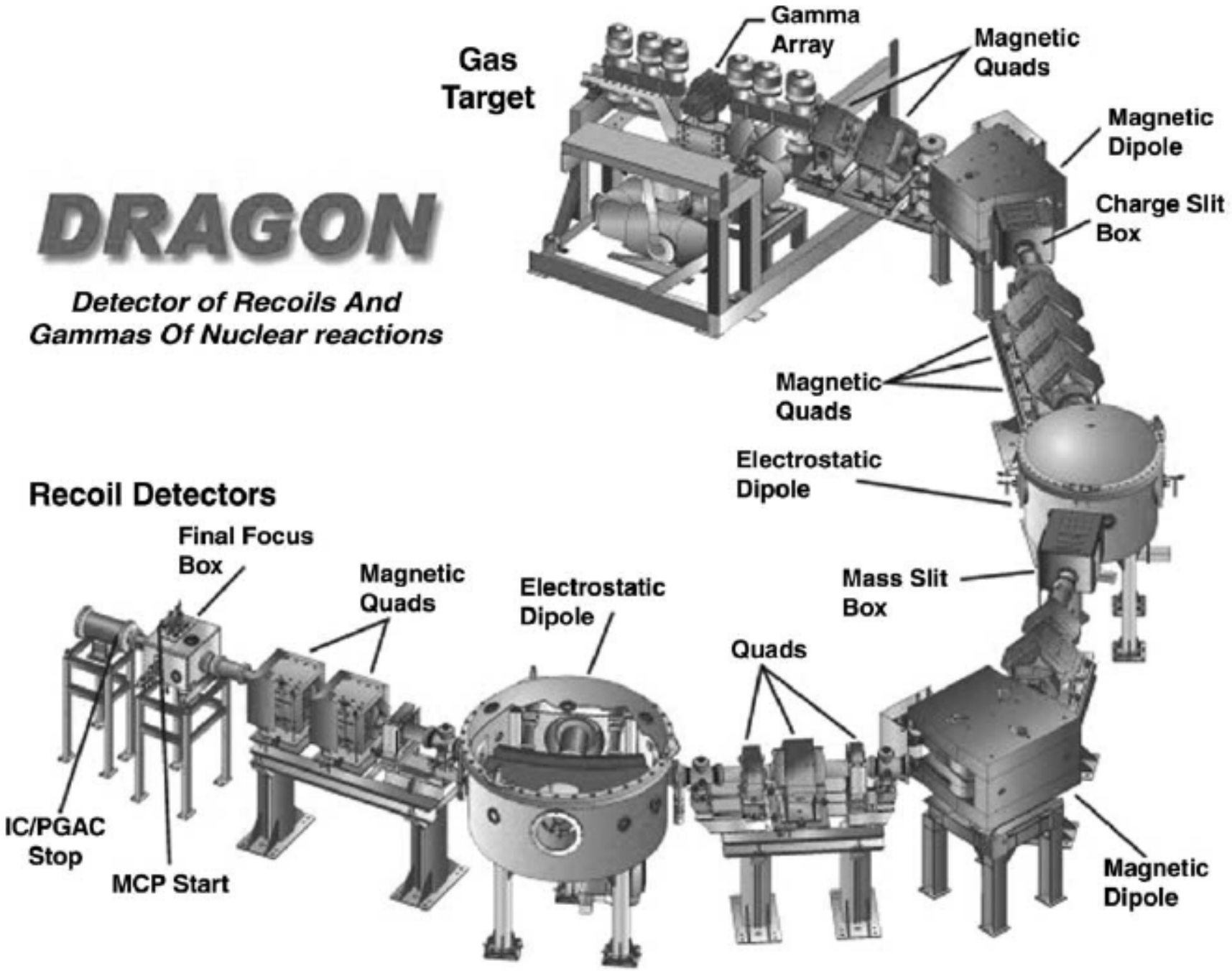

D. Hutcheon, Nucl. Instr. Meth. A498 (2003) 190.

Spallation + Fragmentation + Fission

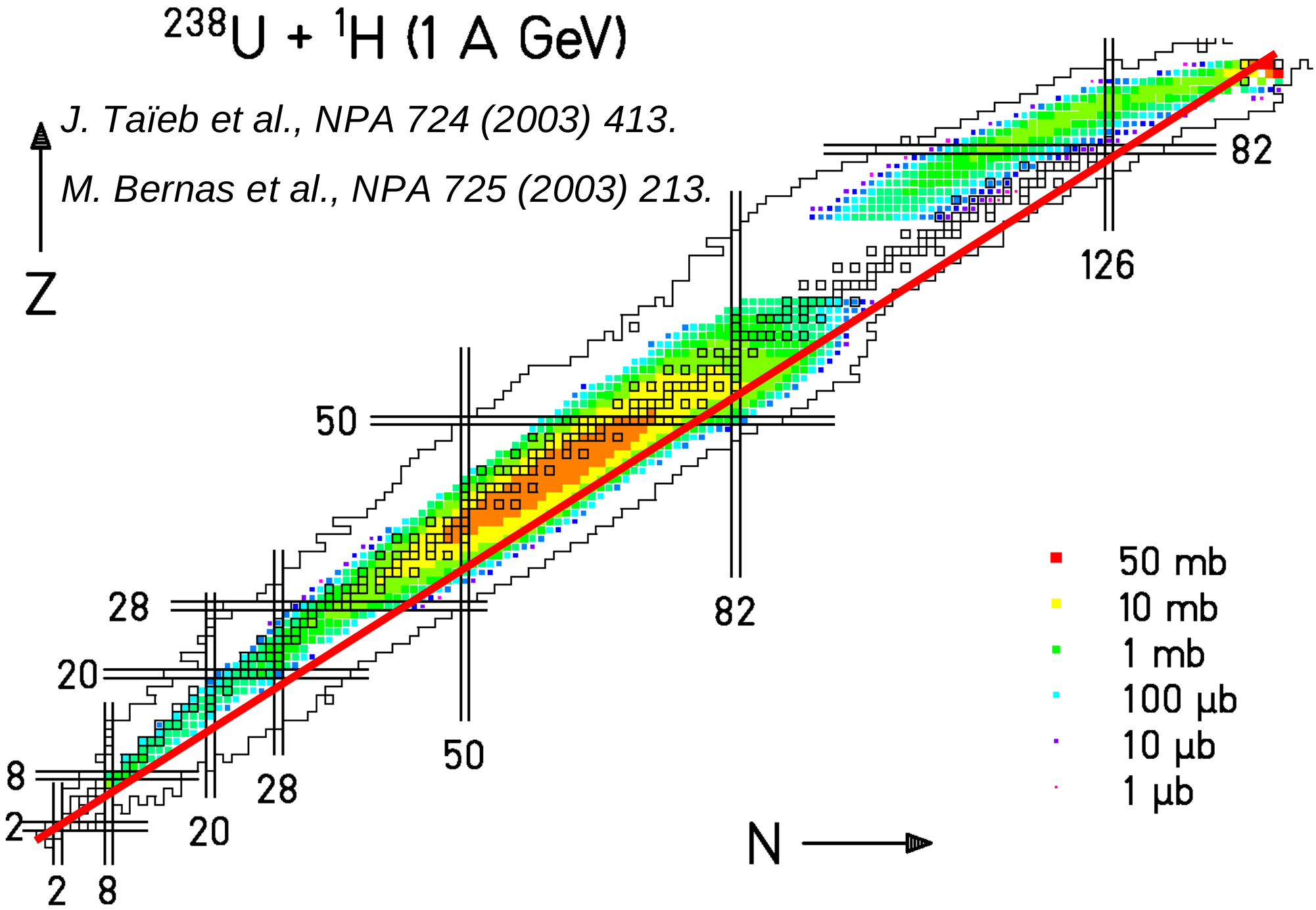

Normal kinematics: n, p or light ions on heavy target

- “conventional” accelerator providing “easily” high beam intensity
- dedicated target required
- reaction products emitted into 4π

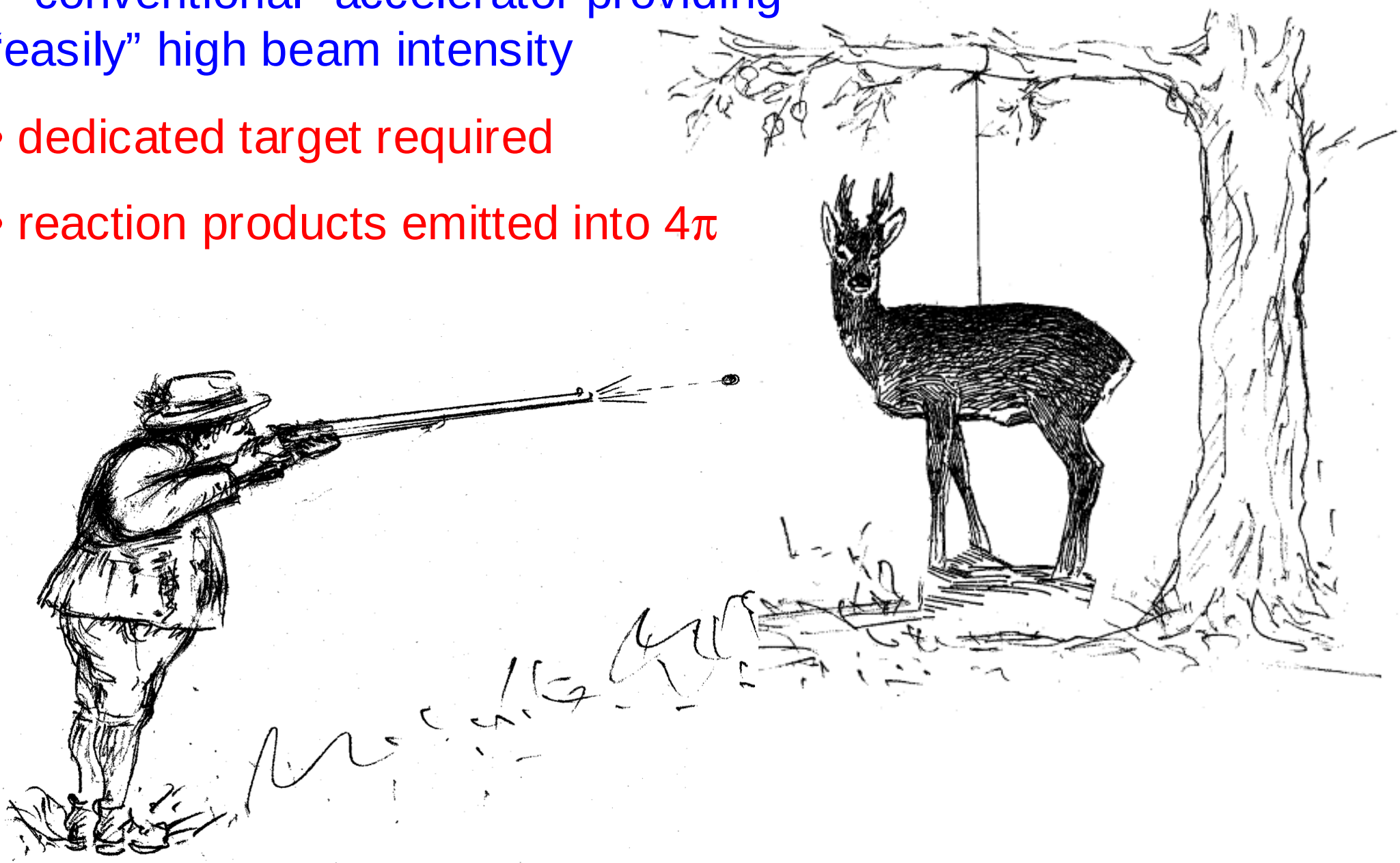

Inverse kinematics: heavy ions on light target

- complex and expensive accelerator
- reaction products forward focused

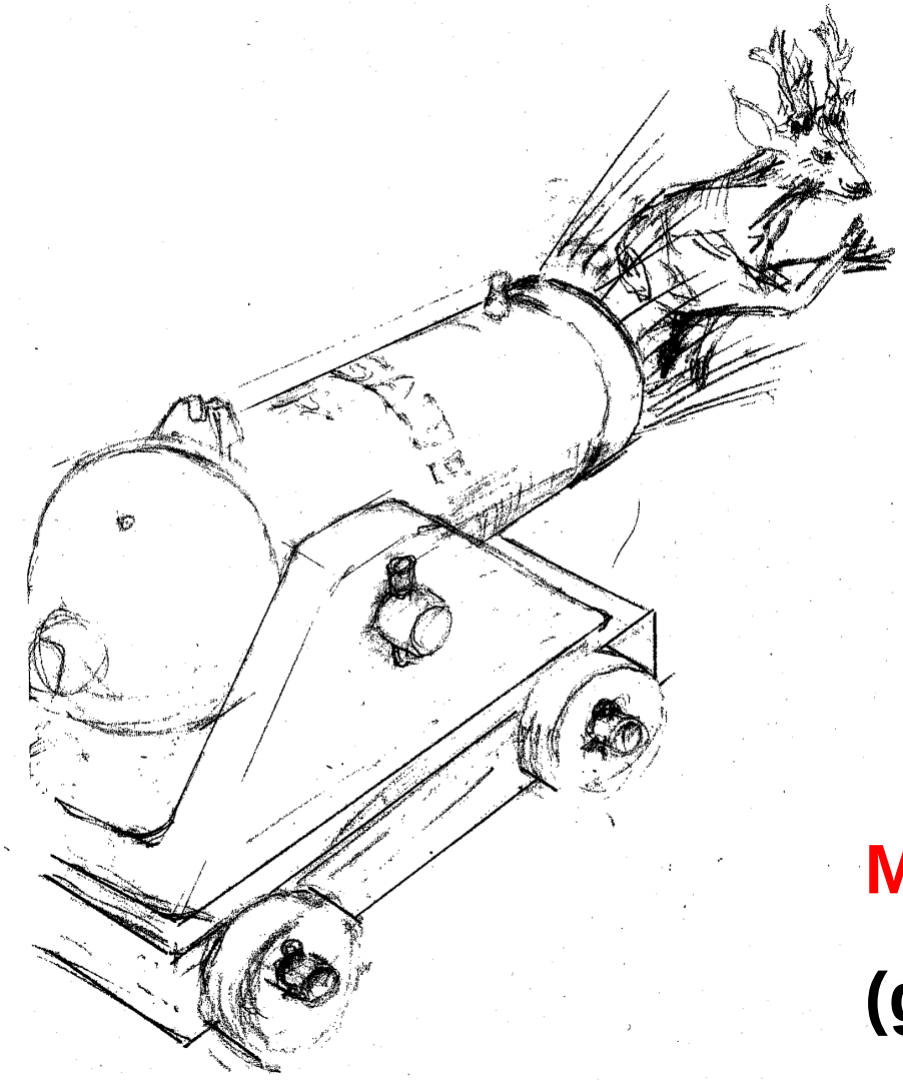

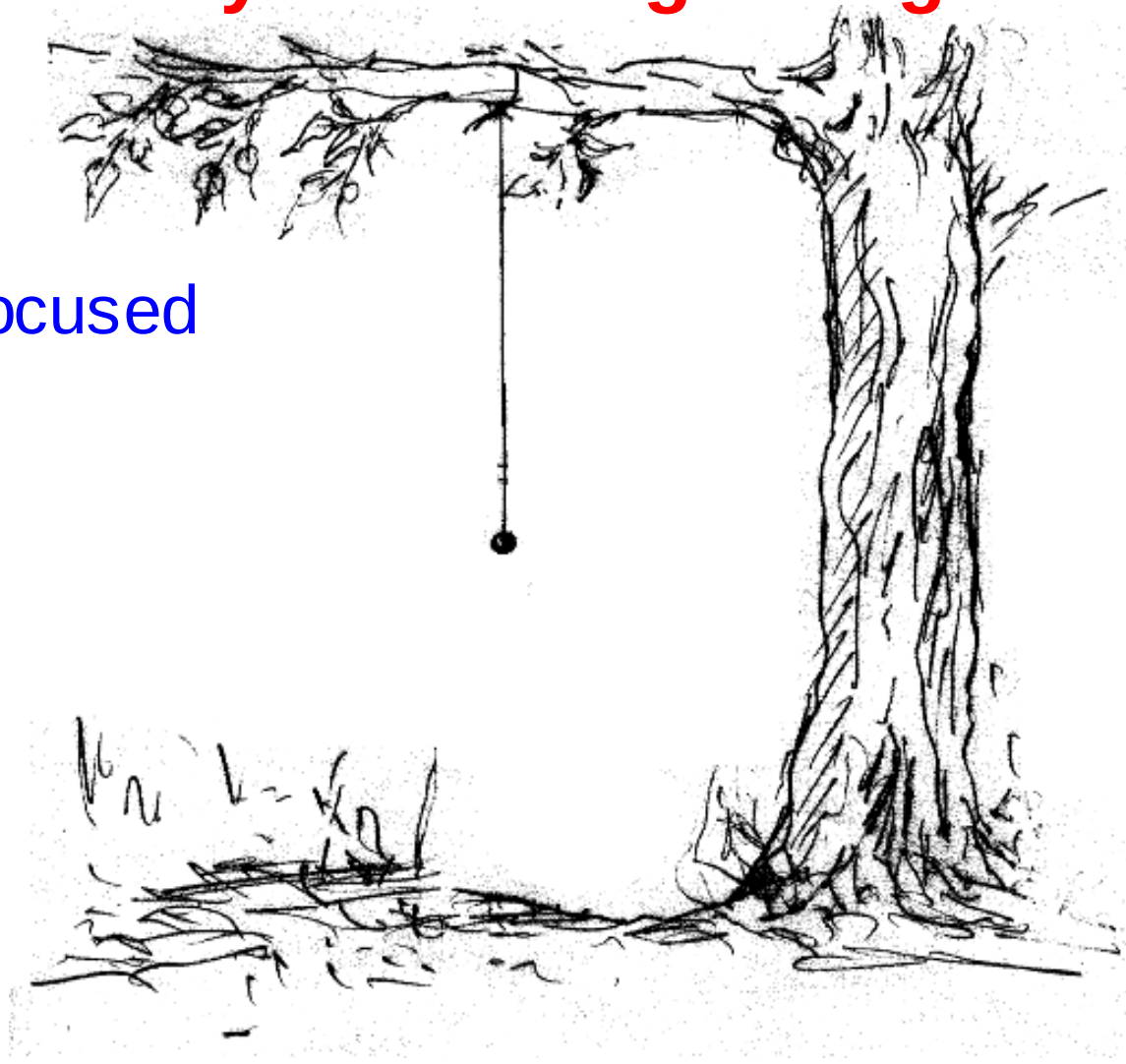

Mind the losses during stopping!

(graphical representation censored)

Spallation + Fragmentation + Fission

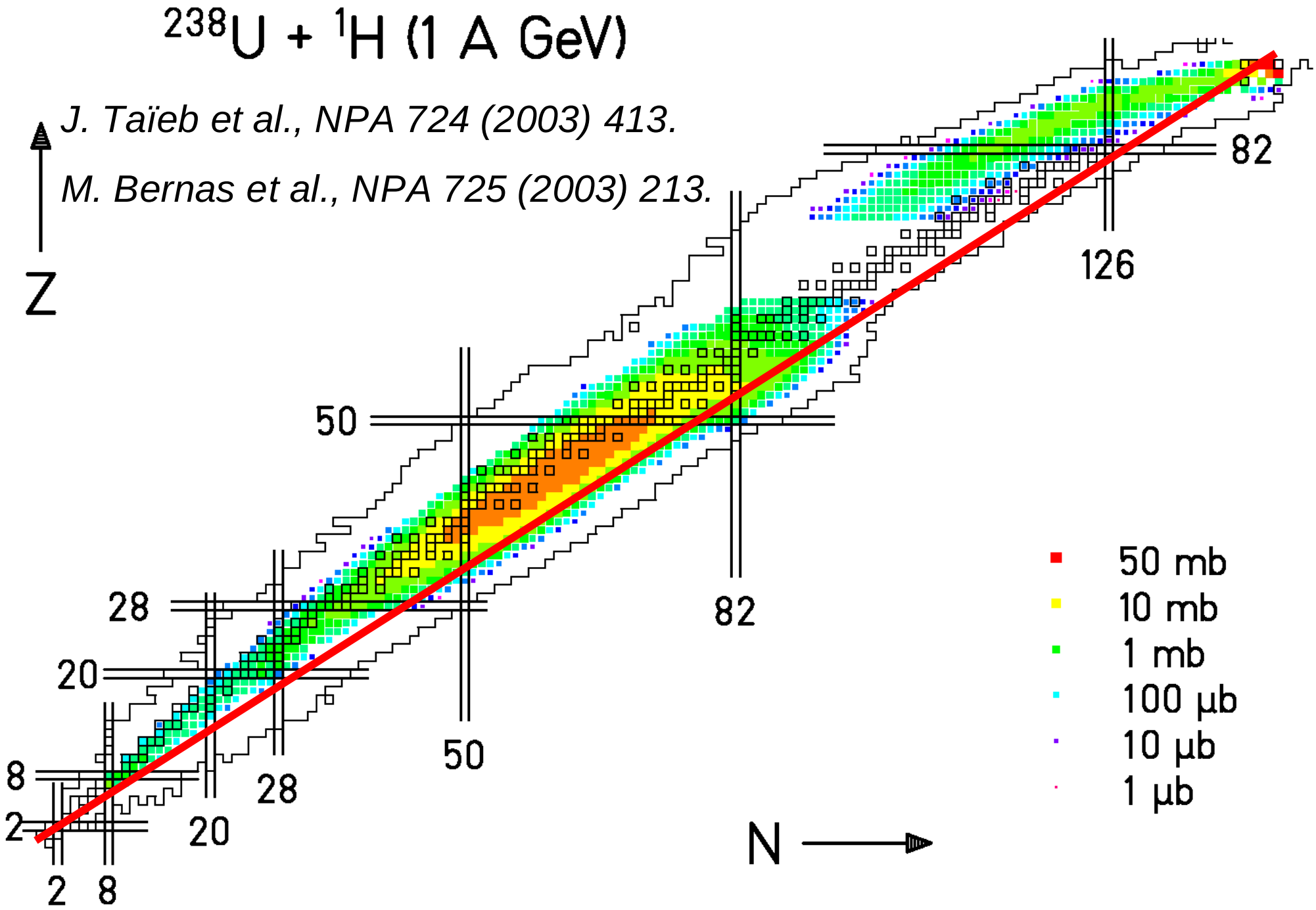

Momentum-loss achromat (Wedge separation)

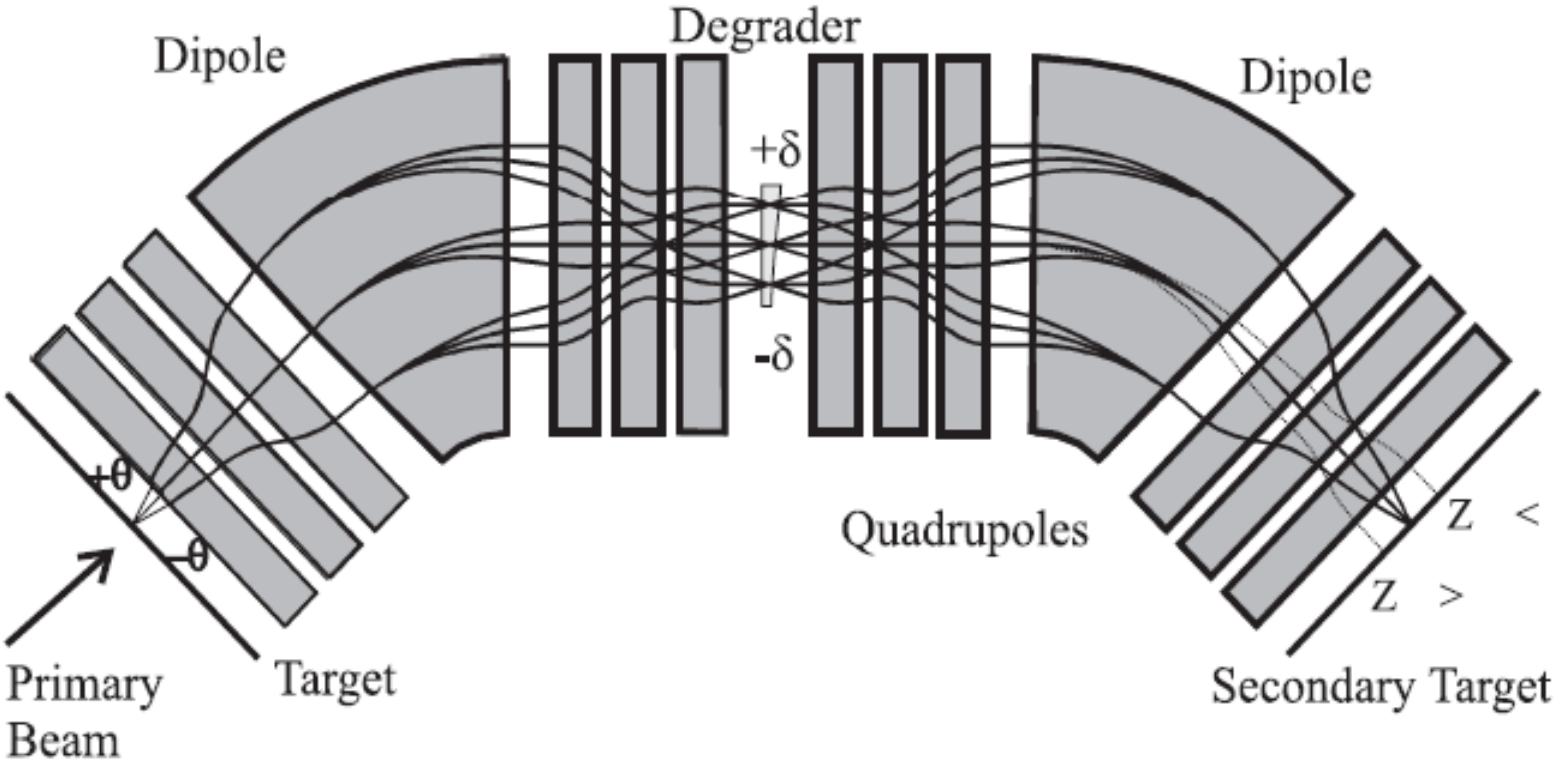

Fig. 4. Schematic representation of the ion-optics used in a momentum-loss achromat to separate projectile fragments.

D.J. Morrissey and B.M. Sherill, Lecture Notes in Physics 651 (2004) 113.

LISE

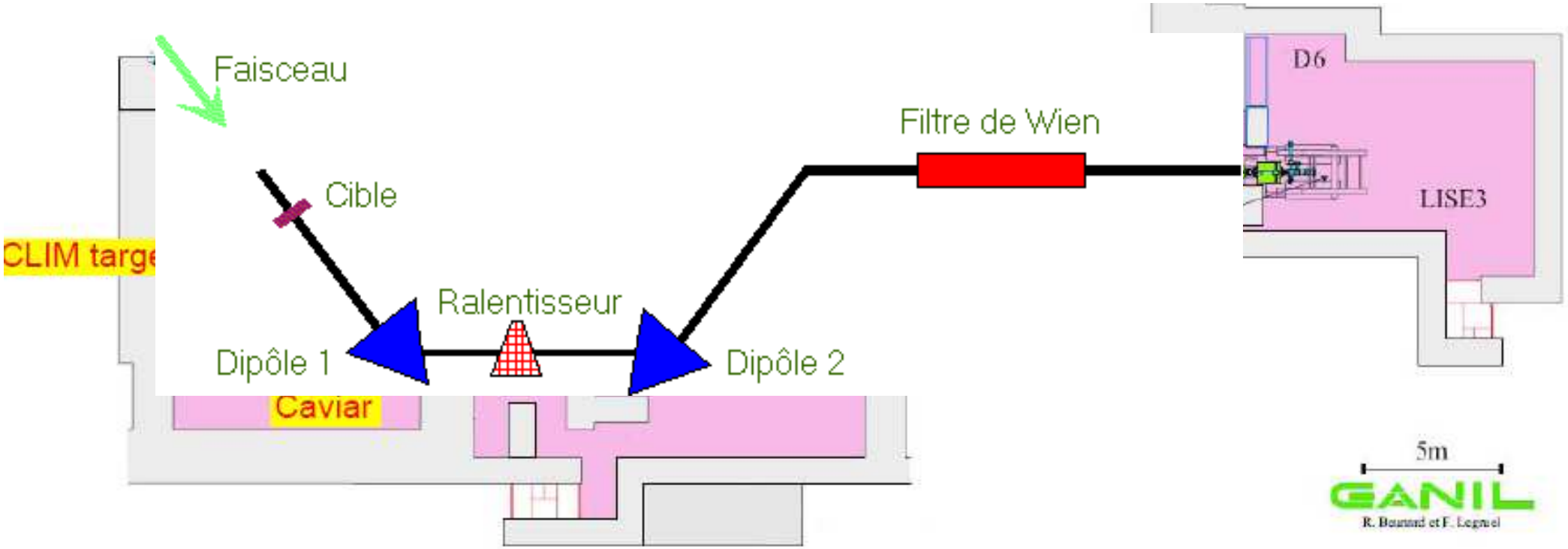

R. Anne et al., Nucl. Instr. Meth. A257 (1987) 215.

R. Anne et al., Nucl. Instr. Meth. B70 (1992) 276.

Dispersive ion optical elements

- magnets are momentum dispersive
- electrostatic deflectors are energy dispersive
- Wien filters are velocity dispersive
- achromatic wedges are dispersive in mZ^2/E or (Z/v)2
- RF kicker are flight time selective

Effect of wedge selection

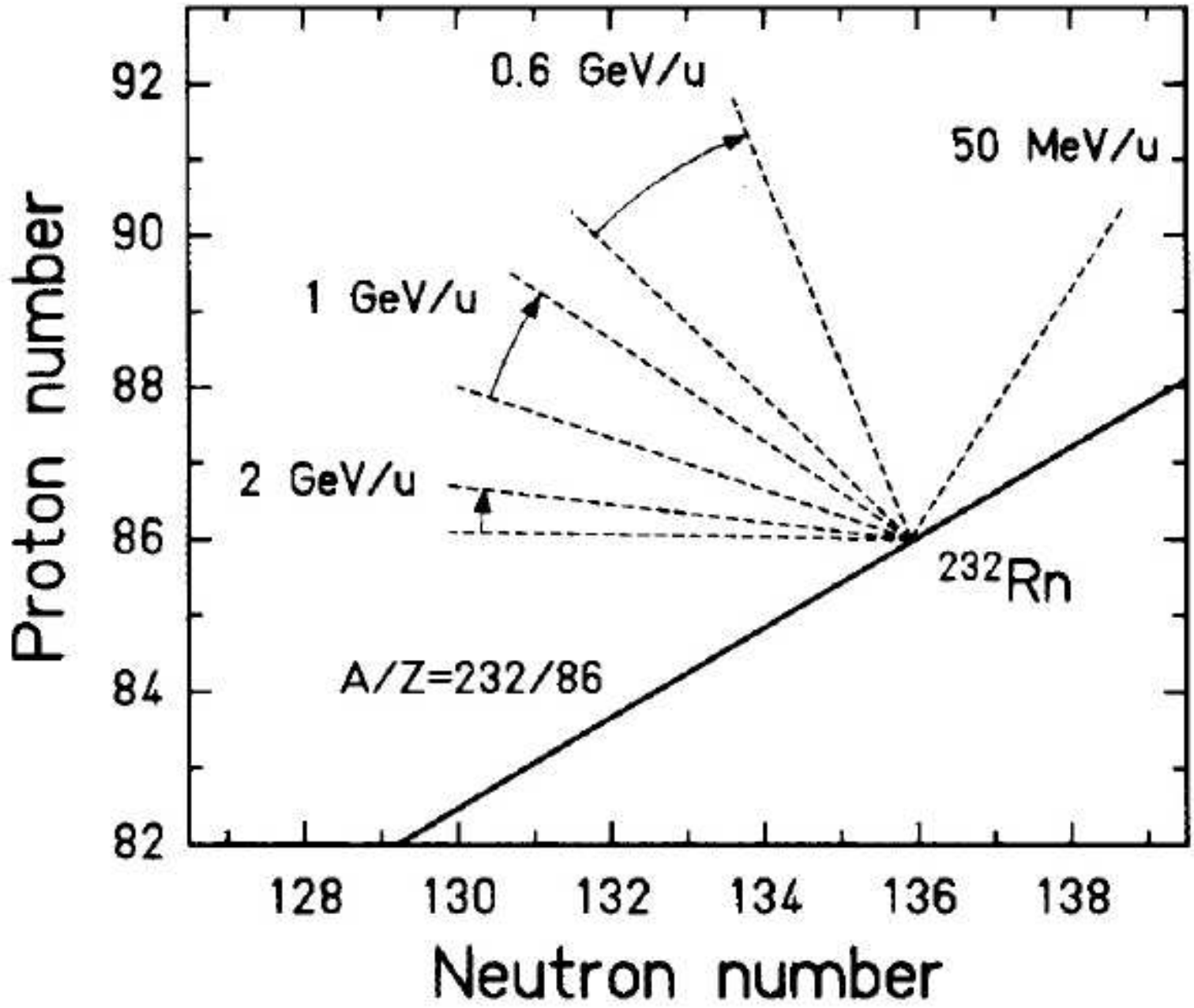

K.H. Schmidt et al., Nucl. Instr. Meth. A260 (1987) 287.

Effect of wedge selection

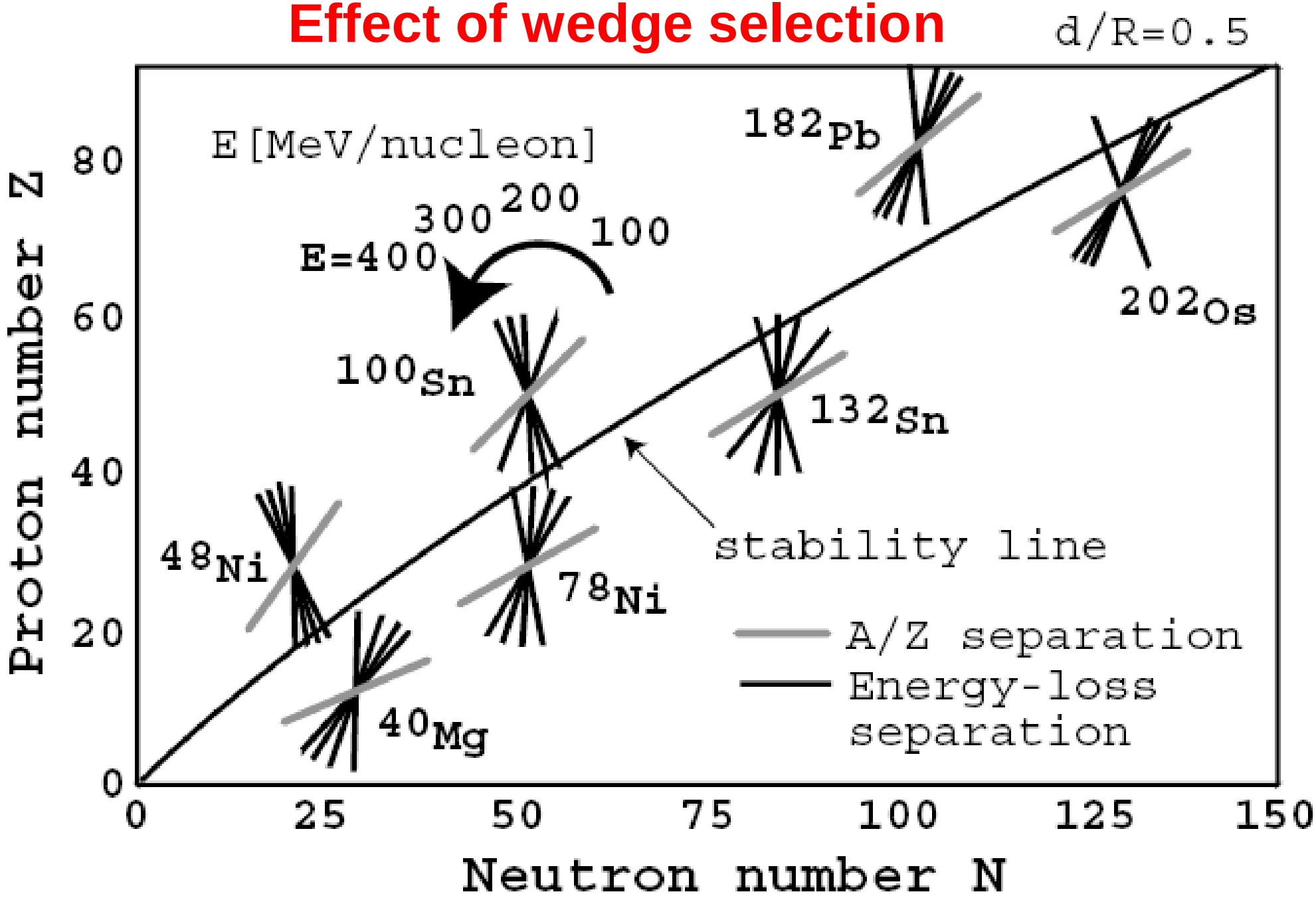

T. Kubo, Nucl. Instr. Meth. B204 (2003) 97.

In-flight production of rare isotopes

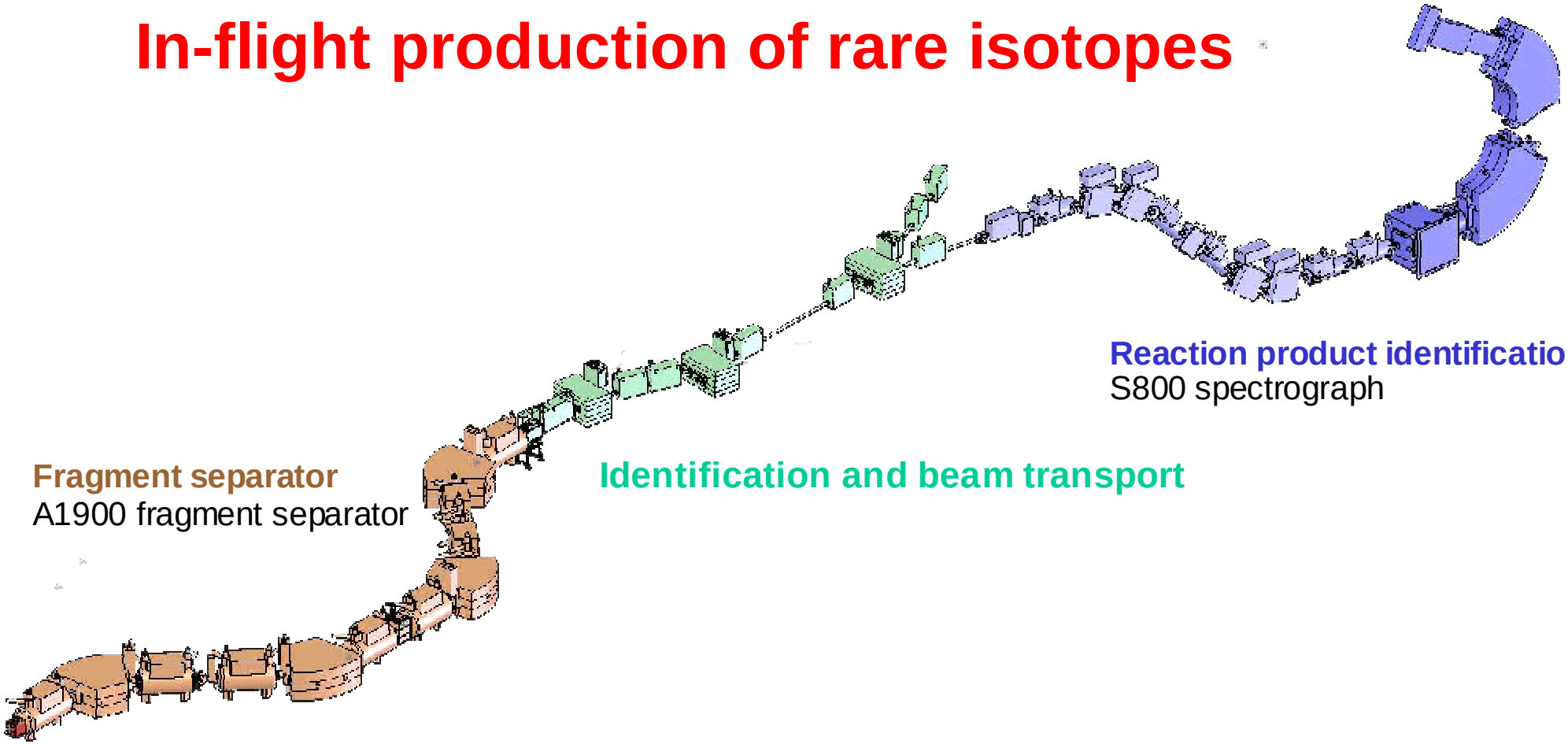

Driver accelerator (v = 0.25-0.6 c)

- **Fragment separator (A1900 NSCL, FRS GSI, BigRIPS RIKEN, ALPHA spectrometer/LISE GANIL)**
- **Identification and beam transport**
  - Stopped beam experiments, reaccelerated beam experiments
  - Fast beam experiments
    - Secondary reaction
    - Reaction product identification (S800 spectrograph, CATE/Aladin, Silicon telescopes/TOF wall, SPEG)

In-flight production of rare isotopes

Example: ^{78}Ni from ^{86}Kr at NSCL

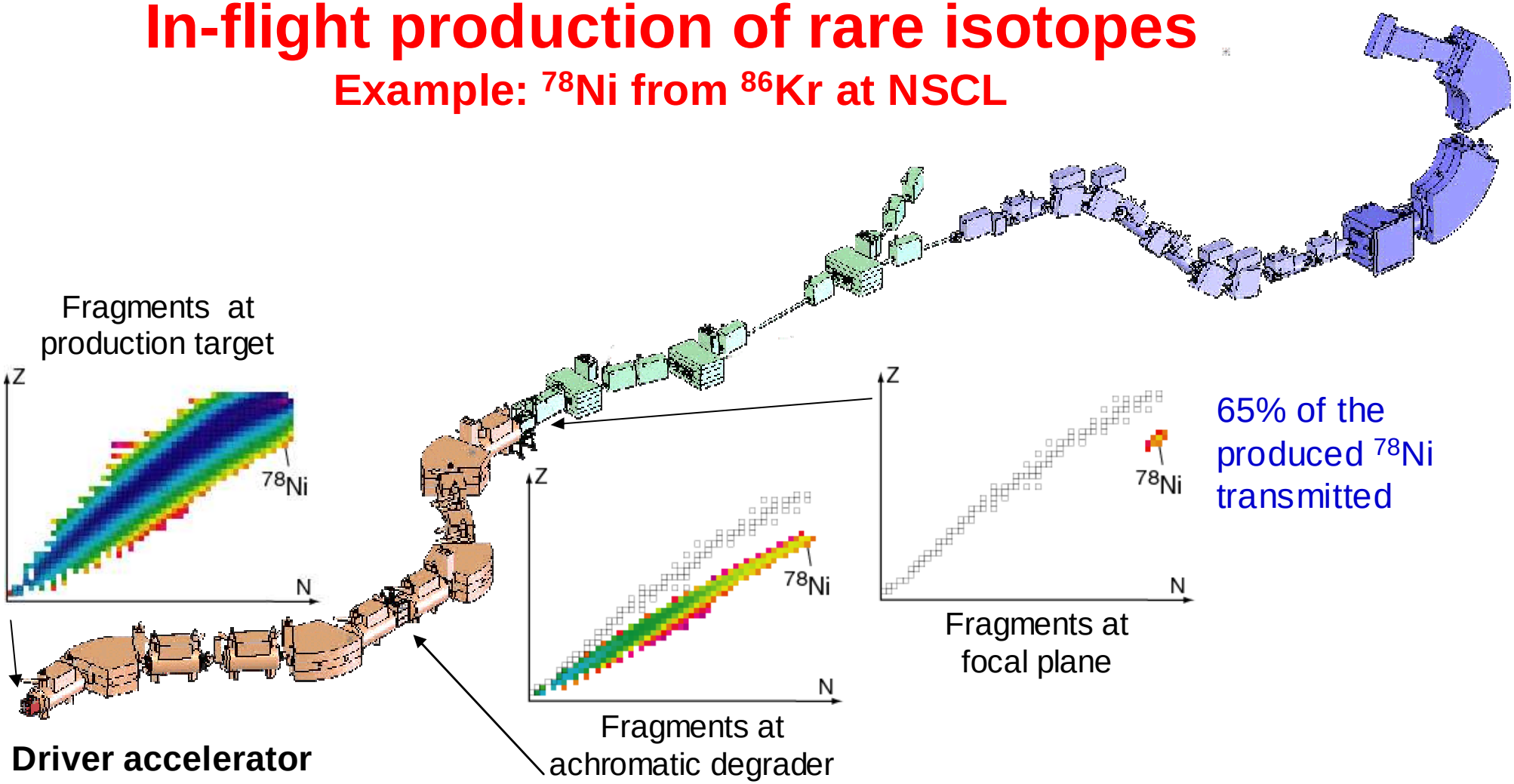

- **Fragment separator (A1900 NSCL, FRS GSI, BigRIPS RIKEN, ALPHA/LISE GANIL)**
- **Identification and beam transport**
  - Stopped beam experiments
  - Fast beam experiments
    - Secondary reaction
    - Reaction product identification (S800 spectrograph, CATE/Aladin, Silicon telescopes/TOF wall, SPEG)

Isotope selection at (high E) in-flight separators

- Ionization to q = Z (high energies!)
- A/Z selection by magnetic deflection
- $B\rho \propto A/Z\ v\ \gamma$
- v can be measured by time of flight or selected by Wien filter

Z selection by specific energy loss

$\Delta E \approx C\ Z^2/v^2$ (Bethe-Bloch)

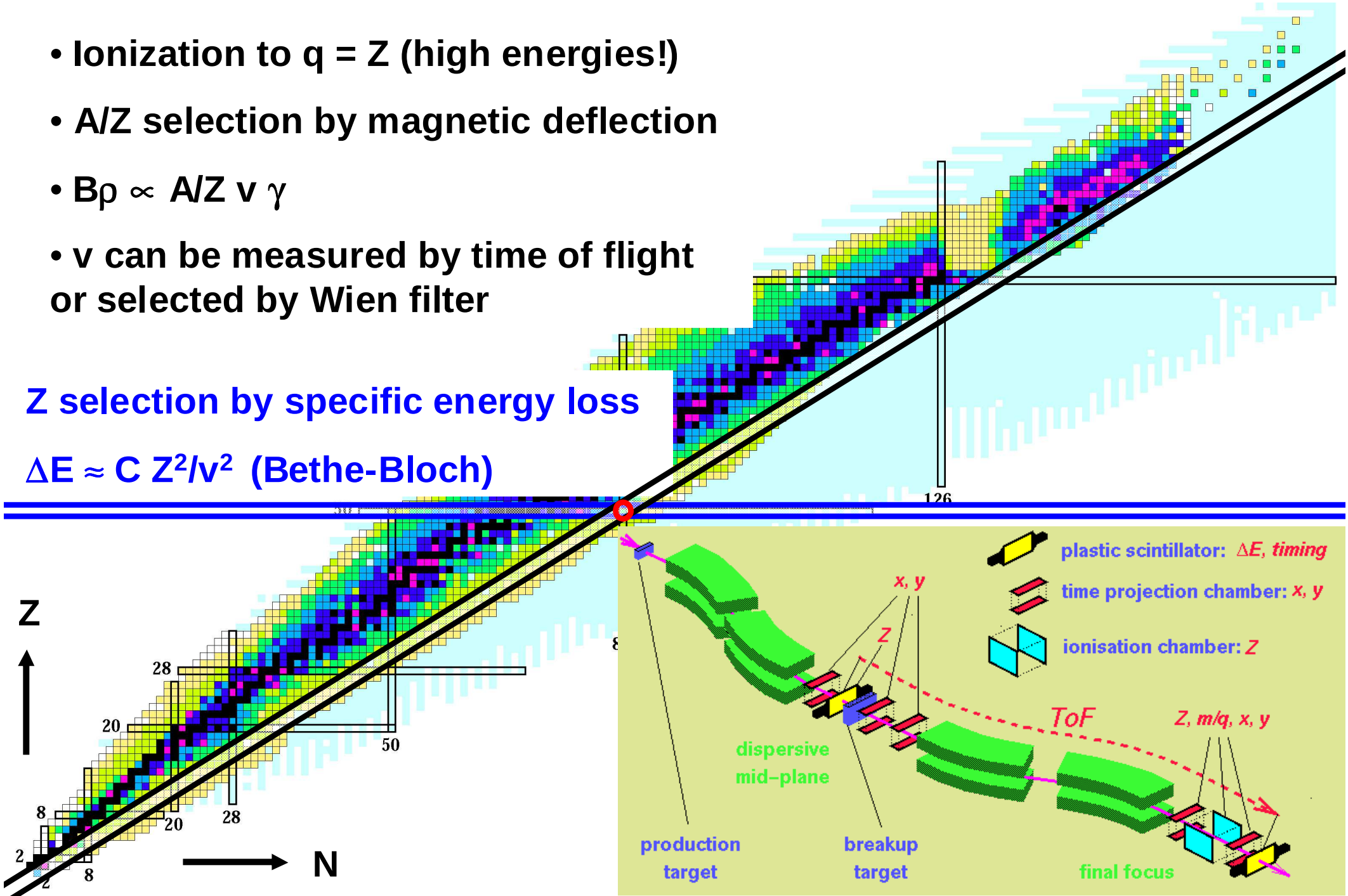

Perfect isotope identification at high energy

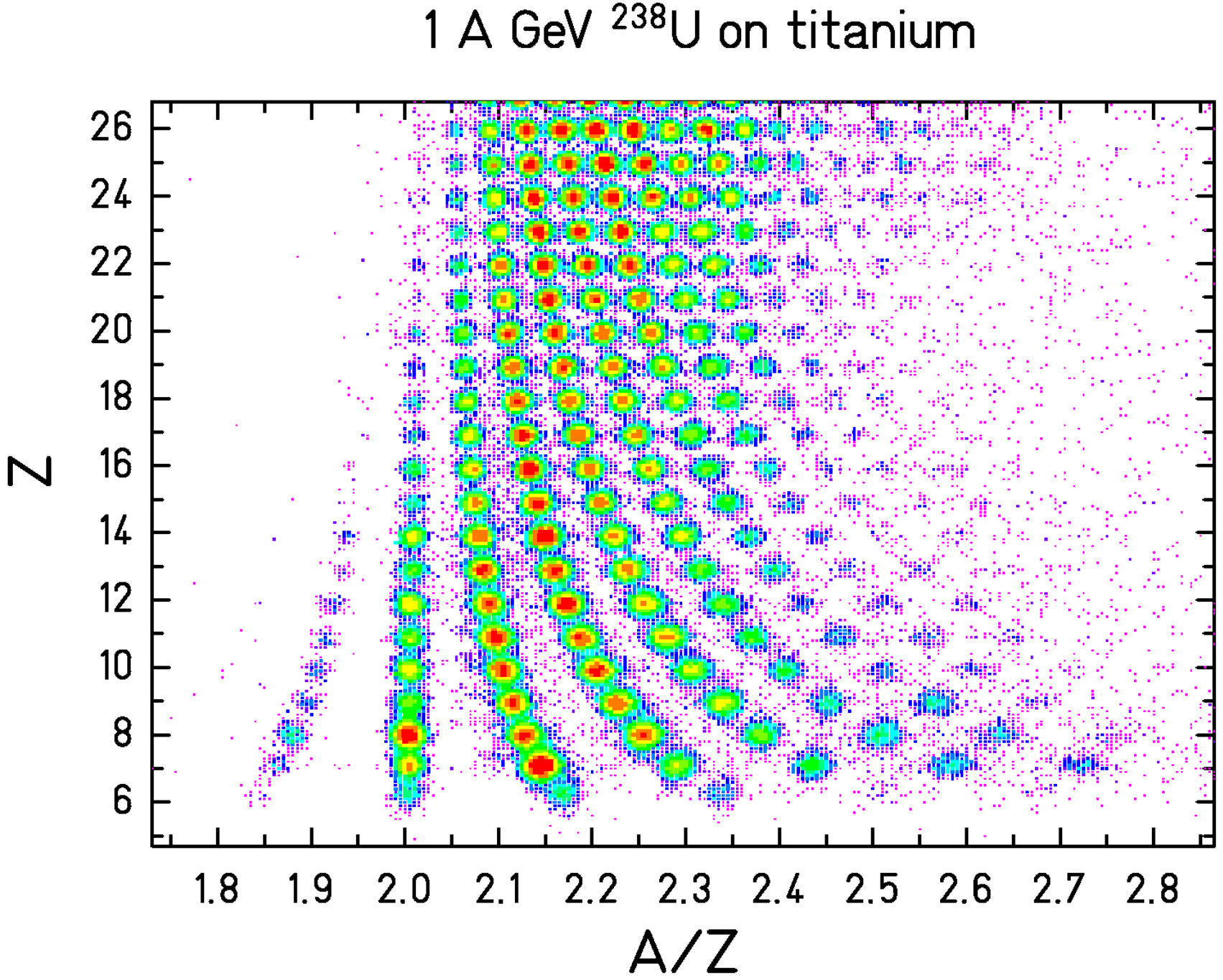

M.V. Ricciardi et al.,Nucl. Phys. A733 (2004) 299.

Optimum energy for FRS-like momentum achromat

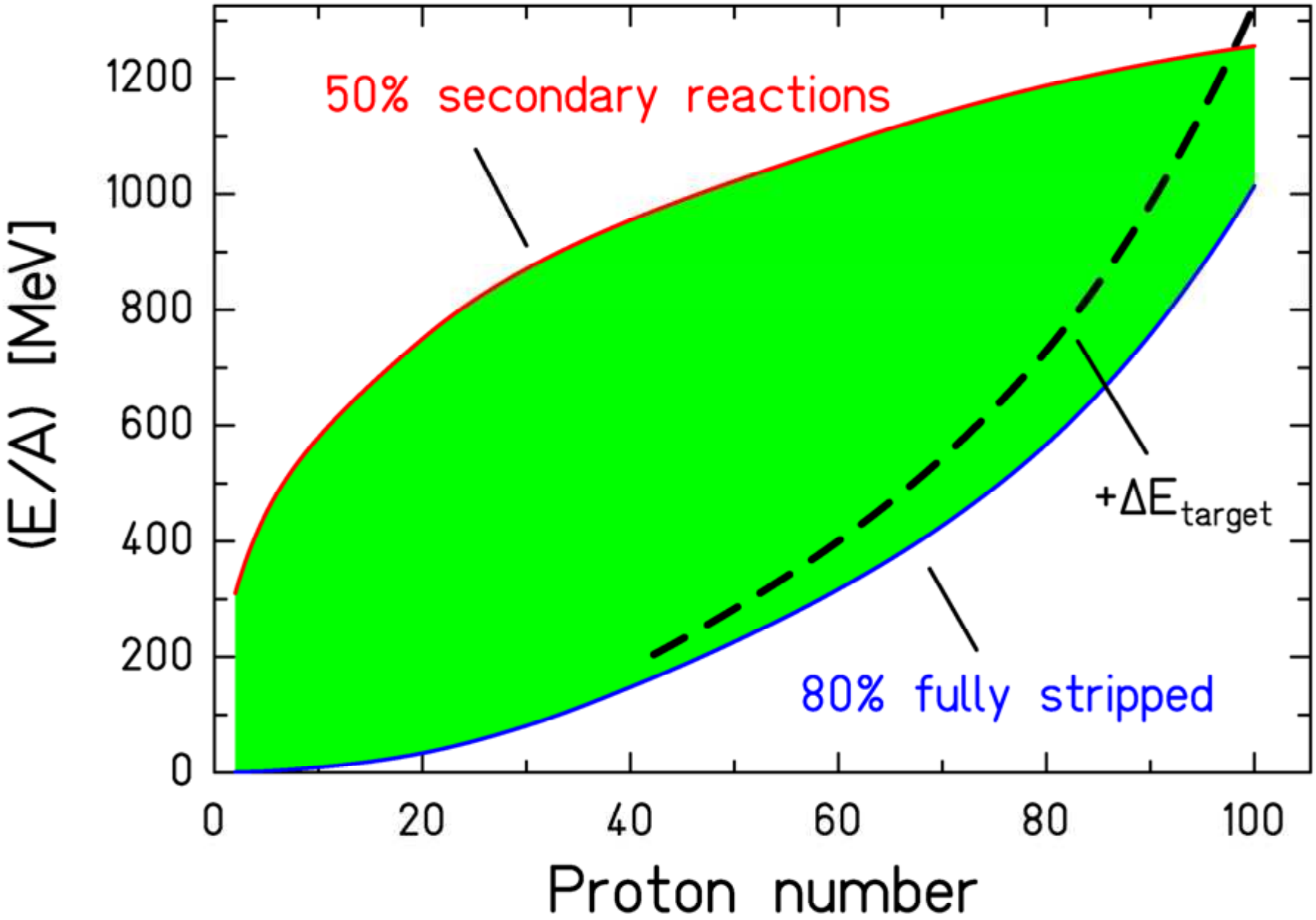

K.H. Schmidt, Euroschool Leuven 2000.

BigRIPS at RIKEN, Japan

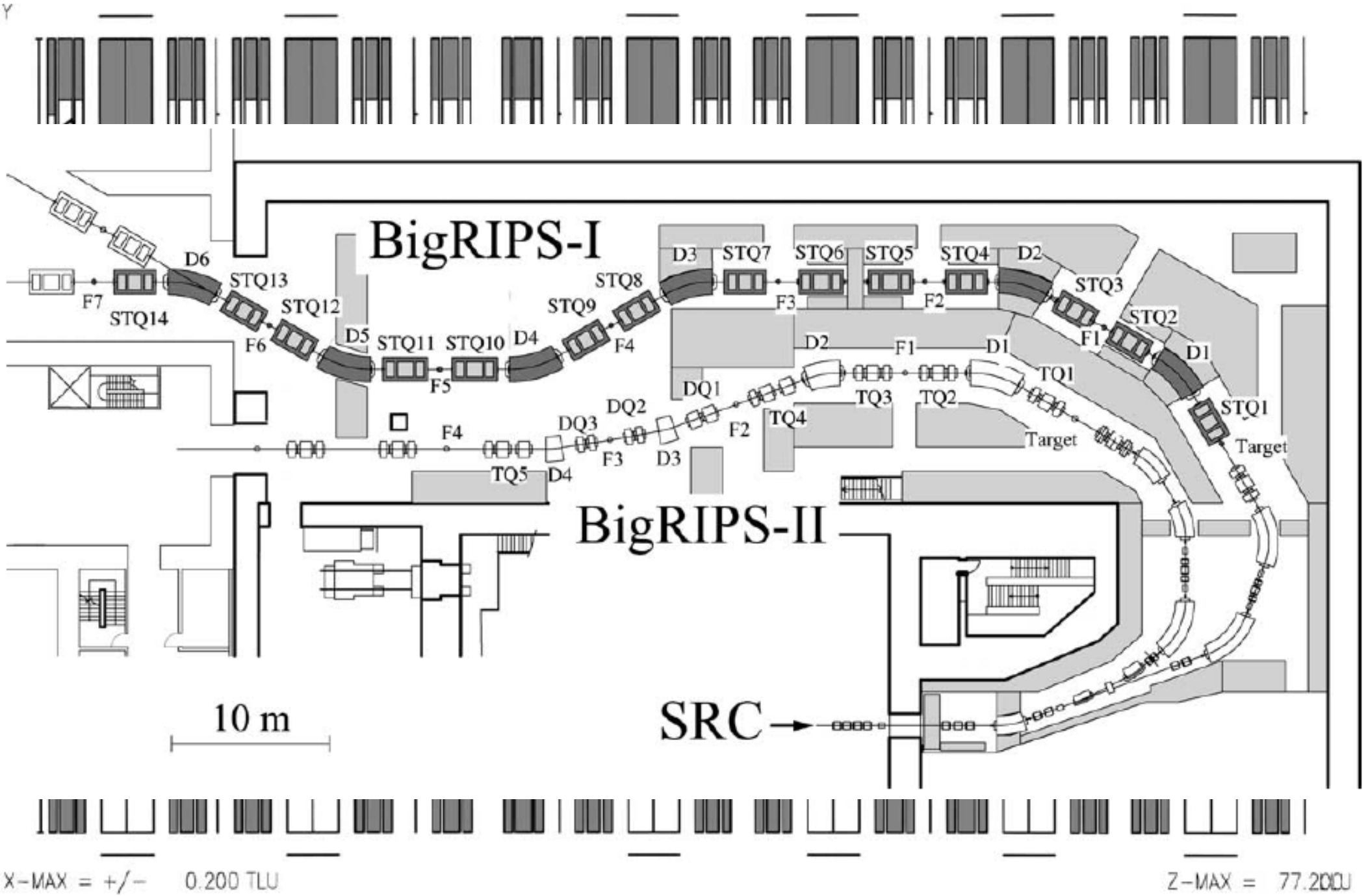

X-MAX = +/- 0.200 TLU

Z-MAX = 77.200U

Super-FRS at FAIR, Darmstadt

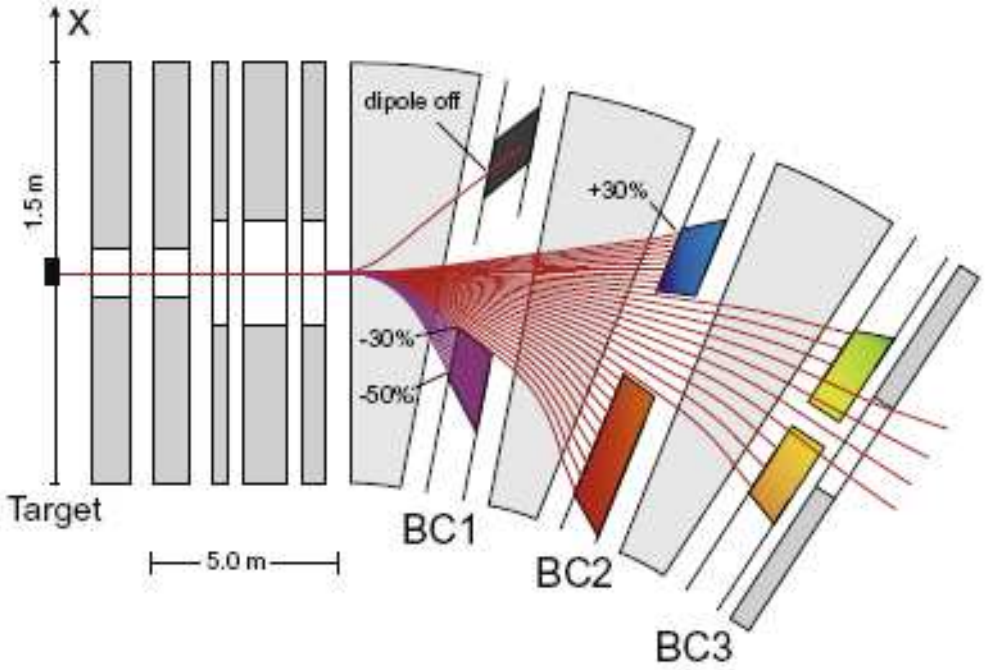

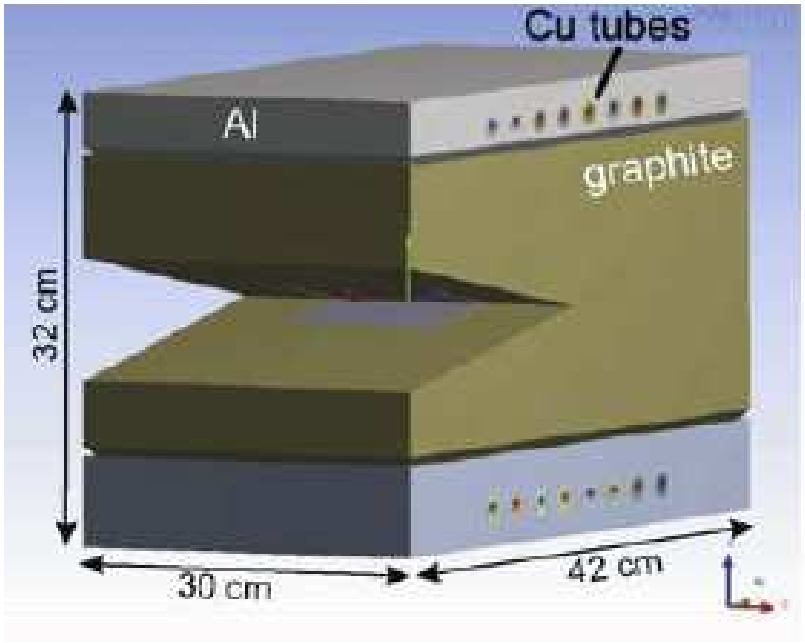

Fig. 4. Beam catcher locations in the first dipole stage of the pre-separator. Depending on the fragment setting the primary beam will be dumped at the position given by the relative difference in magnetic rigidity. Plotted are trajectories of primary beams with different $\delta_{B\rho}$ values in steps of 1%.

Fig. 5. Layout of the front part of the beam catcher. The V-shaped graphite block will absorb the beam energy of up to 50 kW and is actively cooled.

M. Winkler et al., Nucl. Instr. Meth. B266 (2008) 4183.

BigRIPS at RIKEN, Japan

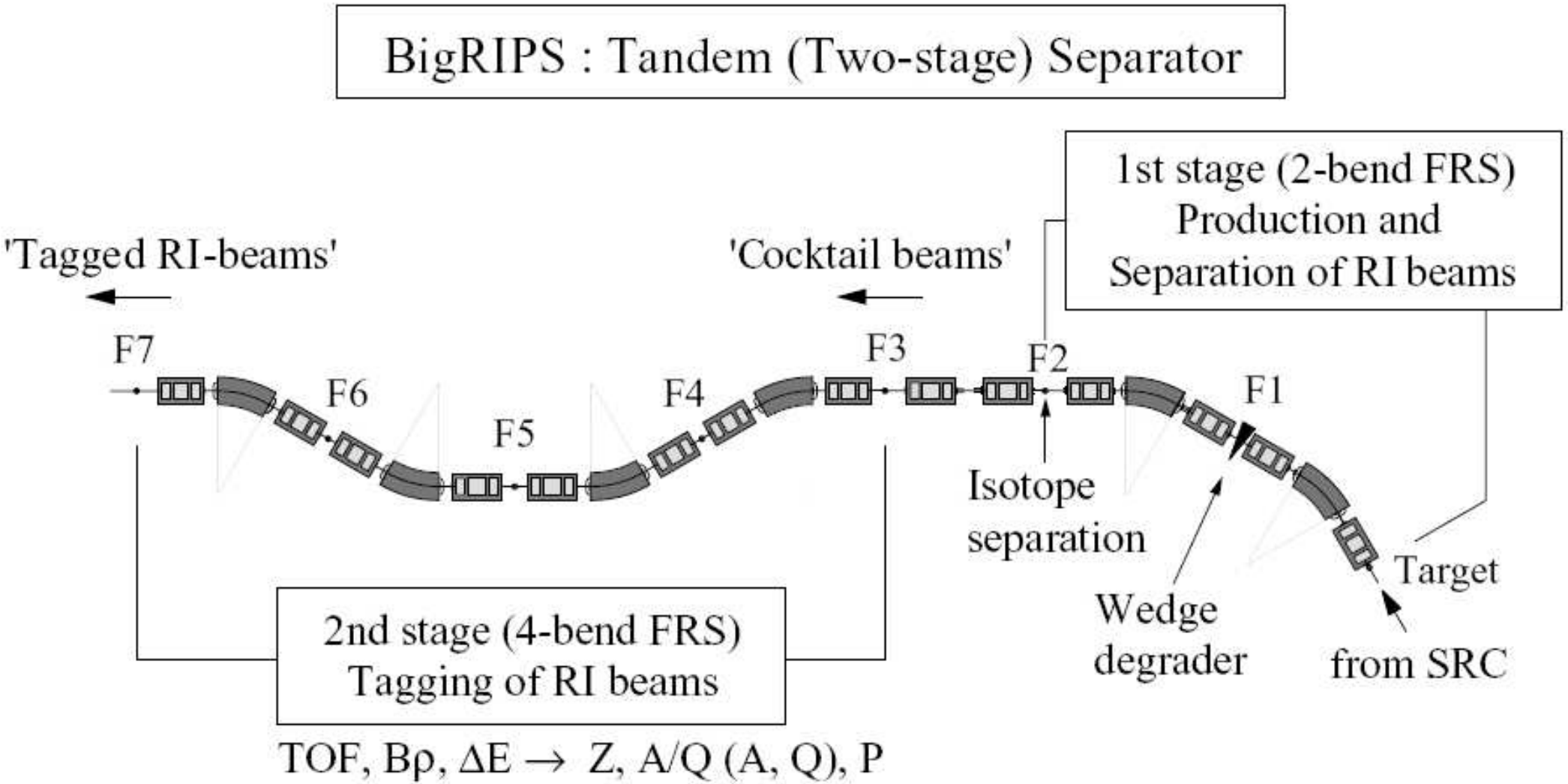

T. Kubo, Nucl. Instr. Meth. B204 (2003) 97.

Q3D Spectrometer

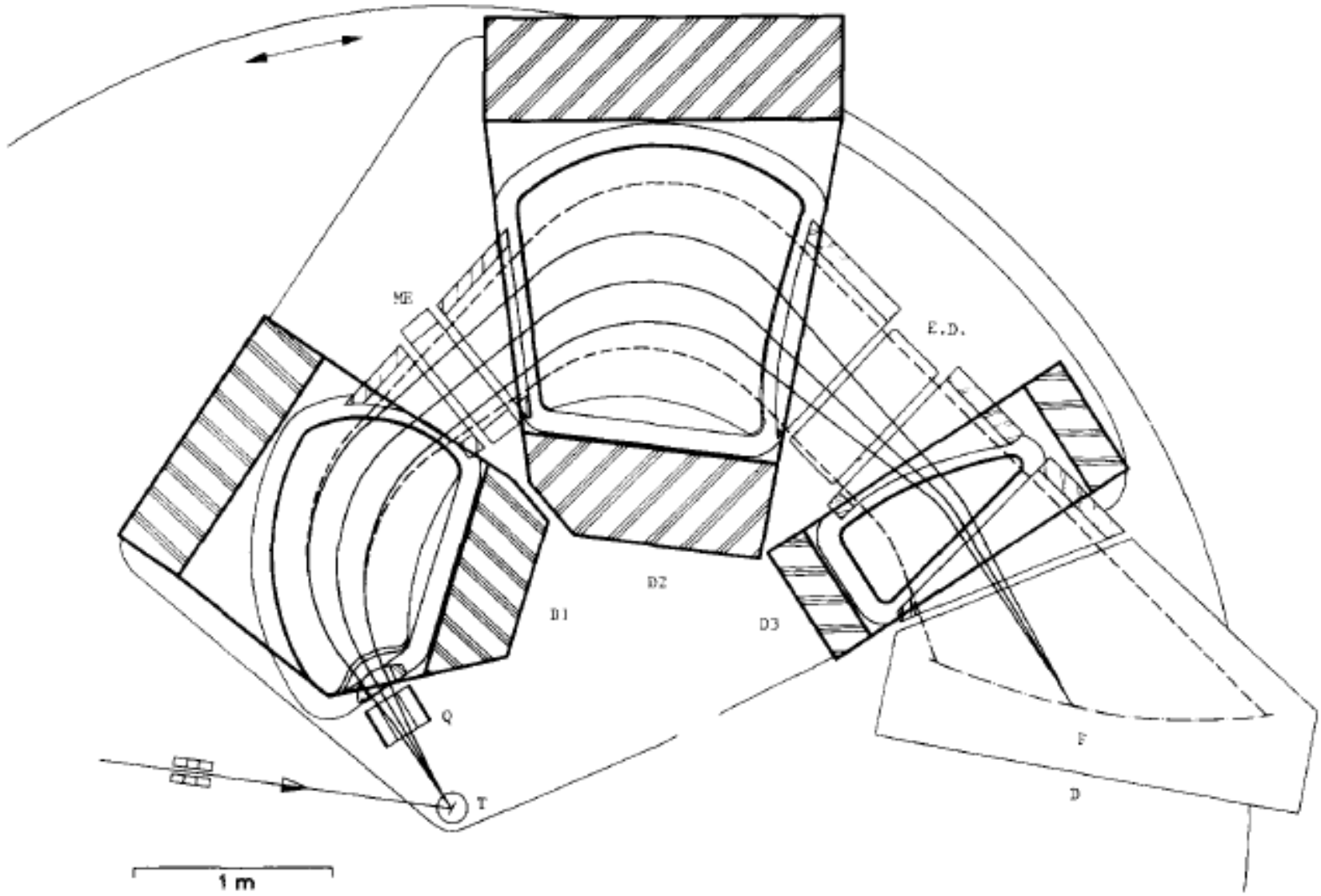

Fig. 1. Ion optical layout of the QDDD spectrograph. T – target chamber; ME – multipole element; D1, D2, D3 – dipole magnets; E.D. – electrostatic deflector; F – focal surface; D – detector chamber.

M. Löffler et al., Nucl. Instr. Meth. 111 (1973) 1.

Example spectrum ^{180}Hf(d,p)

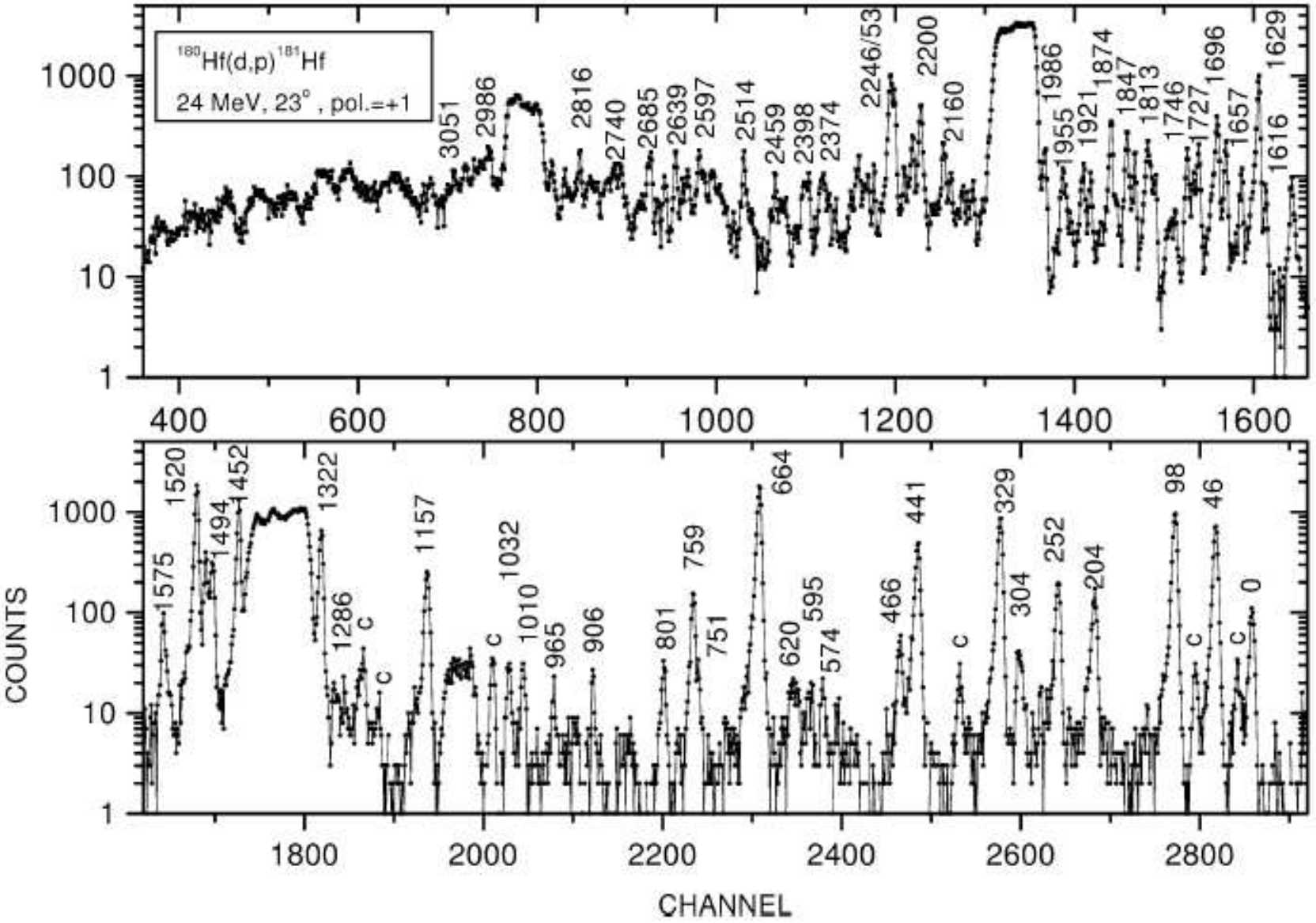

Fig. 3. An example of proton spectra from the reaction ^{180}Hf($\vec{d}$, p)^{181}Hf. The peaks are labelled by the excitation energy in keV. The proton groups labeled with 'c' belong to contaminant isotopes.

The SPEG spectrometer at GANIL

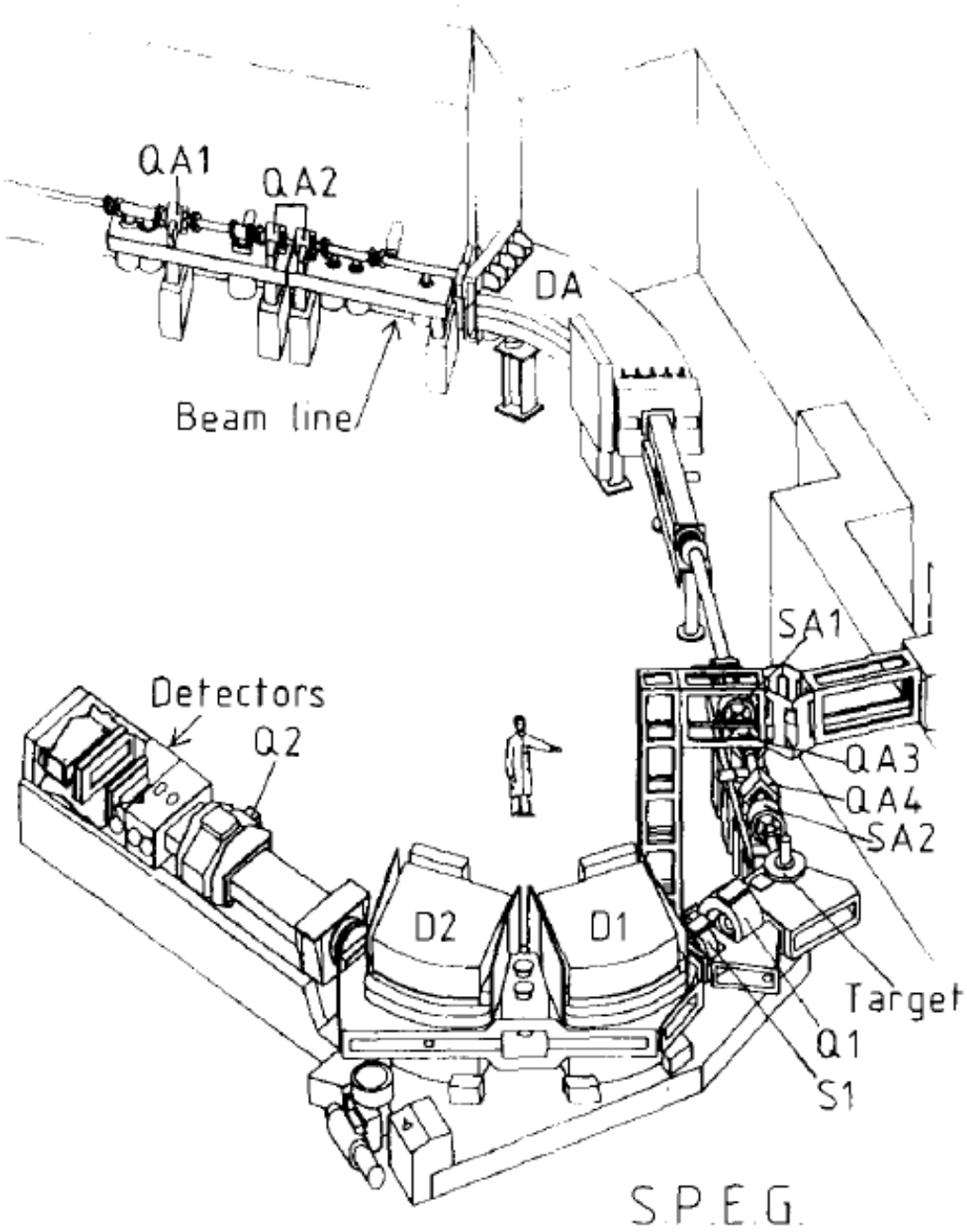

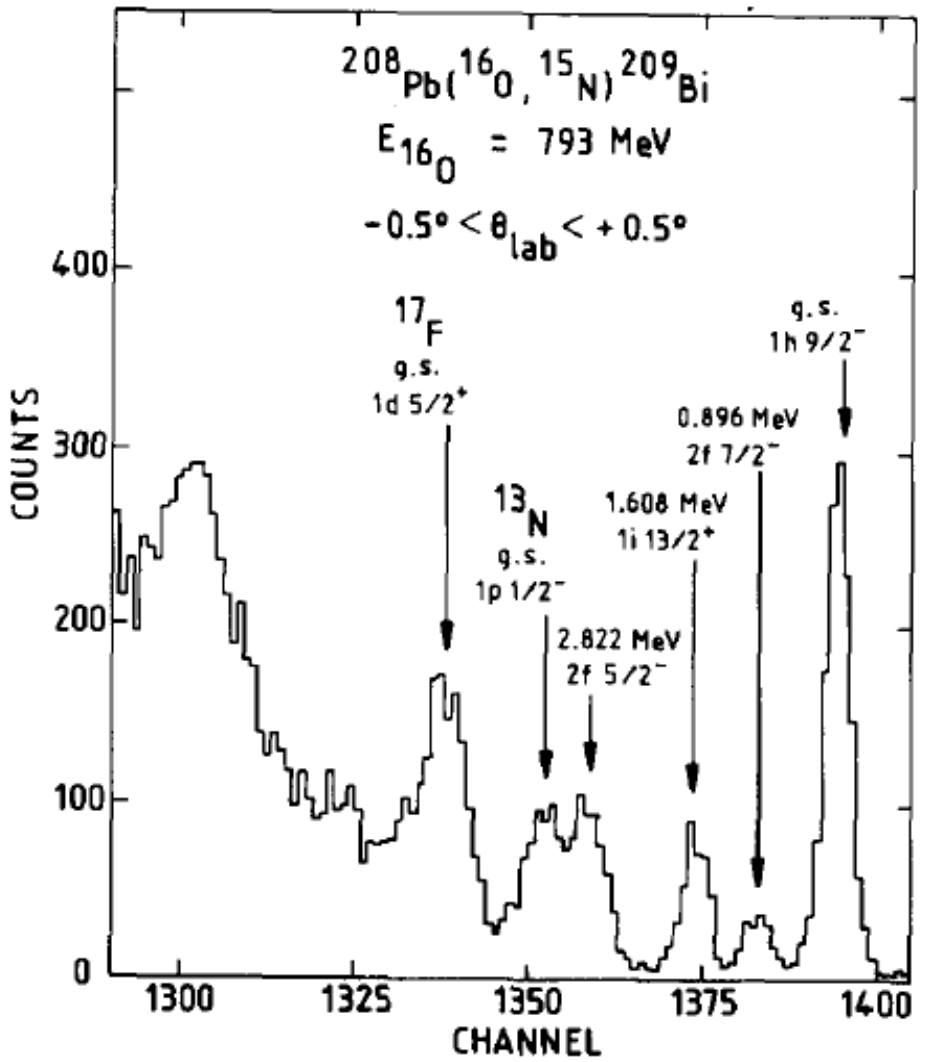

Fig. 20. Zero degree spectrum measured for the $^{208}Pb(^{16}O, ^{15}N)^{209}Bi$ reaction.

L. Bianchi et al., Nucl. Instr. Meth. A276 (1989) 509.

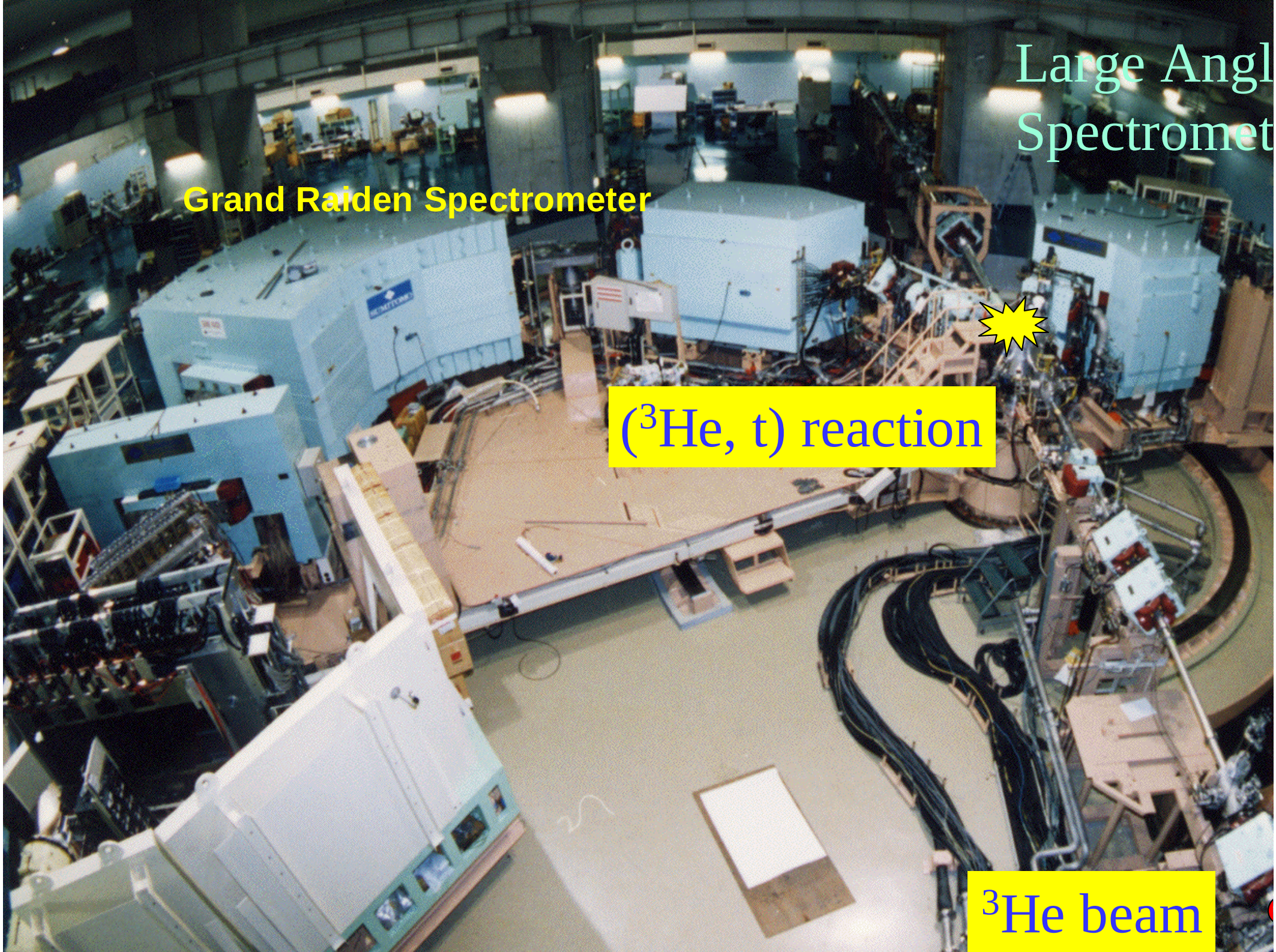
Large Angl
Spectromet
Grand Raiden Spectrometer
(^{3}He, t) reaction
^{3}He beam

Beam line WS-course at RCNP

T. Wakasa et al., NIM A482 (’02) 79.

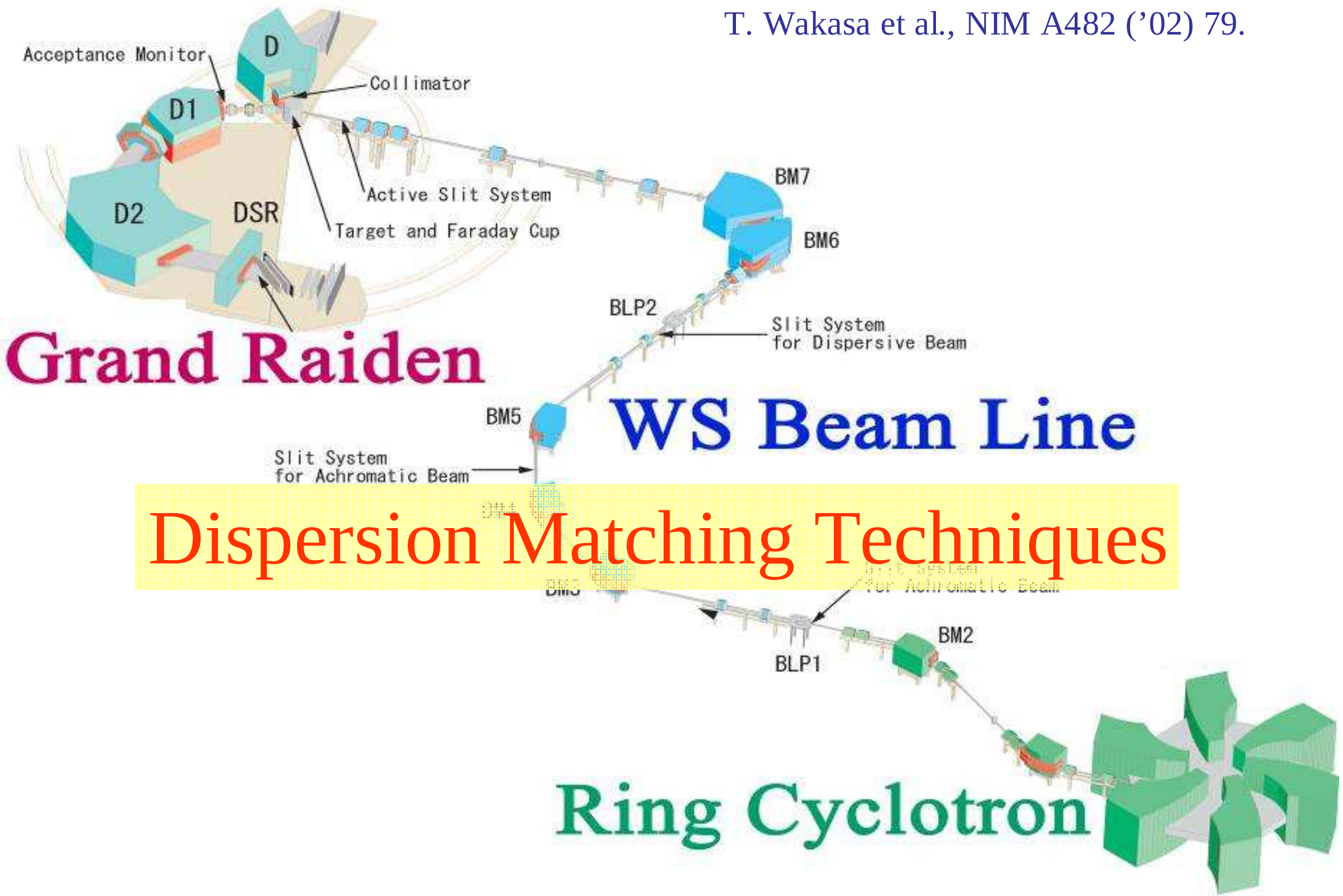

$^{9}Be(^{3}He,t)^{9}B$ spectrum (at various scales)

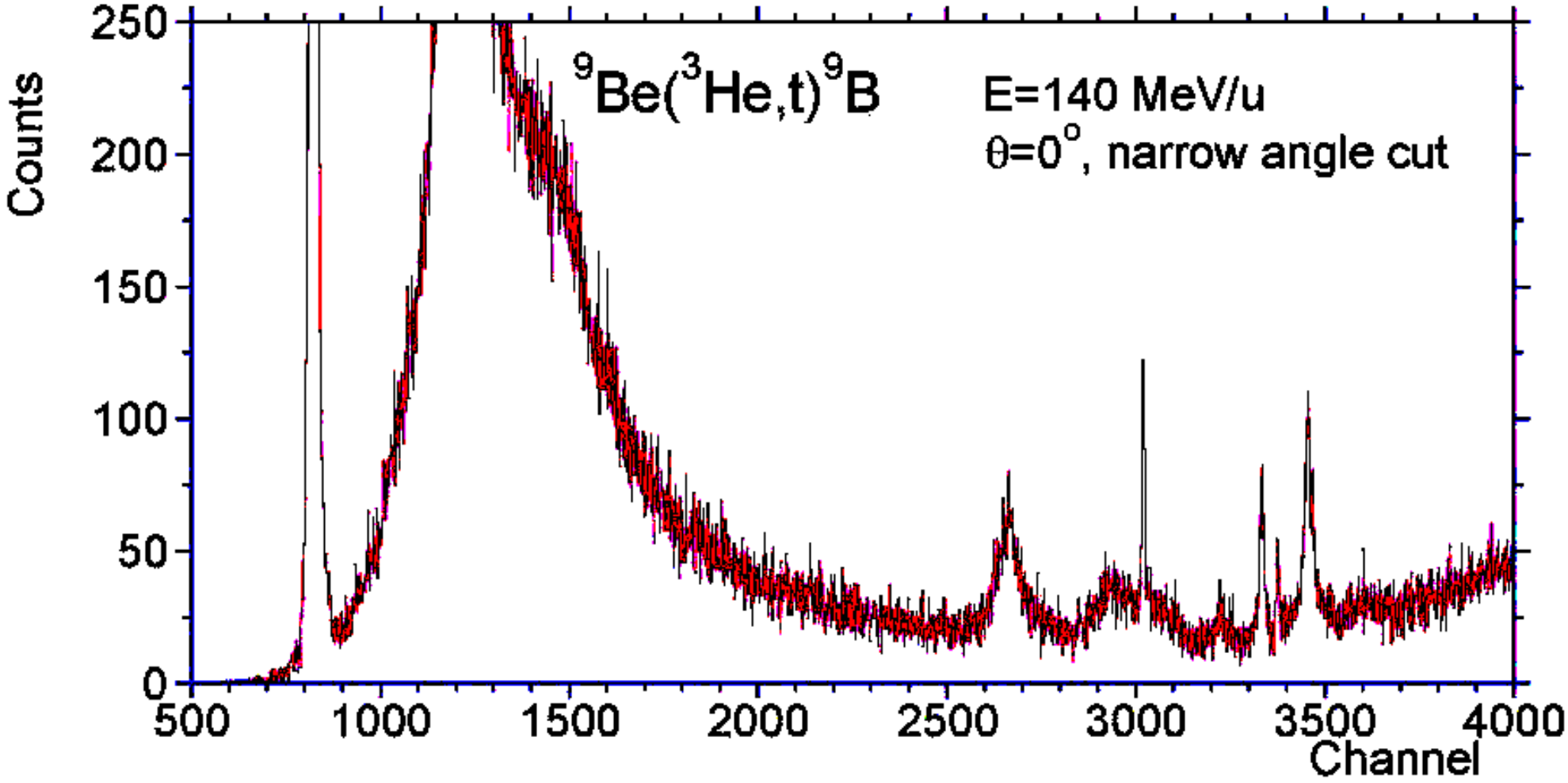

Y. Fujita

^{9}Be(^{3}He,t)^{9}B spectrum (II)

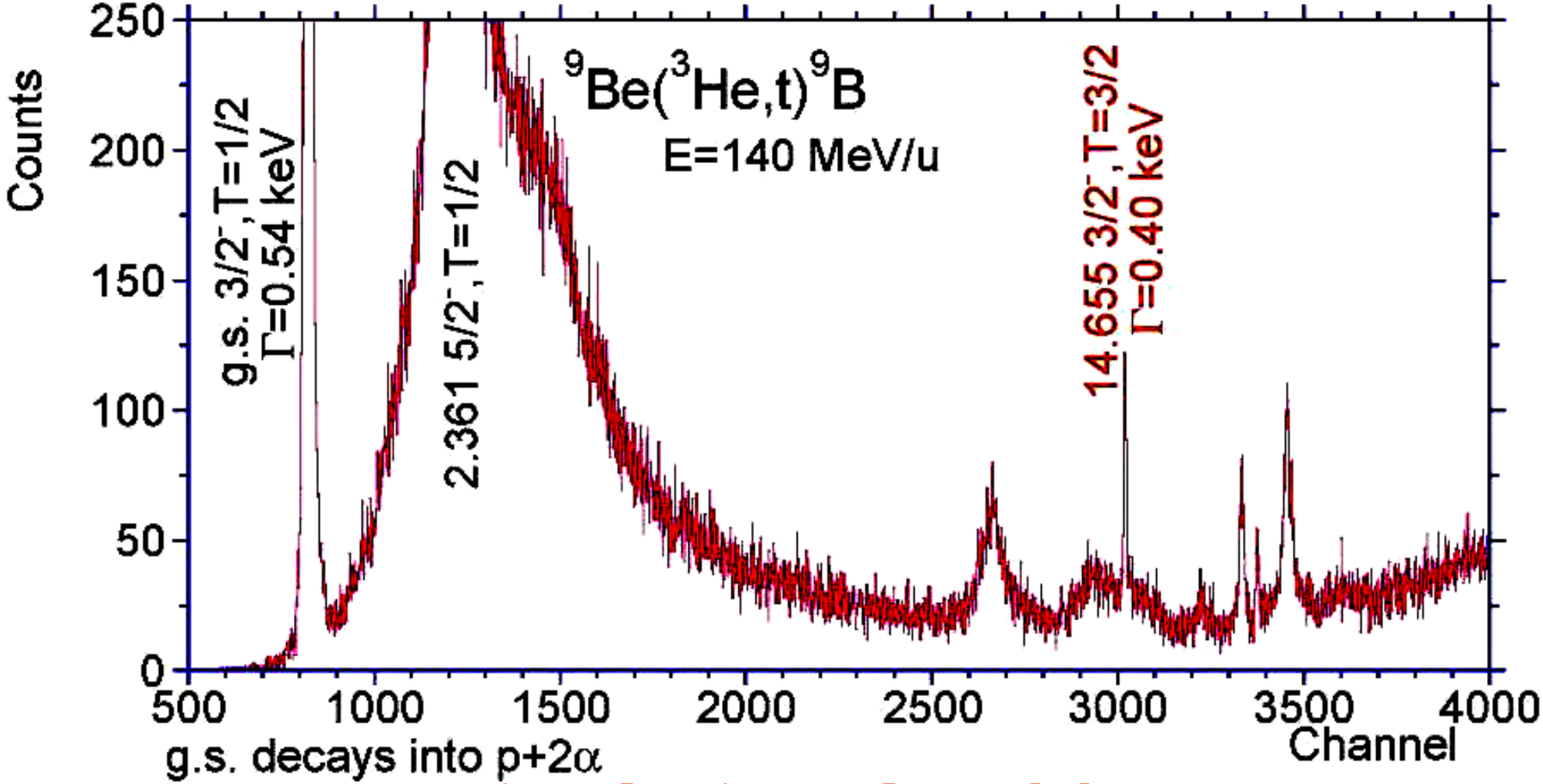

Isospin selection rule prohibits

proton decay of **T=3/2** state!

C. Scholl, Köln

References

- **Inorganic Mass Spectrometry: Principles and Applications, Sabine Becker, Wiley, 2007.**
- **Optics of Charged Particles, Hermann Wollnik, Academic Press 1987.**
- **Mass spectroscopy, H.E. Duckworth et al., Cambridge Univ. Press, 1986.**
- **The transport of charged particle beams, A.P. Banford, E. & F.N. Spon, 1966.**
- **Proceedings of the EMIS (Electromagnetic Isotope Separation) Conferences:**
  Nucl. Instr. Meth. B266, NIM B204, NIM B126, NIM B70, …